Max-Planck-Institut
für Plasmaphysik

Annual Report 2014

Replacement of an ICRF antenna inside the vacuum vessel of the ASDEX Upgrade tokamak. During plasma operation the antenna radiates electromagnetic waves at power levels of about one MW, which are absorbed by the confined plasma. Shown on the left is an ICRF antenna nearly assembled. Its frame is covered by protection tiles. The three technicians are transporting a return-conductor structure of another ICRF antenna.

The inner wall of the tokamak on the right is partly covered by protection tiles. The copper ring at the top belongs to a passive saddle coil which supports the stabilisation of the plasma position. In front of the ring there are active saddle coils fixed in steel casings. They are used to control plasma instabilities and magnetic field errors.

Annual Report 2014

The Max-Planck-Institut für Plasmaphysik is an institute of the Max Planck Gesellschaft, part of the European Fusion Programme and an associate member of the Helmholtz-Gemeinschaft Deutscher Forschungszentren.

In Greifswald, the commissioning of Wendelstein 7-X is now at the centre of attention. The cryostat has been successfully evacuated and its structural integrity has been confirmed. The normally conducting coils have already passed their commissioning tests and the superconducting coil system has proved to be Paschen-tight under non-cryogenic conditions. The next important commissioning step, in early 2015, will be the cool-down of the magnet system to liquid helium temperatures of four kelvin.

Meanwhile, the Wendelstein 7-X team continues to work with great dedication in order to keep to the tight schedule: The periphery assembly with its extensive pipework and the installation of several thousand cables still requires great efforts from the assembly crew. Engineers, technicians and scientists are working hard to wrap up the control systems, to deliver a comprehensive set of diagnostics and to prepare the heating system for the first plasma operation. Also, the vacuum, cryo and heating teams are putting in many night shifts to watch over the commissioning progress or perform tests.

Even though the remarkable achievements made in the construction of the Wendelstein 7-X machine outshine the surrounding events, it is more than a side note to state that IPP in Greifswald is undergoing a transformation: While the future completion of Wendelstein 7-X to a steady-state machine will still require extensive assembly effort, the focus of the institute must now shift more and more towards the scientific exploitation of the machine. The first meeting of the international programme committee in March 2015 is a significant milestone on this route.

At IPP's Garching site in 2014 about half of the operational time of ASDEX Upgrade was devoted to the Medium Sized Tokamak campaign of the EUROfusion consortium. Over the year, an impressive number of roughly 200 collaborators came to Garching to participate in these experiments, and IPP scientists also had a significant share. Results from both the MST and the IPP internal part of the ASDEX Upgrade programme continue to support preparation of ITER and address key issues for the European DEMO.

Scientifically, one of the highlights of the ASDEX Upgrade programme was the exploration of low collisionality ELM mitigation using RMP coils, which was made possible by slowly varying the poloidal spectrum of the perturbation field, allowing an adiabatic scan of plasma response at fixed toroidal mode number. Stationary ELM mitigation was demonstrated, albeit at the price of reduced energy confinement. Analysis shows that the optimum phasing for mitigation is the one where the peeling component of the plasma response is optimized. Another highlight was the achievement of stationary power and particle exhaust at a world record value of $P_{sep}/R=10$ MW/m, i.e. two thirds of the value for ITER, by means of feedback controlled impurity seeding. The newly installed solid tungsten tiles in the outer divertor performed without any problem, as did the two rings of P92 steel tiles on the inner heat shield, which serve as a mockup of the EUROFER steel, which is the structural material candidate for the European DEMO.

Turbulent transport has been studied with various newly installed reflectometry systems to measure simultaneously a large spectrum of fluctuation parameters for comparison with turbulence codes. A first result is that scale-resolved turbulence levels in H-mode discharges compare quite well with GENE simulations in the transition range from ion-temperature-gradient to trapped-electron-mode turbulence. A breakthrough was achieved in clarifying the role of filamentary transport in L-mode plasmas. In agreement with analytical models, the radial propagation velocity is found to increase when the filaments detach from the divertor, leading to a radial shoulder in the SOL density profile. For the first time, fully detached stationary H-mode discharges were achieved relying on nitrogen seeding to increase the radiative divertor losses. The discharges were modelled with SOLPS, and the important role of a radiation zone above the X-point in the detachment process was consistently identified in simulations and by bolometry. The evolution of the injected nitrogen in the tokamak vessel was investigated by experiments on ASDEX Upgrade and in the laboratory in combination with the WallDYN and DIVIMP codes describing the migration of nitrogen. The nitrogen content in the outer tungsten surfaces was found to saturate quickly, while a measurable fraction of the nitrogen is converted to ammonia.

The operation of JET with the ITER-like wall was successfully continued in 2014 under the new umbrella of the EUROfusion consortium. One of the main focuses of the IPP contribution was the physics of power exhaust, guided by a scientific team active in JET and ASDEX Upgrade exploiting the European platform in the best manner. Experiments aiming to reach the highest possible radiation fraction in the ITER-like wall were carried out and assessed as a scenario for both the planned DT campaign in JET and future reactor-sized devices like ITER. Studies on transient divertor heat loads due to energy losses from the pedestal region by ELMs, started in 2008, were completed and eventually resulted, again in conjunction with ASDEX Upgrade results, in improved predictive capability of these burst-like thermal loads towards ITER.

Efforts by the ITER cooperation project at IPP continued with major contributions to the development of heating systems, diagnostics and plasma control as well as theoretical investigations. The ELISE test facility successfully investigated operation parameters for H and D in a caesiated source. This is accompanied by supporting investigations at smaller facilities and theoretical modelling. The contributions to the consortium for the development of the ITER ICRF antenna and ECRH Upper Launcher continue. For the latter the impact of the deposition profile on performance and the behaviour of MHD instabilities has been analyzed. Within the Framework Partnership Agreement for the ITER Diagnostic Pressure Gauges the detailed project planning was concluded and system level design was started. Based on the agreement on the development of the ITER bolometers work on detailed system assessment and project planning has begun within the consortium headed by IPP. Also, optimization of collimators in order to define desired viewing geometries while reducing stray light and reflections was achieved. Work on the Plasma Control System Simulation Platform for ITER continues on its way towards the preliminary design review. Furthermore, as part of a contract with ITER the ASTRA and STRAHL codes have been used to set up a simulation of the pre-thermal quench phase of disruptions in ITER and benchmark it successfully to experimental data from ASDEX Upgrade.

There are three theoretical divisions at IPP, two in Garching and one in Greifswald, which work on advancing the basic understanding of plasma theory, develop novel mathematical methods, and lend theoretical support to the experiments. For several decades, it has been very difficult to make simulations of electromagnetic instabilities and turbulence using particle-in-cell codes because of a famous "cancellation problem" in the equations, but in 2014 this Gordian knot was finally untied by the development of a new algorithm that enables such simulations to be carried out much more robustly and at less computational expense than before. Using this method, it is possible to make accurate simulations of both microinstabilities, which cause turbulence, and large-scale instabilities, which set plasma operating limits in tokamaks. On this subject, first simulations of the spontaneous growth of tearing modes in the presence of electromagnetic turbulence were achieved and showed that growth and saturation are fundamentally affected by the presence of the small-scale fluctuations. Moreover, simulations of magnetohydrodynamic instabilities for ITER parameters indicated the importance of global effects for the transport of alpha particles from the core to the edge.

On behalf of the Directorate and the Board of Scientific Directors I would like to thank all members of the institute for their substantial contribution to the success of fusion research at IPP in the last year.
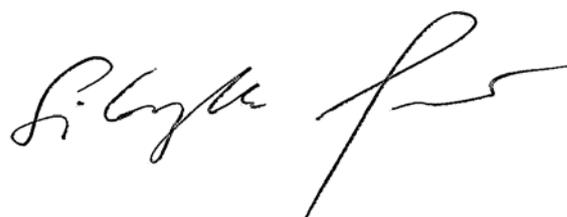
Scientific Director Sibylle Günter

Content

Tokamak Research

ASDEX Upgrade

Head: Prof. Dr. Arne Kallenbach

1 Overview

ASDEX Upgrade (AUG) operation was conducted from February till end of October 2014 with 70 experiment days and 1227 useful plasma discharges. 592 discharges were performed for the new EUROfusion MST1 program, while 541 covered internal proposals. The major enhancements for 2014, the massive tungsten divertor III and the large scale divertor manipulator DIM-II performed very well, and the new B-coil AC power supply BUSSARD was successfully commissioned. Parallel to the plasma operation, procedures for program planning, conduction and evaluation were developed and refined with a focus on facilitating the smooth integration of MST1 and the internal program. The expansion of the infrastructure to provide for up to 40 MST1 guest scientists on site simultaneously had to be completed in early 2014 on the fly during the first MST1 experiments. The start of the campaign appeared somewhat turbulent, since early hardware failures such as the damage of the gate valve of NBI box II required a substantial re-organization of the program. Due to the strong commitment of the people involved as well as the patience and endurance of experiment proponents, a smooth end very successful campaign could finally be established by late spring. Nearly all international AUG collaborations have been integrated into the new MST1 scheme, securing EU funding for these important activities (see also section 2).

The ASDEX Upgrade experimental program is devoted to the preparation of ITER operation, research for basic physics understanding and the design of a prototype fusion reactor, DEMO. In 2014, ASDEX Upgrade operated seven months, in equal shares for IPP-internal and the new EUROfusion MST1 programs. The 2013 extensions, notably the full tungsten divertor III, performed very well. In November, a vent for installation of two new ICRF antennas has started.

1.1 Major Physics Results

Progress in physics understanding and technical developments has been achieved on various topics as power exhaust and divertor physics, pedestal physics, MHD control, ELM mitigation, turbulence studies and ITER scenario development.

Divertor dissipation of very high power levels was demonstrated up to P_{sep}/R values of 10 MW/m, which corresponds to 2/3 of the value foreseen for ITER, while keeping the target peak power load below 5 MW/m^2. This new record level could be achieved in combination with a high divertor neutral particle pressure, facilitated by a new helium valve introduced in the cryo pump for pumping speed variation.

Pedestal studies benefited from the recent enhancement of the edge CXRS diagnostic, enabling stability studies with different impurity seeding species and conditions. The reduction of the edge bootstrap current by the Z_{eff} increase due to seed impurities was identified as an important player for the impurity-induced changes of energy confinement and ELM characteristics. The versatile MHD real-time control system has been further enhanced by new controllers and matured into a general-purpose tool, with applications ranging for NTM stabilisation and disruption avoidance to central electron temperature control as required for studies of the NBI current drive efficiency.

ELM mitigation by magnetic perturbations (MP) could be achieved in 2014 for the first time in AUG under low collisionality conditions, allowing comparisons with other machines like DIII-D or MAST. In course of collaboration with CCFE in the MST1 framework, MP penetration calculations were performed with the MARS-F code, which take into account the linear response of the plasma to the external perturbations. In experiments varying the phase between the upper and lower B-coil rows, a clear phase shift of the plasma response was indeed observed. Plasma slowing down by resonant MP (RMP) interaction was investigated in the context of the study of neoclassical tearing modes (NTMs). The changes of plasma rotation were attributed to local torques on several resonant surfaces, while braking caused by non-resonant components via the neoclassical toroidal viscous torque (NTV) appeared negligibly small for the present experimental conditions. As a result of the considerable number of RMP experiments and extensive modelling work, a much clearer physics picture of the effect of MPs with different resonance conditions is currently evolving, taking into account both the screening but also the amplification of perturbations by the plasma.

Turbulence studies were continued from edge to plasma core, exploiting many new diagnostics which were recently installed at AUG in the framework of the Helmholtz virtual institute (VI). Comparisons with first principle codes like GENE and GEM-R revealed overall good agreement, but also significant deviations like the different response of small and large scale structures on changes of the temperature gradient drive were identified. Refined GENE calculations have been initiated to disentangle the origin of the deviations observed.

In 2014, investigations of the ITER baseline scenario were continued. Under baseline conditions, very large, low-frequency ELMs occurred which were resilient against the AUG ELM mitigation toolset. Modifications to the baseline scenario were investigated and showed promising initial results. Operation at a higher safety factor at reduced plasma current resulted in smaller ELMs, which also appeared to be more susceptible to mitigation. In addition, better energy confinement, related to the higher β at lower plasma current, was achieved. Such an alternative baseline scenario may be very attractive for ITER, since it ameliorates both the ELM power load problem as well as the disruption forces.

In 2014 also a number of new diagnostics were brought into operation. Examples are the first channel of the polarimetry and several new reflectometry diagnostics, which have been installed in the framework of the Helmholtz VI. The collective Thomson scattering diagnostic (CTS), which had been advanced by the Danish collaborators for a number of years, has matured now into a validated tool for the measurement of fast ion velocity distributions and isotope ratios.

1.2 Machine Enhancements

The major enhancement for the 2014 campaign was the installation of the massive tungsten divertor III with its large scale divertor manipulator DIM-II and a liquid helium valve allowing the reduction of the cryo pumping speed, which is required to obtain the high divertor neutral pressure necessary for high power exhaust. While divertor III performed very well during operation, vertical cracks were detected on many tungsten tiles after vessel opening. These have been attributed to the combination of thermal stresses and electromagnetic forces exerted on the tiles during plasma discharges, which exceeded the stresses produced before in GLADIS tests. Neither the cracks nor the leading edges which occurred after small segment de-localisations lead to increased tungsten concentrations in the core plasma, showing again the good divertor retention for local tungsten sources.

The installation of 2 new 3-strap ICRF antennas for reduced tungsten release has been started with the de-mounting of the old antennas in December 2014. The installation of the antennas and related diagnostics is the major activity of the present machine vent. AUG restart is foreseen in June 2015.

1.3 Preparation of the 2015 Experimental Campaign

Preparation of the 2015 program was started with the call for participation in the MST1 programme in October. The internal Call is to follow in February 2015 after the General Planning Meeting in Lausanne, January 19-23, 2015. 56 experimental days are foreseen for 2015, to be equally distributed between MST1 and IPP-internal program. Both, MST and internal program building will cover experiments till end of April 2016. 40 experimental days are foreseen in early 2016, after which a major vent is planned until end of October 2016.

2 The New European MST Project

A new European activity started 2014 involving 333 scientists, 24 laboratories, 3 tokamaks in 3 different countries (AUG in Germany, TCV in Switzerland and MAST in the UK). These numbers witness the international effort of the EUROfusion Medium Size Tokamak (MST) Task Force, which started its first experimental campaign in AUG.

The MST 2014 campaign in AUG has been interwoven and fully synergic with the domestic one. The strong collaboration and support of the IPP domestic team has been key for its success.

The international community strong interest was concretely expressed with 3000 plasma discharges proposed in the MST experiment call, which exceeded the available MST allocation by about a factor of five. The proposals were discussed in the first MST General Planning Meeting held in Beilngries, Germany. As a result 41 experiments were selected for the MST campaign and organized under three main blocks: 1) scenario and confinement, 2) MHD, 3) plasma-wall-interaction and edge physics. 11 modelling tasks have been defined.

To ensure the best integration with the local team, two scientific coordinators have been selected for many of the 41 experiments, usually with one from IPP and one from one of the other participating laboratories.

The MST experimental campaign produced 592 good AUG discharges performed over 70 run days.

The main achievements of the 2014 MST campaign are summarised in the following. More details are in the following chapters.

The ITER baseline plasma scenario was previously established at plasma current of 1.2 MA, with high triangularity δ=0.35, safety factor q_{95}=3, β_N = 1.8, and Greenwald density fraction f_{GW}=0.8. To make it stationary, high gas fuelling (Γ_D=3×10^{22} D/s) was required and as a result only a low normalised confinement of H_{98}=0.8 was achieved. Moreover, this scenario features large undesirable ELMs with a typical energy $\Delta W_{ELM}/W_{ped}$>20 % and low frequency of 10-20 Hz, where so far mitigation with RMP has not been successful. Hence the development of an alternative scenario at lower plasma current (1 MA) has been started with higher edge safety factor q_{95}=3.6. This scenario looks promising as lower fuelling rates are required to obtain a stationary plasmas with H_{98}=1.0.

The effect of impurity seeding on plasma confinement has been studied in plasmas with q_{95}=4.5 and I_p=1 MA. The results show that both in low (0.2) and high (0.35) triangularity plasmas, nitrogen seeding increases the pedestal temperature by 2 % at constant density and hence leads to a beneficial effect on confinement. An orthogonal effect is seen by changing the triangularity from δ~0.2 to 0.35, which increases the plasma density by 3 % at constant temperature. These results contrast experiments on JET with a Be/W wall, where the pedestal temperature is also increased up to 40 % by nitrogen seeding in high triangularity plasmas, whereas in low triangularity plasmas only a small ~10 % beneficial effect is observed. Triangularity in JET did not show any beneficial effect on confinement in plasmas without seeding. Better understanding is key to extrapolate the beneficial effects to ITER.

In the field of ELM control the efforts were focussed towards ELM mitigation using resonant three-dimensional magnetic perturbation (RMP) and ELM pacing via pellet injection. Six experiments where supported to study ELM mitigation at low and high collisionality using RMP, aiming

at characterising the L-mode response of such perturbations, investigating the effect of impurity seeding and pedestal evolution on ELM mitigation by pellets, comparing the pedestal evolution in hydrogen and deuterium and looking at the effect of the divertor geometry on L-H transitions. The international team extended successfully the operating regime with mitigated ELMs to pedestal top electron collisionalities below $\nu^* \leq 0.4$ at q_{95}=3.8 into the region where full ELM suppression is observed on DIII-D. An increase of the ELM frequency up to a factor of 9 and a drop of energy fluence to the target of a factor 4 is observed, but without suppression. However, the remaining small ELMs are sometimes observed in between the large ELMs and could be of a different type. Experiments varying the differential phase of the perturbation field revealed the importance of the plasma response. The best mitigation was achieved at a phase angle shifted by 60˚ with respect to the vacuum approximation agreeing with the theoretical prediction. In all cases the mitigation is accompanied with a strong density pump-out and a loss of confinement by 30 %, though refuelling by pellets can partially restore the confinement whilst retaining mitigation.

The studies on ELM pacing focused on the time lag that needs to pass after an ELM before a small pellet is able to trigger the next ELM, thereby limiting the achievable pacing frequency. This lag time is found in all metal wall devices such as AUG and JET and can be as long as the natural ELM period. The role of intrinsic impurities such as nitrogen or carbon is crucial for pedestal stability and 'zero' lag time – as observed with carbon wall – is recovered with nitrogen puffing to levels that also show increased pedestal confinement.

Experiments on disruptions aimed at assisting ITER in defining its Disruption Mitigation System design. With the use of Massive Gas Injection (MGI) to mitigate disruptions, the competition between radiation and conduction has been studied, investigating also the magnitude of toroidal asymmetry of radiated power with up to two injecting valves. Systematic scans of gas type, quantity, thermal energy and q_{95} have been performed, which constitute a good base for modelling, already started with ASTRA-STRAHL and with JOREK. Disruption prediction activities – under a dedicated task – followed three approaches: search for MHD signature carrying predictive information, mapping of disruption causes for dedicated predictors based on a multi-machine approach and development of predictors from scratch needing a learning process with low number of samples.

For the first time a scenario reproducibly producing a runaway electron beam has been set-up and successful runaway electron suppression via MGI has been achieved in the same discharges.

Experiments on avoidance – or delaying – of disruption focused on stabilisation of MHD modes through the localised injection of electron cyclotron waves. This needs eventually to be combined with a soft plasma termination strategy.

Core MHD stability and its control has been addressed by several successful experiments that (a) optimised the real-time control of Neoclassical Tearing Modes (NTM) via Electron Cyclotron Current Drive, in particular in terms of robustness and power/alignment/timing requirements; (b) explored the interaction between NTM stability and external static and dynamic magnetic perturbation and the NTM onset at low rotation; (d) probed via resonant field amplification the no-wall stability β-limit with conducting structures – a regime particularly interested in perspectives of high β-scenarios towards steady state; (e) contributed to the development of active real-time sawtooth control techniques. Full 3-dimensional electro-magnetic modelling of AUG with the CARIDDI and CAFE codes has been completed and it is ready for exploitation with the CarMa code using realistic 3D conducting structures aiming at quantifying plasma stability with realistic electromagnetic boundary conditions.

Experiments on fast ion physics, supported by extensive modelling, focused on the effect of both micro-turbulence and MHD on fast ion transport and on the neutral beam current drive efficiency and distribution, as well as on the MHD modes excited by the fast particles themselves. Radial transport of fast ions is significantly enhanced by large-scale MHD events. The internal redistribution of fast ions by sawtooth crashes is found to be described well by the basic Kadomtsev reconnection model assuming simple particle convection along the reconnected field lines. No anomalous transport is observed during the reheating phase. The effect of micro-turbulence alone was investigated specifically in MHD-quiescent, high-power NBI discharges. While a clear outward shift of the current profile is observed in going from on- to off-axis heating, anomalous effects do occur, consistent with a radial diffusion coefficient of order 0.5 m^2/s. An investigation of Alfvén Eigen-mode (AE) excitation and of the effect of AEs on fast ions was carried out at varying density, beam energy and deposition location, yielding rich results on both TAEs and RSAEs.

Significant progress was made in integrating the real-time transport code RAPTOR into the AUG discharge-control environment. Improvements in q-profile modelling were demonstrated, as well as robust protection strategies against diagnostic faults. State estimates are now produced by RAPTOR every 10 ms, and real-time control tests can commence shortly.

The fundamental O-mode (O1) ECRH heating scheme envisioned for ITER was investigated at high field (2.9 T) with 105 GHz gyrotrons.

A variety of experiments have been performed focusing on the physics of detachment, high radiation scenarios, erosion of PFCs and filamentary transport.

The formation of the High Field Side High Density (HFSHD), situated in the inner scrape-off-layer (SOL) occurs when the inner divertor is detached while the outer one is attached.

A clear dependence of the magnitude and spatial extend of the HFSHD on the power in the SOL and the neutral pressure in the HFS far SOL is found. Impurity seeding leads to a reduction or even suppression of the HFSHD. Experiments varying plasma current studied the influence of the connection length on the HFSHD.

A scenario at the highest heating power was developed to match reactor relevant SOL plasma conditions (P_{heat}/R>12 MW/m). In this scenario it is possible to reduce the power load on the divertor targets to a minimum by radiation cooling. This was achieved with either nitrogen or krypton seeding and leads to a detached divertor, with power mainly dissipated by radiation inside the confined region.

The new divertor manipulator DIM-II was used to expose W-coated marker probes to low-density and high-temperature L-mode plasmas at the outer strike point. The net erosion rate of the W markers was 0.04-0.13 nm/s while some 30 % of the eroded W atoms had been promptly re-deposited in a shallow trench downstream of the markers. Good agreement with spectroscopy says that the estimated gross erosion rate is >0.07 nm/s at the strike point.

The experiment on SOL filamentary transport aimed to establish the role of effective collisionality and detachment condition in the observed SOL saturation at high density. The experiment revealed that in L-mode the transition is clearly governed by divertor parameters independently from the applied heating scheme. Furthermore the momentum flux in the SOL has been estimated by changing the momentum input and the ion/electron heating scheme, showing a more skewed probability distribution function of momentum flux in NBI heated plasma with respect to ECRH. Investigation of the SOL saturation in high-density regime and at ITER relevant condition in terms of P/R showed a tendency to develop a density shoulder at high density, with more intermittent filamentary behaviour.

3 Turbulence Experiments and Simulations

The HGF Virtual Institute on Advanced Microwave Diagnostics, hosted by IPP, promotes focused studies on plasma turbulence through the support of PhD/Postdocs and the development of new diagnostics. With EU/US partners several new diagnostics were commissioned on AUG, including: (a) An ultra-fast-swept reflectometer (CEA) providing first core to SOL density profiles, their dynamics, and turbulence radial wave-number spectra. (b) A multi-antenna correlation reflectometer (FZJ) for poloidal/toroidal turbulence structure and propagation studies, as well as B-field pitch angles. Both systems complement an extended set of five Doppler reflectometers with: (c) two additional systems (LPP) allowing fine-scale $k_\perp$-spectra, radial correlation lengths and their ρ^*-scaling, as well as multipoint measurements of GAMs and E×B flows. On the GAMs a particular

effort was a result comparison from AUG, TCV, TS and TEXTOR. (d) A Correlation ECE receiver (MIT) was also installed, which is producing first data on core T_e-fluctuations. New diagnostic concepts have also been advanced in the form of phased-array-antennas for non-mechanical reflectometer beam steering. Two phasing schemes have been prototyped and tested: a 32 element helical serial feeder (IGVP) with frequency keying; and a frequency independent parallel-feeder with piezo-driven phase shifters (TUM). A complete in-vessel bi-static antenna system is scheduled for installation in AUG early 2015. The synergy provided by a comprehensive diagnostic set together with emphasis on experimental & numerical comparisons, has lead to significant progress in physics understanding on several fronts.
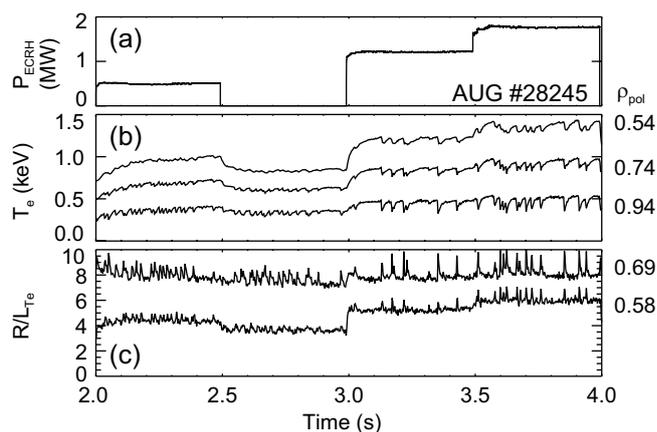

Figure 1: Time traces of (a) ECRH power, (b) T_e, (c) normalised T_e-gradient. The turbulence drive R/L_{Te} is locally modified using ECRH.

One of those projects is the investigation of turbulence and its associated transport, which has not only to be understood from a basic physics point of view, but is of particular importance to develop good confidence in turbulent transport predictions for future experiments. To understand turbulent core transport and predict plasma performance, gyrokinetic codes are currently used. While substantial effort has been dedicated to the verification of the technical validity of the codes, a careful validation including measurements of microturbulence and comparison with results from non-linear simulations, has only started in recent years.

As a first step in this direction, density fluctuations are specifically investigated using Doppler reflectometry. The information obtained is used to compare with the accompanying gyrokinetic simulations, for which the GENE code is employed. Of particular interest is the reaction of the fluctuations to local modifications of the turbulence drive term R/L_{Te}=-$R\nabla T_e/T_e$, which is achieved with the application of additional electron cyclotron resonance heating (ECRH) at mid-radius.

Figure 1 shows time traces of an NBI-heated H-mode discharge from 2 to 4 seconds, where ECRH power steps (a) are applied at $\rho_{pol}^{ECRH}=0.5$, where ρ_{pol} is the normalised poloidal flux radius. The electron temperature T_e at different radii follows P_{ECRH} (b). In (c), the temporal evolution of R/L_{Te} is shown for two radial positions in the plasma. R/L_{Te} is most affected by P_{ECRH} at the inner position ($\rho_{pol}=0.58$), while further outside it remains roughly constant. Hence the most prominent change in direct turbulence measurements is to be expected at radial positions close to $\rho_{pol}=0.58$.
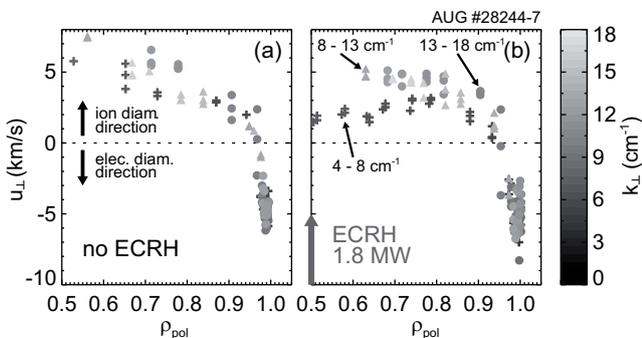

Figure 2: Radial $u_\perp$-profile without (a) and with (b) additional ECRH.

Figure 2 depicts the perpendicular velocity of density fluctuations $u_\perp$ for cases without (a) and with 1.8 MW (b) additional ECRH at $\rho_{pol}^{ECRH}=0.5$ (indicated by the grey arrow) and different turbulence scales (different symbols/colours). Both profiles (from $\rho_{pol}\approx0.5$ to the separatrix) show positive $u_\perp$ from mid-radius to the pedestal top and a well in the edge gradient region around $\rho_{pol}=0.99$.

In figure 2(a) (no ECRH), large, intermediate and small structure sizes (different symbols) propagate with the same $u_\perp$. Adding 1.8 MW of ECRH (b), small and intermediate scales continue to propagate with roughly 5 km/s in the core, while large structures propagate slower. This change in $u_\perp$ at $\rho_{pol}<0.8$ with P_{ECRH} could be related to a change in phase velocity v_{ph} of large-scale turbulent structures, consistent with a change in turbulence properties. The change in $u_\perp$ can be compared to the expected phase velocity of the turbulence, which is generally of the order of $v_{ph}\approx3\rho_s c_s/R$. At $\rho_{pol}=0.6$ this gives a value of $v_{ph}\approx1.6$ km/s. This is less than, but of the same order of magnitude, as the experimentally observed difference of 3 km/s, showing that the observed effect could indeed be due to a modification of v_{ph} of large structures.

Figure 3 shows turbulence levels ñ for different ECRH power levels ($P_{ECRH}<1$ MW: dots, $P_{ECRH}>1$ MW: crosses). In (a), ñ is shown for the largest investigated turbulence structures with $k_\perp=4$-8 cm^{-1}. As a general observation, from the core towards the edge, ñ increases up to roughly $\rho_{pol}=0.98$. In the very edge ($\rho_{pol}=0.99$) a significant reduction of turbulence is observed close to the position of the E_r shear layer.
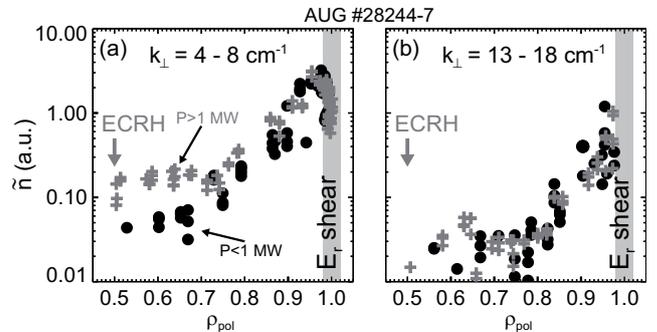

Figure 3: Radial turbulence level profile with $P_{ECRH}<1$ MW (dots) and $P_{ECRH}>1$ MW (crosses) for large structures (a) and small structures (b).

An influence of the additional ECRH power on the turbulence level is observed around mid-radius, close to the ECRH deposition location. For $P_{ECRH}>1$ MW ($R/L_{Te}>5$) an increase in turbulence level in a radial region from $\rho_{pol}\approx0.50$-0.75 with respect to the profile with $P_{ECRH}<1$ MW (dots) is seen. Towards the edge, the influence of additional ECRH decreases and the turbulence level profiles are unchanged for $\rho_{pol}>0.75$. The increase in ñ close to the ECRH deposition radius could be related to the increase in R/L_{Te} as observed in figure 1(c), where the largest R/L_{Te} increase is at the innermost observed radius ($\rho_{pol}=0.58$) at $P_{ECRH}>1$ MW. The turbulence level profiles for smaller scales ($k_\perp=13$-18 cm^{-1}) are shown in (b). Similarly, the general trend is an increase of ñ from the core to the edge. At comparable radii, ñ decreases from large turbulence scales towards smaller scales (a) to (b). For the smallest scales investigated, measurements close to the E_r shear layer were not possible due to loss of the Doppler shifted component.
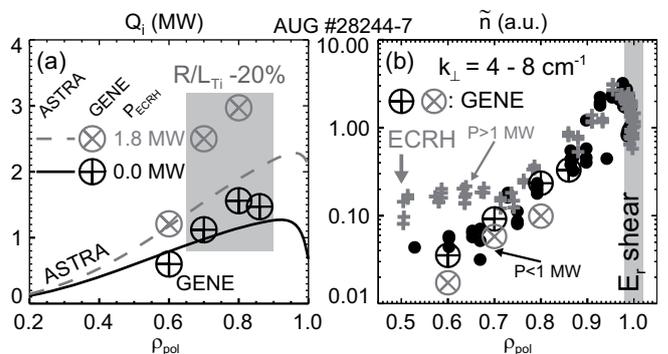
Figure 4: Matching of gyrokinetic simulation to ion heat fluxes (a) and comparison of radial turbulence level profiles from experiment and simulation.

For the different heating powers used in the experiment, figure 4(a) shows the ion heat flux Q_i as obtained from power balance analysis with the ASTRA code (lines). In addition, results from non-linear gyrokinetic simulations in the flux-tube limit are shown as plus symbols and crosses for 0 and 1.8 MW additional input power, respectively.

In order to match the heat fluxes, R/L_{Ti} had to be reduced by 20 % at radii $\rho_{pol} \geq 0.7$. In general, good agreement is obtained between gyrokinetic heat fluxes and the power balance result from ASTRA for the P_{ECRH}=0 MW case, while the P_{ECRH}=1.8 MW case is somewhat overpredicted. Taking into account the stiffness of the profiles, the overprediction is not very pronounced, since a further minor change to the gradients would match the experimental heat fluxes.

Figure 4(b) compares the radial turbulence level profile for the largest scales investigated ($k_\perp$=4-8 cm^{-1}) with results from the corresponding gyrokinetic simulations (pluses and crosses). The experimental points, which are in arbitrary units, have been multiplied by a common factor to give a reasonable match to the absolute ñ values obtained from the GENE simulation. At first sight, the basic trend of an increase of turbulence level from the core to the edge, is reproduced. From ρ_{pol}=0.5 to 0.9, both the measurement and the simulations show roughly an increase of a factor of five in ñ, which is a good achievement. However, the GENE simulation with P_{ECRH}=1.8 MW yields lower turbulence levels than the one with P_{ECRH}=0 MW, which is in contradiction to the measurement and under investigation.

4 ELM Mitigation and Refuelling with MP at Low ν*

Significant progress was made in 2014 towards mitigation of Edge Localised Modes (ELMs) at low plasma collisionality, ν*. In low ν* plasmas with a minimum of deuterium fuelling and significant central ECR heating, ion pedestal collisionalities down to $\nu^*_{i,ped}$=0.1 have been obtained.
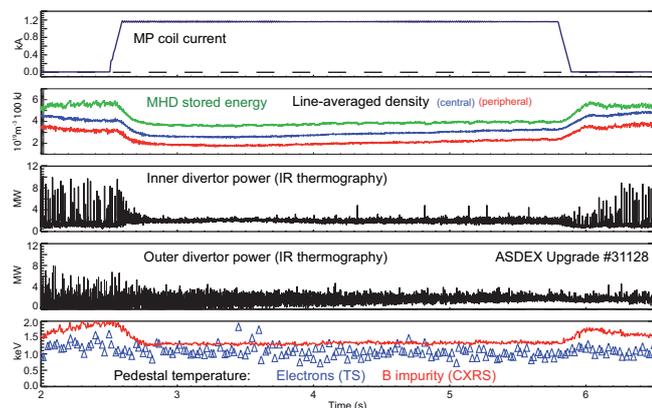

Figure 5: A long time interval with ELM mitigation is obtained by application of n=2 MP. Also n_e, W_{MHD}, and (to a lesser extend) the pedestal T_i drops.

Under these conditions, a significant reduction of the ELM energy loss for extended stationary phases is obtained by application of n=2 magnetic perturbations (MP) with the in-vessel saddle coils (figure 5). The ELM frequency increases by up to a factor of 6 and the peak ELM power in the inner divertor drops by a similar factor. The peak power due to

mitigated ELMs in the inner and outer divertor is comparable with the inter-ELM power. The MP also leads to a strong reduction of plasma density ('pump-out', both at the pedestal and in the plasma core) and a moderate reduction of pedestal T_i (measured by charge exchange at boron impurities) towards the pedestal top T_e. This phenomenon results in a reduction of stored energy (and confinement time as the heating power is constant in this example) by about 35 %.

The effect on ELMs and plasma density depends strongly on the poloidal spectrum of the magnetic perturbation. In AUG, two poloidally separated rows of eight toroidally distributed saddle coils each allow to independently select the phase of an n=2 perturbation in the upper and the lower row of coils. The alignment of the perturbation field is varied by ramping the phase in opposite directions in the upper and the lower rows (i.e. by variation of the differential phase angle ΔΦ between the two rows). Figure 6 shows and example of a pulse with a ΔΦ-ramp and otherwise constant settings (no fuelling, constant heating power and magnetic perturbation amplitude).
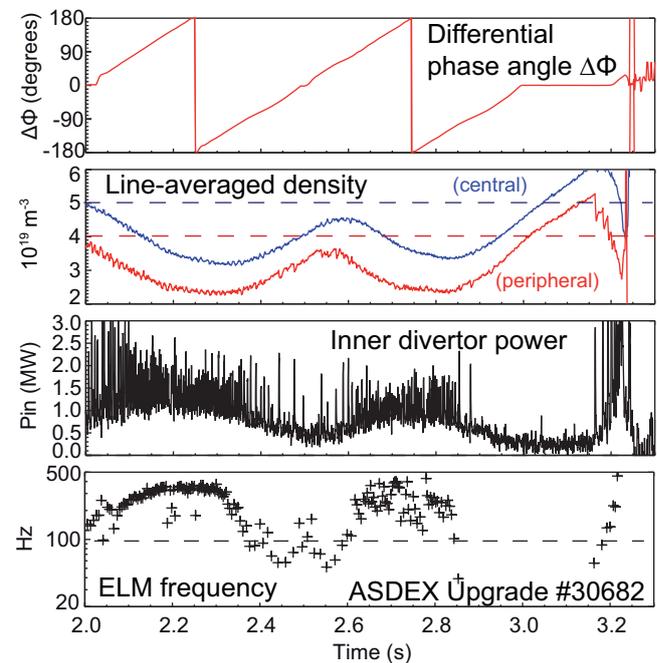
Figure 6: Variation of the differential phase angle ΔΦ between upper and lower coil row n=2 pattern demonstrates the importance of the poloidal spectrum of MP to produce either ELM mitigation and n_e reduction or ELM stabilisation (reduced or zero ELM frequency). Dashed lines indicate initial values with MP off.

Dashed lines indicate the values of central and peripheral line-average density (interferometer) and ELM frequency without magnetic perturbation. For this plasma configuration, the optimum alignment with the unperturbed equilibrium field (often called 'resonant' magnetic perturbation, RMP) is at ΔΦ=30°.

ELM mitigation, combined with ELM frequency increase and density reduction occurs in a wide range of $\Delta\Phi=30° - 180°$ and $\Delta\Phi=-180° - -90°$, while between $\Delta\Phi=-90°$ and $0°$ the ELM frequency is reduced or a classical, non-stationary ELM free phase is triggered. Modelling of the 3D ideal MHD equilibrium with the NEMEC code and the linear plasma response with the MARS-F code indicate that ELM mitigation coincides with a kink-like amplification of a non-resonant component at $m=n\cdot q+2$ in the H-mode barrier region driven by the edge pressure gradient.

Cryogenic deuterium pellets are injected to counteract the density reduction encountered with MP at low plasma collisionality. The pellet diameter was set deliberately rather small at 1.4 mm so that the ratio of pellet to plasma particles was within a factor of 2 similar to that envisaged for ITER. The pellet velocity was set to 560 m/s. Fast camera images show a shallow pellet evaporation depth, r/a>0.8. Owing to the pellet launch geometry, only a modest pellet plasmoid drift is expected and therefore our deposition scheme is mimicking the ITER situation where pellet deposition is rather shallow. Figure 7 shows the successful application of these pellets to refuel the plasma with ELM mitigation by RMP. The size and time-scale of the density drop due to the magnetic perturbation at 2.6 s indicates a pump out rate about 10^{21} atoms/s. This rate is comparable to the fuelling rate from beams and gas. Application of a train of pellets from t=4 s at the rate of up to 16 Hz allows to compensate completely for the pump-out effect. The pellet fuelling rate required to refuel the RMP density drop is similar to the RMP pump-out rate indicating a consistent particle balance. Pellets restore not only the line integrated density but also the density profile. However, the reduction of energy confinement time remains and the energy confinement time is constant during the entire pellet re-fuelling phase. In this pulse, the application of MP increases the ELM frequency from the natural level of 210 Hz to 570 Hz but it drops again during refuelling by pellets. Overall there is still some degree of ELM mitigation left as the density reduction by magnetic perturbations is compensated for by pellet fuelling. Inspection of the post-pellet density transients reveals two time-scales. Edge interferometer, ECE and reflectometer show a fast initial density decay at r/a~0.85, with a decay time of ~8 ms. This value is about one fifth of the energy confinement time and such a fraction is similar to the values observed on MAST for similarly shallow pellets. On a longer timescale between pellets, the density is gradually decreasing across the whole plasma cross-section while a strongly peaked density profile is maintained. This type of evolution is different from that observed in MAST and may point to the role of a pinch for core fuelling in AUG. These experiments on AUG indicate a path towards refuelling in low collisionality ELM mitigation schemes, however, further experiments are needed to demonstrate the full density and ELM control as envisaged for ITER.
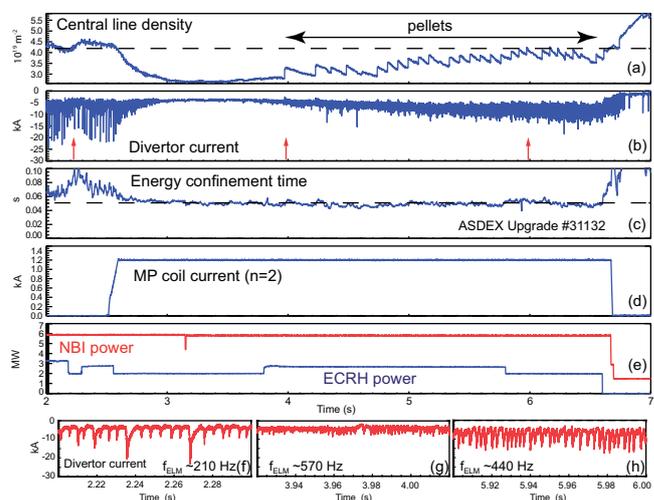
Figure 7: Temporal evolution of plasma parameters with ELM mitigation and pellet refuelling to restore the original n_e. Panels (f-h) zoom into the divertor current signal (ELM monitor) at 3 time windows indicated by the red arrows in (b).

5 Plasma-wall Interactions with N₂-seeding

The power load onto the divertor target plates can be reduced by radiative cooling. Experiments in AUG have demonstrated that the admission of nitrogen to the plasma effectively reduces the peak power fluxes at the divertor. In recent experiments, even detachment of the outer divertor under H-mode conditions was achieved by nitrogen seeding.

However, the chemical reactivity of nitrogen has important consequences for the application of N as seeding gas. Firstly, part of the injected nitrogen is stored in the tungsten wall surfaces by nitride formation and can be released back into the plasma under particle or thermal loads. As the tungsten surfaces have only a limited N storage capacity, excess N is reemitted from the surfaces. Hence, a self-consistent model for the nitrogen wall retention and fluxes to and from the plasma is needed to adjust the nitrogen puff to the value which yields the desired amount of radiation. Secondly, AUG experiments have proven that part of the N is converted to ammonia ($ND_{3-x}H_x$). This could seriously restrict the applicability of nitrogen seeding in the presence of tritium in JET D-T, ITER and DEMO.

To get a better understanding of the interaction between energetic nitrogen ions and tungsten, this system was studied in laboratory experiments. The experiments were performed in an X-ray photoemission spectroscopy (XPS) setup with in situ sample preparation capabilities for multi-species ion implantation at sample temperature up to 900 K. Nitrogen ions with energies from 300 eV to 2500 eV were implanted into tungsten surfaces and the increase of the nitrogen XPS peak intensity with increasing nitrogen fluence was monitored.

These results were compared to results from SDTrimSP, a code which simulates the interaction of energetic particles with matter in the binary collision approximation. Because XPS intensities depend in a complex way on the sample composition, a forward calculation that converts elemental depth profiles calculated with SDTrimSP to XPS intensity ratios was applied to compare experiment and calculation.
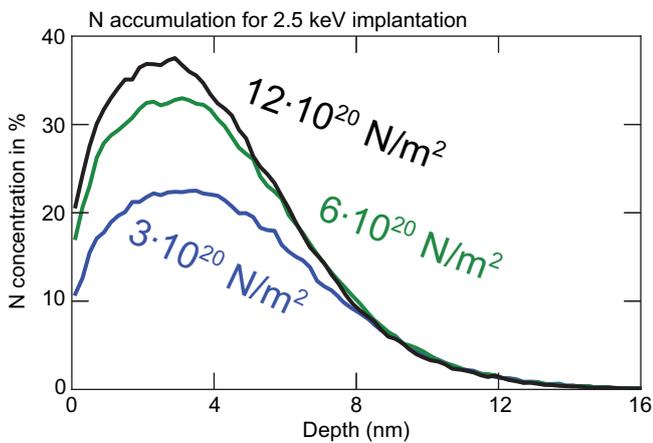

Figure 8: Accumulation of N in a W-surface under 2.5 keV N-bombardment with the fluences given in the figure. The re-erosion limits the maximum local N-concentration.

It was found that the binary collision approximation correctly describes the nitrogen accumulation under bombardment with nitrogen ions with more than 1 keV energy. As can be seen in figure 8, for such high energies the re-erosion of implanted nitrogen by the incoming N-ions is sufficiently high to limit the N-concentration to below 50 % by re-erosion.
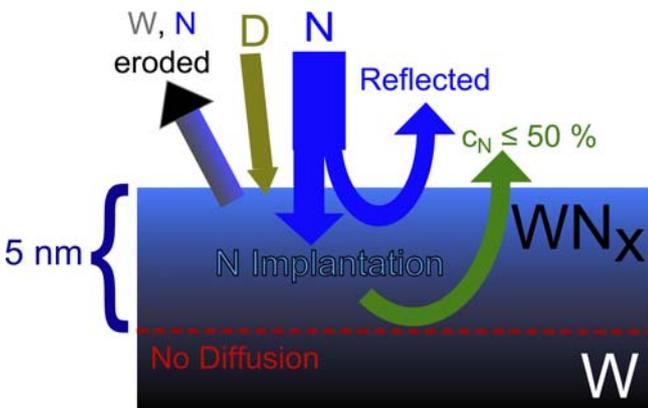
Figure 9: Interaction of N with W-surfaces: Only part of the N-ions impinging on a W-surface is kinetically reflected and the implanted N becomes bound in the form of tungsten-nitride. N does not diffuse in W, so N only accumulates within the implantation range. W and N from the surface are eroded by incoming D- and N-ions. If the N re-erosion by physical sputtering does not restrict the N-concentration to below 50 %, an additional diffusive loss of N from the tungsten-nitride sets in.

At energies below 1 keV the physical processes included in the binary collision approximation employed by SDTrimSP no longer suffice to reproduce the experimentally observed N accumulation. The predicted N-concentrations rise to very high values (up to 100 %) and the predicted nitrogen intensity in the XPS measurements significantly exceeds the measured values. However, it is still possible to reproduce the experimental measurements: SDTrimSP allows specifying a maximum concentration for each element. With a maximum concentration of 50 % for nitrogen, a value corresponding to the stoichiometric nitride WN, SDTrimSP correctly predicts the XPS measurements. The overall physical picture emerging from these experiments is described in figure 9.
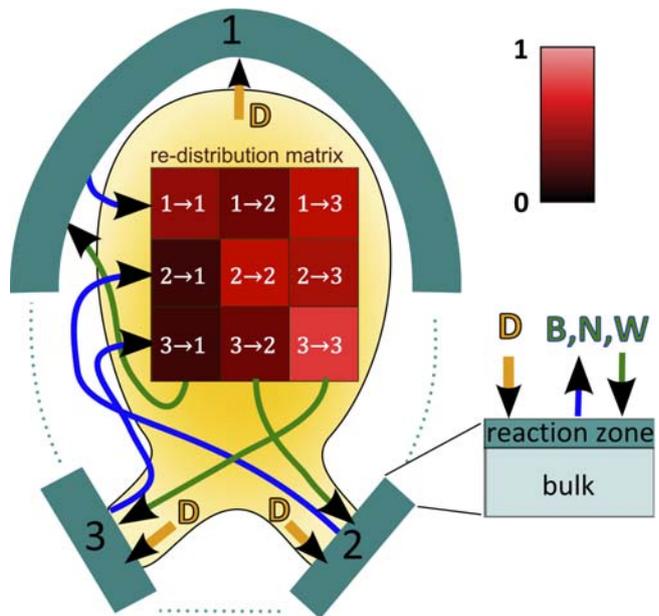
Figure 10: For the WallDYN model the wall is discretised into wall tiles. Each wall tile consists of a bulk and a reaction zone. The composition of the bulk is fixed, the composition of the reaction zone evolves according to the incoming particle fluxes. The transport of the impurities through the plasma is parametrised by the redistribution matrix calculated with DIVIMP. The redistribution matrix states which percentage of the material eroded from a given tile impinges on another tile. Typically the matrix has strong diagonal terms, representing the local redeposition.

In further experiments, the temperature stability of tungsten nitride layers formed by ion implantation was studied. In a first experiment N was implanted into a W-surface at ambient temperature. When the sample temperature is increased, a loss of the N is observed only above 900 K. This is different when the N is implanted into the W-sample at elevated temperature. In this case the N retention is reduced already for an implantation sample temperature of 500 K. This difference indicates that ion bombardment increases the diffusivity of N in tungsten.

To obtain a model for the N wall retention and fluxes in a tokamak, the physical picture derived from the laboratory experiments and SDTrimSP simulations was included in the WallDYN code. WallDYN was developed to simulate the global impurity migration in tokamaks and the resulting evolution of the surface composition. The WallDYN model includes parameterisations for the kinetic interaction of energetic particles with surfaces and for the transport of impurities through the plasma and is illustrated in figure 10.

The interaction of N with W-surfaces and the transport of nitrogen through the plasma were also studied in dedicated AUG experiments. In these experiments, samples were exposed on the divertor manipulator to N_2-seeded L-mode discharges. Afterwards, the nitrogen content of the samples was measured with nuclear reaction analysis at the tandem accelerator at IPP. These measurements showed that the nitrogen content saturated within one discharge. Thus, the saturation areal density is comparable to the one measured in laboratory experiments on smooth samples. This indicates that the roughness of the technical surfaces employed in AUG does not increase the nitrogen retention. This result is currently checked by further experiments based on the new divertor manipulator (DIM-II). With the DIM-II it is possible to expose several samples at the same time, so that it is directly possible to compare samples with a different roughness.
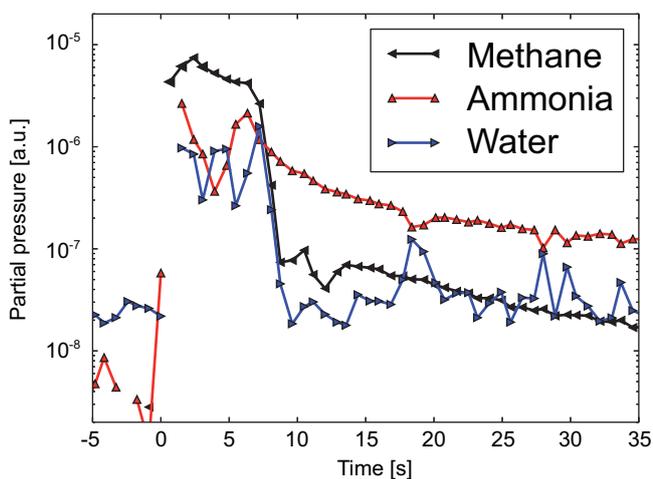
Figure 11: Evolution of the partial pressures of ammonia, methane and water during an N_2-seeded pulse. The ammonia partial pressure is much higher than in a non-seeded discharge. This demonstrates that part of the seeded N_2 is converted to ammonia. After the pulse the ammonia partial pressured decreases only very slowly.

The N-deposition on the divertor manipulator samples and spectroscopic measurements were then compared to WallDYN simulations, employing the surface model deduced from the laboratory experiments. These simulations reproduced most of the experimental findings well. This confirms that the WallDYN model correctly describes N wall retention and fluxes into the plasma. A remaining problem is that, in comparison to measurements with residual gas analysis, WallDYN overestimates the number of N-atoms pumped in the form of N_2 molecules. This deficiency is probably related to the unavailability of a model for the conversion of nitrogen to ammonia.

The main challenge for the quantification of the ammonia production by neutral gas mass spectrometry is the overlap of signal contributions from (deuterated) ammonia with those from (deuterated) methane and water. However, with a new evaluation routine the ability to determine the ammonia partial pressure from a decomposition of mass spectra has been improved. The new routine was successfully applied to seeded and non-seeded discharges, see figure 11. With this improved diagnostic capability it becomes possible to study the dependence of the ammonia formation on plasma parameters and possibly extrapolate the ammonia formation rate to ITER.

In summary, one can say that there is a good agreement between WallDYN simulations and the experiments with respect to the N-migration. This gives confidence in the ability to predict and interpret the plasma-wall interaction in fusion experiments on the basis of well-defined laboratory experiments and computer simulations. Based on the current effort in the detection of produced ammonia, it should soon be possible to study the ammonia generation in more detail and to pave the way for the application of nitrogen seeding in future fusion reactors.

6 ITER Baseline Scenario

The baseline scenario in ITER (ITER BL) aims to achieve 500 MW of fusion power at a plasma current of 15 MA at q_{95}=3. The envisaged plasma density is quantified by the Greenwald fraction f_{GW}=n/n_{GW}=0.85 and the confinement is planned to yield H_{98y2}=1, while β_N is in the range of 1.8. A scaled down scenario is investigated in AUG and a demonstration of simultaneously meeting as many as possible requirements is desired. Such requirements are the dimensionless parameters and the plasma shape, but also stationary behaviour, ELM control, impurity control and power handling. Up to now, no emphasis was put on matching the collisionality of the ITER BL scenario in AUG, as this would sacrifice relevant plasma edge parameters, while many of the encountered challenges originate at the plasma edge.

For the experiments at AUG, an important issue of the ITER BL scenario is the high triangularity of the plasma shape (averaged δ~0.4, upper δ~0.3). First, the strong shaping puts high demands on the vertical field coils, which requires a special setting of coil voltages. Second, the plasma behaviour is characteristically changed by the strong shaping: At high values of δ, the frequency (f_{ELM}) of the edge localized modes (ELMs) is strongly reduced leading to larger individual ELMs.

Probably as a consequence, the plasma density is higher and it is more difficult to keep it stationary. In figure 12, important time traces for an ITER BL discharge are presented and f_{ELM} approaches 10-15 Hz during the flattop phase starting just after t=3 s. In the presented case, a large D_2-fuelling puff prevents f_{ELM} to drop even further and thus, is required for a stationary flattop. However, the strong gas puffing causes the plasma confinement to deteriorate.
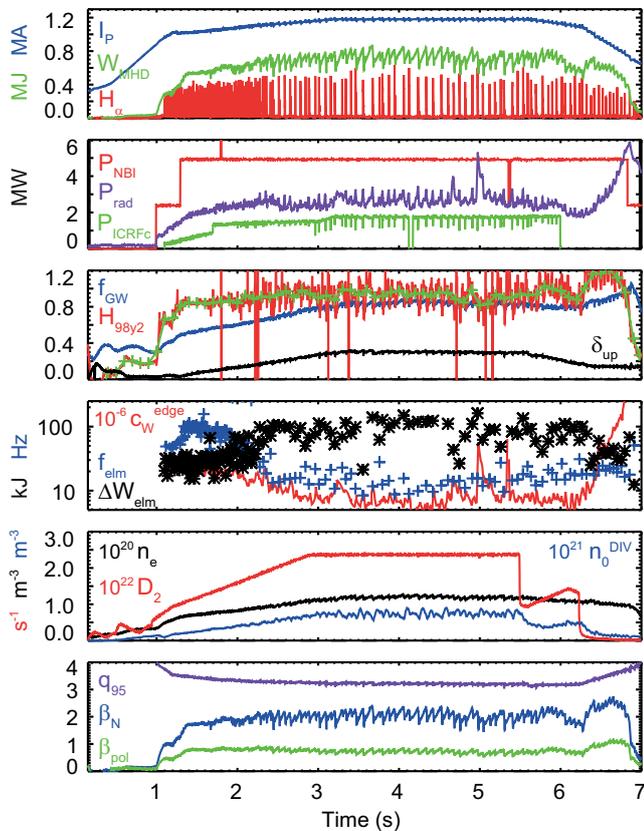
Figure 12: Time traces of #29636 (1.2 MA / 2 T) centrally heated via ICRF.

For the presented case the confinement is at the desired level H_{98y2}=1. However, the plasma pressure is about 20 % too large and this is caused by slightly too much auxiliary heating. It was found earlier in AUG, that the normalised confinement is reduced for lower plasma pressure suggesting that not all dimensionless parameters for an ITER BL discharge may be matched for a stationary discharge. In order to better document this observation, several stationary phases from discharges with slightly different densities and plasma pressures have been investigated in terms of their normalised confinement. The analysis included plasmas with pellets and non-stationary phases from N-seeded discharges. In figure 13, these experiments are summarised. While for an ITER relevant Greenwald fraction f_{GW}, the desired normalised confinement could be achieved (figure 13, left), the ITER relevant β_N~1.8 does not result in sufficient confinement (figure 13, right).

However, at higher β_N sufficient confinement is reliably achieved. This finding provides two remedies for ITER. First, the confinement for the experiments in AUG might be diminished due to the strong D_2-puffing which was necessary for achieving stationary conditions. For an alternative ELM pacing or ELM mitigation strategy, stable discharges may be achieved at better confinement. Second, the beneficial β_N-scaling may allow for an alternative scenario at 12 MA and q_{95}=3.6 with comparable fusion power, simply because β_N achieved by the installed heating power is larger at smaller current. However, the confinement scales approximately with the plasma current, such that H_{98y2}~1.2 and f_{GW}=0.95 would be necessary in order to achieve 500 MW of fusion power in ITER.
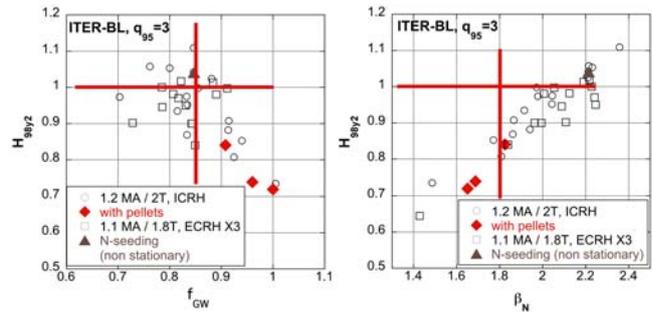
Figure 13: H_{98y2} vs. density f_{GW} (left) and β_N (right) for q_{95}=3 operation. Target values for ITER BL are indicated by red lines.

Experimental investigations of the alternative ITER BL scenario at 12 MA and q_{95}=3.6 have been performed and a more stable behaviour of the discharges allowed for lowering the D_2-puff. A β_N~2.2 is desired for this scenario. Both the lower gas puff and the higher targeted β_N led to improved confinement factors of H_{98y2}>1.0. However, the achieved values for H_{98y2} are still slightly short of the required H_{98y2}~1.2.
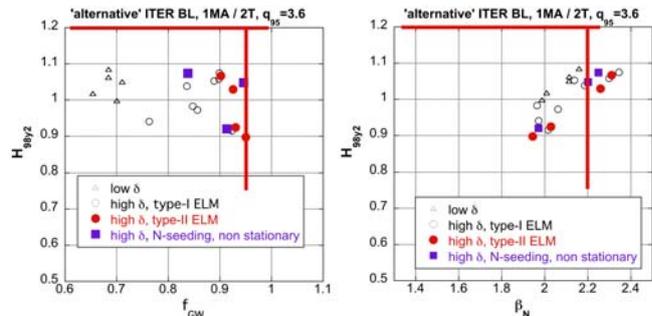
Figure 14: H_{98y2} vs. density f_{GW} (left) and β_N (right) for q_{95}=3.6 operation. Target values for the q_{95}=3.6-scenario are indicated by red lines.

Figure 14 presents data corresponding to that from figure 13, but for the alternative 12 MA and q_{95}=3.6 ITER baseline scenario. Future work may address this alternative scenario,

because it allows for more operational flexibility. Alternatively, lower ν^* may be targeted at the cost of not matching β_N.

Actually, ITER operation will start with a non-nuclear phase in which He plasmas are used to test the safe plasma operation, including ELM mitigation techniques. Thus, the ITER BL scenario for He must also be prepared and investigated in today's devices. To this end, ITER BL discharges in He have been performed at AUG, e.g. #30015 presented in figure 15. The discharges are more stable than in deuterium and density/impurity control seems to be naturally provided. Note that the strong increase in the radiation signal is an artefact
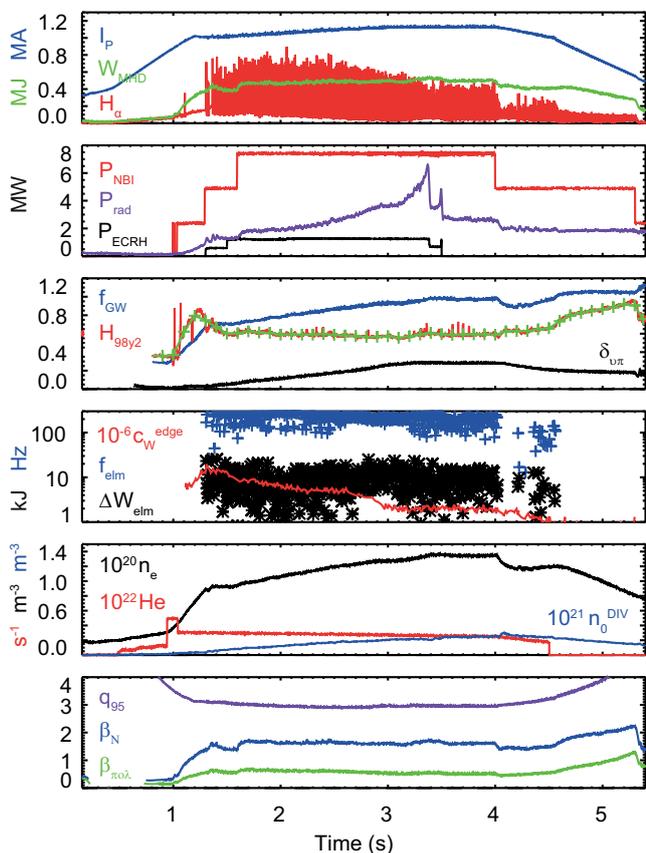

Figure 15: Time traces of the ECRF-heated He-pulse #30015 (1.1 MA / 1.8 T).

due to non-absorbed ECRH. Also note that the ELMs are much smaller in He as f_{ELM} is always above 100 Hz irrespective of δ. On the one hand this suggests a safer operation of He plasmas in ITER, but on the other hand a testing of ELM mitigation in ITER would require access to large, low-frequent ELMs. Possibly the behaviour is influenced by the fact that the investigated He plasmas in AUG are somewhat impure due to the heating by D-beams. Thus, future experiments should aim on improving the purity of the He plasmas, by employing the recently developed He-beams and enhanced wall conditioning.

7 Technical Systems

The experimental campaign 2014 was the first with a massive tungsten divertor. The experimental campaign comprised in total 1641 pulses, with 1227 discharges useful for the physics programme. There were 347 pulses auxiliary heated with more than 10 MW, 105 of them with more than 15 MW. A maximum heating power of 25 MW was applied in two pulses. The experimental campaign was finished with discharge #31766 on October 30th, 2014. A 6 month shut-down began in November to install 2 new 3-strap ICRF-antennas.

7.1 Machine Core

During the operational campaign, two unscheduled vessel openings followed by baking and one short vent was necessary. Shortly after restart, a malfunction of the gate valve of NBI box II was realised, requiring an opening of the vessel. In parallel, the venting was used to replace a damaged Langmuir probe leading to glowing spots in the divertor, isolation sockets at shunts and to modify a few diagnostics. A short, only a few hours lasting vessel vent in May became necessary to replace a leaky diagnostic window. A second unscheduled vessel opening was required during the summer break. One week before the summer break after the disruption of #31355, a protection tile of the inner column fell down into the lower outer divertor. The physics program scheduled until the summer break could be completed by carefully positioning the outer strike line above the broken tile. A one week shut down was used to replace the broken tile. A detailed in-vessel inspection allowed the problems to be identified and to prepare the upcoming shut-down. Broken edges of inner column protection tiles in the vicinity of the ferritic P92 tiles, deep cracks in solid tungsten divertor targets and more serious a divertor tungsten target broken at the clamping were observed. Also, broken graphite protection plates in the NBI box II duct and molten bolts at the NBI dump plates at the inner column were seen. Damaged components were replaced and AUG was operated for another 376 discharges in autumn, with NBI box II being again taken out of operation due to a failure of its gate valve on September 30th.

The solid W-divertor was operated with up to 100 MJ heating energy and a discharge duration of up to 10 s (see figure 16). During operation with high heating power, hot spots occurred at the transition between divertor modules. They were accepted for further plasma operations after careful inspection of the integral target load and possible effects on the plasma performance. The inspection during the summer break revealed that these hot spots were caused by a misalignment of the divertor modules. The alignment was checked during the assembly and before closing the machine. The misalignment is attributed to torque produced by eddy currents induced in the support structure during disruptions.

To avoid this in future campaigns, the preload at the fixing is increased by about a factor 2 and the current flow will be suppressed by isolating one fixing point of the support structure.
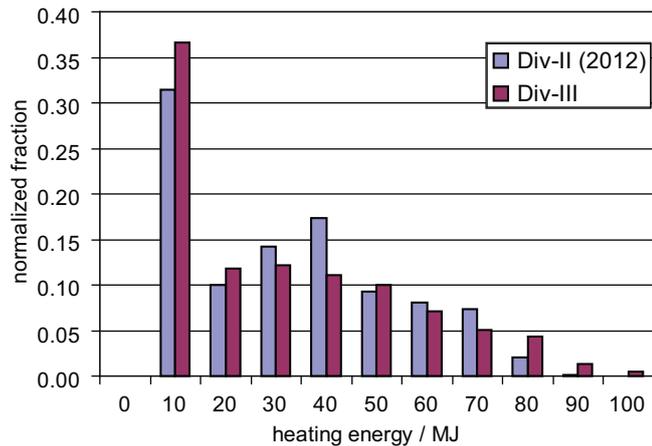

Figure 16: Normalised distribution of plasma heating energy for the last campaign with Div-II and the first Div-III campaign.

7.2 Gas Inlet and Torus Pumping System

Commissioning and operation of the rebuilt gas inlet system (GES) was successfully accomplished. The anticipated benefits from the new wiring of the piezo valves (PV) with the custom-built cable were fully met and the signal noise is strongly reduced. Communication between the discharge control system (DCS) and GES was comprehensively remodelled. Now DCS controls each of the 20 PV independently instead of formerly maximal five valve groups.

The four newly installed mushroom glow discharge anodes were operated over the whole campaign without major problems and do not show any damage after inspection. Software improvements in the control system provide great operational versatility.

The inter-vacuum system has been enhanced considerably. It now completely separates water-cooled in-vessel components and diagnostics. Most of the previously autonomous and unmonitored diagnostics have been integrated in the new installation.

7.3 Failure of a Water Heating/Cooling Circuit on Vessel Shell

Each of the 16 AUG vacuum vessel segments is furnished with four water circuits for vessel baking (150 °C) and cooling. Two circuits on the upper and lower segment, respectively. In April 2014 a locomotive mechanic's level (ML) caused a leak in a lower circuit of segment 10. In addition, the ML destroyed the lower temperature sensors at four toroidal field coils. The origin of the ML is unknown. It was probably lost during the tokamak installation period and trapped for many years between toroidal field coils and the inner vessel shell. The leak cannot be repaired due to limited space. The destroyed water circulation and temperature sensors do not

affect plasma operation. Only the vessel baking procedure is prolonged by roughly half a day. The vessel areas of the defective heating circuit can now be heated only by thermal conduction and radiation. Owing to the temperature differences between the active heated and unheated areas, unacceptable thermal stresses in the shell can arise. To avoid excessive temperature differences and stresses, finite element calculations have been performed with ANSYS. As a result, the vessel heating rate has been reduced from 10 °C/h to 5 °C/h.

7.4 Experimental Power Supply

The first MST1 campaign was very successful from the Experimental Power Supplies (ESV) point of view. There were only few problems affecting the AUG experimental program. The most noticeable fault was a short circuit on a damping choke, resulting in a three week shut-down of generator EZ4.

An important performance step was the transfer of two 15 MVAr reactive power compensation modules from generator EZ3 to EZ4. The successful commissioning was the first milestone implementing a reactive power compensation system on the EZ4 busbar and thus improving the I²t power capabilities of this system.

After four years of operation, a first inspection and overhaul of the new emergency mechanical braking system (MBS) of generator EZ4 was performed. Originally, the MBS applies a continuous torque in engine test cells. At EZ4, the MBS spends most of its time in 'free-wheeling' mode. The maintenance proved the reliability of the system for this special application and inspires confidence for the next ten years of operation of this safety relevant system.

The main project for the high current power supply group was the installation, programming and commissioning of the first four BUSSARD inverter modules feeding the in-vessel B-coils. After intense testing of the power and control systems, towards the end of the experimental campaign BUSSARD could contribute to the physical program providing individual current waveforms to the 4×4 groups of coils. The completion of all 16+1 inverters including an optimisation of the cable input filters and interface boards is scheduled for 2015.

After completion of the new HV building, installation of the high voltage systems for the ECRH3 power supply could start. Since a lot of preparation work was already performed in parallel – e.g. reconstruction of the power stacks from ac to star point controller – activities made significant progress. Commissioning is planned for 2015.

7.5 Neutral Beam Heating

At the beginning of the 2014 campaign, injector II was delayed by altogether seven weeks due to a problem with the large torus gate valve in the beam duct. On first opening

of the valve after AUG vessel baking, the valve's gasket was pulled out of its groove and prohibited any further operation of the injector. The campaign had to be interrupted for two weeks to accommodate for the mechanical repair. One month before the end of the campaign the largely identical incident, although this time with no proceeding vessel baking, occurred again and the injector was no longer available. In the previous campaign a gasket was damaged. The first in-vessel inspection after the end of the campaign revealed that melting by re-ionised beam neutrals had eroded the seal seat of the gate valve. The second gasket loss incident may be related to this damage. An infrared video based interlock is planned to be installed before the next campaign in order to switch off the beams before such damage occurs again.

During the summer break a transformer of the high voltage tetrode that supplies beam source 2 of injector I was found to be defective. Hence, this source could no longer be operated in the remaining part of the campaign.

New automatically operated pneumatic switches were installed for changing the resistivity on the resistors that supply the deceleration grids. These grids serve to suppress backstreaming electrons from being accelerated into the ion source. So far, changing the acceleration voltage from above to below a certain threshold or vice versa had made it necessary to enter the torus hall and manually switch these resistors. This procedure had been time-consuming and often not even possible when access to the torus hall was prohibited because of too high radiation levels.

For the first time on AUG pure helium neutral beams were injected into a discharge. Operation with He is generally complicated by the fact that the NBI's high speed titanium sublimation pumps do not pump He. Nevertheless, 2.4 s of He injection were delivered with up to 2 beams at 36 keV and approximately 0.6 MW per beam in first trial discharges. Improving the performance in He will be a target for the next campaign.

7.6 Ion Cyclotron Heating

Manufacturing, testing and preparation for the integration of 2 new 3-strap antennas, optimised to reduce impurity production is progressing well. This project is an international collaboration with ASIPP Hefei, China and ENEA, Frascati, Italy. Following the acceptance test in Hefei at the end of February, the 2nd antenna was transferred to IPP for further processing. Components of the antenna, made of special materials, were delivered by ENEA. Limiters (W coated C) as well as CuBe springs, became available in time after qualification of the design and manufacturing process. Following validation of the coating process in IPP's GLADIS test facility, Faraday screens made of TZM received the final TiC coating. Complex CuCrZr machined and EB-welded cooling frames passed stringent pressure and hot leak tests.

To prove the compatibility of all components, both antennas were completely assembled during late summer. For further RF tests and to practice the later integration into AUG, the first antenna was installed in an AUG spare octant, see figure 17.
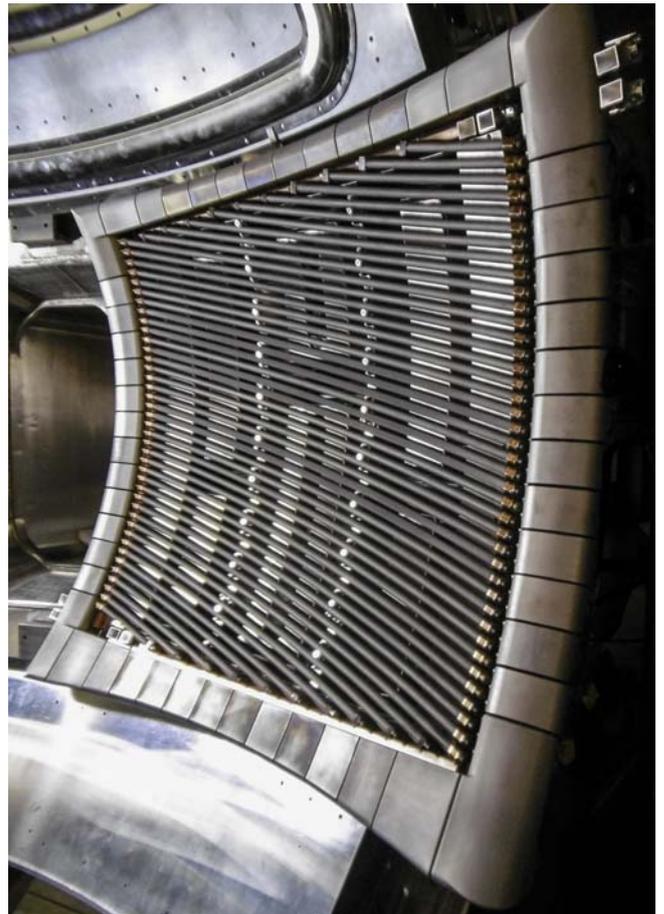
Figure 17: A new 3-strap antenna mounted in the test oktant.

This antenna was then used to thoroughly test the installation of the waveguides for the 10-channel U-band reflectometry, provided by ENEA. Measurements of the ICRF near field distribution in front of the antenna confirmed earlier simulations that were the basis of the design of the antenna. Following the AUG opening in November 2014, two of the existing antennas were removed from the vessel (see IPP report cover picture). The two new antennas, meanwhile disassembled, are scheduled to be installed in the middle of February 2015. This activity supported by staff of ASIPP and ENEA. The additional transmission lines and corresponding tuning systems, required to feed the antenna straps with different phase and amplitude, are already in place and tested. Commissioning and test of the new antennas will start with the new campaign in spring 2015.

7.7 Electron Cyclotron Heating

In 2014, all four ECRH2 units were used together for the first time for plasma operation. Occasionally power was limited by arcing in the transmission line, but otherwise the system has reached a high level of reliability at both frequencies. On request the four old (ECRH1) units were used as well such that record peak levels of 4.4 MW for 2 s of absorbed power were reached. Venting the transmission line with dried air improved the conditioning.

Reliability of the ECRH could be further increased by introducing a gyrotron replacement algorithm for central heating in the discharge control system (see next section). For another application DCS varied directly the beam acceleration voltage of a single gyrotron in order to vary its power. This is used within a real-time controller to keep the electron temperature constant at a predefined radius when replacing on-axis NBI by off-axis NBI (see section 8.10).

Also in 2014, imperfect ECRH absorption was troublesome. Major issues were inadequate plasma position and magnetic field for X3 heating, one case with wrong polarisation at 140 GHz destroying in-vessel optics, and generally faulty polarisation at 105 GHz. The latter was traced back to wrongly marked and mounted polarisers in units 3 and 4 of ECRH2. The polariser settings will be independently cross-checked in the future when a discharge programme is loaded. Still it cannot be excluded that a largely unabsorbed beam hits the vessel walls. Thermal analysis reveals that the insulation bellows behind the inner heat shield are potentially in danger. Since a repair of such a bellow would require a major shut down of AUG, protective measures had to be developed. The tiles on the high field side in the critical sectors will be modified with a labyrinth like overlap. A mock-up was built at IPP and low power measurements at IGVPT Stuttgart revealed that the transmission through the tile gaps is reduced by 15 dB. Together with a copper sheet close to the bellows, this is considered to be sufficient for protection of the bellows.

The ECRH3 project replacing the old ECRH1 system by a new 4 MW, 10 s system has reached its main construction phase in 2014 with expenses of close to 3 M€ and a load of close to 10,000 hours for the central IPP workshops. The project has been rescheduled. The delivery of the first gyrotron was delayed on IPP request by 11 months to September 2015 in order to compensate for planning delays by manufacturing the components for all four units at once. The last gyrotron is still foreseen to be delivered as originally planned in 2017. In 2014 the support structure for the transmission line has been completed, including a removable bridge next to the ICRF system and the holes through the concrete shielding of the torus hall including the radiation safety permit for the modified shielding. Delivery of the wave guides is almost completed. The cooling-system for gyrotrons and subsystems has been completed and tested. It was designed and constructed by ECRH engineers (cutting, welding and mounting: Fa. Reichhardt). The first cryogen-free superconducting 7.2 T magnet from JASTEC (Japan) has been delivered and accepted. It is a copy of the magnets for the Russian ITER gyrotrons. With the 140 GHz gyrotrons it will only be operated at 5.0 T. The new DC cathode heater, developed and manufactured in-house, has been tested successfully. Substantial delays occurred for the delivery of the body modulators (now due February 2015) and the tetrodes and their sockets for the series modulators. Negotiations with Thales Electron devices are ongoing.

7.8 CODAC

Full IT support was provided for the EUROfusion MST campaign at AUG, including 100 new user accounts, a network of SunRay stations, wired and wireless opportunities for laptops, 20 additional offices and 2 video conference rooms. However, during the campaign sometimes performance bottlenecks were evident and, particularly on experiment days, the demand exceeded the available capacity. An upgrade to network and server capabilities is planned for early next year before the new campaign starts.

In terms of real-time control, the collaboration with the WEST project, which was mentioned in last year's report, has begun in earnest. To deploy the real-time software framework in a different environment, the AUG specific parts of the Discharge Control System (DCS) were separated from the core framework. The configuration of several components, user interface, diagnostic management, record archiving, input from sensors, output to actuators, control algorithms as well as timing and event distribution can now be performed by a custom realisation. The core framework retains the basic definitions, infrastructure and function block libraries, essential services for module orchestration, administrative real-time processes and well-defined interfaces to the custom realisations. The restructured framework will be commissioned in February 2015 for our next experimental campaign.

New control algorithms in 2014 focussed on actuator management for ECRH. Tripped gyrotrons can now be replaced in real-time by redundant gyrotrons, thereby keeping the central tungsten concentration low and discharge conditions stable. At least one tripped gyrotron was replaced in 27 pulses since June. Additionally, a cost function was developed to allocate gyrotrons to multiple targets, e.g. central heating and NTMs. It adapts in real-time if new targets emerge or gyrotrons trip.

8 Core Plasma Physics

8.1 Role of the Ion Heat Flux in the L→H Transition

In the paradigm of the L→H transition mechanism, turbulence is reduced by the edge rotation shear induced by the gradient of the radial electric field, E_r. According to the neoclassical theory, E_r is essentially determined by the pressure

gradient of the main ions such that the edge ion heat flux, $q_{i,edge}$, and expected to be a key player in the L→H transition. However, the non-monotonic density dependence of the L→H threshold power, P_{L-H}, with minimum at $n_{e,min}$, is in apparent contradiction with this hypothesis. Recent experimental investigations in the low density range, where the electron and ion heat fluxes can be separated, reveal that the E_r well at the L→H transition is independent of density and that, unexpectedly, P_{L-H} and $n_{e,min}$ increase with plasma current. These observations can be explained by assuming that $q_{i,edge}$ is the main drive for the edge E_r well and they are unified by a single positive linear density dependence of $q_{i,edge}$ at the L→H transition, for a given magnetic configuration and ion isotope. Further, the increase of P_{L-H} towards low density is unambiguously attributed to the decrease of the collisional energy transfer from the electron to the ion channel. Based on this knowledge, considerations on the electron-ion energy exchange yield an analytical expression for $n_{e,min}$ which reproduces the experimental $n_{e,min}$ values in several tokamaks and predicts $n_{e,min}$ in ITER to be close to the density foreseen presently to enter the H-mode.

8.2 H-mode Density Limit

It is desired to operate future fusion power plants in H-mode at the highest density possible. This is limited by the H-mode density limit (HDL). In 2013, four phases were identified on the approach towards the HDL. In 2014, further studies on the HDL were focusing on the possible energy loss channels at this limit. High resolution probe measurements of the SOL plasma were made, which highlight the upcoming of strong filamentary transport to the main chamber wall and a background density evolving in the SOL (see figure 18). Both effects are correlated to the phases of the HDL (3rd and 4th phase (H- and L-mode) have similar SOL characteristics) and explain key issues connected to the observation of these phases.
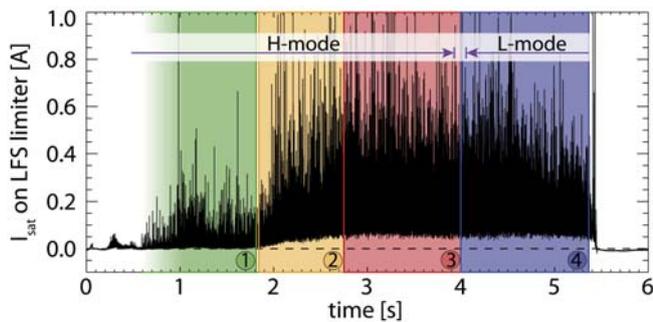
Figure 18: Increasing filamentary transport on the main chamber wall in a gas-ramp pulse. The four phases of the HDL are highlighted.

8.3 Modelling of High Radiation H-modes

In future fusion devices, high radiation losses will be required to reduce the power load in the divertor. To this aim, adequate impurities must be seeded in a controlled way.

Experiments using nitrogen were conducted in AUG H-modes, leading to the expected power load reduction, without confinement degradation. To model these results in a realistic way, time-dependent simulations including both impurity radiation and transport effects are necessary. This has been achieved by coupling the ASTRA and STRAHL codes, which also include the radiation due to the intrinsic impurity tungsten. For the simulations, the following elements must be included in the transport model. The presence of the H-mode transport barrier provides high temperatures and densities leading to a pedestal structure with steep pressure gradients which collapse at each ELM crash and recover during the following inter-ELM phase. This causes strong transport changes in the edge region which highly impact the radiation properties of nitrogen, while tungsten is expected to be less affected. The radiation profiles provided by the simulations agree well with the experimental ones over both radius and time. In particular, the strong enhancement of the nitrogen radiation at the edge caused by the ELM-induced transport is well reproduced, while the radiation properties of tungsten are also well matched. Further, the model also reproduces the increase of the tungsten concentration as the ELM frequency is lowered.

8.4 Toroidal Asymmetries of W-transport
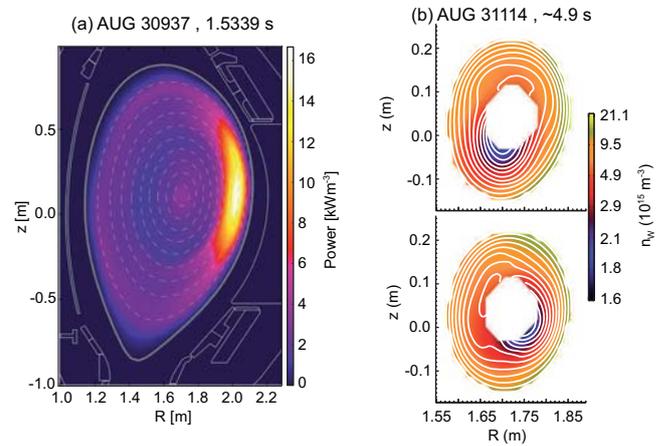
Figure 19: (a) SXR tomographic reconstruction showing strong centrifugal effects and (b) 2D mode-resolved W-density for two mode phases with T_e-contours showing the mode structure.

Two-dimensional impurity transport analyses methods have been developed to study the effects of poloidal asymmetries (due to centrifugal effects and poloidally varying electrostatic potential, figure 19a) and saturated MHD activity (figure 19b) on the transport of W. These methods rely on new advanced SXR tomographic reconstructions and new rotation tomography of 1D-ECE measurements. The effects of different heating methods on impurity asymmetries have been successfully decoupled although discrepancies with theory still need to be explained. In the presence of saturated (1,1) modes,

the W-density is found strongly hollow inside the displaced core. This has triggered new theoretical efforts to study neoclassical and turbulent transport in non-axisymmetric tokamak geometry.

8.5 Helium-transport (FOM-DIFFER)

The importance of understanding the behaviour of helium in fusion plasmas has motivated studies of helium transport, as part of the FOM-DIFFER research programme at AUG. A high étendue CX-spectrometer developed by ITER-NL, suitable for core CXRS measurements on ITER, was installed and utilised for the helium charge exchange measurements. These measurements are not straightforward as recombined helium ions which move along the magnetic field lines provide an additional emission which is not localised at the beam ('plume' effect). To interpret the measured spectra correctly, a model for the helium plume emission was implemented. The model was benchmarked against experimental data and is shown to describe the underlying physics mechanisms accurately, as it can reproduce the experimental helium spectra.

As accurate He densities can now be derived, investigations of He transport have been undertaken. The He-density profiles were found to follow the shape of the electron density, while differences were observed between helium and boron. Theoretical predictions of turbulent transport as calculated via gyrokinetic modelling, which is the dominant transport mechanism, have shown good agreement with the general trends of the measured profiles under certain conditions. However, cases were also found in which strong disagreements were observed. The studies have contributed significantly to the understanding of He transport, but further experimental and theoretical work is necessary.

8.6 β_N-limit

A tokamak plasma is subject to various resistive and ideal MHD instabilities which restrict the operation space of the device. For the largest fusion power production, it is preferable to operate the tokamak close to the stability limit with the maximal possible pressure characterised by the value of β_N. In AUG, this limit is typically set by resistive instabilities (tearing modes). If these instabilities could be prevented, higher values of β_N could be reached. The value of β_N would then be limited by the onset of the ideal kink instability. The actual limit depends on several factors, including the stabilising influence of the conducting components facing the plasma surface. Recently installed internal active coils were used during the last campaign to probe stability of the plasma and identify the β_N limit from plasma response. Analysis of plasma reactions to n=1 DC and n=1 AC external perturbations show a clear enhancement of the plasma reaction with increasing β_N. Moreover, the plasma reaction depends on the pitch angle of the n=1 perturbations. First analysis shows that operation points are around the 'no-wall' limit.

Future investigations will address this point in detail, together with the observed dependence of the plasma rotation on n=1 pitch.

8.7 Sawtooth Crash as Tearing Mode Trigger

Optimisation of the plasma performance is one of the main goals of fusion research. Unfortunately, it is limited by resistive instabilities, usually neoclassical tearing modes. These modes are metastable and can be triggered by other MHD events. Sawtooth crashes provide the strongest internal magnetic perturbations and are able to trigger these modes. Direct measurements show that sawtooth crash triggers the ideal kink mode directly after the crash at the resonant surface. This mode converts into an island only later (figure 20). This is in contradiction to the standard picture of a large island formation directly after the sawtooth crash and gives new insight into the problem.
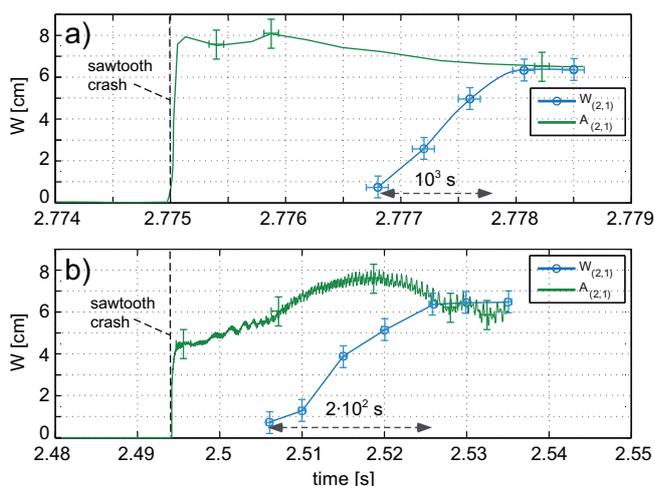
Figure 20: Comparison of the perturbation amplitude for (2,1)-mode from magnetic signal (kink+island), $A_{(2,1)}$, and island width from ECE, $W_{(2,1)}$, for two different cases, #27257: t = 2.77 (a), 2.5 (b) s.

8.8 Plasma Rotation at NTM Onset

Neoclassical tearing modes (NTM) are one of the most serious performance limiting MHD instabilities in a tokamak operating in a conventional plasma scenario, like ITER in the Q=10 operation scenario. One key issue is the rotation dependence of the NTM onset threshold as measured in β. ITER will operate with low plasma rotation, which is different from most present day experiments. The influence of rotation on the NTM onset threshold has been investigated on the basis of a database including around 80 discharges.

This analysis shows that the NTM onset β-threshold increases symmetrically with increasing co- and counter-I_p rotation. The region of minimum onset threshold could be reached and the trend with counter-rotation clearly verified, contrary to previous DIII-D results. Additionally, it shows that NTM limit the maximum achievable β and hence, limit the

plasma operation below the limitations due to technical restrictions such as available heating power. In local parameters taken at the resonant surface, the formation of an upper NTM onset threshold is observed, increasing with normalised plasma rotation, but less distinct at low plasma rotation. This indicates that the NTM behaviour changes at low rotation. This is confirmed by the observation that NTM appearing without any trigger are present mainly at low rotation. Additionally, steeper rotation profiles seem to hamper the appearance of NTM by impeding the triggering process for ELMs and fishbones as a trigger, but this is not the case for sawtooth crashes.

8.9 ICRF 2nd-harmonic D-acceleration during NBI

ICRF is often used to heat the H-minority in a D tokamak plasma. In the presence of a significant fast D-population, a finite D 2nd-harmonic heating is expected because of finite Larmor radius effects. This occurs if T_i is high or the supra-thermal D-tail is significant, like in NBI heated discharges.

The neutron spectrometer installed, based on the liquid scintillator BC501a, detects indeed significant energetic tails in the Pulse Height Spectrum (PHS) of an ICRF+NBI discharge, compared to an NBI-only phase. This is consistent with the enhanced fast D-population predicted by TRANSP with a newly implemented 'RF-kick'-operator. The line-of-sight simulation of the corresponding neutron emission spectra predicted by GENESIS is convolved with the detector's response function to yield PHS in agreement with experimental observations.
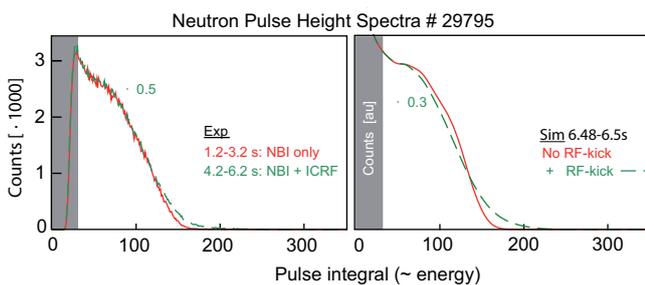
Figure 21: Neutron PH-spectra comparing measured and simulated NBI-phases with and without ICRF.

8.10 Fast-ion Dynamics

The fast-ion diagnostic capabilities have been significantly improved by a newly installed active neutral particle analyser (aNPA) and by an upgraded spectrometer and line of sight setup of the Fast-Ion D_α (FIDA) diagnostic. This made the study of the further acceleration of fast D-ions by second harmonic ICRF possible. Both, the aNPA and FIDA diagnostic measure increased fast-ion energies that are in good agreement with neutron measurements and will be compared with theoretical predictions.

In addition, very strong fast-ion redistribution by sawtooth crashes has been documented. Tomographic reconstructions of the central fast-ion velocity space, which are possible due to the diagnostic upgrades, show that this redistribution is stronger for co-rotating fast ions than for the trapped ones.

The off-axis NBI current drive efficiency has been studied in experiments where 5 MW of on-axis NBI heating power was replaced by 2 off-axis NBI sources. Constant electron temperature profiles were achieved by real-time control of the electron temperature using ECRH. This allows conserving the plasma resistivity while changing the fast-ion current drive profile. The experiments showed a reduction of the loop voltage when applying off-axis NBI, well explained by the tangential geometry of the off-axis NBI sources. However, MSE and first imaging MSE measurements show a weaker effect on the current profiles than expected from neoclassical theory. This observation is in agreement with FIDA measurements and is possibly explained by (1,1)-modes present in the discharges. New experiments are planned in the 2015 campaign with a special focus on avoiding this mode.

8.11 Collective Thomson Scattering (DTU, Denmark)

The collective Thomson scattering (CTS) system, operated by the DTU-group, was used extensively to diagnose the fast-ions dynamics and the plasma ion composition. Experiments were performed where the fast-ion re-distribution due to sawtooth crashes was addressed simultaneously by FIDA and CTS. The information from both diagnostic has been combined by velocity space tomography and a 2D fast-ion distribution function resolved in energy and pitch has been reconstructed just before and just after the crash. Initial comparison between the Kadomtsev sawtooth crash model and the experimental data shows reasonable agreement.

The central minority helium concentration (^{4}He and ^{3}He) has been measured by isotope-CTS with the aim to study the helium transport and to compare the results obtained from CTS and CXRS. Preliminary comparison of the results from the two diagnostics show good agreement.

In collaboration with RFX ENEA (Padova) and ÖAW (Innsbruck), the DTU turbulence group performed investigations of turbulence and transport in the SOL of AUG employing probe measurements at the outboard mid-plane, and at the divertor. The results are compared with numerical simulations applying the global SOL turbulence code HESEL equipped with synthetic probe diagnostics, facilitating the interpretation of the experimental observations and improving the understanding of the underlying SOL-physics.

8.12 ITER-like ECR O1-heating Scheme

An ITER-like O1-heating scheme has been successfully tested with gyrotrons operating at 105 GHz and a nominal magnetic field of 2.9 T. H-mode plasmas with a flat top duration of 4.4 s have been achieved. This scheme has a

high sensitivity to polarisation errors, since any cross polarisation content is reflected directly at the plasma edge and detected as stray radiation.

Applying the O1 scheme, it was found that the measured stray radiation reaches its minimum and levels off, when the model beam polarisation contains is less than 0.5 % of the calculated wrong mode content. Depending on the actual shape of the mode content map as a function of the two polariser angles, this corresponds to a margin of ±2° in the polariser settings. The technical uncertainty is ±0.5°. The measured stray radiation level was within the safe limit for ECE operation. Power modulation experiments were carried out in order to determine the deposition location. Heat wave analysis of ECE channels shows that the power is dominantly absorbed at the first harmonic resonance, located at ρ=0.8. Since the analysis is disturbed by ELMs and STs, minor absorption around ρ=0.6 near the Upper Hybrid Resonance cannot be excluded, as it might occur from the excitation of the parametric decay instability. The latter is also indicated by frequency resolved stray radiation occasionally detected with the CTS system. Discrete peaks similar to a frequency comb were measured intermittently, and this may be linked to secondary waves from parametric decay.

8.13 Disruption Avoidance via ECRF

The work on disruption avoidance with ECCD/ECRH with real-time control on the power and the deposition radius r_{dep} with respect to the resonant surface of the dominant MHD mode (mostly the (2,1)-mode) has been continued. These experiments were performed in high β_N improved H-mode scenarios with early heating (jointly within MST1) and in Ohmically heated L-mode density limits. For the early detection of a still rotating (2,1)-mode the n=1 trigger (NTM scheme) has been used. An offline early detection scheme, based on SVD of magnetics, has been ported from FTU, and is planned for real-time detection of an approaching disruption in future experiments.

In the high β_N scenario the n=1 trigger for applying ECCD led to a recovery of a disruptive discharge for more than 2 s. In these scenarios also the pre-emptive avoidance of the (2,1)-mode has been successfully shown. The best effects could be achieved for r_{dep} slightly outside the nominal resonant surface. Further work is needed on the measurement of the minimal required power and the requirements on the localisation.

In the L-mode density limit, a combination of ECRH at the q=2 surface and the plasma centre, together with a feedback controlled density led reproducibly to a stationary recovery of the discharge at roughly twice the density compared to the onset of the disruption (MARFE, locked (2,1)-mode). Here the core profiles and the presence of sawteeth seem to play a crucial role. This point has to be investigated further in future experiments.

8.14 Disruption Cause Analysis

Most of the existing tokamaks implement disruption protection measurements and can initiate a slow or fast (and mitigated) emergency shut-down. However no reliable disruption prediction system, which is portable to ITER, exists currently in present-day machines. A premise for avoiding or predicting unavoidable disruptions is knowing under which conditions they develop. For this purpose, the causes of disruptions that occurred in 2013 in AUG have been analysed. It is found that 28 % of the discharges with $I_p \geq 0.6$ MA disrupted, and that 74 % of the total disruptions are non-intentional. When possible, disruptions with similar causes were categorised according to the classification system used for JET. The JET classification turned out to be very useful for a preliminary clustering of the AUG disruptions. The same classes are found in both devices; however the likelihood of each class is different, reflecting the diverse heating systems, competences and experimental programme. The most evident difference is the smaller percentage of disruptions during impurity accumulation in AUG, which reflects the capability of this device to centrally heat the plasma with ECRH in most of the experimental scenarios. This work provides a framework for further analysis of the disruptions, on each machine separately, and then jointly. The ultimate aim of this common analysis is the formulation of universal criteria for disruption prediction and avoidance.

8.15 Enhancements of the Real-time Magnetic Equilibrium

Five enhancements of the real-time magnetic equilibrium reconstruction code, JANET, have been implemented. Spline current density basis functions using lookup tables are now used for real-time magnetic equilibrium reconstruction. The transfer function of the fast position control coil has been measured at four frequencies and the oscillations in coil current resulting from ELM's can be properly treated for the low pass response of the magnetic probes inside the vacuum vessel. The introduction of a constraint of the safety factor on the magnetic axis was necessary to predict the location of rational surfaces for NTM stabilisation and disruption avoidance experiments with sufficient accuracy. The external loop voltage measurements can be used for including the modification of the magnetic equilibrium due to vacuum vessel currents during the plasma current ramp. Three rows of ferromagnetic tiles are now installed in the inner heat shield. This requires that the perturbation of the magnetic probe measurements and flux surfaces near these tiles be calculated in real-time. These perturbations can be calculated by a surface current model of ferromagnetic material in a tokamak. The matrices used to calculate the perturbations due to these surface currents and the influence of these currents on neighbouring tiles in real-time need to be computed prior to the discharge.

9 NTM-stabilisation Using High-power Diplexers (Univ. Stuttgart)

The diplexer MkII presently installed at the ECRH2 system was developed for fast switching between two launchers for optimum control of neoclassical tearing modes (NTM), and for separation of a high-power ECRH beam and a low-power ECE signal sharing the same antenna (in-line ECE). In 2014, the control for the resonator tracking with respect to the gyrotron frequency was improved by colleagues from TNO, Delft, to guarantee optimum switching contrast. In addition, polarisation issues were optimised. On AUG, experiments on synchronous stabilisation of NTMs were performed, where the power was toggled between two launchers (L1 and L3) synchronous to the rotation of (3,2) NTM, such that power deposition was always in the O-point of the islands.
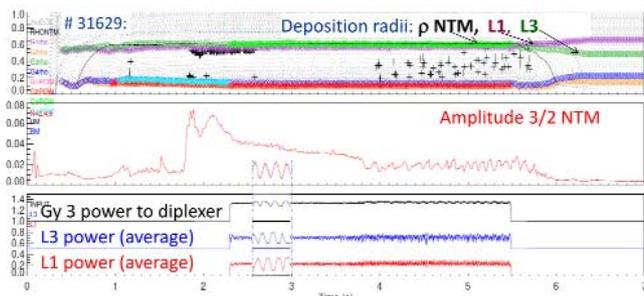

Figure 22: NTM-stabilisation by toggling of the power of a continuously running gyrotron between 2 launchers. Top: Position of the (3,2) NTM, and deposition radii of launchers L1 and L3; middle: amplitude of NTM; bottom: diplexer power signals, input from gyrotron and output to launchers L1 and L3. (Note the temporal averaging of the lower plot. The resolved signals are shown in the insert.).

A clear reduction of the NTM-amplitudes could be demonstrated when the deposition radii of the launchers were equal to the q=1.5 surface. For sufficiently long overlap, complete NTM-stabilisation could be reached, as shown from the data from pulse #31629 in figure 22. These successful experiments are seen as an essential pre-condition for the use of diplexers in the ITER ECRH. The diplexer system is now optimised for experiments with in-line ECE, to detect the position of the NTM islands via a line of sight identical to the ECRH beam, and finally to demonstrate the possibility for feedback launcher control for NTM-stabilisation.

10 Edge and Divertor Physics

10.1 Edge Rotation and in-out Impurity Asymmetries in the Pedestal

The poloidal and toroidal impurity flows in the H-mode pedestal have been studied over a wide range of pedestal top ion collisionalities $\nu_{*,i}$. A comparison of the poloidal rotation data to neoclassical predictions shows good agreement in all cases. The measured edge impurity toroidal rotation is observed to change sign from co- to counter-current with decreasing $\nu_{*,i}$. The switch occurs at the same $\nu_{*,i}$ at which neoclassical theory predicts the main ion poloidal rotation to change from the electron to the ion diamagnetic direction. The behaviour of these two species leads to fairly constant co-current main ion toroidal rotation, which is calculated via radial force balance of both species. Hence, at low $\nu_{*,i}$, due to a lack of frictional coupling, the differential toroidal rotation can be quite large. The behaviour of the impurity flows on a flux surface has also been investigated in detail and it was found that the measurements are consistent with the continuity equation only if the poloidally asymmetric impurity density distribution is taken into account. The measurements were extended to different impurity species and to H-mode plasmas with different $\nu_{*,i}$. The in-out asymmetries in the pedestal are present for both boron and nitrogen, with an impurity localisation at the HFS of ~2.5–3.5.

10.2 Role of T_e in the Edge Particle Transport during Pedestal Evolution

We investigated the effect of T_e on the edge particle transport in the pedestal. For this purpose, we analysed the density build-up after the L→H transition and extended previous analysis methods. ECRH was used to vary the pedestal temperature during its evolution between subsequent H-mode phases. Although the pedestal T_e and its gradients could be varied by a factor of 2, almost no change in the edge density evolution is observed within the measurement uncertainties. ASTRA was used to interpret the measurements and to analyse the dependence of the pedestal particle transport on the T_e-profile. Changes in recycling between the 2 ECRH power steps were small as well as the variation in the ionisation rate. This and the fact, that as the T_e-gradients were varied by a factor 2 already between these 2 power levels, almost no change in the n_e-profiles and their gradients are observed, suggests a minor role of thermo-diffusion in the pedestal during its evolution.

10.3 Impact of MP on Edge E_r & Turbulence

The radial electric field E_r and density turbulence dn_e are particularly good indicators of the MP field penetration and impact on the tokamak edge. As previously reported, using Doppler reflectometry the MP impact is clearly observed in low collisionality L-modes with a near SOL E_r reduction and a reversal of the edge negative well, consistent with field-line ergodisation. The MP impact is very sensitive to the degree of MP resonance with the edge rational field-lines, i.e. to the q-profile and the MP toroidal and poloidal field spectra. Figure 23 compares the edge E_r and short-wavelength dn_e enhancement (with and without MP) from two pulses in a series of low density, ECR heated L-mode discharges, where the relative $\Delta\Phi$ phase between upper and lower B-coil sets is scanned from 0° (even) to 180° (odd parity) for an n=2 MP.

The corresponding MP vacuum spectra show the m=8 & 10 spectral components increasing from weak to strong at the q=-4 and -5 surfaces respectively. All coil parities display some E_r impact, the weakest for the non-resonant case and strongest for the most resonant case. However, dn_e is only enhanced for significantly resonant MP case around the E_r reversal, and reduced when non-resonant. Here, the dn_e enhancement is associated with regions of reduced negative E_r shear.
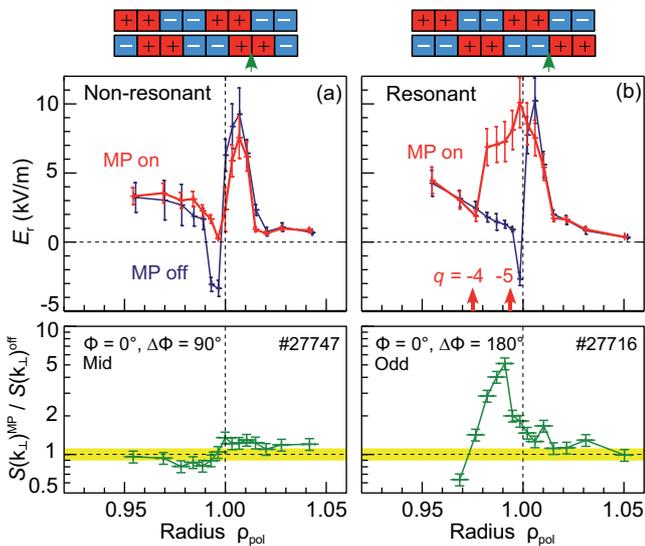
Figure 23: E_r (top) and turbulence ratio (bottom) profiles from matched (-2.3 T, 1.0 MA, P_{ECH}=0.6 MW, 1.3×10^{19}m^{-3}) L-modes for (a) $\Delta\Phi$=90° non-res. & (b) $\Delta\Phi$=180° resonant differential coil phasing with n=2 MP.

10.4 Edge j- & p-profiles during N_2-seeded Improved H-modes

Confinement improvement via N_2-seeding has been the subject of much experimental investigation in recent years. The measured pedestal T_e and n_e-profiles were used as input for the CLISTE equilibrium code to determine the edge current density in reference and seeded phases. The increase of Z_{eff} from N_2-seeding causes a decrease in the efficiency of the bootstrap current drive, resulting in separate behaviours of the local and flux surface averaged edge current density. The local current density always increases, due to higher temperatures associated with confinement improvement, but the average current density is lower than would be expected if Z were not taken into account. This provides a potential confinement improvement mechanism; higher local current density changes the local shear profile, stabilising ballooning modes, while relatively lowered average current density decreases the peeling mode drive. This is in qualitative agreement with peeling-ballooning analysis performed for one discharge, shown in figure 24, where the seeded case is shifted to a higher pressure gradient, but at the same current density. Ballooning modes are further stabilised by an increased Shafranov-shift due to higher global β. A predictive pedestal model is being created to investigate the combination of these effects.
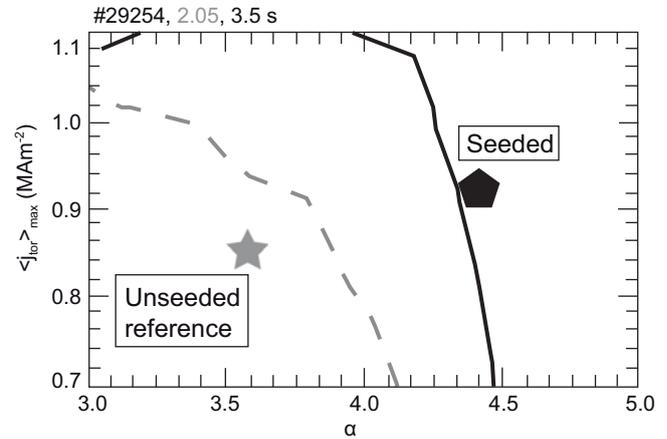
Figure24: Comparison of edge j-profiles with and without N_2-seeding.

10.5 Scaling of Power Spreading in Open/Closed Divertor

We have characterised the power spread (deposited) in the divertor private flux region by the so called S-factor, derived from heat flux profile measurements. An experimental database of the S-factor from AUG and JET outer target data has been gathered and analysed. In terms of main plasma parameters, we find that the poloidal magnetic field plays a major role with S~$1/B_{pol}$ in both L-mode and H-mode plasmas, similarly to the SOL decay length λ_q. Combining JET and AUG data in open divertor H-modes, we obtain a strong and beneficial major radius dependency. For closed AUG DivII configurations in L-mode a larger upstream density clearly broadens S up to 3 times for the same plasma current. Contemporarily, the stronger radiation dissipates a larger fraction of plasma heat. Interestingly, the scaling of S with divertor parameters, reveals that only the target T_e is needed to account for its variation leading the scaling S~$T_e^{0.37}$. SOLPS simulations reproduce most of the observed phenomenology, showing that the degree of divertor closure exerts a strong influence over the neutral density and consequently on the plasma radiation and profile evolution along the field lines. Closed configurations generate larger parallel gradients, lower target T_e and consequently larger S.

10.6 Impact of High n_e-operation on SOL-transport

In the previous year, the onset of the mid-plane density profile flattening observed in high density L-modes and the known as 'shoulder' was linked to the divertor detachment. This was attributed to the increase of perpendicular transport caused by the parallel disconnection of filaments. In order to confirm this, a series of L-mode discharges were realized in which mid-plane collisionality, Λ_{mid}, was kept constant while divertor collisionality, Λ_{div}, was swept by conducting density ramps with different heating power. The results demonstrated that density decay length and filament size scale clearly with Λ_{div} and not with Greenwald density fraction or Λ_{mid}. The same was observed when inducing detachment with N_2-seeding.

Besides, the formation of a density shoulder has been confirmed in ITER-relevant H-modes before divertor detachment, albeit at similar values of Λ_{div} as those encountered in L-mode. These results imply that current models of filament models should be reassessed, as ITER and DEMO will feature collisional divertors leading to enhanced perpendicular transport in the mid-plane.
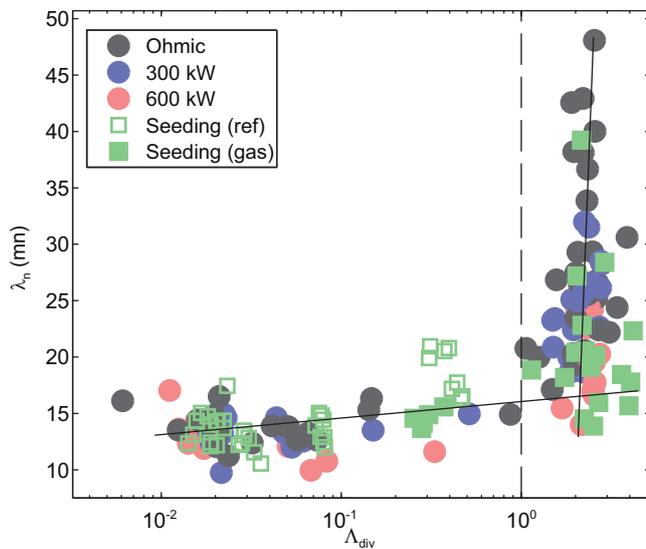
Figure 25: n_e e-folding length λ_n vs. Λ_{div}. 2 clear regimes can be seen separated by $\Lambda_{div}=1$ (same as with N_2-seeding).

10.7 EMC3-EIRENE Simulations of Particle- & Energy-fluxes to Main Chamber- and Divertor PFC

The first EMC3-Eirene simulations with an extended computational grid including both divertor- and main chamber (MC) 3D wall plasma-facing components (PFC) were performed. In a first step the simulations were compared to low-power L-mode discharges before and after the transition from a low- to the high-density regime. For the low-density case the simulations agree quite well up- and downstream with a flat transport profile. In order to explain the upstream far-SOL density profiles of the high density case the MC PFCs needed to be included in the simulations as well as an enhanced transport region at ρ_{pol}=1.01...1.03 consistent with probe measurements of enhanced perpendicular transport. In a 2nd step, particle- and power-fluxes to the limiter for the realistic geometry, for limiters displaced radially inward and for a toroidally symmetric limiter were computed. Almost the same fraction of power as that to the divertor is absorbed by the MC PFCs in the simulation of the high density case.

10.8 Formation of a High n_e-front in the Inner Far SOL

When the inner divertor is strongly detached while the outer one remains attached the ionisation front close to the separatrix has moved to the X-point, i.e. electron densities of the order of 10^{23} m^{-3} are measured spectroscopically at the X-point.

Simultaneously, radiative fluctuations appear in the HFS close to the X-point and another, unexpected high density region forms in the HFS far SOL. In L-mode, this so called HFS high density (HFSHD) is located at ρ_{pol}≈1.02 or ≈5×λ_q and extends from the X-point height ≈20 cm upwards. In H-mode, the HFSHD expands up to ρ_{pol}≈1.05 or ≈10×λ_q into the far SOL and well above the X-point (figure 26a), confirmed by interferometry. The refurbished reflectometry system revealed that the HFSHD even reaches up to the HFS mid-plane, while it is not observed at the LFS mid-plane.

Moreover, the magnitude and spatial extend of the HFSHD scales with power. With increasing heating power the electron density and neutral fluxes in the HFS far SOL increase (figure 26b, c). Seeding of impurities leads to a reduction of the HFSHD. It is important to note that, while the HFSHD increases with heating power or decreases with impurity seeding, the density at the outer mid-plane and the neutral fluxes in the divertor private flux region remain approximately constant.
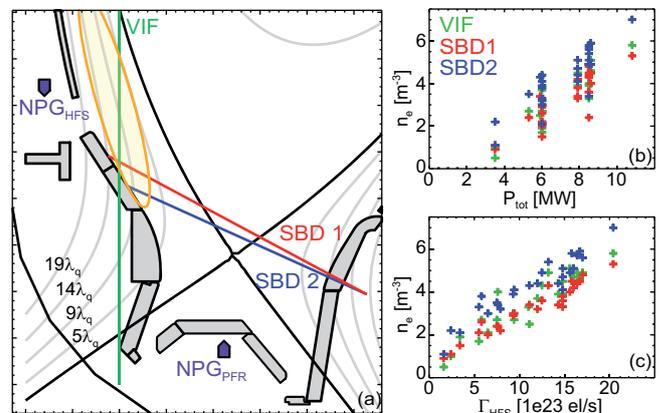
Figure 26: (a) Approximated region of the HFSHD (orange), Stark Broadening LOS (red & blue), vertical interferometer-cord (green) and neutral pressure gauges (purple). HFSHD measured with the according diagnostics in (a) versus the applied heating power (b) and the neutral fluxes in the HFS (c).

10.9 Partial Detachment at High Heating Power

Partial detachment of high power (P_{heat}>20 MW) discharges was obtained by the combination of high deuterium neutral divertor fluxes with N_2-seeding for enhanced divertor radiation and/or Kr-seeding for core plasma radiation. Divertor dissipation of very high power levels was demonstrated up to values of P_{sep}/R of 10 MW/m, corresponding to 2/3 of the value foreseen for ITER, while the target peak power load was simultaneously kept below 5 MW/m^2. Good energy confinement around H_{98}=1 could be maintained during partially detached conditions, i.e. during sustainment of a strong drop of pressure and power flux density along the divertor field lines over the radial extent of a few power decay lengths.

When the detachment is even further pronounced, e.g. by a stronger nitrogen injection, a substantial rise of the pedestal and core density is observed, which correlates with the development of a highly radiating zone in the confined X-point region. This leads to a cooling of the pedestal, but due to a steeper pressure gradient inside the pedestal top, the overall reduction of confinement stays moderate leading to $H_{98}{\sim}0.9$ at substantially increased plasma density (~+30 %).

10.10 Modelling of Complete H-mode Divertor Detachment

Detachment is essential for operating future fusion devices. SOLPS5.0 simulations of high recycling and completely detached high power H-mode discharges in AUG aim at understanding the physical mechanisms of the detachment process. The level of detailed agreement of these simulations with experiment is a novelty. Special features of the completely detached H-mode plasmas such as strongly localised, intense X-point radiation, a related upstream pressure loss and parallel temperature variations (1-100 eV) on closed field lines in the proximity of the X-point are reproduced by the code.

To match the experimental measurements an increased perpendicular transport in the divertor is required in the simulations. In completely detached plasmas with strong N_2-seeding the inclusion of drifts is necessary. A remaining discrepancy consistently manifests in the under-prediction of modelled Balmer-line intensities as well as neutral fluxes and pressures in the divertor. It points to a deficiency of the code to describe the divertor neutral compression and the core plasma fuelling correctly.

10.11 Plasma Operation with Solid W-divertor

The new divertor Div-III was operated for over 800 plasma pulses in 2014. During this campaign pulse lengths of up to 10 s and heating energies of up to 100 MJ were achieved. A cryo-pump by-pass valve was used to achieve the required high divertor neutral particle pressure of more than 4 Pa. The fraction of long lasting discharges and discharges with high heating energy is increased for Div-III compared to the previous Div-II. Safe plasma operation was achieved over the whole campaign supporting the successful design of Div-III. During the Div-III campaign the divertor manipulator DIM-II was used to retract targets and to inspect them. Two findings are obvious as can be seen in figure 27. There is different damage behaviour between the 12 targets tested in the high heat flux facility GLADIS and the targets exposed to the plasma, although the number of high heat load cycles was higher for the test targets. The surface of the plasma exposed target is damaged by a network of shallow cracks in particular in the region close to the region of highest heat load. Whereas these cracks are limited to the surface region a single crack in the centre of the target is through the

whole depth. This deep crack starts at the lower edge of the target below the clamping and propagates poloidally. An in vessel inspection after venting reveals that this finding is typical for about 90 % of the targets. Investigation on the cracking mechanism was started. It should be mentioned that a deep crack in poloidal direction has neither effect on the stability of the mechanical fixing of the target nor did these cracks have had an effect on the plasma performance.
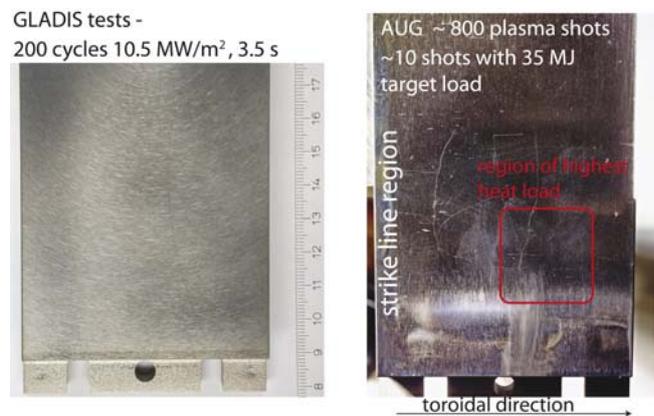
Figure 27: Solid W-tiles after high heat load tests (GLADIS, left) and after one AUG campaign (right).

10.12 Densities from Reflectometry (IST, Portugal)

Physics studies: (i) Density fluctuations: HFS and LFS $\delta n/n$ radial profiles were obtained for L-mode with the profile FMCW reflectometer operated in fixed frequency mode. On the LFS good agreement was found between $\delta n/n$ profiles measured with the LFS frequency hopping reflectometer and the FMCW system. A $\delta n/n$ drop just inside the separatrix is observed in the region of strong E_r-shear. In addition, LFS/HFS asymmetries in $\delta n/n$ were observed, depending on plasma configuration, with larger asymmetries in the SOL for a double-null configuration. RMP coils were also found to cause asymmetries in $\delta n/n$, being more pronounced in the HFS SOL. (ii) Formation of a high density front at the HFS: H-mode density profile studies revealed that the front is formed in the divertor and propagates upwards into the midplane, strongly influencing the ELM dynamics. In L-mode the high density was found to be associated with the divertor detachment.

Diagnostic developments: A new data acquisition system was commissioned and operated during the campaign generating Level-0 shotfiles on a regular basis. Signals from all microwave channels are now acquired for the complete discharge duration with a profile repetition rate (bursts of four sweeps) of 250 µs. Level-1 real-time density profile codes have been ported to the new server architecture and optimized to allow real-time control experiments at HFS/LFS.

11 Scientific Staff

Tokamak Scenario Development (E1): N. Arden, C. Aubanel, K. Bald-Soliman, L. Barrera Orte, F. Bastian, K. Behler, N. Berger, H. Blank, V. Bobkov, A. Bock, F. Braun, A. Burckhart, A. Buhler, L. Casali, M. Dibon, R. Drube, M. Ebner, H. Eixenberger, K. Engelhardt, E. Fable, H. Faugel, S. Fietz, J. C. Fuchs, H. Fünfgelder, T. Franke, L. Giannone, I. Goldstein, A. Gräter, E. Grois, A. Gude, T. Härtl, A. Herrmann, J. Hobirk, V. Igochine, C. Jacob, J. Jacquot, C.-P. Käsemann, A. Kallenbach, A. Kappatou, K. Klaster, B. Kleinschwärzer, A. Kling, J. Kötterl, P. T. Lang, P. Leitenstern, L. Liu, A. Lohs, K. Mank, M. Maraschek, P. de Marné, A. Mayer, R. Merkel, V. Mertens, A. Mlynek, F. Monaco, D. Moseev, S. Müller, G. Neu, H. Nguyen, J.-M. Noterdaeme, R. Ochoukov, B. Plöckl, C. Rapson, G. Raupp, M. Reich, M. Rott, F. Ryter, G. Schall, M. Schandrul, P. A. Schneider, M. Schubert, K.-H. Schuhbeck, J. Schweinzer, G. Sellmair, B. Sieglin, O. Sigalov, M. Sochor, F. Stobbe, J. Stober, W. Suttrop, G. Tardini, W. Treutterer, D. Vezinet, T. Vierle, S. Vorbrugg, D. Wagner, M. Weiland, R. Wenninger, M. Willensdorfer, K. Winkler, B. Wiringer, I. Zammuto, G. Zangl, D. Zasche, T. Zehetbauer, W. Zeidner, H. Zohm.

Plasma Edge and Wall (E2M): M. Balden, J. Bauer, J. Belapure, M. Bernert, G. Birkenmeier, J. Boom, B. Böswirth, D. Brida, J. Brinkmann, D. Carralero, M. Cavedon, G. D. Conway, M. Dunne, R. Dux, T. Eich, S. Elgeti, M. Faitsch, R. Fischer, B. Geiger, H. Greuner, T. Happel, T. Höschen, W. Jacob, F. Koch, K. Krieger, B. Kurzan, A. Lebschy, T. Lunt, H. Maier, A. Manhard, P. Manz, M. Mayer, R. McDermott, A. Medvedeva, G. Meisl, H. W. Müller, R. Neu, M. Oberkofler, T. Odstrcil, S. Potzel, D. Prisiazhniuk, T. Pütterich, F. Reimold, V. Rohde, K. Schmid, A. Scarabosio, T. Schwarz-Selinger, M. Sertoli, L. M. Shao, P. Simon, U. Stroth, K. Sugiyama, H. J. Sun, E. Viezzer, M. Wischmeier, E. Wolfrum.

Tokamak Physics Division: J. Abiteboul, C. Angioni, A. Bergmann, A. Biancalani, R. Bilato, A. Bottino, V. Bratanov, A. de Bustos, A. Chankin, C. P. Coster, T. Görler, J. Grießhammer, S. Günter, M. Hölzl, F. Jenko, O. Kardaun, K. Lackner, P. Lauber, A. Navarro, M. Oberparleiter, G. Pautasso, E. Poli, W. Schneider, M. Schneller, E. Schwarz, B. Scott, A. Stegmeir, E. Strumberger, H.-J. Sun, C. Tichmann, D. Told, Q. Yu, D. Zarzoso.

ITER Technology & Diagnostics: U. Fantz, P. Franzen, M. Fröschle, B. Heinemann, D. Holtum, C. Hopf, C. Martens, H. Meister, R. Nocentini, S. Obermayer, G. Orozco, F. Penzel, R. Riedl, D. Rittich, J. Schäffler, T. Sehmer, D. Wünderlich.

Garching Computer Centre: A. Altbauer, V. Bludov, K. Desinger, R. Dohmen, E. Erastova, C. Guggenberger, C. Hanke, S. Heinzel, J. Kennedy, K. Lehnberger, M. Panea-Doblado, J. Reetz, R. Preuss, M. Rampp, K. Reuter, R. Ritz, A. Schmidt, A. Schott, I. Weidl, M. Zilker.

Integrated Technical Center: R. Blokker, N. Jaksic, R. Jung, M. Kircher, G. Lexa, W. Lösch, J. Maier, A. Pichlmair, H. Pirsch, J. Tretter, H. Tittes, M. Weißgerber, F. Zeus.

IPP Greifswald: O. Ford, R. Wolf.

TUM, München: T. Eibert, C. Koenen, U. Siart.

FZ Jülich: S. Brezinsek, J. Coenen, R. Koslowski, A. Krämer-Flecken, O. Schmitz.

IPF University of Stuttgart: E. Holzhauer, W. Kasparek, A. Köhn, C. Lechte, B. Plaum, M. Ramish, B. Schmid, S. Wolf.

CCFE, Culham, Abingdon, United Kingdom: I. Chapman, C. Challis, P. Jacquet, A. Kirk, Y. Liu, H. Meyer, I. Monakhov.

CEA, Cadarache, France: B. Bottereau, F. Clairet, L. Colas, D. Douai, E. Joffrin, D. Kogut, D. Mazon, D. Molina.

DCU, University College Cork, Ireland: P. McCarthy.

LPP, CNRS, Ecole Polytechnique, Palaiseau, France: P. Hennequin, C. Honoré.

ENEA, Consorzio RFX, Padua, Italy: P. Martin, P. Piovesan, M. Spolaore, N. Vianello.

ENEA, IFP, CNR, Milano, Italy: C. Cazzaniga, G. Croci, G. Gorini, G. Granucci, A. Mancini, M. Nocente, G. Rocchi, O. Tudisco.

DIFFER, Nieuwegein, The Netherlands: A. Bogomolov, M. de Baar, I. Classen, M. Kantor.

HAS, Budapest, Hungary: G. Cseh, A. Fenyvesi, L. Horváth, S. Kálvin, G. Kocsis, N. Lazányi, G. Náfrádi, G. Papp, G. Pokol, G. Pór, T. Szepesi, S. Zoletnik.

Hellenic Republic, Athen, Greece: A. Lazaros.

IPP, Praha, Czech Republic: J. Adamek, M. Komm.

IPPLM, Warsaw University of Technology, Poland: A. Czarnecka, E. Fortuna-Zalesna, M. Rasinski.

IST Lisbon, Portugal: S. da Graca, L. Guimarais, M.-E. Manso, V. Nikolaeva, V. Plyusnin, G. Santos, J. Santos, A. Silva, C. Silva, B. Gonçalves, P. Varela, J. Vicente.

NILPRP, Bucharest, Romania: C. V. Atanasiu.

ÖAW, University of Innsbruck, Austria: S. Costea, C. Ionita, A. Kendl, R. Schrittwieser.

ÖAW, IAP, TU Wien, Austria: F. Laggner, M. Wiesinger.

DTU, Lyngby, Denmark: T. Jensen, S. Nimb, A. Jacobsen, M. Jessen, S.B. Korsholm, F. Leipold, J. Madsen, P. Michelsen, V. Naulin, A. H. Nielsen, S. K. Nielsen, M. L. Magnussen, J. Rasmussen, J. Juul Rasmussen, M. Salewski, M. P. Stejner, L. Tophøj.

TEKES, Aalto University, Espoo, Finland: L. Aho-Mantila, S. Äkäslompolo, M. Airila, O. Asunta, M. Groth, T. Kurki-Suonio, J. Miettunen, T. Tala.

TEKES, VTT, Espoo, Finland: A. H. Hakola, J. Likonen.

University of Nancy, France: I. L. Briançon, F. Brochard, G. Fuchert, A. Shalpegin.

Chalmers Univeristy, Gothenburg, Sweden: O. Yadikin.

University of Seville, Sevilla, Spain: J. Galdón Quiroga, M. Garcia-Muñoz, M. Rodriguez Ramos, L. Sanchis-Sanchez.

University of Strathclyde, Glasgow, United Kingdom: L. Menchero, M. G. O'Mullane, H. P. Summers.

INEEL, Idaho, USA: P. W. Humrickhouse.

University of California, San Diego, USA: S. H. Müller.

JET Cooperation

Head: Dr. Thomas Eich

Experiments aiming to reach the highest possible radiation fraction in the ILW were carried out and assessed as a scenario for both the planned DT campaign in JET and future reactor-sized devices like ITER. Studies on transient divertor heat loads due to energy losses from the pedestal region by ELMs, started in 2008, were completed and resulted eventually, again in conjunction with ASDEX Upgrade results, in an improved predictive capability of these burst-like thermal loads towards ITER. Additionally many other fields of activity were successfully continued with significant IPP involvement during the 2014 JET campaigns. Also in the field of modelling and in the Fusion Technology Task Force IPP involvement did lead to significant scientific progress.

The operation of JET with the ITER-like wall (ILW) was successfully continued in 2014 under the new umbrella of the EUROfusion consortium. One of the main focuses of the IPP contribution was the physics of power and particle exhaust guided by a scientific team active in JET and ASDEX Upgrade exploiting the European platform in the best manner. The latter work did benefit significantly from improving the capabilities of key diagnostics at JET for these and many other studies.

Overview on IPP Involvement

Fortunately, the 2013 campaigns – which had to be stopped owing to technical problems with the neutral beam heating system and reciprocating probe were continued and finalized successfully for most envisaged goals of IPP contributors to the JET programme.

In total 25 IPP scientists were seconded to JET in 2014, leading to a total of ~7 ppy of on-site support for the operation of JET. Two IPP scientists were almost permanently on site, being involved in the management of the JET Task Forces E1 & E2. Eight long-term secondments of IPP staff to the Close Support Unit (2) and to the JET Operator (6) were active in 2014. The majority of the 25 IPP scientists participated in the campaigns C33 – C34 from June to October 2014.

Assessment of FIDA Diagnostic Capabilities

The possibility to measure fast beam ions by the means of spectroscopy has been explored at JET using the charge exchange diagnostic. Strongly Doppler shifted fast-ion D-alpha (FIDA) radiation has been observed when tuning the diagnostics' spectrometer to wavelengths between 656.5 nm and 664 nm (the un-shifted wavelength of the Blamer alpha emission of Deuterium is 656.1 nm). As shown in figure 1, a clear spectral wing is observed between 659 nm and 662 nm which can be attributed to the charge exchange radiation emitted by fast ions. Comparisons of the observed FIDA radiation with theoretical predictions based on the forward modelling tool FIDASIM show good agreement. FIDASIM calculates the attenuation and spectral emission of neutral beams, including charge exchange radiation of thermal and fast ions. The Monte Carlo code has been supplied with simulated fast-ion distribution function from TRANSP to be able to

predict the spectral shape and intensity of the FIDA component. Clearly, the measured spectral wing at 660 nm is well explained by the synthetic FIDA spectrum given in red. In addition, the simulated beam emission and charge exchange emission of thermal Deuterium ions are found in good agreement with the measurement. This shows that the spectra are consistently modeled and proves that FIDA measurements are applicable at JET to characterize fast-ion distribution functions. However, I should be noted that a good signal to noise ratio of this type of spectroscopic measurement is only possible during plasmas that feature low densities and a large fraction of fast-ions. Moreover, significant passive FIDA radiation from the plasma edge has been observed which requires accurate background subtraction by e.g. modulation neutral beam injection.
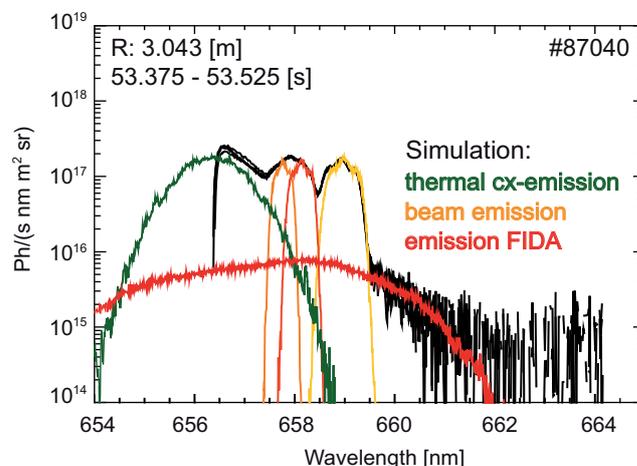
Figure 1: Measured active Balmer Alpha spectra consisting of radiation from beam neutrals, neutralized thermal Deuterium ions and neutralized fast-ions. Predicted spectra from FIDASIM of these contributions are plotted in colour.

Course on Infra-red (IR) Thermography in JET Held by IPP Staff

For the first time a two-weeks course was given by IPP staff to train interested scientists from nine affiliations to learn about IR thermography in tokamaks in general and specifically for JET. IPP did take the lead for IR based studies in the early days of JET EFDA back in 2000 and kept a high level of involvement throughout until today. Infrared (IR) thermography is the main tool to study the heat flux onto the plasma facing components such as the divertor and the first wall. Whereas for small devices the power exhaust from the plasma is still tolerable it becomes challenging for large devices. In order to train new experts in the field of IR thermography a two weeks course was held at JET in July 2014.

The topics of the course included the theoretical basics of thermography, the data evaluation procedures and hands on training at the JET IR system. A special focus was set on the difficulties encountered in a full metal environment where the influence of volumetric radiation and surface reflections need to be treated. Techniques for the correction of camera movement during the discharge were shown. An introduction into the heat flux code THEODOR was given focusing both on the application to data as well as the underlying evaluation algorithm. The course was completed successfully enabling the participants to perform and analyse IR measurements.

ELM Heat Load Scaling Using JET and ASDEX Upgrade Data

ELM induced heat load is a major concern for large fusion devices such as ITER and DEMO. So far no commonly agreed scaling or physics based prediction for the expected target heat load exists. Using well diagnosed JET discharges with both carbon and ITER-like wall (ILW) an attempt is made to correlate the divertor target heat load to the upstream pedestal pressure prior to the ELM crash.

Despite the different ELM behaviour with ILW compared to discharges with carbon plasma facing components the pedestal pressure orders the corresponding ELM deposited energy density measured by infra-red (IR) thermography. It is found that the energy density on target only has a weak dependence on the relative loss in stored energy due to the ELM.

This finding is in agreement with previous findings on DIII-D and JET reporting an increase of the ELM wetted area with the ELM loss energy. In order to extrapolate to large devices it is imperative to include data from different sized devices into the scaling.

For this data from ASDEX Upgrade with combined Thomson-Scattering and IR thermography measurements is used. Preliminary results indicate that ITER operation at half field, half current seems feasible, in terms of divertor heat load for the outer target, with unmitigated type-I ELMs.

This would possibly allow ITER to operate safely in terms of divertor heat load, not exceeding the divertor limits which would result in a reduced component life time, without the need of having a fully developed ELM mitigation technique. However, these studies need to be extended to the inner divertor target for which currently no sufficiently well resolving diagnostic exists. Hence further studies with improved IR diagnostics are planned in 2015/16 for both JET and ASDEX Upgrade, also including the ELM induced load onto the first wall.

Progress on Understanding Detachment

The formation of a high density, being one order of magnitude larger than the separatrix density and situated in the HFS far SOL, has been observed in AUG and JET H-mode and L-mode discharges, which shows that this effect is independent of machine size and confinement mode. In H-mode, the spatial extent into the far SOL is about 10 times λ_q away from the separatrix and more than 20 cm above the X-point, which is much larger compared to L-mode. To trigger the HFSHD the inner divertor has to be detached and the heating power has to be sufficiently high. Detailed power-scans at AUG showed that the electron density and the neutral fluxes in the HFS far SOL increase about linearly with heating power, whereas the neutral fluxes in the PFR and the main plasma density remain unchanged. There is also clear correlation between the HFSHD and the neutral compression ratio in the inner divertor, which decreases with heating power.
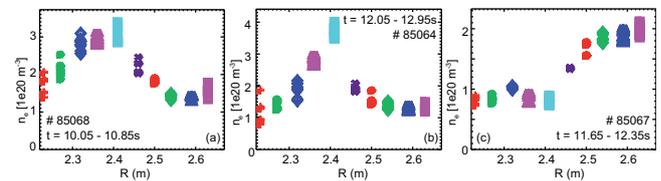
Figure 2: Electron density in the JET HFS SOL measured with KSRD without (a), with medium (b) and high (c) N_2 injection. The colour-code refer to the LOS shown in figure 3.

Figure 2 shows the electron density in the JET HFS SOL measured by Stark broadening of the $D\delta$ line along the lines of sight shown in figure 3 for a discharge without, with medium and with high N_2 injection rate, respectively, and otherwise similar parameters. It can be seen that injecting N_2,
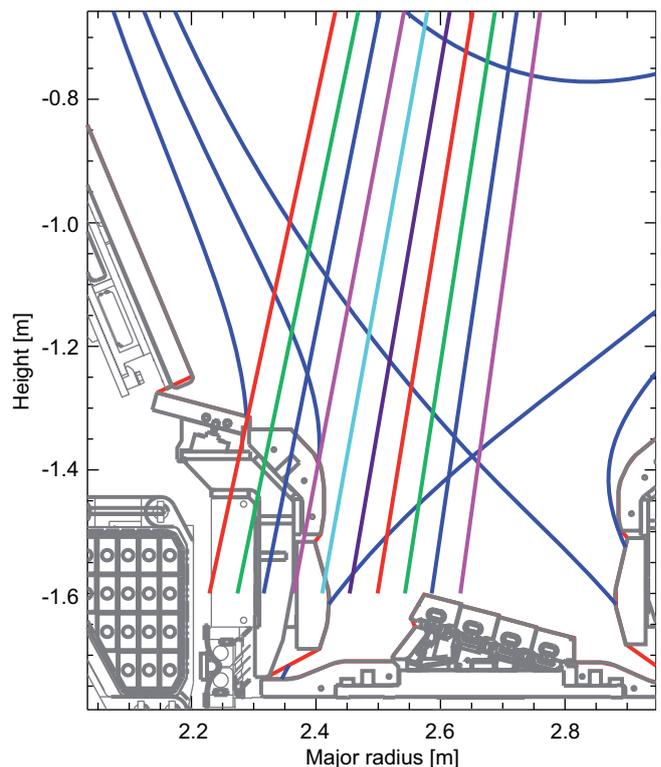
Figure 3: Geometry of the LOS measuring the $D\delta$ line in the JET HFS SOL for Stark broadening analysis.

hence radiating power in the SOL, reduces or suppresses the HFSHD front, depending on the amount of injected N_2, which was also observed in AUG. This further emphasizes the dependence of the HFSHD on the power in the SOL.

Seeding to Achieve Power Plant Like Divertor Conditions

The acceptable limit for erosion under impurity seeded conditions combined with the expected limit on power handling of the divertor components of future large scale fusion devices will demand their operation in the completely detached divertor regime. On JET stable discharges using N_2, Ne, Ar or a combination of N_2 and Ne lead to stable discharges with at the highest seeding levels the radiation peaked around the X-point. The maximum radiation achieved was independent of the heating power and below 75 % of the total heating power. ELMs are mitigated for seeding conditions when the discharge was marginally in H-mode. A stable completely detached inner and outer target was achieved for all seeding gases and the pedestal profile degradation was recovered by steeper profiles in the core at an H_{98y} of 0.7-0.75.

New Light through Old Windows: Improved Bolometer Analysis

Tomographic reconstructions are necessary to obtain the 2D distribution of the total radiation from bolometric measurements. The tomographic code, which is routinely used at ASDEX Upgrade, was tested for the JET bolometry system and is now available as a standard method for data analysis. The new code allows for a local definition of the anisotropy constraints used by the tomographic reconstruction. It also includes different boundary conditions than the existing code, for example no restriction on the radiation at the wall and no penalty of negative radiation are applied any more.
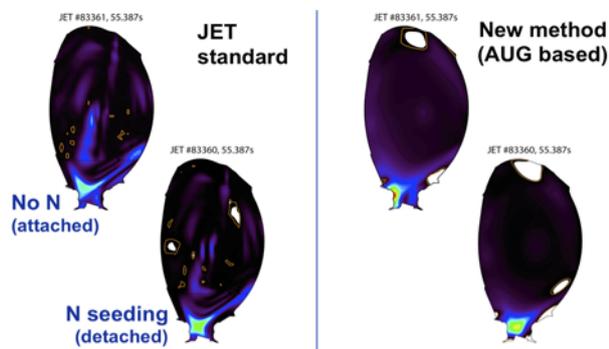
Figure 4: Comparison of the two codes for attached and detached conditions.

The new code shows significant difference to the existing JET method for the radiation distribution in the divertor region. This also impacts the conclusions drawn for different plasma scenarios, e.g. the detached or attached divertor operation (see figure 4). For the latter, radiation was previously falsely always assigned to the X-point region, while the new code could identify this as radiation at the inner target. This change also impacts the physics understanding of the power dissipation in the divertor.

Progress in the Characterization and Modelling of W Transport in the Core of JET-ILW Plasmas

The analysis and modelling activity of W transport in JET-ILW plasmas, which was started in 2013, has been continued and further developed during 2014. Theoretical models and related codes NEO and GKW, successfully applied to the simulation of W accumulation in a hybrid scenario JET-ILW discharge in 2013, have been extended in order to also include the effects of the temperature anisotropy of ion cyclotron resonance heated (ICRH) minority ions. This work has been performed in collaboration with General Atomics for the extension of the drift-kinetic code NEO. The upgraded codes have been applied to the modelling of various JET-ILW plasmas with and without ICRH, in collaboration with CCFE. In this collaborative modelling activity, at IPP we have focused on the validation of specific aspects of the theory of W transport in the presence of poloidal asymmetries of the W density. In usual plasma conditions in JET-ILW baseline scenario the combination of density and temperature gradients, as well as collisionality, of the main plasma where such that the predicted neoclassical convection changed sign from outward to inward over a critical portion of the confinement region when the poloidal asymmetry of the W density generated by centrifugal effects was taken into account.
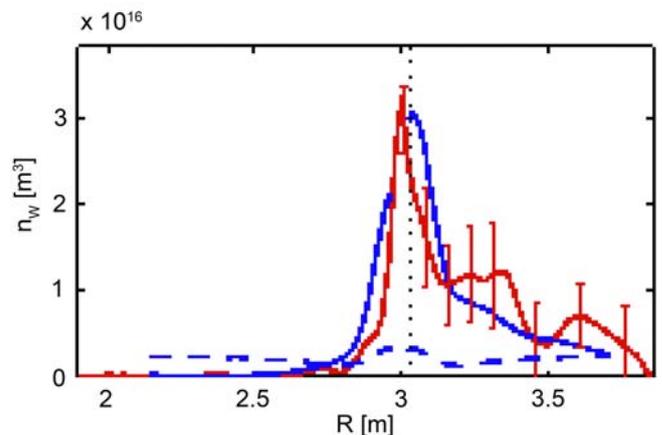
Figure 5: W density profiles as a function of the major radius as obtained by a 2D reconstruction of the W density based on the SXR diagnostic (red line with error bars), as well as obtained by the combination of NEO and GKW results including centrifugal effects (blue solid line) and by the combination of NEO and GKW results when centrifugal effects are neglected. The neglect of poloidal asymmetry of W density leads to a qualitatively wrong description of the W behaviour, predicting absence of W accumulation in conditions where W accumulation is actually taking place.

Thereby, as demonstrated in figure 5, the observed W accumulation was correctly predicted only by the theoretical model which properly includes the impact of poloidal asymmetries on the radial transport, and in particular the consequent relative reduction of the neoclassical temperature screening effect. This result provides first experimental validation of the impact of poloidal asymmetries on the radial transport of heavy impurities. In order to shed light on the transport mechanisms by which ICRH can limit or avoid core W accumulation, an important contribution to JET has been provided by dedicated modelling of the ICRH power densities and temperature anisotropy of the hydrogen minority ions with the full-wave code TORIC coupled to the Fokker-Planck solver SSFPQL. The TORIC/SSFPQL results are used as inputs of the NEO and GKW codes in order to investigate the impact of the presence of the ICRH minority on W. In close collaboration with colleagues at CCFE, we have found that the presence of the minority ions has two important direct effects on the W behavior. As theoretically expected and already observed, the temperature anisotropy of minority ions produces an additional source of poloidal asymmetry. Consistent with an analytical model, simulations show that this can reduce the neoclassical transport if weak high field side asymmetries of W density are achieved, as in the presence of LFS ICRH resonances. In addition, ICRH minority ions can also provide a significant contribution to the neoclassical temperature screening at the radial locations where their effective temperature is still sufficiently close to thermal and their temperature gradient is strong. The gained physical understanding, supported by a simulation activity which is found to reproduce the experimental observations of reconstructed W density in the presence of ICRH, allowed us to realize that the direct impact of ICRH on the W behavior is highly sensitive on the location of the ICRH resonance, and suggests an optimization of the heating set up in order to place the resonance very close to the magnetic axis from the low field side.

Material Erosion and Deposition in the JET Divertor during the First ITER-like Wall Campaign

During JET operation with all-carbon walls prior to 2010 (JET-C) massive re-deposition of carbon was observed in the whole inner divertor, parts of the outer divertor, and in remote divertor areas. Re-deposited layers with thicknesses of up to more than 500 µm were observed. The carbon originated most likely from the main chamber wall, where erosion by physical and chemical sputtering takes place. This massive carbon erosion and subsequent re-deposition was accompanied by a high retention of hydrogen isotopes trapped by co-deposition, resulting in the formation of hydrocarbon layers with high hydrogen concentrations.

With the JET ITER-like wall (ILW) project all plasma-facing carbon was removed and replaced by beryllium and tungsten. Erosion and deposition in the JET divertor were studied during the first JET ITER-like wall (JET-ILW) campaign 2011-2012 by using specially prepared divertor marker tiles, which were analysed before and after the campaign. The erosion/deposition pattern observed with the JET-ILW configuration shows partly drastic changes compared to the pattern observed with JET-C: The total material deposition in the divertor decreased by 1-2 orders of magnitude compared to the deposition of carbon in JET-C. The highest deposition with layer thicknesses of up to 30 µm is now observed on the upper and horizontal parts of the inner divertor. The deposits consist mainly of beryllium with 5-20 at.% of carbon and oxygen, respectively, and small amounts of Ni and W. The deposition of D, Be and C decreased considerably, in particular in the inner and outer divertor corners and in remote areas. At many of these locations deposition is now only observed in valleys of the rough tile surfaces. The vertical part of the inner divertor even turned from a former net deposition area into a net erosion area: Compared to JET-C this is a profound change of the inner divertor behaviour.

This decrease of material deposition in the divertor is probably caused by a decrease of net material erosion at the main chamber walls: At the inner wall of the main chamber a decrease of erosion by a factor of 5-10 was observed. The decreased material deposition is accompanied by a decrease of the total deuterium retention inside the JET vessel by a factor of about 20.

Gaussian Process Tomography

Further work was done for improvements on the applicability and routine usage for the divertor tomography for visible cameras, based on a new Bayesian method (GPT, Gaussian Process Tomography). The latter was developed first for Soft-X tomography and successfully transferred to such an entirely different diagnostic. It additionally did help with the calibration issues of the soft-x system by implementing a forward model and identifying a faulty Gaunt factor model. This work will continue during the 2015 campaign. For both systems IPP staff has also developed and installed software for routine analysis of those diagnostics.

Scientific Staff

Participation in Campaigns C33 – C34: M. Bernert, V. Bobkov, A. Chankin, S. Devaux, P. Drewelow, T. Eich, B. Geiger, J. Hobirk, K. Krieger, P. T. Lang, M. Munoz-Garcia, C. Maggi, S. Marsen, M. Oberkofler, S. Potzel, T. Pütterich, M. Reich, A. Scarabosio, M. Sertoli, B. Sieglin, J. Svensson, E. Viezzer, M. Wischmeier.
Tasks: C. Angioni, A. Chankin, D. P. Coster, K. Krieger, K. Schmid, M. Wischmeier.
IPH Department, PMU Culham: E. Belonohy, K. Gal-Hobirk.
JET Exploitation Unit: J. Boom, S. Devaux, D. Dodt, P. Drewelow, S. Marsen, S. Schmuck.
EUROfusion JET2: M. Mayer.

Stellarator Research

Wendelstein 7-X

Head: Prof. Thomas Klinger

1 Introduction

In 2014 the organisation of the project Wendelstein 7-X (see figure 1) underwent only a few minor changes. In summer 2013 the three design groups in the sub-division "Design and Configuration" were combined into the group "Design and Configuration". In the "Magnets and Cryostat" the department "Cryostat" was dissolved after the mechanical completion of this component.

Design and manufacturing of the different components of the basic device have been brought to a successful end, as described in chapters 2 to 4. Assembly of the stellarator device and the peripheral components have made great progress, as described in chapter 5. The accompanying efforts of the engineering subdivision (chapter 6) and the design and configuration control (chapter 7) are still indispensable. Heating systems (chapter 8) and diagnostics developments (chapter 9) have continued. The development of control systems and data acquisition and the preparation of commissioning are performed in the sub-division "Wendelstein 7-X Operations" (chapter 10).

1.1 Quality Management

The Quality Management (QM) department reports directly to the project director via the associate director coordination. The department organizes the QM system within the project

In March 2014 the last current leads were installed, thereby closing the cryostat. The installation of the in-vessel components continued until December 2014 and assembly of peripheral components (cabling, pipes and structures) is still ongoing. In April 2014 the commission of W7-X started, with the intermediate and cryostat vacuum systems. In July the cryostat was evacuated and the mechanical integrity confirmed. Size fact of 2014 the cryo system is being commissioned.

Wendelstein 7-X and supports the supervision of all external contractors. It has taken over responsibilities for quality assurance during the assembly and commissioning phase of Wendelstein 7-X. In November 2014 the QM system of Wendelstein 7-X has been recertified by the TÜV NORD CERT in a regular annual check.

1.2 Project Coordination

In preparation of the upcoming operation of Wendelstein 7-X during 2014 the project organization was adjusted accordingly by introducing a new subdivision called "Operation" and restructuring a number of departments. Amid these changes the subdivision "Project Co-ordination", too, was restructured and reduced to two remaining departments: Project Control (PC-PS) and Project Documentation (PC-DO) continuing to deal with various coordination activities for the project Wendelstein 7-X. The project control department (PC-PS) remains responsible for the financial planning and control of the investment expenditures and for the time schedule monitoring of all activities within the project. The department monitors and co-ordinates component delivery and supports the component responsible officers and VAD in the handling of external procurement contracts. PC-PS also monitors the assembly and commissioning schedules for the various components and subsystems.
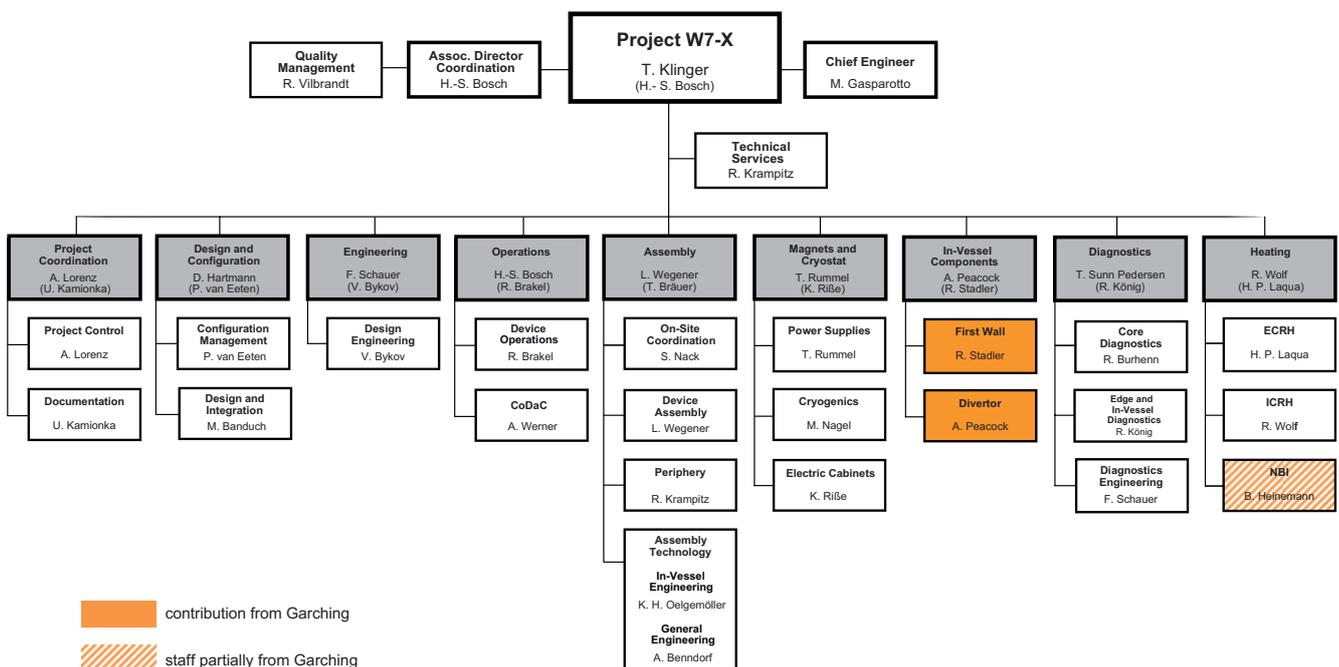

Figure 1: Organigramme of Wendelstein 7-X project as of 31.12.2014.

Furthermore, PC-PS deals with organizational aspects of the project and is responsible for the reporting to all external supervising bodies, especially the supervising body of the financing institutions (project council). The department is using a variety of planning and controlling tools to co-ordinate and to control the Wendelstein 7-X project progress. The Integrated Planning Tool (IPT) consisting of a MS Project based financial and time planning data base, remains the leading planning and controlling tool. The IPT is the routine tool for the responsible officers, their supervisors, but also for the financial reporting to both, the management and the supervising bodies. Preparations have started to upgrade this tool for the new financial framework in the period 2015-2019. In 2014 two other tools were developed and used extensively. First, a design task monitoring tool on MS Excel basis was created jointly with the central design office in order to monitor and co-ordinate the extremely time critical work packages for completion of the W7-X peripheral installations. Secondly, a MS Excel based so called "Monitoring matrix for OP1.1 system completion" was put into use to serve as early warning indicator and to monitor completeness and timely availability of all components and auxiliary systems for W7-X commissioning. The documentation department (PC-DO) is responsible for an independent check of all technical drawings and CAD-models, and for archiving all documents relevant to the project. An electronic documentation system (Agile-PLM) is used for archiving documents and CAD models. PC-DO also deals with the integration of CAD models created by industrial suppliers and other collaborators for some mostly peripheral components. All the models in the archive are imaged into a working directory of all Wendelstein 7-X models, the so-called "Wendelstein 7-X Assembly".

1.3 Schedule

The 2013 revised project schedule has introduced a first three-month phase of plasma operation (OP1.1) starting mid 2015, and this goal was closely pursued in 2014. All assembly milestones scheduled have been achieved. The milestones for completion of the cumbersome installation of in-vessel components and diagnostics were even achieved some weeks earlier than planned as the earlier implemented counter measures, finally showed their effect in the second half of 2014. Just as important was the successful achievement of project milestone M27 called "Completion of Cryostat", triggering the start of the cryostat evacuation phase, the first of six commissioning phases planned for Wendelstein 7-X. The challenge of maintaining the Wendelstein 7-X project schedule in 2014 consisted in managing two ambitious, concurrent schedules: a tight assembly schedule for completing the peripheral installations of supply components, heating systems and diagnostics and a technically complex commissioning schedule with many unknowns. Phase by phase, the details of the commissioning schedule were refined enabling PC-PS to focus on monitoring

critical interfaces between assembly and commissioning. In particular the interaction between in-vessel assembly works and in-vessel access required for commissioning activities had to be followed carefully. A number of potential schedule collisions were identified and mitigation or prevention measures were initiated. During the last months of the year the focus turned to preparation of the first Wendelstein 7-X cool down scheduled for January 2015. Current planning suggests that Wendelstein 7-X is still on track to go into operation in summer of 2015.

2 Magnets and Cryostat

2.1 Magnet System

Wendelstein 7-X has a superconducting magnet system consisting of 50 non-planar coils and 20 planar coils which provides the main magnetic stellarator field. All superconducting coils are finally assembled and placed in their final position in the machine. In addition to the superconducting coils, normal conducting coils were developed to fine tune the magnetic field and to increase the flexibility of the magnetic field configuration. The so called trim coils are mounted on the outer cryostat wall, one coil per each of the five Wendelstein 7-X modules. Due to construction space restrictions two different coil types were developed: four type. A coils and one coil of type B. The type A coil has a nearly rectangular shape with dimensions of 3.5 m × 3.3 m and 48 turns in 8 pancakes. The 110×151 mm^2 coil cross section is comparably compact. The type B coil with outer dimensions of 2.2 m × 2.8 m is smaller than the type A coil. To compensate the smaller size, the B coil has more turns (72 turns) and a higher operational current. In the frame of an international cooperation program of the US Department of Energy (DOE), the US laboratories Princeton Plasma Physics Laboratory (PPPL), Oak Ridge Laboratories (ORNL) and Los Alamos National Laboratories (LANL) received a three years grant to participate in the stellarator research at IPP. PPPL contributes in-kind the five trim coils with their power supplies. The coil delivery was completed with the arrival of the type B coil in April 2013. The assembly of the coils started already in 2013 and was finished in 2014. PPPL has designed and manufactured an Input/Output electronic enclosure (I/O box) which collects and pre-processes the coil sensor data. Ten temperature sensors, eight voltage signals and one flow monitor will be connected to each I/O box. Also these boxes were received and installed in 2014. The five power supplies are also part of the US in-kind contribution to Wendelstein 7-X, whereas the control system, the cooling water units and the grid transformer are part of the IPP. The power supplies are state of the art four quadrant converters with nominal ratings of 2200 Amps and 230 Volts. In 2014 all power supplies have been installed and tested up to the nominal current using dummy loads. The tests were made together with representatives of the manufacturer

Applied Power Systems, from Hicksville, N.Y., USA. The work of the central control system was finished in 2014, too. It allows the operation of the trim coil power supplies either from the main Wendelstein 7-X control room or from the local power supply control room. Finally the commissioning of the complete trim coil system was performed successfully in October and November 2014 with currents which are necessary for the Wendelstein 7-X operation phase OP1.1.

2.2 Cryostat

The plasma is surrounded by the plasma vessel which follows the plasma contour and constitutes the first ultra-high-vacuum barrier. The maximum outer diameter of the helically twisted plasma vessel is approximately 12 m; the minimum inner diameter is 8 m. The plasma vessel is made of the austenitic steel 1.4429 and has a wall thickness of 17 mm. The shape of the plasma vessel cross-section changes within each module from a triangular to a bean form and back again to a triangular form. The outer vessel is designed as a torus with an outer diameter of approximately 16 m. The internal diameter of the cross section is 4.4 m. It is made of austenitic steel 1.4429, the same material as the plasma vessel. The nominal wall thickness of the shell is 25 mm. The entire superconducting coil system is situated in the space between the plasma vessel and the outer vessel. Together with the ports, the two vessels create a cryostat keeping the magnet system at cryogenic temperature and constitute the boundary between the W7-X main device and the external environment. The outer vessel has 524 domes for ports, supply lines, access ports, instrumentation feed through and magnetic diagnostics. The 254 ports give access to the plasma vessel for diagnostics, plasma heating and supply lines. The vessels and the ports are equipped with a thermal insulation to protect the cryogenic components from the heat load of the warm environment. MAN Diesel & Turbo (MAN-DT), Germany, was responsible for the manufacturing and partly also for the assembly of the plasma vessel, the outer vessel and the thermal insulation.

2.2.1 Port Heating and Insulation

A total of 254 ports are used to evacuate the plasma vessel, for plasma diagnostics and heating, as well as for supply lines and sensor cables. The cross sections of the ports range between 100 mm circular up to 400×1000 mm^2 square; the ports are equipped with bellows to compensate deformations and displacements of the plasma vessel with respect to the outer vessel. All ports are surrounded by water pipes in the bellow-area to control their temperature. To generate ultra high vacuum conditions in the plasma vessel the ports, but also supply lines and parts of the plasma diagnostic equipment should be thermally insulated and heated during the baking phase of the plasma vessel. In addition to the heating by hot water, about 197 ports have to be insulated and 149 have to be heated additionally by electrical heaters. In 2014 it turned out that also

the interior or even the connected diagnostic equipment need to be insulated and partially heated. The design work of the insulation has been started and will run until March 2015. By end of 2014 the thermal insulation was designed for 110 ports and delivered for 75 ports. All necessary heating mats have been ordered. In total 380 heating mats will be controlled by five control cubicles and one operator desk integrated into the Wendelstein 7-X control room. The five cubicles were designed, procured and installed in the torus hall in 2014.

2.2.2 Exhaust Gas System

To avoid overpressure in the plasma vessel, safety valves with rupture discs and a piping system were designed to bring the gas outside the torus hall. The required piping was ordered, manufactured and handed over by MC to the assembly sub division. The installation of the system has started. The location for the condenser was changed. This required a modification of the design of some supports. The manufacturing of these parts is scheduled for January 2015. The outer vessel is equipped with pressure caps to avoid overpressure. To avoid human hazard by the gas, exhaust gas chimneys were designed and a technical specification for the procurement was created. The parts were manufactured and delivered to IPP. The installation has started and will be finished in January 2015.

2.2.3 Quench Gas Exhaust System

Helium gas is released by the cryo pipes into the quench pipe system in case of a malfunction. It is guided outside the cryostat via quench pipes or special safety lines. In case of a quench of the superconducting magnet system the expulsed helium gas is collected in a ring manifold outside the cryostat and then transported to the gas storage tanks. In the very unlikely event of a very huge mass flow rate, the helium gas cannot be transported to the gas storage tanks any more. In such a case the expulsed helium will be directly released into the torus hall. The quench gas system consists of the piping with supports (ring manifold, connecting piping), valve groups with safety valves and burst discs, and so called chimneys that guide the expulsed helium to the ceiling in the torus hall. Manufacturing of the quench gas system started in 2013 by KrioSystems in Wrocław. After production the pipe segments were tested according to the pressure vessel standard AD2000 by the manufacturer and then delivered to IPP. Visual inspection, x-ray testing and leak testing was part of the tests. The last components were delivered in the second quarter of 2014. The pipe segments were adjusted, aligned, and finally welded in the torus hall. The onsite welding seams were visually inspected and x-ray testing was done. Each onsite welding seam was also leak tested. Finally, the pipes were thermally insulated with Armaflex insulation. The installation of the pipes on site was done till end of 2014. The last work on the thermal insulation will be finished in February 2015.

2.2.4 Thermal Insulation

The thermal insulation of the Wendelstein 7-X cryostat is fixed at the warm cryostat surfaces (plasma and outer vessel and ports) and protects the cold components against heat loads from the warm surfaces. The thermal insulation consists of a multi-layer insulation (MLI) and a thermal shield. The shield is cooled by helium gas flowing in pipes attached to the shields via copper strips or braids. The mounting of the thermal insulation was finished. Four current lead domes in M2 and M3 were thermally insulated. The very tight space inside and around domes required a sophisticated insulation procedure that was tightly connected with the dome assembly. The last four domes in M2 and M3 were successfully insulated in the first and second quarter of 2014.

2.3 Current Leads

The current leads (CL) are the electrical connection between the cold, superconducting magnet system inside the cryostat and the power supplies outside of the cryostat, operated at room temperature. The main challenge in Wendelstein 7-X is the so-called upside-down orientation of the CL, i.e. the cold end is on top and the warm end is on bottom. In total 14 current leads are needed. The production and the tests were performed by the Karlsruhe Institute of Technology (KIT). In each test campaign, two current leads were connected to form an electrical circuit. After a thorough check under room temperature, the whole test arrangement is cooled down to cryogenic temperature with a rate of 10 Kelvin per hour. After the hydraulic and thermal stabilization, the CLs are loaded several times up to the maximum current of 18.2 kA. The test of a loss-of-Helium-flow accident has demonstrated the ability to de-energize the Wendelstein 7-X magnet system slowly before a quench would occur. The safety margin of the superconducting parts was tested by induced quenches, too. The margin between the operating conditions and the achieved quench temperature meets all requirements. The necessary helium mass flow rates to operate the current leads meet the expectations. After the test under cryogenic conditions, a high voltage test under different environmental pressures is performed. By the end of 2013 all current leads had been finally tested under cryogenic conditions and delivered to IPP. In spring 2014 all current leads were placed at their final position in the Wendelstein 7-X cryostat. Helium which returns from the current lead is fed in separate lines. This lines run from the 14 current leads to the valve rack of the helium refrigerator in the second basement of the torus hall. The installation of the piping was finished in the 3rd quarter of 2014. The piping consists of 14 electrical breaks made of GFRP that electrically isolate the current leads form the ground potential of the piping. The piping was isolated to the environment using shrink tubes starting from the electrical breaks up to the current leads themselves. The electrical breaks were designed and manufactured at ASIPP (Hefei, China).

All these isolators were cooled down to LN2 temperature several times and leak tested at about 80 K. The high voltage tests at 13 kV were passed successfully. In a final assembly steps the temperature and voltage sensor cables and the quench detection cables have been installed. All installation work with respect to the current leads was finished in April 2014. Afterwards the pumping of the isolation vacuum has been started in preparation of the commissioning.

3 Supply Systems

3.1 Helium Refrigerator

The helium refrigerator produces and distributes cold helium required to cool the cold components of Wendelstein 7-X. After the successful acceptance tests of the helium refrigerator the cryo plant was shut down in the first half of 2013 and brought into a safe condition to wait for restart. In 2014 the test boxes that were needed for cryo plant testing were removed. Instead the connection piping was installed from the magnet valve box in the torus hall to Wendelstein 7-X cryostat. The control program of the cryo plant was adjusted to the modified system. The restart of the refrigerator was done in the second half of 2014. Air vented boxes were evacuated again. Step by step the warm cryo plant systems were restarted. The cooling water system, the oil pumps, the compressor systems, and the dryer were put into operation step by step. A first training program for the available operators was carried for the warm system. The start of the compressors, the connection of the dryer and the dryer regeneration were trained. In parallel the commissioning documents were compiled and discussed in the project. The commissioning and acceptance template was prepared and approved for the preparation work and for the cool down activities. The preparation documents contain the following major steps: – Cleaning of the piping inside the cryostat from debris like dust, metal cuts, swarf, etc. by sudden expansion of nitrogen gas. – Finishing the remaining leak tests at connected piping outside the cryostat (at safety valves, burst disc, etc.) – Purging of piping and filling with helium (connection from cryo plant to Wendelstein 7-X, piping inside Wendelstein 7-X, quench gas piping) – Circulation of helium gas from the cryo plant and cleaning of nitrogen impurities with the cold adsorber of cryo plant – Hydraulic checks of different cooling circuits Cleaning of the piping from debris and finishing the leak testing was done in autumn. The circulation of helium gas within the helium piping of the cryostat has been started and will be finalized in January 2015.

3.2 Magnet Power Supply

The superconducting magnet system is divided into seven electrical circuits, five circuits with ten non-planar coils of one type each and two circuits with ten planar coils of one type each. Seven independent power supplies provide direct currents of up to 20 kA at voltages of up to 30 V. Fast and reliable discharge

of the superconducting magnets in case of quenching or severe faults is realised by fast circuit switches which short-circuit the coils and dump the magnetic energy into resistors. The whole system was installed and finally tested already in 2005. In order to prepare the system for the operation phase of Wendelstein 7-X, several tests campaigns have been made also in 2014. In addition the aluminium bus bars which connect the power supplies with the Wendelstein 7-X machine have been installed and insulated. The final connection to the current leads will be made during the commissioning in 2015. The energizing and de-energizing process of the Wendelstein 7-X super conducting magnet system could stress the electrical insulation of the coils, and in the far future lead to cracks in the insulation. This can result in a fault to ground. In case of a fast discharge both events together would lead to a doubled voltage between coil and ground, which should be avoided. To prevent such undesirable occasions, the insulation of the superconducting magnet system shall be monitored by regular high voltage tests with very low energy. The main point is that the check should also be performed after substantial changes of the current which consequently means that the high voltage test shall also be performed when the magnets are energized. The main idea of such an "In-Service-Test" is to induce a high voltage directly into the grounding point of the system and measure the leak current. The measured leak current can then be used to determine any changes in the quality of the insulation. In 2014 the last two of the five units of the In-Service-Test system have been manufactured, tested and installed in the power supply system of the superconducting magnet system. The control system to integrate the system into the overall control system of the magnets has been designed, produced and installed. Functional tests were successfully completed, also with the superconducting coils connected. The system is ready for operation during the commissioning of the magnet system.

3.3 Quench Detection System

The quench detection system of Wendelstein 7-X will permanently check the differential voltages across the double layers of the coils, all sectors of the bus system and the superconducting part of the current leads. The system has to reliably detect millivolt signals in a broadband noise environment. It must operate also at high voltages during a rapid shutdown of the magnets. In total 486 quench detection units are necessary. The quench detection units will be put into ten so-called subsystems. One subsystem contains up to 64 quench detection units and is equipped with an internal AC/DC power supply combined with an uninterruptible power supply to secure the independent operation of the subsystem. For control and data acquisition an internal controller is installed to evaluate and to transmit the quench signals to the magnet safety system and to allow for a full remote control. The fabrication of all subsystems has been finished, and in a steady state test over several months, the faultless operation has been demonstrated.

The signals of the subsystems will be transferred to the magnet protection systems via so-called interface racks. These interfaces combine the signals from the quench detection units and the signals from the monitoring system which checks permanently the proper data transmission and the function of all components. The quench detection system is being controlled by a host control system which allows fully automatic as well as manual operation. The human machine interface has been realized via WinCC. The host control system has been completely manufactured and successfully tested in 2014. The programming of the human machine interface has been finished, too. Starting in autumn the subsystems have been transported from the test bench to the final place in the torus hall. The cabling work has been started. By the end of 2014 the connections between the Quench detection ports at the cryostat and the Quench detection units in the subsystems has been finished in nine of the ten subsystems.

3.4 Machine Instrumentation

The machine instrumentation is a collection of several sensor systems connected to five electronic cubicles for data evaluation and transfer into the Wendelstein 7-X data archive. The following sensor systems are part of the machine instrumentation project: mechanical instrumentation of the magnet system consisting mainly of strain gages and contact sensors on coils, support structures and the plasma vessel; thermocouples on the TDU and NBI beam dump; temperature sensors on the plasma vessel, cryo-shields and ports, PV and cryoleg position monitoring system. In 2014 the work was concentrated to finalise the design work, to manufacture the components for the PV position monitoring system and all control racks, to assemble and route the instrumentation cables and finally to bring the system into operation. The strain gauges on the plasma vessel as the first machine instrumentation system worked well during the first cryostat evacuation mid of 2014. All other systems were brought step by step into operation until end of 2014.

3.5 Engineering and Procurement of Electronic Cubicles

About 30 Wendelstein 7-X projects, mostly diagnostics, announced their need for electrical engineering support and procurement of about 100 electronic cubicles. The cubicles are needed for diagnostic control tasks, for sensor data evaluation, image processing or control of gas inlet valves. Two electrical engineers have been working since October 2013 in a group with the aim to do the electrical engineering, to develop an IPP electrical engineering standard in the projects and finally to procure the designed cubicles in industry. The electrical engineering was accomplished for 38 cubicles e.g. for radiation safety project, for neutron counter, Neutral Beam Injection heating and the diagnostic projects ECE, Video diagnostic, H-alpha and single channel interferometer. 33 cubicles were already manufactured in 2014 under responsibility of this group and handed over to the responsible officers.

4 In-vessel Components

In 2014 the finalisation of the installation of the in-vessel components (IVCs) necessary for operational phase OP1.1 took place. In addition 2014 saw: the completion of the contract with Plansee for the 890 high heat flux (HHF) target elements, the completion of the basic design of the HHF divertor and the completion of the manufacture of the target modules TM9h, TM8h and TM7h. The closure of the contract with Plansee was a particular highlight on the path to a steady state divertor as it had lasted 11 years and now all of the elements are available for the completion of the divertor. In parallel the detailed design, manufacture and testing of the remaining IVCs necessary for the full water cooled phase continued. The IVCs consist of the divertor components (target, baffles, and toroidal closure plates), plasma vessel protection (panels and heat shields), control coils, cryo-pumps, port protections and special port liners for the different heating systems together with the complex system of cooling water supply lines. The high heat flux (HHF) divertor, port protection liners and the cryo-pumps are the main components that still need to be completed.

4.1 Target Elements

For long pulse, high power capability, actively water cooled elements are needed for the HHF divertor. In Wendelstein 7-X these were realised by the production of 890 HHF divertor target elements by Plansee. The elements consist of 8 mm thick carbon fibre reinforced composite (CFC) tiles joined to a water-cooled CuCrZr heat sink. The elements are specified to withstand steady state power fluxes of up to 10 MW/m^2 and to operate with 12 MW/m^2 for a reduced number of cycles. The final batches of elements were delivered in the middle of 2014 and after extensive testing in IPP the contract with Plansee was closed in December 2014. This brought to an end a contract that had been running since 2003. The incoming tests on the newly delivered components showed that they were within the agreed specification. Testing of some of these elements in the GLADIS HHF facility was also performed (see section plasma facing materials and components). For the type 5S target elements of the vertical target 25 elements were so tested. None of the elements showed a problem with the critical joint between CFC and CuCrZr but one element developed a vacuum leak. The leak was originally observed in post GLADIS tests but after careful examination of the recorded vacuum signals in GALDIS it was established that the leak occurred around about pulse 80 of the 100 pulse test programme. The leak is probably caused by a combination of factors. These are believed to be intrinsic issues with the CuCrZr, porosity in the e-beam joint between the CuCrZr and the CFC tiles and a design issue resulting in a small gap between the water cooling circuit and a gap between tiles. These factors and the thermo-mechanical loading of the element in GLADIS had opened up the leak. Different repair methods were proposed and investigated.

One method was identified as being relatively simple and was used on the element that had leaked in GLADIS. This element was then tested in GLADIS for 500 cycles at the location of the leak and found to be sound. The factors that were believed to be responsible for the leak are present in all of the 5S elements so it was decided by the project to pro-phylactically apply the repair technique to all of the 300 5S elements to reinforce them against leaks. The method used for the reinforcement was qualified with the assistance of Plansee.
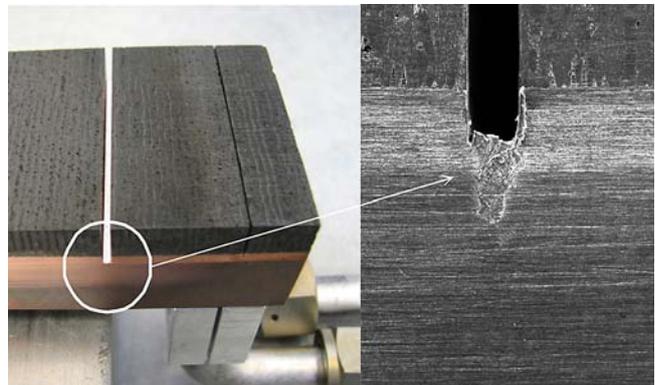
Figure 2: The reinforced element.

For the series reinforcement the activities are being performed in the IPP workshops ITZ and at an external e-beam welding company PTR. ITZ has started the slit machining and preparations are underway for the e-beam welding at PTR. Figure 2 shows the slit machined in the target element through which the e-beam welding is performed.

4.2 Target Modules

The Wendelstein 7-X divertor consists of three main HHF areas: the vertical and main horizontal targets and the high iota tail. These targets are built from target modules; sets of mechanically and hydraulically connected target elements (varying from 6 to 12) forming the physical entities to be installed in Wendelstein 7-X. The high iota tail has three modules:

Figure 3: The plasma facing surface of the three high iota tail modules.

TM7h, TM8h and TM9h; in 2014 the manufacturing of these modules was completed. Figure 3 shows these modules as they are mounted in the divertor.

The vertical target area, also with three modules: TM1v, TM2v and TM3v, was designed in 2013. 2014 saw the production of the manufacturing drawings and the design of the water connections from the modules to the plug-ins and the start of the manufacture of the modules frames, water manifolds and module pipework. The assembly of the vertical modules is likely to be delayed awaiting the reinforcement of the 5S elements. The design of the main horizontal target, with four modules, TMh1 to TMh4 was undertaken in 2014 and approved by the project in a design review. Finalisation of the detailed design and the detailed diagnostic integration were also undertaken. Manufacturing preparation, i.e. production of manufacturing drawings for the 3D machined elements and for the support and module frames also began in 2014. The manufacturing of the target modules is mainly performed in ITZ. Two components are manufactured externally: the water manifolds and the 3D target element machining. For the identification of the company to manufacture the water manifolds for the vertical target a qualification piece from two external companies was requested due to the high tolerance requirements for this welded component. Figure 4 shows the test piece supplied by Dockweiler for the TM3v module. Dockweiler were selected to manufacture the remaining 59 manifolds of the vertical modules and started the work in 2014. Delivery is expected in early 2015.

Figure 4: Water manifold of the TM3v.

4.3 Test Divertor Unit (TDU)

The interim solution for the Divertor to be used during OP1.2 is the TDU. This has the same geometry as the later to be installed HHF divertor but uses inertially cooled graphite tiles instead of water cooled HHF elements. The TDU is already in Greifswald and parts of it (the module support frames, which also acts as a support and conduit for thermocouple wiring) were installed into the machine in 2014.

4.4 Baffle Modules

The manufacture of the main baffle modules was completed in 2013 and final testing successfully performed in 2014. Due to the closure of some plasma vessel ports six new baffle modules were also required. For OP1.2 this closure was temporarily achieved with extended graphite tiles on the existing modules. Due to the introduction of OP1.1 time was available to manu-

facture these six modules before OP1.2. Further investigation, however, revealed that instead of replacing the modules it was possible to adapt the existing modules saving significant resources. This adaption began in 2014 and should be completed by the middle of 2015. The installation in the Wendelstein 7-X machine of part the Rogowski coils showed some deviation to the original geometry. This has the consequence that two further baffle modules need to be adapted. This will take place in parallel to the adaption of the other six modules.

4.5 Wall and Port Protection

Apart from the divertor components the IVCs consist of double walled stainless steel panels (covering approx 70 m² of the plasma vessel) and heat shields (covering approx 50 m²) consisting of water cooled copper plates clad with graphite tiles (similar to the baffles). The completion of the installation of these components (without graphite tiles) was performed in 2014. For OP1.1 local graphite tiles were procured and mounted on the heat shields to form a limiter for the plasma. During steady state full power plasma operation, the inner surfaces of the ports need to be protected in the same way as the inner surfaces of the plasma vessel. Particularly sensitive are the welds between the plasma vessel and the ports. In 2014 work continued to define the exact requirements of these components, to clarify the interfaces with the diagnostic and heating systems (the main users of the ports) and to identify those technologies that could met the identified requirements. For two ports with ECRH systems it was found that the port could be protected by extending the normal port protection. The manufacture of four modified panels is underway. At the end of 2014 a tender was also in preparation to procure demonstration port liner components which will demonstrate the practicality of the presently designed components, taking into account the large spread of port sizes and shapes. During the design of the vertical modules of the HHF divertor, it became clear that some previously designed and procured components surrounding the modules would have to be changed. The pumping gap panels, designed to protect the plasma vessel between the main horizontal and vertical targets, were one such component and at the end of 2014 an outline design for these panel is available. After further checks on manufacture and installation compatibility the panels should start the procurement process in 2015.

4.6 Cryo-pumps

The in-vessel cryo-pumps, located behind the main horizontal HHF divertor target modules, have been designed and partly manufactured. Since the cryo-pumps will not be installed until the just prior to OP2 manufacturing was stopped in 2008. In 2014 the activities associated with the cryopumps were restarted. Modification to the design has taken place to replace vespel components with ceramic materials to reduce the effects of ECRH and to take into account assembly developments and methodologies that have been developed since 2008.

In particular a fully welded design has been developed as well as modified transport and testing frames. The design of the vacuum feed-throughs has also been restarted aiming for procurement in 2015. The parts already prepared for the cryopumps have been in storage for a number of years and due to recent restrictions on the acceptance of welding discolouration it is necessary to clean the existing parts before further assembly of the components. The most successful of a number of methods investigated was high temperature vacuum annealing. Initial concerns that the heat treatment would cause thermal distortion were checked with a suitable test piece and found not to occur. Figure 5 shows some of the parts after cleaning.

Figure 5: Cryopump parts after high temperature heat treatment.

Figure 6: Water baffles after coating with an ECRH absorbent layer.

19 cryo pump water baffles were coated during 2014 with an ECRH absorbent coating. The coating, performed by plasma spray at the University of Stuttgart had previously been qualified by the coating of one water baffle in 2012 and its testing

in Mistral, an ECRH test facility in IPP Greifswald. Some these coated water baffles are shown in figure 6.

4.7 Control Coils
The control coils are supplied by power supplies which are able to provide direct currents of up to 2500 A and alternating currents up to 625 A with frequencies between 1 and 20 Hertz in parallel. In 2014 the test operation of ten power supplies were continued by using dummy loads. The path for the cables from the power supplies to the coils was confirmed, the cable trays have been designed, procured and installed. Per power supply module eight cables with a cross section of 630 mm^2 are being installed. The final connection to the coils will be made with flexible copper braids in March 2015.

4.8 Plug-ins
The in-vessel plug-ins are used to deliver water and, in some cases, diagnostic cabling from the outside of the machine to the inside of the vessel through the supply ports. These plug-ins consist of a set of tubes welded onto a flange through which water is fed to and removed from the IVCs. All 80 plug-ins have been installed in Wendelstein 7-X during 2014. Dependant on whether or not water will flow through the plug-ins during OP1.1 or OP1.2 adaptations of the plug-ins have been performed to ensure that the vacuum integrity of the plasma vessel is maintained.

4.9 Water Supply Lines inside the Plasma Vessel
The cooling supply lines of the in-vessel components run from the plug-ins, via a complicated system of manifolds and pipes, to the various components via flanges. In total 308 cooling circuits are foreseen. In OP1.2 26 cooling circuits will be filled with water. The panels and the heat shields will have their pipework completely welded together before OP1.1 but will not be fully filled with water until OP2. The panel circuits will be filled with inert gas to provide some thermal conduction inside the panels to avoid hot spots.

5 Assembly

In 2014 the qualification and procurement of assembly equipment mainly for the installation of in-vessel components was finalized. Two qualifications were accomplished at the end of the year that are important with regard to the later installation of the TDU: easily installable steps that enable access to the interior of the plasma vessel without damaging the already installed components and, as the second achievement, a method for the installation of the divertor-closure that is compatible with the complex shape of the plasma vessel and with the bad accessibility within the vessel. In November, the assembly of the in-vessel components was brought to completion (figure 7). That comprises also the assembly of 10 heavy control-coils together with their complex plug-ins.

Figure 7: The in-vessel setup for OP1.1. Temporary assembly equipment like the rail system, steps, cables, hoses is removed.

In April the last pair of current leads was completed, the latest weld at the cryostat was made and the vessel closed. The pendulum supports underneath the plasma vessel were activated enabling a vessel movement within the given limits (e.g. through thermal expansion). All remaining auxiliary supports were removed which have been used during the ten years lasting assembly phase. A complex and massive support-structure was completed in the centre of the machine that serves for carrying water-pipes, cable-trays and diagnostics and provides man-access to this machine-area. The work-platform in the experimental hall was fully erected. The mechanical installation of the ECRH and NBI heating system was completed and 15 diagnostic-systems were aligned and fastened to ports or platforms. The inter-vacuum system (provides vacuum for double seals at ports and domes) and the cryo-vacuum system were completed and commissioned. They are already running permanently. The installation of pipes (cooling water, gas, helium transfer line, quench-gas line, exhaust gas), bus-bars (magnet system, control coils and trim coils) and cables (about 5000 for machine instrumentation, diagnostics, heating systems and vacuum systems) in the torus hall was a big challenge because of the pure amount of work within the given time and space. The needed preparation and documentation

for these work packages was unexpectedly large. As usual, last minute changes in design, interfaces and components have permanently enlarged the scope of these peripheral works. They will be accomplished only in spring 2015 – however, without jeopardizing the parallel running commissioning tasks. The global direction of the magnetic field has been successfully checked at room temperature with adequate coil current. The robustness of the insulation of the magnet system was successfully tested under Paschen conditions in the evacuated cryostat at room temperature. The assembly plan was updated and shows now the formal assembly-end in spring 2015. However, that does hardly influence the overall progress of the project since the commissioning of Wendelstein 7-X in parallel has already commenced. A first version of the planning of the upgrade phases towards OP1.2 and OP2 was worked out. The assembly processes, responsibilities and staffing were multiply reorganized during this year according to the frequently and noticeably changing focus of tasks. Personnel for the installation of cables and pipes were massively increased whereas the personnel for complex mechanical works have been reduced. At the end of the year the structure of the assembly organization was modified such that it becomes compatible with the future demands of the operation. Over the year 2014 the number of employees in the assembly division changed from 160 in the beginning to about 130 at the end; most of them are coming from external partners.

5.1 Basic Machine

The last 5 massive auxiliary supports underneath the machine foundation were removed and the setting-behaviour of the machine was comprehensively monitored. Diagonal reinforcements not foreseen in the original design but integrated as an additional safety measure became decisive to limit the machine-deformations to the admissible limit of ~1,5 mm. Another challenge was the activation of the 15 pendulum supports where the plasma vessel (PV) rests on and, simultaneously, the activation of 5 horizontal supports. Horizontal supports keep the PV in lateral position and ensure its centric expansion e.g. due to thermal loads. In addition both, horizontal and pendulum supports enable an initial position-adjustment of the PV within several millimetres in all three axes. During the activation it was revealed that one pendulum was damaged at its spherical bearing. Fortunately, this pendulum is still sufficiently functioning to continue the commissioning and operation of the machine. A repair will be performed later during upgrade phases of the machine. When the above supports took over the dead weight and the lateral forces, the PV deformed slightly at the supported areas. Local values <2 mm were measured. Consequently, the reference marks at the inner wall in the near vicinity of these areas of the PV changed their position and the geometrical reference system needed for the installation of the in-vessel components was disturbed. At this time about 50 % of these components were already installed.

Detailed measurements and analyses were made in terms of the entire reference system, comprising several hundreds of reference marks. It turned out that the global impact onto the installation accuracy was only some tenths of a millimetre since the majority of marks remained unchanged and noticeably changed marks were skipped from the reference system.

5.2 In-vessel Components

In summer 2014 the assembly of in-vessel components (KiP) became stable since nearly all first-of-a-kind work was finished at this time (including last design changes). Series effects and learning curves became fully effective – six months later than planned. Some of the installed plug-ins connecting in-vessel components or in-vessel diagnostics with components outside the machine are not longer dismountable since their dismantling path is blocked now through massive structure components. Experience could already be gathered with the long-term stability of installed components. Heat shields and panels are fastened to the vessel wall via adjustable spring-loaded bearings. Spring-loaded bearings shall ensure a movement through thermal expansion but be robust enough to withstand normal touching or butting during the ongoing assembly work in the narrow plasma vessel. However, it turned out that movements of the assembly personnel and occasional abutting do change the components' position at least twice as much as the given installation tolerances of 1,5 mm. That should not be an issue for heat shields and panels with their moderate thermal loads. But for baffles which are installed in conjunction with the divertor units these bearings must be improved noticeably. A development program is started towards the upgrade for OP1.2 and OP2. Already installed divertor support-frames are more robust and do not show comparable weaknesses. At the end of the KiP assembly a temporary rail system was assembled in the plasma vessel enabling the circulation of a neutron source. It serves the neutron-counter calibration that is performed in the beginning of 2015.

5.3 Periphery

The expenditure for installing pipes and cables had to be doubled during 2014. The detailed layout in the crowded torus hall, additional interface conditions and late design changes were the root cause for that. The number of pipe-welds rose noticeably as well as the associated inspections and x-ray tests. Sometimes already finalized pipes or cables had to be dismantled and newly installed to sidestep clashes with future components. About 5000 cables with average 5 strands per cable are to be installed. That corresponds to about 250 km length and about 50000 strand-ends which have to be connected to cubicles, connection boxes, plugs, etc. In addition hoses for compressed air and fibre optics have to be supplemented. The layout of cable trays is carried out centrally in the design division. Every cable is listed in a cable data base predefining its start and end-point. This data base contains in addition the cable type, its shielding, the maximum length etc.

With these data a detailed installation scheme is made listing exactly the number of tray-sections where the cable must run along. Also the sequence of the cable installation is checked and predefined, if necessary. The expectable as-built cable-length is added to this scheme (enabling a simple cross-check on-site, whether the cable has correctly been routed) and also the wiring-scheme of the strands. With that information the detailed work-flow on-site is planned and the work-progress is monitored on a daily basis. Six engineers are used to provide this preparation work on time and continuously. The complex pipe-work remains time critical. The pipes are being bent in-house by means of computer controlled bending machines. The needed CAD data are provided by the design division or by external companies. Too many data failures led to noticeable extra work. The installation of thermal insulation on the cooling pipes is very time consuming. That is caused through the complex curved routing, the multi-layer design and the bad accessibility. The insulation work is one of the latest work-packages and will last until April 2015.

5.4 Vacuum Technology

Leak-tests accompanying the ongoing assembly were carried out as in the years before. The last Paschen-test of the entire magnet system in the responsibility of the vacuum team was successfully performed in the evacuated cryostat (10E-4 mbar) at room temperature. The completion of the inter-vacuum system and the cryostat vacuum was achieved in the middle of the year with massive assistance from the entire assembly team. During the intensively prepared commissioning of these systems about 20 leaks at the cryostat were identified. Workmanship failures, design imperfections but also leaky components as feed-throughs and one port bellow were the root causes. All leaks were repaired in the course of the year. A special challenge was the setup of the control-equipment for the vacuum systems since its complexity was underestimated and there was and is for that a bottleneck in the availability of skilled personnel. The setup of the vacuum system for the plasma vessel continued as planned (figure 8). Also here challenges are existing with the control equipment. A source of delay is the commenced installation of the gas-inlet system. The procurement contracts were started tardily due to the late availability of the manufacturing design. Increased capacity at the supplier's side shall compensate for that. The associated waste-gas treatment-system will be installed in conjunction with later upgrade phases. The glow discharge system was completed and connected to the power supplies. Altogether, assembly has reached the planned progress in 2014. The cable and pipe installation might be subject to smaller schedule risks. The co-operation with external partners who provide skilled and well-trained technicians and engineers for the realisation of the assembly work on Wendelstein 7-X worked flexible, stabile and smoothly. The conversion of the assembly division towards a future operation organisation has started.

Figure 8: One double vacuum pump-unit out of five at the upper side of the machine; the chimney to the right is the redundancy to the safety-valves that protect the cryostat from over-pressure.

6 Engineering

The sub-division Engineering (EN) provided engineering support to the Wendelstein 7-X project. In 2014 the sub-division comprised the department Design Engineering (EN-DE) only.

6.1 Mechanical, Thermo-mechanical and Thermo-hydraulic Analyses

Considerable analysis work was performed for assembly with respect to new or changed procedures, as well as for in-vessel components, diagnostics and periphery. In the second half of the year emphasis was shifted to preparation of and participation in commissioning like determination of operational limits, prediction of expected signals from the mechanical instrumentation, and cooperation with CoDaC on common interfaces. First successful benchmarking of the cryostat global model with stress and deformation measurement data during evacuation and venting of the cryostat was already possible. Main results of the department's analysis activities were successfully presented at international conferences and published in scientific journals.

6.1.1 Superconducting Magnet System

For analyses of the complex magnet system comprising 70 superconducting coils and their support structure finite element (FE) model trees created with ANSYS and ABAQUS are used. The structure contains many non-linear elements like sliding contact supports with gaps from zero to several millimeters, flanges with possibilities to open, and elements with allowed plastification. The ANSYS and ABAQUS models were further updated and refined. These improvements were necessary for the 72° versions mainly to get more reliable predictions of the machine instrumentation signals. For the 360° versions the updates were needed to derive asymmetric coil deformations due to statistically distributed

variations of gap sizes and friction factors at sliding contacts, differences in bolt preloads, structure material properties throughout the torus, and also due to forces caused by interactions between main magnet and trim coil fields. Very important applications of both 360° models were further analyses of module assembly asymmetries and the thorough investigation – with corresponding benchmarking – of consequences of the asymmetric trim coil fields and forces on the cryo-leg loads (figure 9). Because of its criticality, the analyses of the GRP parts of the cryo-legs were extended to evaluate the behavior under cyclic load conditions. Main result is that there are no restrictions due to the higher than original design cyclic loads, but the safety margins are smaller and more careful monitoring and analysis during MS operation is required. The investigation of special load conditions is still ongoing.
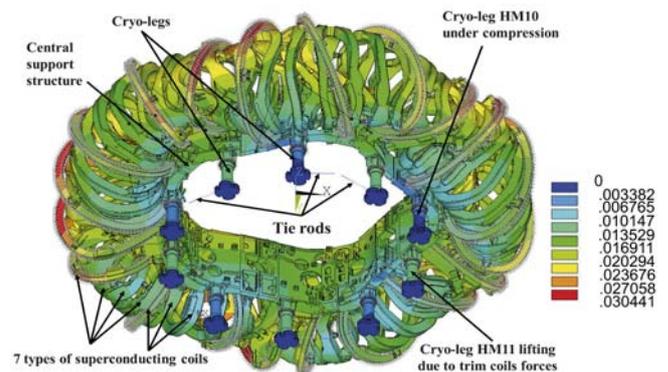
Figure 9: ANSYS 360° global coil system model. Deformation due to EM forces and (asymmetric) raising of the machine base interface by 1 mm at the cryo-leg of half-module HM10 only. Colour code scale in m.

Studies on crack propagation in the weld zone of the lateral support elements (LSE) between the non-planar coils were extended in collaboration with Prof. Citarella, Univ. Salerno, Italy. Mixed cycles for two adjacent cracks were analysed using the code DBEM (figure 10). The previously estimated allowed cycle number does not change under these conditions and remains above the number of specified operation cycles.

Figure 10: DBEM model for adjacent cracks near the lateral support element weld (Univ. Salerno, Italy).

Many activities of EN were specifically devoted to commissioning of different W7-X systems. In order to prepare the commissioning of the MS and its mechanical instrumentation, a detailed post-processing of the Saclay coil acceptance test results and comparison with FE calculations was performed. Generally good agreement between experimental and analysis results were found. The non-planar coils of type 1 (NPC1) showed the most significant deviations. In order to clarify those discrepancies, the NPC1 FE model was refined, and the issue is being analyzed in cooperation with colleagues from ASIPP, Hefei. Another task in context with commissioning was the specification of the coil currents for the initial operation of the individual coil groups. In these commissioning modes the forces and deformations are different, particularly concerning the directions, as compared to the simultaneous operation of the whole magnet system. The commissioning currents of the single NPC1 and NPC5 groups have to be reduced since with full current, corresponding to a plasma axis field of 2.5 T of the complete magnet system, the design values would be exceeded. The evaluation of potential collisions between the magnet and cryostat system due to this special coil operation mode is ongoing.

6.1.2 Cryostat and Periphery

The new cryostat global model (GMCS v3) was updated with vacuum pipes on the pumping ports, and heavily used throughout the year accompanying assembly and commissioning. One important application was the definition of pre-stresses of the diagonal support struts for the machine base cantilevers when removing their temporary supports (figure 11).

support AFF40 slipped out of its recess. The consequences were evaluated and it was found that the given situation can be left as it is for the time being. However, this pendulum force needs to be monitored during cryostat venting and evacuation to make sure that it always stays compressive. In future, under less time pressure, the spherical bearing head can be fed into its cup again which is expected to be a somewhat tedious procedure. Extended analyses were performed in support of dimensioning the heaters for baking the ports and KIP - plug-ins. Other mechanical investigations on components directly related to the cryostat were design calculations for exhaust pipes and their supports, and for forces of such pipes on the heavy duty structure (HDS) in the centre of the torus. During commissioning of the cryostat vacuum, evacuation and venting was supervised via the machine instrumentation and other measurements. The experimental results were evaluated and compared with FE simulations (figure 11). The agreement was generally quite well, and the few deviations could be explained. This work is still ongoing. Other involved linear and non-linear analyses were and are still being performed with an ABAQUS FE model of a rectangular port bellows to assess the consequences of the unexpected buckling of convolutions during evacuation of the cryostat. One aim of this work was to find out the buckling reason in view of the fact that the ports were already tested under vacuum conditions without any abnormal result. Likely causes which can be concluded from the FE analysis are distortions and stresses introduced by the bellows flange to port tube weld on the side of the weaker flange (figure 12).

Figure 11: Cryostat global model: Deformation (in mm) of the cryostat during evacuation. The diagonal support struts are indicated by blue lines.

Figure 12: ABAQUS model of AEE10 bellows. Top: Bellows stresses (in MPa) near the flange, local buckling due to residual stresses of the weld between flange and port tube. Bottom: Local model of the first convolution with imposed deformation according to a scan after evacuation. Buckling can clearly be seen.

Another assembly-related analysis using the GMCS was the preparation of reposition of the plasma vessel (PV) from the sliding bearings on fixed tables to the permanent pendulum supports and the verification of related deformations and loads. During these activities the upper spherical bearings of the pendulum

Another local model of the buckled convolution zone with input from scans of that area after several evacuation and venting cycles allows to simulate the deformations during each cycle and to predict the maximally allowed cycle number. This way it can be decided whether a repair is necessary in future.

Another investigation in support of assembly was, for instance, the analysis of the attachment of the NBI copper cone including some assembly devices. Calculations were also performed to evaluate and allow a simpler bolt preload procedure to facilitate assembly of the ECRH port flanges, and to confirm the structural integrity of ladders and torus hall platform supports.

6.1.3 In-vessel Components (KIPs)

Many analyses on the huge number of in-vessel components are still necessary and will also be needed in future during commissioning and operation. Part of the calculations is dealing with non-conformities resulting from production concerning quality and geometry, or from positioning of these sensitive components which are mostly exposed to high heat loads from the plasma. Small changes of the as-built vs. the design parameters as well as of the predicted plasma energy and particle exhaust distribution can result in large load increases to values well above the allowables. Another part of the work was devoted to evaluation of repair actions and corresponding tests. Extended calculations were also done in support of the limiter design, and for design and test of the TDU scraper element which is being built cooperatively by ORNL, PPPL, and IPP (figure 13).
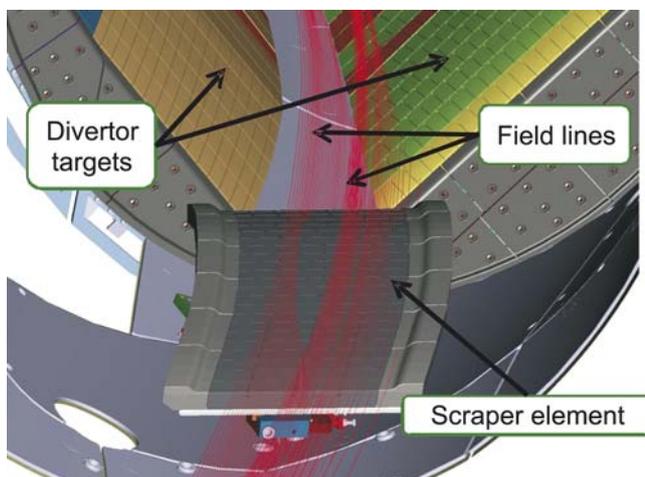

Figure 13: TDU scraper element, toroidally in front of a divertor unit.

Examples of the mentioned works are the evaluation of control coil positioning inaccuracies, the evaluation of small damages of baffle and divertor tiles and, within the scope of a master thesis, of the formation of gaps and steps between baffle and heat shield components as a result of thermo-mechanical strains. In addition, small cracks in the brazing between cooling tubes and heat sinks of baffles were discovered, and crack analysis activities were started together with the In-vessel Components subdivision and Prof. Citarella, Univ. Salerno, Italy. Another work concerning KIPs was the analysis of possible causes and repair proposals of a leakage in a divertor target element of type 5s, and the bench-marking of GLADIS tests of such elements.

Finally, thermo-mechanical analyses on high heat flux (HHF) divertor components are still being performed, and detailed FE models of such divertor modules are being prepared (in cooperation with ASIPP, Hefei) in order to be ready for evaluation of future experimental results.

6.1.4 Diagnostics

Also for diagnostics a number of calculations were carried out like mechanical analyses of the neutron counter supports, of sealing capabilities of CF flanges under mechanical loads, of the integrity of front-end shutters and other components under high cooling water pressure, and of reduced bolt preloads due to stud welding problems of the flux surface measurement manipulator. Thermal-hydraulic studies were done on helium beam diagnostic components, and of the visual diagnostics front shutter including benchmarking with the test. For plasma vessel baking also many port flange areas and protruding diagnostic components need to be heated. Calculations were performed in order to specify the necessary heating powers and heater positions for such components.

6.2 Electromagnetic Analyses

Considerable work was devoted to electromagnetic analyses, particularly concerning eddy currents and related Lorentz forces. Examples are electromagnetic loads on diagnostic components, on port plug-ins, and also on the heavy duty structure in the centre of the torus. A more extended and involved project was the creation of a plasma vessel model for the calculation of electromagnetic forces on the plasma vessel due to eddy currents induced by coil system emergency discharges and plasma current decays. This model served also as input for further refined calculations by LTC, Italy, which are still ongoing (figure 14).
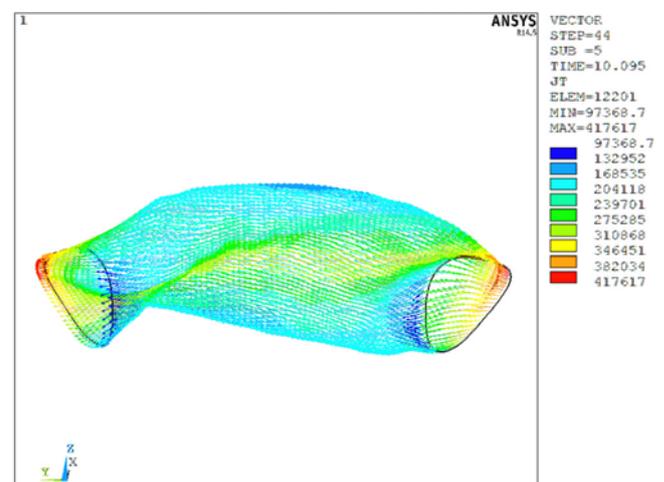

Figure 14: Maximal eddy current densities in the PV wall due to a 100 kA toroidal plasma current decay with the time constant $\tau = 140$ ms (in A/m^2). The results are from the first investigation phase without port holes (LTC comp., Italy).

EM analyses activities were also concerned with calculations of inductive coil couplings between the saddle, trim, control, and superconducting coil systems, as well as with the definition of positive current directions. Other tasks were the determination of Maxwell forces and stray fields as well as evaluation of their consequences. Examples are the estimation of magnetic forces on ferromagnetic objects, the field at the PV wall due to the trim coils, flux density vectors at the neutral gas manometer positions, and EM impacts during commissioning of the trim coils. In order to estimate heat loads due to ECRH stray radiation on in-vessel components, a ray tracing code was developed and applied.

6.3 Field Error Analyses

The estimation of field errors due to manufacturing and assembly tolerances was continuously performed since the start of coil production. These activities allowed correction of errors of a manufacturing or assembly step by definition of new positioning coordinates for the next step. The last correction step was the positioning of the modules on the machine base according to coordinates derived from the error analysis of all previous steps. This way the corresponding field errors could be kept very low. In the reporting period this work was extended to evaluate the consequences of statistical distributions of variations of MS structure parameters like gap sizes and friction factors at sliding contacts, bolt preloads, and Young's moduli. Also the influence of the asymmetrical trim coil forces on the stellarator symmetry of the main field was investigated. The result of these investigations is that the field errors due to all these influences can be easily compensated by the trim coils. Other causes of field errors are ferromagnetic materials, particularly within the PV, which could not and cannot be avoided with reasonable effort. Examples of such permeable components are TDU frame bolts, Ni adapters at the joints between divertor heat sinks and the corresponding cooling pipes, bearing pins at the control coils, bolts of wall panel supports, hose shielding meshworks within ports, different diagnostic components, etc. Examples of relatively large permeable components outside the cryostat which were evaluated with respect to field disturbances are pipe bends and mass flow meters of the water cooling system, and components of the fixed fire-fighting installation. The impact of each permeable component is stored in a database to keep track of the overall disturbance of the EM field.

6.4 Preparation of Commissioning

Specific activities of EN devoted to Wendelstein 7-X commissioning were specifications of mechanical measurements and determination of expected instrumentation signals. This was done for the evacuation and venting of the cryostat, and for the future cool-down and excitation of the magnet system including the trim coils. The strategy for interpretation of the machine instrumentation signals was worked out in detail.

The values for normal operation (green light), for near critical conditions (yellow light: warning), and for allowable limits (red light: stop operation) are being specified. A MATLAB tool for comparison of load cases and to realize the traffic light strategy has partly been developed. Much work has also been put into the development of a MATLAB program to read out the measurement data from the CODAC archive and to evaluate and visualize them. This program is in use already for cryostat evacuation and venting and is being extended for the other upcoming commissioning activities. For the critical cryo-leg movement measurements during magnet cool-down a back-up instrumentation system was developed, together with the Quality Management department, and is being installed for confirmation of the displacements. A procedure to correct cryo-leg movements in case of unexpected behaviour was specified.

6.5 Scraper Element

In addition to the above-mentioned calculations for the design of the TDU scraper element (figure 13) – which is being built cooperatively by ORNL, PPPL and IPP – also other support for this project was provided. This concerns the participation in creating the functional specification as well as in management tasks, and the preparation, determination and specification of heat flux tests of graphite tiles of the scraper element. Change notes were prepared and issued for KIP components at the mechanical interface to the scraper element, and for its instrumentation.

7 Design & Configuration

The subdivision "Design & Configuration" provides the configuration management of Wendelstein 7-X of all its components and design solutions, fabrications drawings and the integration of all components in the torus hall and adjacent areas.

7.1 Design and Integration
7.1.1 Work Organisation

Early in the year 2014 the formerly three design departments within the sub-division Design and Configuration were dismantled and the new department "design and integration" was created. This was done in response to the decreasing design work load in the plasma vessel and for in-port diagnostics and the increasing work load for peripheral components, e.g. cable trays, water pipes, various support structures. In general, the design challenge of these components derives mostly from the need for proper integration into the torus hall and less from meeting complicated functional requirements. Therefore all design personnel were trained in applying the tools developed for the former department Design in the Torus Hall and were organized in only one department to ease internal communication and maintaining the same standards for all design activities. This department is organized with the work flow of a design office: customers issue a design task to the department head.

The department head estimates the total work of the task and assigns it to a designer. The designer details the work together with the customer, performs the task, has it checked internally and delivers the specified output to the customer. The priority, class and status of all design tasks are documented and daily updated in a design task master table. The reduced number of designers and the increasing number of design activities that were considered essential for the first operational phase OP 1.1 requires diligent and transparent setting of the processing sequence. To that purpose each design task is given a priority number by the sub-division Project Coordination that is determined mostly on the purported impact that the task has on the commissioning schedule. The assignment and completion of these tasks is done according to this priority. In particular urgent cases, projects design team were created where one designer was supported by additional designers. The daily updating and the close collaboration between the departments allowed to quickly respond to changing priorities or new design tasks.
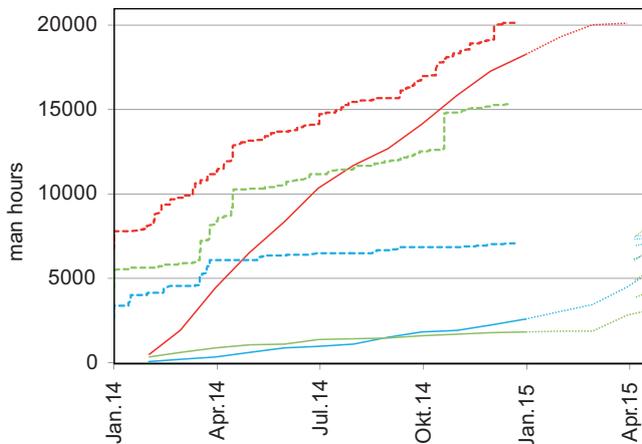

Figure 15: Development of the total amount of design work in 2014 essential for the first operational phase (red), for group B diagnostics (blue), for remaining topics (green). Dashed – work input, solid work done, dotted – work planned.

Figure 15 illustrates the increase of new design tasks essential for OP 1.1 during 2014 (red dashed line) even though at the end of 2013 all responsible officers had been asked to provide the department with a complete list of open design tasks. By the anticipated time of completion of these design tasks in March 2015 the total amount of provided design work will be at least about 2.5 times of what was estimated in January 2014. The work spent on the design tasks is shown as a solid line, the prediction beyond the status date January 2015 of this figure is shown as a dotted line. Similarly the development of the design tasks for the group B diagnostics and for later operational phases are shown in blue and green, resp. The setting of priorities of the design tasks solely on the basis of the commissioning schedule bears various

design quality risks. Firstly, even though the department strives to have an up-to-date digital mock-up of the torus hall and its surrounding, this mock-up was never complete. Due to the urgency of other tasks, observed discrepancies trigger new design tasks that are – in most cases – given a low priority. Secondly, the urgency of the known tasks and the incomplete view of further tasks and requirements prevent a thorough top-down approach that optimizes the usage of the available space and the needs for accessibility and maintenance. Within the project it was decided to take that risk for OP 1.1 in order to meet the mile stones. Close collaboration with the sub-division Assembly was implemented to efficiently deal with installation conflicts that are observed only at the time of installation. These conflicts can have numerous causes, e.g. the incomplete or erroneous digital mock-up, installation of other components outside of their specified tolerance space, fabrication deviations, poor accessibility. Severe conflicts are solved with stop-cards, minor conflicts are solved by jointly developing a solution proposal, fast check by a designer, photo documentation of the final installation and adaptation of the digital mock-up. The frequency of these conflicts occupies one designer for about 25 % of his time. In 2014 for the first time a few designers also took over some responsibilities of project engineers for the fire extinguishing system, the extension of the cold water cooling system for rack and diagnostic cooling, and the installation of an air cooling system for electronic racks. This was done in order to accelerate the preliminary design process of those projects since they have in common a large number of interfaces and thus a high demand on integration and that they require a large number of prefabricated industrial parts. In the past the progress of similar projects, e.g. cooling water routing in the torus hall, were hampered by delays win providing the design departments with all relevant information and thus deterioration of the digital mock-up. In the long run, once the urgency of the design activities subsides, it is planned to apply these extended responsibilities also to other tasks.

7.1.2 Design Tools

The back bone for all design activities is the global digital mock-up of the torus hall and the adjacent areas. This mock-up is updated daily and mirrored to all users. With the help of the well established support by a computer scientist with deep insight in CATIA further automation and adaptation tools were implemented to still be able to efficiently handle the complete digital mock-up for visualization, conflict control and design even though this involves more than 40000 CAD models. Figure 16 shows the complete view of the torus hall with all projects for the operational phase 1.2. Semi-transparent volumes indicate assembly and maintenance areas. The high integration aspect of many of the design tasks in the torus hall involves the generation of assembly documents.
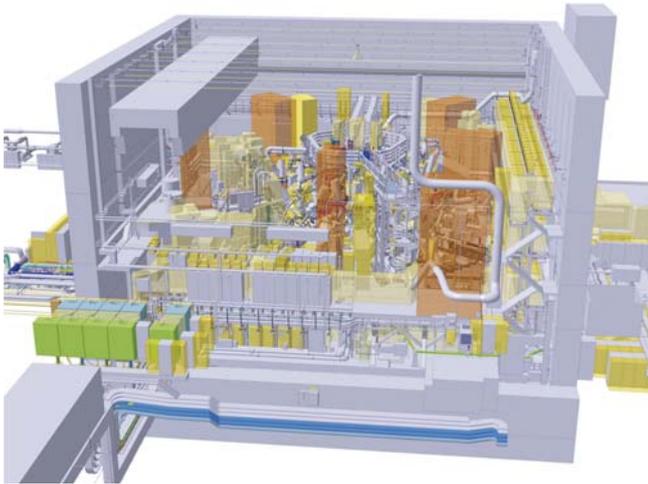
Figure 16: CAD view of the torus hall with all components for the first operational phases.

In the past these assembly documents were painstakingly created by pasting snapshots of the CATIA view on the computer screen with local distance measurements into a bulky document. Now assembly documents for design tasks in the torus hall often consist of the generated CAD models together with relevant neighboring CAD models that are stored in a format that can be visualized by a comfortable, free-of-charge available CAD model viewer. This facilitates maximum flexibility in the assembly process by – in principle – providing all information without limitation to a few selected dimensions. This tool has reduced the required work for generating the assembly documents by typically about 80 % and the results have found wide-spread acceptance in Assembly. Fabrication documents are generated for most of the small diameter (<45 mm) pipes for the gas supply, cooling water etc. since these pipes are constructed in-house. Since bending is done with a fully automated pipe bending device, tools were developed to partition the CAD pipe routing into appropriate pipe sections, check whether the required bending can be performed by the bending device, modify the design, if required, and provide the bending information in the readily readable format. The tools were further optimized to eliminate all tedious and error-prone tasks. The historical incompleteness and inaccuracies of the digital mock-up in particular w.r.t. components that were installed by civil engineering in the past are overcome by using scan data of these areas. To that purpose an external scanning company provided a detailed point data set of all surfaces in the torus hall. This was found very useful in eliminating design iterations and reducing the number of on-site inspections. Figure 17 shows an example of the ceiling of the peripheral diagnostic area where the known CAD models are shown with the juxtaposed point data set derived from the scanning. The deviations of the CAD model from reality and the missing cables and cable trays are clearly visible.
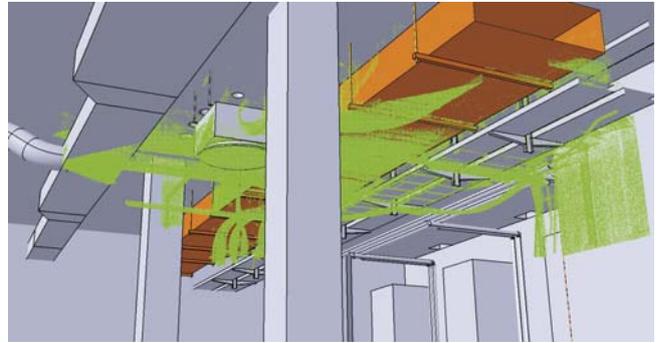

Figure 17: Scan data in the diagnostic area juxtaposed with available CAD data.

7.1.3 Design Examples

In the following some selected design tasks of 2014 are being presented. The total amount of invested design hours was about 23500. About half of that was spent on the design of cable tray routing, the plasma vessel vacuum system, the continuous cold water cooling circuit, the fire extinguishing system, general support structures, the one-channel interferometer, the electron cyclotron emission diagnostic and power cable routing of the trim coils. The fire protection system is a particular example of a system that involved design tasks with a high degree of integration activities.
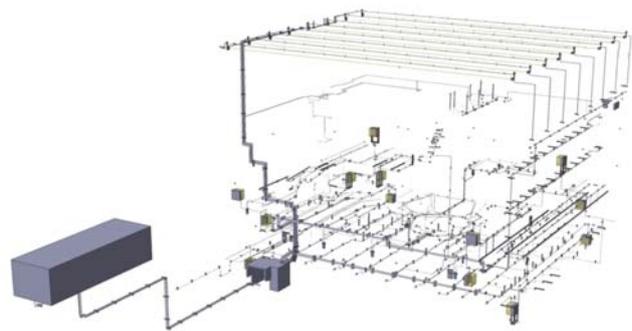

Figure 18: CAD view of the fire extinguishing system in the torus hall.

The final system is shown in figure 18. Due to the safety aspect of this system and the expert knowledge required for the functional layout, external companies were involved in the planning and in the installation. The design interface between these two companies was taken care of by the design department, by developing the concept design and further detailing it until the fabrication documents could be issued. The cold water cooling supply in the torus hall and adjacent areas is another example for a set of design tasks that require a large amount of integration. Also here, a designer took over the responsibility to guide the process from collecting and documenting the detailed requirements up to providing Assembly with the design, the fabrication and assembly documents and hardware.

While the department Configuration Management set out to specify and properly document the needs, the conceptual design started. On that basis the procurement was triggered. As the design progressed, the number of designers was increased to deal with the required detailing. Needed adaptations in the procurement were swiftly implemented.

7.2 Configuration Management

Configuration management for Wendelstein 7-X is done by the department DC-CM. It develops and follows upon the procedures and documents that provide system identification, interface documentation, change request and deviation documentation. The complete device Wendelstein 7-X with all its various components is planned to be completely described for all the various operational phases by a set of so-called "loose leave binders" as a reminiscence of binders that contained sheets with all relevant and up-to-date documentation for past experimental devices. Nowadays they are electronically stored. They describe major components of the machine or certain parameters, definitions or conventions. Usually they contain references to other documents on the original specification, project specification, changes and deviations. Since expert knowledge is needed to write some of the documents they are only as complete as the experts have been able to spend time on their completion. In 2014 the focus was put on the completion of concise loose leave binders that are of particular relevance for the first operational phase. In general, the interfaces between major components, i.e. between components that are described via a loose leave document, are documented and controlled via a set of interface documents that address all facets of these interfaces. The have been further completed with focus on those of relevance for the first operational phase. Intended or unintended deviations of agreed-upon specifications during the design, production and assembly phase are technically discussed and agreed upon with all parties involved and then communicated within the project via change request documents and non-conformity reports, resp. Both set of documents are being filed and completed according to procedures that have been developed together with the department Quality Management. In 2014, the change request procedure has been further refined to also list in detail the various steps needed in order to implement a proposed change. With this change the implementation of changes and its final documentation could be accelerated. Change requests of the past had not been written in such a detailed manner. Therefore there are still some approved, implemented but not fully documented change requests. In 2014, the final documentation check of a number of change notes was limited to sample checks in case of uncritical change requests, to be able to complete the back-log by the start of the first operational phase. Currently 1252 change requests are registered in the database, 87.1 % of the change requests have been accepted, 0.4 % are in the decision process and 12.5 % have either been rejected, withdrawn or became obsolete due to a revision. 93 % of the accepted change requests are implemented and completely documented. The department provided and maintained documents on the usage of ports for the various diagnostics, on the usage of blind flanges, on the number of openings in the torus hall, on the cooling water supply needed by the different users for the various phases of operation, on the chits raised during design reviews (20 design reviews were held in 2014), on the rationales, decisions and actions agreed upon during meetings of the configuration control board (20 topics in 2014).

8 Heating

8.1 Project Microwave Heating for Wendelstein 7-X (PMW)

The PMW project is approaching its end in 2015. Within more than 15 years the ECRH-system has been developed and built as a joint project by the KIT, IPP and IGVP University Stuttgart. The 10 MW cw installation in Greifswald is nearly completed. Even thought the delivery of two gyrotrons is scheduled to 2015, the existing ECRH-system for Wendelstein 7-X is operable and will support the heating requirements in the first Wendelstein 7-X operation phase completely. The microwave power, which is generated by the gyrotrons, is transmitted into the plasma by a quasi-optical transmission line and versatile in-vessel launchers. The four front-steering launchers provide the required launch flexibility for the different heating scenarios in Wendelstein 7-X for up to 12 beams. In addition, [two remote steering launchers (RSL's) supported by the 'Bundesministerium für Bildung und Forschung' (BMBF) in a separate project and located in special ports, enable more sophisticated scenarios in poloidal planes with almost zero-magnetic field gradient. Wendelstein 7-X acts also as a full performance (1 MW, cw) test-bed for this new DEMO-relevant launcher concept.

8.1.1 The Wendelstein 7-X Gyrotrons (KIT/IPP)

Two gyrotrons have been delivered by the THALES company in 2014. The TH1507 SN2i gyrotron successfully passed the final acceptance test in Greifswald in May 2014. The TH1507 SN7 gyrotron was successfully tested at the KIT in October and is presently undergoing its final acceptance test in Greifswald. Five of the seven existing gyrotrons are foreseen for the first Wendelstein 7-X operation.

8.1.2 Transmission Line and Control System (IGVP/IPP)

The Installation of the ECRH-transmission line is almost completed. The multi-beam wave guide system could be successfully aligned with two beams for module 1 and 5 respectively. The retro-reflector units were installed into the ECRH-towers close to the ECRH-ports. They allow to test the performance of the transmission-line with full power over its almost full length. The power measurement system at the M14 mirror, which is the last mirror before the plasma vessel,

has been manufactured at the IGVP and installed on the ECRH-tower. The towers have been equipped with the control system of the transmission line and the data acquisition ECRH-protective diagnostics. The motor drive system of the front steering launcher has been commissioned. The cooling media supply of the launcher and the mirrors has been installed. Most of the mirrors are remotely controlled now. The local ECRH control system has been connected to the Wendelstein 7-X control system. A first synchronized subordinated operation of two gyrotrons was be demonstrated.

8.1.3 ECRH-protective Diagnostic

The ECRH-protective diagnostic should provide safe and reliable ECRH-operation. It is completely installed now. Five sniffer probes, which measure the ECRH stray radiation, are located in each of the five Wendelstein 7-X modules.
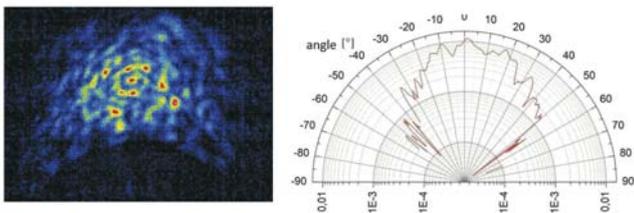

Figure 19: Antenna pattern generated by a Schröder diffusor. Left: Thermal image on a screen in front of the antenna. Right: The analysed angular distribution of the antenna pattern.

Its detection system is equipped with a so called Schroeder diffusor, which provides a wide angle isotropic antenna sensitivity as shown in figure 19. Thermo elements have been brazed-on at the mostly stray radiation exposed port bellows to monitor their temperature during plasma operation. Each ECRH-Launcher is equipped with a near-infrared video camera inside an immersion tube. Even though the field of view was limited by the narrow installation conditions inside the launcher, a complete heat shield observation in front of the launcher could be achieved. For this, the viewing field was divided into a direct field of view and another that observes the lower part of the heat shield in module 1 by a mirror in front of the camera optics (the configuration is reversed in module 5). The camera control system is being developed in collaboration between IPP and CEA-Cadarache in the frame of the EUROfusion-WPS1. The complete equipped and water cooled immersion tube has successfully passed the microwave stray radiation test at the Mistral test chamber. The observation region inside the plasma vessel could be already proved (see figure 20). The video system also allows the full size view on the in-board limiters in modules 1 and 5 during the first Wendelstein 7-X operation phase. Selected tiles in the heat shield are provided with microwave pick-up holes, which are connected with waveguides that bring the signal to detectors outside the plasma vessel. This so called ECA-diagnostic will measure the ECRH-absorption, the beam position and its polarisation. The dedicated 128 amplifiers made by the IGVP have been installed on ECA-ports close to the detectors.
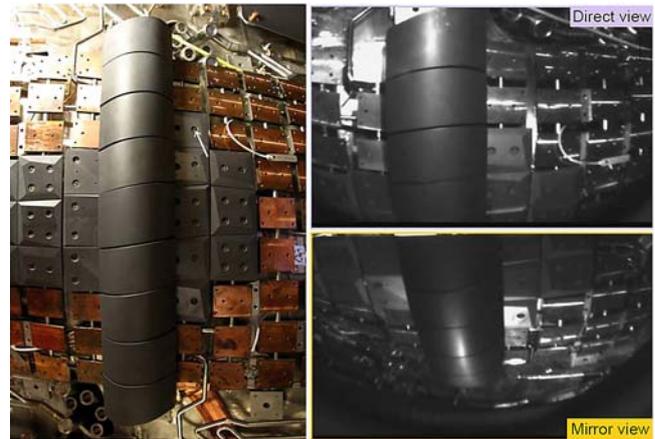
Figure 20: Video observation of the ECRH heat shield and the in-board limiter. Left: Picture of ECRH-heat shield and the in-board limiter inside the plasma vessel. Right: View of the NIR-video camera in the immersion tube with the direct view at the top and the mirror view at the bottom.

8.1.4 In-vessel Components (IPP/IGVP)

The four huge front-steering launchers slipped collision-free into their narrow ports with a clearance of only several mm on their precisely aligned assembly rail system as shown in figure 21.
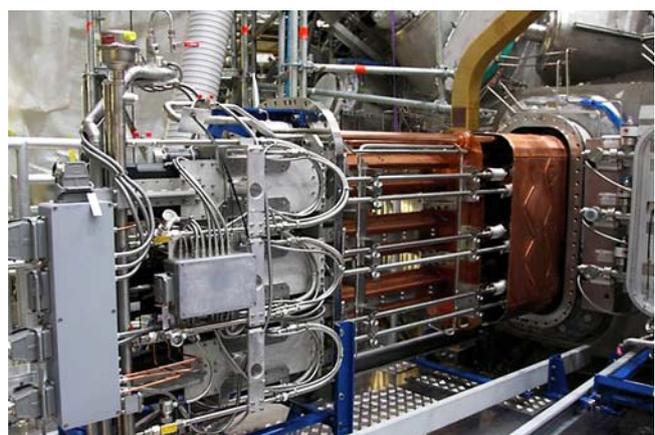

Figure 21: ECRH-launcher on rail system during slip-in into its W7-X port.

Vacuum tightness of their Helicoflex flange connections were achieved. The media connection and commissioning of the launcher are on-going. The launching geometry of the front steering mirrors has been validated inside the plasma vessel. The launching angles were be measured in the real geometry. Opposite to the launcher on the inner wall heat shield, specially shaped reflector tiles have been designed in order to reflect the non-absorbed part of the ECRH-beam a second time through

the plasma center. The reflectors made out of the molybdenum alloy TZM will improve the heating efficiency in case of incomplete single pass absorption ECRH scenarios. These tiles are equipped with a holographic reflection grating and are presently manufactured by the IGVP-Stuttgart.

8.1.5 The Remote Steering Launcher for Wendelstein 7-X

('BMBF-Verbundvorhaben 03FUS0017A', 'Fortgeschrittene Mikrowellen-Heizsysteme für die kontrollierte Kernfusion') Most of the present day high power ECRH-systems (e.g. AUG, Wendelstein 7-X, ITER) are equipped with Front Steering Launchers (FSLs). Movable mirrors inside the vacuum vessel allow steering of the individual rf-beams for on/off axis heating and current drive in a wide toroidal and poloidal angular range. Such FSLs are very flexible and support different plasma heating and current drive scenarios such as X-mode, O-mode, Electron-Bernstein-Wave Heating. FSLs need, however, a sophisticated high precision mirror drive mechanism inside the vacuum vessel with flexible cooling lines and are bulky structures. Figure 22 shows the FSL for Wendelstein 7-X. Three front mirrors are stacked in one port and handle three rf-beams with 1 MW cw power each.
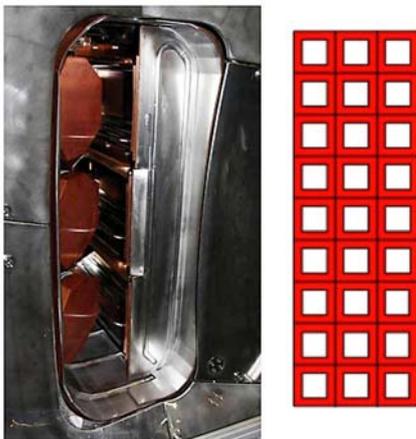

Figure 22: The 3-MW front steering launcher of Wendelstein 7-X (left). The same port area would allow insertion of a 3×9 waveguide array with remote steering for 27 MW rf-power transmission. A scaled sketch is shown on the right.

Although the design is very compact, the antenna occupies a port cross-section area of typically 0.35 m^2. For next step fusion devices such as DEMO with burning plasmas facing the antenna structure, RAMI aspects become of crucial importance and FSLs may no longer be compatible with the demands for robust operation in the hostile radioactive environment. The Remote Steering Launcher (RSL)-concept offers an alternative approach, which is based on multi-mode interference in a square waveguide leading to imaging effects: For a proper length of the waveguide, which matches the Talbot condition, a microwave beam, which is fed at the input of the waveguide with some inclination with respect to the waveguide axis will exit the waveguide

under the same, but opposite angle. The steering mechanism for the microwave beam can then be located remotely outside the vacuum vessel and the cooling structure can bed imbedded in the waveguide wall. The optimization of RSLs with respect to the specific applications, such as high power ECRH and CD, low power diagnostics and/or combination of both, thus attracts increasing interest. The area of the plasma facing RSL front end is small and movable parts and steering mechanisms are avoided inside the vacuum vessel. The rf-power density of RSL-arrays for ECRH is typically 100 MW/m^2 as compared to front steering launchers with about 10-20 MW/m^2. Only small ports are required therefore to supply future fusion devices with the necessary microwave heating power. As sketched in figure 22, an array of 27 RSL-waveguides with 1 MW transmitted power each would fit into one Wendelstein 7-X ECRH port, which houses the FSL with 3 MW port-through power only. The obvious drawback of RSLs is a reduced steering range as compared to front steering launchers and a somewhat larger beam size. An R&D project was thus established in 2012 with preferential support by the BMBF to investigate, develop, manufacture and operate an RSL with extended steering range, low loss, and 1 MW, cw transmission capability. Waveguide-bends, which are mandatory for dogleg structures embedded in radioactive shields of DEMO-type devices, and gaps for integration of fast shutters are part of the design to demonstrate the reactor compatibility. The project combines the expertise of two research laboratories, IGVP and IPP, respectively, and two industrial partners, NTG Neue Technologien GmbH und Co KG and Galvano-T GmbH. The development of waveguide structures with extended steering range and low loss was successfully terminated at IGVP by mid 2014.
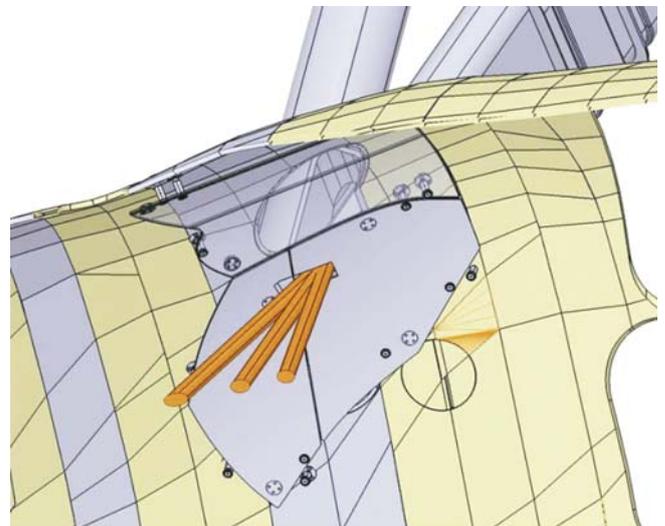

Figure 23: CAD model of the Wendelstein 7-X In-vessel structure in the vicinity of the N-port. The water cooled first wall panel shown in grey has a narrow slit to allow for the beam steering. The rf-beam from the RSL at different steering angles is indicated in orange colour.

The design of the main components was based on these results and the design integration into the Wendelstein 7-X periphery was completed at IPP. As seen from figure 23, very narrow slits are required in the first wall protection panels of Wendelstein 7-X for the beam steering at the N-port position. With the special expertise and experience of the two involved companies on electroforming/electroplating (G-T) as well as custom made high precision machining (NTG) new manufacturing solutions could be realized. The main components such as the corrugated waveguides with thin walls and embedded cooling channels for cw-operation, the mitre bends, the optimized diamond windows and the launching mechanism, respectively, are completed or presently being manufactured. For further details see the report of IGVP, University of Stuttgart, in chapter 8.2. Two RSLs of different size (length and cross-section) are being manufactured and will be fed by two out of the 10 ECRH beams of Wendelstein 7-X. Whereas the FSLs are connected in a standard equatorial plane with tokamak-like magnetic field gradient, the RSL's are connected to narrow N-ports located in a poloidal plane with low or vanishing magnetic field gradient and will thus extend the physics capabilities of ECRH and CD significantly. Theoretical studies show, that particular physics issues such as the confinement of trapped and passing particles can be investigated experimentally by scanning the launch angle of the incident rf-beam in this particular plane.

8.1.6 Staff

Staff at IPP (W7-X-HT and ITZ): B. Berndt, H. Braune, V. Erckmann, F. Hollmann, L. Jonitz, H.P. Laqua, F. Noke, S.Marsen, N. Schneider, M. Preynas, F. Purps, A. Reintrog, T. Schulz, T. Stange, P. Uhren, M. Weissgerber.
Staff at KIT (IHM): K. Baumann, G. Dammertz, G. Gantenbein, M. Huber, H. Hunger, S. Illy, J. Jelonnek, R. Lang, W. Leonhardt, M. Losert, A. Meier (KIT, IAM-AWP), D. Mellein, S. Miksch, I. Pagonakis, A. Papenfuß, A. Samartsev, A. Schlaich, M. Schmid, W. Spiess, T. Scherer (KIT, IAM-AWP), J. Szczesny, M. Thumm, J. Weggen.
Staff at IGVP (Stuttgart University): W. Kasparek, C. Lechte, R. Munk, B. Plaum, Z. Popovic, H. Röhlinger, F. Remppel, K.-H. Schlüter, S. Wolf, A. Zeitler.

8.2 Contributions for ECRH and Microwave Diagnostics (IGVP Stuttgart)

8.2.1 Remote-Steering Launchers for ECRH on Wendelstein 7-X

In the frame of the BMBF-funded "Verbundprojekt FORMIK3", two remote-steering launchers are being built for Wendelstein 7-X by a consortium of IPP Garching and Greifswald, IGVP Stuttgart, and the companies NTG Gelnhausen and Galvano-T, Windeck. Basic facts are described in chapter (Volker Erckmann). For investigations on trapped particles in Wendelstein 7-X as well as a demonstration for a reactor-compatible antenna for ECRH, two N-ports of Wendelstein 7-X will be equipped with "remote-steering" launchers (RSL).

The remote-steering properties are based on multi-mode interference in a square waveguide leading to imaging effects. To improve the angular range of the input beam, non-square cross sections were considered.
The mode dispersion relations of non-square waveguides have been investigated with a comprehensive simulation of the cross-section with IPF-FD3D, and then the resulting modes and propagation constants have been used with PROFUSION to quantify the imaging properties of the whole waveguide.


(1,1) (1,3) (3,3) (1,5) ? ? ? (9,3)
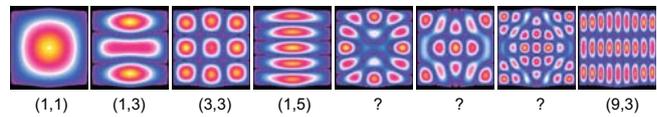
Figure 24: Modes of a deformed waveguide, with corresponding mode numbers for square cross sections.

The deformations were of the form $A \cdot \cos(\pi x/L)^q$, with amplitude A and q=3,4,5. The resulting mode pictures were not always a simple distortion of the square modes, as seen in figure 24 It can be seen that the square waveguide with optimized input coupling ("square with dy" in figure 25) beats the waveguide with the best cosine deformation.
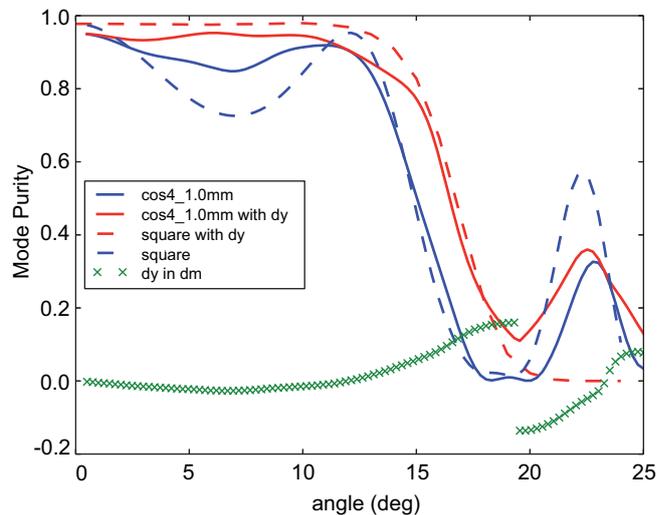

Figure 25: Comparison of imaging quality (Gaussian mode purity of output beam) of square and deformed waveguides. The square waveguide with optimized input coupling (red dashed line, with dy) is best.

The deformation only improves the waveguide at angles around φ≈7. No improvement was seen beyond φ≈14. At all angles, the deformation decreased the effect of the optimised input coupling. Therefore, both Wendelstein 7-X RSLs will be square, with geometrically optimised input coupling, and a length of $3.91 \cdot a^2/\lambda$. The engineering design, which was pursued at IPP Garching, was investigated with respect to possible mode conversions of the RSL waveguide due to various reasons.

As example, figure 26 shows the basic design of RSL 5, where the waveguide is subject to bending due to the fact that the complete antenna is supported basically at two points only. The calculations show that – although bending radii of up to 1200 m can occur – spurious modes are always below the tolerable level.
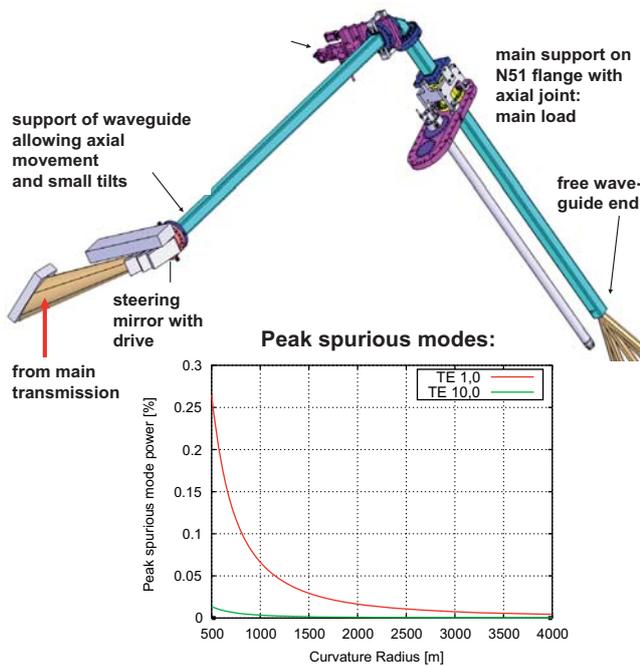

Figure 26: Top: Basic design of the RSL5 showing the supporting points. Bottom: For this geometry, the mode conversion due to bending of the RSL waveguide was calculated, showing negligible effects for the max. radii of 1200 m.

To benchmark calculated results, a fast measurements method is being developed, which is based on resonator techniques. Classical measurements of the launcher performance would employ scans of the antenna patterns at various angles, and subsequent mode analysis of the patterns. For precise results, an input beam with a mode purity of ≥99.8 % was required. In the resonator measurement, a RSL resonator is formed by a waveguide with (half) length of $(3.91/2) \cdot a^2/\lambda$ and a focusing mirror set at an angle φ wrt. the waveguide axis. The focal length of the mirror, its distance to the waveguide, and the steering angle φ determine the parameters of the free-space beam in the resonator, which must be identical to the feed beam in the RSL application. Thus, the gaussian beam efficiency of the corresponding RSL can be directly measured from the Q-factor of this resonator as function of input angle, polarisation, and beam offset.

A preliminary result from a RSL mock-up is shown in figure 27, which demonstrates the optimization for a limited angular range, when the pivot point of the feed beam has a certain lateral offset wrt. the waveguide axis. With an optimized beam coupling, a performance corresponding to the envelope of the measurements can be obtained, yielding steering angles of φ≤14.5.
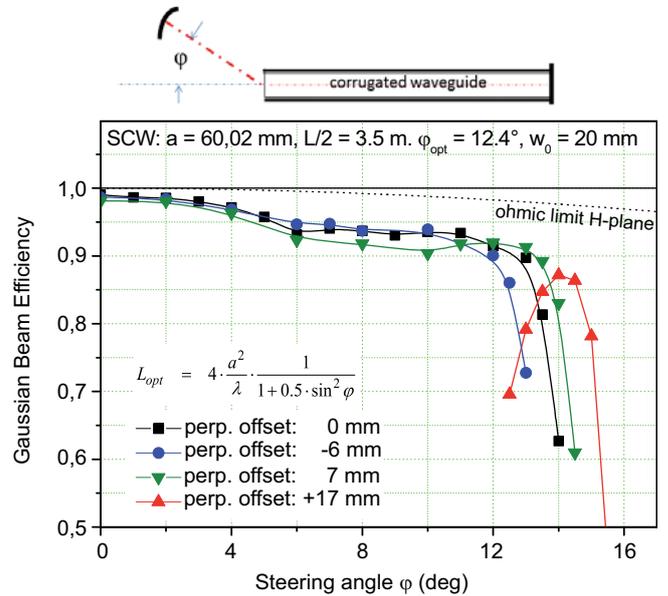

Figure 27: Sketch of measurement set up (top) and measured gaussian beam efficiency (bottom) for a RSL with length of $3.91 \cdot a^2/\lambda$ and various lateral offsets of the feed beam pivot. For an optimized coupling geometry, a performance corresponding to the envelope of the curves can be obtained, yielding steering angles of φ≤14.5.

8.2.2 Series-fed Frequency-steered Array Antennas for Doppler-reflectometry

In 2014, a prototype of the 32-element horn array has been produced. It is shown in figure 28 on the left. Afterwards, the manufacturing process has been substantially improved. To achieve better mechanical precision and simplify the electro-forming, the stack of copper and aluminium sheets is now provided with a support structure. The support structure's transparent PMMA brackets have been designed to indicate the desired shape, thus providing a convenient means of monitoring progress during electro-forming. Prototypes for helical feed networks with an increased diameter of 34.5 mm have been manufactured, shown in figure 28 on the right.
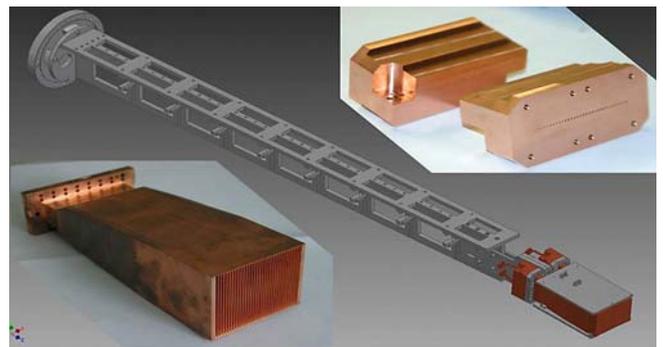

Figure 28: Design of the beam holding a pair of frequency steered array antennas for reflectometry on Wendelstein 7-X. Insert left: Prototype of the 32-element horn array. Insert right: Two helical series feeds for 32-element horn arrays.

Measurements for characterisation have been started and are expected to be completed in January 2015. For the main Reflectometry port on Wendelstein 7-X, a support structure for the installation of an antenna pair through a CF150 flange has been designed (figure 28, centre); manufacturing of this support will be completed shortly. At present, the feeds and the horn arrays are being manufactured, with the goal to be ready for the first operation phase of Wendelstein 7-X.

8.2.3 Investigation of Remote Steering Antennas for ECE
The remote steering principle, which was investigated in detail for high power ECRH applications (see e.g. chapter 8.2.1) can also be used for ECE applications.
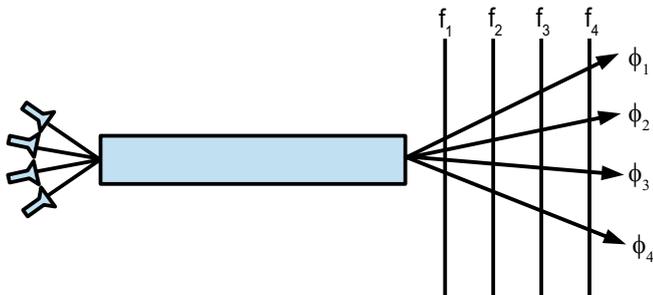

Figure 29: Principle of a remote steering antenna in an ECE imaging system.

The advantage of the remote steering antenna for this application is that radiation can be detected under different angles and frequencies simultaneously while requiring just a small port area (see figure 29). Since the frequency of the ECE radiation depends on the magnetic field, which increases further inside the plasma, this setup allows a 2D imaging. Another advantage is the fact that the actual receiver antennas are placed several meters away from the plasma, where space limitations are less critical.
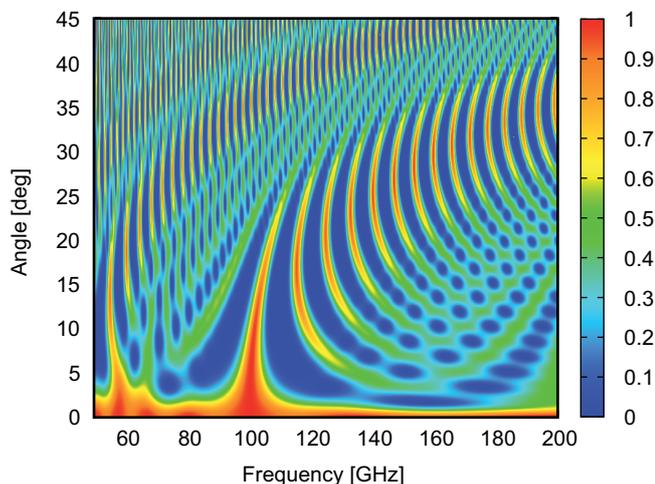

Figure 30: Gaussian efficiency of a remote steering antenna as a function of the angle and frequency.

To explore the possibilities of this method, the Gaussian efficiency of a remote-steering antenna was calculated for a large range of angles and frequencies (figure 30). The design frequency is 100 GHz, here we see the main operating branch near $\varphi=0$. At other angles and frequencies however, we see a large number of areas where an operation with a sufficient efficiency is also possible. For the further development of this method, a realistic investigation of the requirements of such a system based on actual plasma scenarios is necessary.

8.3 Ion Cyclotron Range of Frequency Heating
For the operational phase 1.2 a fully functional ion cyclotron resonance heating (ICRH) system is planned. This system will consist of at least one generator operating at frequencies over the range from 25 to 38 MHz at a maximum power level of 1.5 MW for a maximum pulse length of 10 sec. and two strap antenna with internal pre-matching and the appropriate transmission line and matching system in-between. The whole system is designed, developed, procured, manufactured and integrated within the framework of a collaboration with ERM/KMS Brussels, FZ Jülich and IPP Greifswald. The main purpose of the ICRH system is to create fast particles that can be used as test particles to investigate the predicted improved neoclassical confinement of with increasing plasma beta for some magnetic configurations. Particle energies on the order of 50-100 keV correspond to the energies of alpha particles in a stellarator fusion reactor. The chosen frequency range allows helium 3 and hydrogen minority heating schemes at the standard magnetic field of 2.5 T. both of which generate a high energy tail of fast particles. However, the plasma densities needed to obtain an average plasma beta of several percent constrain the tail energy. In 2014 ERM/KMS proposed a three ion scheme where the concentrations of hydrogen and deuterium are chosen such that the associated ion-ion hybrid resonance coincides with the helium 3 fundamental resonance. Since in the vicinity of this resonance the fast wave polarization is almost circularly polarized in the direction of the ions very strong coupling is predicted. This scheme is planned to be investigated on already running fusion experiments in the near future. In 2014 the preliminary design and partially the detailed design of the major components of the antenna was completed. This included the main support frame, the alignment support frame, the movable antenna unit, the coaxial conductors and mechanical support, the antenna head and the antenna box (see figure 31). The complete antenna including the vacuum feed through is radially movable by 350 mm, driven by a motor that can operate in the ambient magnetic field of Wendelstein 7-X. This is radial movement is necessary to optimize the coupling of the antenna to plasma configurations with inward lying last closed flux surfaces and to reduce the heat load in case that the ICRH system is not part of the experimental program. The antenna head contains the two antenna straps that are shaped to conform to the last closed flux of typical magnetic configurations.

All components of the antenna have to be actively water cooled since for typically discharges the radiation and the convective losses of the plasma surpass the resistive losses in the antenna during ICRH operation. A graphite antenna limiter is planned to be directly mounted onto the water-cooled antenna housing. A dedicated test setup has been prepared to investigate whether this mechanical solution is able to transmitted heat loads on the order of 1 MW/m^2 onto the water cooled housing. Trial runs at the Judith test site in Jülich are planned for 2015. The antenna head also contains provisions to install horns for a microwave reflectometer to allow local density measurements and to install gas valves to locally increase the plasma density in front of the antenna. The detail design of the antenna will be completed in 2015 if the tests of the antenna limiter have shown satisfactory results.
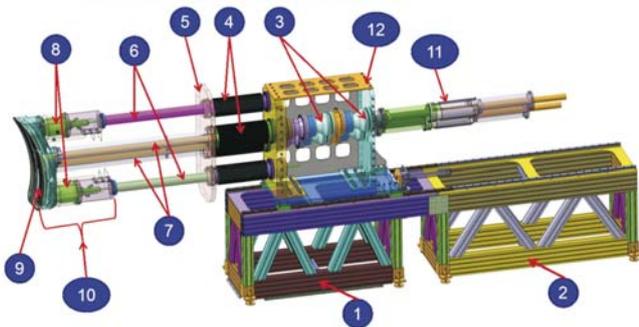

Figure 31: ICRH antenna design for W7-X.

8.4 Neutral Beam Injection

The neutral beam injection (NBI) system for Wendelstein 7-X is planned to go into operation in 2016 during the OP 1.2. In 2014 the Wendelstein 7-X board of management approved additional funding for the installation of two PINI ion sources on each of the two NBI injector boxes. Two PINIs have this year been delivered to Greifswald from Garching by special transport. This allows a total power in D (H) of 10 (7) MW. Work in the group focused on assembling the many components inside the injector boxes and in the box-torus interfaces as well as installing the two injector boxes in the torus hall. In March 2014 the anchorage of the box support structures was installed in the torus hall. This action was delayed by concerns that the torus hall floor steel reinforcement bars would be damaged by drilling the anchor bolts holes. The positions of the reinforcement barswere firstmapped by radar, and holes then were drilled in suitable positions in the torus hall floorand in the feet of the support structures to anchor them. The water pipes for all internal components of the injector boxes, including the new pipe work required for the titanium sublimation pumps, and for the torus hall water piping have been completed.

The torus-box interface element "Bellow unit", manufactured at the ITZ workshop in Garching, and port bellows

protection element "Bellow scraper" (SDMS, France), see figure 32, were delivered to IPP in 2014. Although several technical challenges had to be overcome, installation of these critical elements was completed by the required dates. Manufacturing of the Box-Exit Scrapers (BES) is currently underway (De Pretto, Italy) and installation is planned for 2015.
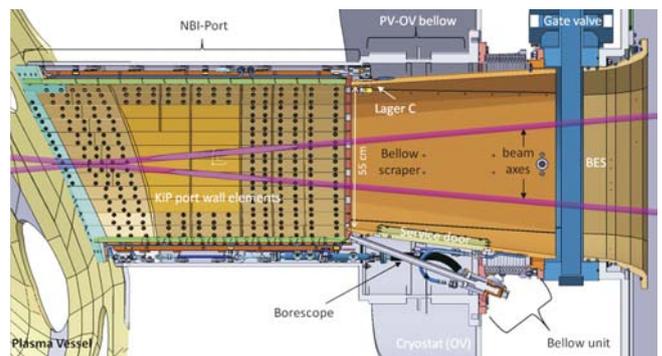
Figure 32: Cross section of the AEK-port detailing the components installed in the NBI-torus interface: various protection elements used to shield it from the NBI beams (KiP port wall elements, bellow scraper (copper cone) and Box-Exit Scraper), diagnostics (borescope), bellow unit, piping for cooling water and gate valve.
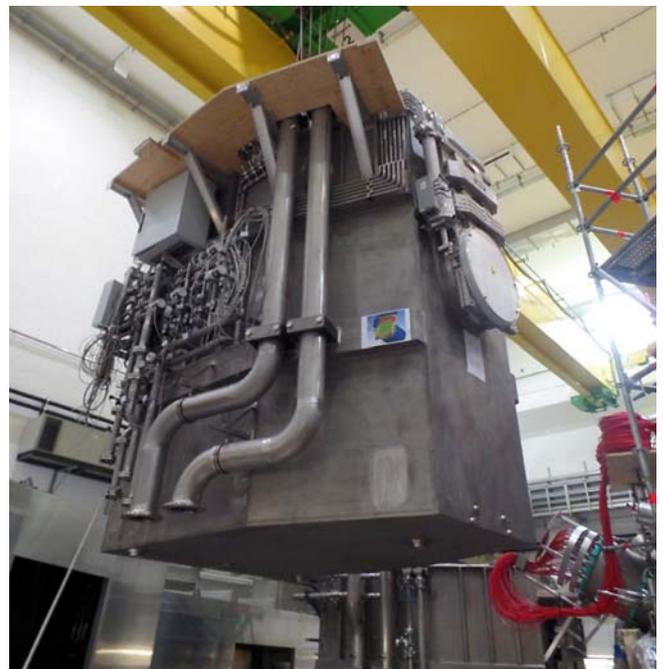
Figure 33: NBI-Box 21 being lowered into position on its support structure in the torus hall. The pipework completed in the NBI pre-assembly hall as well as some of the cabling for the control/DAQ system can be seen.

The thermocouples for monitoring the torus beam dumps and the NBI ducts have been installed and successfully commissioned. All of the port wall protection elements (KiP) have been installed in the NBI ports, including graphite and CFC tiles.

The two injector boxes have been moved from the NBI pre-assembly hall to the torus hall, as shown in Figure 33. They have been connected to the W7-X torus, vacuum leak tested, and aligned with respect to the NBI beam duct, as shown in figure 34. The next steps will be to assemble the periphery of the NBI system, including connection of the injector boxes to the torus hall water piping, to continue the cable routing on the boxes and to the control room and to install the control/DAQ racks and cabinets.

Figure 34:View from inside of bellow scraper in AEK21: two targets are used to align the NBI beam with respect to the duct. Strike points of laser beams for NBI-Box alignment are visible. This picture also shows that the KiP structures including carbon/CFC tiles are installed in the NBI duct.

9 Diagnostics

The work focused strongly on the in-vessel diagnostic components, and the diagnostics necessary for safe operation or indispensable for the physics goals of the first operational phase OP1.1. The following sections briefly summarise the main activities of the Diagnostics subdivision (DIA) which consists of three departments, Edge and In-vessel Diagnostics (DIA-EIV), Core Diagnostics (DIA-COR), and Diagnostic Engineering (DIA-ENG).

9.1 Edge/Divertor and Magnetics Configuration Diagnostics

9.1.1 IR/visible Divertor Observation

The French company Thales-SESO is building two long-pulse-compatible IR/visible endoscopes for divertor temperature control and imaging. The optical design has been completed and manufacturing of the system components has started. The installation of the endoscopes on Wendelstein 7-X for OP1.2 is foreseen by the end of 2015. The company Infratec has delivered the two, fast 3-5 µm infrared cameras and the company Andor two Zyla sCMOS cameras for the visible spectral range for these endoscopes. For OP1.1 a set of ten simplified infrared/visible light (IR/VIS) systems have been installed on Wendelstein 7-X. Each system has one near-infrared (NIR) and two visible light cameras. The cameras are installed directly behind the three observation windows, at the plasma-facing end of a 2 m long immersion tube. Each window is equipped with a rotating shutter. The immersion tubes were manufactured by the company TRINOS. These systems, though designed for divertor observation in OP1.2, also allow observation of the five inboard limiters in OP1.1, but only at a rather shallow angle. An additional 3-5 µm IR camera observation system having a high-resolution perpendicular view on one of the limiters has also been prepared for OP1.1 by LLNL in the US. For OP1.2 high-magnetic-field compatible IR cameras will replace the NIR cameras. The call for tender for these IR cameras was executed and the contract placement is in preparation.

9.1.2 Video Diagnostic

During 2014 the remaining four of the ten front-end components of the video diagnostic were installed on Wendelstein 7-X. Each front-end component consists of a vacuum window, a pinhole, a water-cooled thermal shield and a camera fixture. The video diagnostic camera systems developed by MTA WIGNER RMI, Budapest, Hungary, will be installed in the AEQ ports in all 10 half modules of Wendelstein 7-X, and will enable the observation of almost all of the plasma facing first wall. The two video diagnostic systems that will be used together with the flux-surface measurement system have PCO PixelFly cameras – these were installed and put into trial operation. Four channels using EDICAM were finalised. The installation of the control and data acquisition system for the EDICAM cameras was started: four EDICAM PCs and the VIDACS (the control software for the video diagnostics) PC were taken into operation by installing the necessary software components. The beta version of the VIDACS was installed and offline operation (without trigger and clock input) was demonstrated controlling four EDICAM cameras. The first specification of EDVIS – a multichannel video display and image processing software designed especially for the ten channel video diagnostics – has been completed. The file management, the internal data handler and the GUI module is under development.

9.1.3 Magnetic Diagnostics

The installation of all magnetic diagnostics in Wendelstein 7-X has been completed, see figure 35. The activities now focus on the layout of signal cables in the torus hall and on the electronics and data acquisition. The definition of the interlock system based on the signals of diamagnetic loops and compensation coils has been started.

9.1.4 Flux Surface Mapping

The first two manipulators and the light fibre based reference system were installed at Wendelstein 7-X after separate leak

and baking tests. By means of metrology, the spatial orientation of the sweeping rods, and the position of the reference system have been precisely determined within the plasma vessel, see figure 36. The third and last manipulator was intensively tested at a large vacuum tank and is also ready for installation.
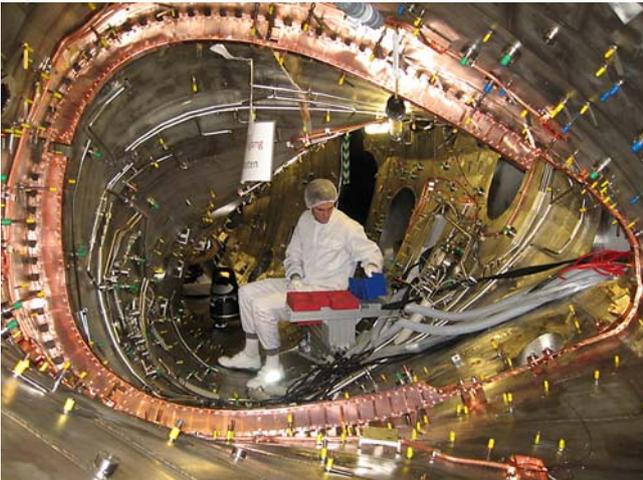

Figure 35: One of the two diamagnetic loops installed in Wendelstein 7-X. The diagnostic indirectly determines the total stored plasma energy by measuring the magnetic flux through the loop – this flux decreases with increasing stored plasma energy. The copper cladding is needed to protect the coil against heat loads during long-pulse operation, primarily coming from stray microwave radiation.
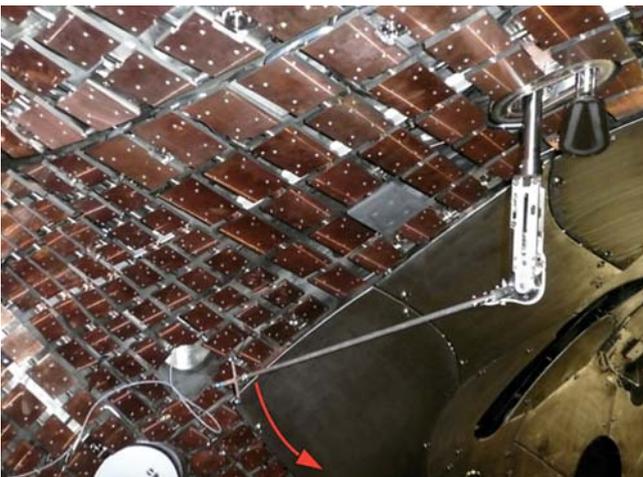

Figure 36: One of the installed flux surface measurement rods during a motion test and metrology measurement inside Wendelstein 7-X, performed under atmospheric pressure. The rotation direction of the rod is indicated with the red arrow. The electron gun will be installed at the tip of the rod, where the four-way cross holds corner cubes in this photo (near the base of the arrow).

9.1.5 Fast Reciprocating Probe System
The design and manufacturing of the support structure for this system has been finished and is ready for installation in the torus hall. The assembly concept has been finalized. The carrier system has been designed and is being manufactured at FZ Jülich. Almost all components have been purchased or manufactured. The assembly is progressing well. In parallel, the control system concept has been developed. The control hardware has been purchased and mounted into cabinets. The system is scheduled for implementation for the first operation phase OP1.1.

9.1.6 Limiter Langmuir Probe Arrays and Target Integrated Flush Mounted Langmuir Probes for TDU Phase
Two arrays of Langmuir-probes have been installed in the limiter of module 5, see figure 37. All in-vessel cables and connectors are installed and tested. The manufacturing of the flush mounted Langmuir-probes for the TDU phase is nearly finished, and the manufacturing of the electronic racks and cables has been started.

9.1.7 Neutral Gas Pressure Gauges
Four immersion systems for the manometer heads have been delivered. They will be completed and installed in Wendelstein 7-X early 2015.

Figure 37: One of the limiter tiles with embedded Langmuir probes, before it was installed on Wendelstein 7-X.

9.1.8 Thermal Helium Beam and Divertor Gas Fuelling System
Both gas manifolds foreseen for OP1.1 have been installed at Wendelstein 7-X. They will be disassembled and improved before OP1.2 in order to meet the leak rate requirements for that phase. The periphery gas station is being assembled. The control software as well as the electronic rack for the periphery gas station and the gas manifolds is being developed by FZ Jülich. The beam emission measurement system is in preparation. It consists of simple camera lenses mounted at the port flanges, with fiberoptic cables transporting the light to a laboratory, where a spectrometer with a CCD camera will analyse the signals.

9.1.9 Thermal He-beam and Visible Spectroscopy Systems
FZ Jülich is developing optical endoscopes as versatile observation systems. The optics design is finalized and integrated

into the mechanical design. The concept for the camera units is complete and some optical components have been purchased. The endoscopes will be used as observation systems for the thermal helium beam diagnostics, employing the versatile gas inlets, as well as for tomographic reconstruction of spectral line emission in the island divertor region.

9.2 Microwave and Laser Based Diagnostics

9.2.1 Interferometry

A dispersion interferometer will be used for the line-integrated density measurement already in OP1.1. The system will be used in later operational phases (OP1.2 and onwards) in the density control feedback circuit. The advantage of the dispersion interferometry technique is that it does not require a reference path, is inherently robust against mechanical vibrations, and even allows an intermittent signal loss during long-pulse discharges. The mechanical support structure of the system, consisting of vertically standing granite plates supported by an aluminium support frame, a retro-reflector on the inboard side, and laser safety protection covers all along the beam path have been prepared and mostly already installed in the torus hall.

9.2.2 Electron Cyclotron Emission (ECE)

The ECE system allows the derivation of the electron temperature from the blackbody cyclotron radiation emitted by the plasma. The 32 channel radiometer and its in-vessel Gauss optics with a slim beam to optimize spatial resolution have been assembled and tested. The received microwave radiation will be guided to the radiometer outside the torus hall by an oversized Cu-transmission line which is prepared for installation. For Wendelstein 7-X strong ECRH stray radiation is expected in particular for ECRH heating at high densities with reduced absorption. To sufficiently suppress the stray radiation a notch filter has been developed which achieves a suppression of the various gyrotron radiation frequencies by more than 40 dB while preserving a low and flat insertion loss characteristic at the ECE channels nearby.

9.2.3 Reflectometry

Three different reflectometry systems will be installed for measuring plasma density profiles, density turbulence and its propagation velocity via microwave signals reflected from the cut-off layers in the plasma. The reflectometry systems are being prepared within the framework of the Helmholtz Virtual Institute on Advanced Microwave Diagnostics, with particular contributions from FZ Jülich and the IGVT Stuttgart, and in a bilateral cooperation with CIEMAT in Spain. A diagnostic plug-in with a fast angular-scan Doppler antenna as K-spectrometer for turbulence measurements is being built at IGVT Stuttgart. A correlation reflectometer is currently being manufactured at FZ-Jülich. It consists of a plug-in that contains the microwave antenna array. The versatile

Gaussian mirror optics developed together with IGVT has been manufactured at IPP. In the first operation phase this optics will be used for the Doppler reflectometer supplied by CIEMAT.

9.2.4 Thomson Scattering

The in-vessel Thomson laser beam path and the observation optics for OP1.1 have been installed and aligned at Wendelstein 7-X. The construction of a new polychromator room has been started.

9.3 Core Spectroscopy

9.3.1 RuDI-X, CXRS, NPA

The Russian Diagnostic Injector for Wendelstein 7-X (RuDI-X) and its high voltage power supply are now ready for the integration into the electronic control and safety system of Wendelstein 7-X, after the successful acceptance tests and commissioning in the diagnostic hall had been performed. RuDI-X provides an energetic beam of neutral particles required for active charge exchange recombination spectroscopy (CXRS) and charge exchange neutral particle analysis (CX-NPA). The quartz fibre array for CXRS had been delivered by an external company, and it was successfully tested in the spectroscopic set-up. The immersion tube for the port AET41 has successfully passed the leak and baking tests.

9.3.2 HEXOS

The electrical installation inside the torus hall for the VUV/EUV spectrometer system HEXOS has been started, including the installation of six electronic racks and the routing and pulling of the cables. The calibration sources have been tested and the commissioning of the HEXOS system is planned for early 2015.

9.3.3 High Resolution X-ray Imaging Spectrometer

The support structure for the high resolution X-ray imaging spectrometer (provided by FZ-Jülich) has been adapted to the available free space. The geometry of the sightline has been calibrated in the laboratory. The beamline components are ready for installation.

9.3.4 X-ray Imaging Crystal Spectrometer

The X-ray imaging crystal spectrometer (XICS) is being prepared in collaboration with PPPL (USA). The design of the spectrometer has been performed by PPPL. The entire system is being manufactured in the USA. Delivery, installation, and commissioning of the spectrometer are planned for spring 2015.

9.3.5 Bolometer

Two bolometers will allow tomographic reconstruction of the total plasma radiation profiles in the triangular plane of

the plasma vessel. Installation of the vertical bolometer in the corresponding port at Wendelstein 7-X has been completed after the successful shutter tests at 150 °C and the integral leak tests of the entire system in vacuum. For the horizontal bolometer system the manufacturing of the cooled front plate, containing the camera pinhole, and the manufacturing of the detector housing have been finished. Assembly and final integral tests in vacuum are planned early 2015.

9.3.6 X-ray Pulse Height Analysis (PHA) and Multi-foil Spectroscopy (MFS)

The pulse height properties of the Silicon Drift Detectors have successfully been tested at IPPLM, Warsaw. The corresponding preamplifier boards were mounted in specially designed housings. Three sets of piezo-slits and a position sensor for the wobble stick have been installed. The data transfer elements have been tested together with the control software of the PHA system. For the MFS system the orientation of the main valve had to be changed to avoid a collision with neighbouring diagnostics. Z_{eff}. During OP1.1 of Wendelstein 7-X, a single line-of-sight of the visible bremsstrahlung will be available for measurements of Z_{eff} using the coaxial port pair AET40/AEZ40. The system will consist of an optical lens at a vacuum window, combined with a fiberoptic cable that transports the measured light to a spectrometer and detector in a laboratory outside the torus hall. The final parts of the system are being prepared.

9.3.7 Neutron Counters

The detector tubes for the neutron monitors and the pulse electronics were delivered to IPP and installed in the neutron monitors. A special in-vessel rail system with a carriage for the calibration source has been developed for the calibration of the neutron detectors. The complete system was set up in a large hall to test the cart motion, the simultaneous position recording with a barcode reader etc. Two of the neutron monitors and the pulse electronics were temporarily transferred to the Physikalische Bundesanstalt in Braunschweig (PTB) for calibration in a low-scattering environment. After this calibration, the neutron monitors were installed at their final location by the Wendelstein 7-X torus. The rail system for the cart motion with the neutron source was installed inside the torus at the end of 2014 in preparation for the neutron calibration, planned for January 2015.

10 Operations

This sub-division was established in October 2013 in order to prepare and conduct the operation of Wendelstein-X. Also the CoDaC-department as a central service group belongs to this division.

10.1 Commissioning

The device operations department is presently preparing and leading the integral commissioning of Wendelstein 7-X. In the beginning of 2014 the newly introduced processes for the commissioning were followed and monitored. After the closure of the cryostat vessel in March, the commissioning of the interspace- and cryostatvacuum was started. A major milestone in July was the first evacuation of the cryostat vessel, see figure 38. In the following weeks, 30 leaks were detected and repaired. Simultaneously, mechanical loads and stresses on the shell structure, resulting in deformations of the vessels and ports and relative movement between the vessels have been measured I the pressure plateaus. Of special interest were the port bellows, specifically those bellows from large oval and rectangular ports where significant deformation is expected due to the vacuum load.
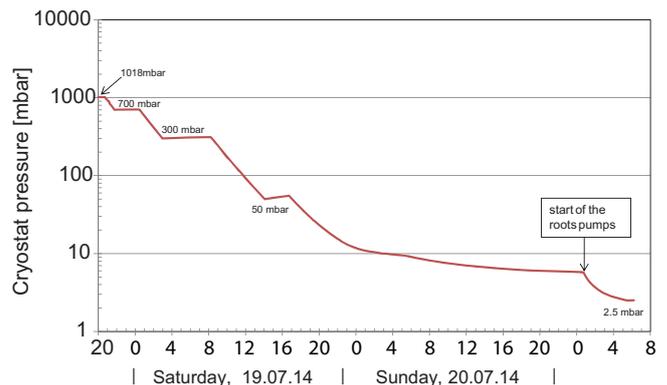
Figure 38: Cryostat-Pumping: Course of the pressure in the W7-X cryostat during the first evacuation. The plateaus at 700, 300 and 50 mbar were introduced to perform mechanical test/measurements on the cryostat.

The measured stresses and deformations were in rather good agreement with the results of the FME-modelling, and confirmed the structural stability of the cryostat, see chapter 6.1.2. The device safety group within OP- Device Operation has continued to evaluate the safety analyses of the main components and systems. In the process of performing the safety assessments, several additional technical and organizational measures to ensure safe operation have been proposed for implementation.

10.2 CoDaC

The department Control, Data Acquisition and Communication (CoDaC) had its focus on the commissioning of Wendelstein 7-X, in particular on the first pump down of the cryostat and the preparation of the cryostat cool down. Main challenges were the continuous data acquisition, the setup of the basic operational management and the setup of the control room.

10.2.1 CoDaC Activities for Commissioning

CoDaC has strongly supported the commissioning of the cryostat vacuum system. The main objectives were the setup

and operation of the machine instrumentation, communication between the local and central control system as well as the reliable data acquisition of all engineering data. The essential machine instrumentation system was required for monitoring of mechanical displacements and stresses of the cryostat. Furthermore, the pressure data of the interspace and cryostat vacuum system has been recorded, which allowed detailed analyses on correlations between pressure and structural changes. The analyses have been performed by the engineering group using interactive analysis tool and a web based data interface (REST API) to the central experimental data archive. With the read-after-write latency of the archive in the order of seconds, the archive could be used for monitoring purposes as well due to the slow characteristic times of the vacuum and mechanical system. The preparation of the calibration of the neutron counters had been almost accomplished, which comprised the provisioning of the system-on-a-chip computer controlled waggon on a rail system carrying the calibration source and the data acquisition for counting and archiving the neutron counter pulses.

10.2.2 Control and Data Acquisition

Beside the direct activities for the commissioning, the control and data acquisition group made a lot of progress in the preparation of further systems. The hardware of the safety control system has been completely implemented. This comprises redundant safety PLCs (programmable logic controller), the cubicles for the safety signal lines and the safety control panel in the control room. Safety warning signalization and emergency stop safety signals to components like vacuum systems, cryo supply and cooling water supply has been prepared. Furthermore, procedures and safety instrumented functions according to the engineering standards EN 61511 have been developed and established. Regarding the central operational management, the status and infrastructure survey of plant systems has been implemented. Electro-technical planning, design and implementation has been performed for the machine and cryo instrumentation, interferometry, ECE, gas feed, video diagnostics and further support for diagnostic systems at lower priority. The data acquisition system has been set into operation for the fully continuous mode. This comprises the data acquisition software "CoDaStation", which can act as a data collector of PLC data as well, and the archive based on application server with the "ArchiveStreamAccess" interface and the GPFS (general parallel filesystem, IBM) as a cluster file system for the elementary storage of data. This system is in continuous operation since April 2014 and since December 2014 it is furthermore equipped with the HPSS (high performance storage system) of the RZG, which receives the data every few hours via a direct 10 Gbit/s data link between Greifswald and Garching (figure 39). Since then, data of the ECRH, the cryo vacuum and the machine instrumentation

has been archived continuously. The development of the new version of the timer-trigger-event system has progressed well. This TTE card uses standard Ethernet for communication with control or data acquisition computer. The prototype could be successfully tested with all functions and series production of this card could be started. The version running on an FPGA development board could be successfully operated for the neutron counter calibration.
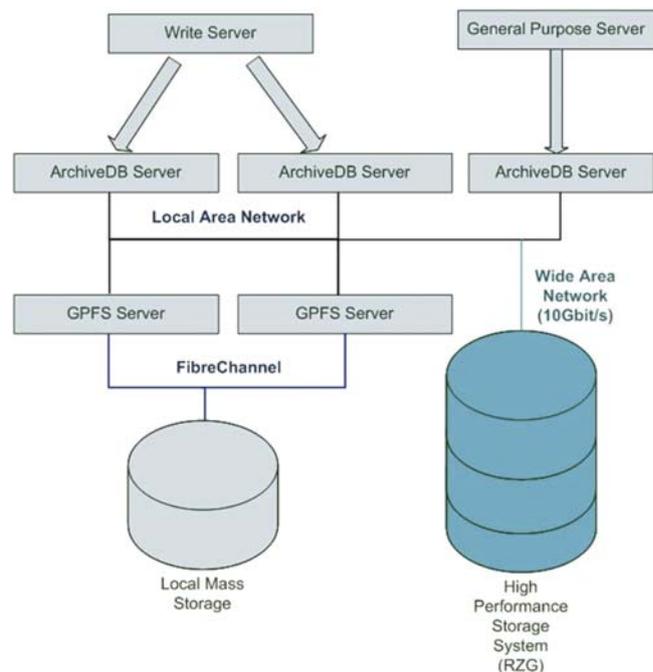
Figure 39: Design of the experiment archive.

10.2.3 Software Development

The software development has focused on finalizing software products. In particular the archive and data acquisition software has been hardened by establishing extensive tests in order to achieve a good reliability for the 24/7 operation. With these tests, the write performance and availability of the archiving system could be much improved and revealed that the read and write processes had to be separated well in order not to disturb the write processes. The archive access API has been expanded by a web version based on RESTful services. This service is mainly for the support of temporary diagnostics, data analysis and fast integration into interactive software tools like MatLab, IDl or LabView. Further progress has been made on the configuration database, which was subject of large software layering refactoring processes and a change from an object database (ObjectivityDB) to a document database (MongoDB). The latter is running now redundantly with three instances. Accompanying to these very basic changes, all applications had to be adapted to the new configuration database. This process has been accomplished on a functional basis and in the next step the performance

will be improved by changing schemas on the persistence, business and application level. The driver development for the new TTE card has been almost completed and versions for the operating systems Windows, Linux and VxWorks have been created.

10.2.4 IT

The IT group has mainly established the infrastructure for the commissioning of Wendelstein 7-X. The control room has been almost fully equipped with zero client workstations for use with the VMware virtual Desktop environment. It has been successfully used for virtual control workstations during the cryostat pump down and further commissioning steps. A video wall has been installed that streams videos and desktop screens solely via standard networks. With this approach, screens of any desktop regardless whether virtual or in hardware can be exposed to the large screens. Furthermore, distant control rooms of ECRH, cryo systems or neutral beam injection can receive and send streams to this display via network. The network system itself has been refined regarding the appropriate network segmentation and many network access systems have been installed in the experiment domain for setting up further Wendelstein 7-X subsystems.

Scientific and Technical Staff

W7-X Subdivisions:
Project Coordination
A. Lorenz, W. Fay, G. Gliege, M. Gottschewsky, D. Haus, R. Herrmann, U. Kamionka, T. Kluck, B. Kursinski, M. Schröder, I. Unmack, H. Viebke, R. Vilbrandt.

Operation
H.-S. Bosch, T. Bluhm, R. Brakel, J.H. Feist, K. Gallowski, M. Grahl, S. Groß, G. Hemmann, C. Hennig, U. Herbst, C. Klug, M. Köppen, M. Kostmann, J. Krom*, G. Kühner, H. Laqua, M. Lewerentz, M. Marquardt, S. Mohr, A. Möller, I. Müller, K. Näckel, D. Naujoks, S. Pingel, H. Riemann, J. Schacht, A. Schütz, H. Schürmann, A. Spring, U. Stridde, S. Valet, A. Werner, A. Wölk.

Engineering
F. Schauer, T. Andreeva, V. Bykov, A. Carls, K. Egorov, J. Fellinger, Tiejun Xu*.

Design and Configuration
D. Hartmann, M. Banduch, Ch. Baylard*, D. Beiersdorf, A. Bergmann, R. Binder, G. Borowitz, T. Broszat, P. v. Eeten, H. Greve, K. Henkelmann, F. Herold, A. Holtz, C. Hühr, J. Knauer, A. Müller, R. Laube, N. Ose, T. Rajna*, S. Renard*, N. Rüter, P. Scholz, K.-U. Seidler, T. Sieber, F. Starke, M. Steffen, T. Suhrow, A. Vorköper, J. Wendorf, U. Wenzel.

Magnets and Cryostat
Th. Rummel, H. Bau, D. Birus, A. Braatz, C. P. Dhard, F. Füllenbach, , K. Hertel, A. Hölting, M. Ihrke, J. Kallmeyer, U. Meyer, B. Missal, T. Mönnich, M. Nagel, M. Nitz, M. Pietsch, K. Riße, M. Schneider, H. Zeplien.

Assembly
L. Wegener, J. Ahmels, H. Bandt, A. Benndorf, T. Bräuer, A. Domscheit, H. Dutz, H. Grote, H. Grunwald, A. Hübschmann, D. Jassmann, H. Jensen*, A. John, R. Krampitz, F. Kunkel, H. Lentz, K. Liesenberg, H. Modrow, J. Müller, S. Nack, U. Neumann, A. Pasyutina, D. Rademann, L. Reinke, K. Rummel, D. Schinkel, U. Schultz, E. Schwarzkopf, O. Volzke, C. von Sehren, K.-D. Wiegand.

Diagnostics
D. Aßmus, J. Baldzuhn, R. Burhenn, D. Chauvin*, A. Dudek, M. Endler, S. Freundt, K. Grosser, H.-J. Hartfuß*, D. Hathiramani, M. Jakubowski, H. Jenzsch, S. Klose, R. König, P. Kornejew, M. Krychowiak, M. Laux, U. Neuner, M. Otte, E. Pasch, T. Sunn Pedersen, D. Pilopp, T. Richert, W. Schneider, B. Standley, S. Thiel, H. Thomsen, U. Wenzel, D. Zhang.

Heating
R. Wolf, H. Braune, V. Erckmann, St. Heinrich, F. Hollmann, L. Jonitz, R. Kairys, H.-P. Laqua, P. McNeely, G. Michel, F. Noke, F. Purps, O. Raths, P. Rong, N. Rust, R. Schroeder, T. Schulz, P. Uhren.

Technical Services (TD)
R. Krampitz, R. Blumenthal, M. Braun, M. Haas, M. Hagen, M. Müller, M. Schülke, M. Stöcker, M. Winkler.

KIP
A. Peacock*, M. Czerwinski, G. Ehrke, P. Junghanns.

Other IPP Divisions
Stellarator Optimization (E3): C. Biedermann, S. Bozhenkov, A. Dinklage, O. Ford, M. Hirsch, A. Kus, A. Langenberg, S. St. Mohr, M. Preynas, T. Stange, F. Warmer.
Stellarator Edge and Divertor Physics (E4): P. Drewelow*, U. Hergenhahn, H. Hölbe, T. Sunn Pedersen, A. Rodatos, H. Saitoh, J. Stanja, E. Stenson, F. Wagner*, E. Winkler.
Stellarator-Dynamics and Transport (E5): B. Buttenschön, N. Fahrenkamp, O. Grulke, T. Klinger, K. Rahbarnia, R. Schwibbe, J. Svensson, D. Wieseler, T. Windisch.
Experimental Plasma Physics I (E1): J. Boscary, A. Eller, H. Faugel, F. Fischer, H. Fünfgelder, C. Li, B. Mendelevitch, J.-M. Noterdaeme, G. Siegl, M. Smirnow, H. Saitoh*, R. Stadler, D. Wegner, G. Zangl.
Plasma Edge and Wall (E2M): M. Balden, B. Böswirth, S. Elgeti, H. Greuner, F. Koch, G. Matern, M. Mayer, R. Neu, V. Rohde, A. Scarabosio.

ITER Technology and Diagnostics (ITED): B. Heinemann, D. Holtum, C. Hopf, W. Kraus, C. Martens, R. Nocentini, S. Obermayer, G. Orozco, R. Riedl, J. Schäffler.
Computer Center Garching (RZG): M. Zilker.
Central Technical Services (ITZ) Garching: J. Adldinger, F. Ascher, B. Brucker, N. Dekorsy, R. Holzthüm, N. Jaksic, J. Maier, O. Sellmeier, A. Pichlmair, H. Pirsch, J. Springer, H. Tittes, M. Weissgerber, J. Tretter, S. Geißler.

Cooperating Research Institutions

Forschungszentrum Jülich (FZJ): J. Assmann, W. Behr, O. Bertuch, W. Biel, V. Borsuk, A. Charl, G. Czymek, P. Denner, A. Freund, F. Harberts, K. P. Hollfeld, M. Knaup, R. Koslowski, A. Krämer-Flecken, Th. Krings, H. T. Lambertz, M. Lennartz, Y. Liang, O. Marchuk, Ph. Mertens, O. Neubauer, G. Offermanns, A. Panin, M. Rack, G. Satheeswaran, H. Schmitz, B. Schweer, A. Terra, J. Thomas.
Karlsruher Institut für Technologie (KIT): K. Baumann, G. Dammertz, G. Gantenbein, M. Huber, H. Hunger, S. Illy, J. Jelonnek, Th. Kobarg, R. Lang, W. Leonhardt, M. Losert, A. Meier, D. Mellein, D. Papenfuß, A. Samartsev, T. Scherer, A. Schlaich, W. Spiess, M. Thumm, S. Wadle, J. Weggen.
Institut für Grenzflächenverfahrenstechnik und Plasmatechnologie, Stuttgart University (IGVP): E. Holzhauer, W. Kasparek, M. Krämer, C. Lechte, R. Munk, B. Plaum, F. Remppel, B. Roth, H. Röhlinger, K.-H. Schlüter, S. Wolf, A. Zeitler.
PTB Physikalische Technische Bundesanstalt Braunschweig, Germany: A. Lücke, A. Pieper, H. Schumacher, B. Wiegel, A. Zimbal.
Universität Rostock/Fachbereich Elektrotechnik: Hr. Timmermann, Hr. Skodzik.
Fraunhofer-Institut für Schicht- und Oberflächentechnik (IST): M. Keunecke.
Fraunhofer-Institut für Werkzeugmaschinen und Umformtechnik (IWU): H.-J. Roscher.
Culham Centre for Fusion Energy (CCFE), Culham, UK: M. Turnyanskiy
FOM-Institute for Plasma Physics, Amsterdam, Netherlands: R. Jaspers.
Technical University Eindhoven, Netherlands: H. Brand, H. Oosterbeek, S. Paqay.
Commissariat á L'Energie Atomique (CEA), Cadarache, France: A. Grosman, V. Moncada, J.M. Trarere.
CIEMAT, Madrid, Spain: E. Ascasibar, E. Blanco, A. Cappa, H. Esteban, T. Estrada, J. Fontdecaba, C. Hidalgo, M. Sanchez, B. van Millingen.
Centro de Fusão Nuclear (CFN/IST), Lissabon, Portugal: H. Fernandes, P. Carvalho, A. da Silva.
Uni Salerno (Italien): R. Citarella, TU Cottbus: M. Führer, ASIPP Hefei (China): Xuebing Peng.
Consorzio RFX Padova, Italy: L. Carraro, A. Fassina, M. Zuin.
CNR Istituto di Fisica del Plasma, Milano, Italy: M. Romé.

University of Opole, Poland: I. Ksiazek, F. Musielok.
The Henryk Niewodniczanski Instiute of Nuclear Physics, (IFJ PAN), Kraków, Poland: A. Czermak, L. Haiduk, Z. Sulek.
IPPLM Institute of Plasma Physics and Laser Microfusion Warsaw, Poland: A. Czarnecka, W. Figacz, A. Galkowski, S. Jablonski, J. Kacmarczyk, M. Kubkowska, L. Ryc, M. Scholz, J. Wolowski.
IPJ Swierk, Poland: M. Barlak, G. Gawlik, J. Jagielski, R. Koziol, P. Kraszewsk.
Warsaw University of Technology: Ł. Ciupiński, G. Krzesinski, P. Marek.
IPP Prague, Czech Republic: J. Preinhaelter, J. Urban, J. Zajac.
Budker Institute of Nuclear Physics, Novosibirsk; Russia: V. I. Davydenko, A. Ivanov, A. Khilchenko, I. V. Shikhovtsev.
Efremov Institute, St. Petersburg, Russia: I. Rodin.
A.F. Ioffe Physico-Technical Institute of the Russian Academy of Sciences, St. Petersburg, Russia: F. Chernyshev, S. Petrov.
Institute of Applied Physics (IAP), Nizhnynovgorod, Russia: L. Lubyako, J. Koshurinov.
Lithuanian Energy Institute, Kaunas, Litauen: R. Alzbutas, G. Dundulis, T. Kaliatka, R. Karalevicius, M. Povilaitis, S. Rimkevicius, E. Urbonavicius.
Research Institute for Particle and Nuclear Physics (KFKI-RMKI), Budapest, Hungary: G. Cseh, T. Ilkei, G. Kocsis, G. Náfrádi, S. Récsei, V. Szabó, T. Szabolics, T. Szetefi, Z. Szökefalvi-Nagy, S. Tulipán, S. Zoletnik.
Princeton Plasma Physics Laboratory (PPPL), USA: T. Brown, D. Gates, P. Heitzenroeder, S. Langish, S. Lazerson, M. Mardenfeld, D. Mikkelsen, H. Neilson, N. Pomphrey, A. Reiman, M. Zarnstorff.
Oak Ridge National Laboratory (ORNL), USA: M. Cole, J. H. Harris, A. Lumsdaine, D. A. Spong.
Los Alamos National Laboratory (LANL), Los Alamos, USA: G. Wurden.
Kyoto University, Japan: T. Mizuuchi, S. Murakami, F. Sano.
National Institute for Fusion Science (NIFS), Toki, Japan: T. Akijama, T. Funaba, K. Ida, T. Morizaki, R. Sakamoto, M. Shoji, N. Tamura, K. Toi, H. Yamada, M. Yokoyama.
Institute of Plasma Physics (ASIPP), Hefei: Wanjiang Pan.

ITER

ITER Cooperation Project

Head: Dr. Hans Meister

The IPP contributions to the ITER Project range from R&D for heating systems and diagnostics to the development of integrated control scenarios and theoretical modelling. In addition, IPP is playing a leading role in contributing to the ITER physics through the International Tokamak Physics Activity (ITPA) and by participating in the EFDA Workprogramme. Furthermore, IPP participates in European training programmes for young scientists and engineers.

Introduction

In 2014 the ITER cooperation project at IPP continued its efforts along the major contributions for the development of heating systems, diagnostics and plasma control as well as theoretical investigations. The ELISE test facility successfully investigated operation parameters for H and D in a caesiated negative ion source for NBI. It is accompanied by supporting investigations at smaller facilities and modelling. The contributions to the CYCLE consortium for the development of the ITER ICRF antenna and to the ECHUL consortium for the ECRH Upper Launcher continue. For the latter the impact of EC deposition profile on performance and the behaviour of MHD instabilities has been analysed. Within the Framework Partnership Agreement (FPA) for the ITER Diagnostic Pressure Gauges the detailed project planning was concluded and system level design has been started. The FPA on the development of the ITER bolometer diagnostic has started its work within the consortium headed by IPP on the detailed system assessment and project planning. Also, the optimisation of collimators in order to define desired viewing geometries while reducing stray light and reflections was achieved. The work on the Plasma Control System Simulation Platform for ITER continues on its way towards the preliminary design review. Furthermore, as part of a contract with ITER the codes ASTRA and STRAHL have been used to set up a simulation of the pre thermal quench phase of disruptions in ITER and benchmark it successfully to experimental data from ASDEX Upgrade.

Heating Systems

Development of RF Driven Negative Hydrogen Ion Sources for ITER

The development of the IPP RF source continued in 2014 with the second experimental year of the half size ITER source at the ELISE test facility with the goal to reach the ITER parameters. At the test facility BATMAN being equipped with the ITER prototype source and at the laboratory experiments at University of Augsburg (see chapter 15) experiments focused on ion source and beam physics, accompanied by ongoing efforts to model the processes related to the extraction of negative ions and the suppression of co-extracted electrons.

At ELISE further experiments towards fulfilling the requirements for the ITER NBI systems have been performed. The very first injection of caesium, needed for achieving the required current densities of negative ions, started in October of 2013. Since then ELISE has been operating routinely with caesium and with medium RF power (≤ 220 kW resulting in ≤ 55 kW/driver). Focus was laid on short pulse operation followed by first steps towards long pulses, i.e. 400 s pulses in hydrogen. Figure 1 shows the dependence of the extracted current densities of negative ions in hydrogen and in deuterium operation on the RF power at the filling pressure of 0.3 Pa (i.e. the ITER value) using short pulse lengths (t_{plasma}=20 s, t_{beam}=10 s). The ratio of co-extracted electrons to extracted ions is plotted as well; this ratio should be kept below one. Operation in hydrogen with a low co-extracted electron current is no issue, as already known from the prototype source, whereas for deuterium the dynamics of the electron to ion ratio is much more pronounced and ratios below one are difficult to achieve. In both hydrogen and deuterium, less filter field as expected is needed: only 2.2 mT and 3.8 mT are used at ELISE, whereas at the prototype source with a different field topology filter fields of 7-10 mT have been used. Consequently, also the integral value along the axial direction from the plasma grid to the driver exit is lower: about 0.4 mTm (hydrogen) and 0.6 mTm (deuterium) in ELISE compared to 1-1.5 mTm at BATMAN.
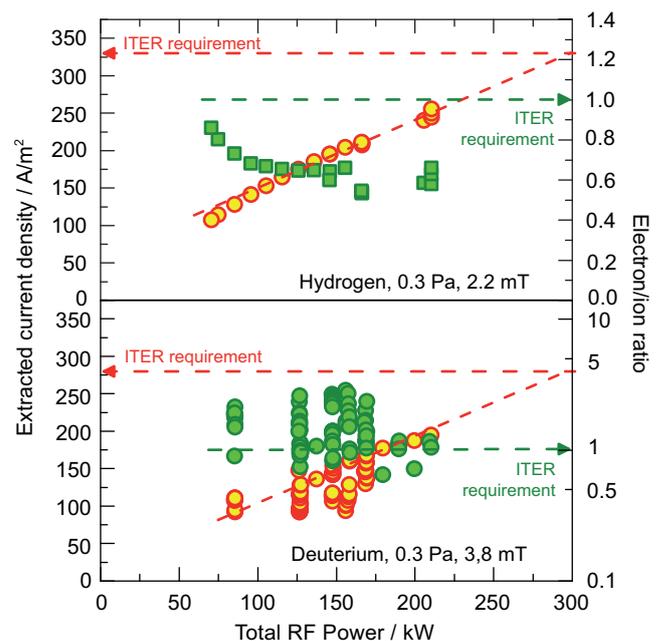

Figure 1: Extracted negative ion current density and the electron-ion ratio versus RF power measured at ELISE in hydrogen and deuterium. Additionally shown are the ITER requirements for both parameters as well as an extrapolation of the current density.

From these quite encouraging results extrapolations of the measured ELISE data to the ITER requirements (horizontal line) are performed: a required RF power of about 70 kW to 80 kW per driver can be expected for the large source which is less than envisaged for the ITER NBI source.

For long pulse operation some issues related to overheating had to be solved first: one concerned the RF transformers that separate parts of the RF circuit being on HV from the grounded RF generator, another the supports of the RF shields around the drivers. Stable negative ion current densities are obtained in long pulses, whereas the co-extracted electrons increase during the pulse and even limit the pulse length, in particular in deuterium. Furthermore, the co-extracted electrons are very sensitive on the RF power and even reveal a vertical asymmetry. Detailed investigations on possible countermeasures have been performed and promising candidates are identified. One example is to fine tune the temperatures of plasma grid and source body which in turn influence the caesium redistribution between these components. These investigations will be continued in 2015 with the aim to achieve pulse lengths of 400 s in hydrogen and one hour in deuterium. After the end of the F4E service contract in November 2014 the experiments at ELISE are funded now up to the end of 2016 within the scope of the Work Program of the NBTF Padua.

For the ELISE campaigns performed so far, evaporation rates of caesium of about 4 mg/h per oven for the hydrogen campaign are obtained for a plasma-on time of 22 hours with about 5 hours beam time. Compared to the prototype sources, evaporation rates are very similar despite the larger source volume, larger grid surface and larger volume-to-surface ratio. Although the size scaling parameter for the caesium consumption is not identified yet, the recent ELISE results indicate low caesium consumption.

At BATMAN the new RF generator based on solid state amplifiers was used to improve substantially the efficiency, reliability and matching properties compared to the free-oscillators used so far in all IPP NBI systems and routine operation could be demonstrated. Experimental studies focussed on beam properties, e.g. the improvement of the beam emission spectroscopy to derive together with the BBC-NI code the beam divergence, stripping fraction and beam homogeneity. Furthermore, experiments on the space charge compensation in the beam have been performed. The results of the latter investigations indicate that the beam of BATMAN is fully compensated for a tank pressure above 0.04 Pa.

The development of a 3D PIC code – the ONIX code – which addresses the physics of formation and extraction of negative hydrogen ions at caesiated sources as well as the amount of co-extracted electrons, made substantial progress. It includes now the bias potential applied to first grid (plasma grid) of the extraction system, and the presence of Cs+ ions in the plasma.

The simulation results show that such aspects play an important role for the formation of an ion-ion plasma in the boundary region by reducing the depth of the negative potential well in vicinity to the plasma grid. This potential well can limit the transport of negative ions from their point of birth at the Cs covered plasma grid surface. With these novelties the simulations provide extracted current densities and co-extracted electron current results which are in better agreement with experimental data.

Furthermore, IPP continued to contribute to the construction of the PRIMA test facilities at RFX Padua (consisting of the full size, full power 1 MeV test facility MITICA and the full size 100 kV ion source test facility SPIDER) in the design of the RF source, the RF circuit and the layout of the source and beam diagnostics. The training of RFX personnel at the operation of the IPP test facilities and the tests of SPIDER and MITICA diagnostic tools together with RFX personnel was extended in 2014 with a total visiting time of about 23 person-months. IPP personnel is also further involved in the tender and procurement of the SPIDER ion source.

Design of the ICRF Antenna for ITER

Since it was agreed in negotiations between CYCLE, F4E and IO that future work for the ITER antenna should take place through a framework contract, a call for such a framework contract was made in 2013 in which CYCLE successfully bid. The framework contract was signed by CCFE on behalf of the consortium partners. Work will concentrate on basic R&D, prototyping and integration, as well as operational testing.

IPP plans to keep involved in this work at the level of 1 ppy.

Upper Launcher for Electron Cyclotron Waves

The development of the upper launcher (UL) for electron-cyclotron (EC) waves, performed in the frame of the ECHUL-Consortium Agreement (involving KIT, CRPP, CNR-IFP, DIFFER and IPP) entered its second phase, which should lead to the final design review in about four years' time, starting from December 2014 under F4E grant 615 (grant 161 until November 2014). The main goal of the involvement of IPP is the analysis of the physics performance of the launcher to assess and guide its design. The main objective of the UL is the control of MHD instabilities, primarily neoclassical tearing modes (NTMs) and sawteeth. Furthermore, the analysis of additional capabilities, like the possibility of triggering the frequently-interrupted NTM regime (FIR-NTM), the stabilization of NTMs at rational surfaces with safety factor q>2 and the influence of edge-localized modes (ELMs), has been performed as part of the task agreement.

In the frequently interrupted regime, (3,2) NTMs do not reach their saturated amplitude because of the concomitant destabilization of an ideal (4,3) mode, which can be achieved

using ECCD to lower the magnetic shear outside the q=4/3 surface. The analysis shows that the power available from the UL should be sufficient to enter FIR-NTMs, but the attractiveness of this regime will have to be checked experimentally, since it could be spoiled by an increased instability of the (3,2) NTM due to ECCD inside the q=3/2 surface. The power available from a given mirror row (13.3 MW) should be enough to also ensure the stabilization of a possible q=3 NTM. On the other hand, extending the steering capabilities of the mirrors up to this surface would imply that the q=3/2 surface cannot be reached during the current ramps, due to the availability of only a limited total steering range. Similar considerations apply even more to the case of beams aiming at the plasma pedestal.

The impact of turbulent transport of current-carrying electrons on the broadening of the EC profiles has been quantified through a detailed gyrokinetic determination of the related velocity-space-resolved diffusion coefficient, for both q=3/2 and q=2 surfaces for a time slice at the end of the flattop phase of the standard scenario. For slightly suprathermal, passing electrons, as those involved in ECCD under ITER conditions, diffusion coefficients of the order of 0.1-0.2 m^2/s are found. These numbers should be interpreted as an upper bound, as the simulations were performed without island, inside which the turbulence level is likely reduced. According to previous Fokker-Planck simulations, a radial electron transport of this size implies a moderate beam broadening due to electron transport (of the order of 10 %).

Diagnostics

ITER Bolometer Diagnostic

The activities within the ITERBolo project continued in 2014 with the optimisation of the collimator design for bolometer cameras. As it became obvious towards the end of the period funded by national funds that improvements in the camera design to reduce stray light and reflections cannot be achieved by the evaluation of lab measurements alone, in collaboration with the Institute for Measurement Systems and Sensor Technology of the Technical University of Munich Monte-Carlo ray tracing methods were implemented for the simulation of the collimator characteristics. In a first approach, simulation parameters related to material properties and surface finishings have been identified by comparing simulations to measurement results of the IBOROB test facility (see chapter 18). In a next step, simulations using the optimised parameters have been applied to various collimator geometries. This allowed identifying quantitatively contributions to stray light and reflections. In particular for the demanding narrow viewing cones of 1° in toroidal direction the deviations in the transmission function from the one expected due to the design turned out to result from a combination of reflections on the inside of apertures and from

light rays passing between apertures. Thus, improvements in the transmission function could be expected by optimising the thickness and number of apertures within a collimator. This led to a revised design featuring 16 apertures of only 0.5 mm thickness as shown in figure 2.
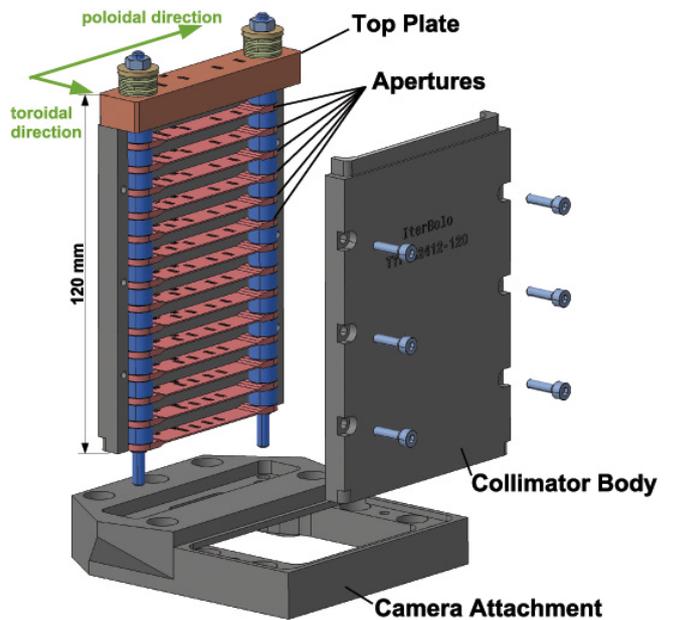
Figure 2: Optimised design for a bolometer collimator with 16 apertures to achieve viewing cones of 1° in toroidal direction.

Figure 3 shows the comparison of the transmission functions as expected in an ideal case (red), measured on a previous prototype (blue) and expected now for the optimised design (green) as presented in figure 2.
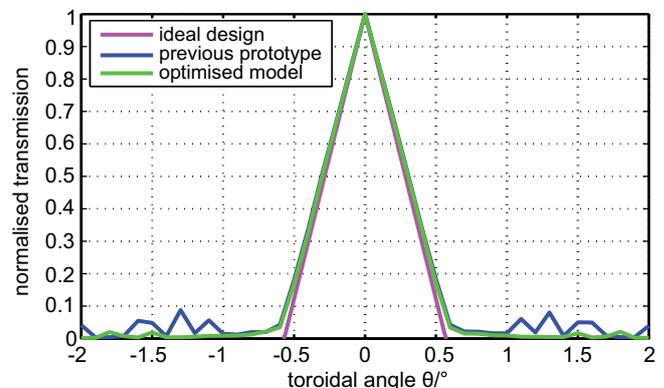
Figure 3: Comparison of simulated transmission functions.

The experience gained in the design of bolometer cameras for ITER has been used to design two new cameras for extending the bolometry system at ASDEX Upgrade. Both cameras will be used to increase the coverage of lines-of-sight (LOS) in the divertor region and around the X-point,

regions featuring strong radiation phenomena and which are of particular interest for transport and power balance studies. A pin-hole camera with 4 LOS observes the outer divertor from the high-field side. A collimator camera with 28 LOS is placed beneath the roof baffle and observes inner and outer divertor regions as well as the X-point.

At the end of June the first Grant within the Framework Partnership Agreement (FPA) for the development of the ITER Bolometer Diagnostic between the ITERBolo consortium (led by IPP) and F4E could be signed. This first Grant is focused on the detailed assessment of the current system status and the planning of all activities within the FPA for the next four years. The first phase of this Grant was completed until the end of 2014. It consisted in the review of the large amount of documentation with ITER and F4E in order to extract the information on requirements, load specifications and interfaces relevant for the bolometry. Additionally, a functional breakdown analysis was carried out to define the main functions and sub-functions of the bolometer diagnostic as well as the flow of signals and the impact of environmental hazards and constraints in an abstract way to prepare the basis for the system level design.

As currently there is no sensor available which is proven to comply with all requirements of ITER operation, a particular focus was laid on the review of the sensor technology available. Sensors based on Au-absorbers on Mica substrates with Au-meanders have proven their capability to cope with high environmental temperatures in JET. However, issues related to radiation stability and reliable detection of high energy photons at sufficient sensitivity are still unresolved for these sensor types. Also, the intrinsic time constant for the heat transfer from absorber to meander does not allow for meeting the time resolution required in ITER. On the other hand, the results from the ITERBolo project demonstrate sensors featuring thick Pt-absorbers on SiN-membranes with Pt-meanders which can detect high energy photons at sufficient sensitivity, meet time resolution requirements and have a high potential for irradiation stability. However, they are not mechanically stable at high operating temperatures. Based on the extensive review of properties for the various candidate materials for absorber, substrate and meander, a recommendation is being compiled for the optimum R&D strategy to follow for arriving at a suitable bolometer sensor for ITER. In order to meet the demanding time constraints of the ITER schedule, parallel investigation of candidate detector types is proposed. Based on the JET-type sensor, a prototype with Au-absorber on a Mica substrate but with Pt-meanders will try to combine the mechanical stability at high temperatures with good sensitivity. However, the relatively long heat transfer times will still be an issue to be solved by complex evaluation methods. On the other hand, based on the results of the ITERBolo project the development of a sensor prototype based on Au-absorbers on SiN-membranes with Pt-absorbers is suggested.

Initial tests promise sufficient mechanical stability which would thus lead to a sensitive sensor meeting all ITER-requirements. A further alternative development path would be to support the absorber not by a thin membrane, but using flexure hinges as suggested at the end of the ITERBolo project (see Annual Report 2013).

Based on these results, the R&D plan for the further development of the ITER bolometer diagnostic will be defined in close cooperation with F4E and ITER. The basis for planning the activities within the FPA has been set. For the sensor development, additional contracts will be placed by F4E also outside the FPA in order to assure a reliable and competitive supply chain. These will have to be supported by the ITERBolo consortium, too.

ITER Diagnostic Pressure Gauges

The planning phase (Specific Grant 01) for the whole FPA-364, which covers the R&D activities for the ITER Diagnostic Pressure Gauges (DPG) within the framework contract with F4E, was successfully concluded in the first quarter of 2014. Two phases of subsequent engineering and testing activities are now planned in order to reach the optimal design within the given time and cost constrains. A total of eight Specific Grants (SG) have been planned and a first draft of the respective Work Breakdown Structure (WBS), schedule and resource estimate (man power and equipment/facilities) has been produced. The subsequent SGs focus on the topics of : System level design & further design of sub-systems, Engineering analyses & performance modelling, Basic testing, Advanced design and specification, Advanced Modelling and Advanced testing & Preparation of fabrication.

Apart from the complete project plan, the initial set of measurement specifications for the DPG was reviewed during SG01 in view of IPP experience with the pressure gauge technology, which constitutes the base (or starting point design) for the DPG, the so called ASDEX pressure gauge. It was concluded that there is no evidence for an a priori impossibility to reach the required performances. The DPG system is also subject to a set of requirements mainly specified by IO in the ITER Sub-system requirement document (SSRD). At present, the SSRD contains a list of both system description and requirements. However, they often fail to specify the origin of the requirements. The SSRD was reviewed and, in some cases, corrected, improved and supplemented some of the requirements by making use of the review of the technical documentation and in-house expertise. The SSRD contained a preliminary list of interfaces with other ITER components. This has been thoughtfully reviewed and agreed in close collaboration with F4E and IO. For the identified interfaces, Interface Control Documents and Interface Sheets have been produced or updated. A preliminary set of interface specifications was provided in these documents which will be further detailed and completed during SG03.

Some preliminary R&D was also conducted in order to early identify critical issues and be able to plan appropriate actions. As prerequisite for this task the starting point design, the ASDEX Pressure Gauge, was reviewed in view of the ITER applications. In the current design the electron source needed for ionisation is obtained using a hot thick filament (typically of doped tungsten material) which has operational temperatures between 1400 and 2000 °C. The filament is subject to (mainly vertical) j×B forces and is easily recognised as the most critical component. Thus initial R&D focused on the following aspects linked to the filament design:

a) Literature research for filament material properties and alternative materials covering e.g. material property data package of doped tungsten and other relevant materials as input for engineering analyses. This data is essential for realistic finite-element modelling as part of the optimisation properties. Unfortunately, within the searched literature, the needed information could not be found. It may be possible that, some industry dealing with these materials, possess such data in an unpublished, perhaps protected, form. An attempt should be made to contact major producers and establish collaborations or even, if possible, buy such data.

b) Study possible designs for fixation of filament (including review of related technologies available in the market if specifications are made freely available). The fixation of the filament to the head baseplate has a strong impact on its mechanical stability. Some ideas were explored but no convincing solution has been found. This activity will have to be continued in future grants.

c) Finite element analysis (ANSYS-like) of present and optimal filament shape, with respect to thermo-mechanical properties (high temperature and J×B forces). Using the pure W thermo-mechanical material properties as working assumption, it was found that the present filament shape may be subject to plastic deformations at magnetic field of 8 T and for filament currents above 18 A. Hence, some problems at the corner of the operations space are possible. This finding has triggered the search for an optimal filament shape which has led to some promising design although in need for further analysis and experimental validation.
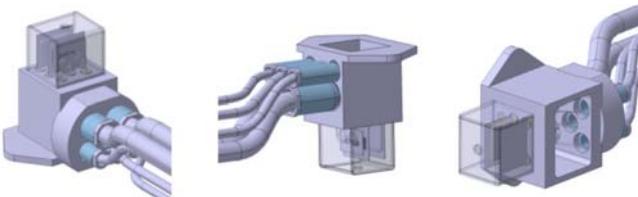
Figure 4: Design study of mounting brackets for the ITER diagnostic pressure gauges.

Finally, a "pre-conceptual design" study of DPG head mounting brackets was performed (see figure 4). The gauge heads are subject to several requirements and constraints on the way they have to be mounted to vacuum vessel structures. None of them, fortunately, seem to constitute an important obstacle for the future development.

In November 2014 the kick-off meeting for SG03 and SG04 took place in IPP a few weeks after signing the contracts. SG03 focuses, initially, on the justification of design axioms (ASDEX pressure gauge) and system level design (SLD). An initial set of system architecture (for both gauge head and electronics) was elaborated and agreed with F4E – subject to further SLD – in December 2014. SG04 (14 months duration) deals with the FEM thermo-mechanical analysis of the DPG components and the numerical simulation of the gauge performance. Most of the foreseen work will be carried out by the engineering company Sgenia, which is part of the consortium coordinated by IPP. The ionisation gauge simulation code originally developed at IPP was successfully transferred to Sgenia's computer cluster and is currently parallelised and improved to allow faster runs and geometrical optimisation of the DPG design.

Control and Data Acquisition (CODAC)

Since summer 2014 IPP leads a consortium consisting of CREATE/Univ. di Napoli (I), CCFE (UK), CEA (F) and General Atomics (US) to assist the ITER Organisation (IO) in the development of the ITER Plasma Control System (PCS) and help prepare the Preliminary Design Review (PDR) expected in 2016/2017. The Task covers five major activities, which are the discharge initiation, scenario control and termination, the disruption and runaway analysis, the development of support functions for error field and shape identification, the architecture concept development, and the development of a control database as central control information repository. All activities focus on the first and initial plasma phases of ITER. The kick-off meeting and the first general progress meeting were held in Cadarache in July and December.

The development activities for the Plasma Control System Simulation Platform (PCSSP) were continued with the partners General Atomics (US, lead) and CREATE/Univ. di Napoli (I), and another task order was issued to the consortium to mature the prototype implementation which had been presented to IO in December 2013.

Simulations for the Pre-thermal Quench Phase of Disruptions in ITER

The duration of the pre- thermal quench (pre-TQ) phase is a design parameter of the ITER Disruption Mitigation System and must be known with good accuracy. The simulation of the pre-TQ phase during massive gas injection (MGI) in ASDEX Upgrade (AUG) with the transport code ASTRA-STRAHL has been carried out in 2014 in the framework of a contract between IPP Garching and the ITER organization.

This work was the first benchmark of ASTRA against detailed MGI experimental measurements. The main focus of these simulations was to determine the dependence of the pre-TQ duration and of the fraction of radiated power on different plasma and gas parameters.

A dedicated experiment, consisting of 11 discharges, was carried out on AUG to document the evolution of the pre-TQ for different plasma (energy and safety factor) and gas (quantity and type; valve position) parameters. The modeling has been set up to exploit the ASTRA-STRAHL code coupling, in particular the multi-species impurity calculations and the self-consistent evolution of plasma temperatures, densities, and current density. The physical assumptions made in the model are presently the most reasonable and include a mock-up of MHD-induced radial transport, which could explain some features observed in the experiment, as e.g. spreading and acceleration of the radiation front. ASTRA-STRAHL neglects the plasma poloidal/toroidal asymmetry, while in reality the parallel propagation and perpendicular penetration of the gas is a 3D phenomenon, accompanied by 3D MHD activity and possible equilibrium distortion.

The simulations – particularly the time scale of the process – show rather good quantitative agreement between modeling and experiment. Energy, safety factor, gas species and gas mixture dependencies have been studied, leading to the identification of physics mechanisms responsible for the observations.

In conclusion, the use of a 1D transport code, despite the simplifications in terms of geometry and MHD stability, has been shown to reproduce experimental observations – and therefore it is suitable for modelling the ITER pre-TQ – probably because of the very "simple" and localized nature of the radiative phenomenon (at least for the high-Z MGI).

Advancement of Young Scientists

The FUSENET (European Fusion Education Network) association, a legal entity created as a continuation of the project funded by the European Commission to support the education of scientist and engineers in the fusion area, was successful in its negotiations with the Commission and EUROFusion to obtain funding to further the stated goals.

In November, it organised a Ph.D. event, attended by 125 participants from all over Europe. In February 2015, FUSENET will have its fourth yearly general assembly. At the meeting, thirteen students from nine different countries in Europe will come together to receive their European Fusion Master's and Doctorate Certificates.

IPP is strongly involved in FUSENET, among others through membership in the Board of Governors and the Academic Council.

In 2014, nine fellowships have been granted in the third cohort of the Fusion-DC (Erasmus Mundus funded) programme. For one of these doctoral students IPP is the home institute, for another one IPP is the host institute.

Scientific Staff

ECRH: C. Angioni, F. Casson, O. Maj, E. Poli, H. Weber, H. Zohm; Members of ECHUL-CA and F4E Teams.
ICRF: J.-M. Noterdaeme.
ITERBolo: C. Gliss, N. Homner, M. Kannamüller, J. Koll, H. Meister, E. Neitzert, F. Penzel, T. Sehmer, S. Shalaby, A. Sigalov; P. Detemple, K. Mpoukouvalas, S. Schmitt (IMM); S. Kalvin, K. Kotrocz, A. Pataki, J. Szücs, G. Veres (Wigner RCP); D. Antok, T. Fekete, G. Gyenes, L. Tatar (MTA EK).
ITER-CODAC: G. Neu, C. Rapson, G. Raupp, W. Treutterer.
ITER-DPG: H. Eixenberger, M. Kannamüller, J. Koll, H. Meister, E. Neitzert, A. Scarabosio, C. Vorpahl; P. Bartholomeus, A. Lobato, O. Paz, D. Portillo, G. Roman (Sgenia Solutiones).
NNBI: S. Briefi, U. Fantz, P. Franzen, R. Friedl, M. Fröschle, B. Heinemann, W. Kraus, U. Kurutz, C. Martens, A. Mimo, S. Mochalskyy, R. Nocentini, S. Obermayer, G. Orozco, M. Ricci, R. Riedl, B. Ruf, L. Schiesko, C. Wimmer, D. Wünderlich; F. Bonomo (RFX Padova).
FUSENET: J.-M. Noterdaeme, H. Zohm.
Fusion-DC: A. Medvedeva, J.-M. Noterdaeme, L. Vela, H. Zohm.

DEMO

DEMO Design Activities

Head: Prof. Dr. Hartmut Zohm

Operating Scenarios for a Tokamak DEMO

As in previous years, these studies aim at assessing a range of possible operating scenarios of a tokamak DEMO by studying two specific cases, a pulsed DEMO based on conservative assumptions and a steady-state DEMO with more advanced assumptions in both physics and technology. This effort is carried out in collaboration with EU partners, largely as part of the PPP&T work programme.

Substantial effort has been devoted to assess the consistency of plasma scenarios for the pulsed DEMO device. Combined ASTRA/STRAHL/TGLF simulations have been performed, which show that the kinetic profiles are mostly determined by stiffness (self-similar gradient lengths) and boundary condition (pedestal top values). This puts some constraints on the minimal pedestal top temperature (>7 keV) to obtain relevant fusion power and gain margin of operation with respect to impurity seeding. The latter has also been studied to clarify which impurity mix could lead to optimized core cooling/edge radiative losses. The impact of core radiation on confinement has at the same time been studied, leading to the result that core radiation is not deleterious to confinement, unless radiative losses are concentrated in the region where the alpha-heating power is deposited.

The high level of core radiation necessary for a tokamak DEMO will also lead to additional power load of the first wall. This has been studied in the framework of a PPP&T project. For the calculation of the heat flux density a Monte Carlo approach based on ray tracing is applied.

The scenario used in these studies contains radiation by the impurities Ar, Xe and W, as well as Bremsstrahlung and Synchro-

The 'DEMO Design Activities' project focuses on aspects of physics and technology relevant for tokamak and stellarator designs, in line with the unique position of IPP following both lines. Many of the activities are carried out under the EUROfusion PPP&T Programme, where substantial EU collaborations exist. On the national level, the German DEMO Working Group joining scientists from FZJ, IPP and KIT serves to strengthen collaboration and strategic planning.

tron radiation. In order to give an upper limit of the heat load, it is assumed that all power transported by the plasma across the separatrix is radiated in the scrape-off layer, i.e. the radiated power fraction is 100 % (realistic estimates presently are in the range of 95 %). For this radiation an exponential decay is assumed leading to a strong contribution around the X-point. Figure 1(a) shows the poloidal radiation distribution calculated from all radiation sources. The corresponding heat flux density on the first wall is shown in figure 1(b). The top and bottom of the first wall receive the highest heat load with a value of around 0.45 MWm^2. Designs of the DEMO blanket will have to take this additional load into account.

Based on reactor-like current profiles, a verification of bootstrap current models has been carried out comparing existing formulas to a first-principle based drift-kinetic code. The comparison has allowed to gain confidence on possible simplified implementation for system codes used for global reactor optimization. This is especially important for the steady-state DEMO, where the bootstrap fraction crucially determines the required current drive power. Studies of such a steady state DEMO based on the 'Improved H-mode regime' have been carried out, assuming a total β_N of 3.8 (thermal β_N of 3.1) and an H-factor of 1.15 (not applying any radiation correction). Under these conditions, and at aspect ratio around 3, the CD power required for Neutral Beam Current Drive (NBCD) at 1.5 MeV is of the order of the power foreseen in ITER phase 2, i.e. 120 MW. Plasma elongation plays a crucial role in achieving the needed bootstrap fraction since it enters in a favorable manner in several ways, most notably in increasing β_p for given β_N, and the operational point mentioned above assumes a κ_x of 1.8. These 0-d studies, carried out within the PPP&T collaboration using the PROCESS code (CCFE) will now be substantiated by an assessment of CD efficiencies using realistic profiled.

Heating and Current Drive

Concerning the stabilisation of Neoclassical Tearing Modes (NTMs) by Electron Cyclotron Current Drive (ECCD), the analysis started last year has been extended for realistic profiles and launching geometries, confirming the previous finding that in the pulsed DEMO, a relatively low power will be sufficient to stabilise NTMs, of the order of 2.5 (3.3) MW for the (3,2) ((2,1)) NTM in the case of flat density profiles. However, for peaked density, these numbers are substantially higher, i.e. 9.5 (11.6) MW, but still this finding means that only a fraction of the installed power (estimated to be of the order of 50 MW) will be required for NTM control.


(a) Radiation distribution.
(b) First wall heat load.

Figure 1: Modelled wall loads due to electromagnetic radiation in a highly radiative DEMO scenario.

For the DEMO Ion Cyclotron Range of Frequencies (ICRF), the full-wave TORIC code has been extended to account for wave absorption by energetic slowing-down alpha particles generated by fusion reactions. With this new version of TORIC, an extensive exploration of the options for current drive with radio-frequency (RF) waves in the ion-cyclotron (IC) range of frequencies for the steady-state and pulsed scenarios presently foreseen in DEMO has been done. These studies show that with an antenna located in the outer midplane, either very low frequencies (<20 MHz) or intermediate frequencies (e.g. 50-70 MHz, depending on B_t) have to be chosen to avoid absorption on the fusion-born α-particles. In these frequency windows, Fast Wave Current Drive (FWCD) can have efficiencies comparable to other H&CD systems. However, as for ECCD, the FWCD efficiency is highest in the centre and off-axis values will be lower due to the lower temperature and the reduction of efficiency by trapped particles. These results confirm earlier conclusions (see 2012 Annual Report).

Also in the ICRF area, work has been started to assess the possibilities to integrate an ICRF antenna in the DEMO blankets. Here, aspects of mechanical engineering as well as neutronics will be examined in a collaboration with Gent University in Belgium.

For the DEMO Neutral Beam Injection (NBI) system, RAMI issues were addressed concerning the RF generators of the RF-driven ion sources. In current systems the power is supplied by tube-based, self-excited RF generators. Efficiency, reliability and matching properties can be improved substantially by replacing these generators by solid state amplifiers, which are based on transmitters used for AM broadcasting. Compared to the tube based generators the efficiency increases from 55 % to more than 90 % and good matching can be achieved for any load. At IPP such a 1 MHz/75 kW amplifier was purchased and has been in routine operation for more than one year with the negative ion source of the BATMAN test stand. Automatic frequency matching and power adjustment is being developed in co-operation with the industrial partner.

Stellarator DEMO Studies

Efforts from the last year to develop stellarator-specific systems codes model have continued. The developed models were implemented in the PROCESS framework – a code maintained at CCFE, UK, which is widely used in the EU for tokamak DEMO design studies. Thus, the stellarator module was extensively tested and in detail verified for different test cases, such as SOL modelling of W7-X with a simplified exhaust model. The verification study showed very good agreement establishing confidence for the use and application of the stellarator module. First studies have been started to characterize the design window of a HELIAS power plant which led to an important first result: The cost level of a HELIAS power plant is comparable to that of an equivalent tokamak. Further and more detailed systems

studies are ongoing including core radiation scenarios and their impact on the ignition window. As an example, in figure 2, the Plasma Operation Contour Analysis is presented for a standard HELIAS scenario with the associated Cordey-Pass on the start-up path to ignition. The required external heating power is very sensitive to the confinement time. Likewise, it is also sensitive to impurities in the start-up phase, e.g. tungsten. Having a radiation maximum at temperatures around 2 keV, the increased radiation losses at low temperatures must consequently be compensated by increased external heating power. Since the confinement properties of the plasma play an important role in these studies, efforts were made to improve the predictive transport models. As it is anticipated that turbulent transport will play a significant role in neoclassically optimized HELIAS configurations, the impact of ITG induced transport has been started to be investigated.

From the stellarator engineering point of view, a new collaborative project has been started with KIT which aims at the development of a technically feasible solution of a breeder blanket configuration for the HELIAS power reactor. This year's activity has been devoted to the development of a 3D neutron source model for the HELIAS. The neutron source distribution has been produced on the basis of a 3D Fourier description assuming nested flux surfaces with constant temperature and density. The HELIAS neutron source model has been adapted for Monte Carlo transport calculations with the MCNP code via an external source routine to represent a cumulative probability distribution for the emission of source neutrons. This approach was successfully tested, verified, and shown to be suitable for predicting the neutron source distribution in the HELIAS plasma chamber. It can be thus applied in the forthcoming neutronic analyses for the design of a breeder blanket configuration for HELIAS.
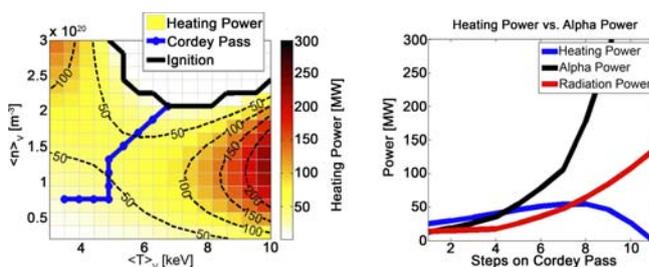
Figure 2: Plasma Operation Contour Analysis for R=22 m, B=5.5 T, P_{fus}=3 GW, and 10 % He-concentration with colour-coded illustration as well as isocontours of required external heating power for power balance. In blue (left) is highlighted the "Cordey-Pass" with minimal heating power for self-sustained ignition (white area). The "Cordey-Pass" is projected along its "steps" with the associated heating, alpha, and radiation powers (right).

Scientific Staff

C. Beidler, R. Bilato, R. Brambilla, L. Casali, A. Dinklage, E. Fable, U. Fantz, R. Kemp (CCFE), W. Kraus, K. Lackner, J.-M. Noterdaeme, E. Poli, F. Schauer, B. Sieglin, G. Tardini, F. Warmer, R. Wenninger, R. Wolf, H. Zohm.

Plasma-Wall Interactions
and Materials

Plasma-Wall Interaction

Head: Prof. Dr. Rudolf Neu

Within the project "Plasma-Wall Interaction" the areas of plasma-surface-interaction studies, material modification under plasma exposure, development of new plasma-facing materials and their characterisation have been merged to form a field of competence at IPP. The work supports exploration and further development of the fusion devices at IPP and also generates basic expertise with regard to PFC-related questions in ITER, DEMO and future fusion reactors.

Surface Processes on Plasma-exposed Materials

Investigation of Low-temperature Ar-H$_2$ Laboratory Plasmas

A rate equation model was devised to study the ion composition of H$_2$-Ar plasmas with different H$_2$-Ar mixing ratios. The model was applied to calculate the various ion densities, the wall loss probability of atomic hydrogen, and the electron temperature T$_e$. The calculated ion densities were compared with experimental results determined by comprehensive plasma characterisation efforts including analyses using an energy-dispersive mass spectrometer (plasma monitor), a retarding field analyser, optical emission spectroscopy, and a Langmuir probe. The production and loss channels of all ions were discussed in detail. With the production and loss rates the density dependence of each ion species on the plasma parameters was explained. The primary ions H$_2$$^+$ and Ar$^+$ which are produced by ionization of the background gas by electron collisions are effectively converted into H$_3$$^+$ and ArH$^+$.

Furthermore, the influence of the electrode cover material on selected line intensities of H, H$_2$, and Ar were determined by optical emission spectroscopy and actinometry for different electrode cover materials. Hydrogen dissociation degrees for the considered conditions were determined experimentally from the measured emission intensity ratios. The surface loss probability of atomic hydrogen, β_H, is correlated with the measured line intensities, but without knowledge of the atomic hydrogen temperature, β_H cannot be determined exactly. However, ratios of β_H values for different surface materials are in first order approximation independent of the atomic hydrogen temperature. Our results show that β_H of copper is equal to the value of stainless steel, β_H of Macor and tungsten is about 2 times smaller and β_H of aluminium about 5 times smaller compared with stainless steel. The latter ratio is in reasonable agreement with literature. The influence of the atomic hydrogen temperature on the absolute value is thoroughly discussed. For an assumption of the atomic hydrogen temperature of 600 K, a β_H value for stainless steel of 0.39±0.13 was determined.

Investigation of Coupled Sputter-diffusion Effects of the Tungsten-iron Model System under Deuterium Ion Bombardment

In the ongoing research for plasma-facing materials suited for fusion reactors it is mandatory to consider the effects of the intended operation temperature of the first wall (around 550 °C) on the performance. At these temperatures migration becomes important in many mixed materials. To take these diffusion effects into account the Monte Carlo code SDTrimSP was enhanced with the capability to compute solid-state diffusion based on Fick's laws. This allows for the first time to consider the coupled effects of implantation, sputtering and diffusion in an integrated way. The new code version SDTrimSP 5.07 has been validated by benchmarking with analytical results from several model systems and by cross-comparison of the simulation data of a tungsten-carbon system with published data. For the iron-tungsten system with diffusion parameters D$_0$=0.015 m^2/s and E$_{act}$=287 kJ/mol the dependence of sputter yield, reflection yield, surface enrichment, and width of the enrichment region have been studied as function of sample temperature in the range of 273-1073 K and deuterium energies in the range of 100-3000 eV. For temperatures below 723 K and deuterium fluxes of 10^{20} at/(m^{2}s) no influence of iron diffusion on the observed quantities can be observed and the results match conventional SDTrimSP simulations. However, for temperatures at and above 773 K a significant, time-, fluence- and energy-dependent change of the sputter yield and surface enrichment can be observed. For example, the calculated steady-state surface enrichment of tungsten of a Fe90W10-sample system under 3 keV deuterium bombardment drops from a tungsten surface concentration of 33 at% at 773 K to less than 17 at% at 1073 K. In contrast to this reduction with increasing temperature the width of the enriched zone (taken as the depth where the concentration deviates less than 2 at% from the initial concentration) is growing from about 1 nm at 773 K to more than 20 nm at 1073 K. An interesting aspect is the influence of the initial composition on the absolute enrichment. For a sample at 773 K with a low initial tungsten concentration of 2 at% the surface tungsten concentration increases under 3 keV deuterium bombardment to slightly below 8 at%, an absolute increase by less than 6 at%. Under identical conditions a Fe90W10 sample shows an increase in tungsten concentration by more than 20 at%. Nevertheless, this considerable difference in enrichment is reduced to about 3 at% at 973 K.

Migration of Materials in Fusion Devices

Experiments with the New Divertor Manipulator System DIM-II in ASDEX Upgrade

Parallel to the installation of massive tungsten target tiles in the outer divertor of ASDEX Upgrade a new manipulator system (DIM-II) was designed, assembled and integrated in the tokamak, which allows exposing two adjacent test target tiles at the outer divertor plate.

The test tiles can be exchanged by means of an airlock system without breaking the vacuum of the ASDEX Upgrade vessel. This allows detailed studies of the influence of plasma-material interactions on the retrieved test tiles using a multitude of ex-situ diagnostics available in the surface analysis laboratories of IPP. Following successful commissioning in the experimental campaign 2014 the first experiment aimed at investigating erosion properties of tungsten. Because the sputtering yield of tungsten varies with the local angle of incidence of projectile ions and because of shadowing effects, surface roughness is expected to increase the erosion rate of tungsten target tiles, particularly at oblique angle of the magnetic field to the tile surface. To quantify the influence of surface roughness on the tungsten erosion yield, W marker layers were deposited on graphite samples with pre-characterised surface roughness. In addition, samples with shallow trenches were prepared. The bottom surface of the trenches provides a shadowed area were re-deposited material is protected from re-erosion, which is essential to quantify deposition rates.
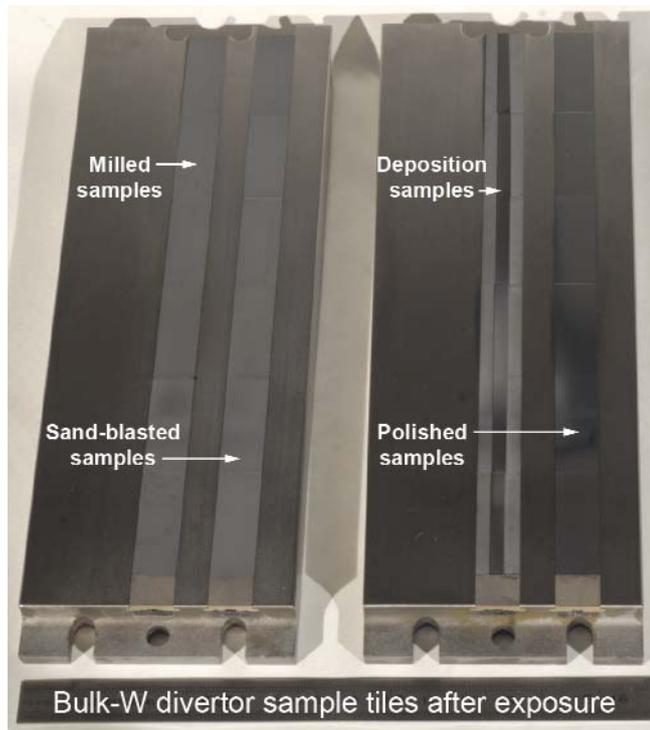

Figure 1: Custom bulk tungsten tiles with tungsten erosion and deposition marker samples installed.

The samples were embedded in two custom bulk tungsten tiles equipped with grooves for insertion of smaller samples (figure 1). Net-erosion rates were quantified by measuring the thickness of respective marker layers before and after plasma exposure using ion beam analysis. This method provides in the same measurement also quantitative information on the deposition rate of other plasma impurities.

Gross-erosion rates were measured spectroscopically from the spectral intensity of the neutral tungsten emission line at 400.9 nm. The post mortem investigations of the samples are ongoing. Both gross- and net-erosion are essential parameters for estimating the life-time of divertor target plates, which contribute significantly to the operating costs of a fusion reactor.

A second experiment with the new manipulator system was performed to investigate the penetration of hot ions in ELM filaments into areas, which are intentionally shadowed from plasma exposure to protect leading edges at gaps between target tiles or tile castellations. Hot ions are expected to partially enter such shadowed zones because of their larger gyro orbit radii. This effect was studied by combining measurements of the lateral distribution of power flux to the divertor target tiles with measurements of the corresponding distribution of tungsten erosion measured by exposure and ex-situ ion beam analysis of tiles with W-marker layers. First results indicate weaker gap penetration as predicted by single-particle orbit calculations. Further analysis is ongoing to confirm these findings and to compare the observations to more sophisticated modelling using PIC simulations.

Size Distribution and Inner Morphology of Dust Particles in ASDEX Upgrade

Dust formation, dust transport as well as final dust distribution inside the device have implications on plasma operation and safety. In order to elucidate which different types of dust particles appear, which processes produce dust particles, and which properties these particles have, dust collection has been performed at AUG particles since 2007 using a closable box holding a Si plate inside. This arrangement allows the collection of dust which is not exposed to plasma after its arrival on the deposition plate. Between three and five collectors at different location were installed in the torus collecting campaign integrated dust particles. This collection method is meanwhile adopted in JET, DIII-D and LHD.

The particles on Si plates are analyzed by optical and scanning electron microscopy (SEM with FIB and EDX) regarding their areal density, shape, elemental composition, and inner and outer morphology. More than 10000 particles are usually analyzed on each Si plate applying an automated routine which allows obtaining statistically significant size distributions of classes of dust particles distinguished by their elemental composition and shape. It turned out that six classes are sufficient to describe 90 % of all particles analyzed: C, B, Fe, Cu dominated irregularly shaped particles and W dominated spherical and non-spherical particles. The size distribution of each dust particle class is best described by a log-normal distribution allowing an extrapolation of the dust volume and surface area. Only for the W-dominated spheroids the maximum of the size distributions is with about 1 μm observed above the resolution limit of 0.28 μm.

The amount of W-containing dust is extrapolated to be less than 300 mg on the horizontal areas of AUG.

By far most of the W-dominated spheroids consist of a solid W core, i.e. solidified W droplets. A part of these particles is coated with a low-Z material; a process that seems to happen presumably in the far scrape-off layer plasma. In addition, some conglomerates of B, C and W appear as spherical particles after their contact with plasma. By far most of the particles classified as B-, C- and W-dominated irregularly shaped particles consist of the same conglomerate with varying fraction of embedded W in the B–C matrix and some porosity, which can exceed 50 %. The fragile structures of many conglomerates confirm the absence of intensive plasma contact. Both the ablation and mobilization of conglomerate material and the production of W droplets are proposed to be triggered by arcing.

Determination of the ^{9}Be(p,p$_0$)^{9}Be Backscattering and ^{9}Be(p,d$_0$)^{8}Be Nuclear Reaction Cross-sections

The quantitative analysis of beryllium with ion-beam analysis methods, for example in samples from JET, requires the precise knowledge of the scattering and nuclear reaction cross-sections. Unfortunately cross-section data for beryllium are scarce and only available at a few angles and in limited energy ranges. The cross-sections for ^{9}Be(p,p$_0$)^{9}Be backscattering and for the ^{9}Be(p,d$_0$)^{8}Be nuclear reaction were measured at a laboratory scattering angle of 165° in the energy range from 400 to 4150 keV. The absolute accuracies are about 4 % for the backscattering and 15 % for the nuclear reaction cross-section. The derived cross-sections were benchmarked in the energy range 1100-4100 keV by comparison to measured spectra from bulk beryllium. The cross-section data have been made available as R33 cross-section data files and can now be used by simulation programs for the analysis of JET samples.

Hydrocarbon Film Deposition inside Cavity Samples in Remote Areas of the JET Divertor

The deposition of hydrocarbon films was studied with cavity samples in remote areas of the inner and outer JET divertor and below the divertor septum during the 1999-2001 and 2005-2009 campaigns, i.e., during JET operation with full carbon walls. Thick hydrocarbon films were formed inside the cavities with high D/C ratios close to 1. The formation of these films is mainly due to sticking of hydrocarbon particles with surface loss probabilities larger than 0.6. The observed surface loss probabilities depend on the position in the divertor and vary during different campaigns. Low sticking species with surface loss probabilities $\beta < 0.01$ cannot be excluded, but they have only a very small contribution to the layer formation in the divertor. The particles responsible for hydrocarbon layer formation originate predominantly from the divertor strike points. This confirms the proposed model,

that thermal decomposition of hydrocarbon layers on divertor tiles by ELM impact is responsible for the formation of hydrocarbon layers in remote areas. Except for the septum cavity the deposition of beryllium inside the cavities was very low and showed a very different distribution from that of deuterium and carbon.

Tritium Inventory – Understanding and Control

Hydrogen Transport Studies in Tungsten

In present-day confinement devices fuel retention in tungsten first wall and divertor targets is very low and mostly limited to near surface areas due to the small ion fluences and the absence of neutron damage. However, in a future fusion device additional defects will be generated in the material which can potentially increase hydrogen isotope retention in tungsten. Neutron bombardment is expected to increase trap densities throughout the bulk so that the material can retain up to one atomic percent of hydrogen isotopes. Besides this steady state value, the key factors for describing the actual retention are the initial uptake of hydrogen, its permeation through the bulk and the release from the front and back surfaces. However, quantitative understanding of the processes involved is still incomplete. For example, deuterium (D) depth profiling of tungsten samples exposed to the high-flux linear plasma generator Pilot-PSI at DIFFER indicated a surprisingly low deuterium uptake which could not be described by the widely-used code TMAP 7. It was proposed that at the very high ion fluxes of about 10^{24} D/m^{2}s an adsorbed deuterium layer reduces the uptake, but pulsed operation and limited temperature control make interpretation of experiments and their modelling challenging. In order to benchmark existing codes, dedicated, well controlled laboratory experiments were conducted at the low-temperature plasma device PlaQ. In all studies so-called self-damaged tungsten was used to mimic neutron-damaged tungsten. For this, mirror polished, 2000 K-annealed, polycrystalline tungsten was implanted with 20 MeV W^{6+} ions at 300 K using the IPP tandem accelerator. The W ion fluence of 8×10^{17} m^{-2} corresponds to a peak damage level of 0.5 dpa. For this energy the damaged zone in these samples has a thickness of approximately 2 μm according to SRIM calculations.

In a first study we concentrated on the hydrogen uptake close to the plasma exposed surface by following the time evolution of the deuterium depth profile within the first 7.5 μm. Samples were exposed to a well characterized D plasma with a constant ion flux of ~10^{20} D/m^2 at a substrate temperature of 450 K. For one experimental series D loading was performed at floating potential to avoid additional damaging of the samples by impinging ions. Another series of implantations was conducted with a d.c. target bias of -100 V. For these two cases maximum ion energies are 15 eV and 115 eV, respectively.

Exposure times were varied from 15 minutes to 3 days corresponding to ion fluences from 8×10^{22} D/m² to 2.3×10^{25} D/m². Deuterium depth profiles were derived by D(^{3}He,p)α nuclear reaction analysis (NRA). For both series, NRA shows that with increasing D ion fluence a D retention front moves into the damaged zone with a maximum D concentration of around 1.4 at%. For the biased case penetration is about ten times faster. The diffusion-trapping code TESSIM was used to describe D uptake and release. From temperature programmed desorption (TPD) measurements of a set of identical samples the dominant de-trapping energies of 1.0 eV and 1.5 eV were derived together with pre-exponential factors of 1×10^{10} s^{-1} and 6×10^{10} s^{-1}, respectively, by measuring the shift of the desorption peak when varying the heating rate from 0.005 to 12 K/s. The initial D implantation profiles as well as the D reflection coefficients were calculated with the Monte Carlo code SDTrimSP. While these calculations are questionable for the floating-potential case they are considered reasonable for the biased case. Quantitative modeling of both series was possible within a factor of two by using a trap density profile fitted to the NRA results and a diffusion coefficient according to Frauenfelder corrected for the heavier mass of deuterium: $D_F=2.9\times10^{-7}$ exp($-0.39/k_BT$) m²s^{-1}. The modeling results clearly showed that the discrepancy observed for exposures in Pilot-PSI is a high-flux effect.

In a second study, we investigated the influence of the sample temperature on the hydrogen uptake at floating potential. The model predicts that between 300 and 400 K the progression of the diffusion front is independent from temperature, which means that the rate-limiting process is not diffusion, but filling of the traps for these energies and particle fluxes. At even higher temperatures, the diffusion front progresses faster because the increasing de-trapping rate reduces the number of trapped deuterium. Similar to the benchmark experiment above, the model describes the experiment within a factor of two without adjusting any free parameters. Better agreement could be obtained by introducing a temperature-dependent effective diffusion. However, a much lower activation energy of only ~0.1 eV (compared to 1 eV derived from the Pilot-PSI experiments) is sufficient to reproduce the observed temperature dependence. The reason for this temperature dependence is not immediately apparent and is currently under investigation.

In addition to these monoatomic retention experiments a third study concentrated on hydrogen isotope exchange in self-damaged tungsten to extend the latest work carried out with low-defect-density polycrystalline tungsten. Samples were prepared in the same way as in the studies described above (20 MeV W^{6+} at room temperature up to a peak damage level of 0.5 dpa) and exposed to D$_2$ and H$_2$ plasmas. First, defects were decorated at a sample temperature of 450 K by exposing the samples at floating potential to a deuterium fluence of 10^{25} D/m². For these fluences all available defects in the damaged zone are filled and the uptake saturates. Isotope exchange was then performed on these samples with H fluences ranging from 1×10^{23} to 2×10^{25} H/m² at the same flux, target temperature, and ion energy. Nuclear reaction analysis was applied to determine the remaining deuterium concentration up to a depth of 7.5 µm. Temperature-programmed desorption spectroscopy was used to determine the total amounts. Similarly to the previous experiments on the low defect density tungsten, hydrogen isotope exchange is very efficient even for these low ion energies. Deuterium removal by H clearly progresses from the surface into the damaged zone with increasing H fluence. The reverse sequence of hydrogen isotopes loading and exchange allowed the analysis of the replacing isotope and showed that the total number of hydrogen isotopes is preserved. The deuterium depth profiles reveal that retention of the replacing isotope starts at the surface even though all traps were filled before with the other isotope. In addition, both sequences together reveal the dynamics of the exchange. Surprisingly the removal of the retained protium by the incoming deuterium proceeds with the same speed as the uptake of deuterium in previously protium loaded tungsten. There is no isotope effect visible as can be seen in figure 2.
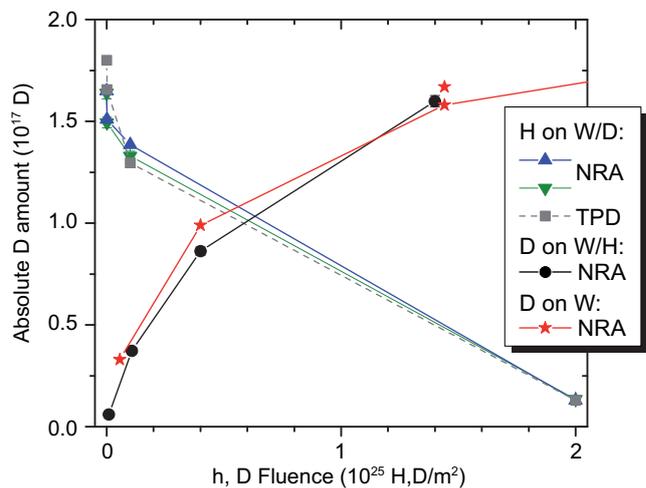
Figure 2: Absolute deuterium amounts retained in self damaged tungsten for three different experimental sequences: Uptake as function of D fluence for a) virgin and b) H saturated samples and deuterium removal as function of H fluence for deuterium saturated samples. All exposures were conducted at 450 K with energies below 5 eV/atom and a flux of 5×10^{19} m^{-2}s^{-1}.

In addition, the uptake of deuterium in hydrogen-free self-damaged tungsten is also plotted in figure 2. It proceeds with the same velocity, too. Obviously the commonly used assumption in modelling, i.e., that occupied traps are considered inactive is not valid. Therefore, presently used diffusion trapping codes must fail when describing the isotope exchange experiments at low enough temperature where no

de-trapping occurs because no interaction between the different hydrogen isotopes can take place. Only within the ion range the collision cascade can lead to de-trapping. But this effect is negligible for these experiments.

To explain the exchange in the bulk one can invoke an ad-hoc exchange between trapped and solute species which would not be visible in a mono-isotopic experiment. A possible explanation for this ad-hoc exchange would be traps that can contain multiple H atoms with fill-level-dependent de-trapping energies: Thus, adding H to a trap containing D would allow the D to de-trap with a lower energetic barrier.

A new diffusion trapping model based on fill-level-dependent de-trapping energies was proposed and implemented in the TESSIM code. The fill-level dependence of the de-trapping energies allows explaining the low temperature isotope experiments as follows: During the D-loading phase, all traps are filled to a maximum fill level in equilibrium with the solute D. Once the D incident flux is switched off the highest fill levels are depopulated by thermal de-trapping due to their low binding energies and the lack of solute D to repopulate them. This leaves the traps in the system filled with D to a level where the corresponding de-trapping energy is too high to de-trap at the current temperature. Once the H flux is turned on the traps are re-populated by the replenished solute population, now consisting dominantly of H. This means that now the traps are filled with a mixture of D and H in equilibrium with the solute population. This equilibrium is a dynamic one: De-trapping from low binding energy high fill level states into the solute is compensated by trapping from the solute into the traps. Therefore, there is an exchange between the mixture of D and H in the traps with the solute, i.e., there is isotope exchange even at low temperature where the highest detrapping energies (low fill levels) would normally not allow exchange with the solute.

Electrochemical Measurement of Hydrogen Permeation

Nowadays, a considerable amount of experimental data on hydrogen isotope diffusion and retention for a wide range of temperatures is available. Unfortunately, this is not the case for explicit measurements of diffusivity and permeability of hydrogen isotopes through tungsten, which may be a concern with regard to fusion fuel escaping through the reactor walls after being implanted into the first wall material. So far, well-accepted diffusion and permeation data exists only for high temperatures above 1100 K. Below this temperature data becomes increasingly sparse and scattered. However, thinking of water-cooled components, temperatures nearly down to room temperature are of interest. In order to measure the small permeation fluxes of hydrogen through tungsten at low temperatures of the order of 300 K, an electrochemical double cell for the measurement of hydrogen permeation was recently commissioned. We studied the temperature dependence of hydrogen permeability through a 3.5 µm thick,

magnetron-sputtered film of tungsten deposited onto a 25 µm thick palladium support. Because of its much higher permeability, palladium has a negligible effect on the permeation signal compared to tungsten. We found that in the temperature range between 265 and 333 K, there is indication for two different permeation channels with different activation energies. Due to the fine-grained, columnar microstructure of the W film, we attribute the permeation channel with the lower activation energy to fast transport along grain boundaries, which becomes increasingly important at low temperatures. The permeation channel with the higher activation energy dominates hydrogen transport at elevated temperatures and is attributed to permeation through bulk grains of tungsten. In addition, electrochemical permeation measurements through a 6.5 µm thick W film produced in the same manner as described above were compared with plasma-driven permeation through an identical W film in the HiFIT experiment at Osaka University. The data from both measurement methods agree well, but both show an unexpected temperature dependence, which is currently being investigated in more detail.

Deuterium Retention in Tungsten Films after Different Heat Treatments

Tungsten films deposited by magnetron sputtering on polycrystalline tungsten substrates were used as a model system to study the influence of the film microstructure on deuterium retention behavior. Different microstructures were produced by annealing the films up to recrystallization temperature and the corresponding structural changes were investigated by scanning electron microscopy combined with focused ion beam (FIB) cross sectioning. The influence of the induced structural changes on D retention was investigated by both nuclear reaction analysis and temperature-programmed desorption. D concentration in the investigated W films is higher than in polycrystalline bulk tungsten by a factor of 3. D retention in the films decreases as a function of annealing temperature. After annealing at 2000 K, FIB cross-section images reveal that cavities appeared at the grain boundaries within the film and at the initial interface between the W film and W substrate. This new microstructure strongly affects the D depth profile and leads to the increase of D retention. Although a further increase of the holding time at 2000 K or an increase of the annealing temperature to 2150 K lead to the reduction of the retained D amount, the D concentration in the recrystallized W films cannot be reduced to a level as low as that of bulk W recrystallized at 2000 K for 30 min.

Influence of MeV Helium Implantation on Deuterium Retention in Damaged Tungsten

Transmutation of wall constituents can result in the accumulation of helium in wall materials. The influence of helium on deuterium retention in damaged tungsten was investigated;

the damage was introduced into the material using self-ion implantation of 20 MeV W ions into W. Two different cases – low (0.02 dpa) and high (0.89 dpa) W damage levels were investigated. Helium was introduced into the resulting damage zone using MeV ion implantation. Different He fluences were applied to investigate the He concentration dependency between 0 and 1000 ppm. D and He retention was investigated by ion beam analysis and thermal desorption spectroscopy. No helium desorption under thermal treatment up to 2000 K was observed which means that such deep implanted He cannot be thermally released. In both high and low damage level cases He does not affect the maximum D concentration within the damaged zone. For the 0.89 dpa and high He fluence samples a significant enhancement of D concentration behind the damaged zone was observed. In the lower damage case D transport within the damaged zone and further into the bulk was slowed down significantly even by low He concentrations.

Flux Effect of the Surface Morphology and Deuterium Retention of Tungsten

Polycrystalline tungsten shows under various hydrogen plasma exposure conditions the formation of blisters on the surface. These blisters are partially plastic deformations and hydrogen gas-filled cavities beneath the surface. Therefore, their appearance has to be taken into account for assessment of the hydrogen retention. In a cooperation with FOM/DIFFER, the dependence of these surface morphological changes on the flux (and fluence) of the deuterium plasma exposure as well as the retained deuterium amount were investigated. The flux varied by four orders of magnitude; 10^{20}-10^{24} D/(m²s). The impact energy of the deuterium ions was fixed to ~40 eV/D and the samples temperature during exposure to around 500 K. For all experiments the same material grade was used. This is important because it was shown that the grade, i.e., the microstructure, has an effect on surface morphological changes and deuterium retention.

The samples exposed to low-flux up to 10^{26} D/m² are mostly smooth with only a few blisters (50-500 μm), while the samples exposed to high flux show a high number of smaller blisters (1-10 μm) and in addition even smaller protrusions. The measured depth profiles of the retained deuterium beyond the D implantation depth of about 10 nm are in agreement with the anticipated retention due to blisters: The low-flux samples show a roughly constant concentration of ~10^{-4} D/W up to the detection range of ~10 μm, while the high-flux samples have a higher concentration close to the surface (first microns) dropping with depth below the level of the low-flux samples. For extrapolation to ITER and beyond, beside the flux also the time available for diffusion at elevated temperature has to be taken into account for retention assessments.

Development of Oxidation-resistant Tungsten Alloys

Besides its use for divertor plasma-facing components, tungsten is also a candidate material to protect the main chamber surfaces of a thermonuclear fusion power plant against erosion by energetic hydrogen. A tungsten armor layer of about 1-2 mm thickness on the blanket of a future fusion demonstration reactor (DEMO) enables 5 years of operation without replacement. The use of pure tungsten could lead to a safety problem in case of a potential loss of coolant accident. Depending on the construction of such a reactor the nuclear decay heat could cause a temperature increase of the surface up to 1500 K within 30 days. Additional air ingress into the vessel could cause the oxidation of the whole tungsten armor. Since WO_3 is rather volatile at this temperature, part of the highly activated tungsten armor could be mobilized. To reduce the risk of radioactive release during such a scenario self-passivating tungsten alloys have been developed. During the normal operation of a fusion power reactor these alloys show a nearly pure tungsten surface due to preferential sputtering of the alloying elements. Upon accidental air ingress with elevated temperatures the additives form an oxide layer at the surface protecting the tungsten alloy against fast oxidation and sublimation of tungsten oxide. Studies on thin films, a few μm deposited by magnetron sputtering, show the best results for the system W-Cr-Ti. In collaboration with the Louis Renner GmbH in Dachau Germany and the CEIT research institute in San Sebastian Spain the production of bulk W-Cr-Ti alloys was investigated by different powder metallurgical processes. The oxidation behavior of the bulk alloys and the thin films was compared by thermogravimetric analysis. Despite of different micro structures the mechanism of oxidation protection was similar for all materials. At the surface a thin protecting scale of Cr_2O_3 was formed. Below it was formed a mixed phase of WCr_2O_6 and WO_{3-x}. Compared to pure tungsten, the oxidation rate could be reduced by 3-4 orders of magnitude.

Cyclic Loads and Damage Tolerance in Tungsten-fibre-reinforced Tungsten Composites

A severe problem for the use of tungsten in a future fusion reactor is its inherent brittleness and its further embrittlement during operation. During the recent years it could be demonstrated that the reinforcement of tungsten with drawn tungsten wires is a viable solution to overcome this problem. These tungsten fibre-reinforced tungsten composites (W_f/W) utilize the so called extrinsic toughening which is well known from ceramic fibre-reinforced ceramics. The main problem of a brittle material is that stress cannot be redistributed and therefore an overload even if appearing only locally leads to a catastrophic failure. On the other hand,

tough materials can redistribute stress by local processes e.g. plastic deformation and therefore exhibit damage tolerance. W_f/W features the same behaviour due to stress redistribution by extrinsic mechanisms like fibre bridging or plastic fibre deformation as shown in mechanical cycling: In a first step a bulk W_f/W sample with a fibre volume fraction of 0.3 was damaged by controlled crack propagation during a bending test. This sample was then exposed to cyclic loading (5 cycles of loading and unloading) in steps of 50 N up to 90 % of the damaging load. In all cases the hysteresis of loading and unloading showed a stable or decreasing width and a stable gradient. This is a strong indication that a steady-state-like behaviour is reached and no further damage occurs as long as the sample is not overloaded again. Obviously it exhibits damage tolerance and allows overload to a certain extend not necessarily leading to catastrophic failure as in the brittle case. Consequently, defects caused by a local event or by a manufacturing flaw will not affect the rest of the structure as local stress peaks can be relaxed and the structure can still be used without severe limitation. This behaviour of W_f/W will allow applying design strategies used for ductile materials and therefore provide new possibilities to use tungsten as a structural material in future fusion reactors.

Fatigue Crack Growth of Steel First Wall under Cyclic Heat Flux Loads

Recently, the idea of bare steel first wall (FW) is drawing attention, where the surface of the steel is to be directly exposed to heat fluxes. Hence, the thermo-mechanical impacts on the bare steel FW will be different from those of the tungsten-coated one. In the case of reduced activation steel EUROFER97, a candidate structural material for the DEMO FW, there is no report on high heat flux tests yet.
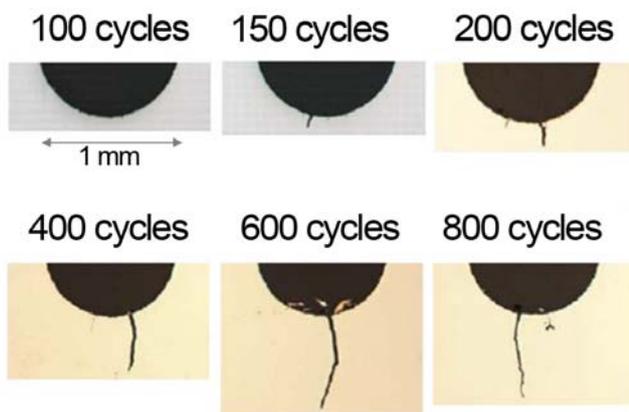

Figure 3: Formation and propagation of cracks at the root of the surface notch of a water-cooled EUROFER steel first wall mock-up during high heat flux fatigue test (3.5 MW/m²).

Thus, the issue of thermal fatigue behavior of EUROFER steel is of interest. To this end, we conducted a series of electron beam irradiation tests with heat flux load of 3.5 MW/m² on a water-cooled FW mock-up made of EUROFER steel with an engraved thin notch on the surface. After the heat flux fatigue test it was found that the notch root region exhibited high density of damage in form of micro-cracks whereas the notch-free surface manifested no sign of crack formation at least until 800 load cycles. In the course of cyclic heat-flux loading, a main crack was preferred among numerous micro-cracks and grew stably in proportion to the number of load cycles indicating a typical fatigue fracture behavior (figure 3). However, the crack extension ceased to continue after around 600 load cycles. The observed damage pattern agrees well with the prediction of finite element simulation based on visco-plastic continuum damage mechanics.

High Heat Flux Facility GLADIS

The high heat flux (HHF) test facility GLADIS offers testing of large water-cooled plasma-facing components (PFCs) as well as small samples with heat and particle loads similar to the expected operating conditions in current and future fusion experiments. In 2014, the major test campaigns were focussed on the assessment of the produced W7-X divertor target elements, the evaluation of the thermo-mechanical behaviour of newly developed plasma-facing materials and PFCs in the framework of the DEMO development and the experimental investigation of surface modifications of tungsten due to hydrogen or mixed hydrogen/ helium particle bombardment.

The main GLADIS contribution to the manufacturing of the W7-X long pulse divertor is the quality assessment of the delivered target elements. The production of the actively water-cooled elements was concluded and the quality assessment was almost finished in 2014 (see section Wendelstein 7-X, 4.1). For the series production, the local surface temperature evolution of the CFC tiles during 100 pulses at 10 MW/m² was analysed. The resulting Gaussian distribution of the temperature increase of the individual CFC tiles describes the thermal performance of the elements. The assessment of total 82 elements (about 10 % of series production) shows no degradation of the manufacturing quality which would result in in a broadening or shift of the Gaussian distribution. No defective tile was detected. On the basis of the statistical assessment, we can conclude that the risk of an undetected defective CFC tile is negligible.

Reliable joining of tungsten to copper is a major issue in the design of water-cooled divertor components for future fusion reactors. A design concern is the large mismatch in the coefficients of thermal expansion between W and Cu which is likely to produce high stresses during HHF loading.

Thus, the performance of the target component relies on the quality of the joining and reduction of mismatch stress between W armour and Cu heat sink. One of the suggested advanced engineering solutions is to use functionally graded composite interlayers. A novel processing route for fabricating graded W/CuCrZr composites using a vacuum melt infiltration was developed in close cooperation with the Dresden University of Technology, the Fraunhofer Institute for Manufacturing and Advanced Materials (Dresden) and the IPP (see Annual Report 2010). A three-layer composite system (W volume fraction: 70/50/30 %) was manufactured as graded interlayer between the W armour and CuCrZr heat sink. Three flat-tile mock-ups with W/CuCrZr multilayers have been tested in GLADIS. W-Tiles and multilayers were joined onto an actively water-cooled heat sink made of CuCrZr via electron beam welding. Cycling tests at 10 MW/m^2 and screening tests up to 20 MW/m^2 were successfully performed and confirmed the expected thermal performance of the compound. The thermal behaviour is in good agreement with the FEM predicted temperatures during the heat flux loading. Furthermore, microscopic investigation showed that the implementation of the novel functionally graded interlayer was successful. The highly stressed composite survived without damage as shown in Figure 4.


Figure 4: Cross section of the W/CuCrZr composite after heat loading up to 20 MW/m². The lower part of the image shows the CuCrZr layer. The pure W plasma-facing material is visible on the top.

Integration of and Collaboration in the EU Programs

With the transition from EFDA to EUROfusion the European programme was newly organized. Many members of the project are involved in the scientific exploitation of the European tokamaks under the Taskforces WPJET1 and WPMST1.

However, the project's main activities within the research along the European Fusion Roadmap are centred within the work packages WPPFC, WPMAT, WPDIV and WPJET2.

Work Package Plasma Facing Materials (WPPFC)

The work with WPPFC comprises six subprojects dealing with subjects centred around investigations on plasma material interaction mostly in linear and laboratory devices. IPP is strongly involved in five of the subprojects and provides the subproject leaders for 'Erosion, deposition and mixing' and 'Fuel retention, fuel removal and damage'.

Work Package Materials (WPMAT)

Within WPMAT materials for a Demonstration Fusion Power Plant are developed. The work of IPP concentrates on the development of high heat flux materials namely tungsten fibre-reinforced tungsten and copper as well as the self-passivating tungsten alloys as an armour material for the main chamber plasma-facing components.

Work Package Divertor (WPDIV)

The scope of the Divertor Project (WPDIV) covers all elements of conceptual design for the whole divertor system of the first DEMO reactor. IPP provides the project leader of WPDIV and in future a significant amount of mock-up testing in GLADIS is foreseen.

Work Package JET2 (WPJET2)

The work package JET2 (WPJET2) aims at the exploitation of the JET ITER-Like Wall (ILW) in view of the erosion – deposition pattern and fuel inventory of the beryllium and tungsten plasma facing components. IPP is responsible for the nuclear reaction analysis of specific tungsten components.

Scientific Staff

V. Alimov, N. Ashikawa, M. Avello de Lama, M. Balden, J. Bauer, N. Bobyr, B. Böswirth, J. Brinkmann, R. Brüderl, L. Buzi, J. Dorner, P. Douglas, T. Dürbeck, R. Dux, T. Eich, S. Elgeti, O. Encke, K. Ertl, A. Friedrich, G. Fuchert, M. Fuhr, M. Fusseder, L. Gao, M. Gloc, H. Greuner, A. Hakola, Y. Han, Al. Herrmann, R. Hoffmann, T. Hoffmann, W. Hohlenburger, F. Hoppe, T. Höschen, E. Huber, W. Jacob, B. Jasper, S. Kapser, F. Koch, A. Kallenbach, K. Krieger, S. Krat, R. Lang, M. Laux, P. Leitenstern, C. Li, H. Maier, A. Manhard, E. Markina, G. Matern, J. Mayer, M. Mayer, G. Meisl, S. Müller, M. Muñoz, R. Neu, D. Nille, M. Oberkofler, O. Ogorodnikova, S. Potzel, F. Reimold, J. Riesch, V. Rohde, J. Roth, J. Schäftner, S. Schindler, K. Schmid, T. Schwarz-Selinger, B. Sieglin, M. Sode, R. Strasser, U. Stroth, K. Sugiyama, T. van Lochem, A. von Müller, U. von Toussaint, T. Wegener, A. Weghorn, M. Westermeier, B. Wielunska, M.Wischmeier, Z. Yang, J.-H. You, P. Zhao, M. Zibrov.

Plasma Theory

Theoretical Plasma Physics

Heads: Prof. Dr. Per Helander, Prof. Dr. Karl Lackner, Dr. Emanuele Poli, Prof. Dr. Eric Sonnendrücker

Tokamak Physics Division

Head: Prof. Dr. Karl Lackner,
Dr. Emanuele Poli (from 1 November)

Tokamak Edge Physics

Transport in the edge plasma is thought to be a combination of anomalous perpendicular transport, convection driven by drifts and classical parallel transport. For typical divertor conditions on present and future tokamaks, kinetic effects might play an important role which is not fully captured by the kinetic corrections that have been implemented in the fluid plasma treatment in SOLPS. Therefore work started a few years ago on implementing a 1D parallel code (KIPP) to treat the electrons kinetically. This work is continued to explore options for coupling KIPP to SOLPS. To address a better treatment for the drift terms in SOLPS, a collaboration was started with the NMPP division. Significant effort went into supporting and developing the SOLPS package, including a cooperation with the RZG and the EUROfusion High Level Support Team (HLST) to parallelize the B2 component of SOLPS.

Work started three years ago to develop a new turbulence code (GRILLIX) capable of treating the edge plasma including the separatrix to address the important issue of anomalous transport in the edge and divertor regions of the tokamak. In the framework of GRILLIX a numerical concept has been designed, which is aimed for simulation of turbulence around the separatrix in divertor geometry. The domain is covered with a cylindrical grid, which is Cartesian within poloidal planes. The discretisation of perpendicular operators is straight forward and parallel operators are discretised via a field line map approach, i.e. a finite difference along magnetic field lines, which requires a field line tracing from plane to plane and an interpolation. The usually employed field aligned coordinate systems, which become ill-defined on the separatrix, are thereby avoided. Ultimately, tokamak geometries with arbitrary poloidal cross sections can be treated. Due to the interpolation process, a numerical perpendicular coupling among distinct field lines arises unavoidably in the approach. This introduces a resolution dependent erroneous perpendicular diffusion. With the application of the support operator method to the parallel diffusion operator, a numerical scheme was constructed, which exhibited very low numerical diffusion. In order to study first generic effects of the diverted geometry on turbulence, the Hasegawa-Wakatani (HW) model was implemented in GRILLIX. It has been observed that the filament structures are strongly damped towards the X-point region. Therefore, the X-point tends to disconnect turbulent structures. This observation can be explained by the fact that the strong local magnetic shear leads to an increase of the perpendicular wave-vector of the filament structures towards the X-point and therefore (within the HW model) dissipation becomes dominant near the X-point. As this mechanism is similar to the previously found resistive X-point mode, this behavior might indicate a generic property of the X-point.

The project "Theoretical Plasma Physics" is devoted to first-principle based model development with emphasis on magnetic confinement. It combines the efforts of the divisions Tokamak Physics, Stellarator Theory and Numerical Methods in Plasma Physics, of a Junior Research Group and of the HLST Core Team of the EFDA HPC Initiative. It is also a major partner in the Max Planck Princeton Center for Plasma Physics.

Figure 1: Snapshot (φ = 0 plane) of GRILLIX turbulence simulation in axial diverted geometry. Left: normalized density fluctuation, right: electrostatic potential.

The effect of a sequence of mitigated ELMs on ITER was simulated using SOLPS. The results, reported at the PSI Conference in Japan, were as follows. Under conditions where the engineering target heat flux limit of 10 MW/m^2 was achieved, steady state W contamination is usually not an issue; in such conditions, the neoclassical transport of W in the pedestal transport barrier leads to hollow W density profiles in this region due to the associated pinch of W being directed outwards from the plasma. If a simple model for the prompt redeposition of W is included, W contamination of the core plasma during ELMs is strongly reduced. Including additional effects into the prompt redeposition model will give a similar strong reduction of W in the core plasma. Without prompt redeposition, the ensuing contamination of the plasma by ELMs depends strongly on the model for W expulsion by ELMs due to the edge W profiles between ELMs being hollow. For "diffusive" ELMs (where W expulsion by ELMs is modelled by an increase in the particle diffusion coefficient) the core W concentration increases with ELM frequency while for "convective" ELMs (where W expulsion by ELMs is modelled by an increased outward plasma velocity) the core W concentration decreases with ELM frequency.

In order to clarify the physics of classical drift effects on divertor and target asymmetries, a detailed analysis of convective fluxes caused by E×B drifts in a realistic JET

configuration, based on a series of EDGE2D-EIRENE code runs, was carried out. The EDGE2D runs included all drifts, E×B as well as ∇B and centrifugal drifts. Particle sources created by divergences of radial and poloidal components of the E×B drift were separately calculated for each flux tube in the divertor. It was demonstrated that in high recycling divertor conditions radial E×B drift creates particle sources in the common flux region (CFR) consistent with experimentally measured divertor and target asymmetries, with the poloidal E×B drift creating sources of an opposite sign but smaller in absolute value. That is, the experimentally observed asymmetries in the CFR are the opposite to the result of simple models for the role of the poloidal E×B developed in the 90's. In the private flux region (PFR), the situation is reversed, with poloidal E×B drift being the dominant. In this region poloidal E×B drift by itself contributes to experimentally observed asymmetries. Thus, in each region the dominant component of the E×B drift acts so as to create density (and temperature) asymmetries observed both in experiment and in 2D edge fluid codes.

MHD Theory
Equilibrium Calculation and Stability Analysis
Equilibria with applied RMP fields were simulated with the 3D ideal-MHD code NEMEC and compared to experimental data. As a basis for the computations served the reconstructed axisymmetric equilibrium of AUG shot 30835 at t=3.2 s. 3D equilibria were computed for various differential phases $\Delta\Phi$ of the RMP coil currents. The comparison of the numerically determined corrugation of the flux surfaces with the ELM behaviour observed in AUG implies that a non-stationary ELM-free H-mode ($\Delta\Phi = -90°$) appears when the corrugation is concentrated around the outer midplane, while the best ELM mitigation is observed when the largest corrugation develops at the top and the bottom of the plasma ($\Delta\Phi = 90°$). These results are in good agreement with the findings of the code MARS-F.

The code CASTOR3D is a hybrid of the codes CASTOR_3DW and STARWALL. It solves an extended eigenvalue problem consisting of the plasma part defined by the weak form of the per-turbed single-fluid magneto-hydro-dynamic (MHD) equations (CASTOR_3DW), and a vacuum part (STARWALL) which is derived from an energy functional. This new code takes wall resistivity and plasma inertia simultaneously into account. Furthermore, additionally to the straight field line coordinates used so far, general flux coordinates were implemented which are more appropriate for the description of instabilities located close to the separatrix, e.g. edge localized modes (ELMs). The formulation of the eigenvalue problem in the new coordinates is not limited to axisymmetric equilibria, so that, finally, stability studies of resistive and rotating 3D equilibria will become possible.

Nonlinear MHD
A benchmark comparison between the non-linear code JOREK and the linear code CASTOR has been carried out for the linear phase of peeling-ballooning instabilities in simplified geometry. Growth rates agree well at moderate Lundquist numbers, while computational limitations of the non-linear code lead to deviations at large Lundquist numbers. In previous MHD simulations of the early ELM phase we have shown the non-linear drive of low-n harmonics to large amplitudes by a coupling between two linearly dominant harmonics. A similar mechanism has now been demonstrated, where a single linearly dominant harmonic with mode number n_1 drives two subdominant harmonics n_2 and n_3 with $n_1=n_2\pm n_3$. Both coupling mechanisms lead to a broadening of the non-linear mode spectrum compared to that from linear simulations. This might be responsible for the experimentally observed temporal evolution of the dominant mode numbers during an ELM crash. We also performed non-linear studies of ELMs in ASDEX Upgrade including diamagnetic drift effects, which act stabilizing onto high-n harmonics such that a maximum linear growth rate at n=10 was observed similar to experimental observations.

Based on a recent theory of the effect of resonant magnetic perturbations (RMPs) on particle confinement, corresponding experiments have been carried out at the tokamak J-TEXT using an externally applied rotating m/n=2/1 RMP. It is found that the RMP improves (degrades) particle confinement when its frequency is higher (lower) than the natural m/n=2/1 tearing mode frequency. This is in agreement with the theoretical prediction and with new numerical results obtained from two-fluid equations for J-TEXT parameters.

The nonlinear growth of the internal kink mode was studied. As has been reported previously, in the framework of two-fluid equations the experimentally observed reconnection rates during sawteeth can be reproduced. Furthermore, local sheared plasma flow is driven during non-linear growth due to the difference between the mode frequency and the electron fluid frequency. The strength and the direction of the generated shear flow are in agreement with corresponding observations on TCV.

Energetic Particle Physics
A linear, global, gyrokinetic stability analysis including multiple background ion species (deuterium, tritium, helium, beryllium) and energetic particle (EP) species (α, NBI ions) was carried out with the LIGKA code aimed at studying EP transport due to Alfvén eigenmodes (AEs) in an ITER 15MA standard scenario. The mode structures and damping rates were used for non-linear, perturbative studies employing the code HAGIS. It was found that kinetic effects (trapped kinetic ions, inclusion of diamagnetic effects, dilution and impurities) typically reduce the damping of AEs and thus lead to a more unstable spectrum of modes, e.g. for toroidal AEs (TAEs) between 5<n<35. Also higher order TAE branches

(m+1/m+2; m+2/m+3,...) can be very weakly damped. After a successful linear benchmark of HAGIS and LIGKA for the EP drive, non-linear simulations were carried out. Although the linear phases in single-mode vs. multi-mode simulations are very similar, the non-linear phase differs significantly due to non-linear phase space coupling effects. The saturation amplitudes are considerably higher and linearly subdominant modes can become dominant in the non-linear phase.

The effect of radial mode structure evolution on the saturation mechanism has been investigated by comparing simulation results of XHMGC with those of HAGIS. Nonlinear wave-particle interaction was calculated for a fixed mode structure provided by XHMGC. Non-perturbative EP responses and finite radial fluctuation structures in non-uniform plasmas were found increasingly more important for increasing EP drive. Using a Hamiltonian mapping diagnostics for resonant particles, nonlinear benchmarks of codes XHMGC, LIGKA-HAGIS and CKA-EUTERPE have been systematically carried out. The formation of phase space zonal structures (PSZS) was observed with common features for all the codes. Both XHMGC and LIGKA-HAGIS show resonance splitting within PSZS formation and the consequent resonant particle density flattening. The radial extension of the density flattening is set, at saturation, by the mode width (radial decoupling) rather than by the finite wave-EP interaction length (resonance detuning).

The electromagnetic PIC code NEMORB was further benchmarked and applied to the problem of EP-driven electrostatic and electromagnetic instabilities. Good agreement between analytic theory and numerical simulation results for EGAMs (EP-driven geodesic acoustic modes) was found and a further understanding of the EGAM-ITG interaction channels was obtained. Concerning Alfvén instabilities, successful benchmarks with NEMORB for the TAE case of the International Tokamak Physics Activity were carried out.

Kinetic Theory and Wave Physics

The full-wave TORIC code has been extended to account for wave absorption by energetic slowing-down alpha particles generated by fusion reactions. With this new version of TORIC, we have done an extensive exploration of the options for current drive with radio-frequency (RF) waves in the ion-cyclotron (IC) range of frequencies for the steady-state and pulsed scenarios presently foreseen in DEMO (figure 2; see also section on DEMO). In cooperation with PPPL, a benchmark activity has been started between TORIC and the AORSA (ORNL) full-wave codes. In particular, we have systematically compared the results of the two codes for high-harmonic scenarios in spherical tokamaks (NSTX-like plasmas). On the side of numerical schemes implemented in TORIC, a simple and accurate algorithm to evaluate the Hilbert transform of a real function was developed using interpolations with piecewise-linear functions. An appropriate matrix representation reduces the complexity of this algorithm to the

complexity of matrix-vector multiplication, which in turn is reduced to O(N log N), with N being the dimension of the core matrix. This has been made possible by the anti-symmetric Toeplitz nature of the core matrix, for which discrete trigonometric transforms are suitable. A consistent set of equations has been derived to model poloidal density asymmetries induced by temperature anisotropies in tokamak rotating plasmas. The model can be applied to compute poloidal density asymmetry of highly charged impurities due to additional plasma heating, such as ICRF.
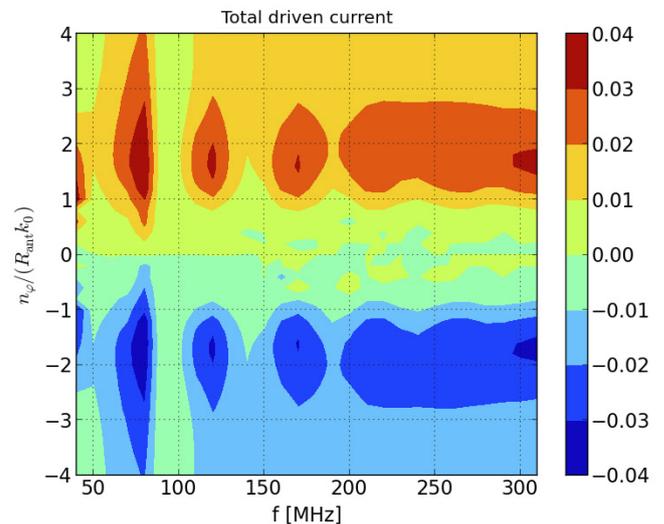
Figure 2: Current driven by fast wave injection (MA per MW coupled to the plasma) as a function of the injection frequency and of the toroidal wave-number. Good efficiency is obtained in frequency windows where absorption on ions is avoided. The optimum wave number results from a compromise between significant electron Landau damping and the need to avoid particle trapping.

The investigation of scattering effects on electron cyclotron beams by electron density fluctuations has continued. A thorough verification and benchmarking of the new code WKBeam has been carried out, in order to assess the correctness of the preliminary results obtained previously. Particularly, in the frame of a collaboration with the Ioffe Institute, St. Petersburg, the results of WKBeam have been compared to analytical solutions valid in a simplified geometry. In most of the cases, we obtain excellent agreement, but the analysis is still continuing. We identified the correct limit which reduces the scattering operator implemented in WKBeam to the one used in the analytical models, thus providing a strong theory basis to our benchmark. The code structure has been improved and allows us to build diagnostics easily as well as to apply the code to various toroidal plasmas with different equilibria (not necessarily tokamak-like). E.g., within an Enabling Research project under the lead of CRPP Lausanne, the configuration of a "simple magnetized torus" has been added in order to simulate the scattering of radio-frequency beams in the TORPEX device.

The degree of density flattening inside a rotating island in the presence of ion-temperature-gradient turbulence has been studied through gyrokinetic simulations In the presence of an imposed island structure. Previous results (excluding turbulence) have shown a complete density flattening for islands rotating at the ion diamagnetic frequency, no flattening in the case of rotation at the electron frequency, when the overlap between ion orbits and the island is significant. These results are confirmed in the presence of ITG turbulence. Also the level of turbulence inside the island is seen to depend on the rotation direction. These results confirm that the neoclassical drive at small island widths depends on the island rotation direction, even in the presence of turbulent transport in the island region. Also the study of the self-consistent evolution of a tearing mode in gyrokinetic simulation, for both the linear and the non-linear phase has been continued. For further results on this topic, see the section Cooperation with University of Bayreuth.

The acceleration of a plasma confined by a cusp magnetic field by the j×B force due to a current between two electrodes was studied with PIC simulations resolving the gyro motion. The goal is to find out where how much momentum can be transferred to the plasma. A slab model was used with two electrodes floating in the plasma with a given potential difference between them. The results show that even with an electron emitting cathode a large current can only flow if a sufficiently strong plasma source is present in the right place for delivering the electrons that are collected by the anode and the ions that carry the current across the field lines and neutralize the electrons coming from the cathode. Higher forces are obtained if the electrodes are closer to the magnets, but further away than the source. Important parameters are the gyro radii for particles with energy equal to the potential difference between the electrodes, rho_eU, rho_iU. For strong current flow across the field lines $rho\_iU>d$ is required, but $rho\_eU<<d$ (this is the case in the experiments). If the electrons are unmagnetized, $rho\_eU>d$, a large fraction of the cross-field current is carried by them; they are accelerated by j×B, but the momentum is then deposited onto the electrodes.

Transport Analysis

In the framework of the development and validation of realistic models of tungsten transport, applications to ASDEX Upgrade and JET plasmas with ion cyclotron resonance heating (ICRH) have been performed with the NEO and GKW codes, taking into account the presence of energetic minority ions. Although the results reveal a strong sensitivity on the profiles of the perpendicular and parallel temperatures of the minority ions predicted with the TORIC/SSFPQL package, qualitative evidence of the need of including these effects to correctly predict the tungsten density profile has been obtained. Other applications have been dedicated to plasmas with neutral beam injection (NBI) heating only, featuring

strong (in ASDEX Upgrade hybrid scenario) or weak (in JET baseline scenario) core ion temperature gradients. The results not only confirmed the experimental importance of neoclassical temperature screening to prevent accumulation in the presence of strong ion temperature gradients, but also validated the theoretical prediction that the relative strength of the temperature screening is reduced in the presence of poloidal asymmetries, as produced by centrifugal effects, which can lead to accumulation. These specific studies, performed on JET plasmas, have produced first experimental validation of the theoretically predicted impact of poloidal asymmetries on the radial transport of heavy impurities. A parallel activity dedicated to helium and boron transport has confirmed the dominance of turbulent transport in the confinement region for these light impurities, but has also revealed discrepancies between the predictions and the measured profiles, which are bigger than those obtained in previous recent works. In particular, although some trends are qualitatively reproduced, the helium density is predicted to be less peaked than observed.

In the framework of theory-based tokamak scenario modelling, substantial effort has been dedicated to assess the consistency of plasma scenarios of a future fusion reactor, such as DEMO. Combined simulations with ASTRA/STRAHL/TGLF have been performed in order to identify acceptable ranges of operation in terms of values of pedestal pressure and amounts of impurity seeding. More detail on the results is presented in the DEMO section. In parallel, a verification of the bootstrap current models is performed for applications to reactor relevant current density profiles. This, in combination with the goal of increasing the modelling capabilities of heavy impurity transport, presently motivates the coupling of the drift-kinetic code NEO to ASTRA. Finally, to improve the predictive capability of ASTRA, a generic, theory-based, toroidal momen-tum transport equation has been derived, suited for implementation in 1D transport codes in axisymmetric geometry. The contributions of E×B, diamagnetic, and poloidal flows are retained for multi-species plasmas. The terms appearing in the expression of the turbulence-driven part of the flux are consistently obtained from standard gyrokinetic theory.

Turbulence Theory

We have been active in both theory and computation, with an emphasis on using computation to understand physical mechanisms rather than on modelling. Relaxation to equilibrium was a main point, as a means towards computational models which carry the MHD and flow equilibrium self-consistently and can be run on the confinement time scale as well as resolving skin-depth scale electromagnetic turbulence. Collaboration with Princeton Plasma Physics Laboratory continued on two projects: plasma micro-turbulence, and edge plasma simulation.

Relaxation to equilibrium was studied using gyrokinetic field theory as a basis and simplified, axisymmetric gyrofluid computation as an example. The neoclassical approach considers drift orbits in a tokamak and collisions, given a background Maxwellian with zonal (flux surface averaged) parameters. In gyrokinetic or fluid theory this translates to the assumption that the total divergences of flows, currents, and heat fluxes are zero and forces due to parallel and toroidal drift motion are balanced, what we mean by "sideband equilibrium". Zonal quantities evolve by transport only, except the electric field which is relaxed by collisions. The various processes occur on different time scales: after Alfvén and acoustic relaxation times have passed the divergence/force balances are established, and then the zonal flow and radial electric field relax with the bootstrap current with ion collisions. If all conserved quantities, including toroidal angular momentum, are specified, then the poloidal rotation and radial electric field are determined once collisional relaxation has finished. Then, transport of the zonal quantities as radial densities of conserved quantities takes place on the longer time scale with all other components evolving in quasi-static equilibrium. This was demonstrated in the fluid drift model (including parallel heat fluxes as dependent variables), without making approximations about time scales except for the basic ones underlying gyrokinetic theory (gyro-frequency, fast-wave Alfvén compression, and anything faster is removed by taking quasi-neutrality and the gyrokinetic gauge transform on the field/particle system Lagrangian).

The latter result depends on an upgrade to the gyrofluid model. The Landau closure previously used damps the parallel dynamics only. However, the total divergence of conductive heat flux in each species should be zero in equilibrium. Hence, the closure model was updated so that this total divergence is damped. Therefore the damping is zero in equilibrium, but oscillations are damped independent of the collision frequency, as expected from Landau damping in finite but arbitrarily small collisionality. Then, neoclassical viscosity is admitted as parallel dissipation, but since it acts on a relaxed force/divergence balance, its effect is to relax the perpendicular rotation as neoclassical theory expects. Provided that the dissipation-free part of the equations conserves fluctuation free energy, and that each dissipation channel (Landau closure, Braginskii collisions, neoclassical viscosity) obeys an H-theorem (dissipation is a positive-definite quantity preceded by a minus sign in the energy theorem), and that these provisos are exact, then there is no barrier to running a self consistent computation of turbulence, flows, and MHD equilibrium for arbitrarily long time while resolving the fastest and smallest scales due to drift wave turbulence.

Representation gyrofluid/fluid total-f version: work done in collaboration with N. Miyato and M. Yagi (JAEA/Rokkasho) on the gyrofluid field theory demonstrated the equivalence of the results concerning flows in the various representations –

exact on an order-by-order basis. The divergences of the toroidal drift of gyro-centres and of the diamagnetic fluid flow were shown to be equal, as is known, while the actual flux of a diamagnetic flow is equivalent to a magnetisation flux in the gyrofluid representation. One step further, the polarisation drift of the fluid was shown to be equivalent to a higher-order $E{\times}B$ term in the magnetisation flux. This elucidates the role of representation: a magnetised fluid has a polarisation drift, while a gyrofluid has a polarisation density, and it also has a magnetisation flux which covers the polarisation flux in the fluid model. The density difference is well known, going back to the work by W.W. Lee (1983). Now we have the end of the story on the fluxes, and there is no mystery about the presence of the polarisation current in a gyrofluid model. Our previous work had already shown the equivalence in the time derivative of the gyrofluid polarisation density and the divergence of the polarisation current. This work shows the equivalence without resorting to the divergences, namely, the zero-divergence part in the magnetisation flux covers the difference in the two representations.

The particle-in-cell (PIC) model for electromagnetic gyrokinetic computation has received improved mathematical basis. Starting from a discrete Lagrangian in terms of finite elements for gyro-centres and field variables, the model was re-derived as a set of Euler-Lagrange equations with a field theoretical basis. A new dissipation mechanism, based on a quad-tree algorithm has been developed and compared with traditional methods. The quad-tree is less computationally intense and allows for a more accurate control of the rate of dissipation introduced in the system. Verification tests on Alfvén continuum damping and geodesic acoustic damping have proceeded with the gyrokinetic PIC code NEMORB as well as the gyrofluid code GEMZ and the above-mentioned neoclassical relaxation fluid model.

Scientific Staff

C. Angioni, A. Bergmann, A. Biancalani, R. Bilato, A. Bottino, A. Chankin, D. Coster, T. Görler, J. Grießhammer, S. Günter, M. Hölzl, F. Jenko, O. Kardaun, K. Lackner, P. Lauber, A. Lessig, P. Merkel, G. Pautasso, G. Papp, E. Poli, J. Regana, W. Schneider, M. Schneller, B. Scott, A. Stegmeir, E. Strumberger, X. Wang, Q. Yu, D. Zarzoso, R. Zille.

Guests

L. Aho-Mantila, VTT Research Insitute, FIN; R. Aledda, Univ. of Cagliari, IT; C. V. Atanasiu, Inst. of Atomic Physics, Bukarest, RO; L. Horvath, HAS, Budapest, HUN; D. Mazon, CEA Cadarache, FR; P. McCarthy, Univ. College, Cork, IR; V. Rozhansky, Techn. Univ., St. Petersburg, RU; S. Shinsuke, NIFS, Gifu, JP; S. Voskoboynikov, Techn. Univ., St. Petersburg, RU.

Stellarator Theory Division

Head: Prof. Dr. Per Helander
Scenario Development for W7-X

Stellarator Theory is playing an important role in planning plasma discharges for W7-X, and this was the topic for an invited plenary talk at the EPS Conference. To ensure proper operation of the island divertor, it is particularly important to identify scenarios with nearly vanishing toroidal plasma current. The neoclassical transport code NTSS, the equilibrium code VMEC, and the DKES code for calculating databases of (mono-energetic) neoclassical transport coefficients were used within an iteration loop. In scenarios without ECCD, the toroidal mirror term was adjusted to make the bootstrap current sufficiently small. Here, only a few iteration steps were necessary. Alternatively, ECCD can be employed to cancel out the bootstrap current, but such scenarios are more difficult to establish. In particular, the rotational transform tends to become significantly reduced close to the ECCD position, leading to a strong increase of the bootstrap current density, and sufficient current drive is often only obtained in X2-mode at low plasma density.

Helias Reactor Optimisation

The satisfactory confinement of fast alpha particles is essential to the design of any viable fusion reactor. Additionally, high-beta equilibria with plasma edge topologies conducive to particle and energy exhaust by means of an island divertor are most readily achieved under current-free conditions, which requires (near) elimination of the bootstrap current, I_{bs}. During 2014, the software package ROSE (ROSE Optimises Stellarator Equilibria) has therefore undergone further development with the ultimate goal of identifying attractive Helias reactor configurations which accomplish both of these goals. It is known that the toroidal and helical components of a stellarator's magnetic field make, respectively, positive and negative contributions to I_{bs}, so that an iterative adjustment of the ratio of these two components can be expected to yield configurations with arbitrarily small levels of bootstrap current. This ratio was included as a target function in ROSE, enabling Helias equilibria with negligible I_{bs} to be realized without adversely affecting fast-particle confinement (for which minimisation of the effective helical ripple serves as proxy during the optimisation). Various measures were introduced to influence the external current distribution consistent with the equilibrium to simplify coil design. The goals here are to reduce: the harmonic content of the current potential, the residual field errors of the filament solution, the 3D and geodesic curvature of current lines and the ratio between the highest and lowest values of local current density. Additionally, the appearance of current "islands" must be avoided as these would necessitate the use of saddle coils. Coil sets obtained to date are more complicated than desired, however, so that efforts at simplification will have high priority during the coming year.

Basic Theory of ITG Modes in Stellarators

The linear theory of ion temperature gradient (ITG) driven micro-instabilities has been extensively studied in both uniform and axisymmetric magnetic field geometry. Yet less is known fundamentally about how this and other instabilities behave in non-axisymmetric stellarator configurations. The possibility of optimizing stellarator geometry for turbulent transport makes it especially timely to revisit the ITG mode and determine the aspects of geometry that control the instability. New first principles models of the ITG mode have been derived directly from gyrokinetic ballooning theory. Areas of strong local magnetic shear, characteristic of stellarator geometries, are shown to localize the ITG mode, effectively "boxing" it in to regions bounded by shear spikes. If the perpendicular wavelength is larger than the ion Larmor scale, the magnetic geometry enters a single quantity in the gyrokinetic description, namely the magnetic drift frequency. This leads naturally to idea of a "drift well", analogous to a quantum mechanical potential well, around which the mode structures are peaked. To investigate the ITG mode in W7-X, numerical simulations using a W7-X geometry are compared with a model tokamak equilibrium with equivalent local instability parameters, i.e. magnetic curvature, temperature gradient, etc. The computed growth rates match well, suggesting that the ITG mode growth rate is well characterized by local scale lengths. Overall, the findings suggest that, for purposes of turbulence optimization, the stabilization of the ITG mode may be achieved by reducing the magnitude of normal magnetic curvature, or by shortening the extent of drift wells along the magnetic field.

Fast Particle Physics and Micro-instabilities with PIC Codes
Non-linear Interaction between Fast Particles and MHD Modes

A non-linear version of the CKA-EUTERPE code has been developed. This code follows fast-particle orbits in a wave field calculated by reduced MHD equations, and a tokamak benchmark with the HMGC code from ENEA Frascati is underway. It has been observed that the mode amplitude does not saturate without a damping of the mode which had to be implemented in the model. With a damping comparable to those of the HGMC code and the MEGA code, a similar level of the saturation amplitude has been obtained. After saturation, a splitting of the mode frequency has been observed (figure 3). Using experience from the ENEA group, a phase space diagnostic has been implemented which allows to analyse the saturation mechanism in more detail (figure 3).

A fluid-electron, gyrokinetic-ion model for electromagnetic gyrokinetic simulations, called FLU-EUTERPE, was implemented for the code EUTERPE. This model offers improved numerical robustness, avoiding the cancellation problem and loosening the time step requirement compared with fully gyrokinetic electromagnetic codes. The cost of these improvements is the neglect of electron kinetic effects, and the requirement to adopt truncated fluid closures.
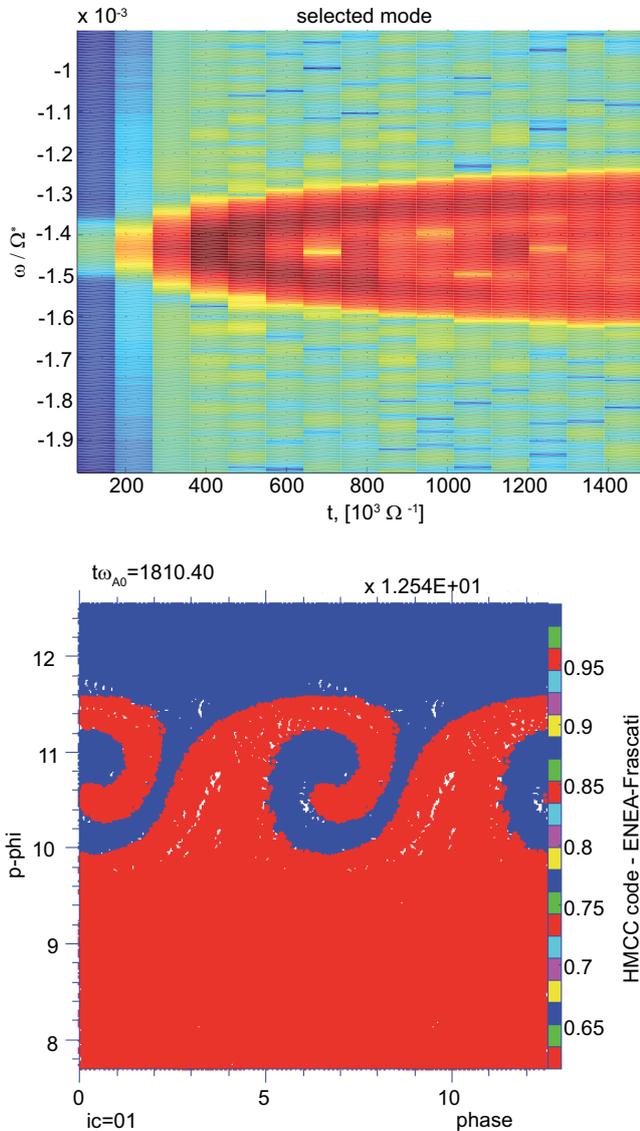
Figure 3: Simulation results from the non-linear CKA-EUTERPE code. Top: frequency splitting during the non-linear part of the mode saturation. Bottom: phase space, P_φ vs. phase Θ, during the wave evolution.

Currently simple closures are used, so that finite $E_\parallel$ effects, such as electron inertia effects, electron Landau damping and resistivity, are neglected entirely. In future work this treatment will be extended.

The implementation has been successfully benchmarked against other gyrokinetic codes for a Toroidal Alfvén Eigenmode case (ITPA benchmark with n=–6, m=10) showing good agreement in both frequency and growth rate. It has subsequently been employed to model the internal kink mode in tokamaks of increasingly realistic geometry, from a large-aspect-ratio circular case to a case with aspect ratio 3.0 and elongation 1.85, comparable to current large tokamaks.

Both the fluid kink and the effect of gyrokinetic bulk ions on the kink mode have been studied. Finally, the effect of gyro-kinetic fast ions has been considered, permitting simulations of the linear stage of the fishbone cycle. Both, kink mode stabilisation by fast particles and the n=1 Energetic Particle Mode have been observed.
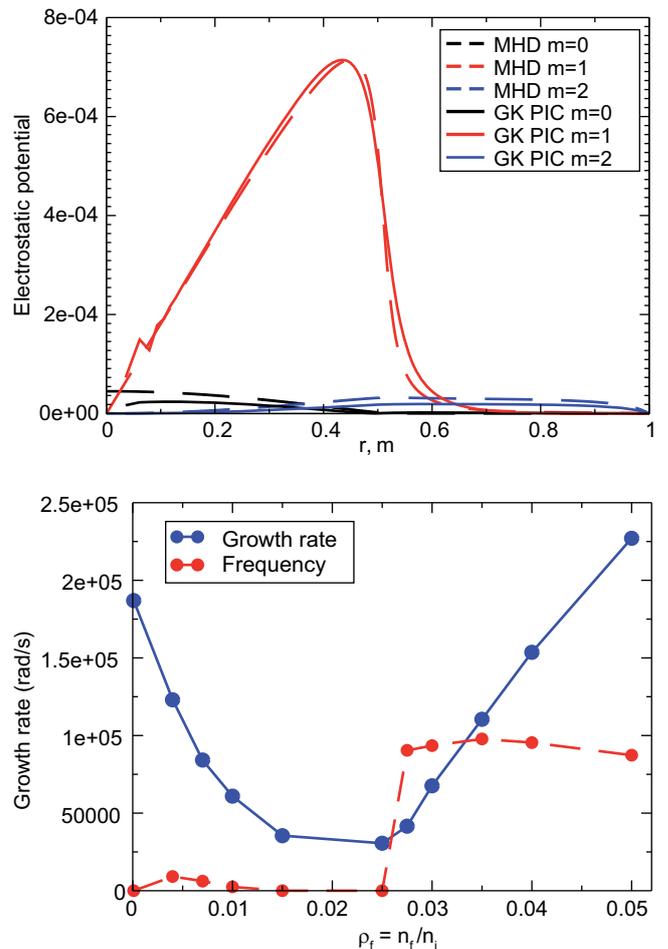
Figure 4: Fast particle stabilization of an internal kink mode simulated with the FLU-EUTERPE code. With sufficiently high fast particle density, a fishbone mode emerges. Top: mode structure of the kink mode compared with the result from an MHD code. Bottom: frequency and growth rate vs. normalized fast particle density.

Gyro-kinetic Simulation of TAE Coupling with the Continuum

First-principle gyrokinetic particle-in-cell simulations of a global Toroidal Alfvén Eigenmode (TAE) have been undertaken in the presence of a strong coupling with the continuum. Effects of the bulk plasma temperature on the interplay between the TAE and Kinetic Alfvén Waves (KAW) have been investigated. A global TAE-KAW structure has been identified which appears to be more unstable with respect to the fast ions than a simple (fluid-like) TAE mode.

New Variables for Gyrokinetic Electromagnetic Simulations
It has been shown that a considerable improvement in global gyrokinetic electromagnetic simulations can be achieved by a slight modification of the simulation scheme. The new scheme has been verified, simulating a Toroidal Alfvén Eigenmode in tokamak geometry at low perpendicular mode numbers. Electromagnetic drift mode simulations in stellarator plasmas are shown to be possible.

Simulations of Gyrokinetic Energetic Ions in W7-X Like Geometries
Simulations of gyrokinetic energetic ions interacting with magneto-hydrodynamic (MHD) Alfvén Eigenmodes have been performed. The effect of finite fast-ion orbit width and finite fast-ion gyro-radius, of the equilibrium radial electric field, as well as that of anisotropic fast particle distributions (loss-cone and ICRH-type distributions), have been studied in Wendelstein 7-X geometry using a combination of gyrokinetic particle-in-cell and reduced MHD eigenvalue codes. A preliminary stability analysis of a HELIAS reactor configuration has been undertaken.
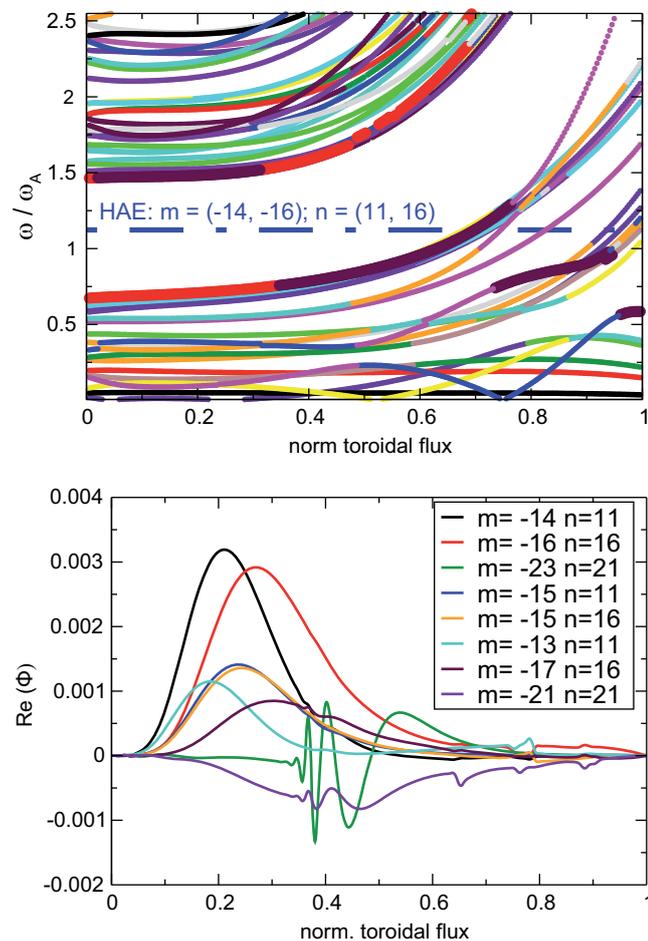

Figure 5: Alfvén continuum (top) and mode structure (bottom) for an unstable HAE found in a HELIAS configuration with γ= 17874 rad/s, ω= 410523.29 rad/s.

Linear Ion-temperature-gradient (ITG) Driven Modes
Linear ITG modes in Wendelstein 7-X (W7-X) and in the Large Helical Device (LHD) have been simulated gyro-kinetically. The studies considered a typical finite-beta equilibrium configuration for each device and were restricted to the electrostatic case with adiabatic electrons. Systematic scans over temperature and density gradients were performed to measure linear growth rates and gain further information about the mode structure. In the absence of kinetic electrons, there is a threshold for the ITG instability at $\eta_i=1$ in both devices. Results were obtained first using simplified temperature and density profiles, which were taken to be independent of the underlying (VMEC) equilibrium pressure profile. With a view to realistic modelling of future experimental situations, a next step was taken by using temperature and density profiles derived from the equilibrium pressure. Results obtained for LHD show broadened (more realistic) mode structures. The effect of the radial electric field on the growth rate of ITG modes was also studied in a series of simulations performed on a W7-X reference case using two different models, with and without rotation shear. In both cases, the electric field mostly leads to a damping of the instability and to a Doppler shift of the frequency. Future simulations should include kinetic electrons, so that trapped-particle modes can be modelled in global 3D geometry.

Neoclassical PIC Simulations
Neoclassical PIC simulations have been performed to calculate the variation of the electrostatic potential over flux surfaces in various stellarators. The results have been compared to experimental floating potential measurements at distant probe locations of the same flux surface in the TJ-II stellarator. The experimental observations have great uncertainties, but the calculations give the correct order of magnitude for the overall variation in potential and predict trends correctly.

ITG Turbulence Simulations
We have employed novel Petaflop-scale gyrokinetic GENE simulations to predict the distribution of turbulence fluctuations and the related transport scaling on entire stellarator magnetic surfaces. The strongest fluctuations caused by Ion Temperature Gradient (ITG) driven turbulence in W7-X are localised along a thin stripe on the outboard side, leaving the rest of the surface relatively quiescent. Similar localization is found also for a quasi-axisymmetric stellarator configuration. This feature, which is not found in tokamaks, appears to affect the scaling of the transport with the normalized gyroradius, which differs from the gyro-Bohm scaling reported from flux tube simulations. The uneven distribution of curvature on the stellarator surface localises the turbulence by imposing a characteristic length corresponding to the variation of curvature on the surface in the direction perpendicular to the magnetic field. In W7-X, this length is

considerably shorter than in typical tokamaks, where the fluctuations cover almost the entire outboard side. These results have implications for transport stiffness. Indeed, as shown in figure 6 the ion heat flux scaling over the normalised ion temperature gradient from flux surface GENE simulations becomes milder as the gyroradius increases, and therefore nonlocal phenomena become more important.
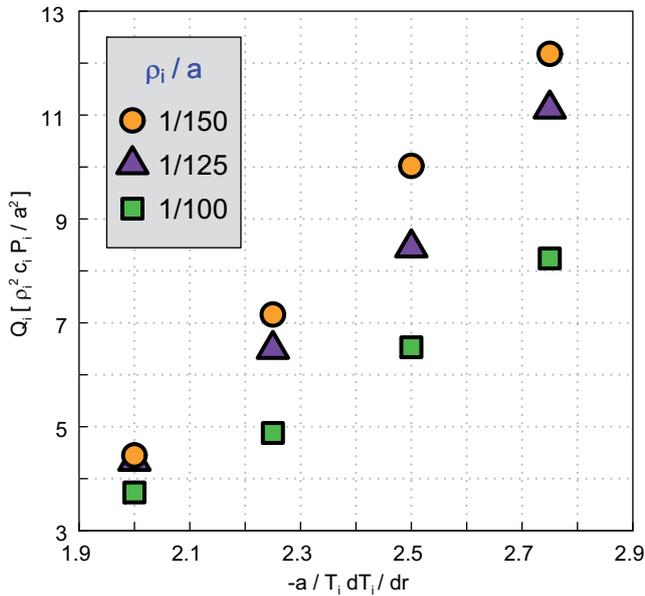

Figure 6: Ion heat flux scaling with the normalized ion temperature gradient from flux surface GENE simulations.

Edge Physics

The EMC3-Eirene code has been employed to assist the design of local limiters for the initial operation phase (OP1.1) of W7-X to enable a meaningful scientific program in an environment of incomplete in-vessel components. Here, in particular, the not-yet-tiled metal divertor frame must be protected from thermal load and sputtering. The size of the limiters is restricted by the available space in the machine. A parameter scan is carried out in order to clarify how the limiter plasma decays and interacts across SOL regions of different connection lengths. The limiters are optimized for a standard configuration with 13 % field contribution from the planar coils, which shifts the ι=5/5 resonance outwards far beyond the limiters. They are positioned in the inboard midplane of the bean-shaped cross-section, touching the $r_{eff} \sim 50$ cm flux surface over several decay lengths in front of the divertor frame. 99 % of the SOL power and more than 97 % of the ion efflux are intercepted by the limiters, while the remaining ions practically do not contribute to sputtering processes on the metal in-vessel components.

The performance of the limiter plasma in OP1.1 in terms of refuelling and sputtering is expected to be affected by recycling neutrals. In comparison to the more sophisticated divertor modules installed later, the inboard limiters are much closer to the plasma centre and cover much less of the plasma. Moreover, no specific baffle arrangement is taken to prevent the limiter-recycled and the charge-exchange (CX) induced neutrals from escaping from the recycling zone into the main chamber. EMC3-Eirene simulations show that the limiter-recycled neutrals provide a central particle refuelling rate which is almost two orders of magnitude larger than that from the divertor. The high refuelling capability of the limiter neutrals restricts the limiter SOL plasmas in a low-density, high-temperature range above the threshold energy of physical sputtering processes on the graphite limiter surface. In addition, the high SOL temperature enriches the high-energy CX-neutral population and thereby increases the impurity yields from metal in-vessel components in the main chamber. The refuelling and sputtering capabilities of the recycling and CX-neutrals have been evaluated for the limiter and compared to a divertor configuration.

Stochastic Heating of Thermal Ions by Compressional Alfvén Eigenmodes in NSTX

In collaboration with PPPL, a project has been launched to investigate if compressional Alfvén eigenmodes (CAEs) can be responsible for excess heating in the National Spherical Tokamak Experiment (NSTX). The background is that in neutral-beam-heated NSTX discharges, the observed ion temperature is sometimes higher than expected from the balance between collisional heating by fast ions, transport losses and collisions with electrons. When the beams are switched on, the ion temperature can rise on time scales shorter than the beam-ion slowing-down time, which implies that there exists a source of heating in excess of the collisional beam ion heating. It has been proposed that this heating originates from interaction with CAEs, which are commonly observed in beam-heated discharges. In this model, the energy is transferred from the fast ions to the waves by resonance, and from the waves to the thermal ions by stochastic heating. The latter is a non-resonant process, which is possible in these discharges because several Alfvén eigenmodes exist simultaneously at around half the ion cyclotron frequency when the beams are turned on.

In the present study, the process is modelled quantitatively, by tracking the orbits of thermal ions in the CAE eigenmodes calculated with the eigenmode code CAE3B (from IPP). A large number of ions are followed in the full gyro-orbit code Gyroxy (from PPPL) under influence of the eigenmodes, and the evolution of the kinetic energy is monitored. Presently, the eigenmode amplitude is treated as a free input parameter, but it is planned to determine the experimental CAE amplitudes from density fluctuation measurements with the high-k diagnostic. Then it will be possible to assess if the proposed heating mechanism can supply the excess heating inferred from transport modelling.

Preliminary calculations are consistent with previously published simulations in slab geometry, but the heating effect is relatively small for expected values of the eigenmode amplitudes.

Micro-Stability of Electron-positron Plasmas

Since experimental efforts are underway to create magnetically confined electron-positron plasmas at IPP, the gyrokinetic theory of micro-instabilities in such plasmas has been explored. Because of the absence of ions in pure electron-positron plasmas there are no drift waves, and any instability must therefore involve magnetic curvature. Furthermore, since the expected density is so small that the Debye length is several orders of magnitude larger than the gyroradius, all instabilities with perpendicular wavelengths comparable to the gyroradius are stabilised. Many of the micro-instabilities plaguing fusion plasmas are thus predicted to be absent in the planned electron-positron plasma experiments.

Scientific Staff

C. D. Beidler, T. Bird, M. Borchardt, M. Cole, M. Drevlak, Y. Feng, J. Geiger, P. Helander, R. Kleiber, A. Könies, H. Maaßberg, N. Marushchenko, A. Mishchenko, C. Nührenberg, J. Nührenberg, G. Plunk, J. Proll, J. Riemann, A. Runov, F. Sardei, H. Smith, T. Stoltzfus-Dueck, Y. Turkin, P. Xanthopoulos, O. Zacharias, A. Zocco.

Guests

S. Äkäslompolo (Aalto University), K. Aleynikova (ITER Organization), P. Aleynikov (ITER Organization), G. Bowden (Australian National University Canberra), F. Busse (University Bayreuth), J. Connor (CCFE Culham), P. Cottier (CEA Cadarache), F. Effenberg (FZ Jülich), B. Faber (University of Wisconsin), J. Hansom (Auburn University), G. Herdrich (University Stuttgart), P. Holmvall (Chalmers University of Technology Gothenburg), R. Kamendje (IAEA Vienna), G. Kawamura (NIFS), W. Kernbichler (ÖAW Graz), T. Kurki-Suonio (Aalto University), F. Manke (Imperial College London), M. Meschede (Greifswald University), M. Mikhailov (Kurchatov Institute Moscow), A. Móllen (Chalmers University of Technology Gothenburg), S. Murakami (NIFS), D. Narita (Kile Institute for World Economy), S. Newton (CCFE Culham), S. Nishimura (NIFS), K. Pawelzik (University Bremen), H. Peraza (Universidad Carlos III Madrid), G. Pełka (Institute of Plasma Physics and Laser Microfusion Krakow), O. Renn (University Stuttgart), P. Ricci (CRPP Lausanne), M. Rodi (Greifswald University), E. Sanchez (CIEMAT Madrid), M. Sauter (University Göttingen), C. Slaby (Greifswald University), Y. Suzuki (NIFS), Hirohiko Tanaka (NIFS), C. Volkhausen (Greifswald University), L. Warr (Greifswald University), H. Yamaguchi (Kyoto University), R. Zagorski (Institute of Plasma Physics and Laser Microfusion Krakow).

Numerical Methods in Plasma Physics

Head: Prof. Dr. Eric Sonnendrücker

The division "Numerical Methods in Plasma Physics" is devoted to the development of efficient and robust computational methods and algorithms for applications in plasma physics and more specifically for the models and problems of interest to other divisions of IPP.

Structure of the Division

The emphasis of the division lies on the development, optimization and analysis of numerical methods and is tightly coupled with the group "Numerical methods in plasma physics" at the Mathematics Center of the TU Munich. In addition to inventing some new methods specifically for the problem at hand, the division aims to maintain a knowledge of state of the art methods in the general area of numerical mathematics and scientific computing in order to be able to adapt them where needed to plasma physics problems. The division consists of four research groups: Kinetic Modelling and Simulation, Fluid Modelling and Simulation, Plasma-Material Modelling and Foundations, Zonal Flows and Structure Formation in Turbulent Plasmas. Moreover the EFDA High Level Support Team (HLST) is attached to the division.

Kinetic Modelling and Simulation

The work in this group was performed within the EUROfusion Enabling Research project WP14-ER-01/IPP-03 entitled "Verification of global gyrokinetic codes and development of new algorithms for gyrokinetic and kinetic codes".

Verification of Gyrokinetic Codes

The first step of this project was to define a set of verification tests for gyrokinetic. This work has been structured around two workshops organised in Garching: the AMVV workshop in April 2014 in order to organise the verification effort and the NumKin Workshop in October 2014 (see below) in which all partners participated to present the state of their work.

The verification and benchmarking problems have been cast in five work packages. 1) Verification of fundamental equations recently implemented in major European codes (NEMORB, EUTERPE, GENE, GYSELA). 2) Benchmark for the adiabatic electrons case (GENE, NEMORB, EUTERPE). 3) Global linear electromagnetic ITG benchmark. 4) EGAMS investigation (GYSELA). 5) General geometry (NEMORB & GENE).

A major effort in our group was to make the link between gyrokinetic theory and the models implemented in the different codes. In modern gyrokinetic theory, the approximations are performed on a field theoretic Lagrangian, however, for different reasons, some of the terms obtained in the theory are hard to implement and further approximations need to be made. For obtaining energy consistent numerical

models, care must be taken to perform these approximations directly on the Lagrangian. With this technique, we could ensure that the PIC codes used at IPP obey a semi-discrete variational principle before time discretisation. Variational integrators as described below can then be used to maintain conservation properties at the fully discrete level.

Variational Integrators for Plasma Physics

In the field of geometric integrators we made progress on several fronts. In our variational Vlasov-Poisson code, a fast preconditioner based on a tensor product decomposition of the linear matrix was implemented. Coupled with an iterative solver like GMRES, this brings the typical runtime of the code down to or below that of an explicit Runge-Kutta method. This is the prerequisite for the extension of variational integrators to higher dimensional versions of the Vlasov-Poisson and Vlasov-Maxwell systems. Further, new one-step integrators for the guiding-centre system where derived and implemented. While previous multi-step variational integrators show perfect conservation of momentum, good conservation of energy, and better long time stability than standard methods, they tend to eventually break down due to errors made in the initialisation of the schemes. The new integrators show the same favourable conservation properties but lack the initialisation problem and therefore show superior long-time stability for extremely long simulation times. This lays the groundwork for the development of geometric particle-in-cell methods for gyrokinetics.

On the theory side, the geometric framework of conservation laws for formal Lagrangians was developed together with its discrete counterpart. It became clear that in the realms of finite-differences the analysis of discrete conservation laws is often not feasible, especially for nonlinear problems, due to the lack of a discrete Leibniz-rule. Promising first results where obtained in an attempt to overcome these limitations by moving to the Galerkin framework using splines as basis functions.

Specific Methods for High Dimensions

A major challenge in simulations of the Vlasov equation stems from the fact that the problem is posed in a six-dimensional phase space. On the other hand, there are classes of methods that are especially designed to efficiently solve high-dimensional problems. We have been investigating the use of such methods for the Vlasov-Poisson equation. The idea of the so-called sparse grid method is to sparsify the high-dimensional mesh in a systematic way such that functions of bounded mixed-derivatives are represented in an economic way. A more recent and less mature technique for high-dimensional problems is the tensor train method. In this method, a high-dimensional function is represented by a nested sum of tensor products. As opposed to the sparse grid method, the compression is not fixed but adapted to the solution.

Semi-Lagrangian solvers for the Vlasov-Poisson equation in both tensor train and sparse grid format have been derived and tested for the Landau and two-stream instability test case in four and six dimensions. In both cases, efficient algorithms have been developed and implemented. The numerical studies have shown compression by a factor of 1E5-1E6 for the solution of the 6D equations in tensor train format. With the sparse grid method, it is more difficult to achieve considerable compression, especially in velocity dimensions. To improve compression for the case of a solution close to an equilibrium, a multiplicative delta-f method has been derived.

Arbitrary Equilibria and Field Aligned Semi-Lagrangian Methods

A hybrid semi-Lagrangian method based on a general mapped mesh in physical space has been developed to treat complex geometries as encountered for tokamak poloidal cross-sections, namely D-shape configurations. An elliptic solver in generalized coordinates based on B-splines tensor product has been implemented in SELALIB, the library that is being developed in the group together with Inria in France for kinetic simulations. Two hybrid semi-Lagrangian codes have been developed and are presently tested: the first code simulates the 4D Vlasov-Poisson problem and the second code is adapted to 4D drift-kinetic slab ITG simulations. In both cases, SELALIB is used as an external library to mimic the development scheme for the GYSELA code.

Another innovative approach using hexagonal meshes based on three directional box-splines for the poloidal plane is under development. A new elliptic solver has been developed to extend the use of B-splines on triangulations, which overcome the restriction of B-splines to Tensor products.

A locally field aligned interpolation for Semi-Lagrangian schemes, adapting a method developed by Hariri-Ottaviani to the semi-Lagrangian context, has been introduced. This approach has been validated on the constant oblique advection equation and on a 4D drift kinetic model with oblique magnetic field in cylindrical geometry. The strength of this method is that one can reduce the number of points in the longitudinal direction. Extension to the tokamak configuration in toroidal geometry is the next step of this study. An asset of this approach is that the magnetic field is always well defined locally, that means between two poloidal planes, and can also be used close to and across the separatrix, which is not the case of classical field aligned coordinate systems.

Fluid Modelling and Simulation
Improved Stability for the Non Linear Reduced MHD Code JOREK

JOREK implements the nonlinear resistive reduced MHD equations. It is discretised in space using a small amount of Fourier modes in the toroidal direction and Finite Elements in the poloidal plane. This yields a nonlinear system of differential equations in time. The classical energy dissipation

properties of the full MHD model can be lost when some terms are neglected in the reduced MHD limit. We have performed a careful derivation for several of the models implemented in JOREK making sure that the dissipation properties are retained and the models are stable. Neglected terms have been added in the code where necessary. The adaptive nonlinear Newton scheme developed last year has be improved and extended to different models. All this makes JOREK more robust and stable. We have now started to investigate efficiency issues in both, computing time and memory consumption. The idea is to make the code more efficient by introducing a new preconditioner for the GMRES iterations using a Schur complement method to transform the iteration operator so that multigrid iterations converge faster. This can be implemented with a matrix free Jacobian computation, thus avoiding the need to assemble and store the Jacobian matrix, resulting in reduced memory requirements.

Improved Models for the SOLPS Code
There is a severe limitation in the time-step observed in the computational-fluid-dynamics kernel of SOLPS related to drift physics, which seems to require a significantly smaller time step than an equivalent simulation without drifts. With the aim of identifying the cause we performed a theoretical analysis of a simplified but relevant model, which enabled us to identify a few issues that might cause the problem. Firstly, without an ad-hoc anomalous perpendicular current density the equation for the electrostatic potential is ill-posed. Secondly, the convergence of the iteration between the evaluation of the drift velocity and the electric current density cannot be guaranteed a priori. And finally, in the derivation of the model a few approximations that break the equivalence with the Braginskii equations have been applied. In order to test whether any of these points is problematic, we developed a stand-alone code based on stabilized finite elements to understand and analyze (a) the coupling between the electron pressure gradient and the electric potential and (b) to isolate the complicated coupling between parallel momentum and current density. Both models are as simple as possible and can be extended later if needed.

Plasma-Material Modelling and Foundations
Uncertainty Quantification for the Two-dimensional Vlasov-Poisson System
The numerical simulation of fusion plasmas involves field quantities, which are hampered by noise – in time or in space or in both. In order to compare results from experiment and model, or to have an estimation of the spread of model predictions, uncertainty quantification is necessary. However, even for a moderate number of uncertain input parameters the convenient approach of Monte Carlo sampling is no longer feasible and more efficient methods need to be applied.

A relatively new and promising approach is based on a suitable spectral expansion of the input parameter distribution. Here the underlying assumption is, that the functional properties of the stochastic processes influencing the input variables are to some extend preserved by the (system of) differential equations in the model (e.g. that Gaussian noise in the input leads to approximately Gaussian distributed fluctuations in the output). This can be exploited for the computation of model predictions. A functional representation, which allows us to investigate the uncertainty propagation through the forward model, was generated by employing a nonintrusive polynomial chaos expansion. For the case of Gaussian noise, it is expedient to choose Hermite functions for the orthonormal basis of our spectral decomposition and to perform the required integrals by Gauss-Hermite quadrature. For first investigations with the newly implemented algorithm the two-dimensional Vlasov-Poisson system is chosen. As a simple test case, we applied a static external electric field distorted with Gaussian noise to a ring (i.e. periodic boundary conditions) of 16 sites and analysed the model response with a focus on the electric field at each site. The data have been computed with three different approaches. The most straightforward way is to sample over the distribution of possible inputs and analyse the distribution of the output electric field establishing thereby the 'exact' result without any additional approximations. This provides also the benchmark the other approaches can be compared with. However, this approach is not suited for more sophisticated models, since the computation time becomes intractable large. The results are shown in the left panel of figure 7 for two time points (T_{upper}=1.44 s, T_{lower}=3.72 s). Particularly interesting is that at some sites the uncertainty becomes smaller at a later time – a fact not expected by common error propagation and a consequence of the nonlinear behaviour of the Vlasov-Poisson system.

On the right side of figure 7 we depict the results for the nonintrusive polynomial chaos expansion method with a spatially randomly varying (but constant in time) input variable at the same time points as for the 'exact' result. While the computation time decreased to a few minutes instead of hours for the left panel, the results agree with each other, underlining the efficiency of the approach.

We pursued a third way considering the random variable to be uncertain at each time step, which establishes a random field over the time incidences and independent random variables of the non-intrusive polynomial chaos expansion. To avoid the parameterization of the random field becoming extensively large one applies a Karhunen-Loève expansion to form a reduced orthonormal basis. Though larger time evolutions result nevertheless in massive computations as well, we found excellent agreement with the sampling approach for times up to 0.5s.
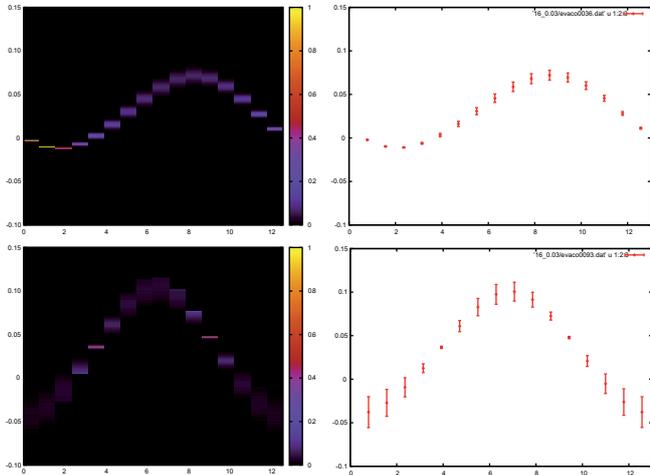
Figure 7: Electric field E(T) obtained by solving the one-dimensional Vlasov-Poisson system for 16 sites with periodic boundary conditions after superimposing an external electric field of $E_{ext}=0.03$ with standard deviation of 0.003 (10 %). Upper row: T=1.44s. Lower row: T=3.72s. Left panel: Resulting distribution with 100000 samples. Right panel: Nonintrusive polynomial chaos expansion letting E_{ext} uncertain but constant throughout time evolution. Depicted is the expectation value of E(T) and its standard deviation (error bar). The agreement of the nonintrusive approach (right) with the 'exact' result (left) is excellent.

Zonal Flows and Structure Formation in Turbulent Plasmas
Zonal Flows

Using the NAN anelastic planetary turbulence code comparison runs have been set up between giant gas planets on the one hand and tokamak core and slab plasma convective turbulence on the other hand. Realistic planetary turbulence simulations are started from a neutral entropy profile, and are driven by a constant cooling rate localized at the surface of the planet. For sufficiently high spin rate of the planet and sufficiently low turbulence drive, zonal flows (ZF) are generated (figure 8). Similar to ZFs in the plasma turbulence (figure 9), the planetary ZFs grow first at relatively short scales. Due to the geometry of the planet, a positive (eastward) flow is always generated at the equator (equatorial super-rotation). With time the flows slowly shift around, showing clear evidence of an effective repulsive force. Different from the plasma scenarios, the ZFs converge to just one equatorial jet and a counter rotation of the rest of the planet. The annihilation of the multiple flows in favour of just one equatorial flow is incompatible with the observations of the large giant planets – it may however rather represent the solar tachocline. It is likely that at different parameters one might recover a behaviour similar to the tokamak core, where a finite ZF wavelength results. In addition bursts of turbulence activity are occurring and sudden increases in the ZFs (which are driven by the turbulence).

The bursts are essentially caused by a threshold in the gradient drive of the turbulence, which varies in time as here the cooling rate is kept constant.
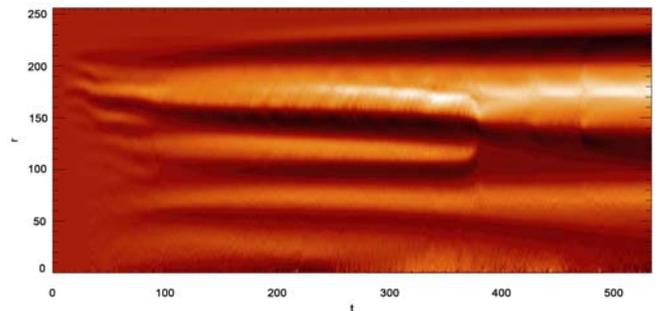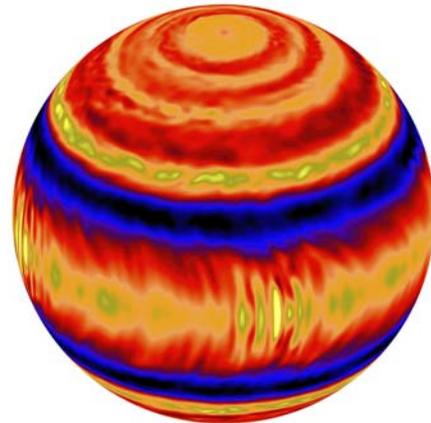
Figure 8: Zonal Flow and turbulence simulations. Top panel: Colour coded zonal flow velocity on the planetary surface. Bottom panel: Time evolution of average vorticity versus distance from planetary axis.
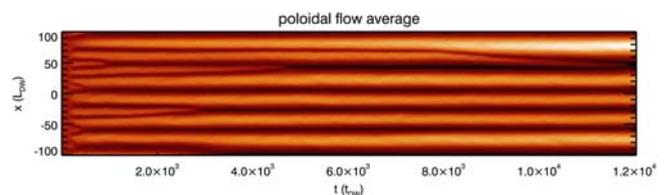
Figure 9: Comparison flows in slab drift wave plasma turbulence simulation.

Workshop on Algorithm and Model Verification and Validation for Kinetic and Gyrokinetic Plasma Simulation Codes (AMVV 14)

As a kick-off meeting for the EUROfusion Enabling Research project WP14-ER-01/IPP-03, we hosted a workshop on verification and validation in Garching from April 8-10 2014, with the aim of coming up with a set of verification tests for kinetic and gyrokinetic codes. There were around 40 participants, which included the participants in the ER project as well as other researchers from Europe and the USA.

Workshop on Numerical Methods for Kinetic Equations (NumKin 14)

A workshop devoted to Numerical Methods for the Kinetic Equations of Plasma Physic was organized by the division. It was hosted on the IPP site from October 20-24 2014. It involved around 50 mathematicians and physicists interested in numerical methods for different kinetic models such as Vlasov, Boltzmann, and Fokker-Planck-Landau as well as reduced models and gyrokinetic models with or without collisions. Different numerical methods including Particle-In-Cell and several semi-Lagrangian and Eulerian techniques were considered.

Scientific Staff

J. Ameres, C. Caldini-Queiros, A. Dodhy-Würsching, E. Franck, Y. Güçlü, K. Hallatschek, H. Heumann, F. Hindenlang, A. Kammel, K. Kormann, M. Kraus, O. Maj, M. Mehrenberger, L. Mendoza, H. Oberlin, R. Preuss, A. Ratnani, M. Restelli, G. Strohmayer, U. von Toussaint, N.Tronko, A. Wacher.

Guests

S. Espinosa, CIEMAT Madrid, SP; G. Latu, CEA, FR; O. Laffite, Univ. Paris 13, FR; M. Mehrenberger, Univ. Strasbourg, FR; A. Hamiaz, Univ. Strasbourg, FR; P. Navaro, CNRS, Strasbourg, FR; A. Ratnani, CEA, FR; C.-D. Munz, Univ. Stuttgart; C. Klingenberg, Univ. Würzburg; P. Helluy, Univ. Strasbourg, FR; C. Steiner, Univ. Strasbourg, FR; V. Grandgirard, CEA, FR; J. V. Gutierrez Santacreu, Univ. Sevilla, SP; J.-L. Vay, Lawrence Berkeley National Laboratory, USA; P. Morrison, Univ. of Texas at Austin, USA; B. Ayuso de Dios, Centre de Recerca Matemàtica, Barcelona, SP; E. Chacon-Golcher, Inria, Strasbourg, FR; M. Campos Pinto, CNRS, Paris 6, FR.

High Level Support Core Team

Head: Dr. Roman Hatzky

Tasks of the High Level Support Team

The High Level Support Team (HLST) provides support to scientists from all Research Units of EUROfusion for the development and optimization of codes to be used on the HELIOS supercomputer system at the Computational Simulation Centre of International Fusion Energy Research Centre (IFERC-CSC), Aomori, Japan. The HLST consists of a core team based at IPP Garching and of staff members provided by the other Research Units. The former has six members and the latter contributes with an additional four scientists. This year the HLST core team was involved in eleven different projects submitted by scientists from all over Europe. By way of example, we present here an overview of the work being done for three projects.

PARSOLPS Project

The SOLPS code package is widely used to simulate Scrape-Off Layer (SOL) plasmas, and two main components of this package are the B2 and the EIRENE codes. B2 is a plasma fluid code to simulate edge plasmas and EIRENE is a kinetic Monte-Carlo code for describing neutral particles. While EIRENE is parallelized with MPI, the B2 code is only partially parallelized using OpenMP. The aim of the PARSOLPS project is to speed up the B2 code and consequently also the coupled B2-EIRENE system.

According to Amdahl's law, the maximum achievable speedup is determined by how large the parallel fraction of the code is. In the frame of the PARSOLPS project, this fraction was significantly increased in the B2 code. The difficulty was that there are many subroutines which take a small share of the CPU time. More than 20 subroutines have been parallelized, and 91% of parallelism has been reached in the whole code. With these changes a speedup of a factor of six can be achieved for the ITER test case when executed on one HELIOS computer node. The execution time scales well for most of the subroutines as we increase the number of threads. The OpenMP regions were introduced in a way to avoid large overheads. It was identified that a large part of the code is memory bandwidth limited. Several of the subroutines were optimized to reach a speedup which is close to the bandwidth limit. The individual subroutines have been tested separately to ensure the correctness of the modified code and to measure the speedup. To aid this work, an automatic unit test generation framework has been created. The project continues in the next year by investigating distributed memory parallelism and coupling the improved version of B2 with the EIRENE code.

HIMAT Project

For the HIMAT project we used the HLib library to get a framework for H-matrix approximations. As test cases we

used the Poisson problem being discretised with the Finite Difference Method (FDM), the linear, bilinear, and trilinear Finite Element Method (FEM) without overlapping elements and the cubic B-spline FEM with overlapping elements. In both 2D and 3D we used a geometric bisection clustering and in 3D in addition a domain-decomposition clustering. Wherever possible, we tried to use the H-matrix format to approximate the inverse matrix and the Cholesky (or LDL) decomposition which we both tested as a preconditioner for the GEMRES iterative solver.

Especially for the Cholesky and LDL decomposition we could achieve very good results in terms of memory consumption and speed for the FDM and linear, bilinear, and trilinear FEMs. The larger the number of degrees of freedom (DoF), the smaller the memory consumption becomes in the case of the H-matrix format compared to the original one. This is even more pronounced for the 3D case compared to the 2D case. For the inverse matrix in H-matrix format a similar behavior can be observed, however less pronounced. Nevertheless, the situation is not that positive when it comes to the Cholesky and LDL decomposition for the cubic B-spline FEM with overlapping elements. For this case the domain-decomposition clustering does not work due to the overlap. Unfortunately, also the geometric bisection clustering fails for larger number of DoF. Therefore, further investigation has to be done on this issue.

REFMUL2P Project

Simulation of x-mode reflectometry using a finite-difference time-domain (FDTD) code is one of the most popular numerical techniques. However, the simulations can become quite demanding. The REFMUL2P project and its predecessor (REFMULXP) were devised to circumvent these questions by implementing a parallel version of the x-mode REFMULx C-code.

The code was first profiled, revealing the numerical kernel as the hot-spot cost-wise, as expected. Then, the single-core performance of these code regions was improved by restricting the scope of the pointers therein to be non-aliased and by re-writing the corresponding numerical expressions such to minimize the number of floating-point operations inside the loops. Both modifications together aided the compiler optimization tasks and resulted in a speedup factor of eight. The development of parallelization strategy followed with the OpenMP threaded version as the first implemented. Then, the full MPI task parallelization was made, which included the domain decomposition and inter-task communication. This required significant, but necessary changes to the source code. Finally, both paradigms were combined to yield a hybrid MPI/OpenMP version.

The scaling measurements made within a single node of HELIOS showed similar behaviour for the pure threaded and pure multi-tasked codes, provided that the process affinity was managed optimally. A maximum speedup of 50 was obtained. For inter-node scaling studies the pure MPI and hybrid parallel codes were used. They showed similar behaviour up to 512 with fixed problem size. The speedup obtained was over 400, meaning that, a run which took over four hours to finish originally could run in half a minute. Using higher numbers of cores required bigger problem sizes. So, a weak scaling study was made, where the problem size increased proportionally to the core-count. The scaling was made up to 4096 cores on HELIOS with a problem size 256 times bigger than the original. The exercise served as a basic proof-of-principle for the applicability of the parallelization techniques developed here to a planned three dimensional code that will employ much bigger grid-counts. It further became clear that parallel I/O must be addressed at some point, which, despite being beyond the scope of this project, provides a useful hint for future developments.

Scientific Staff

T. Fehér, M. Haefele, K. S. Kang, M. Martone, T. Ribeiro.

Turbulence in Laboratory and Astrophysical Plasmas

Head: Prof. Dr. Frank Jenko

The main goal of our research efforts is to better understand the important unsolved problem of plasma turbulence in the context of magnetic confinement fusion science as well as astrophysics. Spanning a wide range of approaches, from simple analytical models to simulations on massively parallel computers, we address both fundamental issues as well as applications to specific experiments. Below, a few current projects are briefly described. For a more complete overview and details, please visit the website http://www.ipp.mpg.de/~fsj.

Direct Comparison of Gyrokinetic Turbulence Simulations with Tokamak Experiments

Over the last few years, gyrokinetic turbulence simulation has matured to a point where the nonlinear simulation results can be directly compared with tokamak experiments, allowing for a constructive dialogue between first-principles theory and measurements. Several projects in our group have been dedicated to exploring new opportunities at the interface of state-of-the-art computing and diagnostics. In one project, we investigated recent claims regarding a systematic underprediction of the ion heat transport level in the outer-core region of L-mode discharges. This so-called transport shortfall would imply that at this point no reliable theoretical predictions can be made in the outer core of many tokamak discharges, and it has even called into question the very validity of gyrokinetic theory. In a dedicated set of simulations with the GENE code based on the plasma parameters of a specific DIII-D L-mode discharge, this claim could not be confirmed, however. Instead, it was possible to match the inferred fluxes from the experiment out to about r/a=0.9. Also, via the use of synthetic diagnostics, it was possible to reproduce the experimental Correlation Electron Cyclotron Emission (CECE) measurements with a high degree of accuracy.

In another study with GENE we simulated an ASDEX Upgrade discharge, analysing various fluctuating quantities and comparing them to experimental measurements carried out via Doppler reflectometry. The heat fluxes in the nonlinear simulations could be matched to the experimental values by varying the logarithmic ion temperature gradient within the expected experimental error bars. The radial dependence of the density fluctuation amplitudes could also be reproduced. Fur-thermore, the simulations predict that the wave number spectra for the density fluctuations should exhibit power laws with non-universal scaling exponents as well as turbulent cross phases between density and electron temperature fluctuations which are well characterised by their respective linear values. These quantities will be measured in future campaigns, providing valuable tests for our theoretical understanding of turbulence in magnetised fusion plasmas.

Yet another study based on GENE focussed on electromagnetic effects on turbulent transport in high-performance ASDEX Upgrade discharges. Modern tokamak H-mode discharges routinely operate at high plasma beta. Dedicated experiments performed on multiple machines measure contradicting dependence of the plasma confinement on this important parameter. In view of designing high-performance scenarios for next-generation devices like ITER, a fundamental understanding of the involved physics is crucial. Theoretical results – most of which obtained for simplified setups – indicate that increased beta does not only modify the characteristics of micro-turbulence, but also potentially introduces fundamentally new physics. Empowered by highly accurate measurements at ASDEX Upgrade, the turbulence code GENE is used to perform a comprehensive gyrokinetic study of dedicated H-Mode plasmas. We find the stabilization of ion-temperature-gradient driven turbulence to be the most pronounced beta effect in these experimentally relevant cases. The resulting beta-improved core confinement should thus be considered for extrapolations to future machines.

Fundamental Properties of Turbulence in Laboratory and Astrophysical Plasmas

Turbulence is widely recognized as one of the most important open problems in modern physics, and turbulence in magnetized plasmas is at the heart of countless important processes in natural and laboratory plasmas. Therefore, its study is of great interest from both a fundamental and an applied perspective. One main goal in this context was to better understand the nonlinear redistribution and dissipation of free energy in turbulent magnetised plasmas. We continued the application of advanced analysis techniques from fluid turbulence to plasma physics and further developed so-called Large Eddy Simulation (LES) techniques in the context of plasma micro-turbulence. Moreover, we started to explore the issue of the small-scale termination of the turbulent energy cascade in collisionless plasmas which is widely viewed nowadays as a key challenge in space plasma physics and plasma astrophysics. By means of GENE simulations with unprecedented numerical resolution, we were able to provide novel insights into the multi-scale nature of dissipation processes at kinetic scales between the ion and electron gyroradii. Moreover, simulation studies with a hybrid Vlasov-Maxwell code highlighted the role of strong current sheets where magnetic reconnection occurs within a turbulent environment as well as the role of the formation of shock structures.

Scientific Staff

J. Abiteboul, P. Astfalk, A. Bañón Navarro, V. Bratanov, A. de Bustos Molina, S. Cerri, H. Doerk, K. Finke, T. Görler, M. Oberparleiter, D. Told, M. Weidl.

Max Planck Princeton Cooperation

Max Planck Princeton Research Center for Plasma Physics

Head: Prof. Dr. Sibylle Günter

Plasma Turbulence

Within the MPPC, fundamental aspects of plasma turbulence as well as applications to fusion research or space and astrophysics have been investigated in close collaboration between scientists at IPP, MPS, PPPL, and Princeton University. In this context, it was often possible to transfer tools and insights from one area to another, exploiting synergies which were hitherto neglected.

The gyrokinetic code GENE has been used, among other things, to shed new light on the energetic coupling between various degrees of freedom in turbulent plasmas [1]. This allows for the construction of reduced models for the prediction of turbulent transport in fusion experiments [2], and it forms the basis for a much deeper understanding of dissipation mechanisms in solar wind turbulence [3] as well as of the interaction between turbulence and magnetic reconnection in space plasmas [4]. Also, the newly developed full-flux-surface version of GENE has been used to predict the anomalous transport in future Wendelstein 7-X experiments, based on the first simulations of this kind [5].

It has recently been shown analytically and in linear gyrokinetic GENE simulations that it is beneficial for trapped-electron-mode (TEM) stability to have a high fraction of trapped particles that experience good average curvature, because they stabilize the modes. This is particularly true in perfectly quasi-isodynamic stellarators with the maximum-J property, but configurations that are only approximately quasi-isodynamic, like W7-X, can also benefit from reduced TEM growth rates. From this, two important questions arise: does the enhanced linear stability result in reduced transport levels? And can this knowledge be used to optimise stellarators not only for neoclassical, but also for turbulent transport?

Both questions were addressed in 2014. We achieved first-of-a-kind turbulence simulations of both ion-temperature-gradient (ITG) driven and density-gradient driven TEM turbulence where the electrons were treated kinetically. We found that the heat fluxes for purely temperature-gradient-driven ITG turbulence are broadly similar in W7-X and in typical tokamaks, if the difference in surface-to-volume ratio of these devices is accounted for. In simulations of density-gradient-driven TEMs, however, W7-X has much lower transport levels. These findings motivate the optimisation method for configurations like the TEM-

In the 3rd year of the MPPC a large number of projects on fundamental aspects of experimental and theoretical plasma physics have been continued based on cross-Atlantic collaborations. Over 70 publications acknowledging the MPPC have been published and numerous short and long-term visits were facilitated by the center. One workshop in Berlin with ca. 80 participants has been organised, that attracted also a broader community outside the MPPC.

dominated stellarator HSX, where the growth rates of TEMs are significantly higher than in W7-X. A "proxy" function was designed to estimate the TEM growth rate, allowing optimal configurations for TEM stability to be determined with the STELLOPT code.

Magnetic Reconnection

Operation of VINETA II continued throughout the last year, during which research focused on the experimental studies of electromagnetic fluctuations within the reconnection current sheet. The fluctuation amplitude linearly correlates with the local mean current density within the sheet. This has shown not to be a particular feature of the reconnection geometry, but has been reproduced by an electrostatically driven current in VINETA II without X-point magnetic field topology. The spectra of the perpendicular magnetic fluctuations are generally broadband and display a power law decrease throughout the entire spectral range of the diagnostics, indicating strongly turbulent fluctuations. However, the spectra consistently feature a breaking slope behavior at the lower-hybrid frequency with a larger spectral index at higher frequencies. As displayed in figure (a) this holds for all cases, for which the lower-hybrid frequency is changed by operation parameters, as, e.g., the magnetic guide field (shown in figure (a)), or the ion mass. The detailed physical mechanisms are under investigation but it strongly suggests either an increased wave energy dissipation or an instability drive at this particular frequency, as has been suggested to be the lower-hybrid drift instability. However, the measured dispersion relation of fluctuations, shown in figure (b), agrees well with linear whistler wave calculations, which can couple to lower-hybrid waves and might represent a dissipation mechanism.

The seeding mechanism for the onset of tearing modes which is directly linked to the fundamental problem of the magnetic reconnection in fusion plasmas was investigated via direct measurements in ASDEX Upgrade (AUG). The strong perturbation from internal sawtooth crash triggers first an ideal kink mode

[1] Teaca et al., Phys. Plasmas 21, 072308 (2014);
    Hatch et al., J. Plasma Phys. 80, 531 (2014).

[2] Bañón Navarro et al., Phys. Plasmas 21, 032304 (2014).

[3] Cerri et al., Phys. Plasmas 21, 082305 (2014).

[4] Pueschel et al., ApJS 213, 30 (2014).

[5] Xanthopoulos et al., Phys. Rev. Lett. 113, 155001 (2014).
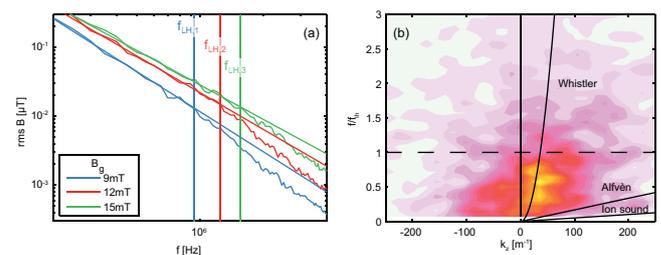
Figure: (a) Fluctuation power spectra of magnetic fluctuations for three different magnetic guide fields. The respective lower-hybrid frequency is indicated by the vertical lines. (b) Result of the dispersion measurement and comparison to linear wave calculations of ions sound, Alfvén and whistler waves.

directly after the crash. The tearing mode appears to be the result of slow conversion from the ideal mode into a resistive mode. Several factors such as the perturbation amplitude and differential rotation are important for this process and determine this conversion time. New experiments and numerical simulations with the non-linear two fluid MHD code M3D-C1 are aimed to identify the main players of the seeding process.

Using the recently developed multiregion, relaxed MHD (MRxMHD) theory, which bridges the gap between Taylor's relaxation theory and ideal MHD, a thorough analytical and numerical proof of the formation of singular currents at rational surfaces in non-axisymmetric ideal MHD equilibria has been constructed. These include the force-free singular current density represented by a Dirac δ-function, which presumably prevents the formation of islands, and the Pfirsch-Schlüter singular current, which arises as a result of finite pressure gradient. An analytical model based on linearized MRxMHD is derived that can accurately (1) describe the formation of magnetic islands at resonant rational surfaces, (2) retrieve the ideal MHD limit where magnetic islands are shielded, and (3) compute the subsequent formation of singular currents. The analytical results are benchmarked against numerical simulations carried out with a fully nonlinear implementation of MRxMHD.

Magneto-rotational Instability

The magneto-rotational instability (MRI) is of central astrophysical importance for the process of accreting matter on a central gravitating object such as a black hole or a newly forming protostar. This phenomenon is investigated by the plasma-astrophysics group at Technische Universität Berlin in collaboration with Princeton University and Princeton Plasma Physics Laboratory. Turbulence driven by the MRI is expected to enhance the outward transport of angular momentum in accretion disks necessary for astronomically observed accretion rates. A fundamental problem which defies resolution since early numerical shearing-box studies of MRI turbulence, is the dependence of the nonlinear saturation level on the Reynolds number, Re: increasing Re diminishes the resulting turbulence amplitude. Only additional constraints imposed on the system such as a mean magnetic field, density stratification, or an elongation of the simulation volume along one spatial direction eliminate this unexpected behaviour. To tackle the problem, a new parallel high-precision magnetohydrodynamics simulation code, csmhd, had been implemented. The finite-volume central-scheme approach, in combination with the constrained transport method to ensure vanishing divergence of magnetic fields, has been chosen because of expected performance benefits compared to standard Godunov-like upwind methods. First comparison runs with a standard implementation of ATHENA, a modern Godunov-class simulation tool developed by our collaborators at Princeton university showed a significantly higher efficiency of csmhd. In addition, the csmhd code achieves

superior precision for smooth solutions while being slightly more dissipative in the case of discontinuities. The program has been debugged and extensively tested and is now ready for production runs and further optimization.

Energetic Particles

The acceleration and propagation of energetic particles in background MHD turbulence has been studied, with applications to cosmic ray physics in mind. In particular, the impact of a deviation from the usual simplifying assumption of balanced turbulence was investigated, and significant effects regarding the transport of the fast particles have been found [6]. In a related project, the acceleration of cosmic rays in shock fronts has been studied via a novel combination of fluid and particle techniques, providing new insights into the generation of cosmic energetic particles.

The numerical tools used for runaway electron (RE) modeling were further developed, e.g. HAGIS was extended to include relativistic physics, and the coupling between the CODE and GO was finished. We analysed the interaction of post-disruption plasma waves with runaway electrons on TEXTOR. In agreement with experimental observations we identified these waves as toroidal Alfvén eigenmodes (TAE), possibly driven by a spatial gradient of the background electron distribution. We applied GO to ITER disruptions to give predictive figures for typical disruption scenarios in terms of quench times and most dominant runaway generation mechanisms [7]. GO was extended to describe the effect of RMPs on runaway confinement in a self-consistent way. We found that RMPs on themselves will not be strong enough to suppress runaway generation in ITER [8]. A reliable scenario was established at AUG for runaway research. The suppression of REs is achievable with a secondary Argon injection during the plateau.

The benchmark concerning Alfvénic modes based on a well-diagnosed AUG discharge was revisited and modified in order to accommodate a wider range of codes. Excellent agreement was for the linear mode properties in appropriate limits and the influence of kinetic effects was documented in a detailed way.

Scientific Staff

P. Astfalk, H. Bohlin, V. Bratanov, A. de Bustos Molina, S. Cerri, J. Clementson, N. Fahrenkamp, O. Grulke, T. Görler, S. Günter, P. Helander, V. Igochine, F. Jenko, T. Klinger, K. Lackner, Ph. Lauber, J. Loizu, D. Meshcheriakov, D. Milojevich, W.-C. Müller, A. Banon Navarro, G. Papp, G. Plunk, J. Proll , K. Rahbarnia, I. Shesterikov, P. Singh Verma, A. von Stechow, D. Told, M. Weidl, T. Windisch, P. Xanthopoulos.

[6] Teaca et al., Phys. Rev. E 90, 021101 (2014); Weidl et al., submitted to ApJ.

[7] E. M. Hollmann,G. Papp et al., POP 021802 (2015).

[8] G. Papp et al., submitted to JPP.

Supercomputing

Computer Center Garching

Head: Dipl.-Inf. Stefan Heinzel

Introduction

The Rechenzentrum Garching (RZG) provides supercomputing and archival services for the IPP and other Max Planck Institutes throughout Germany. Besides operation of the systems, application support is given to Max Planck Institutes with high-end computing needs in fusion research, materials science, astrophysics, and other fields. Moreover, the RZG provides data visualization services for the exploration and quantitative analysis of simulation results. Data management and long-term storage services are provided for large sets of experimental data, supercomputer simulation data, and data from the humanities for many Max Planck Institutes. In addition, the RZG provides network and standard IT services for the IPP and other MPIs at the Garching site. The experimental data acquisition software development group XDV for both the Wendelstein 7-X fusion experiment and the current ASDEX Upgrade fusion experiment operates as part of the RZG. Furthermore, the RZG is engaged in several large MPG, national and international projects in collaboration with other scientific institutions.

Systems

The RZG operates the Max Planck and IPP supercomputer named "Hydra" with an aggregated peak performance of 2.8 PFlop/s with more than 80,000 compute cores and Mellanox InfiniBand FDR14 interconnect technology. It consists of an Intel Sandy Bridge based part (with 200 TFlop/s peak, since 2012), an Intel Ivy Bridge processor based system with 1.6 PFlop/s peak, and an Intel Ivy Bridge processor based system (350 compute nodes) equipped with 676 NVidia Kepler K20X GPUs and 24 Intel Xeon Phi cards, respectively. Hydra is highly used by many Max Planck Institutes. Furthermore, a series of different mid-range Linux clusters are operated for the IPP and further Max Planck Institutes, and also the ITM gateway computer for the European fusion research community is operated by the RZG. A graphics system for remote visualization services with fast access to the Hydra file systems is also maintained. Tape libraries for mass storage are maintained locally at the IPP and at the LRZ (Leibniz Rechenzentrum) for the second tape copies of archival data, for protection against physical damage, with a dedicated network connection of 10 Gb/s. HPSS is used for archive data, while TSM (Tivoli Storage Manager) is used for backups. For storage of Wendelstein 7-X experiment data, a dedicated HPSS instance was created at the RZG. The RZG also operates the complex network infrastructure for Max Planck Institutes

The RZG supports optimization of complex applications from plasma physics, astrophysics, materials science, and other disciplines for supercomputers and offers data management services and infrastructure. Moreover, the RZG provides data visualization services for the exploration and quantitative analysis of simulation results and plays a leading role in several large MPG, national and international projects in collaboration with other scientific institutions.

at the campus Garching and the access of other Munich Max Planck Institutes via the Munich Science Network provided by the LRZ to the RZG and to the German Science Network of DFN for general internet access.

High-Performance Computing

Support in the field of high-performance computing (HPC) is a central mission of the RZG. Major tasks are the optimization of codes and participation in visualization and graphical preparation of data, also for computer architectures and systems, which are not running at the RZG, but at other institutes and computing centres world-wide. In the course of 2014 among others significant contributions have been made to the following applications: parallelization of methods recently integrated in the FHI-aims code of the FHI, increase of the parallel scalability of the supernova code VERTEX from the MPI for Astrophysics up to 131,000 cores, algorithmic developments related to stellarator geometry for the micro-turbulence code GENE of the IPP, parallelization of the edge plasma simulation code SOLPS from the IPP, porting of compute-intensive routines of the DFT class library S/PHI/nX from the MPI für Eisenforschung to GPUs, developments for the class library H5xx for data input and output from the MPI for Intelligent Systems, hybrid parallelization of the dynamo code MagIC from the MPI for Solar System Research, distributed parallelization of the new C++ code BioEM for Bayesian modelling of electron-microscopical pictures from the MPI of Biophysics. In the following selected projects are presented in more detail.

GENE Code

GENE is one of the leading codes for gyrokinetic plasma turbulence simulations. GENE is widely used for different physics applications and runs on all major supercomputer platforms. During the last year, GENE has been extended to overcome the assumption of toroidal periodicity (which is usually fulfilled in tokamak scenarios) to make the code ready for full-3D magnetic geometries. This is mainly necessary for the simulation of gyrokinetic plasma turbulence in stellarators, but also for the investigation of perturbations in the tokamak's magnetic field. The implementation of the 3D case was carried out in collaboration with the NMPP department and led to the introduction of an object hierarchy realized with new Fortran 2003/2008 features. The main challenge of the 3D geometry is to use a grid in real space also for the y direction. By that, the gyro-averaging procedure and the field solve become matrix-vector multiplication and solution of a linear system of equations, respectively.

The gyromatrix and the matrix for the linear solver are sparse and hence suitable parallelized sparse linear solvers have to be employed. It was decided to use Petsc for the sparse-matrix format and the matrix-vector multiplication, and as a first approach the MUMPS package has been used for the direct solution of the field equation. For the derivatives in y direction, standard finite differences as in the other directions have been successfully used. With these extensions it was possible to reproduce linear ITG simulations with adiabatic electrons from the local and x-global mode with the new full-3D physical grid. For full functionality the work has to be continued to include physical boundary conditions, electromagnetic effects, and kinetic electrons.

SOLPS Code

The SOLPS code is used to simulate the important scrape-off layer in tokamak experiments such as ASDEX Upgrade (AUG). SOLPS consists of several components, most importantly the plasma fluid module B2 and the Monte-Carlo transport code Eirene for neutral species. Starting out from an existing, preliminary OpenMP parallelization of B2 which showed only very modest speedups, the RZG together with the European High-Level Support Team (HLST) has substantially improved and extended the parallelization of B2 and demonstrated speedups of a factor of 5-6 with respect to the serial production version used at AUG. Verification of the new parallel B2 code module is almost completed and the code is about to be released to AUG users. Corresponding to B2's runtime share of about 50 %, SOLPS production runs are expected to be faster by a factor of 2 to 3. Work has begun to identify a suitable version in the existing zoo of Eirene variants which provides the necessary functionality for AUG applications and at the same time supports MPI-parallel operation. After coupling to the parallel B2 code, SOLPS production runs will be able to take full advantage of the 5-6-fold speedups that have been achieved for the B2 module.

IDE Code

At the ASDEX Upgrade (AUG) experiment tokamak magnetic equilibria are calculated with the equilibrium code IDE (integrated data equilibrium) which employs a Grad-Shafranov solver together with a comprehensive set of external (magnetic) and internal constraints. Depending on the chosen time resolution, the IDE analysis of a typical AUG discharge requires roughly 45 minutes of computing time, or approximately 2 seconds per time point. Trivial parallelization over individual time points and distribution over the cores of a compute cluster so far allowed completing the post processing of a discharge well within the experiment cycle, i. e. in a few minutes. However, latest physics improvements to IDE, specifically the introduction of a current diffusion term which supplements the set of internal constraints, entail a numerical coupling between subsequent time points, and hence new, non-trivial levels of

parallelism have to be exploited in order to meet the runtime requirements for post processing. To this end, the relevant routines of the IDE code have recently been substantially optimized and OpenMP parallelized at the RZG. On 10 cores of a modern CPU the entire IDE analysis now takes roughly 0.2 s per time point, which enables routine post-processing of AUG discharges employing the new physics description of IDE and using an up to 10-fold increased time resolution.

ELPA, a Library of Scalable Eigenvalue Solvers

Highly-scalable direct eigenvalue solvers for symmetric matrices had been developed through a BMBF project coordinated by the RZG. The software called ELPA, which is publicly available under an LGPL license, is in world-wide usage in different simulation software packages and meanwhile is packaged with major Linux distributions. ELPA is maintained in a GIT repository for public use and was further optimized in collaboration with the TU Munich.

GPU and Many-Core Computing Technologies for HPC Applications

The RZG supports the development of GPU and Many-Core applications and the assessment and operation on the large GPU partition of the HPC system Hydra (with 676 Nvidia K20x GPUs) and on various departmental clusters. In the course of the year 2014, RZG's application support group has actively contributed to porting and benchmarking of the following codes to GPU and/or to Intel's Many-Core architecture: GENE (IPP), S/PHI/nX (MPI für Eisenforschung), BioEM (MPI of Biophysics), MNDO (MPI für Kohlenforschung), GROMACS and NAMD (in collaboration with the MPI of Biophysics and the MPI for Biophysical Chemistry), and ELPA (in collaboration with Nvidia).

PRACE

The RZG continued as Tier-1 partner together with the Gauss Centre for Supercomputing (GCS) in the EU FP7 PRACE-3IP project where many European supercomputing centres collaborate for the support of excellent simulation projects from all over Europe. The RZG had a leading role in the organization and conduction of the international "HPC Summer School in Computational Sciences", which was held in June 2014 in Budapest for 80 Canadian, European, Japanese and US American postgraduate students and postdocs with PRACE financing the European participants. Four participants came from the MPG.

Scientific Visualization

The RZG operates a central visualization infrastructure for the Max Planck Society and the IPP. It enables scientists to efficiently perform interactive remote visualization of large data sets generated at the supercomputer Hydra or at the Linux clusters, in particular without the need to transfer the data to local workstations. The RZG supports scientists with the use of these

resources and also takes over concrete visualization projects. As an example, the figure shows snapshots from the temporal evolution of turbulent structures in a highly resolved turbulence simulation of a model of a cold accretion disc. The simulations were performed by the MPI for Dynamics and Self-Organization in the context of the PRACE/DECI project HYDRAD which received visualization and code-optimization support from the RZG.
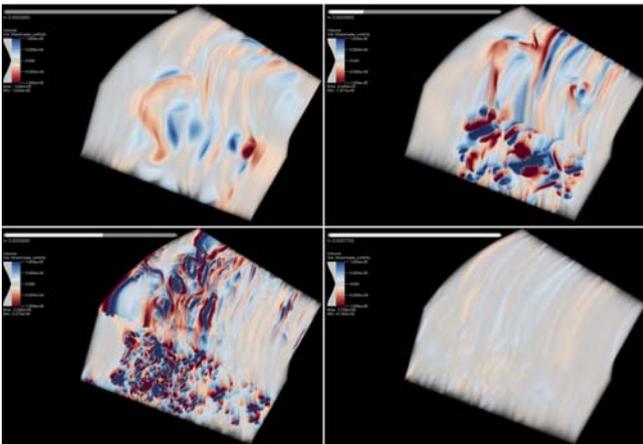
© Data: MPI for Dynamics and Self-Organisation; Visualization: Markus Rampp, RZG.

Figure: Temporal evolution of the vorticity in a representative spatial section of a model of a protoplanetary accretion disc.

Data Services

Within the past few years, services around the handling of scientific data have gained more and more importance and the RZG has addressed this by establishing a new group in 2013 dedicated to the topic. The RZG now provides a variety of services all the way from offering several storage systems for different needs through the provisioning of Persistent Identifiers (PID) to handling metadata. Through the participation in national and international projects the RZG gains new experiences and expands its know-how to improve its service portfolio. Many of these services are also of interest to the fusion community. In the following several examples will be given to illustrate this.

Tape Library and Migrating File Systems
For long-term archiving the RZG operates a tape library which in late 2011 was switched to using IBM's High Performance Storage System (HPSS). By now most data have been migrated to using the new system. HPSS offers a variety of interfaces out of which the GPFS-HPSS-Interface (GHI) to IBM's General Parallel File System (GPFS) which provides concurrent high-speed file access to applications executing on multiple nodes of clusters allows for a seamless integration between the RZG's most powerful file system and the tape archive. The fusion experiment Wendelstein 7-X has its own dedicated GHI system at the RZG to fully support the amount of data expected to arise from the upcoming measurements.

In addition, the RZG has worked on a convenient web interface to the archive that is expected to be placed into production during 2015.

Sync&Share
With the increasing prevalence of mobile and hand-held devices cloud-based sync&share solutions are getting more and more popular. People appreciate the convenience of services like Dropbox and expect similar offerings in their work environment. To this end the RZG has set up an in-house private storage cloud using the ownCloud software stack. All users with an account at the RZG can use this service after subscribing to it. A web interface provides convenient access to files and folders uploaded to this site from anywhere through a web browser. In addition, there are desktop as well as mobile clients to keep local copies of selected folders in synchrony across multiple devices. Controlled sharing with colleagues is also supported including collaborators outside the MPG. More information on this new service is available at https://www.rzg.mpg.de/services/data/share.

Databases
Providing databases as a service is among the core offerings of RZG's data group. This includes not only the provisioning and management of several database management systems, but also support with regard to long-term maintenance or the evaluation of potential alternatives.

Comptel
In the late 1990s the MPI for Extraterrestrial Physics developed COMPASS, a system for the processing and analysis of data from COMPTEL, a gamma-ray telescope that was put into orbit on board the NASA Gamma-Ray Observatory. Since then the data were managed and made available using an Oracle database together with the Fortran-based Oracle FORMS which will soon reach their end of lifetime. To make the system future-proof the RZG supported the MPE in 2014 to migrate all data to the open-source RDBMS MySQL and to re-implement the user interface using a modern Java-based web application framework (ZK Toolkit).

Movebank
Movebank is a free, online database of animal tracking data hosted by the MPI for Ornithology in Radolfzell. Movebank is an international project with over four thousand users, including people from research and conservation groups around the world. During 2014 the RZG has deployed a clustered NoSQL database, namely HBASE, for evaluation by the Movebank developers. After an initial test phase yielding positive results for both functionality and performance, plans are now discussed for the deployment of a production HBASE system for the Movebank project. This system will address performance and scalability issues which have been identified with the current system that relies on a PostgreSQL database server.

IPP/AUG

In preparation for an upgrade of both the Oracle software and Linux operating system a test/mimic instance of the Oracle database was deployed on a virtual machine. The upgrade of the OS as well as major, and subsequent minor, updates to the Oracle software have been tested on this mimic system. This allows to ensure a smooth and fast upgrade process on the production system.

International Data-intensive Projects
CLARIN

The RZG is a member of the CLARIN project (Common Language Resources and Technology Infrastructure) which aims at providing easy and sustainable access for scholars in the humanities and social sciences to digital language data (in written, spoken, video or multimodal form) and advanced tools to discover, explore, exploit, annotate, analyse or combine them, independent of where they are located. To this end CLARIN is building a networked federation of European data repositories, service centres and centres of expertise – one of which being the RZG – with single-sign-on access for all members of the academic community in all participating countries. Tools and data from different centres are made interoperable, so that data collections can be combined and tools from different sources can be chained to perform complex operations to support researchers in their work.

RDA

The RZG continues to actively contribute to the Research Data Alliance (RDA) including its European branch RDA-Europe. RDA's mission is to build the social and technical bridges that enable open sharing of research data on a global scale and across all disciplines. Members of the RZG are actively involved in several working and interest groups as well as in the RDA Technical Advisory Board and the RDA Secretariat. In addition, the RZG has organized the first RDA Science Workshop in February 2014 at the headquarter of the Max Planck Society in Munich as well as the first national RDA meeting in November in Potsdam.

EUDAT

The RZG is also engaged in the EUDAT project, a pan-European data initiative that started in October 2011. EUDAT brings together a unique consortium of 25 partners – including research communities, national data and high-performance computing (HPC) centres including the RZG, technology providers, and funding agencies – from 13 countries. EUDAT is tasked to build a sustainable cross-disciplinary and cross-national data infrastructure that provides a set of shared services for accessing and preserving research data from all disciplines. The RZG participates in the requirements analysis, service development and service enabling, and it is coordinating the operation of the EUDAT infrastructure with its distributed services. To illustrate the usage of these services the RZG has established a collaboration with the Museum of Natural History in Berlin which manages and hosts an Animal Sound Archive. All underlying data as well as the software stack used to make these data web accessible are replicated to the RZG using EUDAT services thereby providing a fallback site to further increase the security and robustness of the *Tierstimmenarchiv*.

Virtual Hosting Environment

The RZG operates a virtual hosting environment based on VMware vSphere. This approach allows for a quick and flexible allocation of resources (virtual machines) for small to medium-sized projects. Currently, the platform is hosting a variety of services on more than 100 virtual machines. These range from services operated by the RZG like the GIT hosting service over services of the IPP (various web sites and web services) to projects by various Max Planck Institutes and national and international data projects like CLARIN, DARIAH, EUDAT and RDA-Europe. For the virtual machines, the user has the choice of either SuSE Linux Enterprise Server or Scientific Linux as the operating system. Generally, the operating system is managed and kept up-to-date by the RZG, while the user/service admin is granted root access to deploy and manage their service. Working together with other groups at the RZG, assistance can be offered each step of the way.

Data Acquisition for Plasma Fusion Experiments

The XDV group is engaged in data processing of the large-scale experiments of the IPP and supports the CODAC group of Wendelstein 7 X with the development of the data acquisition system of the experiment W7-X. In 2014 an ATCA-ADC prototype board and a standard ADC module designed for data acquisition of magnetic and ECE diagnostics was successfully tested, and the series production of further 14 boards and 500 modules was initiated. To evaluate the data acquisition system for the Thomson-Scattering diagnostic, a 4-channel high-speed MTCA.4-standard based system was acquired and installed, and a technical specification was compiled which serves as basis for a call for tenders for a data acquisition system.

Staff

A. Altbauer, F. Baruffa, D. Beckert, V. Bludov, G. Bronold, T. Dannert, C. delle Fratte, K. Desinger, R. Dohmen, E. Erastova, C. Falls-Rodriguez, K. Gross, C. Guggenberger, C. Hanke, S. Heinzel, F. Hinterland, L. Hüdepohl, F. Kaiser, J. Kennedy, T. Khan, H. Lederer, K. Lehnberger, A. Marek, L. Mazzaferro, W. Nagel, M. Panea-Doblado, F. Paulus, E. Pfannenstein, M. Rampp, J. Reetz, K. Reuter, K. Ritter, R. Ritz, B. Sanchez, A. Schmidt, A. Schott, J. Schuster, S. Wangnett, I. Weidl, T. Zastrow, K. Zilker.
XDV Data Acquisition Group: M. Zilker.

PAX, APEX

Head: Prof. Dr. Thomas Sunn Pedersen

PAX/APEX

It has been predicted for more than two decades that turbulence and plasma waves in pair plasmas will show a behaviour which is completely different from conventional plasmas. In 2014, in the stellarator theory department of IPP, an important breakthrough was achieved, as an analytical theory for electron-positron plasmas showed the nearly complete absence of microinstabilities which drive turbulence in electron-ion plasmas (see this report). Our work will permit tests of these predictions in an experiment.

Work associated with this activity during 2014 took place at the Garching campus of IPP, the positron beamline NEPOMUC of the FRM II neutron source in Garching, and in Greifswald. NEPOMUC currently is the most intense source for cold positrons world-wide, and will host a permanent installation of the APEX experiment once sufficient laboratory space becomes available. Meanwhile, experimental work is being conducted on a temporary basis at the so-called open beam-port of the NEPOMUC facility.

The experimental project APEX (A Positron-Electron Experiment) aims to create the first confined electron-positron plasma in a laboratory. It is complemented by the Positron Accumulation Experiment (PAX), in which positron accumulation techniques are being developed in order to achieve a higher plasma density. Both of these experiments are motivated by significant theoretical interest in the properties of pair plasmas in general, and of electron-positron plasmas in particular.

but are starting with a dipole ('APEX-D'), because good confinement for pure electron plasmas has been shown in this configuration. As the confinement volume must be free from material objects, we plan to produce the magnetic field with a magnetically levitated super-conducting current loop. In 2014, we have done parameter studies on the dimensions of the coil and on methods to achieve stable levitation. More importantly, we have used the dipole field of a permanent magnet to test techniques for injection (using electrons) into the confinement volume.

The confinement region of a levitated dipole consists of a set of closed magnetic field lines that link the coil. Injection of charged particles from the outside into the confinement region is a non-trivial problem. One problem that must be overcome is the magnetic mirror effect, which tends to reflect many of the weakly magnetized positrons coming from the NEPOMUC beamline. In order to study the issues associated with injection we constructed a prototype for APEX-D that uses the dipole field of a rare earth permanent magnet (figure 1).

We are currently exploring two techniques to transport charged particles into the confinement region where particles mirror reflected near the poles of the magnet are confined in the equatorial region. These are fundamentally different: (1) "Drift injection" uses a set of E×B plates at a suitable position with respect to the confinement volume to induce cross-field drift onto trapped orbits. (2) "Remoderation" employs the known effect whereby an energetic positron beam (keV) that impinges on a metal surface results in re-emission of some percentage of thermalized positrons. This process can be efficient (more than 10 %). We are designing a set-up using a tungsten crystal as a reflection remoderator in the prototype experiment.

Experiments on cross-field drift injection were conducted with both electrons (figure 2) and positrons (see below). For electrons, confinement times of 160 ms were demonstrated.

APEX
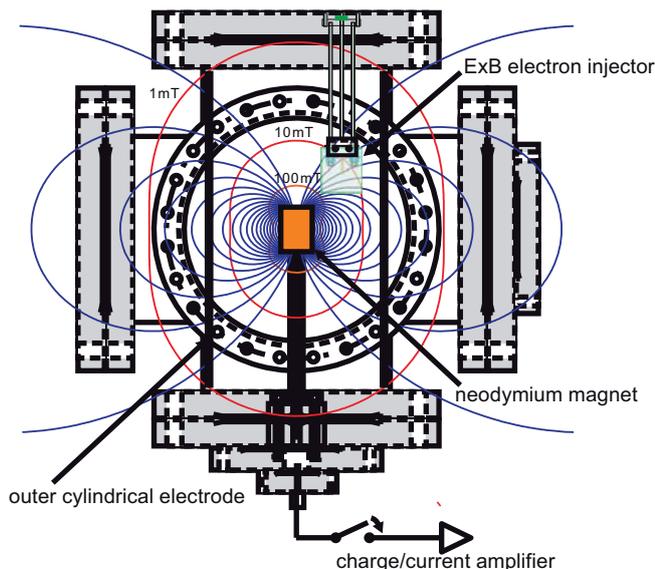
*Figure 1: Setup of the dipole prototype device used for injection experiments. For positron experiments at NEPOMUC, the electron gun is replaced by the positron beam.*

Magnetic configurations that are promising for confining an electron-positron plasma are stellarators and dipole magnetic fields. We aim to use both variants in our experiments,
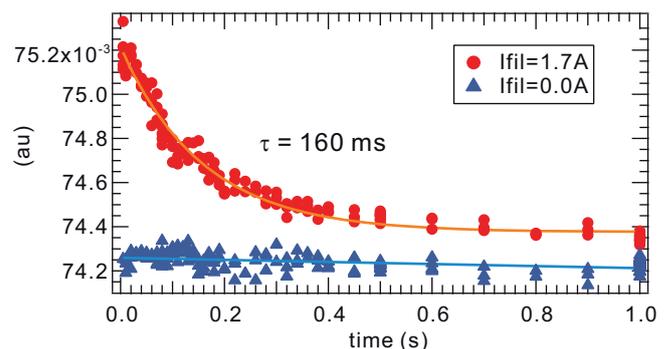

Figure 2: Confinement of electrons in the prototype dipole device.

Positron Experiments at NEPOMUC

Fourteen days of beamtime for positron experiments were allocated to this activity in 2014. We installed the prototype dipole trap, and a retarding field energy analyzer (RFA) at the open beam port. Specifically, (1) we investigated the beam profile, flux and parallel and perpendicular energy spread of the positron beam using the RFA with a variable field gradient. Then (2) we conducted drift injection and positron trapping experiments in the prototype dipole field, using the E×B drift produced by a pair of oppositely biased plates.
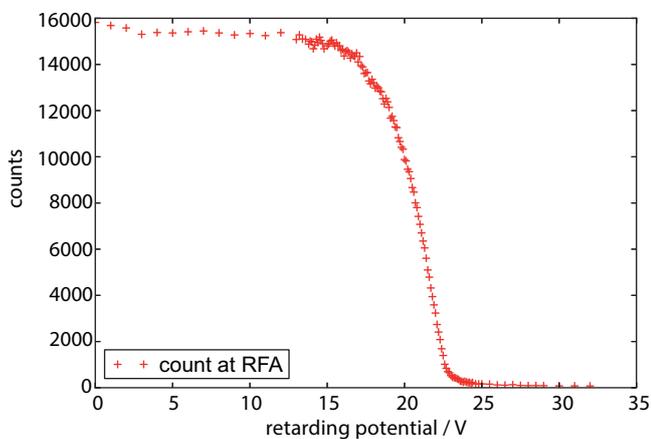

Figure 3: RFA measurement of a 20 eV positron beam.

(1) The RFA allows measurement of the parallel and perpendicular energy of the positron beam, which are important input parameters for our experiments. With the RFA, we measured the parallel energy distribution of beams with nominal parallel kinetic energies of 12, 20, 400, 600, and 1000 eV. Energy profiles of low energy ("remoderated") beams with 12 and 20 eV, and of the 1 keV primary beam were analyzed in different field gradients in order to obtain the perpendicular temperatures. Typical RFA data are shown in figure 3. To determine the intensity of the beams, annihilation gamma ray counts were measured at the RFA and the x-y target plates. We will obtain the absolute intensity of each of the beams from the comparison with properties of previously measured beams and with direct beam current measurements.

(2) In the dipole experiment, we applied DC bias voltages to the E×B plates and measured gamma counts with various collimators in order to identify the approximate location of annihilation events. By applying appropriate electric fields in the dipole magnetic field, positrons were successfully transported into a strong field region and annihilated on the magnet case. Quantitative analysis of these experiments and comparison with orbit calculations are underway. We also attempted to assess the confinement properties of positrons after pulsed injection, but the trapped component of the signal

was below the detection limit, indicating that further optimizations of the injection and trapping schemes are needed.

PAX Experiments

A quick estimate shows that even at very good injection and confinement efficiency, the DC beam even of the NEPOMUC source is only sufficient to create very thin pair plasmas. To overcome this limitation, efficient schemes for accumulation of large numbers of positrons are mandatory. We are developing these techniques in Greifswald. Work in 2014 focused on experiments in a Penning-Malmberg trap, using electrons as a proxy for positrons. The temporal properties of electron confinement were measured by filling the trap with an electron gun, and dumping the integrated charge after a holding time t onto a grounded collector. Stable confinement of more than 10^8 electrons was achieved for up to an hour (figure 4).
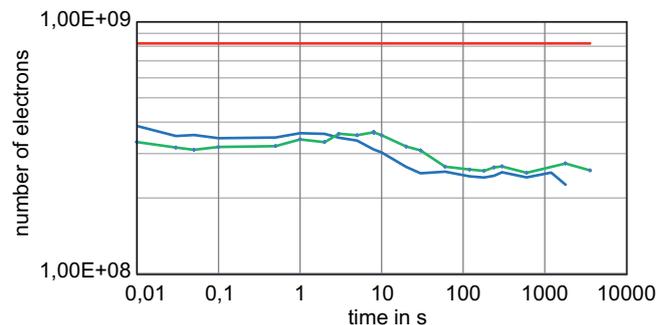
Figure 4: Number of stored electrons vs. time in a Penning-Malmberg trap of length 89 mm inside a 2.3 T magnetic field (blue and green: measured data, red: space charge limit given by trapping potential).

In conclusion, significant progress toward production of the world's first laboratory electron-positron plasma took place during 2014. Experimental measurements of the intense NEPOMUC positron beam characteristics, tests of electron confinement and positron injection into a prototype dipole trap, and development of positron accumulation and storage techniques were conducted at IPP Greifswald, IPP Garching, and the Technische Universität München (FRM II experimental reactor).

Scientific Staff

T. Sunn Pedersen, H. Saitoh, U. Hergenhahn, E. Stenson, J. Stanja, H. Niemann, N. Paschkowski, K. Pal Singh.

VINETA

Head: Dr. Olaf Grulke

Magnetic Reconnection

Major progress has been made in the understanding of the space-time evolution of the current sheet during driven magnetic reconnection in VINETA II. The setup is shown in figure 1. A pair of axial conductors (X-drive) generates an in-plane X-point magnetic field topology. A second pair of conductors (reconnection drive) is used to drive magnetic reconnection. The plasma gun located on the X-line provides the plasma current in response to the inductive electric field. The reconnection current closes via the vacuum vessel walls, thereby forming a current loop with its characteristic inductance being much larger than the intrinsic plasma inductance due to electron inertia. Consequently, the reconnection current is phase-shifted by $\pi/2$ to the inductive electric field at the X-line. The in-plane reconnection magnetic field together with the homogenous axial guide magnetic guide field leads to a strongly elongated sheet geometry along the X-line due to the magnetic field pitch angle. A measurement of the current sheet profile at three axial positions is depicted in figure 1. In addition the current sheet is not in force balance with the magnetic field and consequently expands perpendicular to the separatrix, thereby causing an axial gradient of the reconnection rate.

Within the current sheet broadband electromagnetic fluctuations are observed. The fluctuation spectrum displays a power-law decrease $S(f) \sim f^{-\alpha}$ without signatures of coherent modes. The fluctuations display an only slightly larger coherence length along the magnetic field when compared to the perpendicular direction. A striking feature in all cases is a breaking-slope behavior of the spectrum at the lower-hybrid frequency f_{LH}. This behavior is robust against parameter variations which change the lower-hybrid frequency as, e.g., guide field variations or changes of the ion mass. Comparisons of the experimental results with nonlinear reconnection simulations are ongoing to clarify the underlying instability mechanisms. Although the spectrum is broadband measurements of the wavelength parallel to the magnetic field yields a dispersion relation of the fluctuations, which agrees fairly well with a whistler wave propagating
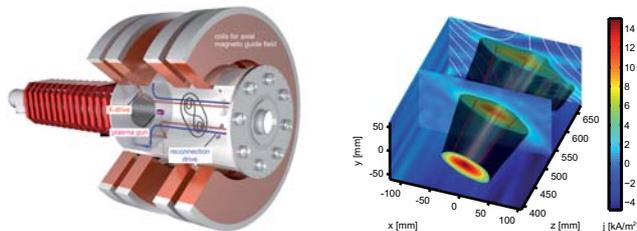
The scientific program at VINETA has been the continuation of studies of driven magnetic reconnection and the development of a high density helicon discharge. In magnetic reconnection the dynamics of the current sheet on a macroscopic and microscopic scale has been characterized. Unparalleled plasma densities have been achieved in the helicon discharge.

in the direction of the electron drift within the current sheet.

High Density Helicon Discharge

The primary goal is to demonstrate the feasibility of the prototype helicon discharge for the advanced plasma-based particle-driven accelerator AWAKE currently under construction at CERN.

Three fundamental requirements must be met: (i) scalability of the discharge to a length of L$\approx$10 m, (ii) a peak plasma density of $n_{nom} \geq 7 \cdot 10^{20}$ m^{-3} sustained over a sufficient time, and (iii) sufficient axial plasma density homogeneity. The first aspect is intrinsically provided by the modular prototype setup using an array of axially distributed helicon antennas. In the 1 m long prototype experiment four helicon antennas are used, which can be individually powered with up to 12 kW, respectively. Power balance calculations indicate that the heating power is mostly radiated by excited neutrals and plasma ions with only little power loads to the axially bounding walls. Figure 2 (left) shows the results of the peak plasma density as measured by a CO_2 interferometer and scaled by the density profile for different magnetic field strength and rf power levels. In both cases a linear dependency is observed, which is in agreement with the linear helicon wave dispersion relation. Already for an rf power level of $P_{rf}=27$ kW the nominal plasma density of $n \approx 7 \cdot 10^{20}$ m^{-3} is achieved. Over an rf pulse cycle the temporal peak plasma density evolution is characterized by an initial density peak and subsequent density decrease (figure 2). The temporal width of the initial density peak is compatible with the short time scales of the accelerator concept. The fast decrease of the plasma density is attributed to neutral gas pumping out of the plasma center, which has often been discussed as a major density limitation for helicon discharges.
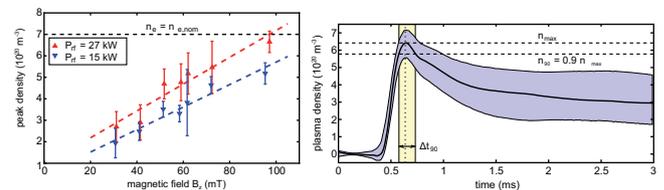
Figure 2: Left – Measurements of the dependence of the peak plasma density on magnetic field strength for two different rf power levels. Right – temporal evolution of the peak plasma density over an rf pulse. The shaded area indicates variations over an ensemble of individual discharges with nominally constant operation parameters.

Scientific Staff

H. Bohlin, B. Buttenschön, J. Clementson, N. Fahrenkamp, O. Grulke, T. Klinger, D. Milojevich, K. Rahbarnia, T. Schröder, I. Shesterikov, A. von Stechow, T. Windisch.


Figure 1: Left – Reconnection setup including the plasma gun, the X-drive, and reconnection drive conductors. Right – Measurements of the azimuthal current density profile at three axial positions (colour coded) and some example magnetic field lines (red). The X-point topology is shown as white contour lines.

Electron Spectroscopy

Head: Dr. Uwe Hergenhahn

The electron spectroscopy group is active in developing advanced spectroscopic techniques and in their application to current topics in electron dynamics of molecules, clusters and liquids. In 2014, the focus of our research was on fast autoionization channels, like Auger decay and Intermolecular Coulombic Decay (ICD). These activities are a part of a Research Unit on ICD, funded by the Deutsche Forschungsgemeinschaft.

A Magnetic Bottle Spectrometer for Research on Liquids

Conventional (e.g. hemispherical) electron spectrometers typically only use on the order of 1 % of the available signal. Several alternative types of spectrometers allow for more efficient detection. Among them, so-called magnetic bottle spectrometers offer an attractive mix of properties. These instruments use a magnetic field configuration reminiscent of 'magnetic bottle' devices from the early years of fusion research, but cut into half. In effect, electrons that are produced at the point of strongest magnetic field are guided into regions of weaker field, where a detector (electron multiplier, e.g. a microchannel plate) is placed. The electron spectroscopy group has several years of experience in operating a magnetic bottle spectrometer for research on clusters. In 2014, a new instrument was constructed and commissioned, which is adapted to the use together with a liquid jet. In these experiments, a liquid jet source is used to spray a thin (10 µm) jet of a liquid or solvent into a vacuum chamber. This allows the study of the liquid-vacuum interface by electron spectroscopy.

instrument are the spectroscopy of substances with low solulibility, such as biomolecules, spectroscopy of photoelectron lines near to their respective thresholds, and electron, electron coincidence spectroscopy. Our new design (figure 1) is particularly adapted to the high background pressure that is inevitable when experimenting with liquid substances in vacuum.
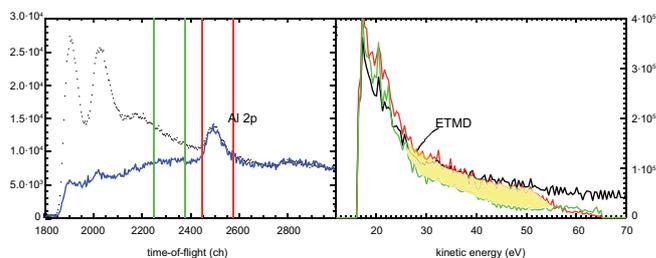
Figure 2: Left panel: Electron spectrum (dots) and electron-electron coincidence spectrum (blue line showing the fast electron) of a 1.5 M solution of Al_2Cl_3 in water recorded by $h\nu= 170.2$ eV photons. Spectra were normalized to equal background height. Red bars mark the Al 2p photoelectrons. Right panel: Secondary electrons arriving in coincidence with Al 2p photoelectrons (red trace, for primary electrons between the red bars in left panel), or with electrons not due to the Al solute (green trace, for primary electrons between the green bars). The difference between red and green trace can be attributed to the decay of the Al vacancy by ETMD.


Figure 1: Detail from the construction of the spectrometer. The electrostatic potential of the drift tube is provided by thin wires, through which differential pumping of the spectrometer volume is not inhibited. As a result, the drift tube is guiding electrons, but is fully transparent for molecules. A valve at the entrance into the drift tube allows to vent the jet chamber while keeping the detector evacuated.

Experiments with the new instrument were conducted in collaboration with the group of Bernd Winter, Helmholtz-Zentrum Berlin, who provided the liquid jet technology. First measurements focussed on autoionization phenomena in neat water and solutes. Generally, after photoionization with energetic radiation, an excited vacancy state is created that can decay by either fluorescence or autoionization. Research oportunities on these phenomena have greatly improved by the invention of liquid jets. In particular, autoionization by non-local mechanisms (Intermolecular Coulombic Decay or Electron Transfer Mediated Decay, ICD or ETMD) has become a topic of recent interests. First results have been obtained about ETMD of an Al 2p vacancy in a solute of AlCl (figure 2). In solution, Al (electron configuration $3s^23p$) is found in the form of Al^{3+} ions. This suggests that after core level (Al 2p) ionization, the vacancy decays by ETMD from the surrounding water molecules. Data in figure 2 provide experimental evidence for this assumption.

The new instrument will allow for large solid angle detection of electrons with acceptable kinetic energy resolution. Magnetic bottle spectrometers are also known for robust detection of slow (sub eV) electrons. Visions associated with the new

Scientific Staff

U. Hergenhahn, M. Förstel.

University Contributions to IPP Programme

Cooperation with Universities

Author: Gregor Neu

Teaching and Mentoring

IPP is highly interested in fostering national and international students' interest in high-energy plasma physics and other fusion-relevant fields like plasma-material interaction. This interest is reflected in the long-term endeavour of teaching plasma physics at various universities in Germany and abroad. In 2014, 25 members of IPP taught at universities or universities of applied sciences: Many of the IPP staff are Honorary Professors, Adjunct Professors or Guest Lecturers at various universities and give lectures on theoretical and experimental plasma physics, fusion research, data analysis and materials science. The table gives an overview. The teaching programme has been highly successful over the years and many students who first came into contact with plasma physics through lectures given by IPP staff have later done thesis work and even taken up a career in fusion research.

Lecturing at and cooperation with universities are supplemented by IPP's Summer Uni-versity in Plasma Physics:

Many important goals in plasma physics, technology and materials science have to be attained on the way to a fusion power plant. Since this process will last another generation, IPP attaches great importance to training young scientists. Close interaction with universities in teaching and research is therefore an important part of IPP's mission. Moreover, joint projects with several universities form an integral part of IPP's research programme.

one week of lectures given by IPP staff and lecturers from partner institutes providing detailed tuition in nuclear fusion – in 2014 for the 29th time in Garching (alternating with Greifswald). Most of the about 70 participants are from Europe but there is also a number of attendees from abroad. Some of them take part in the "European Doctorate in Fusion" programme. A "European Doctorate" title is awarded to PhD students in parallel to a conventional one. This requires spending a significant part of the work on their subject at another European university or research centre. The European Doctorate in Fusion was initiated six years ago and is presently supported by institutions in Germany, Italy (University of Padua), and Portugal (Instituto Superior Técnico). With the organisation of the yearly "Advanced Courses in Fusion" IPP provides a major contribution to this programme.

The international character of fusion research is also reflected in the countries of origin of graduate students at IPP: one-fifth of the postgraduates and approximately two-thirds of the postdocs are from abroad. In the year 2014 a total of 74 postgraduates were supervised, 10 of them successfully completing their theses.

Joint Appointments, Grown and Growing Cooperation

IPP closely cooperates with universities in joint appointment programmes: three W3 appointments at the University of Greifswald, a W3 and a W2 appointment at the Technical University of Berlin, and two W3 and a W2 appointment at the Technical University of Munich, mark the successful implementation of these programmes.

Another example of a close cooperation is that with the Institute of Interfacial Process Engineering and Plasma Technology (IGVP) of the University of Stuttgart. The cooperation focusses on the development of novel microwave components and high power microwave transmission systems for the heating of fusion plasmas. IGVP also participates in ASDEX Upgrade experiments for the investigation of ECR heating processes, the influence of ECR current drive on neoclassical tearing modes and in the interpretation of microwave diagnostic data through „full-wave codes".

Networking

In addition, IPP uses specific instruments developed by the Max Planck Society, the Helmholtz Association, Deutsche Forschungsgemeinschaft (DFG), Leibniz-Gemeinschaft or

University	Members of IPP staff
University of Greifswald	Dr. Hans-Stephan Bosch Dr. Andreas Dinklage Prof. Per Helander Prof. Thomas Klinger Dr. Heinrich Laqua Prof. Thomas Sunn Pedersen
Technical University of Berlin	Prof. Robert Wolf
Technical University of Munich	Prof. Sibylle Günter Dr. Klaus Hallatschek Dr. Philipp Lauber Prof. Rudolf Neu Prof. Eric Sonnendrücker Prof. Ulrich Stroth
University of Munich	Dr. Thomas Pütterich Dr. Jörg Stober Prof. Hartmut Zohm
University of Augsburg	Prof. Ursel Fantz Dr. Marco Wischmeier
University of Ulm	Dr. Thomas Eich Prof. Frank Jenko Dr. Emanuele Poli Dr. Jeong-Ha You
Technical University of Graz	Dr. Udo v. Toussaint
University of Bayreuth	Dr. Wolfgang Suttrop
University of Gent	Prof. Jean-Marie Noterdaeme

Table: IPP staff who taught courses at universities in 2014.

the German government for more intensive networking with universities on a constitutional basis – partly in conjunction with non-university research partners and industrial partners.

Organisation of or participation in graduate schools:
- The International Helmholtz Graduate School for Plasma Physics (HEPP), started in October 2011, which is a graduate school for doctoral candidates at the Max-Planck-Institute for Plasma Physics (IPP) and their partner universities the Technical University of Munich (TUM) and the Ernst-Moritz-Arndt University of Greifswald (EMAU). Associated partners are the Leibniz Institute for Plasma Science and Technology (IPN) in Greifswald and the Leibniz Computational Center (LRZ) in Garching. HEPP aims to provide a coherent framework at IPP and the participating universities for qualifying a new generation of internationally competitive doctoral candidates in the field of plasma physics, fusion research, computational physics, and surface science.

Young investigators groups:
- A Helmholtz Young Investigator Group on the "Macroscopic Effects of Microturbulence Investigated in Fusion Plasmas" led by Dr. Rachael McDermott and doted with a financial support of 250 k€ until December 2017. The University partner is the University of Augsburg.
- The European Research Council (ERC) (Starting / Consolidator) Grant and on "Plasma Turbulence in Laboratory and Astrophysical Plasmas" headed by Professor Dr. Frank Jenko, which runs out in November 2016.

Research partnerships:
- DFG Research Training Group on "Intermolecular and Interatomic Coulombic Decay", together with the Goethe University Frankfurt, the University of Innsbruck, the University of Heidelberg, the University of Hamburg, and the Helmholtz-Zentrum Berlin. The research unit focusses on the investigation of a mechanism for the transformation of electronic energy created by excitation or ionization with radiation in the UV and far beyond, or with energetic particles.

Virtual institutes:
- Helmholtz Virtual Institute "Plasma Dynamical Processes and Turbulence Studies using Advanced Microwave Diagnostics" where IPP cooperates in basic research of plasmadynamics and the development of novel microwawe diagnostics with the University of Stuttgart, the Technical University of Munich, the École Polytechnique, Palaiseau (F), the Ecole Polytechnique Féderale de Lausanne (CH), and the Plasma Science and Fusion Center of the Massachusetts Institute of Technology (US).

When the decision was made to build ITER, it became clear that training of young scientists and engineers had to be intensified.

A European Fusion Education Network (FuseNet) was therefore formed in the 7th EU Framework Programme (FP7, 2007-2013). FuseNet currently consists of 13 research organisations – one of them IPP – and 35 universities from 20 European countries. Throughout the 8th Framework Programme, Horizon 2020 (2014-2020), FuseNet will be funded by the EUROfusion consortium.

IPP is also one of the nine partners of the Joint Doctoral College in Fusion Science and Engineering (FUSION-DC), which has been approved under the auspices of Erasmus Mundus, the European programme to promote training schemes. The doctoral college founded in October 2011 is being supported with about five million Euros and provides 40 doctoral scholarships for work in the field of fusion research.

Universität Augsburg
AG Experimentelle Plasmaphysik (EPP)

Head: Prof. Dr.-Ing. Ursel Fantz

Developments for Negative Hydrogen Ion Sources

In negative hydrogen ion sources for fusion negative ions are produced at a low work function surface, which is generated by covering the converter surface with caesium. The experiments at the IPP test facilities showed that the performance of the sources strongly depends on the caesium

The research at the University of Augsburg focusses on diagnostics of low temperature plasmas, on investigations of the plasma chemistry in molecular plasmas and on plasma surface interaction. For that purpose several different low pressure plasma experiments are available. Fundamental studies for the development of negative hydrogen ion sources for ITER and DEMO are carried out in close collaboration with the ITER Technology & Diagnostics Division of IPP.

dynamics. Therefore, fundamental investigations are carried out at the flexible laboratory experiment ACCesS (Augsburg Comprehensive Cesium Setup) which has vacuum and plasma conditions comparable to the IPP prototype source. The planar ICP is equipped with multiple diagnostics which can be applied simultaneously.

In continuation of the investigations on the work function of caesiated materials (Annual Report 2013) the influence of the interaction with hydrogen and deuterium plasmas is studied (figure 1). The minimal achievable work function under ion source relevant vacuum conditions is χ_{vac}=2.75 eV, which is considerably higher than for pure Cs layers and is attributed to the formation of compounds with the residual gases. Due to the steady deterioration of the Cs layer during storage in vacuum the work function degrades to values slightly above 3 eV. The interaction with the hydrogen plasma leads to a decrease of the work function below the minimal vacuum value: within the error margins about 2.6 eV can be attained for both isotopes. Additional Cs evaporation leads to a further decrease of the work function down to the value of pure Cs (χ_{Cs}=2.14 eV). After caesiation the hydrogen plasma counteracts a degradation of the Cs layer, which leads to a stable work function. Switching off the plasma yields directly a degradation of the Cs layer.

The achieved work function values indicate that for both, H_2 and D_2, the plasma surface interaction effectively cleans the Cs layer such that the work function of pure Cs can be achieved. Such fundamental investigations will be continued including the influence of biasing the sample surface with respect to the plasma.

To overcome caesium related issues affecting the RAMI requirements for DEMO NBI sources, caesium-free alternative materials for negative hydrogen ion formation are investigated at a flexible ECR discharge. The effect of different converter materials on the negative hydrogen ion density is investigated by means of laser photodetachment in hydrogen and deuterium at ion source relevant pressures. Promising materials like tantalum, tungsten, LaB_6 and different types of carbon materials have been investigated as a function of sample temperature, distance to sample and sample bias. However, for none of the materials an increase in the negative ion density in the vicinity of the surface is observed, in other words, the volume formation of negative ions is still dominant. In order to assess the required enhancement of negative ion formation experiments with caesium are currently investigated. In a next step other caesium-free materials like diamond with different dopants are scheduled.

Concerning a neutral beam system for DEMO the applicability of a laser neutralizer is investigated in laboratory scale aiming at proof-of-principle demonstration. Therefore, a medium power continuous wave (cw) laser has to be resonantly coupled into an enhancement cavity, which is to be achieved by utilizing the Pound-Drever-Hall locking technique. In order to determine the particular constraints on the specific optical components, the Gaussian beam propagation is calculated by ray transfer matrix analysis. The results include a required accuracy of alignment of about 0.5 mm and the optical components need to withstand optical power densities of up to 900 W/mm². Purchase of the required optical components satisfying these conditions is completed, now starting the setup and alignment.

Low Temperature Plasmas

Helicon RF coupling which relies on wave heating mechanisms in cylindrical magnetized discharges is well known for its efficient plasma generation. To explore the fundamental feasibility of Helicon coupling for the molecular gases hydrogen and deuterium, an experimental setup is available (see Annual Reports 2011-2013) which can be operated either with an inductive coil (ICP mode) or with a specially shaped Helicon RF antenna. Radial emission profiles are measured applying the Abel inversion technique.

Figure 1: Influence of a H_2 and a D_2 plasma on the work function of a caesiated stainless steel surface before, during and after caesiation.

In figure 2, the normalized emission profile of the H_β line in ICP and Helicon mode is shown, both measured at 3.5 mT and 1 Pa. For the ICP, a broad maximum is observed whereas a hollow profile with a distinct minimum at the cylinder axis occurs in Helicon mode which indicates a significant change in the plasma heating for the two modes. To gain further insight in the formation of the profiles and for measuring the electron temperature and density with spatial resolution, Langmuir probes and microwave interferometry are going to be realized. Furthermore, different discharge vessel materials are investigated concerning their influence on the dissociation degree due to the material dependent reformation efficiency of hydrogen atoms to molecules. An Al_2O_3 ceramic tube was installed, but no significant difference to quartz could be observed at 0.3 Pa for varying magnetic field strengths.
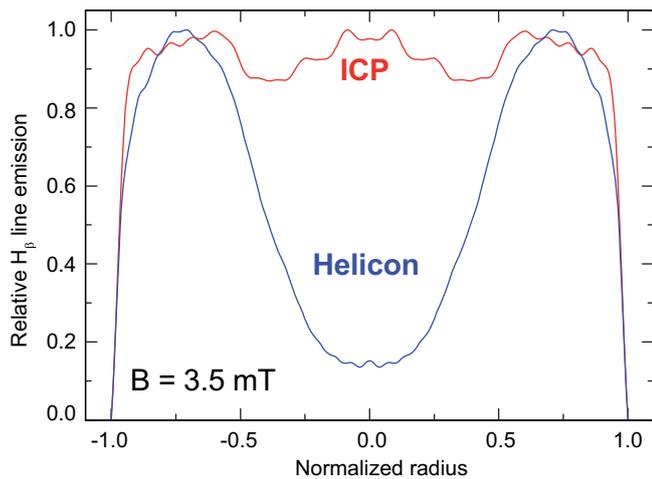

Figure 2: Radial emission profiles in hydrogen plasmas using either the ICP antenna or a Helicon antenna (Nagoya-type-III). An axial magnetic field of 3.5 mT is applied in both cases.

The influence of the RF frequency on spatial profiles of electron temperature and density is investigated at a planar ICP where the planar coil is located on top of a quartz window which separates the cylindrical discharge vessel (height 10 cm, diameter 15 cm) from ambient pressure. By changing the frequency from 27.12 MHz to 2 MHz measurements carried out at pressures of 5, 7.5 and 10 Pa in Argon at 200 W of RF power using a Langmuir probe revealed that profiles of the electron temperature and density both in radial and axial direction are virtually unaffected.

The spectroscopic investigations of an atmospheric plasmoid generated by a water discharge – an IPP experiment – have been continued using a calibrated photodiode system with high temporal and some spatial resolution. Figure 3 shows an example of the temporal evolution of the signals. On the whole it can be stated, that emission from the OH radical is predominant during the entire duration of the discharge. Atomic hydrogen radiation (H_α) is most intense during the

first 50 ms, whereas emission from sodium exhibits a distinct afterglow. These results emphasize the perception of the plasmoid as an ascending water plasma in atmospheric air, in which water molecules and the dissolved salts are dissociated and influence the whole discharge characteristics.
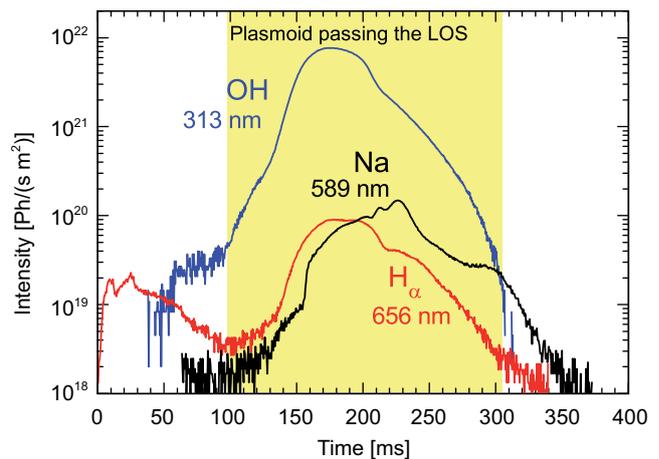
Figure 3: Signals from the photodiode system at the plasmoid experiment taken at a height of 20 cm above the water surface using three different interference filters.

Theses

B. Ruf: Reconstruction of Negative Hydrogen Ion Beam Properties from Beamline Diagnostics. (PhD Thesis)
C. Wimmer: Characteristics and Dynamics of the Boundary Layer in RF-driven Sources for Negative Hydrogen Ions. (PhD Thesis)
P. Gutmann: Vergleich zylindrischer Wasserstoffplasmen (H_2, D_2) im ICP- und Helikon-Setup. (Master Thesis)
D. Rauner: Cavity-Ring-Down-Spektroskopie zur Quantifizierung negativer Wasserstoffionen in einem ECR Plasma. (Master Thesis)
J. Doerfler: Vergleich der Plasmaparameter induktiv gekoppelter Niederdruckplasmen bei 27.12 MHz und bei 2 MHz. (Master Thesis)
I. Pilottek: Optimierung einer Photodiodendiagnostik und Bestimmung der zeit- und ortsaufgelösten Emission eines atmosphärischen Plasmoids. (Bachelor Thesis)
T. Springer: Optimierung und Automatisierung eines Mikrowelleninterferometers zur Diagnostik an Niederdruckplasmen. (Bachelor Thesis)
S. Kurt: Vermessung der radialen Emissionsprofile an einer Helikon-Entladung mittels Abel-Inversion. (Bachelor Thesis)

Scientific Staff

U. Fantz, S. Briefi, S. Cristofaro, J. Doerfler, R. Friedl, P. Gutmann, S. Kurt, U. Kurutz, M. Müller, I. Pilottek, D. Rauner, D. Schmid, T. Springer.

Universität Bayreuth
Lehrstuhl für Theoretische Physik V

Head: Prof. Dr. Arthur G. Peeters

In June 2010 the University of Bayreuth opened a new Chair researching the physics of high temperature plasmas. The Chair is financially supported by the University, the 'Volkswagen-Stiftung', through a Lichtenberg Professorship of Prof. A.G. Peeters, and the IPP. Through this Chair the University and the IPP continue and strengthen their long term collaboration. The dedication to the collaboration is also expressed through the involvement of an IPP employee, PD Dr. W. Suttrop, in the teaching at the University. It is also evident from the multiple collaborative projects between the University and the IPP. The projects deal with toroidal momentum transport, micro-instabilities and the interaction of small scale turbulence with large scale MHD modes. Below the progress in 2014 on the study of the interaction of turbulence with the tearing mode, is briefly discussed. Magnetic islands in a tokamak can lead to loss of confinement or even disruptions of the plasma. In particular it is expected that the neoclassical tearing mode (NTM) sets the beta limit in a reactor. The study of the tearing mode is an ongoing collaborative research project. In previous work the influence of a (stationary) tearing mode on micro-turbulence has been investigated. The further development of the nonlinear gyro-kinetic GKW code in 2013 and 2014 has enabled the study of the self-consistent tearing mode evolution in toroidal geometry for realistic parameters (i.e mass ratio, collisionality).

The linear studies show that toroidal geometry and collisionality have a significant influence on the growth rate and rotation frequency. At low collisionalities the mode rotates in the electron diamagnetic direction, as expected, but at higher collisionalities the mode rotation reverses direction and is found to rotate in the ion diamagnetic direction.

In the nonlinear case, the mode evolution was investigated in the presence of electromagnetic micro-turbulence. Turbulent fluctuations seed the island through nonlinear energy exchange from turbulent modes, generating islands sizes of the order of the ion Larmor radius on a timescale much shorter than the linear tearing growth. Turbulent fluctuations do not destroy the growing island early in its development, which maintains a coherent form as it grows, with its rotation frequency determined by the nonlinear interaction. A large degree of stochastisation around the separatrix and a complete breakdown of the X-point is observed, which significantly reduces the effective island width. A turbulent modification of the electrostatic field in and around the island greatly affects the size of the singular layer width, and the island is observed to grow at the linear rate even though the island is significantly wider than the singular layer width. The singular layer width is the maximum island size at which linear theory is considered to be valid and, therefore, a nonlinear modification of the Rutherford mechanism or threshold is observed.

Through the Chair for theoretical plasma physics, the university of Bayreuth and the IPP continue and strengthen their collaboration, which focuses on the kinetic description of transport processes, small-scale instabilities and their interaction with long-wavelength instabilities. Recent progress in the numerical investigation of tearing modes in the presence of plasma microturbulence are presented.

The impact of rotating magnetic islands on background radial profiles in the presence of strong turbulent transport has been analysed, with particular emphasis on island widths of the order of a few ion Larmor radii, i.e. 6-10 ion Larmor radii. These studies were made using the flux-tube approximation, which is lighter computationally than the global case. So far only the case of ion temperature gradient (ITG) turbulence has been considered. It has been shown that magnetic islands rotating in the ion diamagnetic direction lead to a strong reduction of fluctuations inside the separatrix, when the island width is close to the radial correlation length of turbulence (see figure). Surprisingly, this reduction has been found not to be related to the reduction of the ion temperature gradient. Instead, a nonlinear transfer of energy from the turbulent to the island modes might be responsible for the stabilization of the turbulence at radial scales close to the correlation length of turbulence. When the island width is large enough, the standard profile flattening leading to a linear stabilization of turbulence dominates, independent of the islands' rotation frequency. Finally, the density flattening due to the adiabatic response of trapped ions in the presence of small-intermediate magnetic islands survives the radial turbulent transport, representing a destabilizing effect for a bootstrap-driven magnetic island rotating in the ion diamagnetic direction, while it is stabilising otherwise.
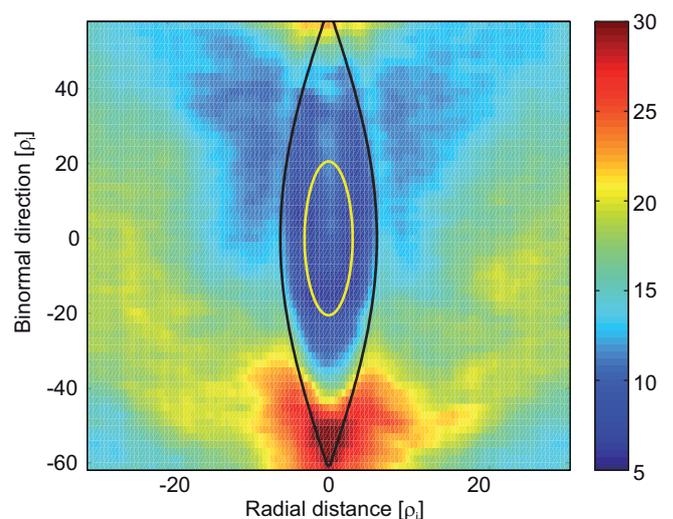

Figure: Mean turbulence amplitude in the presence of a rotating magnetic island.

Scientific Staff

C. Angioni, A. Bottino, R. Buchholtz, S. Grosshauser, W. A. Hornsby, P. Migliano, A. G. Peeters, E. Poli, D. Strintzi, W. Suttrop, A. Weikl, D. Zarzoso.

Technische Universität Berlin
Plasmaphysik, Plasma-Astrophysik

Prof. Dr. Robert Wolf, Prof. Dr. Wolf-Christian Müller

Lagrangian Statistics of Turbulence

The transport properties of turbulent media are most naturally analyzed in the co-moving Lagrangian frame of reference. The Lagrangian theory of turbulence has consequently experienced a tremendous growth of importance, knowledge, and impact over the last decade. The pioneering activities by some members and collaborators of the plasma-astrophysics group have led to an international scientific collaboration involving this group and researchers based in the United Kingdom, in particular at the universities of Glasgow, Exeter and Warwick (Center for Fusion, Space, and Astrophysics). The research project has begun in the course of 2014 and focuses on a rather new theoretical concept in turbulence theory: the convex hull of an ensemble of passive tracers advected by the turbulent flow. This object combines a number of properties which render it very useful for the analysis of turbulent flows with embedded coherent structures on larger spatial scales. Convex-hull analysis offers access to Lagrangian statistical properties of the ensemble enclosed by the hull as well as the ensemble representing the hull. Compared to standard volume averaging, convex-hull statistics is additionally associated with a local position (of the hull's center) as well as a spatial scale (the hull's diameter). It is, moreover, suited for anisotropic systems. Thus, standard Lagrangian statistics has a similar relationship to convex-hull statistics as has the Fourier to the wavelet transform.
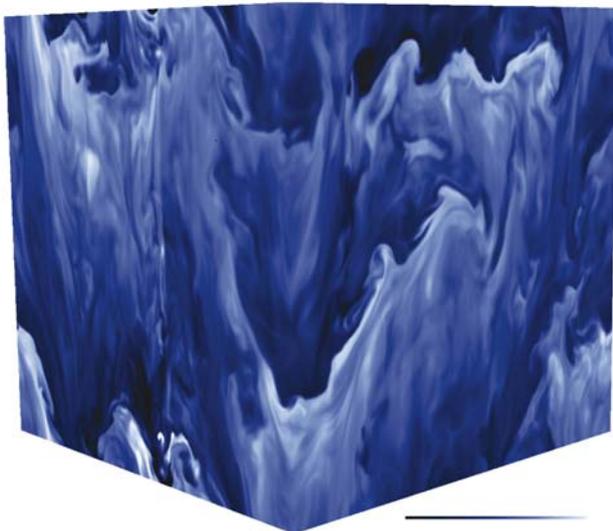
The collaboration of the Technical University of Berlin (TUB) and IPP has led to the founding of the research groups Plasma Physics (2011) and Plasma-Astrophysics (2013) within the Centre for Astronomy and Astrophysics (ZAA). This fosters interdisciplinary research and university teaching incorporating the physics of high-energy and laboratory plasmas as well as of fundamental, and thus also astrophysically relevant, nonlinear plasma dynamics.

The new statistical concept will, for a start, be applied to magneto-hydrodynamic turbulence in a mean magnetic field and to MHD Boussinesq convection (see figure 1). The latter introduces a constant mean temperature gradient and, thus, in addition to the magnetic field a second characteristic direction. During 2014 the computational resources of about 14.5×10^6 CPUh, required for the initial phase of the project have been granted for the year 2015 by the North-German Supercomputing Alliance.

MHD Turbulence in Strong Magnetic Fields

The work on magnetohydrodynamic turbulence in a strong mean magnetic field, B_0, has been continued. The new regime of weakened MHD turbulence that develops under certain conditions (isotropic scaling w.r.t. the mean field direction, scale-independent fluctuation anisotropy $\sim b_{rms}/B_0$, significant field parallel energy transport) is shown to depend on the ratio of kinetic to magnetic energy at the largest scales of the flow. To this end, the imposed large-scale equipartition of both energies is relaxed in free turbulence decay where a secular build-up of excess magnetic energy at large scales is generated self-consistently by the turbulence. For magnetic energy a factor of 2-3 larger than kinetic energy the system switches from the new regime to standard critically balanced turbulence. This non-universality is relevant for explaining observations made in the solar wind where signatures of both regimes are reported under varying large-scale conditions.

Figure 1: Thermal fluctuations during stationary MHD convection (brighter colours corresponding to higher values).
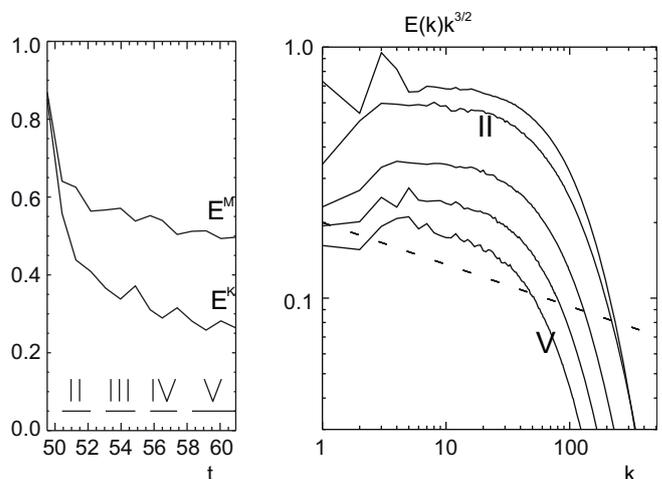
Figure 2: Temporal evolution of total kinetic and magnetic energy in the course of freely decaying turbulence (left) starting from a state of newly discovered turbulence (energy spectrum $E(k) \sim k^{-3/2}$) (right, uppermost curve), eventually turning into critically balanced turbulence ($E(k) \sim k^{-5/3}$, dashed line).

Modeling ECRH Plasma-startup in Wendelstein 7-X

Quantitative modeling of the plasma driven by electron cyclotron radiation heating (ECRH) in a stellarator device is of importance for the upcoming start of operation of the Wendelstein 7-X experiment. In the framework of a Diploma thesis carried out at TU Berlin under the joint supervision of R. Wolf and W.-C. Müller, work has begun on an idealized numerical rate-equation model. The energy supplied to the plasma by ECRH is calculated using the ray-tracing code TRAVIS developed and maintained at IPP Greifswald which will be coupled to the numerical plasma model.

Technische Universität München
Lehrstuhl für Messsystem- und Sensortechnik
Head: Prof. Dr.-Ing. Alexander W. Koch

ITER Bolometer Camera Development

Most of the ITER bolometer cameras will be realized as a collimator construction type because the viewing cones of the lines of sight (LOS) in ITER will have to pass through very narrow gaps between the plasma facing components which provide the neutron shielding of the vessel components. Due to the limited installation space in ITER, the camera size is restricted. Thus it is very challenging to achieve the narrow viewing cone characteristics of up to 0.5°. Multiple apertures have to be integrated into the camera in order to define accurately the LOS and to mitigate unwanted stray light. In the past, different camera prototype designs have been assessed in order to develop a camera suitable for the harsh ITER conditions, e.g. high temperatures and high neutron flux. The camera design of 2014 is shown in figure 1.
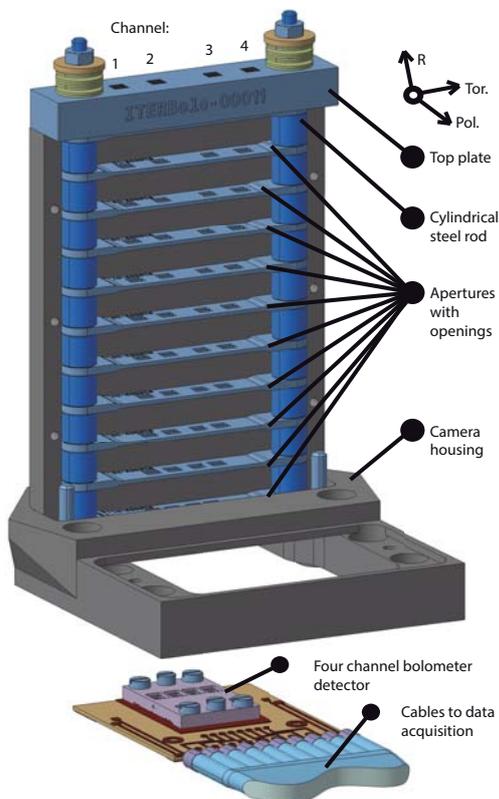
There has been a continuous cooperation of IPP and the TUM Institute for Measurement Systems and Sensor Technology in the past. Thermography and speckle interferometry have been a field of broad research. For four years now, the focus has been on the bolometer development in collaboration with the ITER Diagnostics Group of the ITER Technology & Diagnostics division of IPP.

ITER Bolometer Robot Test Rig: IBOROB

The ITER Bolometer Robot Test Rig (IBOROB) was developed in order to measure and analyze the LOS characteristics of the different collimator versions necessary for the ITER bolometer diagnostic and to serve as a proof of concept for a future device envisaged for ITER. For two years it has been used as a regular measurement device to quantify the design changes of the collimator prototypes manufactured as part of the development for the ITER bolometer diagnostic (see chapter 4). The device helped to assess the impact of stray light, evaluated the geometrical parameters of multiple bolometer collimator channels and could identify design imperfections of the camera concerning the LOS alignment. Thus, IBOROB significantly influenced the collimator design development for the ITER bolometer cameras. During last year's regular maintenance shutdown of ASDEX Upgrade, it was also successfully installed in the vessel in order to perform in situ measurements of the pin hole type bolometer cameras.

Influence of Calibration Errors on the Transmission Measurements

The experience from the usage of IBOROB demonstrated that there are several parameters which influence the transmission measurement results. It was shown that the accuracy of the initial calibration of the laser source has to be taken into account in order to correctly interpret the obtained results. During a measurement, the laser beam is supposed to be oriented always onto the center of the bolometer aperture. However, the only possibility to check if the setup is correct is by eye and through the laser protection glasses, which results in a certain degree of uncertainty. Therefore, in order to investigate the influence of a constant laser positioning inaccuracy on the transmission measurements, multiple one-dimensional toroidal measurements with a laser beam shifted gradually (1 mm steps) in the toroidal (horizontal) plane have been performed. The laser was shifted from an offset of -5 mm to +5 mm. The bar-graph in figure 2 (top) shows the maximum transmission values in relation to the different laser offset positions. The signals are normalized to the maximum transmission value. In parallel, a calculation (simulation) was performed based on the one-dimensional convolution of a Gauss-function (Laser diameter 27 mm) having the same offset values with a rectangular function (toroidal aperture opening 4 mm). The simulation shows a symmetric decrease of the maximum transmission values for both offset directions, which is as expected.

Figure 1: Isometric view of the current collimator prototype with 12 apertures mounted on two cylindrical steel rods.

The main bolometer camera components are the detector, the camera housing, the collimator top plate and two cylindrical steel rods, on which the apertures (max. 12) can be fitted on.
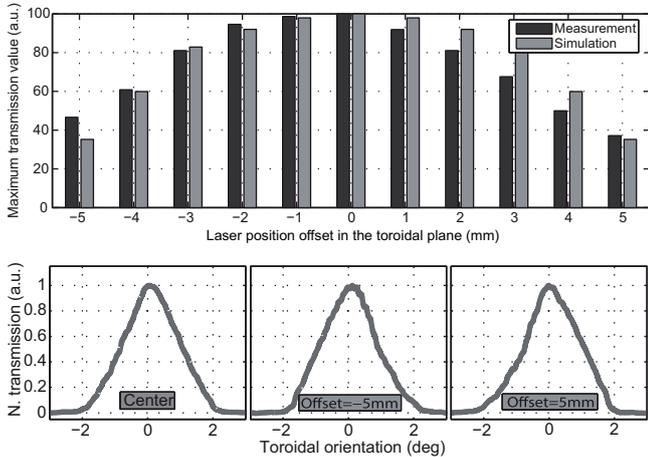
Figure 2: The bar-graph (top) shows the normalized maximum transmission values of different laser offset positions in the toroidal plane. The measurements can be compared with a simulation of the laser offset. Here, a shift of -0.8 mm can be determined. The toroidal transmission measurements (bottom) show the changing characteristics of an incorrectly calibrated laser. The plot on the left shows the original trapezoidal characteristics, the transmission with the offsets (middle and right) are changing to a breaking wave form.

This is in contrast to the measurements, which are displaced to the left in the bar-graph and correspond approximately to a shift of -0.8 mm. Figure 2 (bottom) shows the normalized transmission measurements from both extreme values and the center value. Here, the effect on the transmission characteristics can be analyzed. The trapezoidal signal changes into a form of a breaking wave, for -5 mm in the positive toroidal orientation and for +5 mm in the negative orientation. The signal decrease and increase towards its maximum is enhanced on its respective side. Here, the effect is relatively small, in particular considering that an offset of 5 mm is a worst case deviation for the ITER prototype measurements conducted in the laboratory. However, for larger aspect ratios of aperture and laser beam and more difficult measurement environments as the measurements conducted in AUG, this effect has to be taken into account.

Monte Carlo Ray Tracing of Bolometer LOS

IBOROB can be considered as an efficient tool to measure the current state of the LOS characteristics. However, separating individual optical effects of the camera or performing an optimization of the camera configurations (e.g. number of apertures) is complex and time demanding. Multiple measurements have to be compared with each other and it has to be taken into account that the manufacturing and modification of several prototypes is costly. Therefore, Monte Carlo ray tracing (MCRT) based methods have been used to perform optical simulations of the transmission measurements.

But simulations have the inherent disadvantage that they strongly depend on the boundary conditions, such as the set of optical absorption and scattering properties of the camera housing and aperture material. Here, the results from IBOROB helped to estimate these parameters by comparing MCRT calculations with corresponding transmission measurements. Once a certain parameter set had been deduced, further modification of the camera parameters could be performed in order to calculate an optimized configuration.
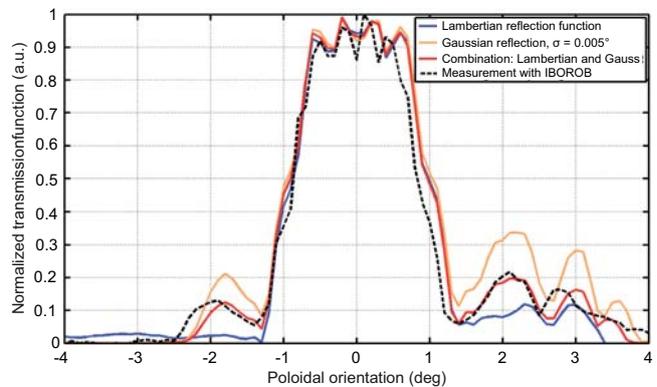
Figure 3: Normalized poloidal transmission function of an ITER prototype collimator camera. The measurement with IBOROB can be compared to Monte Carlo Ray Tracing calculations of three different reflection characteristics.

Figure 3 shows the measurement of a normalized poloidal transmission function of an ITER prototype collimator camera and Monte Carlo Ray Tracing calculations of three different reflection characteristics. The camera material is modelled having a Lambertian reflection characteristic (blue), a Gaussian reflection characteristic (yellow) with $\sigma = 0.005°$ and with a combination of both characteristics (red). The combination shows the best match with the measurement (see the modulations on the signal), demonstrating that reflections in the camera are neither purely diffusive nor purely Gaussian. This parameter set is now used as reference for further calculations.

Theses

S. Shalaby: Parameterstudien für Monte Carlo Ray Tracing von ITER Bolometer Sichtliniencharakteristiken. (Bachelor Thesis)

Scientific Staff

TUM: S. Shalaby, M. Jakobi.
IPP: F. Penzel, H. Meister, T. Sehmer, M. Kannamüller, J. Koll.

Universität Stuttgart
Institut für Grenzflächenverfahrenstechnik und Plasmatechnologie (IGVP)

Head: Prof. Dr. Thomas Hirth

ECRH in Over-dense Plasmas

The electrostatic electron Bernstein waves (EBWs) have no high-density cut-off and are very well absorbed at the electron cyclotron resonance (ECR) layer and its harmonics. They provide a method to heat over-dense plasmas, which are otherwise inaccessible to electromagnetic waves. Because of their electrostatic nature they need to be coupled to injected electromagnetic waves. The O-SX-B mode conversion process is such a coupling process, which is successfully applied at the stellarator TJ-K with an 8 GHz microwave heating system. After plasma start-up at the fundamental ECR, it is possible to continuously reduce the background magnetic field B_0 by almost a factor of five. The reduction of B_0 is accompanied by a continuous decrease of the broadband turbulence. Figure 1 shows spectra of the ion-saturation current obtained from Langmuir-probe measurements at the plasma boundary: the low-frequency, broadband component decreases with a reduced value of B_0. In turn, a dominant peak around 4 kHz with a large number of harmonics develops. The energy seems to be transferred from the broadband turbulence into a coherent mode extended over the whole plasma cross section.

The joint program between IGVP and IPP on ECRH systems for AUG, W7-X, and ITER as well as contributions to the experimental program of AUG can be found on the respective pages of this report. Here is summarized the part of the program carried out at IGVP: the development of new mm-wave components, investigations of plasma waves and turbulent transport. Experiments are carried out on the torsatron TJ-K, which is operated with a magnetically confined low-temperature plasma.

microwaves in a 2D geometry. The effect of a single blob was studied first. The density perturbations were then extended to consist of fluctuations generated from a Hasegawa-Wakatani drift-wave turbulence model within the BOUT++ framework. Parameter scans are performed, in which the scattering of a traversing microwave beam is studied as a function of the average size and amplitude of the density fluctuations. These investigations are of relevance for both, heating scenarios, in which mode conversion processes at the plasma boundary are involved, and scenarios, in which very localized absorption in the plasma centre is desired.

Global Turbulence and Confinement Studies

In TJ-K, a poloidal probe array was employed to study statistical properties of zonal flows. Therefor, an average (zonal) potential was deduced from all probes of the array and taken as trigger signal to reveal the related, conditionally averaged dynamics in the poloidal cross-section in some toroidal distance. In particular, the zonal feature, which was mapped over to the observed cross-section via long-range correlations, could clearly be demonstrated. They appear to propagate radially inwards and are associated with a decrease in radial correlation length of ambient turbulence, possibly reflecting the tilt of vortices in the shear flow. The distribution of zonal amplitudes over positive and negative events is asymmetric. Zonal amplitudes tend to decrease with increasing electron collision rate (see figure 2).

Figure 1: Spectra of the ion-saturation current in EBW-heated discharges for varying values of the background magnetic field as indicated by the different colours.

The mode conversion into EBWs usually takes place at the plasma boundary, where density perturbations due to broadband plasma turbulence occur. Depending on their average size and amplitude, they can significantly distort microwaves traversing them. The full-wave code IPF-FDMC is used to study the influence of these perturbations on propagating

Figure 2: Radial profiles of zonal potential amplitudes in dependence of the electron collision rate ν. The amplitude decreases with increasing ν.

Reynolds-stress drive and flow acceleration are positively correlated with both having comparable absolute values. The contribution of geodesic damping is currently under investigation. An asymmetry in the poloidal Reynolds-stress distribution was found similar to turbulent transport.

Furthermore, magnetic field-line curvature was studied as driving mechanism of blobs in the scrape-off layer of TJ-K. To this end, blobs were tracked in the 2D poloidal cross-section by means of Langmuir probes and the conditional averaging technique. Along their trajectory, blob velocity components were deduced at centre of mass coordinates and compared to the associated field-line averaged normal and geodesic curvature components. Background E×B flows, measured with emissive probes, were also taken into account. Radial and poloidal velocity components were found to compare reasonably well with simple estimates from an analytical model. I.e., in particular, the relation of radial propagation to the normal curvature could be confirmed. Moreover, first results indicate that the poloidal propagation could in part be attributed to the geodesic curvature drive, with influence also from equilibrium E×B flows. However, the blob velocities – as measured in discharges with varied ρ_s – show large scatter around the predicted values, which complicates the discrimination between curvature driven components and background flows. In the next step, geodesic curvature will be controlled actively in TJ-K for a clearer determination of the dynamical poloidal velocity component. In addition, the scrape-off layer width can be increased, allowing for a larger observation region, in which to track blobs for longer and obtain better statistics.

Doppler Reflectometry Simulations with IPF-FD3D

In collaboration with G. Conway and T. Görler (IPP), the fullwave code IPF-FD3D is used to simulate Doppler reflectometry on ASDEX Upgrade, in close coupling with experimental investigations and with incorporation of simulated plasma turbulence using the gyrokinetic turbulence code GENE. This synthetic diagnostic is used to understand the experimentally observed fluctuation spectra. Figure 3 shows the resulting spectrum of the density fluctuations from IPF-FD3D fullwave simulations for X mode reflectometry.

In order to gain good turbulence data as input to IPF-FD3D, the equilibrium and relevant profiles from the experimental Doppler shots are taken from the AUG database and used as input to GENE. The turbulence simulations are run by IPP. They are tweaked so that the turbulent transport matches the measured transport from experiment. It is then assumed that the turbulence characteristics (fluctuation strength, knee position, spectral index) in the GENE data correspond to the experiment.

The equilibrium and background density are combined with the GENE turbulence data and input to the full-wave code,

which is run at IGVP. It produces the fluctuation spectra from the Doppler measurements, just like in the experiment. For this, hundreds of time slices of turbulence are used to get a statistical measure of the Doppler spectrum. It is estimated that for more reliable statistics, 1000 to 2000 turbulence realizations may be needed.
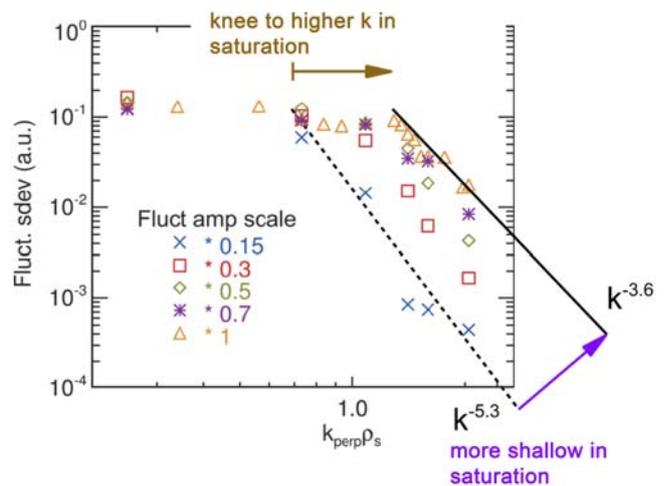
Figure 3: Doppler spectra from IPF-FD3D for GENE turbulence in an L mode scenario. Scaling the absolute fluctuation strength shows the non-linear influence on the knee position in the resulting IPF-FD3D spectra.

In the GENE data, the knee is in the wavenumber region corresponding to ITG modes. In the experimental data, it is at much larger wavenumbers. Since the knee position is closely related to the wavenumber where the turbulent drive is occurring, this is a significant discrepancy. It was now possible to show that this is a characteristic of the Doppler diagnostic. The figure shows that when the turbulence strength is scaled down before input into the IPF-FD3D full-wave simulation, the knee position moves to lower wavenumbers. The reason for this is non-linear saturation of the Doppler signal. At the scaled down strength, the linear response is recovered, with the knee position much nearer to the one seen in the GENE data directly. As the fluctuation strength is increased, the signal goes into saturation at the lower wavenumbers, but not the higher ones, squishing the spectrum against the limit and causing the knee to move to higher wavenumbers.

More simulations with different experimental data are underway. It is also considered to investigate the difference between O and X mode reflectometry, which have different thresholds concerning the onset of non-linear saturation.

Scientific Staff

S. Garland, E. Holzhauer, W. Kasparek, A. Köhn, C. Lechte, B. Plaum, M. Ramisch, K. Rumiantcev, B. Schmid, P. Simon, S. Wolf, A. Zach.

Publications

Publications

Articles, Books and Inbooks

Adamek, J., Horacek, J., Seidl, J., Müller, H. W., Schrittwieser, R., Mehlmann, F., Vondracek, P., Ptak, S., COMPASS Team, and ASDEX Upgrade Team: Direct Plasma Potential Measurements by Ball-pen Probe and Self-emitting Langmuir Probe on COMPASS and ASDEX Upgrade. Contributions to Plasma Physics **54**, 279-284 (2014).

Afeyan, B., Casas, F., Crouseilles, N., Dodhy, A., Faou, E., Mehrenberger, M., and Sonnendrücker, E.: Simulations of kinetic electrostatic electron nonlinear (KEEN) waves with variable velocity resolution grids and high-order time-splitting. The European Physical Journal D: Atomic, Molecular and Optical Physics **68**, 295 (2014).

Alimov, V. K., Hatano, Y., Sugiyama, K., Balden, M., Höschen, T., Oyaidzu, M., Roth, J., Dorner, J., Fußeder, M., and Yamanishi, T.: Surface modification and deuterium retention in reduced activation ferritic martensitic steels exposed to low-energy, high flux D plasma and D_2 gas. Physica Scripta **T159**, 014049 (2014).

Alimov, V. K., Hatano, Y., Sugiyama, K., Balden, M., Oyaidzu, M., Akamaru, S., Tada, K., Kurishita, H., Hayashi, T., and Matsuyama, M.: Surface morphology and deuterium retention in tungsten and tungsten–rhenium alloy exposed to low-energy, high flux D plasma. Journal of Nuclear Materials **454**, 136-141 (2014).

Anderson, J., Halpern, F. D., Xanthopoulos, P., Ricci, P., and Furno, I.: Statistical analysis and modeling of intermittent transport events in the tokamak scrape-off layer. Physics of Plasmas **21**, 122306 (2014).

Angioni, C., and Helander, P.: Neoclassical transport of heavy impurities with poloidally asymmetric density distribution in tokamaks. Plasma Physics and Controlled Fusion **56**, 124001 (2014).

Angioni, C., Mantica, P., Pütterich, T., Valisa, M., Baruzzo, M., Belli, E. A., Belo, P., Casson, F. J., Challis, C., Drewelow, P., Giroud, C., Hawkes, N., Hender, T. C., Hobirk, J., Koskela, T., Lauro Taroni, L., Maggi, C. F., Mlynar, J., Odstrcil, T., Reinke, M. L., Romanelli, M., and JET EFDA Contributors: Tungsten transport in JET H-mode plasmas in hybrid scenario, experimental observations and modelling. Nuclear Fusion **54**, 083028 (2014).

Arevalo, J., Alonso, J. A., McCarthy, K. J., Velasco, J. L., Garcia-Regana, J. M., and Landreman, M.: Compressible impurity flow in the TJ-II stellarator. Nuclear Fusion **54**, 013008 (2014).

Arion, T., Takahashi, O., Püttner, R., Ulrich, V., Barth, S., Lischke, T., Bradshaw, A. M., Förstel, M., and Hergenhahn, U.: Conformational and nuclear dynamics effects in molecular Auger spectra: fluorine core-hole decay in CF_4. Journal of Physics B **47**, 124033 (2014).

Arnoux, G., Balboa, I., Clever, M., Devaux, S., De Vries, P., Eich, T., Firdaouss, M., Jachmich, S., Lehnen, M., Lomas, P. J., Matthews, G. F., Mertens, P., Nunes, I., Riccardo, V., Ruset, C., Sieglin, B., Valcarcel, D. F., Wilson, J., Zastrow, K.-D., and JET-EFDA Contributors: Power handling of the JET ITER-like wall. Physica Scripta **T159**, 014009 (2014).

Assmann, R., Bingham, R., Bohl, T., Bracco, C., Buttenschön, B., Butterworth, A., Caldwell, A., Chattopadhyay, S., Cipiccia, S., Feldbaumer, E., Fonseca, R. A., Goddard, B., Gross, M., Grulke, O., Gschwendtner, E., Holloway, J., Huang, C., Jaroszynski, D., Jolly, S., Kempkes, P., Lopes, N., Lotov, K., Machacek, J., Mandry, S. R., McKenzie, J. W., Meddahi, M., Militsyn, B. L., Moschuering, N., Muggli, P., Najmudin, Z., Noakes, T. C. Q., Norreys, P. A., Öz, E., Pardons, A., Petrenko, A., Pukhov, A., Rieger, K., Reimann, O., Ruhl, H., Shaposhnikova, E., Silva, L. O., Sosedkin, A., Tarkeshian, R., Trines, R. M. G. N., Tückmantel, T., Vieira, J., Vincke, H., Wing, M., Xia, G., and AWAKE Collaboration: Proton-driven plasma wakefield acceleration: a path to the future of high-energy particle physics. Plasma Physics and Controlled Fusion **56**, 084013 (2014).

Ayten, B., Westerhof, E., and ASDEX Upgrade Team: Nonlinear effects in electron cyclotron current drive applied for the stabilization of neoclassical tearing modes. Nuclear Fusion **54**, 073001 (2014).

Balden, M., Endstrasser, N., Humrickhouse, P. W., Rohde, V., Rasinski, M., Toussaint, U. v., Elgeti, S., Neu, R., and ASDEX Upgrade Team: Collection strategy, inner morphology, and size distribution of dust particles in ASDEX Upgrade. Nuclear Fusion **54**, 073010 (2014).

Balden, M., Manhard, A., and Elgeti, S.: Deuterium retention and morphological modifications of the surface in five grades of tungsten after deuterium plasma exposure. Journal of Nuclear Materials **452**, 248-256 (2014).

Baldwin, M. J., Schwarz-Selinger, T., and Doerner, R. P.: Experimental study and modelling of deuterium thermal release from Be–D co-deposited layers. Nuclear Fusion **54**, 073005 (2014).

Banon Navarro, A., Teaca, B., Jenko, F., Hammett, G. W., Happel, T., and ASDEX Upgrade Team: Applications of large eddy simulation methods to gyrokinetic turbulence. Physics of Plasmas **21**, 032304 (2014).

Barradas, N. P., Mayer, M., Reis, M. A., and Schiettekatte, F.: IBA Software. In: Ion Beam Analsis: Fundamentals and

Applications. (Ed.) M. Nastasi. CRC Press, Taylor & Francis Group, London, 339-370 (2014).

Bécoulet, M., Orain, F., Huijsmans, G. A., Pamela, S., Cahyna, P., Hoelzl, M., Garbet, X., Franck, E., Sonnendrücker, E., Dif-Pradalier, G., Passeron, C., Latu, G., Morales, J., Nardon, E., Fil, A., Nkonga, B., Ratnani, A., and Grandgirard, V.: Mechanism of Edge Localized Mode Mitigation by Resonant Magnetic Perturbations. Physical Review Letters **113**, 115001 (2014).

Behler, K., Blank, H., Buhler, A., Drube, R., Eixenberger, H., Engelhardt, K., Lohs, A., Merkel, R., Raupp, G., Treutterer, W., ASDEX Upgrade Team, and Rechenzentrum Garching: Update on the ASDEX Upgrade data acquisition and data management environment. Fusion Engineering and Design **89**, 702-706 (2014).

Belli, E. A., Candy, J., and Angioni, C.: Pfirsch-Schlüter neoclassical heavy impurity transport in a rotating plasma. Plasma Physics and Controlled Fusion **56**, 124002 (2014).

Bergsaker, H., Possnert, G., Bykov, I., Heinola, K., Petersson, P., Miettunen, J., Widdowson, A., Riccardo, V., Nunes, I., Stamp, M., Brezinsek, S., Groth, M., Kurki-Suonio, T., Likonen, J., Coad, J., Borodin, D., Kirschner, A., Schmid, K., Krieger, K., and JET EFDA Contributors: First results from the ^{10}Be marker experiment in JET with ITER-like wall. Nuclear Fusion **54**, 082004 (2014).

Berkel, M. v., Zwart, H. J., Hogeweij, G. M. D., Vandersteen, G., Brand, H. v. d., Baar, M. R. d., and ASDEX Upgrade Team: Estimation of the thermal diffusion coefficient in fusion plasmas taking frequency measurement uncertainties into account. Plasma Physics and Controlled Fusion **56**, 105004 (2014).

Bernert, M., Eich, T., Burckhart, A., Fuchs, J. C., Giannone, L., Kallenbach, A., McDermott, R. M., Sieglin, B., and ASDEX Upgrade Team: Application of AXUV diode detectors at ASDEX Upgrade. Review of Scientific Instruments **85**, 033503 (2014).

Beurskens, M. N. A., Frassinetti, L., Challis, C., Giroud, C., Saarelma, S., Alper, B., Angioni, C., Bilkova, P., Bourdelle, C., Brezinsek, S., Buratti, P., Calabro, G., Eich, T., Flanagan, J., Giovannozzi, E., Groth, M., Hobirk, J., Joffrin, E., Leyland, M. J., Lomas, P., Luna, E. d. l., Kempenaars, M., Maddison, G., Maggi, C., Mantica, P., Maslov, M., Matthews, G, Mayoral, M.-L., Neu, R., Nunes, I., Osborne, T., Rimini, F., Scannell, R., Solano, E. R., Snyder, P. B., Voitsekhovitch, I., Vries, P. d., and Jet-EFDA Contributors: Global and pedestal confinement in JET with a Be/W metallic wall. Nuclear Fusion **54**, 043001 (2014).

Biancalani, A., Bottino, A., Lauber, P., and Zarzoso, D.: Numerical validation of the electromagnetic gyrokinetic code NEMORB on global axisymmetric modes. Nuclear Fusion **54**, 104004 (2014).

Bilato, R., and Brambilla, M.: Toroidal trapping effects in the surface-averaged Fokker-Planck SSFPQL solver. Radiofrequency Power in Plasmas: Proceedings of the 20th Topical Conference. (Eds.) A. Tuccillo, S. Ceccuzzi. AIP Conference Proceedings **1580**. American Institute of Physics, Melville, TN, 306-309 (2014).

Bilato, R., Brambilla, M., and Fable, E.: Simulations of fast-wave current drive in pulsed and steady-state DEMO designs. Journal of Physics: Conference Series **561**, 012001 (2014).

Bilato, R., Brambilla, M., and Poli, E.: On the approximations of the distribution function of fusion alpha particles. Physics of Plasmas **21**, 104502 (2014).

Bilato, R., Coster, D., Dumont, R., Johnsson, T., Klingshirn, H. J., Lerche, E., Sauter, O., Brambilla, M., Figini, L., Van Eester, D., Villard, L., Farina, D., and ITM-TF Contributors: ICRF-code benchmark activity in the framework of the European task-force on integrated Tokamak Modelling. Radiofrequency Power in Plasmas: Proceedings of the 20th Topical Conference. (Eds.) A. Tuccillo, S. Ceccuzzi. AIP Conference Proceedings **1580**. American Institute of Physics, Melville, TN, 291-294 (2014).

Bilato, R., Maj, O., and Angioni, C.: Modelling the influence of temperature anisotropies on poloidal asymmetries of density in the core of rotating plasmas. Nuclear Fusion **54**, 072003 (2014).

Bilato, R., Maj, O., and Brambilla, M.: An algorithm for fast Hilbert transform of real functions. Advances in Computational Mathematics **40**, 1159-1168 (2014).

Bird, T., and Hegna, C. C.: Controlling tokamak geometry with three-dimensional magnetic perturbations. Physics of Plasmas **21**, 100702 (2014).

Birkenmeier, G., Laggner, F. M., Willensdorfer, M., Kobayashi, T., Manz, P., Wolfrum, E., Carralero, D., Fischer, R., Sieglin, B., Fuchert, G., Stroth, U., and ASDEX Upgrade Team: Magnetic field dependence of the blob dynamics in the edge of ASDEX upgrade L-mode plasmas. Plasma Physics and Controlled Fusion **56**, 075019 (2014).

Bluhm, T., Heimann, P., Hennig, C., Kühner, G., Kroiss, H., Krom, J., Laqua, H., Lewerentz, M., Maier, J., Riemann, H., Schacht, J., Spring, A., Werner, A., and Zilker, M.: Wendelstein 7-X's CoDaStation: A modular application for scientific data acquisition. Fusion Engineering and Design **89**, 658-662 (2014).

Bobkov, V., Stepanov, I., Jacquet, P., Monakhov, I., Bilato, R., Colas, L., Czarnecka, A., Dux, R., Faugel, H., Kallenbach, A., Müller, H. W., Noterdaeme, J.-M., Potzel, S., Pütterich, T., Suttrop, W., and ASDEX Upgrade Team: Influence of gas injection location and magnetic perturbations on ICRF antenna performance in ASDEX Upgrade. Radiofrequency Power in Plasmas: Proceedings of the 20th Topical Conference. (Eds.) A. Tuccillo, S. Ceccuzzi. AIP Conference Proceedings **1580**. American Institute of Physics, Melville, TN, 271-274 (2014).

Bohlin, H., Stechow, A. v., Rahbarnia, K., Grulke, O., and Klinger, T.: VINETA II: A linear magnetic reconnection experiment. Review of Scientific Instruments **85**, 023501 (2014).

Bonomo, F., Agostini, M., Brombin, M., Fantz, U., Franzen, P., Pasqualotto, R., Wünderlich, D., and NNBI Team: Tomography feasibility study on the optical emission spectroscopy diagnostic for the negative ion source of the ELISE test facility. Plasma Physics and Controlled Fusion **56**, 015006 (2014).

Borgdorff, J., Ben Belgacem, M., Bona-Casas, C., Fazendeiro, L., Groen, D., Hoenen, O., Mizeranschi, A., Suter, J. L., Coster, D., Coveney, P. V., Dubitzky, W., Hoekstra, A. G., Strand, P., and Chopard, B.: Performance of distributed multiscale simulations. Philosophical Transactions of the Royal Society of London, Series A: Mathematical and Physical Sciences **372**, 20130381 (2014).

Borodin, D., Brezinsek, S., Miettunen, J., Stamp, M., Kirschner, A., Björkas, C., Groth, M., Marsen, S., Silva, C., Lisgo, S. W., Matveev, D., Airila, M., Philipps, V., and JET-EFDA Contributors: Determination of Be sputtering yields from spectroscopic observations at the JET ITER-like wall based on three-dimensional ERO modelling. Physica Scripta **T159**, 014057 (2014).

Boscary, J., Peacock, A., Smirnow, M., and Tittes, H.: Summary of Research and Development Activities for the Production of the Divertor Target Elements of Wendelstein 7-X. IEEE Transactions on Plasma Science **42**, 533-538 (2014).

Bosch, H.-S., Brakel, R., Gasparotto, M., Grote, H., Hartmann, D., Herrmann, R., Nagel, M., Naujoks, D., Otte, M., Riße, K., Rummel, T., and Werner, A.: Transition from Construction to Operation Phase of the Wendelstein 7-X Stellarator. IEEE Transactions on Plasma Science **42**, 432-438 (2014).

Bourdelle, C., Maggi, C. F., Chone, L., Beyer, P., Citrin, J., Fedorczak, N., Garbet, X., Loarte, A., Millitello, F., Romanelli, M., Sarazin, Y., and JET EFDA Contributors: L to H mode transition: on the role of Z_{eff}. Nuclear Fusion **54**, 022001 (2014).

Bowden, G. W., Könies, A., Hole, M. J., Gorelenkov, N. N., and Dennis, G. R.: Comparison of methods for numerical calculation of continuum damping. Physics of Plasmas **21**, 052508 (2014).

Braeuer, T., Havemeister, R., Henkel, A., and Müller, J.: Interaction of Metrology and Assembly at W7-X. IEEE Transactions on Plasma Science **42**, 1943-1950 (2014).

Brendel, A., Paffenholz, V., and Kimmig, S.: Fracture behaviour of SiC monofilament reinforced copper – an acoustic emission study. Journal of Composite Materials **48**, 835-842 (2014).

Brezinsek, S., Stamp, M. F., Nishijima, D., Borodin, D., Devaux, S., Krieger, K., Marsen, S., O'Mullane, M., Bjoerkas, C., Kirschner, A., and JET EFDA Contributors: Study of physical and chemical assisted physical sputtering of beryllium in the JET ITER-like wall. Nuclear Fusion **54**, 103001 (2014).

Briefi, S., and Fantz, U.: Simulation of the A–X and B–X transition emission spectra of the InCl molecule in low pressure plasmas. Journal of Quantitative Spectroscopy and Radiative Transfer **133**, 551-558 (2014).

Briguglio, S., Wang, X., Zonca, F., Vlad, G., Fogaccia, G., Di Troia, C., and Fusco, V.: Analysis of the nonlinear behavior of shear-Alfvén modes in tokamaks based on Hamiltonian mapping techniques. Physics of Plasmas **21**, 112301 (2014).

Brombin, M., Spolaore, M., Serianni, G., Barzon, A., Franchin, L., Pasqualotto, R., Pomaro, N., Schiesko, L., Taliercio, C., and Trevisan, L.: Electrostatic sensors for SPIDER experiment: Design, manufacture of prototypes, and first test. Review of Scientific Instruments **85**, 02A715 (2014).

Brombin, M., Spolaore, M., Serianni, G., Pomaro, N., Taliercio, C., Dalla Palma, M., Pasqualotto, R., and Schiesko, L.: Langmuir probes for SPIDER (source for the production of ions of deuterium extracted from radio frequency plasma) experiment: Tests in BATMAN (Bavarian test machine for negative ions). Review of Scientific Instruments **85**, 11D832 (2014).

Brunner, K. J., Grulke, O., Niemczyk, D., and Klinger, T.: Ion Drift Measurements around a Grounded Sphere in Magnetized Sub-sonic Plasma Flows. Contributions to Plasma Physics **54**, 802-811 (2014).

Buchholz, R., Camenen, Y., Casson, F. J., Grosshauser, S. R., Hornsby, W. A., Migliano, P., and Peeters, A. G.: Toroidal momentum transport in a tokamak due to profile shearing. Physics of Plasmas **21**, 062304 (2014).

Bulanin, V. V., Wagner, F., Varfolomeev, V. I., Gusev, V. K., Kurskiev, G. S., Minaev, V. B., Patrov, M. I., Petrov, A. V., Petrov, Y. V., Prisyazhnyuk, D. V., Sakharov, N. V., Tolstyakov, S. Y., Khromov, N. A., Shchegolev, P. B., and Yashin, A. Y.: Observation of geodesic acoustic modes in the Globus-M spherical Tokamak. Technical Physics Letters **40**, 375-377 (2014).

Bykov, V., Fellinger, J., Schauer, F., Köppen, M., Egorov, K., Eeten, P. v., Dudek, A., and Andreeva, T.: Specific Features of Wendelstein 7-X Structural Analyses. IEEE Transactions on Plasma Science **42**, 690-697 (2014).

Campergue, A.-L., Jacquet, P., Bobkov, V., Milanesio, D., Monakhov, I., Colas, L., Arnoux, G., Brix, M., Sirinelli, A., and JET-EFDA Contributors: Characterization of local heat flux around ICRF antennas on JET Radiofrequency Power in Plasmas: Proceedings of the 20th Topical Conference. (Eds.) A. Tuccillo, S. Ceccuzzi. AIP Conference Proceedings **1580**. American Institute of Physics, Melville, TN, 263-266 (2014).

Carralero, D., Birkenmeier, G., Müller, H. W., Manz, P., De Marne, P., Müller, S. H., Reimold, F., Stroth, U., Wischmeier, M., and Wolfrum, E.: An experimental investigation of the high density transition of the scrape-off layer transport in ASDEX Upgrade. Nuclear Fusion **54**, 123005 (2014).

Casali, L., Bernert, M., Dux, R., Fischer, R., Kallenbach, A., Kurzan, B., Lang, P., Mlynek, A., McDermott, R., Ryter, F., Sertoli, M., Tardini, G., Zohm, H., and ASDEX Upgrade Team: Transport analysis of high radiation and high density plasmas in the ASDEX Upgrade tokamak. EPJ Web of Conferences **79**, 01007 (2014). http://dx.doi.org/10.1051/epjconf/20137901007.

Cerri, S. S., Banon Navarro, A., Jenko, F., and Told, D.: Collision-dependent power law scalings in two dimensional gyrokinetic turbulence. Physics of Plasmas **21**, 082305 (2014).

Cerri, S. S., Pegoraro, F., Califano, F., Del Sarto, D., and Jenko, F.: Pressure tensor in the presence of velocity shear: Stationary solutions and self-consistent equilibria. Physics of Plasmas **21**, 112109 (2014).

Chankin, A. V., and Coster, D. P.: Benchmarks of KIPP: Vlasov-Fokker-Planck Code for Parallel Plasma Transport in the SOL and Divertor. Contributions to Plasma Physics **54**, 493-497 (2014).

Chankin, A. V., Coster, D. P., and Dux, R.: Monte Carlo simulations of tungsten redeposition at the divertor target. Plasma Physics and Controlled Fusion **56**, 025003 (2014).

Chapman, I. T., Becoulet, M., Bird, T., Canik, J., Cianciosa, M., Cooper, W. A., Evans, T., Ferraro, N., Fuchs, C., Gryaznevich, M., Gribov, Y., Ham, C., Hanson, J., Huijsmans, G., Kirk, A., Lazerson, S., Liang, Y., Lupelli, I., Moyer, R. A., Nührenberg, C., Orain, F., Orlov, D., Suttrop, W., Yadykin, D., ASDEX Upgrade Team, DIII-D Team, MAST Team, NSTX Team, and EFDA-JET Contributors: Three-dimensional distortions of the tokamak plasma boundary: boundary displace-ments in the presence of resonant magnetic perturbations. Nuclear Fusion **54**, 083006 (2014).

Citrin, J., Jenko, F., Mantica, P., Told, D., Bourdelle, C., Dumont, R., Garcia, J., Haverkort, J. W., Hogeweij, G. M. D., Johnson, T., Pueschel, M. J., and JET-EFDA Contributors: Ion temperature profile stiffness: non-linear gyrokinetic simu-lations and comparison with experiment. Nuclear Fusion **54**, 023008 (2014).

Classen, I. G. J., Domier, C. W., Luhmann Jr., N. C., Bogomo-lov, A. V., Suttrop, W., Boom, J., Tobias, B. J., Donne, A. J. H., and ASDEX Upgrade Team: Dual array 3D electron cyclotron emission imaging at ASDEX Upgrade. Review of Scientific Instruments **85**, 11D833 (2014).

Clementson, J., Beiersdorfer, P., Brage, T., and Gu, M. F.: Atomic data and theoretical X-ray spectra of Ge-like through V-like W ions. Atomic Data and Nuclear Data Tables **100**, 577-649 (2014).

Clementson, J., Rahbarnia, K., Grulke, O., and Klinger, T.: Design of A, B, and C Pulse Forming Networks Using the VINPFN Application. IEEE Transactions on Power Elec-tronics **29**, 5673-5679 (2014).

Coad, J. P., Alves, E., Barradas, N. P., Baron-Wiechec, A., Catarino, N., Heinola, K., Likonen, J., Mayer, M., Matthews, G. F., Peterson, P., Widdowson, A., and JET-EFDA Contributors: Surface analysis of tiles and samples exposed to the first JET campaigns with the ITER-like wall. Physica Scripta **T159**, 014012 (2014).

Coenen, J. W., De Temmerman, G., Federici, G., Philipps, V., Sergienko, G., Strohmayer, G., Terra, A., Unterberg, B., Wegener, T., and Van den Bekerom, D. C. M.: Liquid metals as alternative solution for the power exhaust of future fusion devices: status and perspective. Physica Scripta **T159**, 014037 (2014).

Colas, L., Bobkov, V., Carralero, D., Kocan, M., Müller, H. W., Manz, P., Kubic, M., Gunn, J. P., Herrmann, A., Rohde, V., and ASDEX Upgrade Team: 2-dimensional mapping of ICRF-induced scrape-off layer modifications with a retarding field analyser on ASDEX-Upgrade Radiofrequency Power in Plasmas: Proceedings of the 20th Topical Conference. (Eds.) A. Tuccillo, S. Ceccuzzi. AIP Conference Proceedings **1580**. American Institute of Physics, Melville, TN, 259-262 (2014).

Cole, M., Mishchenko, A., Könies, A., Kleiber, R., and Borchardt, M.: Fluid electron, gyrokinetic ion simulations of linear internal kink and energetic particle modes. Physics of Plasmas **21**, 072123 (2014).

Cole, M., Newton, S. L., Cowley, S. C., Loureiro, N. F., Dickinson, D., Roach, C., and Connor, J. W.: Electromagnetic effects in the stabilization of turbulence by sheared flow. Plasma Physics and Controlled Fusion **56**, 015007 (2014).

Cottier, P., Bourdelle, C., Camenen, Y., Gürcan, Ö. D., Casson, F., Garbet, X., Hennequin, P., and Tala, T.: Angular momentum transport modeling: achievements of a gyrokinetic quasi-linear approach. Plasma Physics and Controlled Fusion **56**, 015011 (2014).

Craciunescu, T., Murari, A., Sieglin, B., Matthews, G., and JET EFDA Contributors: An Original Method for Spot Detection and Analysis for Large Surveys of Videos in JET. IEEE Transactions on Plasma Science **42**, 1358-1366 (2014).

Crouseilles, N., Glanc, P., Hirstoaga, S. A., Madaule, E., Mehrenberger, M., and Pétri, J.: A new fully two-dimensional conservative semi-Lagrangian method: applications on polar grids, from diocotron instability to ITG turbulence. The European Physical Journal D: Atomic, Molecular and Optical Physics **68**, 252 (2014).

Crouseilles, N., Navaro, P., and Sonnendrücker, E.: Charge-conserving grid based methods for the Vlasov–Maxwell equations. Comptes Rendus Mécanique **342**, 636-646 (2014).

Czarnecka, A., Bobkov, V., Coffey, I. H., Colas, L., Jacquet, P., Lawson, K. D., Lerche, E., Maggi, C., Mayoral, M.-L., Pütterich, T., Van Eester, D., and JET-EFDA Contributors: Spectroscopic investigation of heavy impurity behaviour during ICRH with the JET ITER-like wall. Radiofrequency Power in Plasmas: Radiofrequency Power in Plasmas: Proceedings of the 20th Topical Conference. (Eds.) A. Tuccillo, S. Ceccuzzi. AIP Conference Proceedings **1580**. American Institute of Physics, Melville, TN, 227-230 (2014).

D'Inca, R., Noterdaeme, J.-M., and ASDEX Upgrade Team: Characterization of the fast ions distribution from ion cyclotron emission measurements. Radiofrequency Power in Plasmas: Proceedings of the 20th Topical Conference. (Eds.) A. Tuccillo, S. Ceccuzzi. AIP Conference Pro ceedings **1580**. American Institute of Physics, Melville, TN, 243-246 (2014).

Danielis, P., Skodzik, J., Altmann, V., Schweissguth, E. B., Golatowski, F., Timmermann, D., and Schacht, J.: Survey on real-time communication via Ethernet in industrial automation environments. Proceedings of the 2014 IEEE Emerging Technology and Factory Automation (ETFA). IEEE, Piscataway, NJ (2014).

Dannert, T., Marek, A., and Rampp, M.: Porting Large HPC Applications to GPU Clusters: The Codes GENE and VERTEX. Parallel Computing: Accelerating Computational Science and Engineering (CSE). (Eds.) G. Bader, A. Bode, H.-J. Bungartz et al. IOS Press, Amsterdam, 305-314 (2014).

De Muri, M., Cavallin, T., Pasqualotto, R., Dalla Palma, M., Cervaro, V., Fasolo, D., Franchin, L., Tollin, M., Greuner, H., Böswirth, B., and Serianni, G.: High energy flux thermo-mechanical test of 1D-carbon-carbon fibre composite prototypes for the SPIDER diagnostic calorimeter. Review of Scientific Instruments **85**, 02A718 (2014).

De Muri, M., Pavei, M., Rizzolo, A., Bonomo, F., Franzen, P., Riedl, R., Ruf, B., Schiesko, L., Valente, M., Cervaro, V., Fasolo, D., Franchin, L., Tollin, M., Pasqualotto, R., and Serianni, G.: Prototype of a Diagnostic Calorimeter for BATMAN: Design and Preliminary Measurements. IEEE Transactions on Plasma Science **42**, 1032-1035 (2014).

Dejarnac, R., Podolnik, A., Komm, M., Arnoux, G., Coenen, J. W., Devaux, S., Frassinetti, L., Gunn, J. P., Matthews, G. F., Pitts, R. A., and JET-EFDA Contributors: Numerical evaluation of heat flux and surface temperature on a misaligned JET divertor W lamella during ELMs. Nuclear Fusion **54**, 123011 (2014).

Devynck, P., Maddison, G., Giroud, C., Jacquet, P., Lehnen, M., Lerche, E., Matthews, G. F., Neu, R., Stamp, M. F., Van Eester, D., and JET-EFDA Contributors: Comparing the bulk radiated power efficiency in carbon and ITER-like-wall environments in JET. Plasma Physics and Controlled Fusion **56**, 075026 (2014).

Dobes, K., Köppen, M., Oberkofler, M., Lungu, C. P., Porosnicu, C., Höschen, T., Meisl, G., Linsmeier, C., and Aumayr, F.: Interaction of nitrogen ions with beryllium surfaces. Nuclear Instruments and Methods in Physics Research Section B: Beam Interactions with Materials and Atoms **340**, 34-38 (2014).

Doerk, H., and Jenko, F.: Towards optimal explicit time-stepping schemes for the gyrokinetic equations. Computer Physics Communications **185**, 1938-1946 (2014).

Doerner, R. P., Nishijima, D., and Schwarz-Selinger, T.: Impact of surface morphology on sputtering during high-fluence plasma exposure. Physica Scripta **T159**, 014040 (2014).

Drevlak, M., Geiger, J., Helander, P., and Turkin, Y.: Fast Particle Confinement with Optimized Coil Currents in the W7-X Stellarator. Nuclear Fusion **54**, 073002 (2014).

Dux, R., Loarte, A., Fable, E., and Kukushkin, A.: Transport of tungsten in the H-mode edge transport barrier of ITER. Plasma Physics and Controlled Fusion **56**, 124003 (2014).

Erckmann, V., Braune, H., Gantenbein, G., Jelonnek, J., Kasparek, W., Laqua, H. P., Lechte, C., Marushchenko, N. B., Michel, G., Plaum, B., Thumm, M., Wolf, R., and W7-X ECRH Team: ECRH and W7-X: An intriguing pair. Radiofrequency Power in Plasmas: Proceedings of the 20th Topical Conference. (Eds.) A. Tuccillo, S. Ceccuzzi. AIP Conference Proceedings **1580**. American Institute of Physics, Melville, TN, 542-545 (2014).

Falchetto, G. L., Coster, D., Coelho, R., Scott, B. D., Figini, L., Kalupin, D., Nardon, E., Nowak, S., Alves, L. L., Artaud, J. F., Basiuk, V., Bizarro, J. P. S., Boulbe, C., Dinklage, A., Farina, D., Faugeras, B., Ferreira, J., Figueiredo, A., Huynh, P., Imbeaux, F., Ivanova-Stanik, I., Jonsson, T., Klingshirn, H.-J., Konz, C., Kus, A., Marushchenko, N. B., Pereverzev, G., Owsiak, M., Poli, E., Peysson, Y., Reimer, R., Signoret, J., Sauter, O., Stankiewicz, R., Strand, P., Voitsekhovitch, I., Westerhof, E., Zok, T., Zwingmann, W., ITM-TF Contributors, ASDEX Upgrade Team, and JET-EFDA Contributors: The European Integrated Tokamak Modelling (ITM) effort: achievements and first physics results. Nuclear Fusion **54**, 043018 (2014).

Falchetto, G. L., Coster, D., Coelho, R., Scott, B. D., Figini, L., Kalupin, D., Nardon, E., Nowak, S., Alves, L. L., Artaud, J. F., Basiuk, V., Bizarro, J. P. S., Boulbe, C., Dinklage, A., Farina, D., Faugeras, B., Ferreira, J., Figueiredo, A., Huynh, P., Imbeaux, F., Ivanova-Stanik, I., Jonsson, T., Klingshirn, H.-J., Konz, C., Kus, A., Marushchenko, N. B., Pereverzev, G., Owsiak, M., Poli, E., Peysson, Y., Reimer, R., Signoret, J., Sauter, O., Stankiewicz, R., Strand, P., Voitsekhovitch, I., Westerhof, E., Zok, T., Zwingmann, W., ITM-TF Contributors, ASDEX Upgrade Team, and JET-EFDA Contributors: Corrigendum: The European Integrated Tokamak Modelling (ITM) effort: achievements and first physics results (2014 Nucl. Fusion 54 043018). Nuclear Fusion **54**, 099501 (2014).

Fantz, U., Briefi, S., Friedl, R., Kammerloher, M., Kolbinger, J., and Oswald, A.: Initial Phase of a Large Atmospheric Plasmoid Generated above a Water Surface. IEEE Transactions on Plasma Science **42**, 2624-2625 (2014).

Fantz, U., Franzen, P., Heinemann, B., and Wünderlich, D.: First results of the ITER-relevant negative ion beam test facility ELISE (invited). Review of Scientific Instruments **85**, 02B305 (2014).

Fantz, U., Schiesko, L., and Wünderlich, D.: Plasma expansion across a transverse magnetic field in a negative hydrogen ion source for fusion. Plasma Sources Science and Technology **23**, 044002 (2014).

Farina, D., Henderson, M., Figini, L., Saibene, G., Goodman, T., Kajiwara, K., Omori, T., Poli, E., Strauss, D., and

Takahashi, K.: Optimization of the ITER EC H&CD functional capabilities while relaxing the engineering constraints. Radiofrequency Power in Plasmas: Proceedings of the 20th Topical Conference. (Eds.) A. Tuccillo, S. Ceccuzzi. AIP Conference Proceedings **1580**. American Institute of Physics, Melville, TN, 175-182 (2014).

Fasshauer, E., Förstel, M., Pallmann, S., Pernpointner, M., and Hergenhahn, U.: Using ICD for structural analysis of clusters: A case study on NeAr clusters. New Journal of Physics **16**, 103026 (2014). http://iopscience.iop.org/1367-2630/16/10/103026.

Faugel, H., Bobkov, V., Eixenberger, H., Podoba, Y., and Stepanov, I.: Upgrading the ICRF data aquisition system at ASDEX Upgrade. Radiofrequency Power in Plasmas: Proceedings of the 20th Topical Conference. (Eds.) A. Tuccillo, S. Ceccuzzi. AIP Conference Proceedings **1580**. American Institute of Physics, Melville, TN, 378-381 (2014).

Fellinger, J., Egorov, K., Kallmeyer, J. P., Bykov, V., and Schauer, F.: Asymmetry of W7-X magnet system introduced by torus assembly. Fusion Engineering and Design **89**, 2189-2193 (2014).

Feng, Y., Frerichs, H., Kobayashi, M., Bader, A., Effenberg, F., Harting, D., Hoelbe, H., Huang, J., Kawamura, G., Lore, J. D., Lunt, T., Reiter, D., Schmitz, O., and Sharma, D.: Recent Improvements in the EMC3-Eirene Code. Contributions to Plasma Physics **54**, 426-431 (2014).

Fernández-Menchero, L., and Otranto, S.: Fully and double differential cross sections for the single ionization of H_2O by bare ion impact. Journal of Physics B **47**, 035205 (2014).

Förstel, M., Arion, T., and Hergenhahn, U.: Reprint of Measuring the efficiency of interatomic coulombic decay in Ne clusters. Journal of Electron Spectroscopy and Related Phenomena **196**, 54-57 (2014).

Fortuna-Zalesna, E., Grzonka, J., Rasinski, M., Balden, M., Rohde, V., Kurzydlowski, K. J., and ASDEX Upgrade Team: Characterization of dust collected after plasma operation of all-tungsten ASDEX Upgrade. Physica Scripta **T159**, 014066 (2014).

Franke, T., Barbato, E., Cardinali, A., Ceccuzzi, S., Cesario, R., Eester, D. V., Lerche, E., Mayoral, M.-L., Mirizzi, F., Nightingale, M., Noterdaeme, J.-M., Poli, E., Tuccillo, A. A., Wenninger, R., and Zohm, H.: RF H&CD systems for DEMO – Challenges and opportunities. Radiofrequency Power in Plasmas: Proceedings of the 20th Topical Conference. (Eds.) A. Tuccillo, S. Ceccuzzi. AIP Conference Proceedings **1580**. American Institute of Physics, Melville, TN, 207-210 (2014).

Franzen, P., and Fantz, U.: On the NBI system for substantial current drive in a fusion power plant: Status and R&D needs for ion source and laser neutralizer. Fusion Engineering and Design **89**, 2594-2605 (2014).

Franzen, P., Wünderlich, D., Fantz, U., and NNBI Team: On the electron extraction in a large RF-driven negative hydrogen ion source for the ITER NBI system. Plasma Physics and Controlled Fusion **56**, 025007 (2014).

Frerichs, H., Schmitz, O., Reiter, D., Evans, T. E., and Feng, Y.: Striation pattern of target particle and heat fluxes in three dimensional simulations for DIII-D. Physics of Plasmas **21**, 020702 (2014).

Friedl, R., and Fantz, U.: Fundamental studies on the Cs dynamics under ion source conditions. Review of Scientific Instruments **85**, 02B109 (2014).

Fuchert, G., Birkenmeier, G., Carralero, D., Lunt, T., Manz, P., Müller, H. W., Nold, B., Ramisch, M., Rohde, V., and Stroth, U.: Blob properties in L- and H-mode from gas-puff imaging in ASDEX Upgrade. Plasma Physics and Controlled Fusion **56**, 125001 (2014).

Fuchs, V., Laqua, H. P., Krlin, L., Panek, R., Preinhalter, R., Seidl, J., and Urban, J.: Lower hybrid wavepacket stochasticity revisited. Radiofrequency Power in Plasmas: Proceedings of the 20th Topical Conference. (Eds.) A. Tuccillo, S. Ceccuzzi. AIP Conference Proceedings **1580**. American Institute of Physics, Melville, TN, 442-445 (2014).

Fuchs, V., Laqua, H. P., Seidl, J., Krlin, L., Panek, R., Preinhaelter, J., and Urban, J.: Relativistic Fermi-Ulam map: Application to WEGA stellarator lower hybrid power operation. Physics of Plasmas **21**, 061513 (2014).

Füllenbach, F., Rummel, T., Mönnich, T., and Köster, E.: Design and Prototype of the High Voltage In-service-tests on the Superconducting Magnet System of Wendelstein 7-X. IEEE Transactions on Applied Superconductivity **24**, 0502604 (2014).

Gantenbein, G., Samartsev, A., Aiello, G., Dammertz, G., Jelonnek, J., Losert, M., Schlaich, A., Scherer, T. A., Strauss, D., Thumm, M., and Wagner, D.: First Operation of a Step-frequency Tunable 1-MW Gyrotron with a Diamond Brewster Angle Output Window. IEEE Transactions on Electron Devices **61**, 1806-1811 (2014).

Gao, L., Jacob, W., Schwarz-Selinger, T., and Manhard, A.: Deuterium implantation into tungsten nitride: Negligible diffusion at 300 K. Journal of Nuclear Materials **451**, 352-355 (2014).

Gao, L., Jacob, W., Wang, P., Toussaint, U. v., and Manhard, A.: Influence of nitrogen pre-implantation on deuterium retention in tungsten. Physica Scripta **T159**, 014023 (2014).

Gao, L., Toussaint, U. v., Jacob, W., Balden, M., and Manhard, A.: Suppression of hydrogen-induced blistering of tungsten by pre-irradiation at low temperature (Letters). Nuclear Fusion **54**, 122003 (2014).

García-Rosales, C., López-Ruiz, P., Alvarez-Martín, S., Calvo, A., Ordás, N., Koch, F., and Brinkmann, J.: Oxidation behaviour of bulk W-Cr-Ti alloys prepared by mechanical alloying and HIPing. Fusion Engineering and Design **89**, 1611-1616 (2014).

Gasparotto, M., Baylard, C., Bosch, H.-S., Hartmann, D., Klinger, T., Vilbrandt, R., Wegener, L., and W7-X Team: Wendelstein 7-X – Status of the project and commissioning planning. Fusion Engineering and Design **89**, 2121-2127 (2014).

Geiger, B., Garcia-Munoz, M., Dux, R., Ryter, F., Tardini, G., Barrera Orte, L., Classen, I. G. J., Fable, E., Fischer, R., Igochine, V., McDermott, R., and ASDEX Upgrade Team: Fast-ion transport in the presence of magnetic reconnection induced by sawtooth oscillations in ASDEX Upgrade. Nuclear Fusion **54**, 022005 (2014).

Ghendrih, P., Norscini, C., Cartier-Michaud, T., Dif-Pradalier, G., Abiteboul, J., Dong, Y., Garbet, X., Gürcan, O., Hennequin, P., Grandgirard, V., Latu, G., Morel, P., Sarazin, Y., Storelli, A., and Vermare, L.: Phase space structures in gyrokinetic simulations of fusion plasma turbulence. The European Physical Journal D: Atomic, Molecular and Optical Physics **68**, 303 (2014).

Ghezzi, F., Caniello, R., Giubertoni, D., Bersani, M., Hakola, A., Mayer, M., Rohde, V., Anderle, M., and ASDEX Upgrade Team: Deuterium depth profile quantification in a ASDEX Upgrade divertor tile using secondary ion mass spectrometry. Applied Surface Science **315**, 459-466 (2014).

Girardo, J.-B., Zarzoso, D., Dumont, R., Garbet, X., Sarazin, Y., and Sharapov, S.: Relation between energetic and standard geodesic acoustic modes. Physics of Plasmas **21**, 092507 (2014).

Görler, T., White, A. E., Told, D., Jenko, F., Holland, C., and Rhodes, T. L.: A flux-matched gyrokinetic analysis of DIII-D L-mode turbulence. Physics of Plasmas **21**, 122307 (2014).

Granucci, G., Ricci, D., Cavinato, M., Farina, D., Figini, L., Mattei, M., Stober, J., and Tudisco, O.: EC assisted start-up experiments reproduction in FTU and AUG for simulations of the ITER case. Radiofrequency Power in Plasmas: Proceedings of the 20th Topical Conference. (Eds.) A. Tuccillo,

S. Ceccuzzi. AIP Conference Proceedings **1580**. American Institute of Physics, Melville, TN, 494-497 (2014).

Greenwald, M., Bader, A., Baek, S., Bakhtiari, M., Barnard, H., Beck, W., Bergerson, W., Bespamyatnov, I., Bonoli, P., Brower, D., Brunner, D., Burke, W., Candy, J., Churchill, M., Cziegler, I., Diallo, A., Dominguez, A., Duval, B., Edlund, E., Ennever, P., Ernst, D., Faust, I., Fiore, C., Fredian, T., Garcia, O., Gao, C., Goetz, J., Golfinopoulos, T., Granetz, R., Grulke, O., Hartwig, Z., Horne, S., Howard, N., Hubbard, A., Hughes, J., Hutchinson, I., Irby, J., Izzo, V., Kessel, C., LaBombard, B., Lau, C., Li, C., Lin, Y., Lipschultz, B., Loarte, A., Marmar, E., Mazurenko, A., McCracken, G., McDermott, R., Meneghini, O., Mikkelsen, D., Mossessian, D., Mumgaard, R., Myra, J., Nelson-Melby, E., Ochoukov, R., Olynyk, G., Parker, R., Pitcher, S., Podpaly, Y., Porkolab, M., Reinke, M., Rice, J., Rowan, W., Schmidt, A., Scott, S., Shiraiwa, S., Sierchio, J., Smick, N., Snipes, J. A., Snyder, P., Sorbom, B., Stillerman, J., Sung, C., Takase, Y., Tang, V., Terry, J., Terry, D., Theiler, C., Tronchin-James, A., Tsujii, N., Vieira, R., Walk, J., Wallace, G., White, A., Whyte, D., Wilson, J., Wolfe, S., Wright, G., Wright, J., Wukitch, S., and Zweben, S.: 20 years of research on the Alcator C-Mod tokamak. Physics of Plasmas **21**, 110501 (2014).

Greuner, H., Böswirth, B., Eich, T., Herrmann, A., Maier, H., and Sieglin, B.: Experimental determination of the transient heat absorption of W divertor materials. Physica Scripta **T159**, 014003 (2014).

Greuner, H., Maier, H., Balden, M., Böswirth, B., Elgeti, S., Schmid, K., and Schwarz-Selinger, T.: Surface morphology changes of tungsten exposed to high heat loading with mixed hydrogen/helium beams. Journal of Nuclear Materials **455**, 681-684 (2014).

Grünhagen Romanelli, S., Brezinsek, S., Butler, B., Coad, J. P., Drenik, A., Giroud, C., Jachmich, S., Keenan, T., Kruezi, U., Mozetic, M., Oberkofler, M., Parracho, A., Romanelli, M., Smith, R., Yorkshades, J., and JET-EFDA Contributors: Gas analyses of the first complete JET cryopump regeneration with ITER-like wall. Physica Scripta **T159**, 014068 (2014).

Grulke, O., Terry, J. L., Cziegler, I., LaBombard, B., and Garcia, O. E.: Experimental investigation of the parallel structure of fluctuations in the scrape-off layer of Alcator C-Mod. Nuclear Fusion **54**, 043012 (2014).

Grzonka, J., Ciupinski, L., Smalc-Koziorowska, J., Ogorodnikova, O., Mayer, M., and Kurzydlowski, K. J.: Electron microscopy observations of radiation damage in irradiated and annealed tungsten. Nuclear Instruments and Methods in Physics Research Section B: Beam Interactions with Materials and Atoms **340**, 27-33 (2014).

Guillemaut, C., Pitts, R. A., Kukushkin, A. S., Gunn, J. P., Bucalossi, J., Arnoux, G., Belo, P., Brezinsek, S., Brix, M., Corrigan, G., Devaux, S., Flanagan, J., Groth, M., Harting, D., Huber, A., Jachmich, S., Kruezi, U., Lehnen, M., Marsen, S., Meigs, A. G., Meyer, O., Stamp, M., Strachan, J. D., Wischmeier, M., and JET EFDA Contributors: Influence of atomic physics on EDGE2D-EIRENE simulations of JET divertor detachment with carbon and beryllium/tungsten plasma-facing components. Nuclear Fusion **54**, 093012 (2014).

Hakola, A., Karhunen, J., Koivuranta, S., Likonen, J., Balden, M., Herrmann, A., Mayer, M., Müller, H. W., Neu, R., Rohde, V., Sugiyama, K., and ASDEX Upgrade Team: Long-term erosion of plasma-facing materials with different surface roughness in ASDEX Upgrade. Physica Scripta **T159**, 014027 (2014).

Hallatschek, K.: An ultra-fast smoothing algorithm for time-frequency transforms based on Gabor functions. Applied and Computational Harmonic Analysis **36**, 158-166 (2014).

Hatch, D. R., Jenko, F., Bratanov, V., and Banon Navarro, A.: Phase space scales of free energy dissipation in gradient-driven gyrokinetic turbulence. Journal of Plasma Physics **80**, 531-551 (2014).

Havlickova, E., Fundamenski, W., Wischmeier, M., Fishpool, G., and Morris, A. W.: Investigation of conventional and Super-X divertor configurations of MAST Upgrade using scrape-off layer plasma simulation. Plasma Physics and Controlled Fusion **56**, 075008 (2014).

Havlickova, E., Wischmeier, M., and Fishpool, G.: Modelling the Effect of the Super-X Divertor in MAST Upgrade on Transition to Detachment and Distribution of Volumetric Power Losses. Contributions to Plasma Physics **54**, 448-453 (2014).

Helander, P.: Microstability of Magnetically Confined Electron-Positron Plasmas. Physical Review Letters **113**, 135003 (2014).

Helander, P.: Theory of plasma confinement in non-axisymmetric magnetic fields (Review Article). Reports on Progress in Physics **77**, 087001 (2014).

Hennig, C., Bluhm, T., Kühner, G., Laqua, H., Lewerentz, M., Müller, I., Pingel, S., Riemann, H., Schacht, J., Spring, A., Werner, A., and Wölk, A.: MobileCoDaC – A transportable control, data acquisition and communication infrastructure for Wendelstein 7-X. Fusion Engineering and Design **89**, 689-692 (2014).

Heyn, M. F., Ivanov, I. B., Kasilov, S. V., Kernbichler, W., Leitner, P., Nemov, V. V., Suttrop, W., and ASDEX Upgrade

Team: Quasilinear modelling of RMP interaction with a tokamak plasma: application to ASDEX Upgrade ELM mitigation experiments. Nuclear Fusion **54**, 064005 (2014).

Hirsch, M., Laqua, H. P., Hathiramani, D., Oosterbeek, J., Baldzuhn, J., Biedermann, C., Brand, H. v. d., Cardella, A., Erckmann, V., Jimenez, R., König, R., Köppen, M., Parquay, S., Zhang, D., and W7-X Team: The impact of microwave stray radiation to in-vessel diagnostic components. Fusion Reactor Diagnostics: Proceedings of the International Conference. (Eds.) G. Gorini, F. P. Orsitto, C. Sozzi, M. Tardocchi. AIP Conference Proceedings **1612**. American Institute of Physics, Melville, TN, 39 (2014).

Hoelzl, M., Huijsmans, G. T. A., Merkel, P., Atanasiu, C., Lackner, K., Nardon, E., Aleynikova, K., Liu, F., Strumberger, E., McAdams, R., Chapman, I., and Fil, A.: Non-linear Simulations of MHD Instabilities in Tokamaks Including Eddy Current Effects and Perspectives for the Extension to Halo Currents. Journal of Physics: Conference Series **561**, 012011 (2014).

Hofsäss, H., Zhang, K., and Mutzke, A.: Simulation of ion beam sputtering with SDTrimSP, TRIDYN and SRIM. Applied Surface Science **310**, 134-141 (2014).

Hu, Q., Yu, Q., and Hu, X.: Linear and nonlinear effect of sheared plasma flow on resistive tearing modes. Physics of Plasmas **21**, 122507 (2014).

Hu, Q., Yu, Q., Wang, N., Shi, P., Yi, B., Ding, Y., Rao, B., Chen, Z., Gao, L., Hu, X., Jin, H., Li, M., Li, J., Yu, K., Zhuang, G., and J-TEXT Team: Influence of rotating resonant magnetic perturbations on particle confinement. Nuclear Fusion **54**, 122006 (2014).

Hu, Q., Zhuang, G., Yu, Q., Rao, B., Gao, L., Wang, N., Jin, W., Yi, B., Zeng, W., Chen, W., Ding, Y., Chen, Z., Hu, X., and J-TEXT Team: Enhanced particle transport caused by resonant magnetic perturbations in the J-TEXT tokamak. Nuclear Fusion **54**, 064013 (2014).

Huang, J., Feng, Y., Wan, B., Liu, S., Chang, J., Wang, H., Gao, W., Zhang, L., Gao, W., Chen, Y., Wu, Z., Wu, C., and EAST Team: Implementation and first application of EMC3-EIRENE to EAST double-null divertor. Plasma Physics and Controlled Fusion **56**, 075023 (2014).

Igochine, V., Gude, A., Günter, S., Lackner, K., Yu, Q., Barrera Orte, L., Bogomolov, A., Classen, I., McDermott, R. M., Luhmann, N., and ASDEX Upgrade Team: Conversion of the dominantly ideal perturbations into a tearing mode after a sawtooth crash. Physics of Plasmas **21**, 110702 (2014).

Imrisek, M., Weinzettl, V., Mlynar, J., Odstrcil, T., Odstrcil, M., Ficker, O., Pinzon, J. R., Ehrlacher, C., Panek, R., and Hron, M.: Use of soft x-ray diagnostic on the COMPASS tokamak for investigations of sawteeth crash neighborhood and of plasma position using fast inversion methods. Review of Scientific Instruments **85**, 11E433 (2014).

Jacquet, P., Bobkov, V., Brezinsek, S., Brix, M., Campergue, A.-L., Colas, L., Czarnecka, A., Drewelow, P., Graham, M., Klepper, C. C., Lerche, E., Mayoral, M.-L., Meigs, A., Milanesio, D., Monakhov, I., Mlynar, J., Pütterich, T., Sirinelli, A., Van Eester, D., and JET-EFDA Contributors: ICRF heating in JET during initial operations with the ITER-like wall. Radio-frequency Power in Plasmas: Proceedings of the 20th Topical Conference. (Eds.) A. Tuccillo, S. Ceccuzzi. AIP Conference Proceedings **1580**. American Institute of Physics, Melville, TN, 65-72 (2014).

Jacquet, P., Bobkov, V., Colas, L., Czarnecka, A., Lerche, E., Mayoral, M.-L., Monakhov, I., Van-Eester, D., Arnoux, G., Brezinsek, S., Brix, M., Campergue, A.-L., Devaux, S., Drewelow, P., Graham, M., Klepper, C. C., Meigs, A., Milanesio, D., Mlynar, J., Pütterich, T., Sirinelli, A., and JET-EFDA Contributors: Ion cyclotron resonance frequency heating in JET during initial operations with the ITER-like wall. Physics of Plasmas **21**, 061510 (2014).

Jacquot, J., Milanesio, D., Colas, L., Corre, Y., Goniche, M., Gunn, J., Heuraux, S., and Kubič, M.: Radio-frequency sheaths physics: Experimental characterization on Tore Supra and related self-consistent modeling. Physics of Plasmas **21**, 061509 (2014).

Jaksic, N., Herrmann, A., and Greuner, H.: Transient Thermal and Structural Mechanics Investigation of the New Solid Tungsten Divertor Tile for Special Purposes at ASDEX Upgrade. IEEE Transactions on Plasma Science **42**, 1790-1795 (2014).

Jelonnek, J., Albajar, F., Alberti, S., Avramidis, K., Benin, P., Bonicelli, T., Cismondi, F., Erckmann, V., Gantenbein, G., Hesch, K., Hogge, J.-P., Illy, S., Ioannidis, Z. C., Jin, J., Laqua, H., Latsas, G. P., Legrand, F., Michel, G., Pagonakis, I. G., Piosczyk, B., Rozier, Y., Rzesnicki, T., Tigelis, I. G., Thumm, M., Tran, M. Q., and Vomvoridis, J. L.: From Series Production of Gyrotrons for W7-X toward EU-1 MW Gyrotrons for ITER. IEEE Transactions on Plasma Science **42**, 1135-1144 (2014).

Joffrin, E., Baruzzo, M., Beurskens, M., Bourdelle, C., Brezinsek, S., Bucalossi, J., Buratti, P., Calabro, G., Challis, C. D., Clever, M., Coenen, J., Delabie, E., Dux, R., Lomas, P., Luna, E. d. l., Vries, P. d., Flanagan, J., Frassinetti, L., Frigione, D., Giroud, C., Groth, M., Hawkes, N., Hobirk, J., Lehnen, M., Maddison, G., Mailloux, J., Maggi, C. F.,

Matthews, G., Mayoral, M., Meigs, A., Neu, R., Nunes, I., Pütterich, T., Rimini, F., Sertoli, M., Sieglin, B., Sips, A. C. C., Rooij, G. v., Voitsekhovitch, I., and JET-EFDA Contributors: First scenario development with the JET new ITER-like wall. Nuclear Fusion **54**, 013011 (2014).

Kang, K. S.: A Parallel Multigrid Solver on a Structured Triangulation of a Hexagonal Domain. Domain Decomposition Methods in Science and Engineering XXI. (Ed.) J. Erhel. Springer International Publishing, Cham, 789-797 (2014).

Kantor, M., Moseev, D., and Salewski, M.: On bias of kinetic temperature measurements in complex plasmas. Physics of Plasmas **21**, 023701 (2014).

Karhunen, J., Hakola, A., Likonen, J., Lissovski, A., Paris, P., Laan, M., Piip, K., Porosnicu, C., Lungu, C. P., and Sugiyama, K.: Development of laser-induced breakdown spectroscopy for analyzing deposited layers in ITER. Physica Scripta **T159**, 014067 (2014).

Kasilov, S. V., Kernbichler, W., Martitsch, A. F., Maaßberg, H., and Heyn, M. F.: Evaluation of the toroidal torque driven by external non-resonant non-axisymmetric magnetic field perturbations in a tokamak. Physics of Plasmas **21**, 092506 (2014).

Kawamura, G., Feng, Y., Kobayashi, M., Shoji, M., Morisaki, T., Masuzaki, S., and Tomita, Y.: First EMC3-EIRENE Simulations with Divertor Legs of LHD in Realistic Device Geometry. Contributions to Plasma Physics **54**, 437-441 (2014).

Kim, K., Na, Y.-S., Kim, H.-S., Maraschek, M., Park, Y. S., Stober, J., Terzolo, L., and Zohm, H.: Time-dependent simulations of feedback stabilization of neoclassical tearing modes in KSTAR plasmas. Fusion Engineering and Design **89**, 859-866 (2014).

Kiptily, V. G., Beaumont, P., Belli, F., Cecil, F. E., Conroy, S., Craciunescu, T., Garcia-Munoz, M., Curuia, M., Darrow, D., Ericsson, G., Fernandes, A. M., Giacomelli, L., Gorini, Murari, A., Nocente, M., Pereira, R. C., Perez Thun, C. v., Popovichev, S., Riva, M., Santala, M., Soare, S., Sousa, J., Syme, D. B., Tardocchi, M., Zoita, V. L., Chugunov, I. N., Gin, D. B., Khilkevich, E., Shevelev, A. E., Goloborod'ko, V., Sharapov, S. E., Voitsekhovitch, I., Yavorskij, V., and JET-EFDA Contributors: Fusion alpha-particle diagnostics for DT experiments on the joint European torus. Fusion Reactor Diagnostics: Proceedings of the International Conference. (Eds.) G. Gorini, F. P. Orsitto, C. Sozzi, M. Tardocchi. AIP Conference Proceedings **1612**. American Institute of Physics, Melville, TN, 87 (2014).

Kirk, A., Dunai, D., Dunne, M., Huijsmans, G., Pamela, S., Becoulet, M., Harrison, J. R., Hillesheim, J., Roach, C., and

Saarelma, S.: Recent progress in understanding the processes underlying the triggering of and energy loss associated with type I ELMs. Nuclear Fusion **54**, 114012 (2014).

Klämpfl, T. G., Shimizu, T., Koch, S., Balden, M., Gemein, S., Li, Y.-F., Mitra, A., Zimmermann, J. L., Gebel, J., Morfill, G. E., and Schmidt, H.-U.: Decontamination of Nosocomial Bacteria Including Clostridium Difficile Spores on Dry Inanimate Surface by Cold Atmospheric Plasma. Plasma Processes and Polymers **11**, 974-984 (2014).

Knie, A., Hans, A., Förstel, M., Hergenhahn, U., Schmidt, P., Reiß, P., Ozga, C., Kambs, B., Trinter, F., Voigtsberger, J., Metz, D., Jahnke, T., Dörner, R., Kuleff, A. I., Cederbaum, L. S., Demekhin, P. V., and Ehresmann, A.: Detecting ultrafast interatomic electronic processes in media by fluorescence. New Journal of Physics **16**, 102002 (2014). http://iopscience.iop.org/1367-2630/16/10/102002.

Kobayashi, T., Birkenmeier, G., Wolfrum, E., Laggner, F. M., Willensdorfer, M., Stroth, U., Inagaki, S., Itoh, S.-I., and Itoh, K.: Method for estimating the propagation direction of a coherent plasma structure using a one-dimensional diagnostic array. Review of Scientific Instruments **85**, 083507 (2014).

Kobayashi, M., Feng, Y., Yamada, I., Hayashi, H., and Kawamura, G.: Benchmark of Monte Carlo Scheme of EMC3 Dealing with Non-Uniform Cross-Field Transport Coefficients and Implementation in LHD. Contributions to Plasma Physics **54**, 383-387 (2014).

König, R., Biel, W., Biedermann, C., Burhenn, R., Cseh, G., Czarnecka, A., Endler, M., Estrada, T., Grulke, O., Hathiramani, D., Hirsch, M., Jablonski, S., Jakubowski, M., Kaczmarczyk, J., Kasparek, W., Kocsis, G., Kornejew, P., Krämer-Flecken, A., Krychowiak, M., Kubkowska, M., Langenberg, A., Laux, M., Liang, Y., Lorenz, A., Neubauer, O., Otte, M., Pablant, N., Pasch, E., Pedersen, T. S., Schmitz, O., Schneider, W., Schuhmacher, H., Schweer, B., Thomsen, H., Szepesi, T., Wiegel, B., Windisch, T., Wolf, S., Zhang, D., and Zoletnik, S.: Status of the diagnostics development for the first operation phase of the stellarator Wendelstein 7-X. Review of Scientific Instruments **85**, 11D818 (2014).

Kraus, W., Briefi, S., Fantz, U., Gutmann, P., and Doerfler, J.: Ways to improve the efficiency and reliability of radio frequency driven negative ion sources for fusion. Review of Scientific Instruments **85**, 02B309 (2014).

Kreter, A., Dittmar, T., Nishijima, D., Doerner, R. P., Baldwin, M. J., and Schmid, K.: Erosion, formation of deposited layers and fuel retention for beryllium under the influence of plasma impurities. Physica Scripta **T159**, 014039 (2014).

Landreman, M., Smith, H., Mollén, A., and Helander, P.: Comparison of particle trajectories and collision operators for collisional transport in nonaxisymmetric plasmas. Physics of Plasmas **21**, 042503 (2014).

Lang, P. T., Burckhart, A., Bernert, M., Casali, L., Fischer, R., Kardaun, O., Kocsis, G., Maraschek, M., Mlynek, A., Plöckl, B., Reich, M., Ryter, F., Schweinzer, J., Sieglin, B., Suttrop, W., Szepesi, T., Tardini, G., Wolfrum, E., Zasche, D., Zohm, H., and ASDEX Upgrade Team: ELM pacing and high-density operation using pellet injection in the ASDEX Upgrade all-metal-wall tokamak. Nuclear Fusion **54**, 083009 (2014).

Langer, G., Erdelyi, G., Csik, A., Tskhakaya, D., Coster, D., and Tökesi, K.: Interaction of low energy carbon ions with tungsten surface. Journal of Physics: Conference Series, **488**, 132009 (2014).

Laqua, H. P., Chlechowitz, E., Otte, M., and Stange, T.: Stochastic acceleration of relativistic electrons and plasma heating and current drive with 2 (2014).45 GHz frequency at the WEGA stellarator. Plasma Physics and Controlled Fusion **56**, 075022 (2014).

Lasa, A., Schmid, K., and Nordlund, K.: Modelling of W–Be mixed material sputtering under D irradiation. Physica Scripta **T159**, 014059 (2014).

Latu, G., Grandgirard, V., Abiteboul, J., Crouseilles, N., Dif-Pradalier, G., Garbet, X., Ghendrih, P., Mehrenberger, M., Sarazin, Y., and Sonnendrücker, E.: Improving conservation properties of a 5D gyrokinetic semi-Lagrangian code. The European Physical Journal D: Atomic, Molecular and Optical Physics **68**, 345 (2014).

Laux, M., Balden, M., and Siemroth, P.: Modification of arc emitted W particles in a model scrape-off layer plasma. Physica Scripta **T159**, 014026 (2014).

Leins, M., Kopecki, J., Gaiser, S., Schulz, A., Walker, M., Schumacher, U., Stroth, U., and Hirth, T.: Microwave Plasmas at Atmospheric Pressure. Contributions to Plasma Physics **54**, 14-26 (2014).

Lerche, E., Van Eester, D., Jacquet, P., Mayoral, M.-L., Bobkov, V., Colas, L., Czarnecka, A., Crombé, K., Monakhov, I., Rimini, F., Santala, M., and JET-EFDA Contributors: Impact of minority concentration on fundamental (H)D ICRF heating performance in JET-ILW. Nuclear Fusion **54**, 073006 (2014).

Lerche, E., Van Eester, D., Jacquet, P., Mayoral, M.-L., Bobkov, V., Colas, L., Czarnecka, A., Graham, M., Matthews, G.,

McCormick, K., Monakhov, I., Neu, R., Pütterich, T., Rimini, F., Vries, P. d., and JET-EFDA Contributors: Statistical comparison of ICRF and NBI heating performance in JET-ILW L-mode plasmas. Radiofrequency Power in Plasmas: Proceedings of the 20th Topical Conference. (Eds.) A. Tuccillo, S. Ceccuzzi. AIP Conference Proceedings **1580**. American Institute of Physics, Melville, TN, 235-238 (2014).

Lerche, E., Van Eester, D., Messiaen, A., Franke, T., and EFDA-PPPT Contributors: Fast wave current drive in DEMO. Radiofrequency Power in Plasmas: Proceedings of the 20th Topical Conference. (Eds.) A. Tuccillo, S. Ceccuzzi. AIP Conference Proceedings **1580**. American Institute of Physics, Melville, TN, 338-341 (2014).

Li, C., Boscary, J., Dekorsy, N., Junghanns, P., Mendelevitch, B., Peacock, A., Pirsch, H., Sellmeier, O., Springer, J., Stadler, R., and Streibl, B.: Production management and quality assurance for the fabrication of the In-vessel components of the stellarator Wendelstein 7-X. Fusion Engineering and Design **89**, 981-984 (2014).

Li, C., Greuner, H., Yuan, Y., Luo, G. N., Böswirth, B., Fu, B. Q., Xu, H. Y., Jia, Y. Z., and Liu, W.: Effects of temperature on surface modification of W exposed to He particles. Journal of Nuclear Materials **455**, 201-206 (2014).

Li, E., Igochine, V., Dumbrajs, O., Xu, L., Chen, K., Shi, T., and Hu, L.: The non-resonant kink modes triggering strong sawtooth-like crashes in the EAST tokamak. Plasma Physics and Controlled Fusion **56**, 125016 (2014).

Li, M., Werner, E., and You, J.-H.: Fracture mechanical analysis of tungsten armor failure of a water-cooled divertor target. Fusion Engineering and Design **89**, 2716-2725 (2014).

Linden, W. v. d., Dose, V., and Toussaint, U. v.: Basic definitions for frequentist statistics and Bayesian inference. Bayesian Probability Theory: Applications in the Physical Sciences. (Eds.) W. v. d. Linden, V. Dose, U. v. Toussaint. Cambridge University Press, Cambridge, 15-32 (2014).

Linden, W. v. d., Dose, V., and Toussaint, U. v.: Bayesian experimental design. Bayesian Probability Theory: Applications in the Physical Sciences. (Eds.) W. v. d. Linden, V. Dose, U. v. Toussaint. Cambridge University Press, Cambridge, 491-505 (2014).

Linden, W. v. d., Dose, V., and Toussaint, U. v.: Bayesian inference. Bayesian Probability Theory: Applications in the Physical Sciences. (Eds.) W. v. d. Linden, V. Dose, U. v. Toussaint. Cambridge University Press, Cambridge, 33-46 (2014).

Linden, W. v. d., Dose, V., and Toussaint, U. v.: Bayesian parameter estimation. Bayesian Probability Theory: Applications in the Physical Sciences. (Eds.) W. v. d. Linden, V. Dose, U. v. Toussaint. Cambridge University Press, Cambridge, 227-235 (2014).

Linden, W. v. d., Dose, V., and Toussaint, U. v. (Eds.): Bayesian Probability Theory: Applications in the Physical Sciences. Cambridge University Press, Cambridge, 649 p. (2014).

Linden, W. v. d., Dose, V., and Toussaint, U. v.: The Bayesian way. Bayesian Probability Theory: Applications in the Physical Sciences. (Eds.) W. v. d. Linden, V. Dose, U. v. Toussaint. Cambridge University Press, Cambridge, 255-275 (2014).

Linden, W. v. d., Dose, V., and Toussaint, U. v.: The central limit theorem. Bayesian Probability Theory: Applications in the Physical Sciences. (Eds.) W. v. d. Linden, V. Dose, U. v. Toussaint. Cambridge University Press, Cambridge, 139-146 (2014).

Linden, W. v. d., Dose, V., and Toussaint, U. v.: Change point problems. Bayesian Probability Theory: Applications in the Physical Sciences. (Eds.) W. v. d. Linden, V. Dose, U. v. Toussaint. Cambridge University Press, Cambridge, 409-430 (2014).

Linden, W. v. d., Dose, V., and Toussaint, U. v.: Combinatorics. Bayesian Probability Theory: Applications in the Physical Sciences. (Eds.) W. v. d. Linden, V. Dose, U. v. Toussaint. Cambridge University Press, Cambridge, 47-70 (2014).

Linden, W. v. d., Dose, V., and Toussaint, U. v.: Comparison of Bayesian and frequentist hypothesis tests. Bayesian Probability Theory: Applications in the Physical Sciences. (Eds.) W. v. d. Linden, V. Dose, U. v. Toussaint. Cambridge University Press, Cambridge, 324-330 (2014).

Linden, W. v. d., Dose, V., and Toussaint, U. v.: Consistent inference on inconsistent data. Bayesian Probability Theory: Applications in the Physical Sciences. (Eds.) W. v. d. Linden, V. Dose, U. v. Toussaint. Cambridge University Press, Cambridge, 364-395 (2014).

Linden, W. v. d., Dose, V., and Toussaint, U. v.: Continuous distributions. Bayesian Probability Theory: Applications in the Physical Sciences. (Eds.) W. v. d. Linden, V. Dose, U. v. Toussaint. Cambridge University Press, Cambridge, 92-138 (2014).

Linden, W. v. d., Dose, V., and Toussaint, U. v.: The Cramer-Rao inequality. Bayesian Probability Theory: Applications in the Physical Sciences. (Eds.) W. v. d. Linden, V. Dose, U. v. Toussaint. Cambridge University Press, Cambridge, 248-254 (2014).

Linden, W. v. d., Dose, V., and Toussaint, U. v.: Frequentist parameter estimation. Bayesian Probability Theory: Applications in the Physical Sciences. (Eds.) W. v. d. Linden, V. Dose, U. v. Toussaint. Cambridge University Press, Cambridge, 236-247 (2014).

Linden, W. v. d., Dose, V., and Toussaint, U. v.: The frequentist approach. Bayesian Probability Theory: Applications in the Physical Sciences. (Eds.) W. v. d. Linden, V. Dose, U. v. Toussaint. Cambridge University Press, Cambridge, 276-283 (2014).

Linden, W. v. d., Dose, V., and Toussaint, U. v.: Function estimation. Bayesian Probability Theory: Applications in the Physical Sciences. (Eds.) W. v. d. Linden, V. Dose, U. v. Toussaint. Cambridge University Press, Cambridge, 431-450 (2014).

Linden, W. v. d., Dose, V., and Toussaint, U. v.: Global smoothness. Bayesian Probability Theory: Applications in the Physical Sciences. (Eds.) W. v. d. Linden, V. Dose, U. v. Toussaint. Cambridge University Press, Cambridge, 215-223 (2014).

Linden, W. v. d., Dose, V., and Toussaint, U. v.: Integral equations. Bayesian Probability Theory: Applications in the Physical Sciences. (Eds.) W. v. d. Linden, V. Dose, U. v. Toussaint. Cambridge University Press, Cambridge, 451-469 (2014).

Linden, W. v. d., Dose, V., and Toussaint, U. v.: Limit theorems. Bayesian Probability Theory: Applications in the Physical Sciences. (Eds.) W. v. d. Linden, V. Dose, U. v. Toussaint. Cambridge University Press, Cambridge, 83-91 (2014).

Linden, W. v. d., Dose, V., and Toussaint, U. v.: Mathematical compendium. Bayesian Probability Theory: Applications in the Physical Sciences. (Eds.) W. v. d. Linden, V. Dose, U. v. Toussaint. Cambridge University Press, Cambridge, 595-610 (2014).

Linden, W. v. d., Dose, V., and Toussaint, U. v.: The meaning of 'probability'. Bayesian Probability Theory: Applications in the Physical Sciences. (Eds.) W. v. d. Linden, V. Dose, U. v. Toussaint. Cambridge University Press, Cambridge, 3-14 (2014).

Linden, W. v. d., Dose, V., and Toussaint, U. v.: Model selection. Bayesian Probability Theory: Applications in the Physical Sciences. (Eds.) W. v. d. Linden, V. Dose, U. v. Toussaint. Cambridge University Press, Cambridge, 470-490 (2014).

Linden, W. v. d., Dose, V., and Toussaint, U. v.: Monte Carlo methods. Bayesian Probability Theory: Applications in the Physical Sciences. (Eds.) W. v. d. Linden, V. Dose, U. v. Toussaint. Cambridge University Press, Cambridge, 537-571 (2014).

Linden, W. v. d., Dose, V., and Toussaint, U. v.: Nested sampling. Bayesian Probability Theory: Applications in the Physical

Sciences. (Eds.) W. v. d. Linden, V. Dose, U. v. Toussaint. Cambridge University Press, Cambridge, 572-594 (2014).

Linden, W. v. d., Dose, V., and Toussaint, U. v.: Numerical integration. Bayesian Probability Theory: Applications in the Physical Sciences. (Eds.) W. v. d. Linden, V. Dose, U. v. Toussaint. Cambridge University Press, Cambridge, 509-536 (2014).

Linden, W. v. d., Dose, V., and Toussaint, U. v.: Poisson processes and waiting times. Bayesian Probability Theory: Applications in the Physical Sciences. (Eds.) W. v. d. Linden, V. Dose, U. v. Toussaint. Cambridge University Press, Cambridge, 147-164 (2014).

Linden, W. v. d., Dose, V., and Toussaint, U. v.: Prior probabilities by transformation invariance. Bayesian Probability Theory: Applications in the Physical Sciences. (Eds.) W. v. d. Linden, V. Dose, U. v. Toussaint. Cambridge University Press, Cambridge, 165-177 (2014).

Linden, W. v. d., Dose, V., and Toussaint, U. v.: Quantified maximum entropy. Bayesian Probability Theory: Applications in the Physical Sciences. (Eds.) W. v. d. Linden, V. Dose, U. v. Toussaint. Cambridge University Press, Cambridge, 201-214 (2014).

Linden, W. v. d., Dose, V., and Toussaint, U. v.: Random walks. Bayesian Probability Theory: Applications in the Physical Sciences. (Eds.) W. v. d. Linden, V. Dose, U. v. Toussaint. Cambridge University Press, Cambridge, 71-82 (2014).

Linden, W. v. d., Dose, V., and Toussaint, U. v.: Regression. Bayesian Probability Theory: Applications in the Physical Sciences. (Eds.) W. v. d. Linden, V. Dose, U. v. Toussaint. Cambridge University Press, Cambridge, 333-363 (2014).

Linden, W. v. d., Dose, V., and Toussaint, U. v.: Sampling distributions and common hypothesis tests. Bayesian Probability Theory: Applications in the Physical Sciences. (Eds.) W. v. d. Linden, V. Dose, U. v. Toussaint. Cambridge University Press, Cambridge, 284-323 (2014).

Linden, W. v. d., Dose, V., and Toussaint, U. v.: Selected proofs and derivations. Bayesian Probability Theory: Applications in the Physical Sciences. (Eds.) W. v. d. Linden, V. Dose, U. v. Toussaint. Cambridge University Press, Cambridge, 611-618 (2014).

Linden, W. v. d., Dose, V., and Toussaint, U. v.: Testable information and maximum entropy. Bayesian Probability Theory: Applications in the Physical Sciences. (Eds.) W. v. d. Linden, V. Dose, U. v. Toussaint. Cambridge University Press, Cambridge, 178-200 (2014).

Linden, W. v. d., Dose, V., and Toussaint, U. v.: Unrecognized signal contributions. Bayesian Probability Theory: Applications in the Physical Sciences. (Eds.) W. v. d. Linden, V. Dose, U. v. Toussaint. Cambridge University Press, Cambridge, 396-408 (2014).

Loarte, A., Koechl, F., Leyland, M. J., Polevoi, A., Beurskens, M., Parail, V., Nunes, I., Saibene, G. R., Sartori, R. I. A., and JET EFDA Contributors: Evolution of plasma parameters in the termination phase of high confinement H-modes at JET and implications for ITER. Nuclear Fusion **54**, 123014 (2014).

Lore, J. D., Andreeva, T., Boscary, J., Bozhenkov, S., Geiger, J., Harris, J. H., Hölbe, H., Lumsdaine, A., McGinnis, D., Peacock, A., and Tipton, J.: Design and Analysis of Divertor Scraper Elements for the W7-X Stellarator. IEEE Transactions on Plasma Science **42**, 539-544 (2014).

Luce, T. C., Challis, C. D., Ide, S., Joffrin, E., Kamada, Y., Politzer, P. A., Schweinzer, J., Sips, A. C. C., Stober, J., and ASDEX Upgrade Team: Development of advanced inductive scenarios for ITER. Nuclear Fusion **54**, 013015 (2014).

Lumsdaine, A., Boscary, J., Clark, E., Ekici, K., Harris, J., McGinnis, D., Lore, J. D., Peacock, A., Tipton, J., and Tretter, J.: Modeling and Analysis of the W7-X High Heat-Flux Divertor Scraper Element. IEEE Transactions on Plasma Science **42**, 545-551 (2014).

Lunt, T., Canal, G. P., Feng, Y., Reimerdes, H., Duval, B. P., Labit, B., Vijvers, W. A. J., Coster, D., Lackner, K., and Wischmeier, M.: First EMC3-Eirene simulations of the TCV snowflake divertor. Plasma Physics and Controlled Fusion **56**, 035009 (2014).

Lyssoivan, A., Van Eester, D., Wauters, T., Bobkov, V., Vervier, M., Douai, D., Kogut, D., Kreter, A., Moiseenko, V., Möller, S., Noterdaeme, J.-M., Philipps, V., Rohde, V., Schneider, P., Sergienko, G., Van Schoor, M., TEXTOR Team, and ASDEX Upgrade Team: RF physics of ICWC discharge at high cyclotron harmonics. Radiofrequency Power in Plasmas: Proceedings of the 20th Topical Conference. (Eds.) A. Tuccillo, S. Ceccuzzi. AIP Conference Proceedings **1580**. American Institute of Physics, Melville, TN, 287-290 (2014).

Ma, R., Chavdarovski, I., Ye, G., and Wang, X.: Linear dispersion relation of beta-induced Alfvén eigenmodes in presence of anisotropic energetic ions. Physics of Plasmas **21**, 062120 (2014).

Madaule, E., Restelli, M., and Sonnendrücker, E.: Energy conserving discontinuous Galerkin spectral element method for the Vlasov-Poisson system. Journal of Computational Physics **279**, 261-288 (2014).

Maddison, G. P., Giroud, C., Alper, B., Arnoux, G., Balboa, I., Beurskens, M. N. A., Boboc, A., Brezinsek, S., Brix, M., Clever, M., Coelho, R., Coenen, J. W., Coffey, I., Silva Aresta Belo, P. C. d., Devaux, S., Devynck, P., Eich, T., Felton, R. C., Flanagan, J., Frassinetti, L., Garzotti, L., Groth, M., Jachmich, S., Järvinen, A., Joffrin, E., Kempenaars, M. A. H., Kruezi, U., Lawson, K. D., Lehnen, M., Leyland, M. J., Liu, Y., Lomas, P. J., Lowry, C. G., Marsen, S., Matthews, G. F., McCormick, K., Meigs, A. G., Morris, A. W., Neu, R., Nunes, I. M., Oberkofler, M., Rimini, F. G., Saarelma, S., Sieglin, B., Sips, A. C. C., Sirinelli, A., Stamp, M. F., Rooij, G. J. v., Ward, D. J., Wischmeier, M., and JET EFDA Contributors: Contrasting H-mode behaviour with deuterium fuelling and nitrogen seeding in the all-carbon and metallic versions of JET. Nuclear Fusion **54**, 073016 (2014).

Maggi, C. F., Delabie, E., Biewer, T. M., Groth, M., Hawkes, N. C., Lehnen, M., Luna, E. d. l., McCormick, K., Reux, C., Rimini, F., Solano, E. R., Andrew, Y., Bourdelle, C., Bobkov, V., Brix, M., Calabro, G., Czarnecka, A., Flanagan, J., Lerche, E., Marsen, S., Nunes, I., Van Eester, D., Stamp, M. F., and JET EFDA Contributors: L–H power threshold studies in JET with Be/W and C wall. Nuclear Fusion **54**, 023007 (2014).

Maier, H., Greuner, H., Balden, M., Böswirth, B., Elgeti [Lindig], S., Toussaint, U. v., and Linsmeier, C.: Tungsten erosion under combined hydrogen/helium high heat flux loading. Physica Scripta **T159**, 014019 (2014).

Manz, P., Boom, J. E., Wolfrum, E., Birkenmeier, G., Classen, I. G. J., Luhmann Jr, N. C., Stroth, U., and ASDEX Upgrade Team: Velocimetry analysis of type-I edge localized mode precursors in ASDEX Upgrade. Plasma Physics and Controlled Fusion **56**, 035010 (2014).

Marek, A., Blum, V., Johanni, R., Havu, V., Lang, B., Auckenthaler, T., Heinecke, A., Bungartz, H.-J., and Lederer, H.: The ELPA library: scalable parallel eigenvalue solutions for electronic structure theory and computational science. Journal of Physics: Condensed Matter **26**, 213201 (2014).

Marek, A., Rampp, M., Hanke, F., and Janka, H.-T.: Towards Petaflops Capability of the VERTEX Supernova Code. Parallel Computing: Accelerating Computational Science and Engineering (CSE). (Eds.) G. Bader, A. Bode, H.-J. Bungartz et al. Advances in Parallel Computing **25**. IOS Press, Amsterdam, 712-721 (2014).

Markelj, S., Ogorodnikova, O., Pelicon, P., Schwarz-Selinger, T., Vavpetic, P., and Cadez, I.: In situ nuclear reaction analysis of D retention in undamaged and self-damaged tungsten under atomic D exposure. Physica Scripta **T159**, 014047 (2014).

Markina, E., Mayer, M., Elgeti [Lindig], S., and Schwarz-Selinger, T.: Influence of MeV helium implantation on deu-terium retention in self-ion implanted tungsten. Physica Scripta **T159**, 014045 (2014).

Martone, M.: Efficient multithreaded untransposed, transposed or symmetric sparse matrix–vector multiplication with the Recursive Sparse Blocks format. Parallel Computing **40**, 251-270 (2014).

Marushchenko, N. B., Erckmann, V., Beidler, C. D., Geiger, J., Laqua, H., Helander, P., Maaßberg, H., and Turkin, Y.: Selective ECR heating of trapped/passing electrons in the W7-X stellarator. Radiofrequency Power in Plasmas: Proceedings of the 20th Topical Conference. (Eds.) A. Tuccillo, S. Ceccuzzi. AIP Conference Proceedings **1580**. American Institute of Physics, Melville, TN, 518-521 (2014).

Marushchenko, N. B., Turkin, Y., and Maaßberg, H.: Ray-tracing code TRAVIS for ECR heating, EC current drive and ECE diagnostic. Computer Physics Communications **185**, 165-176 (2014).

Matthews, G. F., Brezinsek, S., Chapman, I., Hobirk, J., Horton, L. D., Maggi, C. F., Nunes, I., Rimini, F. G., Sips, G., Vries, P. d., and EFDA-JET Contributors: The second phase of JET operation with the ITER-like wall. Physica Scripta **T159**, 014015 (2014).

Matveev, D., Kirschner, A., Schmid, K., Litnovsky, A., Borodin, D., Komm, M., Van Oost, G., and Samm, U.: Estimation of the contribution of gaps to tritium retention in the divertor of ITER. Physica Scripta **T159**, 014063 (2014).

Mavridis, M., Isliker, H., Vlahos, L., Görler, T., Jenko, F., and Told, D.: A study of self organized criticality in ion temperature gradient mode driven gyrokinetic turbulence. Physics of Plasmas **21**, 102312 (2014).

Mayer, M.: Improved physics in SIMNRA 7 (2014). Nuclear Instruments and Methods in Physics Research Section B: Beam Interactions with Materials and Atoms **332**, 176-180 (2014).

Mayoral, M.-L., Bobkov, V., Czarnecka, A., Day, I., Ekedahl, A., Jacquet, P., Goniche, M., King, R., Kirov, K., Lerche, E., Mailloux, J., Van Eester, D., Asunta, O., Challis, C., Ciric, D., Coenen, J. W., Colas, L., Giroud, C., Graham, M., Jenkins, I., Joffrin, E., Jones, T., King, D., Kiptily, V., Klepper, C. C., Maggi, C., Maggiora, R., Marcotte, F., Matthews, G., Milanesio, D., Monakhov, I., Nightingale, M., Neu, R., Ongena, J., Pütterich, T., Riccardo, V., Rimini, F., Strachan, J., Surrey, E., Thompson, V., Rooij, G. v., and JET EFDA Contributors: On the challenge of plasma heating with the JET metallic wall. Nuclear Fusion **54**, 033002 (2014).

Mayoral, M.-L., Pütterich, T., Jacquet, P., Lerche, E., Van Eester, D., Bobkov, V., Bourdelle, C., Colas, L., Czarnecka, A.,

Mlynar, J., Neu, R., and JET-EFDA Contributors: Comparison of ICRF and NBI heated plasmas performance in the JET ITER-like wall. Radiofrequency Power in Plasmas: Proceedings of the 20th Topical Conference. (Eds.) A. Tuccillo, S. Ceccuzzi. AIP Conference Proceedings **1580**. American Institute of Physics, Melville, TN, 231-234 (2014).

McDermott, R. M., Angioni, C., Conway, G. D., Dux, R., Fable, E., Fischer, R., Pütterich, T., Ryter, F., Viezzer, E., and ASDEX Upgrade Team: Core intrinsic rotation behaviour in ASDEX Upgrade ohmic L-mode plasmas. Nuclear Fusion **54**, 043009 (2014).

Mehlmann, F., Costea, S., Schrittwieser, R., Naulin, V., Rasmussen, J. J., Müller, H. W., Nielsen, A. H., Carralero, D., Rohde, V., Lux, C., Ionita, C., and ASDEX Upgrade Team: Electric Probe Measurements of the Poloidal Velocity in the Scrape-off Layer of ASDEX Upgrade. Contributions to Plasma Physics **54**, 273-278 (2014).

Meisl, G., Schmid, K., Encke, O., Höschen, C., Gao, L., and Linsmeier, C.: Implantation and erosion of nitrogen in tungsten. New Journal of Physics **16**, 093018 (2014). http://iopscience.iop.org/1367-2630/16/9/093018.

Meister, H., and Kalvin, S.: Optimisation of design parameters for collimators and pin-holes of bolometer cameras. Fusion Engineering and Design **89**, 3039-3045 (2014).

Menmuir, S., Giroud, C., Biewer, T. M., Coffey, I. H., Delabie, E., Hawkes, N. C., Sertoli, M., and JET EFDA Contributors: Carbon charge exchange analysis in the ITER-like wall environment. Review of Scientific Instruments **85**, 11E412 (2014).

Meyer-Spasche, R.: Cosmopolitan Oscar Buneman (1913-1993): his serpentine path from Milan to Stanford. Almagest **5**, 26-39 (2014).

Miettunen, J., Airila, M. I., Makkonen, T., Groth, M., Lindholm, V., Björkas, C., Hakola, A., Müller, H. W., and ASDEX Upgrade Team: Dissociation of methane and nitrogen molecules and global transport of tracer impurities in an ASDEX Upgrade L-mode plasma. Plasma Physics and Controlled Fusion **56**, 095029 (2014).

Mikhailov, M. I., Nührenberg, J., and Zille, R.: Near-magnetic-axis geometry of a closely quasi-isodynamic stellarator. Plasma Physics Reports **40**, 83-87 (2014).

Mikhailov, M. I., Shchepetov, S. V., Drevlak, M., Nührenberg, C., and Nührenberg, J.: Stability of Global Magnetohydrodynamic Modes in the L-5 Compact Torsatron. Plasma Physics Reports **40**, 781-789 (2014).

Milligen, B. P. v., Birkenmeier, G., Ramisch, M., Estrada, T., Hidalgo, C., and Alonso, A.: Causality detection and turbulence in fusion plasmas. Nuclear Fusion **54**, 023011 (2014).

Mishchenko, A., Cole, M., Kleiber, R., and Könies, A.: New variables for gyrokinetic electromagnetic simulations. Physics of Plasmas **21**, 052113 (2014).

Mishchenko, A., Könies, A., Feher, T., Kleiber, R., Borchardt, M., Riemann, J., Hatzky, R., Geiger, J., and Turkin, Y.: Global hybrid-gyrokinetic simulations of fast-particle effects on Alfvén Eigenmodes in stellarators. Nuclear Fusion **54**, 104003 (2014).

Mishchenko, A., Könies, A., and Hatzky, R.: Gyrokinetic particle-in-cell simulations of Alfvén eigenmodes in presence of continuum effects. Physics of Plasmas **21**, 052114 (2014).

Mishchenko, A., Könies, A., Kleiber, R., and Cole, M.: Pullback transformation in gyrokinetic electromagnetic simulations. Physics of Plasmas **21**, 092110 (2014).

Missal, B., Leher, F., Schiller, T., Friedrich, P., and Capriccioli, A.: Pendulum support of the W7-X plasma vessel: Design, tests, manufacturing, assembly, critical aspects, status. Fusion Engineering and Design **89**, 1820-1825 (2014).

Mlynek, A., Casali, L., Ford, O., Eixenberger, H., and ASDEX Upgrade Team: Fringe jump analysis and implementation of polarimetry on the ASDEX Upgrade DCN interferometer. Review of Scientific Instruments **85**, 11D408 (2014).

Mochalskyy, S., Wünderlich, D., Ruf, B., Fantz, U., Franzen, P., and Minea, T.: On the meniscus formation and the negative hydrogen ion extraction from ITER neutral beam injection relevant ion source. Plasma Physics and Controlled Fusion **56**, 105001 (2014).

Mochalskyy, S., Wünderlich, D., Ruf, B., Franzen, P., Fantz, U., and Minea, T.: 3D numerical simulations of negative hydrogen ion extraction using realistic plasma parameters, geometry of the extraction aperture and full 3D magnetic field map. Review of Scientific Instruments **85**, 02B301 (2014).

Mollen, A., Landreman, M., and Smith, H. M.: On collisional impurity transport in nonaxisymmetric plasmas. Journal of Physics: Conference Series **561**, 012012 (2014).

Morita, S., Wang, E. H., Kobayashi, M., Dong, C. F., Oishi, T., Feng, Y., Goto, M., Huang, X. L., Masuzaki, S., Murakami, I., Suzuki, Y., Watanabe, T., and LHD Experiment Group: Two-dimensional study of edge impurity transport in the Large Helical Device. Plasma Physics and Controlled Fusion **56**, 094007 (2014).

Müller, H. W., Carralero, D., Birkenmeier, G., Conway, G. D., Fischer, R., Happel, T., Manz, P., Suttrop, W., Wolfrum, E., and ASDEX Upgrade Team: Characterization of Scrape-off Layer Turbulence Changes Induced by a Non-axisymmetric Magnetic Perturbation in an ASDEX Upgrade Low Density L-mode. Contributions to Plasma Physics **54**, 261-266 (2014).

Müller, S. H., Conway, G. D., Birkenmeier, G., Carralero, D., Happel, T., Herrmann, A., Manz, P., Marné, P. d., Mlynek, A., Müller, H. W., Potzel, S., Rohde, V., Stroth, U., Tsalas, M., Tynan, G. R., Wolfrum, E., and ASDEX Upgrade Team: Direct observations of L-I-H and H-I-L transitions with the X-point reciprocating probe in ASDEX Upgrade. Physics of Plasmas **21**, 042301 (2014).

Murari, A., Gelfusa, M., Peluso, E., Gaudio, P., Mazon, D., Hawkes, N., Point, G., Alper, B., Eich, T., and JET-EFDA Contributors: Improved equilibrium reconstructions by advanced statistical weighting of the internal magnetic measurements. Review of Scientific Instruments **85**, 123507 (2014).

Mynick, H., Xanthopoulos, P., Faber, B., Lucia, M., Rorvig, M., and Talmadge, J. N.: Turbulent optimization of toroidal configurations. Plasma Physics and Controlled Fusion **56**, 094001 (2014).

Neu, R., Brezinsek, S., Beurskens, M., Bobkov, V., Vries, P. d., Giroud, C., Joffrin, E., Kallenbach, A., Matthews, G. F., Mayoral, M.-L., Pautasso, G., Pütterich, T., Ryter, F., Schweinzer, J., ASDEX Upgrade Team, and JET EFDA Contributors: Experiences with Tungsten Plasma Facing Components in ASDEX Upgrade and JET. IEEE Transactions on Plasma Science **42**, 552-562 (2014).

Nocentini, R., Fantz, U., Franzen, P., Fröschle, M., Heinemann, B., Riedl, R., and NNBI-Team: Toward a Large RF Ion Source for the ITER Neutral Beam Injector: Overview of the ELISE Test Facility and First Results. IEEE Transactions on Plasma Science **42**, 616-623 (2014).

Nold, B., Manz, P., Ribeiro, T., Fuchert, G., Birkenmeier, G., Müller, H. W., Ramisch, M., Scott, B. D., and Stroth, U.: Turbulent transport across shear layers of magnetically confined plasmas. Physics of Plasmas **21**, 102304 (2014).

Nornberg, M. D., Taylor, N. Z., Forest, C. B., Rahbarnia, K., and Kaplan, E.: Optimization of magnetic amplification by flow constraints in turbulent liquid sodium. Physics of Plasmas **21**, 055903 (2014).

Norscini, C., Ghendrih, P., Cartier-Michaud, T., Dif-Pradalier, G., Milelli, D., Sarazin, Y., Abiteboul, J., Estève, D., Garbet, X., Grandgirard, V., and Latu, G.: Turbulent transport close to mar-ginal instability: role of the source driving the system out of equilibrium. Journal of Physics: Conference Series **561**, 012013 (2014).

Noterdaeme, J.-M.: Introduction to the Physics and Technology of Radio-frequency Heating and Current Drive. Fusion Science and Technology **65**, 164-165 (2014).

Odstrcil, M., Mlynar, J., Weinzettl, V., Hacek, P., Odstrcil, T., Verdoolaege, G., Berta, M., Szabolics, T., and Bencze, A.: Plasma tomographic reconstruction from tangentially viewing camera with background subtraction. Review of Scientific Instruments **85**, 013509 (2014).

Ogorodnikova, O. V., Gasparyan, Y., Efimov, V., Ciupiński, Ł., and Grzonka, J.: Annealing of radiation-induced damage in tungsten under and after irradiation with 20 MeV self-ions. Journal of Nuclear Materials **451**, 379-386 (2014).

Ongena, J., Messiaen, A., Dumortier, P., Durodie, F., Kazakov, Y. O., Louche, F., Schweer, B., Vervier, M., Van Eester, D., Koch, R., Krivska, A., Lyssoivan, A., Van Schoor, M., Wauters, T., Borsuk, V., Neubauer, O., Schmitz, O., Offermans, G., Altenburg, Y., Baylard, C., Birus, D., Bozhenkov, S., Hartmann, D. A., Kallmeyer, J., Renard, S., and Wolf, R.: The dedicated ICRH system for the stellarator Wendelstein 7-X. Radiofrequency Power in Plasmas: Proceedings of the 20th Topical Conference. (Eds.) A. Tuccillo, S. Ceccuzzi. AIP Conference Proceedings **1580**. American Institute of Physics, Melville, TN, 105-112 (2014).

Ongena, J., Messiaen, A., Van Ester, D., Schweer, B., Dumortier, P., Durodie, F., Kazakov, Y. O., Louche, F., Vervier, M., Koch, R., Krivska, A., Lyssoivan, A., Van Schoor, M., Wauters, T., Borsuk, V., Neubauer, O., Schmitz, O., Offermans, G., Altenburg, Y., Baylard, C., Birus, D., Bozhenkov, S., Hartmann, D., Kallmeyer, J., Renard, S., Wolf, R. C., and Fülöp, T.: Study and design of the ion cyclotron resonance heating system for the stellarator Wendelstein 7-X. Physics of Plasmas **21**, 061514 (2014).

Orozco, G., Fröschle, M., Heinemann, B., Hopf, C., Nocentini, R., Riedl, R., and Stäbler, A.: AC operation of large titanium sublimation pumps in a magnetic field: results of the test stand for the W7-X neutral beam injectors. Fusion Engineering and Design **89**, 3070-3077 (2014).

Paneta, V., Axiotis, M., Gastis, P., Kokkoris, M., Kontos, A., Lagoyannis, A., Mayer, M., Misaelides, P., Perdikakis, G., and Vlastou, R.: Determination and theoretical analysis of the differential cross sections of the ^{2}H(d,p) reaction at energies and detection angles suitable for NRA (Nuclear Reaction Analysis). EPJ Web of Conferences **66**, 10009 (2014). http://dx.doi.org/10.1051/epjconf/20146610009.

Peacock, A., Boscary, J., Czerwinski, M., Ehrke, G., Greuner, H., Junghanns, P., Mendelevitch, B., Smirnow, M., Stadler, R., Tittes, H., and Tretter, J.: Status of High Heat Flux Components at W7-X. IEEE Transactions on Plasma Science **42**, 542-532 (2014).

Peeper, K., Moser, M., Reichart, P., Markina, E., Elgeti [Lindig], S., Balden, M., Schwarz-Selinger, T., Mayer, M., and Dollinger, G.: Three-dimensional microscopy of deuterium in tungsten. Physica Scripta **T159**, 014070 (2014).

Peng, X. B., Hirsch, M., Köppen, M., Fellinger, J., Bykov, V., Schauer, F., and Vliegenthart, W.: Thermo-mechanical behavior of retro-reflector and resulting parallelism error of laser beams for Wendelstein 7-X interferometer. Fusion Engineering and Design **89**, 318-323 (2014).

Penzel, F., Meister, H., Bernert, M., Sehmer, T., Trautmann, T., Kannamüller, M., Koll, J., Koch, A. W., and ASDEX Upgrade Team: Automated in situ line of sight calibration of ASDEX Upgrade bolometers. Fusion Engineering and Design **89**, 2262-2267 (2014).

Petersson, P., Rubel, M., Possnert, G., Brezinsek, S., Kreter, A., Möller, S., Hakola, A., Mayer, M., Miettunen, J., Airila, M. I., Makkonen, T., Neu, R., Rohde, V., and ASDEX Upgrade Team: Overview of nitrogen-15 application as a tracer gas for material migration and retention studies in tokamaks. Physica Scripta **T159**, 014042 (2014).

Pflüger, D., Bungartz, H.-J., Griebel, M., Jenko, F., Dannert, T., Heene, M., Kowitz, C., Parra-Hinojosa, A., and Zaspel, P.: EXAHD: An Exa-scalable Two-Level Sparse Grid Approach for Higher-Dimensional Problems in Plasma Physics and Beyond. Euro-Par 2014: Parallel Processing Workshops. (Eds.) L. Lopes, J. Žilinskas, A. Costan. Springer International Publishing, Cham, 565-576 (2014).

Pinto, M. C., Jund, S., Salmon, S., and Sonnendrücker, E.: Charge-conserving FEM–PIC schemes on general grids. Comptes Rendus Mécanique **342**, 570-582 (2014).

Plunk, G., Helander, P., Xanthopoulos, P., and Connor, J. W.: Collisionless microinstabilities in stellarators. III. The ion-temperature-gradient mode. Physics of Plasmas **21**, 032112 (2014).

Potzel, S., Dux, R., Müller, H. W., Scarabosio, A., Wischmeier, M., and ASDEX Upgrade Team: Electron density determination in the divertor volume of ASDEX Upgrade via Stark broadening of the Balmer lines. Plasma Physics and Controlled Fusion **56**, 025010 (2014).

Potzel, S., Wischmeier, M., Bernert, M., Dux, R., Müller, H. W., Scarabosio, A., and ASDEX Upgrade Team: A new experimental classification of divertor detachment in ASDEX Upgrade. Nuclear Fusion **54**, 013001 (2014).

Preuss, R., and Toussaint, U. v.: Prediction of plasma simulation data with the Gaussian process method. Bayesian Inference and Maximum Entropy Methods in Science and Engineering: Proceedings of the 33rd International Workshop on Bayesian Inference and Maximum Entropy Methods in Science and Engineering (MaxEnt 2013). (Eds.) R. K. Niven, B. Brewer, D. Paull et al. AIP Conference Proceedings **1636**. American Institute of Physics, Melville, TN, 118 (2014).

Preynas, M., Goniche, M., Hillairet, J., Litaudon, X., and Ekedahl, A.: Experimental characterization and modeling of non-linear coupling of the LHCD power on Tore Supra. Radiofrequency Power in Plasmas: Proceedings of the 20th Topical Conference. (Eds.) A. Tuccillo, S. Ceccuzzi. AIP Conference Proceedings **1580**. American Institute of Physics, Melville, TN, 418-421 (2014).

Preynas, M., Laqua, H. P., Otte, M., Stange, T., Wauters, T., and Assmus, D.: Study of plasma start-up initiated by second harmonic electron cyclotron resonance heating on WEGA experiment. Radiofrequency Power in Plasmas: Proceedings of the 20th Topical Conference. (Eds.) A. Tuccillo, S. Ceccuzzi. AIP Conference Proceedings **1580**. American Institute of Physics, Melville, TN, 498-501 (2014).

Pueschel, M. J., Told, D., Terry, P. W., Jenko, F., Zweibel, E. G., Zhdankin, V., and Lesch, H.: Magnetic Reconnection Turbulence in Strong Guide Fields: Basic Properties and Application to Coronal Heating. The Astrophysical Journal Supplement Series **213** : 30 (2014).

Qin, C. M., Braun, F., Zhao, Y. P., Wan, B. N., Li, J., Zhang, X. J., Yang, Q. X., Yuan, S., Noterdaeme, J.-M., Kasahara, H., and ICRF Team on EAST: A new radiation stripline ICRF antenna design for EAST tokamak. Radiofrequency Power in Plasmas: Proceedings of the 20th Topical Conference. (Eds.) A. Tuccillo, S. Ceccuzzi. AIP Conference Proceedings **1580**. American Institute of Physics, Melville, TN, 346-349 (2014).

Rack, M., Sieglin, B., Eich, T., Pearson, J., Liang, Y., Balboa, I., Jachmich, S., Wingen, A., Pamela, S. J. P., and JET EFDA Contributors: Findings of pre-ELM structures through the observation of divertor heat load patterns at JET with applied n=2 perturbation fields (Letter). Nuclear Fusion **54**, 072004 (2014).

Rack, M., Sieglin, B., Pearson, J., Eich, T., Liang, Y., Denner, P., Wingen, A., Zeng, L., Balboa, I., Jachmich, S., and JET-EFDA Contributors: Modified heat load deposition of the ELM crash due to n=2 perturbation fields at JET. Nuclear Fusion **54**, 064012 (2014).

Rapson, C., Carvalho, P., Lüddecke, K., Neto, A., Santos, B., Treutterer, W., Winter, A., and Zehetbauer, T.: Coupling DCS and MARTe: two real-time control frameworks in collaboration. Fusion Engineering and Design **89**, 3125-3130 (2014).

Rapson, C., Giannone, L., Maraschek, M., Reich, M., Stober, J., Treutterer, W., and ASDEX Upgrade Team: Amplitude based feedback control for NTM stabilisation at ASDEX Upgrade. Fusion Engineering and Design **89**, 568-571 (2014).

Rapson, C., Grulke, O., Matyash, K., and Klinger, T.: The effect of boundaries on the ion acoustic beam-plasma instability in experiment and simulation. Physics of Plasmas **21**, 052103 (2014).

Rasmussen, J., Nielsen, S. K., Stejner, M., Salewski, M., Jacobsen, A. S., Korsholm, S. B., Leipold, F., Meo, F., Michelsen, P. K., Moseev, D., Schubert, M., Stober, J., Tardini, G, Wagner, D., and ASDEX Upgrade Team: Improved Collective Thomson Scattering measurements of fast ions at ASDEX upgrade. Fusion Reactor Diagnostics: Proceedings of the International Conference. (Eds.) G. Gorini, F. P. Orsitto, C. Sozzi, M. Tardocchi. AIP Conference Proceedings **1612**. American Institute of Physics, Melville, TN, 117 (2014).

Rathgeber, S. K., Barrera, L., Birkenmeier, G., Fischer, R., Suttrop, W., and ASDEX Upgrade Team: Investigations on the edge kinetic data in regimes with type-I and mitigated ELMs at ASDEX Upgrade. Nuclear Fusion **54**, 093011 (2014).

Raupp, G., Walker, M. L., Ambrosino, G, Tommasi, G. d., Humphreys, D. A., Mattei, M., Neu, G, Treutterer, W., and Winter, A.: Event generation and simulation of exception handling with the ITER PCSSP. Fusion Engineering and Design **89**, 523-528 (2014).

Ribeiro, T., and Haefele, M.: NEMORB's Fourier Filter and Distributed Matrix Transposition on Petaflop Systems. Parallel Computing: Accelerating Computational Science and Engineering (CSE). (Eds.) M. Bader, A. Bode, H.-J. Bungartz. IOS Press, Amsterdam, 415-426 (2014).

Riesch, J., Höschen, T., Linsmeier, C., Wurster, S., and You, J.-H.: Enhanced toughness and stable crack propagation in a novel tungsten fibre-reinforced tungsten composite produced by chemical vapour infiltration. Physica Scripta **T159**, 014031 (2014).

Riße, K., Füllenbach, F., Rummel, T., Mardenfeld, M., and Zhao, X.: Wendelstein 7-X Trim Coils – Component Safety Aspects and Commissioning Strategy. IEEE Transactions on Plasma Science **42**, 449-452 (2014).

Roth, J., Wampler, W. R., Oberkofler, M., Deusen, S. v., and Elgeti, S.: Deuterium retention and out-gassing from berylli-

um oxide on beryllium. Journal of Nuclear Materials **453**, 27-30 (2014).

Roth, J., Sugiyama, K., Alimov, V., Höschen, T., Baldwin, M., and Doerner, R.: EUROFER as wall material: reduced sputtering yields due to W surface enrichment. Journal of Nuclear Materials **454**, 1-6 (2014).

Rummel, K., John, A., and Hajduk, L.: Installation of the Superconducting Bus Bar System of Wendelstein 7-X. IEEE Transactions on Plasma Science **42**, 1958-1963 (2014).

Rummel, T., Riße, K., Füllenbach, F., Köppen, M., Kißlinger, J., Brown, T., Hatcher, R., Langish, S., Mardenfeld, M., and Neilson, H.: The Wendelstein 7-X Trim Coil System. IEEE Transactions on Applied Superconductivity **24**, 4200904 (2014).

Rummel, T., Schauer, F., Mönnich, T., Buscher, K.-P., Fietz, W. H., and Heller, R.: Current Leads for the Wendelstein 7-X Superconducting Magnet System. IEEE Transactions on Plasma Science **42**, 2146-2153 (2014).

Ruset, C., Maier, H., Grigore, E., Matthews, G. F., De Temmerman, G., Widdowson, A., and JET-EFDA Contributors: Tungsten coatings under high thermal loads in JET and Magnum-PSI. Physica Scripta **T159**, 014025 (2014).

Rycerz, K., Ciepiela, E., Pawlik, M., Hoenen, O., Harezlak, D., Wilk, B., Gubala, T., Meizner, J., Coster, D., and Bubak, M.: Enabling Multiscale Fusion Simulations on Distributed Computing Resources. eScience on Distributed Computing Infrastructure. (Eds.) M. Bubak, J. Kitowski, K. Wiatr. Springer, Heidelberg, 195-210 (2014).

Ryter, F., Barrera Orte, L., Kurzan, B., McDermott, R., Tardini, G, Viezzer, E., Bernert, M., Fischer, R., and ASDEX Upgrade Team: Experimental evidence for the key role of the ion heat channel in the physics of the L–H transition. Nuclear Fusion **54**, 083003 (2014).

Saitoh, H., Pedersen, T. S., Hergenhahn, U., Stenson, E., Paschkowski, N., and Hugenschmidt, C.: Recent status of A Positron-Electron Experiment (APEX). Journal of Physics: Conference Series **505**, 012045 (2014).

Saitoh, H., Yano, Y., Yoshida, Z., Nishiura, M., Morikawa, J., Kawazura, Y., Nogami, T., and Yamasaki, M.: Observation of a new high-β and high-density state of a magnetospheric plasma in RT-1 (2014). Physics of Plasmas **21**, 082511 (2014).

Salewski, M., Geiger, B., Jacobsen, A. S., García-Muñoz, M., Heidbrink, W. W., Korsholm, S. B., Leipold, F., Madsen, J., Moseev, D., Nielsen, S. K., Rasmussen, J., Stejner, M.,

Tardini, G., Weiland, M., and ASDEX Upgrade Team: Measurement of a 2D fast-ion velocity distribution function by tomographic inversion of fast-ion D-alpha spectra. Nuclear Fusion **54**, 023005 (2014).

Salewski, M., Geiger, B., Moseev, D., Heidbrink, W. W., Jacobsen, A. S., Korsholm, S. B., Leipold, F., Madsen, J., Nielsen, S. K., Rasmussen, J., Stejner, M., Weiland, M., and ASDEX Upgrade Team: On velocity-space sensitivity of fast-ion D-alpha spectroscopy. Plasma Physics and Controlled Fusion **56**, 105005 (2014).

Sato, R., Chikada, T., Matsuzaki, H., Suzuki, A., Terai, T., and Sugiyama, K.: Measurement of hydrogen isotope concentration in erbium oxide coatings. Fusion Engineering and Design **89**, 1375-1379 (2014).

Schacht, J., Pingel, S., Wölk, A., Raußeck, R., and CoDaC Team: Gate valve and shutter control system of the fusion experiment Wendelstein 7-X. Fusion Engineering and Design **89**, 588-594 (2014).

Schmid, K., Toussaint, U. v., and Schwarz-Selinger, T.: Transport of hydrogen in metals with occupancy dependent trap energies. Journal of Applied Physics **116**, 134901 (2014).

S*chneider, P., Wolfrum, E., Dunne, M., Dux, R., Gude, A., Kurzan, B., Pütterich, T., Rathgeber, S., Vicente, J., Weller, A., Wenninger, R., and ASDEX Upgrade Team:* Observation of different phases during an ELM crash with the help of nitrogen seeding. Plasma Physics and Controlled Fusion **56**, 025011 (2014).

Schröder, T., Grulke, O., Klinger, T., Boswell, R. W., and Charles, C.: Collisionless expansion of pulsed rf plasmas. Journal of Physics D: Applied Physics **47**, 055207 (2014).

Senichenkov, I. Y., Kaveeva, E. G., Rozhansky, V. A., Voskoboynikov, S. P., Molchanov, P. A., Coster, D. P., Pereverzev, G. V., ASDEX Upgrade Team, and Globus-M Team: Integrated modeling of H-mode tokamak discharges with ASTRA and B2SOLPS numerical codes. Plasma Physics and Controlled Fusion **56**, 055002 (2014).

Seo, J., Chang, C. S., Ku, S., Kwon, J. M., Choe, W., and Müller, S. H.: Intrinsic momentum generation by a combined neoclassical and turbulence mechanism in diverted DIII-D plasma edge. Physics of Plasmas **21**, 092501 (2014).

Sergienko, G., Arnoux, G., Devaux, S., Matthews, G. F., Nunes, I., Riccardo, V., Sirinelli, A., Huber, A., Brezinsek, S., Coenen, J. W., Mertens, P., Philipps, V., Samm, U., and JET EFDA Contributors: Movement of liquid beryllium during melt events in JET with ITER-like wall. Physica Scripta **T159**, 014041 (2014).

Serianni, G., De Muri, M., Muraro, A., Veltri, P., Bonomo, F., Chitarin, G., Pasqualotto, R., Pavei, M., Rizzolo, A., Valente, M., Franzen, P., Ruf, B., and Schiesko, L.: First negative ion beam measurement by the Short-Time Retractable Instrumented Kalorimeter Experiment (STRIKE). Review of Scientific Instruments **85**, 02A736 (2014).

Sertoli, M., Flannegan, J. C., Cackett, A., Hodille, E., Vries, P. d., Sieglin, B., Marsen, S., Brezinsek, S., Matthews, G. F., Coenen, J. W., and JET-EFDA Contributors: Transient impurity events in JET with the new ITER-like wall. Physica Scripta **T159**, 014014 (2014).

Shabbir, A., Verdoolaege, G., Kardaun, O., Noterdaeme, J.-M., and JET-EFDA Contributors: Visualization of the operational space of edge-localized modes through low-dimensional embedding of probability distributions. Review of Scientific Instruments **85**, 11E819 (2014).

Shimizu, S., Barczyk, S., Rettberg, P., Shimizu, T., Klaempfl, T., Zimmermann, J. L., Höschen, T., Linsmeier, C., Weber, P., Morfill, G. E., and Thomas, H. M.: Cold atmospheric plasma – A new technology for spacecraft component decontamination. Planetary and Space Science **90**, 60-71 (2014).

Sigalov, A., Eixenberger, H., and Käsemann, C.-P.: Datenerfassungssystem des Vierquadranten-Stromrichters für die Plasma-Lageregelung von ASDEX Upgrade. Virtuelle Instrumente in der Praxis 2014. Begleitband zum 19. VIP-Kongress. (Eds.) R. Jamal, R. Heinze. VDE-Verlag, Berlin, 6-9 (2014).

Silva, C., Arnoux, G., Devaux, S., Frigione, D., Groth, M., Horacek, J., Lomas, P. J., Marsen, S., Matthews, G., Meneses, L., and Pitts, R. A.: Characterization of scrape-off layer transport in JET limiter plasmas. Nuclear Fusion **54**, 083022 (2014).

Simon, P., Ramisch, M., Beletskii, A. A., Dinklage, A., Endler, M., Marsen, S., Nold, B., Stroth, U., Tamain, P., and Wilcox, R.: Scaling and transport analyses based on an international edge turbulence database. Plasma Physics and Controlled Fusion **56**, 095015 (2014).

Singh, R., Brunner, S., Ganesh, R., and Jenko, F.: Finite ballooning angle effects on ion temperature gradient driven mode in gyrokinetic flux tube simulations. Physics of Plasmas **21**, 032115 (2014).

Smirnow, M., Kuchelmeister, M., Boscary, J., Tittes, H., and Peacock, A.: Mechanical analysis of the joint between Wendelstein 7-X target elements and the divertor frame structure. Fusion Engineering and Design **89**, 1037-1041 (2014).

Sode, M., Schwarz-Selinger, T., Jacob, W., and Kersten, H.: Surface loss probability of atomic hydrogen for different

electrode cover materials investigated in H_2-Ar low-pressure plasmas. Journal of Applied Physics **116**, 013302 (2014).

Sode, M., Schwarz-Selinger, T., Jacob, W., and Kersten, H.: Wall loss of atomic nitrogen determined by ionization threshold mass spectrometry. Journal of Applied Physics **116**, 193302 (2014).

Sommer, F., Stober, J., Angioni, C., Fable, E., Bernert, M., Burckhart, A., Bobkov, V., Fischer, R., Fuchs, C., McDermott, R., Suttrop, W., Viezzer, E., and ASDEX Upgrade Team: H-mode characterization for dominant ECRH and comparison to dominant NBI and ICRF heating at ASDEX Upgrade. Radiofrequency Power in Plasmas: Proceedings of the 20th Topical Conference. (Eds.) A. Tuccillo, S. Ceccuzzi. AIP Conference Proceedings **1580**. American Institute of Physics, Melville, TN, 153-160 (2014).

Soto-Chavez, A. R., Wang, G., Bhattacharjee, A., Fu, G. Y., and Smith, H.: A model for falling-tone chorus. Geophysical Research Letters **41**, 1838-1845 (2014).

Spitsyn, A. V., Golubeva, A. V., Bobyr, N. P., Khripunov, B. I., Cherkez, D. I., Petrov, V. B., Mayer, M., Ogorodnikova, O. V., Alimov, V. K., Klimov, N. S., Putrik, A., Chernov, V. M., Leontieva-Smirnova, M. V., Gasparyan, Y. M., and Efimov, V. S.: Retention of deuterium in damaged low-activation steel Rusfer (EK-181) after gas and plasma exposure. Journal of Nuclear Materials **455**, 561-567 (2014).

Stegmeir, A., Coster, D., Maj, O., and Lackner, K.: Numerical Methods for 3D Tokamak Simulations Using a Flux-Surface Independent Grid. Contributions to Plasma Physics **54**, 549-554 (2014).

Stejner, M., Nielsen, S., Jacobsen, A. S., Korsholm, S. B., Leipold, F., Meo, F., Michelsen, P. K., Moseev, D., Rasmussen, J., Salewski, M., Schubert, M., Stober, J., Wagner, D., and ASDEX Upgrade Team: Resolving the bulk ion region of millimeter-wave collective Thomson scattering spectra at ASDEX Upgrade. Review of Scientific Instruments **85**, 093504 (2014).

Stepanov, I., Noterdaeme, J.-M., Bobkov, V., Coster, D., Faugel, H., Bilato, R., Brambilla, M., Suttrop, W., Kallenbach, A., Schweinzer, J., Wolfrum, E., Fischer, R., Mlynek, A., Nikolaeva, V., Guimarais, L., Milanesio, D., and ASDEX Upgrade Team: Improved measurements of ICRF antenna input impedance at ASDEX Upgrade during ICRF coupling studies. Radiofrequency Power in Plasmas: Proceedings of the 20th Topical Conference. (Eds.) A. Tuccillo, S. Ceccuzzi. AIP Conference Proceedings **1580**. American Institute of Physics, Melville, TN, 275-278 (2014).

Strauss, D., Aiello, G., Bruschi, A., Chavan, R., Farina, D., Figini, L., Gagliardi, M., Garcia, V., Goodman, T. P., Grossetti, G., Heemskerk, C., Henderson, M. A., Kasparek, W., Krause, A.,

Landis, J.-D., Meier, A., Moro, A., Platania, P., Plaum, B., Poli, E., Ronden, D., Saibene, G., Sanchez, F., Sauter, O., Scherer, T., Schreck, S., Serikov, A., Sozzi, C., Spaeh, P., Vaccaro, A., and Weinhorst, B.: Progress of the ECRH Upper Launcher design for ITER. Fusion Engineering and Design **89**, 1669-1673 (2014).

Strumberger, E., Günter, S., Merkel, P., and Tichmann, C.: Linear stability studies including resistive wall effects with the CASTOR/STARWALL code. Journal of Physics: Conference Series **561**, 012016 (2014).

Strumberger, E., Günter, S., and Tichmann, C.: MHD instabilities in 3D tokamaks. Nuclear Fusion **54**, 064019 (2014).

Sudhir, D., Bandyopadhyay, M., Kraus, W., Gahlaut, A., Bansal, G., and Chakraborty, A.: Online tuning of impedance matching circuit for long pulse inductively coupled plasma source operation – An alternate approach. Review of Scientific Instruments **85**, 013510 (2014).

Sugiyama, K., Mayer, M., Herrmann, A., Krieger, K., Rohde, V., Balden, M., Lindig, S., Neu, R., Müller, H. W., and ASDEX Upgrade Team: Deuterium retention in tungsten used in ASDEX Upgrade: comparison of tokamak and laboratory studies. Physica Scripta **T159**, 014043 (2014).

Sun, Y., Chen, Z. P., Zhu, T. Z., Yu, Q., Zhuang, G., Nan, J. Y., Ke, X., Liu, H., and J-TEXT Team: The influence of electrode biasing on plasma confinement in the J-TEXT tokamak. Plasma Physics and Controlled Fusion **56**, 015001 (2014).

't Hoen, M. H. J., Balden, M., Manhard, A., Mayer, M., Elgeti, S., Kleyn, A. W., and Zeijlmans van Emmichoven, P. A.: Surface morphology and deuterium retention of tungsten after low- and high-flux deuterium plasma exposure. Nuclear Fusion **54**, 083014 (2014).

Takahashi, H., Shimozuma, T., Kubo, S., Yoshimura, Y., Igami, H., Ito, S., Kobayashi, S., Mizuno, Y., Okada, K., Mutoh, T., Nagaoka, K., Murakami, S., Osakabe, M., Yamada, I., Nakano, H., Yokoyama, M., Ido, T., Shimizu, A., Seki, R., Ida, K., Yoshinuma, M., Kariya, T., Minami, R., Imai, T., Marushchenko, N. B., Turkin, Y., and LHD Experiment Group: Extension of high T_e regime with upgraded electron cyclotron resonance heating system in the Large Helical Device. Physics of Plasmas **21**, 061506 (2014).

Tasso, H., and Throumoulopoulos, G.: Tokamak-like Vlasov equilibria. The European Physical Journal D: Atomic, Molecular and Optical Physics **68**, 175 (2014).

Teaca, B., Banon Navarro, A., and Jenko, F.: The energetic coupling of scales in gyrokinetic plasma turbulence. Physics of Plasmas **21**, 072308 (2014).

Teaca, B., Weidl, M. S., Jenko, F., and Schlickeiser, R.: Acceleration of particles in imbalanced magnetohydrodynamic turbulence. Physical Review E **90**, 021101(R).

Tenfelde, J., Mackel, F., Ridder, S., Tacke, T., Kempkes, P., and Soltwisch, H.: Apex expansion of magnetized plasma loops in a laboratory experiment. Plasma Physics and Controlled Fusion **56**, 055011 (2014).

Terry, P. W., Makwana, K. D., Pueschel, M. J., Hatch, D. R., Jenko, F., and Merz, F.: Mode-space energy distribution in instability-driven plasma turbulence. Physics of Plasmas **21**, 122303 (2014).

Tökesi, K., Salamon, P., Tskhakaya, D., and Coster, D.: Universal functional formula of atomic elastic cross sections. The case of the hydrogen target. Journal of Physics: Conference Series **488**, 042011 (2014).

Tökesi, K., Tskhakaya, D., and Coster, D.: Atomic data for integrated tokamak modelling – Fermi-shuttle type ionization as a possible source of high energy electrons. EPJ Web of Conferences **79**, 02003 (2014).
http://dx.doi.org/10.1051/epjconf/20137902003.

Toussaint, U. v., and Gori, S.: Modeling hydrogen transport in large disordered systems. Physica Scripta **T159**, 014058 (2014).

Träbert, E., Beiersdorfer, P., Clementson, J., and Laska, A.: O VIII H_α and Ly_β Transitions as an XUV/EUV Branching Ratio Tool. The Astrophysical Journal Supplement Series **212**, 20 (2014).

Tretter, J., Boscary, J., Mendelevitch, B., Peacock, A., and Stadler, R.: Configuration Space Control Using the Example of In-vessel Components for Wendelstein 7-X. IEEE Transactions on Plasma Science **42**, 675-681 (2014).

Treutterer, W., Cole, R., Lüddecke, K., Neu, G., Rapson, C., Raupp, G., Zasche, D., Zehetbauer, T., and ASDEX Upgrade Team: ASDEX Upgrade Discharge Control System – A real-time plasma control framework. Fusion Engineering and Design **89**, 146-154 (2014).

Treutterer, W., Humphreys, D., Raupp, G., Schuster, E., Snipes, J., De Tommasi, G., Walker, M., and Winter, D.: Architectural concept for the ITER Plasma Control System. Fusion Engineering and Design **89**, 512-517 (2014).

Tripsky, M., Wauters, T., Lyssoivan, A., Koch, R., Bobkov, V., Vervier, M., Van Oost, G., Van Schoor, M., ASDEX Upgrade Team, and TEXTOR Team: Monte Carlo simulation of initial breakdown phase for magnetised toroidal ICRF discharges.

Radiofrequency Power in Plasmas: Proceedings of the 20th Topical Conference. (Eds.) A. Tuccillo, S. Ceccuzzi. AIP Conference Proceedings **1580**. American Institute of Physics, Melville, TN, 334-337 (2014).

Tskhakaya, D., Coster, D., and ITM-TF Contributors: Implementation of PIC/MC Code BIT1 in ITM Platform. Contributions to Plasma Physics **54**, 399-403 (2014).

Tsujii, N., D'Inca, R., Noterdaeme, J.-M., Bilato, R., Bobkov, V. V., Brambilla, M., Van Eester, D., Harvey, R. W., Jaeger, E. F., Lerche, E. A., Schneider, P., and ASDEX Upgrade Team: Effect of collisional heat transfer in ICRF power modulation experiment on ASDEX-Upgrade. Radiofrequency Power in Plasmas: Proceedings of the 20th Topical Conference. (Eds.) A. Tuccillo, S. Ceccuzzi. AIP Conference Proceedings **1580**. American Institute of Physics, Melville, TN, 239-242 (2014).

Tudisco, O., Silva, A., Ceccuzzi, S., D'Arcangelo, O., Rocchi, G., Fünfgelder, H., Bobkov, V., Cavazzana, R., Conway, G. D., Friesen, J., Goncalves, B., Mancini, A., Meneses, L., Noterdaeme, J.-M., Siegl, G., Simonetto, A., Tsujii, N., Tuccillo, A. A., Vierle, T., Zammuto, I., ASDEX Upgrade Team, and FTU Team: A multichannel reflectometer for the density profile measurements in front of the new ICRF antenna in ASDEX Upgrade. Radiofrequency Power in Plasmas: Proceedings of the 20th Topical Conference. (Eds.) A. Tuccillo, S. Ceccuzzi. AIP Conference Proceedings **1580**. American Institute of Physics, Melville, TN, 566-569 (2014).

Valcarcel, D. F., Alves, D., Card, P., Carvalho, B. B., Devaux, S., Felton, R., Goodyear, A., Lomas, P. J., Maviglia, F., McCullen, P., Reux, C., Rimini, F., Stephen, A., Zabeo, L., Zastrow, K.-D., and JET EFDA Contributors: The JET real-time plasma-wall load monitoring system. Fusion Engineering and Design **89**, 243-258 (2014).

Van Eester, D., Lerche, E., Jacquet, P., Bobkov, V., Czarnecka, A., Coenen, J. W., Colas, L., Crombé, K., Graham, M., Jachmich, S., Joffrin, E., Klepper, C. C., Kiptily, V., Lehnen, M., Maggi, C., Marcotte, F., Matthews, G., Mayoral, M.-L., Mc Cormick, K., Monakhov, I., Nave, M. F. F., Neu, R., Noble, C., Ongena, J., Pütterich, T., Rimini, F., Solano, E. R., and Rooij, G v.: Effect of the minority concentration on ion cyclotron resonance heating in presence of the ITER-like wall in JET. Radiofrequency Power in Plasmas: Proceedings of the 20th Topical Conference. (Eds.) A. Tuccillo, S. Ceccuzzi. AIP Conference Proceedings **1580**. American Institute of Physics, Melville, TN, 223-226 (2014).

Van Zeeland, M. A., Ferraro, N. M., Heidbrink, W. W., Kramer, G. J., Pace, D. C., Chen, X., Evans, T. E., Fisher, R. K., Garcia-Munoz, M., Hanson, J. M., Lanctot, M. J., Lao, L. L., Moyer, R. A., Nazikian, R., and Orlov, D. M.: Modulation of

prompt fast-ion loss by applied n=2 fields in the DIII-D tokamak. Plasma Physics and Controlled Fusion **56**, 015009 (2014).

Vicente, J., Conway, G. D., Manso, M. E., Müller, H. W., Silva, C., Da Silva, F., Guimarais, L., Silva, A., and ASDEX Upgrade Team: H-mode filament studies with reflectometry in ASDEX Upgrade. Plasma Physics and Controlled Fusion **56**, 125019 (2014).

Vicente, J., Silva, F. d., Heuraux, S., Manso, M. E., Conway, G. D., Silva, C., and ASDEX Upgrade Team: A numerical study of fixed frequency reflectometry measurements of plasma filaments with radial and poloidal velocity components. Review of Scientific Instruments **85**, 11D817 (2014).

Viezzer, E., Pütterich, T., Angioni, C., Bergmann, A., Dux, R., Fable, E., McDermott, R. M., Stroth, U., Wolfrum, E., and ASDEX Upgrade Team: Evidence for the neoclassical nature of the radial electric field in the edge transport barrier of ASDEX Upgrade. Nuclear Fusion **54**, 012003 (2014).

Viezzer, E., Pütterich, T., McDermott, R., Conway, G. D., Cavedon, M., Dunne, M., Dux, R., Wolfrum, E., and ASDEX Upgrade Team: Parameter dependence of the radial electric field in the edge pedestal of hydrogen, deuterium and helium plasmas. Plasma Physics and Controlled Fusion **56**, 075018 (2014).

Vilbrandt, R., Bosch, H.-S., and Feist, J.-H.: Quality Management System in Fusion Research – Experience from W7-X. IEEE Transactions on Plasma Science **42**, 3644-3649 (2014).

Voitsekhovitch, I., Belo, P., Citrin, J., Fable, E., Ferreira, J., Garcia, J., Garzotti, L., Hobirk, J., Hogeweij, G., Joffrin, E., Köchl, F., Litaudon, X., Moradi, S., Nabais, F., JET-EFDA Contributors, and EU-ITM ITER Scenario Modelling Group: Modelling of JET hybrid scenarios with GLF23 transport model: E×B shear stabilization of anomalous transport. Nuclear Fusion **54**, 093006 (2014).

Voitsenya, V. S., Balden, M., Bardamid, A. F., Belyaeva, A. I., Bondarenko, V., Skoryk, O. O., Shtan, A. F., Solodovchenko, S. I., Sterligov, V. A., and Tyburska-Püschel, B.: Effect of sputtering on self-damaged ITER-grade tungsten. Journal of Nuclear Materials **453**, 60-65 (2014).

Vries, P. C. d., Baruzzo, M., Hogeweij, G. M. D., Jachmich, S., Joffrin, E., Lomas, P. J., Matthews, G. F., Murari, A., Nunes, I., Pütterich, T., Reux, C., Vega, J., and JET-EFDA Contributors: The influence of an ITER-like wall on disruptions at JET. Physics of Plasmas **21**, 056101 (2014).

Wagner, D., Stober, J., Leuterer, F., Monaco, F., Müller, S., Münich, M., Rapson, C., Reich, M., Schubert, M., Schütz, H.,

Treutterer, W., Zohm, H., Thumm, M., Scherer, T., Meier, A., Gantenbein, G., Jelonnek, J., Kasparek, W., Lechte, C., Plaum, B., Litvak, A. G., Denisov, G. G., Chirkov, A., Popov, L. G., Nichiporenko, V. O., Myasnikov, V. E., Tai, E. M., Solyanova, E. A., and Malygin, S. A.: Operation and Upgrade of the ECRH System at ASDEX Upgrade. 39th International Conference on Infrared, Millimeter, and Terahertz Waves (IRMMW-THz). IEEE, Piscataway, NJ, (2014).

Wagner, F.: Considerations for an EU-wide use of renewable energies for electricity generation. The European Physical Journal Plus **129**, 219 (2014).

Wagner, F.: Electricity by intermittent sources: An analysis based on the German situation 2012 (2014). The European Physical Journal Plus **129**, 20 (2014).

Walker, M. L., Ambrosino, G., De Tommasi, G., Humphreys, D. A., Mattei, M., Neu, G., Raupp, G., Treutterer, W., and Winter, A.: A simulation environment for ITER PCS development. Fusion Engineering and Design **89**, 518-522 (2014).

Wang, P., and Jacob, W.: Deuterium diffusion and retention in a tungsten-carbon multilayer system. Nuclear Instruments and Methods in Physics Research Section B: Beam Interactions with Materials and Atoms **329**, 6-13 (2014).

Wang, P., Jacob, W., and Elgeti, S.: Deuterium retention in tungsten films after different heat treatments. Journal of Nuclear Materials **456**, 192-199 (2014).

Wang, P., Jacob, W., Gao, L., Elgeti [Lindig], S., and Balden, M.: Deuterium retention in tungsten films deposited by magnetron sputtering. Physica Scripta **T159**, 014046 (2014).

Wanner, M., Riße, K., and Rummel, T.: Analysis of the Interlayer Joint Resistance of the Superconducting Coils of W7-X. Fusion Science and Technology **65**, 391-398 (2014).

Wauters, T., Laqua, H. P., Otte, M., Preynas, M., Stange, T., Urlings, P., Altenburg, Y., Assmus, D., Birus, D., and Louche, F.: Ion and electron cyclotron wall conditioning in stellarator and tokamak magnetic field configuration on WEGA. Radiofrequency Power in Plasmas: Proceedings of the 20th Topical Conference. (Eds.) A. Tuccillo, S. Ceccuzzi. AIP Conference Proceedings **1580**. American Institute of Physics, Melville, TN, 187-190 (2014).

Webster, A. J., Dendy, R. O., Calderon, F. A., Chapman, S. C., Delabie, E., Dodt, D., Felton, R., Todd, T. N., Maviglia, F., Morris, J., Riccardo, V., Alper, B., Brezinsek, S., Coad, P., Likonen, J., Rubel, M., and JET EFDA Contributors: Time-resonant tokamak plasma edge instabilities? Plasma Physics and Controlled Fusion **56**, 075017 (2014).

Wehner, S., Cisternas, J., Descalzi, O., and Küppers, J.: Noisy CO oxidation on Iridium(111) surfaces. European Physical Journal – Special Topics **223**, 21-41 (2014).

Wenninger, R., Bernert, M., Eich, T., Fable, E., Federici, G., Kallenbach, A., Loarte, A., Lowry, C., McDonald, D., Neu, R., Puetterich, T., Schneider, P., Sieglin, B., Strohmayer, G., Reimold, F., and Wischmeier, M.: DEMO divertor limitations during and in between ELMs. Nuclear Fusion **54**, 114003 (2014).

Widdowson, A., Alves, E., Ayres, C. F., Baron-Wiechec, A., Brezinsek, S., Catarino, N., Coad, J. P., Heinola, K., Likonen, J., Matthews, G. F., Mayer, M., Rubel, M., and JET-EFDA Contributors: Material migration patterns and overview of first surface analysis of the JET ITER-like wall. Physica Scripta **T159**, 014010 (2014).

Wiegel, B., Schneider, W., Grünauer, F., Burhenn, R., Schuhmacher, H., and Zimbal, A.: Monitoring of the neutron production at the Wendelstein 7-X stellarator. Radiation Protection Dosimetry **161**, 326-330 (2014).

Willensdorfer, M., Birkenmeier, G., Fischer, R., Laggner, F. M., Wolfrum, E., Veres, G., Aumayr, F., Carralero, D., Guimarais, L., Kurzan, B., and ASDEX Upgrade Team: Characterization of the Li-BES at ASDEX Upgrade. Plasma Physics and Controlled Fusion **56**, 025008 (2014).

Winkler, K., Shannon, M., and Lockley, D.: Thermo-structural development of the ITER ICRF strap housing module. Radiofrequency Power in Plasmas: Proceedings of the 20th Topical Conference. (Eds.) A. Tuccillo, S. Ceccuzzi. AIP Conference Proceedings **1580**. American Institute of Physics, Melville, TN, 366-369 (2014).

Wünderlich, D., Mochalskyy, S., Fantz, U., Franzen, P., and NNBI Team: Modelling the ion source for ITER NBI: from the generation of negative hydrogen ions to their extraction. Plasma Sources Science and Technology **23**, 015008 (2014).

Wünderlich, D., Wimmer, C., and Friedl, R.: A collisional radiative model for low-pressure hydrogen–caesium plasmas and its application to an RF source for negative hydrogen ions. Journal of Quantitative Spectroscopy and Radiative Transfer **149**, 360-371 (2014).

Xanthopoulos, P., Mynick, H., Helander, P., Turkin, Y., Plunk, G., Jenko, F., Görler, T., Told, D., Bird, T., and Proll, J.: Controlling Turbulence in Present and Future Stellarators. Physical Review Letters **113**, 155001 (2014).

Xu, G. S., Wang, H. Q., Xu, M., Wan, B. N., Guo, H. Y., Diamond, P. H., Tynan, G. R., Chen, R., Yan, N., Kong, D. F.,

Zhao, H. L., Liu, A. D., Lan, T., Naulin, V., Nielsen, A. H., Juul Rasmussen, J., Miki, K., Manz, P., Zhang, W., Wang, L., Shao, L. M., Liu, S. C., Chen, L., Ding, S. Y., Zhao, N., Li, Y. L., Liu, Y. L., Hu, G. H., Wu, X. Q., and Gong, X. Z.: Dynamics of L–H transition and I-phase in EAST. Nuclear Fusion **54**, 103002 (2014).

Xufei, X., Nocente, M., Bonomo, F., Franzen, P., Fröschle, M., Grosso, G., Grünauer, F., Pasqualotto, R., Tardocchi, M., Fan, T., and Gorini, G.: Neutron measurements from beam-target reactions at the ELISE neutral beam test facility. Review of Scientific Instruments **85**, 11D864 (2014).

Yamamoto, T., Shibata, T., Ohta, M., Yasumoto, M., Nishida, K., Hatayama, A., Mattei, S., Lettry, J., Sawada, K., and Fantz, U.: Modeling of neutrals in the Linac4 H$^-$ ion source plasma: Hydrogen atom production density profile and H$_\alpha$ intensity by collisional radiative model. Review of Scientific Instruments **85**, 02B118 (2014).

Yamoto, S., Hoshino, K., Toma, M., Homma, Y., Hatayama, A., Bonnin, X., Coster, D., and Schneider, R.: Systematic Study of Tungsten Impurity Transport in Representative Regimes of Divertor Plasma. Contributions to Plasma Physics **54**, 421-425 (2014).

Yang, Q. X., Song, Y. T., Wang, Y. S., Noterdaeme, J.-M., and Fünfgelder, H.: EBW Technology Applied on the ICRF Antenna Component. IEEE Transactions on Plasma Science **42**, 1421-1424 (2014).

Yao, W., Krill III, C. E., Albinski, B., Schneider, H.-C., and You, J. H.: Plastic material parameters and plastic anisotropy of tungsten single crystal: a spherical micro-indentation study. Journal of Materials Science **49**, 3705-3715 (2014).

Yashin, A. Y., Bulanin, V. V., Gusev, V. K., Khromov, N. A., Kurskiev, G. S., Minaev, V. B., Patrov, M. I., Petrov, A. V., Petrov, Y. V., Prisyazhnyuk, D. V., Sakharov, N. V., Shchegolev, P. B., Tolstyakov, S. Y., Varfolomeev, V. I., and Wagner, F.: Geodesic acoustic mode observations in the Globus-M spherical tokamak. Nuclear Fusion **54**, 114015 (2014).

You, J. H.: Damage and fatigue crack growth of Eurofer steel first wall mock-up under cyclic heat flux loads. Part 2: Finite element analysis of damage evolution. Fusion Engineering and Design **89**, 294-301 (2014).

You, J. H., Höschen, T., and Pintsuk, G.: Damage and fatigue crack growth of Eurofer steel first wall mock-up under cyclic heat flux loads. Part 1: Electron beam irradiation tests. Fusion Engineering and Design **89**, 284-288 (2014).

Yu, J. H., Doerner, R. P., Dittmar, T., Höschen, T., Schwarz-Selinger, T., and Baldwin, M. J.: ITER-relevant transient heat loads on tungsten exposed to plasma and beryllium. Physica Scripta **T159**, 014036 (2014).

Yu, Q., Günter, S., and Lackner, K.: Formation of plasmoids during sawtooth crashes (Letter). Nuclear Fusion **54**, 072005 (2014).

Yuan, Y., Xu, B., Fu, B. Q., Greuner, H., Böswirth, B., Xu, H. Y., Li, C., Jia, Y. Z., Qu, S. L., Luo, G.-N., Lu, G. H., and Liu, W.: Suppression of cavitation in melted tungsten by doping with lanthanum oxide. Nuclear Fusion **54**, 083026 (2014).

Zacharias, O., Comisso, L., Grasso, D., Kleiber, R., Borchardt, M., and Hatzky, R.: Numerical comparison between a gyrofluid and gyrokinetic model investigating collisionless magnetic reconnection. Physics of Plasmas **21**, 062106 (2014).

Zarzoso, D., Biancalani, A., Bottino, A., Lauber, P., Poli, E., Girardo, J.-B., Garbet, X., and Dumont, R. J.: Analytic dispersion relation of energetic particle driven geodesic acoustic modes and simulations with NEMORB. Nuclear Fusion **54**, 103006 (2014).

Zayachuk, Y., Manhard, A., 't Hoen, M. H. J., Jacob, W., Zeijlmans van Emmichoven, P. A., and Oost, G. v.: Depth profiling of the modification induced by high-flux deuterium plasma in tungsten and tungsten-tantalum alloys. Nuclear Fusion **54**, 123013 (2014).

Zhang, X. J., Zhao, Y. P., Wan, B. N., Ding, B. J., Xu, G. S., Gong, X. Z., Li, J. G., Lin, Y., Taylor, G., Noterdaeme, J.-M., Braun, F., Wukitch, S., Magne, R., Litaudon, X., Kumazawa, R., Kasahara, H., and EAST Team: LHCD and ICRF heating experiments in H-mode plasmas on EAST. Radiofrequency Power in Plasmas: Proceedings of the 20th Topical Conference. (Eds.) A. Tuccillo, S. Ceccuzzi. AIP Conference Proceedings **1580**. American Institute of Physics, Melville, TN, 49-56 (2014).

Zhao, Y. P., Zhang, X. J., Mao, Y. Z., Yuan, S., Xue, D. Y., Deng, X., Wang, L., Ju, S. Q., Cheng, Y., Qin, C. M., Chen, G., Lin, Y., Li, J. G., Wan, B. N., Song, Y. T., Braun, F., Kumazawa, R., and Wukitch, S.: EAST ion cyclotron resonance heating system for long pulse operation. Fusion Engineering and Design **89**, 2642-2646 (2014).

Zibrov, M., Mayer, M., Markina, E., Sugiyama, K., Betzenbichler, M., Kurishita, H., Gasparyan, Y., Ogorodnikova, O., Manhard, A., and Pisarev, A.: Deuterium retention in TiC and TaC doped tungsten under low-energy ion irradiation. Physica Scripta **T159**, 014050 (2014).

Zivelonghi, A., and You, J.-H.: Mechanism of plastic damage and fracture of a particulate tungsten-reinforced copper composite: A microstructure-based finite element study. Computational Materials Science **84**, 318-326 (2014).

Conference Papers

Adamek, J., Müller, H. W., Horacek, J., Schrittwieser, R., Vondracek, P., Kurzan, B., Bilkova, P., Böhm, P., Aftanas, M., Panek, R., COMPASS Team, and ASDEX Upgrade Team: Radial profiles of the electron temperature on COMPASS, and ASDEX Upgrade from ball-pen probe and Thomson scattering diagnostic. 41st EPS Conference on Plasma Physics, (Eds.) S. Ratynskaia, P. Mantica, A. Benuzzi-Mounaix et al. ECA **38F**, European Physical Society, Geneva, P2.011 (2014).

Aho-Mantila, L., Coster, D. P., Wischmeier, M., and ASDEX Upgrade Team: On the role of drifts in the divertor power load distribution in ASDEX Upgrade. 41st EPS Conference on Plasma Physics, (Eds.) S. Ratynskaia, P. Mantica, A. Benuzzi-Mounaix et al. ECA **38F**, European Physical Society, Geneva, O4.120 (2014).

Alegre, D., Oberkofler, M., Drenik, A., Kruezi, U., Brezinsek, S., Tabares, F. L., Maddison, G., Reux, C., and JET EFDA Contributors: Gas exhaust study by RGA in JET after disruptions and impurity seeding. 41st EPS Conference on Plasma Physics, (Eds.) S. Ratynskaia, P. Mantica, A. Benuzzi-Mounaix et al. ECA **38F**, European Physical Society, Geneva, P1.027 (2014).

Bergmann, A., and Lackner, K.: Force by a cross-field current between electrodes on a plasma confined by a cusp magnetic field. 41st EPS Conference on Plasma Physics, (Eds.) S. Ratynskaia, P. Mantica, A. Benuzzi-Mounaix et al. ECA **38F**, European Physical Society, Geneva, P4.142 (2014).

Bogomolov, A. V., Classen, I. G. J., Boom, J., Donné, A. J. H., Wolfrum, E., Suttrop, W., Luhmann Jr., N. C., and ASDEX Upgrade Team: Study of the ELM fluctuation characteristics during the mitigation of type-I ELMs. 41st EPS Conference on Plasma Physics, (Eds.) S. Ratynskaia, P. Mantica, A. Benuzzi-Mounaix et al. ECA **38F**, European Physical Society, Geneva, P2.009 (2014).

Bozhenkov, S., Effenberg, F., Feng, Y., Geiger, J., Hartmann, D. A., Hölbe, H., Pederson, T. S., and Wolf, R. C.: Limiter for the early operation phase of W7-X. 41st EPS Conference on Plasma Physics, (Eds.) S. Ratynskaia, P. Mantica, A. Benuzzi-Mounaix et al. ECA **38F**, European Physical Society, Geneva, P1.080 (2014).

Brochard, F., Drevlak, M., Helander, P., Bonhomme, G., Faudot, E., Heuraux, S., Lemoine, N., Kißlinger, J., Mikhailov, M., Nührenberg, C., Nührenberg, J., Turkin, Y., and Kelbert, E.: Physics and Engineering Design of ESTELL Quasi-axisymmetric Stellarator. 41st EPS Conference on Plasma Physics, (Eds.) S. Ratynskaia, P. Mantica, A. Benuzzi-

Mounaix et al. ECA **38F**, European Physical Society, Geneva, P2.081 (2014).

Buttenschön, B., Kempkes, P., Grulke, O., and Klinger, T.: A high power helicon discharge as a plasma cell for future plasma wakefield accelerators. 41st EPS Conference on Plasma Physics, (Eds.) S. Ratynskaia, P. Mantica, A. Benuzzi-Mounaix et al. ECA **38F**, European Physical Society, Geneva, P2.102 (2014).

Casali, L., Fable, E., Dux, R., Bernert, M., Fischer, R., Kallenbach, A., Kurzan, B., Mlynek, A., McDermott, R. M., Ryter, F., Sertoli, M., Tardini, G., and ASDEX Upgrade Team: Transport analysis and modelling of high radiation and high density plasmas at ASDEX Upgrade. 41st EPS Conference on Plasma Physics, (Eds.) S. Ratynskaia, P. Mantica, A. Benuzzi-Mounaix et al. ECA **38F**, European Physical Society, Geneva, P2.005 (2014).

Cesario, R., Amicucci, L., Artaserse, G., Chapman, I. T., Marinucci, M., Jenko, F., Lupelli, I., Romanelli, M., Saarelma, S., Told, D., and JET EFDA Contributors: Initial low recycling improving confinement and current drive in advanced tokamak (AT) and hybrid scenarios. 41st EPS Conference on Plasma Physics, (Eds.) S. Ratynskaia, P. Mantica, A. Benuzzi-Mounaix et al. ECA **38F**, European Physical Society, Geneva, P1.016 (2014).

Clementson, J., Lewerentz, L., Grulke, O., Schneider, R., Sydora, R. D., and Klinger, T.: Gyrokinetic simulations of magnetic reconnection in non-uniform plasmas. 41st EPS Conference on Plasma Physics, (Eds.) S. Ratynskaia, P. Mantica, A. Benuzzi-Mounaix et al. ECA **38F**, European Physical Society, Geneva, P4.118 (2014).

Costea, S., Nielsen, A. H., Naulin, V., Rasmussen, J. J., Müller, H. W., Conway, G. D., Vianello, N., Carralero, D., Schrittwieser, R., Mehlmann, F., Lux, C., Ionita, C., and ASDEX Upgrade Team: Investigations of poloidal velocity and shear in the SOL of ASDEX Upgrade. 41st EPS Conference on Plasma Physics, (Eds.) S. Ratynskaia, P. Mantica, A. Benuzzi-Mounaix et al. ECA **38F**, European Physical Society, Geneva, P2.001 (2014).

Crombé, K., Jacquot, J., Louche, F., and Van Eester, D.: Numerical Challenges in Modelling Near-antenna Field Behaviour in Cold Plasmas. 41st EPS Conference on Plasma Physics, (Eds.) S. Ratynskaia, P. Mantica, A. Benuzzi-Mounaix et al. ECA **38F**, European Physical Society, Geneva, P1.03 (2014).

Devynck, P., Maddison, G., Giroud, C., Jacquet, P., Lehnen, M., Lerche, E., Matthews, G. F., Neu, R., Stamp, M. F., Van Eester, D., and JET EFDA Contributors: Comparing the bulk radiated power efficiency in carbon and ITER-like-wall environments in JET. 41st EPS Conference on Plasma Physics,

(Eds.) S. Ratynskaia, P. Mantica, A. Benuzzi-Mounaix et al. ECA **38F**, European Physical Society, Geneva, P1.009 (2014).

Drevlak, M., Beidler, C. D., Geiger, J., Helander, P., and Turkin, Y.: Quasi-isodynamic Configuration with Improved Confinement. 41st EPS Conference on Plasma Physics, (Eds.) S. Ratynskaia, P. Mantica, A. Benuzzi-Mounaix et al. ECA **38F**, European Physical Society, Geneva, P1.070 (2014).

Dunne, M. G., Wolfrum, E., Burckhart, A., Fischer, R., Giannone, L., McCarthy, P. J., Viezzer, E., and ASDEX Upgrade Team: Edge current density and pressure profile evolution during nitrogen seeded improved H-mode scenarios on ASDEX Upgrade. 41st EPS Conference on Plasma Physics, (Eds.) S. Ratynskaia, P. Mantica, A. Benuzzi-Mounaix et al. ECA **38F**, European Physical Society, Geneva, P2.017 (2014).

Farina, D., Poli, E., Figini, L., Maj, O., Mariani, A., Weber, H., Goodman, T., Sauter, O., Cavinato, M., Saibene, G., and Henderson, M.: ECCD requirements and criteria for NTM stabilization in ITER scenarios. 41st EPS Conference on Plasma Physics, (Eds.) S. Ratynskaia, P. Mantica, A. Benuzzi-Mounaix et al. ECA **38F**, European Physical Society, Geneva, P5.007 (2014).

Felici, F., Geelen, P., Giannone, L., Kim, D., Maljaars, E., Piovesan, P., Piron, C., Rapson, C., Sauter, O., Teplukhina, A., Treutterer, W., Barrera, L., Fable, E., Reich, M., Tardini, G., and ASDEX Upgrade Team: First results of real-time plasma state reconstruction using a model-based dynamic observer on ASDEX-Upgrade. 41st EPS Conference on Plasma Physics, (Eds.) S. Ratynskaia, P. Mantica, A. Benuzzi-Mounaix et al. ECA **38F**, European Physical Society, Geneva, P2.002 (2014).

Feng, Y., Bozhenkov, S., Effenberg, F., Hoelbe, H., Reiter, D., and Turkin, Y.: Neutral transport behavior expected for the first limiter plasmas in W7-X. 41st EPS Conference on Plasma Physics, (Eds.) S. Ratynskaia, P. Mantica, A. Benuzzi-Mounaix et al. ECA **38F**, European Physical Society, Geneva, P1.079 (2014).

Février, O., Maget, P., Lütjens, H., Luciani, J. F., Decker, J., Giruzzi, G., Reich, M., Beyer, P., and ASDEX Upgrade Team: Modeling of magnetic island modifications by ECCD using XTOR-2F. 41st EPS Conference on Plasma Physics, (Eds.) S. Ratynskaia, P. Mantica, A. Benuzzi-Mounaix et al. ECA **38F**, European Physical Society, Geneva, P2.057 (2014).

Fietz, S., Maraschek, M., Zohm, H., Barrera, L., McDermott, R. M., Reich, M., and ASDEX Upgrade Team: Study of the onset of neoclassical tearing modes at the ASDEX Upgrade tokamak. 41st EPS Conference on Plasma Physics, (Eds.) S. Ratynskaia, P. Mantica, A. Benuzzi-Mounaix et al. ECA **38F**, European Physical Society, Geneva, P2.003 (2014).

159

Figueiredo, A. C. A., Giroud, C., Hawkes, N., Hillesheim, J., Leyland, M., Meneses, L., Poli, E., and JET EFDA Contributors: Observation of nitrogen seeding effects on density fluctuations at the edge pedestal by radial correlation reflectometry in JET. 41st EPS Conference on Plasma Physics, (Eds.) S. Ratynskaia, P. Mantica, A. Benuzzi-Mounaix et al. ECA **38F**, European Physical Society, Geneva, P1.032 (2014).

Fil, A., Nardon, E., Beyer, P., Becoulet, M., Dif-Pradalier, G., Grandgirard, V., Guirlet, R., Hoelzl, M., Huijsmans, G. T. A., Latu, G., Lehnen, M., Loarte, A., Orain, F., Pamela, S., Passeron, C., Reux, C., Saint-Laurent, F., Tamain, P., and JET EFDA Contributors: Modeling of disruption mitigation by massive gas injection. 41st EPS Conference on Plasma Physics, (Eds.) S. Ratynskaia, P. Mantica, A. Benuzzi-Mounaix et al. ECA **38F**, European Physical Society, Geneva, P1.045 (2014).

Frassinetti, L., Joffrin, E., Tamain, P., Maget, P., Saarelma, S., Boom, J., Flanagan, J., Giroud, C., Delabie, E., Kempenaars, M., Lomas, P., Maggi, C., Menes, L., Nunes, I., and JET EFDA Contributors: Effect of the divertor geometry on the pedestal confinement in JET-ILW. 41st EPS Conference on Plasma Physics, (Eds.) S. Ratynskaia, P. Mantica, A. Benuzzi-Mounaix et al. ECA **38F**, European Physical Society, Geneva, P1.030 (2014).

Frerichs, H., Schmitz, O., Reiter, D., Evans, T. E., Feng, Y., and Ferraro, N. M.: Impact of an M3D-C1 modeled plasma response on simulations of the DIII-D plasma edge with EMC3-EIRENE. 41st EPS Conference on Plasma Physics, (Eds.) S. Ratynskaia, P. Mantica, A. Benuzzi-Mounaix et al. ECA **38F**, European Physical Society, Geneva, P2.025 (2014).

Fuchert, G, Birkenmeier, G., Carralero, D., Lunt, T., Manz, P., Müller, H. W., Nold, B., Ramisch, M., Rohde, V., Stroth, U., and ASDEX Upgrade Team: Blob properties in L- and H-mode plasmas of ASDEX Upgrade. 41st EPS Conference on Plasma Physics, (Eds.) S. Ratynskaia, P. Mantica, A. Benuzzi-Mounaix et al. ECA **38F**, European Physical Society, Geneva, P2.007 (2014).

Fuchs, J. C., Suttrop, W., Barrera Orte, L., Cavedon, M., Birkenmeier, G., Giannone, L., Guimarais, L., Kirk, A., Kurzan, B., McCarthy, P. J., Nikolaeva, V., Wolfrum, E., Viezzer, E., and ASDEX Upgrade Team: Investigation of the boundary distortions in the presence of rotating external magnetic perturbations on ASDEX Upgrade. 41st EPS Conference on Plasma Physics, (Eds.) S. Ratynskaia, P. Mantica, A. Benuzzi-Mounaix et al. ECA **38F**, European Physical Society, Geneva, P2.004 (2014).

Giannone, L., Fischer, R., Fuchs, C. J., Lackner, K., Maraschek, M., McCarthy, P. J., Schuhbeck, K. H., Suttrop, W., Zammuto, I., and ASDEX Upgrade Team: Enhancements of the real-time magnetic equilibrium on ASDEX Upgrade. 41st EPS Conference on Plasma Physics, (Eds.) S. Ratynskaia, P. Mantica, A. Benuzzi-Mounaix et al. ECA **38F**, European Physical Society, Geneva, P2.013 (2014).

Goniche, M., Lerche, E., Jacquet, P., Van Eester, D., Bobkov, V., Brezinsek, S., Colas, L., Czarnecka, A., Drewelow, P., Dumont, R., Fedorczak, N., Giroud, C., Graham, M., Graves, J. P., Monakhov, I., Monier-Garbet, P., Noble, C., Pütterich, T., Rimini, F., Valisa, M., and JET EFDA Contributors: Optimization of ICRH for tungsten control in JET H-mode plasmas. 41st EPS Conference on Plasma Physics, (Eds.) S. Ratynskaia, P. Mantica, A. Benuzzi-Mounaix et al. ECA **38F**, European Physical Society, Geneva, O4.129 (2014).

Hender, T. C., Alper, B., Angioni, C., Baranov, Y., Baruzzo, M., Buratti, P., Casson, F. J., Challis, C. D., Mantica, C., Romanelli, M., Sharapov, S., and JET-EFDA Contributors: Influence of MHD on impurity peaking in JET. 41st EPS Conference on Plasma Physics, (Eds.) S. Ratynskaia, P. Mantica, A. Benuzzi-Mounaix et al. ECA **38F**, European Physical Society, Geneva, P1.011 (2014).

Hirsch, M., Burhenn, R., Estrada, T., Hartfuss, H.-J., Kasparek, W., Krämer-Flecken, A., Köppen, M., Kornejew, P., Lechte, C., Neuner, U., Plaum, B., Standley, B., Stange, T., Trimino-Mora, H., Windisch, T., Wagner, D., and Wolf, S.: Microwave and Interferometer Diagnostics for Wendelstein 7-X. 41st EPS Conference on Plasma Physics, (Eds.) S. Ratynskaia, P. Mantica, A. Benuzzi-Mounaix et al. ECA **38F**, European Physical Society, Geneva, P1.069 (2014).

Hobirk, J., Buratti, P., Challis, C. D., Coffey, I., Drewelow, P., Joffrin, E., Lauro-Taroni, L., Mailloux, J., Nunes, I., Pucella, G., Pütterich, T., Vries, P. C. d., and JET EFDA Contributors: Analysis of plasma termination in the JET hybrid scenario. 41st EPS Conference on Plasma Physics, (Eds.) S. Ratynskaia, P. Mantica, A. Benuzzi-Mounaix et al. ECA **38F**, European Physical Society, Geneva, P1.003 (2014).

Hornung, G., Hoste, S., Verdoolaege, G., Ghendrih, P., Sarazin, Y., and Noterdaeme, J.-M.: A blob tracking algorithm for the study of turbulence-flow interaction. 41st EPS Conference on Plasma Physics, (Eds.) S. Ratynskaia, P. Mantica, A. Benuzzi-Mounaix et al. ECA **38F**, European Physical Society, Geneva, P1.050 (2014).

Horvath, L., Pokol, G. I., Papp, G, Por, G, Lauber, P., Gude, A., and Igochine, V.: Changes in the radial structure of EPMs during the chirping phase taking the uncertainties of the time-frequency transforms into account. 41st EPS Conference on Plasma Physics, (Eds.) S. Ratynskaia, P. Mantica, A. Benuzzi-Mounaix et al. ECA **38F**, European Physical Society, Geneva, P2.008 (2014).

Huber, A., Wischmeier, M., Lowry, C. G., Brezinsek, S., Maggi, C. F., Reinke, M. L., Sergienko, G., Aho-Mantila, L., Arnoux, G., Beurskens, M. N. A., Clever, M., Devaux, S., Esser, H. G, Giroud, C., Groth, M., Jachmich, S., Järvinen, A., Linsmeier, C., Lipschultz, B., Matthews, G. F., Maddison, G., Marsen, S., Meigs, A. G, Mertens, P., Nave, M. F. F., Philipps, V., Stamp, M., Wiesen, S., and JET-EFDA Contributors: Impact of strong impurity seeding on the radiation losses in JET with ITER-like Wall. 41st EPS Conference on Plasma Physics, (Eds.) S. Ratynskaia, P. Mantica, A. Benuzzi-Mounaix et al. ECA **38F**, European Physical Society, Geneva, P1.031 (2014).

Igochine, V., Gude, A., Günter, S., Lackner, K., Yu, Q., Barrera Orte, L., Bogomolov, A., Classen, I., McDermott, R., Luhmann Jr., N. C., and ASDEX Upgrade Team: Slow conversion of the ideal MHD perturbations into a tearing mode after a sawtooth crash. 41st EPS Conference on Plasma Physics, (Eds.) S. Ratynskaia, P. Mantica, A. Benuzzi-Mounaix et al. ECA **38F**, European Physical Society, Geneva, O4.117 (2014).

Kammel, A., and Hallatschek, K.: Mechanisms of drift wave based zonal flow transitions and bifurcations. 41st EPS Conference on Plasma Physics, (Eds.) S. Ratynskaia, P. Mantica, A. Benuzzi-Mounaix et al. ECA **38F**, European Physical Society, Geneva, P2.023 (2014).

Komm, M., Kocan, M., Carralero, D., Müller, H. W., Stöckel, J., Rea, C., COMPASS Team, and ASDEX Upgrade Team: Fast measurements of ion temperature fluctuations in COMPASS and ASDEX Upgrade scrape-off layer. 41st EPS Conference on Plasma Physics, (Eds.) S. Ratynskaia, P. Mantica, A. Benuzzi-Mounaix et al. ECA **38F**, European Physical Society, Geneva, P5.026 (2014).

Krebs, I., Jardin, S. C., Igochine, V., Günter, S., Hoelzl, M., and ASDEX Upgrade Team: Studying Incomplete Sawtooth Reconnection in ASDEX Upgrade with the Non-linear Two-fluid 3D MHD Code M3D-C[1]. 41st EPS Conference on Plasma Physics, (Eds.) S. Ratynskaia, P. Mantica, A. Benuzzi-Mounaix et al. ECA **38F**, European Physical Society, Geneva, P2.022 (2014).

Labit, B., Canal, G. P., Lunt, T., Reimerdes, H., Vijvers, W. A. J., Coda, S., Duval, B. P., De Temmerman, G., Morgan, T. W., Tal, B., and TCV Team: Overview of recent snowflake divertor studies in TCV. 41st EPS Conference on Plasma Physics, (Eds.) S. Ratynskaia, P. Mantica, A. Benuzzi-Mounaix et al. ECA **38F**, European Physical Society, Geneva, P5.021 (2014).

Lang, P. T., Meyer, H., Birkenmeier, G., Burckhart, A., Carvalho, I., Delabie, E., Frassinetti, L., Huijsmans, G., Kocsis, G., Loarte, A., Maggi, C. F., Plöckl, B., Rimini, F., Ryter, F., Saarelma, S., Szepesi, T., Wolfrum, E., ASDEX Upgrade Team, and JET EFDA Contributors: ELM control at the L-H transition achieved by pellet pacing in the all-metal wall tokamaks ASDEX Upgrade and JET. 41st EPS Conference on Plasma Physics, (Eds.) S. Ratynskaia, P. Mantica, A. Benuzzi-Mounaix et al. ECA **38F**, European Physical Society, Geneva, O3.114 (2014).

Langenberg, A., Thomsen, H., Burhenn, R., Marchuk, O., Svensson, J., Pedersen, T. S., and Wolf, R. C.: Forward Modeling of a High Resolution X-ray Imaging Crystal Spectrometer for the Wendelstein 7-X Stellarator. 41st EPS Conference on Plasma Physics, (Eds.) S. Ratynskaia, P. Mantica, A. Benuzzi-Mounaix et al. ECA **38F**, European Physical Society, Geneva, P1.074 (2014).

Laqua, H. P., Chlechowitz, E., Dostal, M., Otte, M., and Stange, T.: The Generation and Confinement of Relativistic Electrons at the WEGA Stellarator. 41st EPS Conference on Plasma Physics, (Eds.) S. Ratynskaia, P. Mantica, A. Benuzzi-Mounaix et al. ECA **38F**, European Physical Society, Geneva, P1.071 (2014).

Lazerson, S. A., Gates, D. A., Neilson, H., Otte, M., Bozhenkov, S., Pedersen, T. S., Geiger, J., and Lore, J.: Error field and magnetic diagnostic modeling for W7-X. 41st EPS Conference on Plasma Physics, (Eds.) S. Ratynskaia, P. Mantica, A. Benuzzi-Mounaix et al. ECA **38F**, European Physical Society, Geneva, P1.073 (2014).

Lechte, C., Conway, G. D., Görler, T., Tröster, C., and ASDEX Upgrade Team: Doppler Reflectometry Simulations for ASDEX Upgrade. 41st EPS Conference on Plasma Physics, (Eds.) S. Ratynskaia, P. Mantica, A. Benuzzi-Mounaix et al. ECA **38F**, European Physical Society, Geneva, O3.115 (2014).

Lewerentz, L., Clementson, J., Schneider, R., Sydora, R. D., Grulke, O., and Klinger, T.: A gyrokinetic model for studies of magnetic reconnection in periodic and bounded plasmas. 41st EPS Conference on Plasma Physics, (Eds.) S. Ratynskaia, P. Mantica, A. Benuzzi-Mounaix et al. ECA **38F**, European Physical Society, Geneva, P1.144 (2014).

Liu, F., Huijsmans, G. T. A., Loarte, A., Garofalo, A. M., Solomon, W. M., Snyder, P. B., and Hoelzl, M.: Nonlinear MHD simulations of QH-mode plasmas in DIII-D. 41st EPS Conference on Plasma Physics, (Eds.) S. Ratynskaia, P. Mantica, A. Benuzzi-Mounaix et al. ECA **38F**, European Physical Society, Geneva, O5.135 (2014).

Lux, H., Kemp, R., Ward, D. J., and Sertoli, M.: Impurity Radiation in DEMO. 41st EPS Conference on Plasma Physics, (Eds.) S. Ratynskaia, P. Mantica, A. Benuzzi-Mounaix et al. ECA **38F**, European Physical Society, Geneva, P5.016 (2014).

Lyssoivan, A., Wauters, T., Tripský, M., Bobkov, V., Crombé, K., Douai, D., Kreter, A., Nicolai, D., Noterdaeme, J.-M.,

Rohde, V., Schneider, P., Van Eester, D., Van Schoor, M., Vervier, M., TEXTOR Team, and ASDEX Upgrade Team: Wave aspect of neutral gas breakdown with ICRF antenna in ICWC operation mode. 41st EPS Conference on Plasma Physics, (Eds.) S. Ratynskaia, P. Mantica, A. Benuzzi-Mounaix et al. ECA **38F**, European Physical Society, Geneva, P2.030 (2014).

Maggi, C. F., Meyer, H., Bourdelle, C., Delabie, E., Drewelow, P., Carvalho, I. S., Rimini, F., Siren, P., and JET EFDA Contributors: Role of low-Z impurities in L-H transitions in JET. 41st EPS Conference on Plasma Physics, (Eds.) S. Ratynskaia, P. Mantica, A. Benuzzi-Mounaix et al. ECA **38F**, European Physical Society, Geneva, P1.004 (2014).

Mailloux, J., Beurskens, M., Chapman, I., Nunes, I., Alper, B., Baruzzo, M., Belo, P. S. A., Belonohy, E., Bernardo, J., Buratti, P., Challis, C. D., Luna, E. d. l., Frassinetti, L., Garcia, J., Giroud, C., Hawkes, N., Hobirk, J., Joffrin, E., Keeling, D., Lennholm, M., Lomas, P. J., Luce, T., Mantica, P., Marchetto, C., Maslov, M., Pucella, G., Saarelma, S., Sharapov, S., Solano, E. R., Sozzi, C., Szepsi, G., Tsalas, M., and JET EFDA Contributors: Effect of 'baseline' and 'hybrid' operational parameters on plasma confinement and stability in JET with a Be/W ITER-like Wall. 41st EPS Conference on Plasma Physics, (Eds.) S. Ratynskaia, P. Mantica, A. Benuzzi-Mounaix et al. ECA **38F**, European Physical Society, Geneva, O4.127 (2014).

Mantica, P., Angioni, C., Casson, F. J., Pütterich, T., Valisa, M., Baruzzo, M., Silva Aresta Belo, P. C. d., Coffey, I., Drewelow, P., Giroud, C., Hawkes, N. C., Hender, T. C., Koskela, T., Lauro Taroni, L., Lerche, E., Maggi, C. F., Mlynar, J., O'Mullane, M., Puiatti, M. E., Reinke, M. L., Romanelli, M., and JET EFDA Contributors: Understanding and Controlling Tungsten Accumulation in JET Plasmas with the ITER-like Wall. 41st EPS Conference on Plasma Physics, (Eds.) S. Ratynskaia, P. Mantica, A. Benuzzi-Mounaix et al. ECA **38F**, European Physical Society, Geneva, P1.017 (2014).

Martitsch, A. F., Kasilov, S. V., Kernbichler, W., and Maassberg, H.: Evaluation of non-ambipolar particle fluxes driven by external non-resonant magnetic perturbations in a tokamak. 41st EPS Conference on Plasma Physics, (Eds.) S. Ratynskaia, P. Mantica, A. Benuzzi-Mounaix et al. ECA **38F**, European Physical Society, Geneva, P1.049 (2014).

Marushchenko, N. B., Beidler, C. D., Erckmann, V., Geiger, J., Laqua, H. P., Maaßberg, H., and Turkin, Y.: ECRH scenarios with transition from X2 to O2 mode in W7-X Stellarator. 41st EPS Conference on Plasma Physics, (Eds.) S. Ratynskaia, P. Mantica, A. Benuzzi-Mounaix et al. ECA **38F**, European Physical Society, Geneva, P1.084 (2014).

Meyer, H., Delabie, E., Maggi, C. F., Bourdelle, C., Drewelow, P., Carvalho, I., Lang, P., Rimini, F., and JET EFDA Contributors: The role of divertor and SOL physics for access to H-mode on JET. 41st EPS Conference on Plasma Physics, (Eds.) S. Ratynskaia, P. Mantica, A. Benuzzi-Mounaix et al. ECA **38F**, European Physical Society, Geneva, P1.013 (2014).

Milligen, B. P. v., Birkenmeier, G., Ramisch, M., Estrada, T., Hidalgo, C., and Alonso, A.: Causality detection and turbulence in fusion plasmas. 41st EPS Conference on Plasma Physics, (Eds.) S. Ratynskaia, P. Mantica, A. Benuzzi-Mounaix et al. ECA **38F**, European Physical Society, Geneva, P2.034 (2014).

Monreal, P., Sánchez, E., Calvo, I., Bustos, A., Könies, A., Kleiber, R., and Görler, T.: Residual zonal flow level in stellarators for arbitrary wavelengths. 41st EPS Conference on Plasma Physics, (Eds.) S. Ratynskaia, P. Mantica, A. Benuzzi-Mounaix et al. ECA **38F**, European Physical Society, Geneva, P2.089 (2014).

Moseev, D., Geiger, B., Strumberger, E., Jacobsen, A. S., Korsholm, S. B., Mochalskyy, S., Nielsen, S. K., Rasmussen, J., Salewski, M., Stejner, M., Weiland, M., and ASDEX Upgrade Team: Influence of neoclassical tearing modes on confined fast ions in ASDEX Upgrade. 41st EPS Conference on Plasma Physics, (Eds.) S. Ratynskaia, P. Mantica, A. Benuzzi-Mounaix et al. ECA **38F**, European Physical Society, Geneva, P2.014 (2014).

Ochoukov, R., Bobkov, V., Bernert, M., Carralero, D., Cavedon, M., Conway, G. D., Dux, R., Guimarais, L., Happel, T., Herrmann, A., Kocan, M., Leitenstern, P., Müller, H. W., Nikolaeva, V., Noterdaeme, J.-M., Puetterich, T., Simon, P., Viezzer, E., Wolfrum, E., and ASDEX Upgrade Team: Experimental study of a possible role of the scrape off layer radial electric field in determining H-mode confinement properties on ASDEX Upgrade. 41st EPS Conference on Plasma Physics, (Eds.) S. Ratynskaia, P. Mantica, A. Benuzzi-Mounaix et al. ECA **38F**, European Physical Society, Geneva, P2.012 (2014).

Papp, G., Lauber, P., Schneller, M., Braun, S., Koslowski, H. R., and TEXTOR Team: Interaction of runaway populations with fast particle driven modes. 41st EPS Conference on Plasma Physics, (Eds.) S. Ratynskaia, P. Mantica, A. Benuzzi-Mounaix et al. ECA **38F**, European Physical Society, Geneva, P2.032 (2014).

Pautasso, G., Vries, P. C. d., and ASDEX Upgrade Team: Disruption causes in ASDEX Upgrade. 41st EPS Conference on Plasma Physics, (Eds.) S. Ratynskaia, P. Mantica, A. Benuzzi-Mounaix et al. ECA **38F**, European Physical Society, Geneva, P2.015 (2014).

Peraza-Rodriguez, H., Sanchez, R., Geiger, J., Reynolds, J. M., and Tribaldos, V.: Application of the SIESTA code to the calculation of MHD equilibria for the Wendelstein 7-X

Stellarator. 41st EPS Conference on Plasma Physics, (Eds.) S. Ratynskaia, P. Mantica, A. Benuzzi-Mounaix et al. ECA **38F**, European Physical Society, Geneva, P2.072 (2014).

Proll, J. H. E., Faber, B. J., Xanthopoulos, P., and Helander, P.: Microturbulence simulations in optimised stellarators. 41st EPS Conference on Plasma Physics, (Eds.) S. Ratynskaia, P. Mantica, A. Benuzzi-Mounaix et al. ECA **38F**, European Physical Society, Geneva, P1.082 (2014).

Rahbarnia, K., Cardella, A., Endler, M., Hathiramani, D., Geiger, J., Grulke, O., Klinger, T., Neuner, U., Pedersen, T. S., Werner, A., and Windisch, T.: Magnetic Diagnostics for Wendelstein 7-X during the first Operation Phase. 41st EPS Conference on Plasma Physics, (Eds.) S. Ratynskaia, P. Mantica, A. Benuzzi-Mounaix et al. ECA **38F**, European Physical Society, Geneva, P1.077 (2014).

Ratynskaia, S., Mantica, P., Benuzzi-Mounaix, A., Dilecce, G., Bingham, R., Hirsch, M., Kemnitz, B., and Klinger, T. (Eds.): 41st EPS Conference on Plasma Physics. ECA **38F**, European Physical Society, Geneva, (2014). http://ocs.ciemat.es/EPS2014PAP/html/index.html.

Riemann, J., Kleiber, R., and Borchardt, M.: Global Simulation of Linear Instability in W7-X and LHD with EUTERPE. 41st EPS Conference on Plasma Physics, (Eds.) S. Ratynskaia, P. Mantica, A. Benuzzi-Mounaix et al. ECA **38F**, European Physical Society, Geneva, P1.081 (2014).

Ryter, F., Barrera Orte, L., Kurzan, B., McDermott, R. M., Tardini, G., Viezzer, E., Bernert, M., Fischer, R., and ASDEX Upgrade Team: Experimental evidence for the key role of the ion heat channel in the physics of the L-H transition. 41st EPS Conference on Plasma Physics, (Eds.) S. Ratynskaia, P. Mantica, A. Benuzzi-Mounaix et al. ECA **38F**, European Physical Society, Geneva, P2.016 (2014).

Salmi, A., Tala, T., Bourdelle, C., Mantica, P., Meneses, L., Mordjick, S., Bufferand, H., Clever, M., Svensson, J., Tamain, P., Groth, M., Hillesheim, J., Maggi, C. F., Maslov, M., Naulin, V., Rasmussen, J. J., Sips, G., Sirinelli, A., Tsalas, M., Weisen, H., Wischmeier, M., and JET EFDA Contributors: Gas puff modulation experiments in JET L- and H-mode plasmas. 41st EPS Conference on Plasma Physics, (Eds.) S. Ratynskaia, P. Mantica, A. Benuzzi-Mounaix et al. ECA **38F**, European Physical Society, Geneva, P1.008 (2014).

Sanchez, E., Calvo, I., Velasco, J. L., Kleiber, R., Hatzky, R., and Borchardt, M.: Simulation of electrostatic instabilities in a heliac configuration. 41st EPS Conference on Plasma Physics, (Eds.) S. Ratynskaia, P. Mantica, A. Benuzzi-Mounaix et al. ECA **38F**, European Physical Society, Geneva, P2.079 (2014).

Satake, S., Velasco, J. L., Dinklage, A., Yokoyama, M., Suzuki, Y., Beidler, C. D., Maaßberg, H., Geiger, J., Wakasa, A., Matsuoka, S., Murakami, S., Lopez-Bruna, D., Pablant, N., LHD Exp. Group, TJ-II Team, and W7-AS Team: Benchmark of local and non-local neoclassical transport calculations in helical configurations. 41st EPS Conference on Plasma Physics, (Eds.) S. Ratynskaia, P. Mantica, A. Benuzzi-Mounaix et al. ECA **38F**, European Physical Society, Geneva, O4.130 (2014).

Schmid, B., Ramisch, M., and Stroth, U.: Zonal flow formation in the stellarator TJ-K. 41st EPS Conference on Plasma Physics, (Eds.) S. Ratynskaia, P. Mantica, A. Benuzzi-Mounaix et al. ECA **38F**, European Physical Society, Geneva, P1.083 (2014).

Schmitz, O., Becoulet, M., Cahyna, P., Evans, T., Feng, Y., Ferraro, N. M., Frerichs, H., Huijsmans, G, Lao, L., Loarte, A., and Reiter, D.: Impact of plasma response models in three-dimensional fluid modeling of divertor heat fluxes in RMP ELM control scenarios at ITER. 41st EPS Conference on Plasma Physics, (Eds.) S. Ratynskaia, P. Mantica, A. Benuzzi-Mounaix et al. ECA **38F**, European Physical Society, Geneva, P5.014 (2014).

Schmuck, S., Svensson, J., Figini, L., Jonsson, T., Fessey, J., Meneses, L., Boom, J. E., and JET EFDA Contributors: Electron Temperature and Density Inferred from JET ECE Diagnostics. 41st EPS Conference on Plasma Physics, (Eds.) S. Ratynskaia, P. Mantica, A. Benuzzi-Mounaix et al. ECA **38F**, European Physical Society, Geneva, P1.025 (2014).

Shabbir, A., Verdoolaege, G, Kardaun, O. J. W. F., Webster, A. J., Dendy, R. O., Noterdaeme, J. M., and JET EFDA Contributors: Discrimination and visualization of ELM types based on a probabilistic description of inter-ELM waiting times. 41st EPS Conference on Plasma Physics, (Eds.) S. Ratynskaia, P. Mantica, A. Benuzzi-Mounaix et al. ECA **38F**, European Physical Society, Geneva, P1.001 (2014).

Solano, R. E., Autricque, E. A., Coffey, I., Delabie, E., Luna, E. d. l., Drewelow, P., Lerche, E., Frassinetti, L., Clever, M., Nunes, I., Loarer, T., Meigs, A., Rimini, F., Stamp, M., Sips, G., Svensson, J., Tamain, P., and EFDA JET Contributors: Effect of fuelling location on pedestal and ELMs in JET. 41st EPS Conference on Plasma Physics, (Eds.) S. Ratynskaia, P. Mantica, A. Benuzzi-Mounaix et al. ECA **38F**, European Physical Society, Geneva, P1.006 (2014).

Stechow, A. v., Bohlin, H., Rahbarnia, K., Grulke, O., and Klinger, T.: Current sheet dynamics in the VINETA II magnetic reconnection experiment. 41st EPS Conference on Plasma Physics, (Eds.) S. Ratynskaia, P. Mantica, A. Benuzzi-Mounaix et al. ECA **38F**, European Physical Society, Geneva, P4.111 (2014).

Tardini, G., Bilato, R., Weiland, M., and ASDEX Upgrade Team: Detection of 2nd harmonic deuterium acceleration by ICRF in ASDEX Upgrade NBI heated discharges via neutron spectrometry. 41st EPS Conference on Plasma Physics, (Eds.) S. Ratynskaia, P. Mantica, A. Benuzzi-Mounaix et al. ECA **38F**, European Physical Society, Geneva, O2.103 (2014).

Thomsen, H., Burhenn, R., Assmann, J., Bertschinger, G., Biel, W., Buttenschön, B., Grosser, K., Hahnke, E., Ksiazek, I., Langenberg, A., Marchuk, O., Pablant, N., Zhang, D., and Pedersen, T. S.: Prospects of the impurity transport diagnostics in Wendelstein 7-X stellarator. 41st EPS Conference on Plasma Physics, (Eds.) S. Ratynskaia, P. Mantica, A. Benuzzi-Mounaix et al. ECA **38F**, European Physical Society, Geneva, P1.075 (2014).

Turkin, Y., Geiger, J., Maaßberg, H., Beidler, C. D., and Marushchenko, N. B.: Transport modelling of operational scenarios in W7-X. 41st EPS Conference on Plasma Physics, (Eds.) S. Ratynskaia, P. Mantica, A. Benuzzi-Mounaix et al. ECA **38F**, European Physical Society, Geneva, P1.086 (2014).

Van Eester, D., Lerche, E., Jacquet, P., Bobkov, V., Czarnecka, A., Colas, L., Crombé, K., Dumont, R., Ericsson, G., Eriksson, J., Giroud, C., Goniche, M., Graham, M., Kiptily, V., Ongena, J., Pütterich, T., Rimini, F., Santala, M., and JET EFDA Contributors: Minority ion cyclotron resonance heating in H-mode in presence of the ITER-like wall in JET. 41st EPS Conference on Plasma Physics (Eds.) S. Ratynskaia, P. Mantica, A. Benuzzi-Mounaix et al. ECA **38F**, European Physical Society, Geneva, P1.002 (2014).

Velasco, J. L., López-Bruna, D., Satake, S., Ascasíbar, E., Dinklage, A., Estrada, T., McCarthy, K. J., Medina, F., Ochando, M., and Yokoyama, M.: Validation of local and non-local neoclassical predictions for the radial transport of plasmas of low ion collisionallity. 41st EPS Conference on Plasma Physics, (Eds.) S. Ratynskaia, P. Mantica, A. Benuzzi-Mounaix et al. ECA **38F**, European Physical Society, Geneva, P2.077 (2014).

Vezinet, D., Decker, J., Peysson, Y., Puetterich, T., Mazon, D., and Meyer, O.: LHCD-induced soft X-ray poloidal asymmetry during tungsten trace injection: investigating radiative processes. 41st EPS Conference on Plasma Physics, (Eds.) S. Ratynskaia, P. Mantica, A. Benuzzi-Mounaix et al. ECA **38F**, European Physical Society, Geneva, P5.056 (2014).

Vries, P. C. d., Pautasso, G., Nardon, E., Cahyna, P., Gerasimov, S., Maraschek, M., Lehnen, M., Huijsmans, G. T. A., Hender, T. C., and JET EFDA Contributors: MHD perturbation amplitudes required to trigger disruptions. 41st EPS Conference on Plasma Physics, (Eds.) S. Ratynskaia, P. Mantica, A. Benuzzi-Mounaix et al. ECA **38F**, European Physical Society, Geneva, O5.133 (2014).

Wolfrum, E., Wiesinger, M., Barrera Orte, L., Bernert, M., Dunne, M., Fischer, R., Potzel, S., Schneider, P. A., Suttrop, W., and ASDEX Upgrade Team: Pedestal properties of mitigated ELMy H-modes at high density at ASDEX Upgrade. 41st EPS Conference on Plasma Physics, (Eds.) S. Ratynskaia, P. Mantica, A. Benuzzi-Mounaix et al. ECA **38F**, European Physical Society, Geneva, P2.006 (2014).

Yu, Q., Günter, S., and Lackner, K.: Numerical studies on sawtooth crashes. 41st EPS Conference on Plasma Physics, (Eds.) S. Ratynskaia, P. Mantica, A. Benuzzi-Mounaix et al. ECA **38F**, European Physical Society, Geneva, P2.020 (2014).

Zeng, L., Koslowski, H. R., Liang, Y., Lvovskiy, A., Lehnen, M., Bozhenkov, S. A., Chen, Z., Dong, Y., Zhang, Y., Gao, X., Denner, P., Pearson, J., and Rack, M.: Experimental observation of magnetic turbulence causing runaway electron losses during tokamak disruptions. 41st EPS Conference on Plasma Physics, (Eds.) S. Ratynskaia, P. Mantica, A. Benuzzi-Mounaix et al. ECA **38F**, European Physical Society, Geneva, O4.123 (2014).

Zhang, D., Dux, R., Burhenn, R., Thomsen, H., Jenzsch, H., König, R., and Pedersen, T. S.: Feasibility Assessment of Bolometry as Impurity Transport Study Tool for the Stellarator W7-X. 41st EPS Conference on Plasma Physics, (Eds.) S. Ratynskaia, P. Mantica, A. Benuzzi-Mounaix et al. ECA **38F**, European Physical Society, Geneva, P1.068 (2014).

Theses

Astfalk, P.: Vlasov-hybrid simulations of firehose-unstable plasmas. Master, Ludwig-Maximilians-Universität München (2014).

Cristofaro, S.: Characterisation of the BATMAN beam properties by H_α-Doppler shift spectroscopy and mini-STRIKE calorimeter. Master, Università degli studi di Padova (2014).

Denk, S.: Non-thermal electron energy distributions in microwave heated plasmas measured via electron cyclotron emission. Master, Technische Universität München (2014).

Dibon, M. M.: Entwicklung und Verbesserung eines Blower Gun Pellet Injektors für die Anwendung in thermonukleren Fusionsanlagen. Master, Technische Universität München (2014).

Dostal, M.: Erzeugung und Einschluss relativistischer Elektronen mit großem parallelem Impuls am Stellarator WEGA. Master, Universität Rostock (2014).

Encke, O.: Interaction of N&D ions with tungsten. Diploma, Universität Ulm (2014).

Eulenberg, P.: Detektionsalgorithmus für Sägezahncrashs in magnetisch eingeschlossenen Fusionsplasmen. Bachelor, Ludwig-Maximilians-Universität München (2014).

Faitsch, M.: Thermographie des oberern Divertors an AUG. Master, Universität Ulm, Ulm (2014).

Fochi, A.: Improvement of microwave Doppler reflectometry analysis methodology. Bachelor, Ludwig-Maximilians-Universität München (2014).

Gallitscher, J.: Einfluss der Lage des Temperaturprofils auf die Auswertung des Randdichteprofils aus der Lithiumstrahldiagnostik am Tokamak ASDEX Upgrade. Bachelor, Technische Universität München (2014).

Guggemos, T.: Entwicklung einer schnellen Messvorrichtung zur Detektion von Fehlerströmen in einer Umrichteranlage des Kernfusionsexperimentes ASDEX Upgrade. Bachelor, Hochschule für angewandte Wissenschaften München (2014).

Haecker, R.: Influence of impurity profiles on the evaluation of density profiles from the Lithium beam diagnostic at the ASDEX Upgrade tokamak. Bachelor, Technische Universität München (2014).

Han, Y.: Investigation of mechanical behaviour of recrystallization stabilized tungsten wire for the application in tungsten fibre-reinforced tungsten composites. Master, Technische Universität München (2014).

Hauertmann, L.: Effect of Plasma Rotation on the Magnetic Equilibrium of Fusion Plasmas. Bachelor, Technische Universität München (2014).

Homner, N.: Kollimatoroptimierung für die ITER-Bolometerdiagnostik mittels Monte-Carlo Raytracing. Bachelor, Ludwig-Maximilians-Universität München (2014).

Köhler, M.: Simulation of the interaction of implantation and diffusion in selected systems using Monte Carlo techniques. Bachelor, Ludwig-Maximilians-Universität München (2014).

Lebschy, A.: Electron density reconstruction using beam emission spectroscopy on a heating beam. Master, Ludwig-Maximilians-Universität München (2014).

Linz, G.: Untersuchung der Spalt und Stufenbildung zwischen Hitzeschutzbauteilen aufgrund thermo-mechanischer Verformung am Fusionsexperiment Wendelstein 7-X. Master, Brandenburgische Technische Universität Cottbus (2014).

Mink, F.: Verbesserung der Bestimmung von Speziesverteilung und Strahlgeometrie der Neutralinjektion an ASDEX Upgrade. Master, Ludwig-Maximilians-Universität München (2014).

Paradela Perez, I.: Study of geometry and plasma current effects on the power spreading in tokamak divertor using SOLPS. Master, Technische Universität München (2014).

Pimazzoni, A.: Investigation of ELISE beam properties by means of the diagnostic calorimeter. Master, Università degli studi di Padova (2014).

Sacco, M.: FEM-BEM approach for crack growth assessment in magnet system of modular stellarator (W7-X) for nuclear fusion. Master, University of Salerno (2014).

Shalaby, S. A.: Parameterstudien für Monte Carlo Ray Tracing von ITER Bolometer. Bachelor, Technische Universität München (2014).

Zolchow, M.: Investigation of an In-situ Calibration Method for the Imaging MSE-Diagnostic on ASDEX Upgrade Utilizing the Edge Zeeman Emission. Master, Ernst-Moritz-Arndt Universität Greifswald (2014).

PhD-Theses

Bohlin, H.: Global dynamics of magnetic reconnection in VINETA II. Ernst-Moritz-Arndt-Universität Greifswald (2014).

Feher, T. B.: Simulation of the interaction between Alfvén waves and fast particles. Ernst-Moritz-Arndt-Universität Greifswald (2014).

Proll, J. H. E.: Trapped-particle Instabilities in Quasi-isodynamic Stellarators. Ernst-Moritz-Arndt-Universität Greifswald (2014).

Reimold, F.: Divertor Detachment of H-mode Plasmas in ASDEX Upgrade. Technische Universität München (2014).

Ruf, B.: Reconstruction of Negative Hydrogen Ion Beam Properties from Beamline Diagnostics. Universität Augsburg (2014).

Schaber, K.: Integration of Variable Renewable Energies in the European power system: a model-based analysis of transmission grid extensions and energy sector coupling. Technische Universität München (2014).

Sieglin, B.: Experimental Investigation of Heat Transport and Divertor Loads of Fusion Plasma in All Metal ASDEX Upgrade and JET. Technische Universität München (2014).

Sode, M.: Quantitative Beschreibung von Wasserstoff-Stickstoff-Argon-Mischplasmen. Christian-Albrechts-Universität Kiel (2014).

Wimmer, C.: Characteristics and Dynamics of the Boundary Layer in RF-driven Sources for Negative Hydrogen Ions. Universität Augsburg (2014).

Patents

Pedersen, T. S., and Paschkowski, N.: Anordnung elektrischer Leiter und Verfahren zur Herstellung einer Anordnung elektrischer Leiter. Die Erfindung wurde vom IPP als in Anspruch genommen. Deutsche Patentanmeldung 10 2014 017 857.9.

Mlynek, A., Ford, O., and Plöckl, B.: Terahertz – Polarimeter. Erfindungsmeldung: 08.12.2014. Eine mögliche Patentierung wird derzeit geprüft.

Hergenhahn, U., and Förstel, M.: Apparat zum Herstellen mikrohydierter Moleküle einer verdampften Substanz (A source for microhydrated biomolecules). Erfindungsmeldung: 08.12.2014. Eine mögliche Patentierung wird derzeit geprüft.

Laboratory Reports

Internal IPP Reports
IPP 1/353
Fietz, S.: Influence of plasma rotation on tearing mode stability on the ASDEX Upgrade. 104 p. (2014).

IPP 1/354
Dibon, M. M.: Entwicklung und Verbesserung eines Blower Gun Pellet Injektors für die Anwendung in thermonukleren Fusionsanlagen. 124 p. (2014)

IPP 1/355
Leuterer, F., and Kaufmann, M.: Interaction between an electron and an electromagnetic wave. 22 p. (2014).

IPP 4/292
Meister, H., and Schmitt, S.: Entwicklung und Test von Prototypkomponenten für die ITER Bolometerdiagnostik. 96 p. (2014).

IPP 4/293
Friedl, R.: Experimental investigations on the caesium dynamics in H_2/D_2 low temperature plasmas. 256 p. (2014).

IPP 12/12
Proll, J. H. E.: Trapped-particle Instabilities in Quasi-isodynamic Stellarators. 128 p. (2014).

IPP 13/22
Feher, T. B.: Simulation of the interaction between Alfvén waves and fast particles. 205 p. (2014).

IPP 13/23
Torrisi, S., and Warmer, F.: Design of an N-Dimensional Parameter Scanner for the Systems Code PROCESS. 37 p. (2014).

IPP 17/40
Dunne, M.: Inter-ELM evolution of the edge current density profile on the ASDEX Upgrade tokamak. 166 p.(2014).

IPP 17/41
Burckhart, A.: Different ELM regimes at ASDEX Upgrade and their linear stability analysis. 110 p. (2014).

IPP 17/42
Sode, M.: Quantitative Beschreibung von Wasserstoff-Stickstoff-Argon-Mischplasmen. 210 p. (2014).

IPP 19/3
Kang, K. S.: The parallel multigrid and domain decomposition methods for an elliptic problem on a hexagonal domain with structured triangular meshes. 61 p. (2014).

Lectures

Aho-Mantila, L., Carralero, D., Conway, G. D., Müller, H. W., Müller, S. H., Potzel, S., Reimold, F., Scarabosio, A., Wischmeier, M., and ASDEX Upgrade Team: Connecting SOL transport with divertor exhaust physics. (19th Joint EU-US Transport Task Force Meeting (TTF 2014), 2014-09-08 to 2014-09-11, Culham).

Aho-Mantila, L., Conway, G. D., Müller, H. W., Müller, S., Potzel, S., Coster, D., Wischmeier, M., Meigs, A., Stamp, M., ASDEX Upgrade Team, and JET-EFDA Contributors: Assessment of Scrape-off Layer Simulations with Drifts against L-mode Experiments in ASDEX Upgrade and JET. (25th IAEA Fusion Energy Conference (FEC 2014), 2014-10-13 to 2014-10-18, Saint Petersburg).

Aho-Mantila, L., Lowry, C., Marsen, S., Müller, H. W., Potzel, S., Wischmeier, M., Bonnin, X., Brezinsek, S., Federici, G., ASDEX Upgrade Team, and JET-EFDA Contributors: Validated model-based radiation scalings for the ITER-like divertors of JET and ASDEX Upgrade. (21st International Conference on Plasma Surface Interactions 2014 (PSI 21), 2014-05-26 to 2014-05-30, Kanazawa).

Albajar, F., Bornatici, M., and Engelmann, F.: EC Radiative Transport and Losses in DEMO-like High-temperature Plasmas. (18th Joint Workshop on Electron Cyclotron Emission and Electron Cyclotron Resonance Heating, 2014-04-22 to 2014-04-25, Nara).

Alcuson, J., Reynolds-Barredo, J. M., Sanchez, R., and Xanthopoulos, P.: Development of tracer technology to characterize radial turbulent transport in stellarator geometry using the GENE gyrokinetic code. (19th Joint EU-US Transport Task Force Meeting (TTF 2014), 2014-09-08 to 2014-09-11, Culham).

Alimov, V. K., Hatano, Y., Roth, J., Sugiyama, K., Oyaidzu, M., Baldwin, M., Doerner, R., 't Hoen, M. H. J., Lee, H. T., Ueda, Y., Matsuyama, M., and Hayashi, T.: Deuterium retention in reduced activation ferritic martensitic steels exposed to D plasmas and irradiated with D ions. (12th International Workshop on Hydrogen Isotopes in Fusion Reactor Materials (HWS-12), 2014-06-02 to 2014-06-04, Toyama).

Alimov, V. K., Hatano, Y., Sugiyama, K., Balden, M., Elgeti, S., Oyaidzu, M., Akamaru, S., Hayashi, T., and Matsuyama, M.: Surface morphology and deuterium retention in tungsten and tungsten-rhenium alloy exposed to low-energy, high flux D plasma. (21st International Conference on Plasma Surface Interactions 2014 (PSI 21), 2014-05-26 to 2014-05-30, Kanazawa).

Alonso, J. A., Garcia-Regana, J. M., Pedrosa, M. A., Hidalgo, C., Velasco, J. L., Calvo, I., Silva, C., Helander, P., and Kleiber, R.: Electrostatic potential variations along flux surfaces as an ingredient of radial impurity transport. (19th Joint EU-US Transport Task Force Meeting (TTF 2014), 2014-09-08 to 2014-09-11, Culham).

Alonso, J. A., Pedrosa, M. A., Hidalgo, C., Garcia-Regana, J. M., Velasco, J. L., Calvo, I., and Silva, C.: In-surface electrostatic potential variations in the TJ-II stellarator. (41st EPS Conference on Plasma Physics, 2014-06-23 to 2014-06-27, Berlin).

Andreeva, T., Bykov, V., Bräuer, T., Egorov, K., Endler, M., Fellinger, J., Kißlinger, J., Köppen, M., and Schauer, F.: Final Assessment of Wendelstein 7-X Magnetic Pertubations Caused by Construction Asymetries. (25th IAEA Fusion Energy Conference (FEC 2014), 2014-10-13 to 2014-10-18, Saint Petersburg).

Angioni, C.: Tungsten Transport in the Core of JET H-mode Plasmas, Experiments and Modelling. (56th Annual Meeting of the APS Division of Plasma Physics, 2014-10-27 to 2014-10-31, New Orleans, LA).

Angioni, C., Belli, E. A., Bilato, R., Casson, F. J., Mazon, D., Odstrcil, T., Pütterich, T., and ASDEX Upgrade Team: Theoretical modelling of W transport in ASDEX Upgrade. (19th Joint EU-US Transport Task Force Meeting (TTF 2014), 2014-09-08 to 2014-09-11, Culham).

Arden, N., Eixenberger, H., Rott, M., Schandrul, M., Suttrop, W., and Teschke, M.: Control system and DC-link supply of the inverter system BUSSARD for ASDEX Upgrade in vessel saddle coils. (28th Symposium on Fusion Technology (SOFT 2014), 2014-09-29 to 2014-10-03, San Sebastian).

Arnoux, G., Coenen, J., Balboa, I., Bazylev, B., Clever, M., Corre, Y., Dejarnac, R., Devaux, S., Eich, T., Gauthier, E., Frassinetti, L., Horacek, J., Jachmich, S., Kinna, D., Marsen, S., Matthews, G. F., Mertens, P., Pitts, R. A., Rack, M., Sergienko, G., Sieglin, B., and Thompson, V.: Thermal analysis of an exposed tungsten edge in the JET divertor. (21st International Conference on Plasma Surface Interactions 2014 (PSI 21), 2014-05-26 to 2014-05-30, Kanazawa).

Bader, A., Stephey, L. A., Anderson, D. T., Feng, Y., Hegna, C. C., Schmitz, O., and Talmadge, J. N.: Simulated Stellarator Edge Behavior with Modified HSX Coils. (56th Annual Meeting of the APS Division of Plasma Physics, 2014-10-27 to 2014-10-31, New Orleans, LA).

Balden, M., Elgeti, S., Alimov, V. K., Sugiyama, K., Roth, J., Ogorodnikova, O., Matern, G., Maier, H., Hatano, Y., Oyaidzu, M., Yamanishi, T., Hayashi, T., Lee, H. T., Ueda, Y., 't Hoen, M. H. J., De Temmerman, G., Rasinski, M.,

Fortuna-Zalesnag, E., Kurzydlowski, K. J., Doerner, R. P., and Baldwin, M. J.: Surface modifications of RAFM steels by deuterium exposure: Variation from coral-like/fuzz-like to blister-like features. (21st International Conference on Plasma Surface Interactions 2014 (PSI 21), 2014-05-26 to 2014-05-30, Kanazawa).

Balden, M., Manhard, A., and Elgeti, S.: Strong influence of the tungsten grade on deuterium retention and on morphological modifications of the surface after deuterium plasma loading. (12th International Workshop on Hydrogen Isotopes in Fusion Reactor Materials (HWS-12), 2014-06-02 to 2014-06-04, Toyama).

Baron-Wiechec, A., Widdowson, A., Alves, E., Ayres, C. F., Barradas, N. P., Brezinsek, S., Catarino, N., Coad, P., Heinola, K., Likonen, J., Matthews, G. F., Mayer, M., Petersson, P., Rubel, M., Renterghem, W. v., and JET-EFDA Contributors: Global erosion and deposition patterns in JET with the ITER-like Wall. (21st International Conference on Plasma Surface Interactions 2014 (PSI 21), 2014-05-26 to 2014-05-30, Kanazawa).

Baruzzo, M., Alper, B., Angioni, C., Baranov, Y., Buratti, P., Casson, F., Hender, T., Mantica, P., Marchetto, C., Taroni, L. L., and Valisa, M.: Neoclassical Tearing Modes characterization in JET ILW operation. (56th Annual Meeting of the APS Division of Plasma Physics, 2014-10-27 to 2014-10-31, New Orleans, LA).

Battes, K., Day, C., and Rohde, V.: Basic considerations on the pump-down time in the dwell phase of a pulsed fusion DEMO. (28th Symposium on Fusion Technology (SOFT 2014), 2014-09-29 to 2014-10-03, San Sebastian).

Bazylev, B., Arnoux, G., Coenen, J. W., Clever, M., Coffey, J., Corre, Y., Dejarnac, R., Devaux, S., Gauthier, E., Horacek, J., Hirai, T., Jachmich, S., Knaup, M., Krieger, K., Marsen, S., Matthews, G., Meigs, A., Mertens, P., Pitts, R., Pütterich, T., Stamp, M., Sergienko, G., Tamain, P., and Thompson, V.: Modelling of Melt Damage of Tungsten Armour under Multiple Transients Expected in ITER and Validations against JET-ILW Experiments. (25th IAEA Fusion Energy Conference (FEC 2014), 2014-10-13 to 2014-10-18, Saint Petersburg).

Bazylev, B., Arnoux, G., Coenen, J. W., Matthews, G. F., Mertens, P., Knaup, M., Jachmich, S., Clever, M., Dejarnac, R., Coffey, I., Corre, Y., Devaux, S., Gauthier, E., Horacek, J., Krieger, K., Marsen, S., Meigs, A., Pitts, R. A., Puetterich, T., Rack, M., Stamp, M., Sergienko, G., Tamain, P., Thompson, V., and JET-EFDA Contributors: MEMOS code validation on JET transient tungsten melting experiments. (21st International Conference on Plasma Surface Interactions 2014 (PSI 21), 2014-05-26 to 2014-05-30, Kanazawa).

Becoulet, M., Orain, F., Morales, J., Garbet, X., Dif-Pradalier, G., Passeron, C., Latu, G., Nardon, E., Fil, A., Grandgirard, V., Huijsmans, G., Pamela, S., Kirk, A., Hoelzl, M., Franck, E., Sonnendrücker, E., Nkonga, B., and Cahyna, P.: Non-linear MHD Modelling of Edge Localized Modes and their Interaction with Resonant Magnetic Perturbations in Rotating Plasmas. (25th IAEA Fusion Energy Conference (FEC 2014), 2014-10-13 to 2014-10-18, Saint Petersburg).

Belonohy, E., Abreu, P., Beurskens, M., Boom, J., Brix, M., Flanagan, J., Gerasimov, S., Kempenaars, M., Luna, E. d. l., Lupelli, I., Maslov, M., Meneses, L., Salmon, R., Schmuck, S., Shaw, S. R., Sirinelli, A., Solano, E. R., and JET EFDA Contributors: The effect of the accuracy of toroidal field measurements on spatial consistency of kinetic profiles at JET. (28th Symposium on Fusion Technology (SOFT 2014), 2014-09-29 to 2014-10-03, San Sebastian).

Bernert, M., Carralero, D., Eich, T., Kallenbach, A., Reimold, F., and ASDEX Upgrade Team: The H-mode density limit at the ASDEX Upgrade tokamak. (41st EPS Conference on Plasma Physics, 2014-06-23 to 2014-06-27, Berlin).

Bertelli, N., Phillips, C. K., Valeo, E. J., Bilato, R., Brambilla, M., Jaeger, E. F., and Bonoli, P. T.: Benchmark of ICRF codes in mid and high harmonic regimes in view of NSTX-U operation. (56th Annual Meeting of the APS Division of Plasma Physics, 2014-10-27 to 2014-10-31, New Orleans, LA).

Biancalani, A., Bottino, A., Briguglio, S., Conway, G. D., Troia, C. D., Kleiber, R., Könies, A., Lauber, P., Mishchenko, A., Scott, B. D., Simon, P., Vlad, G., Wang, X., Zarzoso, D., Zocco, A., Zonca, F., and ASDEX Upgrade Team: Global Gyrokinetic Modeling of Geodesic Acoustic Modes and Shear Alfvén Instabilities in ASDEX Upgrade. (25th IAEA Fusion Energy Conference (FEC 2014), 2014-10-13 to 2014-10-18, Saint Petersburg).

Biancalani, A.: Verification of GK codes on linear collisionless dynamics of axisymmetric modes in tokamaks. (Numerical Methods for the Kinetic Equations of Plasma Physics (NumKin2014), 2014-10-20 to 2014-10-24, Garching).

Biel, W., Baar, M. d., Dinklage, A., Felici, F., König, R., Meister, H., Treutterer, W., and Wenninger, R.: DEMO diagnostics and burn control. (28th Symposium of Fusion Technology (SOFT 2014), 2014-09-29 to 2014-10-03, San Sebastian).

Bilato, R., Brambilla, M., and Fable, E.: Simulations of fast-wave current drive in pulsed and steady-state DEMO designs. (Joint Varenna-Lausanne International Workshop on Theory of Fusion Plasmas, 2014-09-01 to 2014-09-05, Varenna).

Birkenmeier, G., Carralero, D., Komm, M., Müller, H. W., Müller, S. H., Groth, M., Brix, M., Manz, P., Laggner, F. M., Bernert, M., Fuchert, G., Krieger, K., Wolfrum, E., Stroth, U., and ASDEX Upgrade Team: Eperimental results of SOL transport in high and low density discharges. (19th Joint EU-US Transport Task Force Meeting (TTF 2014), 2014-09-08 to 2014-09-11, Culham).

Birkenmeier, G., Manz, P., Carralero, D., Laggner, F., Willensdorfer, M., Wolfrum, E., Fuchert, G., Stroth, U., and ASDEX Upgrade Team: Die Physik intermittenter Transport-prozesse in der Randschicht von Fusionsplasmen. (78. DPG-Jahrestagung und Frühjahrstagung der Sektion AMOP, 2014-03-17 to 2014-03-21, Berlin).

Birkenmeier, G, Manz, P., Carralero, D., Laggner, F., Bernert, M., Kobayashi, T., Fuchert, G., Krieger, K., Reimold, F., Schmid, K., Willensdorfer, M., Wolfrum, E., and Stroth, U.: Filament Transport in the SOL of ASDEX Upgrade. (25th IAEA Fusion Energy Conference (FEC 2014), 2014-10-13 to 2014-10-18, Saint Petersburg).

Bizarro, J. P. S., Köchl, F., Romanelli, M., Challis, C., Hobirk, J., Koskela, T., and JET-EFDA Contributors: Modelling of core connement in JET Carbon vs. ITER-like wall discharges. (19th Joint EU-US Transport Task Force Meeting (TTF 2014), 2014-09-08 to 2014-09-11, Culham).

Blackwell, B., Haskey, S., Howard, J., Pretty, D., Thorman, A., Bertram, J., Hole, M. J., Könies, A., Nührenberg, C., and Dewar, R.: Structure and Scaling of Fluctuations in the MHD Range in the H-1NF HELIAC. (25th IAEA Fusion Energy Conference (FEC 2014), 2014-10-13 to 2014-10-18, Saint Petersburg).

Bobyr, N. P., Alimov, V. K., Khripunov, B. I., Spitsyn, A. V., Hatano, Y., Golubeva, A. V., and Petrov, V. B.: Influence of Helium on Hydrogen Isotope Exchange in Tungsten at Sequential Exposures to Deuterium and Helium-Protium Plasmas. (21st International Conference on Plasma Surface Interactions 2014 (PSI 21), 2014-05-26 to 2014-05-30, Kanazawa).

Bobyr, N. P., Spitsyn, A. V., Golubeva, A., Mayer, M., Hatano, Y., Klimov, N. S., Khripunov, B. I., Alimov, V. K., Cherkez, D. I., Ogorodnikova, O. V., and Chernov, V. M.: Hydrogen Isotopes Retention in Low-activated Structural Materials. (12th International Workshop on Hydrogen Isotopes in Fusion Reactor Materials (HWS-12), 2014-06-02 to 2014-06-04, Toyama).

Bock, A., Stober, J., Fischer, R., McCarthy, P., Reich, M., and ASDEX Upgrade Team: Reconstruction of q-profiles using Monte-Carlo-technique. (78. DPG-Jahrestagung und Frühjahrstagung der Sektion AMOP, 2014-03-17 to 2014-03-21, Berlin).

Bonomo, F., Barbisan, M., Cristofaro, S., Ruf, B., Fantz, U., Franzen, P., Pasqualotto, R., Riedl, R., Schiesko, L., Serianni, G, Wünderlich, D., and NNBI Team: BATMAN Beam Properties Characterization by the Beam Emission Spectrocopy Diagnostic. (4th International Symposium on Negative Ions, Beams and Sources (NIBS 2014), 2014-10-06 to 2014-10-10, Garching).

Borchardt, M., Drevlak, M., Eder, T., Hirsch, M., Kemnitz, B., Kleiber, A., Kleiber, R., Könies, A., and Riemann, J.: Energie-versorgung der Zukunft: Potentiale und Hürden Fortbildung für Lehrerinnen und Lehrer. (Lehrerfortbildung, 2014-02-05, Garching).

Borchardt, M., Drevlak, M., Eder, T., Kemnitz, B., Kleiber, R., Kleiber, A., Könies, A., and Riemann, J.: Energieversorgung der Zukunft: Potentiale und Hürden. (Lehrerfortbildung, 2014-11-21, Greifswald).

Boscary, J., Lore, J., Lumsdaine, A., Maier, M., McGinnis, D., Peacock, A., and Tretter, J.: Development Activities of the High Heat Flux Scraper Element. (28th Symposium on Fusion Technology (SOFT 2014), 2014-09-29 to 2014-10-03, San Sebastian).

Bosch, H.-S.: Struktur der Materie. Vorlesung (SS 2014. Vorlesung, Ernst-Moritz-Arndt Universität Greifswald).

Bosch, H.-S., and W7-X Team: Experience with the comissioning of the superconducting Stellarator Wendelstein 7-X. (28th Symposium on Fusion Technology (SOFT 2014), 2014-09-29 to 2014-10-03, San Sebastian).

Bottino, A.: Introduction to particle-in-cell methods for the simulation of the Vlasov-Maxwell gyrokinetic equations. (7th ITER International School, 2014-08-25 to 2014-08-29, Aix-en-Provence).

Bottino, A., Biancalani, A., Zarzoso, D., and Villard, L.: Simulations of energetic particle driven instabilities in Tokamak. (Platform for Advanced Scientific Computing Conference 2014 (PASC), 2014-06-02 to 2014-06-03, Zurich).

Bourdelle, C., Beyer, P., Chôné, L., Citrin, J., Dif-Pradalier, G., Fedorczak, N., Fuhr, G., Garbet, X., Loarte, A., Maggi, C. F., Militello, F., and Sarazin, Y.: L to H mode transition: Parametric dependencies of the temperature threshold. (19th Joint EU-US Transport Task Force Meeting (TTF 2014), 2014-09-08 to 2014-09-11, Culham).

Bourdelle, C., Fedorczak, N., Loarte, A., Militello, F., Maggi, C., Dif-Pradalier, G, Garbet, X., and Citrin, J.: L to H Mode Transition: Parametric Dependencies of the Temperature Threshold. (25th IAEA Fusion Energy Conference (FEC 2014), 2014-10-13 to 2014-10-18, Saint Petersburg).

Brand, H. v. d., Baar, M. R. d., Berkel, M. v., Bongers, W. A., Doelman, N., Giannone, L., Kasparek, W., Stober, J. K., Wagner, D., Westerhof, E., and ASDEX Upgrade Team: Detection of MHD instabilities with ECE. (18th Joint Workshop on Electron Cyclotron Emission and Electron Cyclotron Resonance Heating, 2014-04-22 to 2014-04-25, Nara).

Bratanov, V., Jenko, F., Hatch, D., and Wilczek, M.: Non-universal power-law spectra in turbulent systems. (78. DPG-Jahrestagung und Frühjahrstagung der Sektion AMOP, 2014-03-17 to 2014-03-21, Berlin).

Bravenec, R., Goerler, T., Told, D., Jenko, F., Pueschel, M. J., McKee, G., Candy, J., Garofalo, A., Smith, S., Staebler, G., Barnes, M., Holland, C., Ding, S., and Rhodes, T.: Benchmarking of the Gyrokinetic Microstability Codes GENE, GS2, and GYRO over a Range of Plasma Parameters. (56th Annual Meeting of the APS Division of Plasma Physics, 2014-10-27 to 2014-10-31, New Orleans, LA).

Brezinsek, S., Philipps, V. P., Matthews, G., Rubel, M., Borodin, D., Schmid, K., Widdowson, A., Mayer, M., Stamp, M., Likonen, J., Baron-Wiechec, A., Coad, P., Garcia-Carasco, A., Heinola, K., Kirschner, A., Krat, S., Linsmeier, C., Lipschultz, B., and Petersson, P.: Beryllium Migration in JET ITER-like Wall Plasmas. (25th IAEA Fusion Energy Conference (FEC 2014), 2014-10-13 to 2014-10-18, Saint Petersburg).

Briefi, S., and Fantz, U.: Alternative RF coupling concepts for H- ion sources. (4th International Symposium on Negative Ions, Beams and Sources (NIBS 2014), 2014-10-06 to 2014-10-10, Garching).

Briefi, S., Gutmann, P., Doerfler, J., and Fantz, U.: Alternative HF-Einkopplungsmethoden für Quellen negativer Wasserstoffionen für die Neutralteilchenheizung von Fusionsexperimenten. (78. DPG-Jahrestagung und Frühjahrstagung der Sektion AMOP, 2014-03-17 to 2014-03-21, Berlin).

Brombin, M., Spolare, M., Serianni, G., Pomaro, N., Taliercio, C., Dalla Palma, M., Pasqualotto, R., and Schiesko, L.: Langmuir probes for SPIDER experiment: tests in BATMAN. (20th Topical Conference on High-Temperature Plasma Diagnostics (HTPD 2014), 2014-06-01 to 2014-06-05, Atlanta, GA).

Bulanin, V, Gusev, V, Iblyaminova, A., Khromov, N., Kurskiev, G, Minaev, V., Patrov, M., Petrov, A., Petrov, Y., Sakharov, N., *Shchegolev, P., Tolstyakov, S., Varfolomeev, V., Wagner, F., and Yashin, A.:* Geodesic Acoustic Mode Investigation in the Spherical Globus-M Tokamak Using a Multi-diagnostic Approach. (25th IAEA Fusion Energy Conference (FEC 2014), 2014-10-13 to 2014-10-18, Saint Petersburg).

Bungartz, H.-J., Görler, T., Jarema, D., Jenko, F., Neckel, T., and Told, D.: Block Structured Grids for GENE (Gyrokinetic Electromagnetic Numerical Experiment). (78. DPG-Jahrestagung und Frühjahrstagung der Sektion AMOP, 2014-03-17 to 2014-03-21, Berlin).

Buttenschön, B.: Plasma Wakefield Acceleration: Ein neues Beschleunigerkonzept zur Erzeugung hochenergetischer Elektronen- und Positronenstrahlen. (Physikalisches Kolloquium, 2014-07-01, Universität Kiel).

Buttenschön, B., Kempkes, P., Grulke, O., and Klinger, T.: A high power helicon discharge as plasma cell for future plasma wakefield accelerators. (5th Conference on Power Electronics for Plasma Engineering (PE2 2014), 2014-05-20 to 2014-05-22, Warsaw).

Buttenschön, B., Kempkes, P., Grulke, O., and Klinger, T.: A high power helicon discharge as prototype for a plasma wakefield accelerator experiment. (78. DPG-Jahrestagung und Frühjahrstagung der Sektion AMOP, 2014-03-17 to 2014-03-21, Berlin).

Bykov, I., Balden, M., Bergsaker, H., Elgeti, S., Manhard, A., and Mayer, M.: Microanalysis of the lateral and depth distributions of deuterium in blistered tungsten. (12th International Workshop on Hydrogen Isotopes in Fusion Reactor Materials, 2014-06-02 to 2014-06-04, Toyama).

Bykov, V., Egorov, K., Fellinger, J., Schauer, F., Kallmeyer, J., and Gasparotto, M.: Engineering Challenges of W7-X: Mechanicel Instrumentation System for Commissioning and Operation. (21st Topical Meeting on the Technology of Fusion Energy (TOFE), 2014-11-09 to 2014-11-13, Anaheim, CA).

Califano, F., Cerri, S. S., Decamillis, S., Pegoraro, F., and Del Sarto, D.: Anisotropy generation by the Kelvin Helmoltz Instability and the role of the plasma pressure tensor. (41st EPS Conference on Plasma Physics, 2014-06-23 to 2014-06-27, Berlin).

Carralero, D., Müller, H. W., Birkenmeier, G., Groth, M., Brix, M., Kallenbach, A., Manz, P., Marné, P. d., Marsen, S., Müller, S., Potzel, S., Reimold, F., Silva, C., Stroth, U., Wischmeier, M., Wolfrum, E., ASDEX Upgrade Team, and JET-EFDA Contributors: Implications of high density operation on SOL transport: a multimachine investigation. (21st Inter-

national Conference on Plasma Surface Interactions 2014 (PSI 21), 2014-05-26 to 2014-05-30, Kanazawa).

Carralero, D., Müller, H. W., Groth, M., Komm, M., Adamek, J., Aho-Mantilla, L., Birkenmeier, G., Brix, M., Janky, F., Hacek, P., Lunt, T., Marsen, S., Reimold, F., Silva, C., Stroth, U., Potzel, S., Wischmeier, M., Wolfrum, E., ASDEX Upgrade Team, COMPASS Team, and JET-EFDA Contributors: First wall flux distribution in DEMO size devices. (22nd European Fusion Program Workshop, 2014-12-01 to 2013-12-03, Split).

Carralero, D., Müller, H. W., Groth, M., Komm, M., Adamek, J., Birkenmeier, G., Brix, M., Jankyc, F., Hacek, P., Marsen, S., Reimold, F., Silva, C., Stroth, U., Wischmeier, M., Wolfrum, E., ASDEX Upgrade Team, COMPASS Team, and JET-EFDA Contributors: The role of divertor collisionality on SOL transport: a study on the ITER stepladder. (56th Annual Meeting of the APS Division of Plasma Physics, 2014-10-27 to 2014-10-31, New Orleans, LA).

Casali, L., Bernert, M., Dux, R., Fischer, R., Kallenbach, A., Kardaun, O., Kurzan, B., Lang, P., Mlynek, A., McDermott, R., Ryter, F., Sertoli, M., Tardini, G., and Zohm, H.: Transport analysis of high radiation and high density plasmas at ASDEX Upgrade. (78. DPG-Jahrestagung und Frühjahrstagung der Sektion AMOP, 2014-03-17 to 2014-03-21, Berlin).

Casali, L., Fable, E., Dux, R., Bernert, M., and Ryter, F.: Modeling of pedestal and core radiation in nitrogen seeded H-modes at ASDEX Upgrade. (56th Annual Meeting of the APS Division of Plasma Physics, 2014-10-27 to 2014-10-31, New Orleans, LA).

Casson, F. J., Angioni, C., Belli, E., Bilato, R., Mantica, P., Valisa, M., Garzotti, L., Giroud, C., Hender, T., Marchetto, C., Pütterich, T., Reinke, M., Belo, P., Drewelow, P., Johnson, T., Koskela, T., Lauro-Taroni, L., Maggi, C., Mlynar, J., Romanelli, M., and JET-EFDA Contributors: Modelling of tungsten transport in the presence of ICRH and NTMs in JET. (19th Joint EU-US Transport Task Force Meeting (TTF 2014), 2014-09-08 to 2014-09-11, Culham).

Casson, F. J., Angioni, C., Belli, E., Hender, T., Koskela, T., Mazon, D., Mantica, P., Pütterich, T., Reinke, M., Sertoli, M., Valisa, M., Vezinet, D., Belo, P., Drewelow, P., Lauro-Taroni, L., Maggi, C., Mlynar, J., Romanelli, M., ASDEX Upgrade Team, and JET-EFDA Contributors: Theoretical description of heavy impurity transport and its application to the modelling of tungsten in JET and ASDEX Upgrade. (41st EPS Conference on Plasma Physics, 2014-06-23 to 2014-06-27, Berlin).

Cavedon, M., Pütterich, T., Viezzer, E., and ASDEX Upgrade Team: Upgrade of the Edge Charge Exchange System at the

ASDEX Upgrade tokamak. (78. DPG-Jahrestagung und Frühjahrstagung der Sektion AMOP, 2014-03-17 to 2014-03-21, Berlin).

Cavedon, M., Pütterich, T., Viezzer, E., Conway, G. D., Happel, T., Ryter, F., Simon, P., Wolfrum, E., and ASDEX Upgrade Team: Fast edge charge exchange measuremnts at the L-H transition in ASDEX Upgrade. (19th Joint EU-US Transport Task Force Meeting (TTF 2014), 2014-09-08 to 2014-09-11, Culham).

Ceccherini, F., Galeotti, L., Brambilla, M., Barnes, D. C., and Yang, X.: Propagation and dynamics of microwaves in the ECRH frequency range for the FRC. (56th Annual Meeting of the APS Division of Plasma Physics, 2014-10-27 to 2014-10-31, New Orleans, LA).

Cerri, S. S., Banon Navarro, A., Doerk, H., Told, D., and Jenko, F.: The role of collisions in 2D gyrokinetic turbulence: the freely decaying electrostatic case. (78. DPG-Jahrestagung und Frühjahrstagung der Sektion AMOP, 2014-03-17 to 2014-03-21, Berlin).

Cerri, S. S., Henri, P., Califano, F., Del Sarto, D., Faganello, M., and Pegoraro, F.: Extended MHD model and shear flow dynamics in magnetized plasmas. (41st EPS Conference on Plasma Physics, 2014-06-23 to 2014-06-27, Berlin).

Challis, C., Dux, R., Hennequin, P., Reich, M., Schneider, P., Schweinzer, J., Stober, J., ASDEX Upgrade Team, Tala, T., and JET Contributors: Report on ITPA-IOS Joint Experiment 4.2. (13th Energetic Particle Physics ITPA TG Meeting, 2014-10-21 to 2014-10-23, Padova).

Challis, C., Garcia, J., Beurskens, M., Buratti, P., Frassinetti, L., Giroud, C., Hawkes, N., Hobirk, J., Joffrin, E., Keeling, D., King, D., Marchetto, C., Mailloux, J., McDonald, D., Ferreira Nunes, I. M., Pucella, G., Saarelma, S., and Simpson, J.: Improved Confinement in JET High Beta Plasmas with an ITER-like Wall. (25th IAEA Fusion Energy Conference (FEC 2014), 2014-10-13 to 2014-10-18, Saint Petersburg).

Chankin, A. V., and Coster, D. P.: On the locality of parallel transport of heat carrying electrons in the SOL. (21st International Conference on Plasma Surface Interactions 2014 (PSI 21), 2014-05-26 to 2014-05-30, Kanazawa).

Chiang, H.-Y., Park, S.-H., Mayer, M., Schmid, K., Balden, M., and Petry, W.: Swift Heavy Ion Irradiaton in a High Fluence: Material Selection of Nuclear Fuel UMo for Research Reactors. (19th International Conference on Ion Beam Modification of Materials (IBMM), 2014-09-14 to 2014-09-19, Leuven).

Chikada, T., Suzuki, A., Terai, T., and Koch, F.: Deuterium permeation in erbium oxide coating and RAFM steel via liquid Li-Pb alloy. (28th Symposium on Fusion Technology (SOFT 2014), 2014-09-29 to 2014-10-03, San Sebastian).

Citrin, J., Garcia, J., Jenko, F., Mantica, P., Told, D., Bourdelle, C., Dumont, R., Haverkort, J. W., Hogeweij, G. M. D., Johnson, T., Pueschel, M. J., and JET-EFDA Contributors: The significant role of fast ions in nonlinear electromagnetic stabilization of tokamak microturbulence. (41st EPS Conference on Plasma Physics, 2014-06-23 to 2014-06-27, Berlin).

Ciupinski, L., Grzonka, J., Ogorodnikova, O. V., Mayer, M., and Kurzydlowski, K. J.: Stem observations of radiation damages in irradiated and annealed tungsten. (20th International Workshop on Inelastic Ion-Surface Collisions (IISC-20), 2014-02-16 to 2014-02-21, Wirrina Cove).

Clark, E., Lumsdaine, A., Boscary, J., Ekiki, K., Harris, J., McGinnis, D., Lore, J., Peacock, A., and Tretter, J.: Multiphysics Analysis of the Wendelstein 7-X Actively Cooled Divertor Scraper Element. (20th Topical Conference on High-Temperature Plasma Diagnostics (HTPD 2014), 2014-06-01 to 2014-06-05, Atlanta, GA).

Clark, E., Lumsdaine, A., Boscary, J., Ekici, K., Harris, J., McGinnis, D., Lore, J., Peacock, A., and Tretter, J.: Thermal-fluid Analysis of the W7-X High Heat-flux Divertor Scraper Element. (28th Symposium on Fusion Technology (SOFT 2014), 2014-09-29 to 2014-10-03, San Sebastian).

Classen, I. G. J., Domier, C. W., Luhmann Jr., N. C., Bogomolov, A. V., Suttrop, W., Boom, J., Tobias, B. J., Donne, A. J. H., and ASDEX Upgrade Team: Dual Array 3D Electron Cyclotron Emission Imaging at ASDEX Upgrade. (20th Topical Conference on High-Temperature Plasma Diagnostics (HTPD 2014), 2014-06-01 to 2014-06-05, Atlanta, GA).

Clementson, J., Lewerentz, L., Grulke, O., Bohlin, H., Kempkes, P., Rahbarnia, K., Schneider, R., Stechow, A. v., Sydora, R., and Klinger, T.: Gyrokinetic investigations of fast magnetic reconnection. (78. DPG-Jahrestagung und Frühjahrstagung der Sektion AMOP, 2014-03-17 to 2014-03-21, Berlin).

Coenen, J. W., Arnoux, G., Matthews, G. F., Mertens, P., Knaup, M., Jachmich, S., Bazylev, B., Clever, M., Dejarnac, R., Coey, I., Corre, Y., Devaux, S., Frassinetti, L., Gauthier, E., Horacek, J., Krieger, K., Marsen, S., Meigs, A., Pitts, R. A., Puetterich, T., Rack, M., Stamp, M., Sergienko, G., Tamain, P., Thompson, V., and JET-EFDA Contributors: ELM induced tungsten melting and its impact on tokamak operation. (21st International Conference on Plasma Surface Interactions 2014 (PSI 21), 2014-05-26 to 2014-05-30, Kanazawa).

Colas, L., Gunn, J. P., Hillairet, J., Litaudon, X., Jacquot, J., Milanesio, D., Lu, L., Bernard, J.-M., Carpentier, S., Corre, Y., Durodie, F., Faudot, E., Firdaouss, M., Goniche, M., Helou, W., Heuraux, S., Kubic, M., Lamalle, P. U., Maggiora, R., and Pitts, R. A.: Self-consistent Modeling of Radio-frequency Sheaths: Comparison with Tore Supra Measurements and Predictability for Future Machines. (25th IAEA Fusion Energy Conference (FEC 2014), 2014-10-13 to 2014-10-18, Saint Petersburg).

Colas, L., Jacquet, P., Van Eester, D., Brix, M., Sirinelli, A., Crombé, K., Křivska, A., Goniche, M., Bobkov, V., Lerche, E., Tamain, P., Marsen, S., Silva, C., Rimini, F., and JET-EFDA Contributors: Localized scrape-off layer density modifications by ion cyclotron near fields in JET L-mode plasmas with ITER-like wall. (21st International Conference on Plasma Surface Interactions 2014 (PSI 21), 2014-05-26 to 2014-05-30, Kanazawa).

Cole, M., and Mishchenko, A.: Electromagnetic simulations of tokamaks and stellarators. (78. DPG-Jahrestagung und Frühjahrstagung der Sektion AMOP, 2014-03-17 to 2014-03-21, Berlin).

Cole, M., and Mishchenko, A.: Simulations of Alfvén eigenmodes in tokamaks and stellarators. (Joint Varenna-Lausanne International Workshop on Theory of Fusion Plasmas, 2014-09-01 to 2014-09-05, Varenna).

Conway, G. D., Müller, H. W., Lunt, T., Suttrop, W., Fietz, S., Simon, P., Maraschek, M., Happel, T., Viezzer, E., and ASDEX Upgrade Team: Recent results on the 3D effects of magnetic perturbation coils on the edge/SOL properties in ASDEX Upgrade. (19th Joint EU-US Transport Task Force Meeting (TTF 2014), 2014-09-08 to 2014-09-11, Culham).

Conway, G. D., Müller, H. W., Lunt, T., Suttrop, W., Simon, P., Maraschek, M., Fietz, S., Happel, T., Viezzer, E., and ASDEX Upgrade Team: 3D effects of magnetic perturbation coils on the edge/SOL properties in ASDEX Upgrade. (41st EPS Conference on Plasma Physics, 2014-06-23 to 2014-06-27, Berlin).

Coster, D. P., Chankin, A. V., Klingshirn, H. J., Dux, R., Fable, E., Bonnin, X., Kukushkin, A., and Loarte, A.: SOLPS modelling of W for ITER. (21st International Conference on Plasma Surface Interactions 2014 (PSI 21), 2014-05-26 to 2014-05-30, Kanazawa).

Czarnecka, A., Bobkov, V., Dux, R., Pütterich, T., Sertoli, M., and ASDEX Upgrade Team: Trends of W behaviour in ICRF assisted discharges in ASDEX Upgrade. (21st International Conference on Plasma Surface Interactions 2014 (PSI 21), 2014-05-26 to 2014-05-30, Kanazawa).

Da Silva, F., Heuraux, S., Ribeiro, T., Despres, B., and Campos Pinto, M.: Materials and medical applications of fintie-differences time-domain codes developed for simulation of radar (reflectometry) experiments in fusion plasmas. (8th Congress of the Portuguese Committee of URSI – "Drones and Autonomous Vehicles: Present and Future Challenges", 2014-11-28, Lisbon).

Dannert, T.: Experiences with porting large HPC applications to GPUs. (International Cluster Workshop on GPUs, 2014-02-15, München).

Dannert, T.: MPI Parallelization of the Dynamo Simulation Code MagIC. (Vortrag. 2014-05-14, Max Planck Institut für Sonnensystemforschung, Göttingen).

Delabie, E., Maggi, C., Meyer, H., Biewer, T. M., Bourdelle, C., Brix, M., Carvalho, I. S., Clever, M., Drewelow, P., Hawkes, N., Hillesheim, J., Meigs, A., Meneses, L., Rimini, F., Siren, P., Solano, E., and Stamp, M.: Overview and Interpretation of L-H Threshold Experiments on JET with the ITER-like Wall. (25th IAEA Fusion Energy Conference (FEC 2014), 2014-10-13 to 2014-10-18, Saint Petersburg).

Delabie, E., Maggi, C. F., Meyer, H., Biewer, T., Bourdelle, C., Brix, M., Carvalho, I., Drewelow, P., Hawkes, N., Hillesheim, J., Meigs, A., Meneses, L., Rimini, F., Solano, E., Stamp, M., and JET EFDA Contributors: L-H Transitions on JET with the ITER-like Wall. (19th Joint EU-US Transport Task Force Meeting (TTF 2014), 2014-09-08 to 2014-09-11, Culham).

Dhard, C. P., Nagel, M., Raatz, S., Nüsslein, U., and Ressel, M.: Final acceptance tests of helium refrigerator for Wendelstein 7-X. (Joint 25th International Cryogenics Engineering Conference (ICEC 25) and 2014 International Cryogenic Materials Conference (ICMC 2014), 2014-07-07 to 2014-07-11, Enschede).

Dibon, M., Baldzuhn, J., Beck, M., Cardella, A., Köchl, F., Kocsis, G, Lang, P., Macian-Juan, R., Plöckl, B., Szepesi, T., and Weisbart, W.: Blower Gun pellet injection system for W7-X. (78. DPG-Jahrestagung und Frühjahrstagung der Sektion AMOP, 2014-03-17 to 2014-03-21, Berlin).

Dibon, M. M., Baldzuhn, J., Beck, M., Cardella, A., Köchl, F., Kocsis, G, Lang, P. T., Macian-Juan, R., Plöckl, B., Szepesi, T., and Weisbart, W.: Blower gun pellet injection system for W7-X. (28th Symposium on Fusion Technology (SOFT 2014), 2014-09-29 to 2014-10-03, San Sebastian).

Dif-Pradalier, G., Sarazin, Y., Ghendrih, P., Norscini, C., Abiteboul, J., Cartier-Michaud, T., Diamond, P. H., Dumont, R., Esteve, D., Garbet, X., Grandgirard, V., Gürcan, Ö. D.,

Hennequin, P., Morel, P., and Vermare, L.: Forcing & Self-Organisation in the Core & Near-Edge Plasma. (19th Joint EU-US Transport Task Force Meeting (TTF 2014), 2014-09-08 to 2014-09-11, Culham).

Dinklage, A., Koenig, R., Maaßberg, H., Sunn Pedersen, T., Warmer, F., Wolf, R. C., Alonso, A., Ascasibar, E., Baldzuhn, J., Beidler, C. D., Biedermann, C., Bosch, H.-S., Brakel, R., Bozhenkov, S., Burhenn, R., Calvo, I., Castejon, F., Drevlak, M., Erckmann, V., Effenberg, F., Estrada, T., Feng, Y., Gates, D., Geiger, J., Grulke, O., Hartmann, D., Helander, P., Hidalgo, C., Hirsch, M., Hölbe, H., Klinger, T., Jakubowski, M., Kocsis, G., Kubkowska, M., Laqua, H., Laux, M., Liang, Y., Marushchenko, N., Moncada, V., Neubauer, O., Ongena, J., Otte, M., Pablant, N., Preynas, M., Puiatti, M.-E., Garcia-Regana, J. M., Schauer, F., Schmitz, O., Smith, H., Stange, T., Thomsen, H., Travere, J.-M., Turkin, Y., Velasco, J.-L., Werner, A., Tanaka, K., Ida, K., Kubo, S., Sakamoto, R., Yamada, H., Yokoyama, M., Yoshinuma, M., W7-X Team, TJ-II Team, and LHD-Experiment Team: The Initial Programme of Wendelstein 7-X on the Way to a HELIAS Fusion Power Plant. (25th IAEA Fusion Energy Conference (FEC 2014), 2014-10-13 to 2014-10-18, Saint Petersburg).

Dittmar, T., Doerner, R. P., Köppen, M., Kreter, A., Linsmeier, C., Oberkofler, M., and Schwarz-Selinger, T.: The material system beryllium-nitrogen-deuterium: review of recent results. (78. DPG-Jahrestagung und Frühjahrstagung der Sektion AMOP, 2014-03-17 to 2014-03-21, Berlin).

Dobes, K., Köppen, M., Oberkofler, M., Lungu, C. P., Porosnicu, C., Höschen, T., Linsmeier, C., and Aumayr, F.: Interaction of nitrogen and deuterium ions with beryllium surfaces. (20th International Workshop on Inelastic Ion-Surface Collisions (IISC-20), 2014-02-16 to 2014-02-21, Wirrina Cove).

Doerk, H., Dunne, M., Görler, T., Hatch, D. R., Jenko, F., Kurzan, B., Navarro, A., McDermott, R., Pueschel, M. J., Ryter, F., Told, D., and ASDEX Upgrade Team: Beta scaling of confinement in fusion plasmas – A gyrokinetic perspective. (U.S. Transport Task Force Workshop (TTF), 2014. 2014-04-22 to 2014-04-25, San Antonio, TX).

Doerner, R. P., Jepu, I., Lasa, A., Nishijima, D., Nordlund, K., Safi, E., and Schwarz-Selinger, T.: The relationship between gross and net erosion of beryllium at elevated temperature. (21st International Conference on Plasma Surface Interactions 2014 (PSI 21), 2014-05-26 to 2014-05-30, Kanazawa).

Dostal, M., Laqua, H. P., and Stange, T.: Einschluss von MeV-Elektronen im Stellarator WEGA. (78. DPG-Jahrestagung und Frühjahrstagung der Sektion AMOP, 2014-03-17 to 2014-03-21, Berlin).

Douai, D., Brezinsek, S., Hagelaar, G. J. M., Hong, S. H., Kogut, D., Lomas, P. J., Lyssoivan, A., Nunes, I., Pitts, R. A., Rohde, V., Vries, P. C. d., Wauters, T., JET EFDA Contributors, and ASDEX Upgrade Team: Wall conditioning for ITER: current experimental and modeling activities. (21st International Conference on Plasma Surface Interactions 2014 (PSI 21), 2014-05-26 to 2014-05-30, Kanazawa).

Douai, D., Kogut, D., Baldwin, M., Brezinsek, S., Doerner, R., Hagelaar, G., Hong, S.-H., Lomas, P., Lyssoivan, A., Ferreira Nunes, I. M., Pitts, R., Rohde, V., Schwarz-Selinger, T., Vries, P. d., and Wauters, T.: Experimental and Modelling Results on Wall Conditioning for ITER Operation. (25th IAEA Fusion Energy Conference (FEC 2014), 2014-10-13 to 2014-10-18, Saint Petersburg).

Drenik, A., Oberkofler, M., Alegre, D., Kruezi, U., Brezinsek, S., Mozetic, M., Nunes, I., Wischmeier, M., Giroud, C., Maddison, G., Reux, C., and JET EFDA Contributors: Mass spectrometry analysis of impurity seeded discharges in JET-ILW. (21st International Conference on Plasma Surface Interactions 2014 (PSI 21), 2014-05-26 to 2014-05-30, Kanazawa).

Du, J., Yuan, Y., Wirtz, M., Linke, J., Liu, W., and Greuner, H.: FEM study of recrystallized tungsten under ELM-like heat loads. (21st International Conference on Plasma Surface Interactions 2014 (PSI 21), 2014-05-26 to 2014-05-30, Kanazawa).

Duval, B., Reimerdes, H., Vijvers, W., Labit, B., Canal, G., and Lunt, T.: Progress in Snowflake Divertor Studies on TCV. (25th IAEA Fusion Energy Conference (FEC 2014), 2014-10-13 to 2014-10-18, Saint Petersburg).

Dux, R., Loarte, A., Kukushkin, A. S., Fable, E., Coster, D., and Chankin, A.: Influence of a Tungsten Divertor on the Performance of ITER H-Mode Plasmas. (25th IAEA Fusion Energy Conference (FEC 2014), 2014-10-13 to 2014-10-18, Saint Petersburg).

Eeten, P. v., Bräuer, T., Bykov, V., Carls, A., and Fellinger, J.: Features and Analyses of W7-X Cryostat System FE Model. (28th Symposium on Fusion Technology (SOFT 2014), 2014-09-29 to 2014-10-03, San Sebastian).

Effenberg, F., Feng, Y., Bozhenkov, S., Frerichs, H., Hölbe, H., Reiter, D., Schmitz, O., and Pedersen, T. S.: Exploration of radiation cooling for startup plasmas at Wendelstein 7-X with EMC3-EIRENE simulations. (78. DPG-Jahrestagung und Frühjahrstagung der Sektion AMOP, 2014-03-17 to 2014-03-21, Berlin).

Effenberg, F., Feng, Y., Bozhenkov, S., Frerichs, H., Hölbe, H., Pedersen, T. S., Reiter, D., and Schmitz, O.: Investigation of impurity radition in Wendelstein 7-X startup plasmas with EMC3-Eirene. (56th Annual Meeting of the APS Division of Plasma Physics, 2014-10-27 to 2014-10-31, New Orleans, LA).

Effenberg, F., Feng, Y., Bozhenkov, S., Frerichs, H., Hölbe, H., Reiter, D., Schmitz, O., and Pedersen, T. S.: Investigation of impurity transport and radiation cooling for startup plasmas at W7-X with EMC3-EIRENE simulations. (41st EPS Conference on Plasma Physics, 2014-06-23 to 2014-06-27, Berlin).

Egorov, K., Bykov, V., Fellinger, J., Schauer, F., and Köppen, M.: Advanced Structural Analysis of Wendelstein 7-X Magnet System Weight Supports. (25th IAEA Fusion Energy Conference (FEC 2014), 2014-10-13 to 2014-10-18, Saint Petersburg).

Eich, T.: ELM heat load multi-machine scaling. (20th ITPA Scrape-off Layer & Divertor Topical Group Meeting, 2014-10-20 to 2014-10-23, Prague).

Eich, T., Sieglin, B., Loarte, A., Matthews, G. F., Herrmann, A., JET-EFDA Team, and ASDEX Upgrade Team: Revisited ELM divertor heat load scaling to ITER with JET and ASDEX Upgrade data. (56th Annual Meeting of the APS Division of Plasma Physics, 2014-10-27 to 2014-10-31, New Orleans, LA).

Elgeti, S., Balden, M., and Manhard, A.: Blister evolution with fluence and temperature of deuterium plasma exposed tungsten. (21st International Conference on Plasma Surface Interactions 2014 (PSI 21), 2014-05-26 to 2014-05-30, Kanazawa).

Fable, E.: Toroidal momentum tranposrt equation for transport codes and consitency with a gyrokinetic model. (19th Joint EU-US Transport Task Force Meeting (TTF 2014), 2014-09-08 to 2014-09-11, Culham).

Fantz, U.: Einführung in die Plasma- und Fusionsphysik. (Lehrerfortbildung für Berufliche Oberschulen Fachrichtung Physik/Technologie, 2014-02-05, IPP Garching).

Fantz, U.: Einführung in die Plasma- und Fusionsphysik. (Lehrerfortbildung für Lehrkräfte Physik an Gymnasien, MB Oberbayern Ost, 2014-11-12, IPP Garching).

Fantz, U.: Das Feuer der Sonne für die Erde: Energiegewinnung durch Kernfusion! (Themenabend Kernfusion, 2014-02-07, Planetarium Laupheim).

Fantz, U.: Das Feuer der Sonne für die Erde: Energiegewinnung durch Kernfusion! (Themenabend Kernfusion, 2014-02-14, Planetarium Laupheim).

Fantz, U.: Das Feuer der Sonne für die Erde: Energiegewinnung durch Kernfusion! (4. Unterfränkisches Ferienseminar für Gymnasiasten, 2014-07-31, Würzburg).

Fantz, U.: Fusionsforschung. (SS 2014. Vorlesung, Universität Augsburg).

Fantz, U.: Niedertemperaturplasmen als industrielle Schlüsseltechnologie. (WS 2013/2014. Seminar, Universität Augsburg).

Fantz, U.: Physikalische Grundlagen der Energieversorgung. (WS 2013/2014. Vorlesung/Seminar, Universität Augsburg).

Fantz, U.: Plasmaphysik. (WS 2013/2014. Vorlesung/Seminar, Universität Augsburg.

Fantz, U., and Briefi, S.: Achievement of high atomic hydrogen densities in cylindrical rf plasmas with magnetic field. (67th Gaseous Electronics Conference (GEC 2014), 2014-11-03 to 2014-11-07, Raleigh, NC).

Fantz, U., Franzen, P., Kraus, W., Schiesko, L., Wimmer, C., and Wünderlich, D.: Size Scaling of Negative Hydrogen Ion Sources for Fusion. (4th International Symposium on Negative Ions, Beams and Sources (NIBS 2014), 2014-10-06 to 2014-10-10, Garching).

Fantz, U., and Schreck, M.: Niedertemperaturplasmen als industrielle Schlüsseltechnologie. (SS 2014. Seminar, Universität Augsburg).

Fantz, U., and Wünderlich, D.: Relevance of Molecules in Ionizing and Recombining Plasmas in the Divertor and in Negative Ion Sources for Fusion. (Decennial IAEA Technical Meeting on Atomic, Molecular and Plasma-Material Interaction Data for Fusion Science and Technology, 2014-12-15 to 2014-12-19, Daejeon).

Fedorczak, N., Monier-Garbet, P., Brezinsek, S., Goniche, M., Joffrin, E., Lerche, E., Lipschultz, B., Luna, E. d. l., Maddison, G., Maggi, C., Matthews, G., Nunes, I., Pütterich, T., Rimini, F., Solano, E. R., Tamain, P., Tsalas, M., Vries, P. d., and JET-EFDA Contributors: Tungsten sources and transport control in JET-ILW H-modes. (21st International Conference on Plasma Surface Interactions 2014 (PSI 21), 2014-05-26 to 2014-05-30, Kanazawa).

Fellinger, J., Egorov, K., Bykov, V., and Schauer, F.: Assessment of instrumentation of the magnet system of W7-X. (28th Symposium on Fusion Technology (SOFT 2014), 2014-09-29 to 2014-10-03, San Sebastian).

Feng, Y.: Features of detached plasmas predicted for W7-X. (24th International Toki Conference (ITC-24), 2014-11-04 to 2014-11-07, Ceratopia Toki, Toki-city, Gifu).

Ferreira Nunes, I. M., Lomas, P., Baruzzo, M., Beurskens, M., Challis, C., Frassinetti, L., Hobirk, J., Joffrin, E., Lowry, C.,

Rimini, F., Sips, A., and Voitsekhovitch, I.: Compatibility of High Performance Operation with JET ILW. (25th IAEA Fusion Energy Conference (FEC 2014), 2014-10-13 to 2014-10-18, Saint Petersburg).

Fietz, S., Maraschek, M., Zohm, H., Barrera, L., McDermott, R. M., Reich, M., and ASDEX Upgrade Team: Study of the onset of neoclassical tearing modes at the ASDEX Upgrade tokamak. (41st EPS Conference on Plasma Physics, 2014-06-23 to 2014-06-27, Berlin).

Figini, L., Farina, D., Poli, E., Bruschi, A., Moro, A., Platania, P., Sozzi, C., Goodman, T., Sauter, O., Cavinato, M., Saibene, G., and Henderson, M. A.: Assessment of the ITER EC Upper Launcher Performance. (18th Joint Workshop on Electron Cyclotron Emission and Electron Cyclotron Resonance Heating, 2014-04-22 to 2014-04-25, Nara).

Fischer, R., Barrera, L., Dux, R., Geiger, B., Giannone, L., Lebschy, A., Rathgeber, S. K., Suttrop, W., Willensdorfer, M., Wolfrum, E., and ASDEX Upgrade Team: Recent Developments of Integrated Data Analysis at ASDEX Upgrade. (8th Workshop on Fusion Data Processing, Validation and Analysis, 2014-11-04 to 2014-11-06, Ghent).

Flanagan, J. C., Sertoli, M., Cackett, A., Hodille, E., Vries, P. d., Coffey, I. H., Sieglin, B., Brezinsek, S., Matthews, G. F., Widdowson, A., Coenen, J. W., Marsen, S., Craciunescu, T., Murari, A., Bacharis, M., Harting, D., and JET-EFDA Contributors: Characterising dust in JET with the new ITER-like wall. (41st EPS Conference on Plasma Physics, 2014-06-23 to 2014-06-27, Berlin).

Förstel, M., Arion, T., Harbo, L., Zhang, C. F., and Hergenhahn, U.: Measuring the efficiency of ICD in neon- and in water clusters. (78. DPG-Jahrestagung und Frühjahrstagung der Sektion AMOP, 2014-03-17 to 2014-03-21, Berlin).

Ford, O. P., Howard, J., Reich, M., Svensson, J., and Wolf, R.: Coherence imaging spectroscopy: A new method for measuring plasma dynamics. (78. DPG-Jahrestagung und Frühjahrstagung der Sektion AMOP, 2014-03-17 to 2014-03-21, Berlin).

Franck, E., Lessig, A., Hölzl, M., Ratnani, A., and Sonnendrücker, E.: Hierarchy of fluid models and numerical methods for the JOREK code. (ITER Seminar, 2014-10-14, LJLL, Jussieu, Paris).

Franck, E., Lessig, A., Hölzl, M., Ratnani, A., and Sonnendrücker, E.: Hierarchy of fluid models and numerical methods for the JOREK code. (TONUS Day, 2014-11-04, IRMA, Strasbourg).

Franck, E., Lessig, A., Hölzl, M., and Sonnendrücker, E.: Preconditioning and nonlinear time solvers for the Jorek MHD code. (10th AIMS Conference on Dynamical Systems, Differential Equations and Applications, 2014-07-07 to 2014-07-11, Madrid).

Franke, T., Barbato, E., Bosia, G., Cardinali, A., Ceccuzzi, S., Cesario, R., Van Eester, D., Federici, G., Gantenbein, G., Helou, W., Hillairet, J., Jenkins, I., Kazakov, Y. O., Kemp, R., Lerche, E., Mirizzi, F., Noterdaeme, J.-M., Poli, E., Porte, L., Ravera, L., Surrey, E., Tardini, G., Tran, M. Q., Tsironis, C., Tuccillo, A. A., Wenninger, R., and Zohm, H.: Technological and Physics Assessments on Heating and Current Drive Systems for DEMO. (28th Symposium on Fusion Technology (SOFT 2014), 2014-09-29 to 2014-10-03, San Sebastian).

Franzen, P., Wünderlich, D., Riedl, R., Nocentini, R., Bonomo, F., Fantz, U., Fröschle, M., Heinemann, B., Martens, C., Kraus, W., Pimazzoni, A., Ruf, B., and NNBI Team: Status of the ELISE Test Facililty. (4th International Symposium on Negative Ions, Beams and Sources (NIBS 2014), 2014-10-06 to 2014-10-10, Garching).

Frassinetti, L., Dunne, M., Beurskens, M., Schneider, P., Giroud, C., Wolfrum, E., Bernert, M., Casali, L., Cavedon, M., Kappatou, A., Laggner, F., McDermott, R., Ryter, F., Saarelma, S., Simpson, J., Tardini, G., Viezzer, E., and ASDEX Upgrade Team: ELM dynamics in AUG and JET with & without Nitrogen seeding. (20th ITPA Scrape-off Layer & Divertor Topical Group Meeting, 2014-10-20 to 2014-10-23, Prague).

Friedl, R., and Fantz, U.: Einfluss von Xenon- und Caesium-Beimischungen auf ein Wasserstoff-Niedertemperatur-plasma. (78. DPG-Jahrestagung und Frühjahrstagung der Sektion AMOP, 2014-03-17 to 2014-03-21, Berlin).

Friedl, R., and Fantz, U.: Temperature and substrate dependencies of the work function of caesiated materials under ion source conditions in vacuum and plasma. (4th International Symposium on Negative Ions, Beams and Sources (NIBS 2014), 2014-10-06 to 2014-10-10, Garching).

Frigione, D., Garzotti, L., Lennholm, M., Alper, B., Artaserse, G., Bennett, P., Eich, T., Kocsis, G., Lang, P. T., Mooney, R., Rack, M., Sips, G., Tvalashvili, G., Wilkes, D., and JET-EFDA Contributors: Divertor Load Footprint of ELMs in Pellet Triggering and Pacing Experiments at JET. (21st International Conference on Plasma Surface Interactions 2014 (PSI 21), 2014-05-26 to 2014-05-30, Kanazawa).

Fröschle, M., Friedl, R., Kammerloher, M., Riedl, R., and Steinberger, J.: Concepts of Caesium Evaporation and Control at IPP. (4th International Symposium on Negative Ions, Beams and Sources (NIBS 2014), 2014-10-06 to 2014-10-10, Garching).

Gao, L., Balden, M., Jacob, W., and Toussaint, U. v.: Temperature-dependent blister nucleation induced by deuterium implantation into tungsten. (12th International Workshop on Hydrogen Isotopes in Fusion Reactor Materials (HWS-12), 2014-06-02 to 2014-06-04, Toyama).

Gao, L., Jacob, W., Manhard, A., Schwarz-Selinger, T., Schmid, K., and Toussaint, U. v.: Characterization of the Deuterium-rich Surface Layer on Tungsten after Deuterium Implantation. (21st International Conference on Plasma Surface Interactions 2014 (PSI 21), 2014-05-26 to 2014-05-30, Kanazawa).

Garcia, J., Citrin, J., Görler, T., Hayashi, N., Jenko, F., Maget, P., Mantica, P., Pueschel, M. J., Told, D., Bourdelle, C., Dumont, R., Giruzzi, G., Haverkort, W., Hogeweij, G., Ide, S., Johnson, T., and Urano, H.: Core Microturbulence and Edge MHD Interplay and Stabilization by Fast Ions in Tokamak Confined Plasmas. (25th IAEA Fusion Energy Conference (FEC 2014), 2014-10-13 to 2014-10-18, Saint Petersburg).

Garcia-Munoz, M., Äkäslompolo, S., Akers, R., Marné, P. d., Dunne, M. G., Ferraro, N. M., Fietz, S., Galdon, J., Garcia-Lopez, J., Geiger, B., Herrmann, A., Hölzl, M., Jimenez-Ramos, M. C., Lazanyi, N., Liu, Y., Nocente, M., Pace, D., Shinohara, K., Suttrop, W., Van Zeeland, M., Strumberger, E., and Wolfrum, E.: Fast-Ion Response to Externally Applied 3D Magnetic Perturbations in ASDEX Upgrade H-Mode Plasmas. (25th IAEA Fusion Energy Conference (FEC 2014), 2014-10-13 to 2014-10-18, Saint Petersburg).

Garcia-Munoz, M., Geiger, B., Pace, D. C., Van Zeeland, M. A., ASDEX Upgrade Team, and DIII-D Teams: Fast-Ion Transport in the AUG and DIII-D Tokamaks. (56th Annual Meeting of the APS Division of Plasma Physics, 2014-10-27 to 2014-10-31, New Orleans, LA).

Gasparyan, Y. M., Ogorodnikova, O. V., Efimov, V. S., Mednikov, A., Marenkov, E. D., Pisarev, A. A., Markelj, S., and Čadež, I.: Deuterium retention and thermal desorption from self-damaged tungsten. (21st International Conference on Plasma Surface Interactions 2014 (PSI 21), 2014-05-26 to 2014-05-30, Kanazawa).

Geiger, J., Beidler, C., Feng, Y., Helander, P., Maaßberg, H., Marushchenko, N. B., Nührenberg, C., Turkin, Y., and W7-X Team: Physics Properties of Magnetic Configurations of Wendelstein 7-X. (24th International Toki Conference (ITC-24), 2014-11-04 to 2014-11-07, Ceratopia Toki, Toki-city, Gifu).

Geiger, B., Classen, I., Garcia-Munoz, M., Hopf, C., Lauber, P., Nielsen, S., Reich, M., Ryter, F., Schneider, P. A., Schneller, M., Tardini, G., Weiland, M., and Salewski, M.: Experimental Quantification of the Impact of Large and Small Scale

Instabilities on Confined Fast Ions in ASDEX Upgrade. (25th IAEA Fusion Energy Conference (FEC 2014), 2014-10-13 to 2014-10-18, Saint Petersburg).

Geiger, B., Classen, I., Garcia-Munoz, M., Lauber, P., Reich, M., Ryter, F., Salewski, M., Schneider, P., Schneller, M., Tardini, G., Weiland, M., and ASDEX Upgrade Team: Quantification of the impact of large and small scale instabilities on the fast-ion confinement in ASDEX Upgrade. (41st EPS Conference on Plasma Physics, 2014-06-23 to 2014-06-27, Berlin).

Geiger, J., and TF Initial Physics Program of Wendelstein 7-X: Physics in the Magnetic Configuration Space of Wendelstein 7-X. (41st EPS Conference on Plasma Physics, 2014-06-23 to 2014-06-27, Berlin).

Geiger, B., Weiland, M., Mlynek, A., Dunne, M., Dux, R., Fischer, R., Hobirk, J., Hopf, C., Reich, M., Rittich, D., Ryter, F., Schneider, P., and Tardini, G.: Fast-ion transport and NBI current drive in ASDEX Upgrade. (56th Annual Meeting of the APS Division of Plasma Physics, 2014-10-27 to 2014-10-31, New Orleans, LA).

Giannone, L., Bernert, M., Fischer, R., Fuchs, C., Gromann, L., Gude, A., Igochine, V., Kallenbach, A., Lackner, K., Lunt, T., Maraschek, M., Martinov, S., McCarthy, P. J., Meister, H., Odstrcil, T., Preuss, R., Rampp, M., Rapson, C., Scarabosio, A., Sigalov, A., Schuhbeck, K.-H., Sieglin, B., Suttrop, W., Zammuto, I., and ASDEX Upgrade Team: Real-time magnetic equilibria on ASDEX Upgrade tokamak. (14th Scientific Research and Big Physics Symposium, 2014-05-15, München).

Girardo, J.-B., Zarzoso, D., Dumont, R., Garbet, X., Sarazin, Y., and Sharapov, S.: Relation between Energetic and Standard Geodesic Acoustic Modes. (19th Joint EU-US Transport Task Force Meeting (TTF 2014), 2014-09-08 to 2014-09-11, Culham).

Giroud, C., Jachmich, S., Jacquet, P., Järvinen, A. E., Lerche, E., Rimini, F., Aho-Mantila, L., Balboa, I., Belo, P., Beurskens, M., Brezinsek, S., Cunningham, G., Delabie, E., Devaux, S., Frassinetti, L., Figueiredo, A., Huber, A., Hillesheim, J., Garzotti, L., Goniche, M., Groth, M., Lomas, P., Maddison, G., Marsen, S., Matthews, G., Menmuir, S., Rooij, G. v., Saarelma, S., and Stamp, M.: Towards Baseline Operation Integrating ITER-relevant Core and Edge Plasma within the Constraint of the ITER-like Wall at JET. (25th IAEA Fusion Energy Conference (FEC 2014), 2014-10-13 to 2014-10-18, Saint Petersburg).

Giruzzi, G., Artaud, J.-F., Ivanova-Stanik, I., Kemp, R., Zagorski, R., Baruzzo, M., Bolzonella, T., Fable, E., Garzotti, L., King, D., Stankiewicz, R., Stepniewski, W., Vincenzi, P., and Ward, D.: Modelling of Pulsed and Steady-state DEMO Scenarios. (25th IAEA Fusion Energy Conference (FEC 2014), 2014-10-13 to 2014-10-18, Saint Petersburg).

Görler, T.: Gyrokinetic benchmark of global electromagnetic microinstabilities. (Numerical Methods for the Kinetic Equations of Plasma Physics (NumKin2014), 2014-10-20 to 2014-10-24, Garching).

Görler, T., Told, D., Jenko, F., Casson, F., Fable, E., White, A. E., and ASDEX Upgrade Team: Outer core L-mode ion heat fluxes matched by nonlinear gyrokinetic simulations. (U.S. Transport Task Force Workshop (TTF 2014), 2014-04-22 to 2014-04-25, San Antonio, TX).

Graves, J. P., Lennholm, M., Chapman, I. T., Lerche, E., Reich, M., Bobkov, V., Dumont, R., Van Eester, D., Faustin, J., Goniche, M., Jacquet, P., Johnson, T., Liu, Y., Nicolas, T., Tholerus, S., Blackman, T., Carvalho, I. S., Felton, R., Kiptily, V., Monakhov, I., Nave, M. F. F., Sozzi, C., Tsalas, M., and JET EFDA Contributors: Sawtooth control in JET with ITER relevant low field side resonance ICRH and ITER like wall. (41st EPS Conference on Plasma Physics, 2014-06-23 to 2014-06-27, Berlin).

Greuner, H., Zivelonghi, A., Böswirth, B., and You, J.-H.: Results of high heat flux testing of W/CuCRZr multilayer composites with percolating microstructure for plasma-facing components. (28th Symposium on Fusion Technology (SOFT 2014), 2014-09-29 to 2014-10-03, San Sebastian).

Grießhammer, J.: Modelling the effect of resonant magnetic perturbations in ASDEX Upgrade with the extented MHD code XTOR-2F. (78. DPG-Jahrestagung und Frühjahrstagung der Sektion AMOP, 2014-03-17 to 2014-03-21, Berlin).

Groth, M., Brezinsek, S., Belo, P., Calabro, G., Corrigan, G., Brix, M., Clever, M., Coenen, J. W., Devaux, S., Drewelow, P., Eich, T., Harting, D., Huber, A., Jachmich, S., Kruezi, U., Lawson, K. D., Lehnen, M., Maggi, C. F., Marchetto, C., Marsen, S., Maviglia, F., Meigs, A. G, Sergienko, G., Sieglin, B., Silva, C., Stamp, M. F., and Wiesen, S.: Divertor plasma conditions and neutral dynamics in semi-horizontal and vertical divertor configurations in JET-ILW low confinement plasmas. (21st International Conference on Plasma Surface Interactions 2014 (PSI 21), 2014-05-26 to 2014-05-30, Kanazawa).

Groth, M., Clever, M., Lawson, K., Meigs, A., Stamp, M., Svensson, J., Belo, P., Brezinsek, S., Brix, M., Coenen, J., Corrigan, G., Eich, T., Giroud, C., Harting, D., Huber, A., Jachmich, S., Uron, K., Lehnen, M., Lowry, C., Maggi, C., Marsen, S., Sergienko, G., Sieglin, B., Rooij, G. v., and Wiesen, S.: Steps in Validating Scrape-off Layer Simulations of Detached Plasmas in the JET ITER-like Wall Configuration.

(25th IAEA Fusion Energy Conference (FEC 2014), 2014-10-13 to 2014-10-18, Saint Petersburg).

Grulke, O., Bohlin, H., Milojevic, D., Rahbarnia, K., Shesterikov, I., and Stechow, A. v.: Dynamics of the current sheet during driven guide-field reconnection. (56th Annual Meeting of the APS Division of Plasma Physics, 2014-10-27 to 2014-10-31, New Orleans, LA).

Günter, S.: Introducing EUROfusion. (EUROfusion Launch Event, 2014-10-09, Brussels).

Günter, S.: Kernfusion – Wie lässt sich die Energiequelle der Sterne auf der Erde nutzen? (Vortrag, 2014-02-17, Carl-Orff-Gymnasium Unterschleißheim).

Günter, S.: Physics basis of magnetic fusion power plants. (Kolloquium, 2014-06-10, Universität Mainz).

Günter, S.: Physics basis of magnetic fusion power plants. (Kolloquium Fachbereich Physik, 2014-12-11, Universität Rostock).

Günter, S., Yu, Q., Lackner, K., Bhattacharjee, A., and Huang, Y.-M.: Fast sawtooth reconnection at realistic Lundquist numbers. (41st EPS Conference on Plasma Physics, 2014-06-23 to 2014-06-27, Berlin).

Günter, S., and Lauber, P.: Plasmaphysik I. (WS 2013/2014. Vorlesung, Technische Universität München).

Günter, S., and Lauber, P.: Plasmaphysik II. (SS 2014. Vorlesung, Technische Universität München).

Gusev, V., Bakharev, N., Ber, B., Bondarchuk, E., Bulanin, V., Bykov, A., Chernyshev, F., Demina, E., Dyachenko, V., Goncharov, P., Gorodetsky, A., Gusakov, E., Iblyaminova, A., Irzak, M., Kaveeva, E., Khitrov, S., Khokhlov, M., Khromov, N., Krasnov, S., Kurskiev, G., Labusov, A., Lepikhov, S., Litunovsky, N., Mazul, I., Melnik, A., Mikov, V., Minaev, V., Miroshnikov, I., Mukhin, E., Novokhatsky, A., Patrov, M., Petrov, A., Petrov, Y., Rozhansky, V., Sakharov, N., Saveliev, A., Senichenkov, I., Sergeev, V., Shchegolev, P., Shcherbinin, O., Tanchuk, V., Tolstyakov, S., Varfolomeev, V., Vekshina, E., Voronin, A., Voskoboinikov, S., Wagner, F., Yashin, A., Zadvitskiy, G., Zakharov, A., Zalavutdinov, R., and Zhilin, E.: Review of Globus-M Spherical Tokamak Results. (25th IAEA Fusion Energy Conference (FEC 2014), 2014-10-13 to 2014-10-18, Saint Petersburg).

Hakola, A., Koivuranta, S., Likonen, J., Herrmann, A., Maier, H., Mayer, M., Neu, R., and Rohde, V.: Erosion of tungsten and steel in the main chamber of ASDEX Upgrade.

(21st International Conference on Plasma Surface Interactions 2014 (PSI 21), 2014-05-26 to 2014-05-30, Kanazawa).

Hallatschek, K., and Kammel, A.: Evolution and System Dependent Properties of Zonal Flows and GAMs in Tokamaks and Planet Atmospheres. (25th IAEA Fusion Energy Conference (FEC 2014), 2014-10-13 to 2014-10-18, Saint Petersburg).

Hamaji, Y., Torikai, Y., Sugiyama, K., Lee, H. T., Ohtsuka, Y., and Ueda, Y.: Detailed study on carbon deposision/mixing layer formation on tungsten and its impact on retention. (21st International Conference on Plasma Surface Interactions 2014 (PSI 21), 2014-05-26 to 2014-05-30, Kanazawa).

Hans, A., Knie, A., Förstel, M., Schmidt, P., Reiß, P., Jahnke, T., Dörner, R., Kuleff, A. I., Cederbaum, L. S., Demekhin, P. V., Hergenhahn, U., and Ehresmann, A.: Detecting interatomic Coulombic decay in neon clusters by photon measurement. (78. DPG-Jahrestagung und Frühjahrstagung der Sektion AMOP, 2014-03-17 to 2014-03-21, Berlin).

Happel, T., Banon Navarro, A., Conway, G. D., Görler, T., Jenko, F., Ryter, F., Stroth, U., and ASDEX Upgrade Team: Wavenumber-resolved core turbulence studies in the ASDEX Upgrade tokamak and comparison with non-linear gyrokinetic simulations with the GENE code. (56th Annual Meeting of the APS Division of Plasma Physics, 2014-10-27 to 2014-10-31, New Orleans, LA).

Happel, T., Banon Navarro, A., Conway, G. D., Jenko, F., Stroth, U., and ASDEX Upgrade Team: Der Turbulenz auf der Spur durch Vergleiche von Reflektometriemessungen mit gyrokinetischen Simulationen. (78. DPG-Jahrestagung und Frühjahrstagung der Sektion AMOP, 2014-03-17 to 2014-03-21, Berlin).

Harting, D., Wiesen, S., Groth, M., Brezinsek, S., Corrigan, G., Arnoux, G., Boerner, P., Devaux, S., Flanagan, J., Järvinen, A., Marsen, S., Reiter, D., and JET-EFDA Contributors: Intra-ELM phase modelling of a JET ITER-like wall H-mode discharge with EDGE2D-EIRENE. (21st International Conference on Plasma Surface Interactions 2014 (PSI 21), 2014-05-26 to 2014-05-30, Kanazawa).

Härtl, T., Rohde, V., Mertens, V., Bösser, D., Glöckner, T., and ASDEX Upgrade Team: Status and perspectives of the ASDEX Upgrade gas inlet system. (28th Symposium on Fusion Technology (SOFT 2014), 2014-09-29 to 2014-10-03, San Sebastian).

Hatch, D., Dunne, M. G., Doerk, H., Jenko, F., Told, D., Wolfrum, E., and Viezzer, E.: Gyrokinetic Analysis of ASDEX-Upgrade Inter-ELM Pedestal Profile Evolution.

(56th Annual Meeting of the APS Division of Plasma Physics, 2014-10-27 to 2014-10-31, New Orleans, LA).

Hatzky, R.: The High Level Support Team. (IFERC-CSC HELIOS MIC Workshop, 2014-05-14, Gif-sur-Yvette).

Hatzky, R.: The High Level Support Team – A support unit for petaflop computing. (Platform for Advanced Scientific Computing Conference (PASC14), 2014-06-02 to 2014-06-03, Zurich).

Hatzky, R., Borchardt, M., Bottino, A., Kleiber, R., Könies, A., Mishchenko, A., and Sonnendrücker, E.: Reduction of the statistical error in electronmagnetic PIC simulations. (Electromagnetic Gyrokinetic PIC Meeting, 2014-12-09 to 2014-12-11, Princeton, NJ).

Havlíčková, E., Wischmeier, M., Fishpool, G., Meyer, H., and Lipschultz, B.: The effect of the Super-X divert or of MAST Upgrade on impurity radiation modelled by SOLPS. (21st International Conference on Plasma Surface Interactions 2014 (PSI 21), 2014-05-26 to 2014-05-30, Kanazawa).

Heinemann, B., Fantz, U., Franzen, P., Fröschle, M., Kraus, W., Nocentini, R., Riedl, R., and Ruf, B.: Upgrade of BATMAN test facility for H- source development. (4th International Symposium on Negative Ions, Beams and Sources (NIBS 2014), 2014-10-06 to 2014-10-10, Garching).

Heinola, K., Widdowson, A., Likonen, J., Alves, E., Baron-Wiechec, A., Brezinsek, S., Catarino, N., Coad, P., Koivuranta, S., Matthews, G. F., Mayer, M., Petterson, P., and JET-EFDA Contributors: Fuel retention in JET ITER-like wall from post-mortem analysis. (EUROfusion PFC&JET 2 Annual Meeting, 2014-11-24 to 2014-11-27, Jülich).

Heinola, K., Widdowson, A., Likonen, J., Alves, E., Baron-Wiechec, A., Brezinsek, S., Catarino, N., Coad, P., Koivuranta, S., Matthews, G. F., Mayer, M., Petterson, P., and JET-EFDA Contributors: Fuel retention in JET ITER-like wall from post-mortem analysis. (21st International Conference on Plasma Surface Interactions 2014 (PSI 21), 2014-05-26 to 2014-05-30, Kanazawa).

Helander, P.: Forskningsorganisation: Diskussionsunderlag. (Vortrag, 2014-11-18, Königlich Schwedische Akademie der Wissenschaften, Stockholm).

Helander, P.: Hydrodynamik. (WS 2013/2014. Vorlesung, Ernst-Moritz-Arndt-Universität Greifswald).

Helander, P.: Kernfusion – Stand und Perspektiven. (Gemeinsame Sitzung des Themennetzwerks Energie & Ressourcen und Materialwissenschaft & Werkstofftechnik, 2014-11-13, Berlin).

Helander, P., Jenko, F., Kleiber, R., Plunk, G. G., Proll, J. H. E., Riemann, J., and Xanthopoulos, P.: Advances in Stellarator Gyrokinetics. (25th IAEA Fusion Energy Conference (FEC 2014), 2014-10-13 to 2014-10-18, Saint Petersburg).

Helou, W., Colas, L., Hillairet, J., Mollard, P., Argouarch, A., Berger-By, G., Bernard, J.-M., Chen, Z., Delaplanche, J.-M., Durodié, F., Ferlay, F., Jacquot, J., Litaudon, X., Lombard, G., Maggiora, R., Milanesio, D., Patterlini, J.-C., Prou, M., Volpe, R., and Vulliez, K.: Radio-frequency Electrical Design of the WEST Long Pulse and Load-resilient ICRH Launchers. (28th Symposium on Fusion Technology (SOFT 2014), 2014-09-29 to 2014-10-03, San Sebastian).

Hennequin, P., Happel, T., Schneider, P., Conway, G. D., Ryter, F., Stroth, U., Honore, C., Vermare, L., Gürcan, Ö., Morel, P., and ASDEX Upgrade Team: Spatial structure of the turbulence and its scaling with rho*: observations using radial correlation Doppler reflectometry on ASDEX Upgrade. (19th Joint EU-US Transport Task Force Meeting (TTF 2014), 2014-09-08 to 2014-09-11, Culham).

Herb, J., Raeder, J., Weller, A., Wolf, R., Boccaccini, L. V., Carloni, D., Jin, X. Z., Stieglitz, R., and Pistner, C.: Review of the Safety Concept for Fusion Reactor Concepts and Transferability of the Nuclear Fission Regulation to Potential Fusion Power Plants. (25th IAEA Fusion Energy Conference (FEC 2014), 2014-10-13 to 2014-10-18, Saint Petersburg).

Hernandez, C., Richou, M., Firdaouss, M., Vignal, N., Desgranges, C., Cantone, V., Billard, A., Pintsuk, G., Greuner, H., Missirlian, M., Samaille, F., Tsitrone, E., and Bucalossi, J.: Tungsten coating developments on large size and complex geometries CuCrZr elements for the WEST project. (28th Symposium on Fusion Technology (SOFT 2014), 2014-09-29 to 2014-10-03, San Sebastian).

Herrmann, A., Greuner, H., Jaksic, N., Balden, M., Kallenbach, A., Krieger, K., Marne, P. d., Rohde, V., Scarabosio, A., Schall, G., and ASDEX Upgrade Team: Solid Tungsten Divertor-III for ASDEX Upgrade and Contributions to ITER. (25th IAEA Fusion Energy Conference (FEC 2014), 2014-10-13 to 2014-10-18, Saint Petersburg).

Herrmann, A., Jaksic, N., Leitenstern, P., Greuner, H., Krieger, K., Marné, P. d., Oberkofler, M., Rohde, V., Schall, G., and ASDEX Upgrade Team: A large scale divertor manipulator for ASDEX Upgrade. (28th Symposium on Fusion Technology (SOFT 2014), 2014-09-29 to 2014-10-03, San Sebastian).

Hirsch, M., Estrada, T., Hartfuss, H.-J., Kasparek, W., Lechte, C., Krämer-Flecken, A., Kornejew, P., Plaum, B., Stange, T., Windisch, T., Wagner, D., and Wolf, S.: Microwave Diagnostics for Wendelstein 7-X. (41st EPS Conference on Plasma Physics, 2014-06-23 to 2014-06-27, Berlin).

Hölbe, H.: Numerical studies for the nuclear fusion reactor Wendelstein 7-X. (78. DPG-Jahrestagung und Frühjahrstagung der Sektion AMOP, 2014-03-17 to 2014-03-21, Berlin).

Hölzl, M., Merkel, P., Huysmans, G. T. A., Atanasiu, C., Lackner, K., Nardon, E., Strumberger, E., McAdams, R., Liu, F., Chapman, I., and Fil, A.: Non-linear Simulations of MHD Instabilities in Tokamaks Including Eddy Current Effects and Perspectives for the Extension to Halo Currents. (Joint Varenna-Lausanne International Workshop on Theory of Fusion Plasmas, 2014-09-01 to 2014-09-05, Varenna).

Hogeweij, G., Leonov, V., Schweinzer, J., Sips, A., Angioni, C., Calabrò, G., Dux, R., Kallenbach, A., Lerche, E., Maggi, C. F., and Pütterich, T.: Impact of W on Scenario Simulations for ITER. (25th IAEA Fusion Energy Conference (FEC 2014), 2014-10-13 to 2014-10-18, Saint Petersburg).

Hopf, C.: Neutral beam heating and current drive (physics). (Joint European Research Doctorate in Fusion Science and Engineering, Engineering Advanced Course, 2014-10-20 to 2014-10-31, Padova).

Hopf, C.: Neutral Beam Current Drive Experiments on ASDEX Upgrade – A Status Report. (Seminar Talk. Institute for Plasma Research, 2014-09-04, Gandhinagar).

Hornsby, W. A., Buchholz, R., Casson, F. J., Migliano, P., Poli, E., Zarzoso, D., and Peeters, A. G.: Tearing modes within the gyro-kinetic framework. (Joint Varenna-Lausanne International Workshop on Theory of Fusion Plasmas, 2014-09-01 to 2014-09-05, Varenna).

Hubbard, A., Osborne, T., Ryter, F., Gao, X., Ko, J., Churchill, R. M., Cziegler, I., Fenstermacher, M. E., Gerhardt, S., Gohil, P., Hughes, J., Liu, Z., Loarte, A., Maingi, R., Barrera Orte, L., Fischer, R., Manz, P., Marinoni, A., McDermott, R., McKee, G. R., Marmar, E., Rice, J., Schmitz, L., Theiler, C., Viezzer, E., Walk, J., Whyte, D., White, A., Wolfe, S. M., Wolfrum, E., Yan, Z., Zhang, T., and Happel, T.: Multi-device Studies of Pedestal Physics and Confinement in the I-mode Regime. (25th IAEA Fusion Energy Conference (FEC 2014), 2014-10-13 to 2014-10-18, Saint Petersburg).

Huber, A., Brezinsek, S., Sergienko, G., Groth, M., Vries, P. C. d., Arnoux, G., Beurskens, M. N. A., Calabro, G., Clever, M., Esser, H. G., Jachmich, S., Linsmeier, C., Matthews, G. F.,

Marsen, S., Meigs, A. G., Mertens, P., Philipps, V., Stamp, M., Wischmeier, M., Wiesen, S., and JET-EFDA Contributors: Density limit of H-mode plasmas on JET. (21st International Conference on Plasma Surface Interactions 2014 (PSI 21), 2014-05-26 to 2014-05-30, Kanazawa).

Huijsmans, G., Liu, F., Futatani, S., Loarte, A., Köchl, F., Hoelzl, M., Garofalo, A. M., and Nardon, E.: Non-linear MHD Simulations for ITER. (25th IAEA Fusion Energy Conference (FEC 2014), 2014-10-13 to 2014-10-18, Saint Petersburg).

Humphreys, D. A., Walker, M. L., Welander, A. S., Ambrosino, G., Tommasi, G. d., Mattei, M., Neu, G., Rapson, C., Raupp, G., Treutterer, W., and Winter, A.: The ITER Plasma Control System Simulation Platform. (56th Annual Meeting of the APS Division of Plasma Physics, 2014-10-27 to 2014-10-31, New Orleans, LA).

Igochine, V.: Identification and possible extension of the beta limit in ASDEX Upgrade. (19th Workshop on MHD Stability Control, 2014-11-03 to 2014-11-05, Auburn, AL).

Igochine, V.: Slow conversion of ideal MHD perturbations into a tearing mode after a sawtooth crash. (56th Annual Meeting of the APS Division of Plasma Physics, 2014-10-27 to 2014-10-31, New Orleans, LA).

Igochine, V., Gude, A., Günter, S., Lackner, K., Yu, Q., Barrera Orte, L., Bogomolov, A., Classen, I., McDermott, R., Luthmann, N. C., and ASDEX Upgrade Team: Slow conversion of ideal MHD perturbations into a tearing mode after a sawtooth crash. (56th Annual Meeting of the APS Division of Plasma Physics, 2014-10-27 to 2014-10-31, New Orleans, LA).

Iijima, N., Miyamoto, M., Nishijima, D., Baldwin, M. J., Doerner, R. P., Ueda, Y., Sagara, A., and Höschen, T.: Effect of temperature on microstructures and retention of properties in tungsten exposed to D+He+Be mixture plasma in PISCES. (21st International Conference on Plasma Surface Interactions 2014 (PSI 21), 2014-05-26 to 2014-05-30, Kanazawa).

Imrisek, M., Weinzettl, V., Mlynar, J., Odstrcil, T., Odstrcil, M., Ficker, O., Pinzon, J. R., Ehrlacher, C., Panek, R., and Hron, M.: Use of soft x-ray diagnostic on the COMPASS tokamak for investigations of sawteeth crash neighborhood and of plasma position using fast inversion methods. (20th Topical Conference on High-Temperature Plasma Diagnostics (HTPD 2014), 2014-06-01 to 2014-06-05, Atlanta, GA).

Innocente, P., Farthing, J., Giruzzi, G., Ide, S., Joffrin, E., Kamada, Y., Kühner, G., Naito, O., Urano, H., and Yoshida, M.:

Requirements for tokamak remote operation: application to JT-60SA. (28th Symposium on Fusion Technology (SOFT 2014), 2014-09-29 to 2014-10-03, San Sebastian).

Jacob, W.: Beryllium-related PSI-experiments in IPP Garching. (2nd Research Coordination Meeting of the CRP on Data for Erosion and Tritium Retention in Beryllium Plasma-facing Materials, 2014-08-18 to 2014-08-19, Vienna).

Jacob, W.: PSI issues for steel as plasma-facing material. (Consultancy Meeting on Plasma Interaction with Steel Surfaces, 2014-08-20, Vienna).

Jacquet, P., Goniche, M., Bobkov, V., Lerche, E., Colas, L., Hosea, J., Moriyama, S., Pinsker, R., Wang, S., Faugel, H., Monakhov, I., Noterdaeme, J.-M., Petrzilka, V., Pitts, R., Shaw, A., Stepanov, I., Sips, A., Van Eester, D., Wukitch, S., and Zhang, X.: Maximization of ICRF Power by SOL Density Tailoring with Local Gas Injection. (25th IAEA Fusion Energy Conference (FEC 2014), 2014-10-13 to 2014-10-18, Saint Petersburg).

Jacquet, P., Goniche, M., Bobkov, V., Lerche, E., Pinsker, R., Noterdaeme, J.-M., Faugel, H., Stepanov, I., and ASDEX Upgrade Team: Maximization of ICRF Power by SOL Density Tailoring with Local Gas Injection. (12th ITPA Integrated Operation Scenarios Topical Group Meeting (ITPA-IOS-TG), 2014-03-31 to 2014-04-03, Cambridge, MA).

Järvinen, A., Groth, M., Airila, M., Belo, P., Brezinsek, S., Clever, M., Corrigan, G., Devaux, S., Giroud, C., Harting, D., Huber, A., Lawson, K., Lehnen, M., Maddison, G., Maggi, C., Makkonen, T., Marsen, S., Matthews, G. F., Meigs, A. G., Monier-Garbet, P., Moulton, D., Stamp, M., Wiesen, S., and JET EFDA Contributors: Interpretation of radiative divertor studies with impurity seeding in type-I ELMy H-mode plasmas in JET-ILW using EDGE2D/EIRENE. (21st International Conference on Plasma Surface Interactions 2014 (PSI 21), 2014-05-26 to 2014-05-30, Kanazawa).

Jaksic, N., Greuner, H., Herrmann, A., and Böswirth, B.: Final tests and structural analysis of the new solid tungsten divertor tile for ASDEX Upgrade. (28th Symposium on Fusion Technology (SOFT 2014), 2014-09-29 to 2014-10-03, San Sebastian).

Jakubowski, M. W., Biedermann, C., König, R., Lorenz, A., Pedersen, T. S., Rodatos, A., and W7-X Team: Development of infrared and visible endoscope as the safety diagnostic for steady-state operation of Wendelstein 7-X. (12th Quantitative InfraRed Thermography Conference (QIRT 2014), 2014-07-07 to 2014-07-11, Bordeaux).

Jakubowski, M. W., Biedermann, C., König, R., Lorenz, A., Pedersen, T. S., Rodatos, A., and W7-X Team: Development of infrared and visible endoscope as the safety diagnostic for steady-state operation of Wendelstein 7-X. (8th Workshop on Fusion Data Processing, Validation and Analysis, 2014-11-04 to 2014-11-06, Ghent).

Jakubowski, M., Evans, T. E., Kirk, A., McKee, G. R., Schmitz, O., Suttrop, W., Tanaka, K., Canik, J., Dinklage, A., Hidalgo, C., and Jeon, Y.: Influence of Magnetic Perturbations on Particle Pump-out in Magnetic Fusion Devices. (25th IAEA Fusion Energy Conference (FEC 2014), 2014-10-13 to 2014-10-18, Saint Petersburg).

Järvinen, A. E., Groth, M., Silva Arestada Belo, P., Brezinsek, S., Beurskens, M., Corrigan, G., Devaux, S., Giroud, C., Eich, T., Harting, D., Huber, A., Jachmich, S., Lawson, K., Lehnen, M., Lipschultz, B., Maddison, G., Marsen, S., Meigs, A., Moulton, D., Sieglin, B., Stamp, M., Wiesen, S., and Matthews, G.: Comparison of H-mode Plasmas in JET-ILW and JET-C with and without Nitrogen Seeding. (25th IAEA Fusion Energy Conference (FEC 2014), 2014-10-13 to 2014-10-18, Saint Petersburg).

Jenko, F., Citrin, J., Goerler, T., Told, D., Abiteboul, J., Banon Navarro, A., Bourdelle, C., Bravenec, R., Casson, F., Doerk, H., Dumont, R., Fable, E., Garcia, J., Haverkort, W., Hogeweij, D., Howard, N., Johnson, T., Mantica, P., Pueschel, M. J., and White, A.: Can Gyrokinetics Really Describe Transport in L-mode Core Plasmas? (25th IAEA Fusion Energy Conference (FEC 2014), 2014-10-13 to 2014-10-18, Saint Petersburg).

Jia, Y. Z., Li, C., Xu, H. Y., DeTemmerman, G, Greuner, H., and Liu, W.: Grain Orientation Dependence of Tungsten Surface Modifications Induced by Energetic Particles. (20th Topical Conference on High-Temperature Plasma Diagnostics (HTPD 2014), 2014-06-01 to 2014-06-05, Atlanta, GA).

Joffrin, E., Challis, C. D., Frassinetti, L., Garcia, J., Hobirk, J., McDonald, D. C., Sergienko, G., and Tamain, P.: Role of neutrals on the confinement of hybrid scenario in JET-C and JET-ILW. (41st EPS Conference on Plasma Physics, 2014-06-23 to 2014-06-27, Berlin).

Joffrin, E., Garcia, J., Tamain, P., Belonohy, E., Bufferand, H., Buratti, P., Challis, C., Delabie, E., Drewelow, P., Dodt, D., Frassinetti, L., Groth, M., Hobirk, J., Koechl, F., Lipschutz, B., Lomas, P., Luna, E. d. l., Giroud, C., Loarer, T., Matthews, G., Maviglia, F., Nunes, I., Pucella Rimini, F., Solano, E., Sips, A. C. C., Tsalas, M., and Weisen, H.: Impact of divertor geometry on ITER scenarios performance in the JET metallic wall. (25th IAEA Fusion Energy Conference (FEC 2014), 2014-10-13 to 2014-10-18, Saint Petersburg).

Junghanns, P., Boscary, J., and Peacock, A.: Experience gained from the 3D machining of the HHF divertor target elements. (28th Symposium on Fusion Technology (SOFT 2014), 2014-09-29 to 2014-10-03, San Sebastian).

Kallenbach, A., Bernert, M., Casali, L., Giannone, L., Maraschek, M., Potzel, S., Reimold, F., Schweinzer, J., and Tardini, G.: Partial Detachment of High Power Discharges in ASDEX Upgrade. (25th IAEA Fusion Energy Conference (FEC 2014), 2014-10-13 to 2014-10-18, Saint Petersburg).

Kang, K. S.: Multigrid method on Intel Xeon Phi (MIC). (European Multigrid Conference, 2014-09-09 to 2014-09-12, Leuven).

Kang, K. S.: Scalable implementation of the parallel multigrid method on massively parallel computers. (International Conference on "Numerical Methods for Scientific Computations and Advanced Applications" (NMSCAA'14), 2014-05-19 to 2014-05-22, Bansko).

Kappatou, A., McDermott, R., Angioni, C., Pütterich, T., Viezzer, E., Cavedon, M., Fischer, R., Willensdorfer, M., Tardini, G., and ASDEX Upgrade Team: Helium transport investigations in ASDEX Upgrade. (19th Joint EU-US Transport Task Force Meeting (TTF 2014), 2014-09-08 to 2014-09-11, Culham).

Käsemann, C.-P., Jacob, C., Stobbe, F., Mayer, A., Sachs, E., Klein, R., and ASDEX Upgrade Team: New Drive Converter and Digital Control for the Pulsed Power Supply System of ASDEX Upgrade. (28th Symposium on Fusion Technology (SOFT 2014), 2014-09-29 to 2014-10-03, San Sebastian).

Kasparek, W., Lechte, C., Plaum, B., Zeitler, A., Erckmann, V., Laqua, H. P., Weißgerber, M., Bechtold, A., Busch, M., and Szcepaniak, B.: Remote-steering Launchers for the ECRH system on the Stellarator W7-X. (18th Joint Workshop on Electron Cyclotron Emission and Electron Cyclotron Resonance Heating, 2014-04-22 to 2014-04-25, Nara).

Kasparek, W., Plaum, B., Lechte, C., Wu, Z., Wang, H., Maraschek, M., Stober, J., Wagner, D., Schubert, M., Grünwald, G., Monaco, F., Müller, S., Schütz, H., Erckmann, V., Doelman, N., Braber, R. v. d., Klop, W., Brand, H. v. d., Bongers, W., Krijger, B., Petelin, M., Koposova, L., Lubyako, L., Bruschi, A., Sakamoto, K., Teams at the Contributed Institutes, and ASDEX Upgrade Team: Development of Resonant Diplexers for High-power ECRH – Status, Applications, Plans. (18th Joint Workshop on Electron Cyclotron Emission and Electron Cyclotron Resonance Heating, 2014-04-22 to 2014-04-25, Nara).

Kawamura, G., Feng, Y., Kobayashi, M., Shoji, M., Morisaki, T., and Masuzaki, S.: Transport Simulation Analysis of Peripheral Plasma with the Open and the Closed LHD Divertor. (25th IAEA Fusion Energy Conference (FEC 2014), 2014-10-13 to 2014-10-18, Saint Petersburg).

Kernbichler, W., Kasilov, S. V., Kapper, G., and Marushchenko, N. B.: Computation of the Spitzer function in stellarators and tokamaks with finite collisionality. (18th Joint Workshop on Electron Cyclotron Emission and Electron Cyclotron Resonance Heating, 2014-04-22 to 2014-04-25, Nara).

Kirk, A., Chapman, I., Liu, Y., Suttrop, W., Cahyna, P., Eich, T., Jakubowski, M., Saarelma, S., Scannell, R., Harrison, J., Thornton, A., and Valovic, M.: Effect of Resonant Magnetic Perturbations on Low Collisionality Discharges in MAST and a Comparison with ASDEX Upgrade. (25th IAEA Fusion Energy Conference (FEC 2014), 2014-10-13 to 2014-10-18, Saint Petersburg).

Klimov, N. S., Podkovyrov, V. L., Muzichenko, A. D., Zhitlukhin, A. M., Kovalenko, D. V., Putrik, A. B., Barsuk, V. A., Kuprianov, I. B., Linke, J., Bazylev, B. N., Spitsyn, A. V., Ogorodnikova, O., Mayer, M., and Giniyatulin, R. N.: Plasma facing materials performance under ITER-relevant mitigated disruption photonic heat loads. (21st International Conference on Plasma Surface Interactions 2014 (PSI 21), 2014-05-26 to 2014-05-30, Kanazawa).

Klinger, T.: Wendelstein 7-X Approaches Operation – Review of Construction, Status of Commissioning, and Initial Research Plan. (21st Topical Meeting on the Technology of Fusion Energy (TOFE), 2014-11-09 to 2014-11-13, Anaheim, CA).

Kobayashi, M., Feng, Y., Schmitz, O., Liang, Y., Evans, T. E., Frerichs, H., Cui, Z. Y., Reiter, D., Asakura, N., Wenzel, U., Morita, S., Ida, K., Tanaka, H., Masuzaki, S., Yamada, I., Peterson, B. J., Ohnof, N., Pandya, S., Narushima, Y., Suzuki, C., Tamura, N., Tokuzawa, T., Itoh, K., Akiyama, T., Tanaka, K., and Yamada, H.: Impacts of 3D magnetic field structure on boundary & divertor plasmas in stellarator/heliotron devices. (21st International Conference on Plasma Surface Interactions 2014 (PSI 21), 2014-05-26 to 2014-05-30, Kanazawa).

Kobayashi, M., Ida, K., Feng, Y., Schmitz, O., Evans, T. E., Frerichs, H., Liang, Y., Ghendrih, P., Ciraolo, G., Bader, A., Guo, H., Tabares, F., Tafalla, D., Reiter, D., Cui, Z., Xu, Y., Wenzel, U., Asakura, N., Ohno, N., Morita, S., Masuzaki, S., Peterson, B., Itoh, K., and Yamada, H.: 3D Effects of Edge Magnetic Field Configuration on Divertor/SOL Transport and Optimization Possibilities for a Future Reactor. (25th IAEA Fusion Energy Conference (FEC 2014), 2014-10-13 to 2014-10-18, Saint Petersburg).

Koch, F., Brinkmann, J., Siefken, U., Florko, I., Elgeti, S., Matern, G., and Wiltner, A.: Safety improvement of a future nuclear fusion power plant by self-passivating tungsten alloys. (The Nuclear Materials Conference (NuMat 2014), 2014-10-27 to 2014-10-30, Clearwater, FL).

Kocsis, G., Biedermann, C., Bodnár, G., Cseh, G., Ilkei, T., König, R., Otte, M., Szabolics, T., Szepesi, T., and Zoletnik, S.: Overview video diagnostics for W7-X stellarator. (28th Symposium on Fusion Technology (SOFT 2014), 2014-09-29 to 2014-10-03, San Sebastian).

König, R., Biel, W., Biedermann, C., Burhenn, R., Cseh, G., Czarnecka, A., Endler, M., Estrada, T., Grulke, O., Hathiramani, D., Hirsch, M., Jablonski, S., Jakubowski, M., Kaczmarczyk, J., Kasparek, W., Kocsis, G., Kornejew, P., Krämer-Flecken, A., Krychowiak, M., Kubkowska, M., Langenberg, A., Laux, M., Liang, Y., Lorenz, A., Neubauer, O., Otte, M., Pabiant, N., Pasch, E., Pedersen, T. S., Schmitz, O., Schneider, W., Schuhmacher, H., Schweer, B., Thomsen, H., Szepesi, T., Wiegel, B., Windisch, T., Wolf, S., Zhang, D., and Zoletnik, S.: Status of the Diagnostics Development for the First Operation Phase of the Stellarator Wendelstein 7-X. (20th Topical Conference on High-Temperature Plasma Diagnostics (HTPD 2014), 2014-06-01 to 2014-06-05, Atlanta, GA).

König, R., and W7-X Diagnostics Team: Construction and commissioning status of Wendelstein 7-X and prospects for university collaborations. (Workshop on Exploratory Topics in Plasma and Fusion Research (EPR) and US-Japan Compact Torus (CT) Workshop, 2014-08-05 to 2014-08-08, Madison, WI).

König, R., and W7-X Diagnostics Team: Status of the Diagnostics Development for the Stellarator Wendelstein 7-X. (20th Topical Conference on High-Temperature Plasma Diagnostics (HTPD 2014), 2014-06-01 to 2014-06-05, Atlanta, GA).

Konishi, S., Campbell, D., Gasparotto, M., and Giancarli, L.: Status of ITER TBM Program. (21st Topical Meeting on the Technology of Fusion Energy (TOFE), 2014-11-09 to 2014-11-13, Anaheim, CA).

Kormann, K.: A semi-Lagrangian Vlasov solver in tensor train format. (Numerical Methods for the Kinetic Equations of Plasma Physics (NumKin2014), 2014-10-20 to 2014-10-24, Garching).

Kormann, K., and Sonnendrücker, E.: Sparse grids for the Vlasov equation. (Workshop on Sparse Grids and Applications, 2014-09-01 to 2014-09-05, Stuttgart).

Krat, S., Bykov, I., Coad, P., Likonen, J., Mayer, M., Renterghem, W. v., Ruset, C., De Saint-Aubin, G., Widdowson, A., and

JET-EFDA Contributors: Erosion/deposition on JET divertor marker tiles exposed during the first JET ILW campaign. (EUROfusion PFC&JET 2 Annual Meeting, 2014-11-24 to 2014-11-27, Jülich).

Krat, S., Bykov, I., Coad, P., Likonen, J., Mayer, M., Renterghem, W. v., Ruset, C., De Saint-Aubin, G., Widdowson, A., and JET-EFDA Contributors: New results on analysis of JET erosion/deposition samples. (20th ITPA Scrape-off Layer & Divertor Topical Group Meeting, 2014-10-20 to 2014-10-23, Prague).

Krat, S., Bykov, I., Van Renterghem, W., Mayer, M., Widdowson, A., and JET-EFDA Contributors: Erosion and deposition in JET divertor during 2011-2012 campaign. (International Summer School on the Physics of Plasma-Surface Interactions, 2014-07-28 to 2014-08-04, Moscow).

Krat, S., Gasparyan, Y., Pisarev, A., Mayer, M., Toussaint, U. v., Coad, P., Widdowson, A., and JET-EFDA Contributors: Hydrocarbon film deposition inside cavity samples in remote areas of the JET divertor during the 1999-2001 and 2005-2009 campaigns. (21st International Conference on Plasma Surface Interactions 2014 (PSI 21), 2014-05-26 to 2014-05-30, Kanazawa).

Kraus, M.: New Developments in Variational Integrators for Plasma Physics. (Seminar, 2014-05-26, Nagoya).

Kraus, M.: New Developments in Variational Integrators for Plasma Physics. (International Conference on Geometric Algorithms and Methods for Plasma Physics, 2014-05-13 to 2014-05-15, Hefei).

Kraus, M.: New Developments in Variational Integrators for Plasma Physics. (Seminar. National Institute for Fusion Science, 2014-05-28, Oroshi-Cho, Toki-City, Gifu).

Kraus, M.: Unconventional Variationalintegrators and their Application in Plasma Physics. (Seminar, Waseda University, 2014-05-08, Tokyo).

Kraus, M.: Variational Integrators for Nonvarational PDEs. (Journées de Dynamique Non Linéaire, 2014-07-10, Cadarache).

Kraus, M.: Variational Integrators for Nonvarational PDEs. (11th World Congress on Computational Mechanics, 2014-07-20 to 2014-07-25, Barcelona).

Kraus, M.: Variational Integrators in Plasma Physics. (Talk, SFB Seminar Discretization in Geometry and Dynamics, 2014-04-08, München).

183

Kraus, W., Fantz, U., Heinemann, B., and Franzen, P.: Solid State RF Amplifier for Powerful Negative Hydrogen Ion Sources. (4th International Symposium on Negative Ions, Beams and Sources (NIBS 2014), 2014-10-06 to 2014-10-10, Garching).

Krebs, I., Jardin, S. C., Igochine, V., Günter, S., and Hölzl, M.: Investigations on Sawtooth Reconnection in ASDEX Upgrade Tokamak Discharges Using the 3D Non-linear Two-fluid MHD Code M3D-C1. (56th Annual Meeting of the APS Division of Plasma Physics, 2014-10-27 to 2014-10-31, New Orleans, LA).

Krieger, K., ASDEX Upgrade Team, JET-EFDA Contributors, and TEXTOR Team: The impact of tungsten divertors on plasma performance. (41st EPS Conference on Plasma Physics, 2014-06-23 to 2014-06-27, Berlin).

Krieger, K., and Neu, R.: First results of "ELM penetration into shadowed areas" experiment at AUG and "Performance of the new ASDEX Upgrade bulk W divertor (Div III)". (20th ITPA Scrape-off Layer & Divertor Topical Group Meeting, 2014-10-20 to 2014-10-23, Prague).

Krieger, K., and Schmid, K.: Quantitative comparison of measured and predicted Be sources for initial ILW Be migration experiment: WALLDYN modelling for limiter and divertor phases in JET. (20th ITPA Scrape-off Layer & Divertor Topical Group Meeting, 2014-10-20 to 2014-10-23, Prague).

Kurutz, U., and Fantz, U.: Investigations on caesium-free alternatives for H- formation at ion sourc relevant parameters. (4th International Symposium on Negative Ions, Beams and Sources (NIBS 2014), 2014-10-06 to 2014-10-10, Garching).

Kurutz, U., Fantz, U., and Rauner, D.: Volumen und oberflächenunterstützte Erzeugung von negativen Wasserstoffionen in einem Niederdruck-ECR-Plasmaten. (78. DPG-Jahrestagung und Frühjahrstagung der Sektion AMOP, 2014-03-17 to 2014-03-21, Berlin).

Lang, P. T.: DEMO Design Change Request-001: Pellet fuelling guide tube space reservation on the inboard. (PPPT Design Configuration Meeting, 2014-07-01, Garching).

Lang, P. T.: Matter injection in DEMO – Introduction to the project. (Kick-off Meeting of the DEMO Work Package Tritium, Fuelling and Vacuum, 2014-04-29, KIT Karlsruhe).

Lang, P. T.: Matter injection in DEMO: Status of the technology assessment. (DEMO Work Package Tritium, Fuelling and Vacuum Progress Meeting, 2014-11-25, KIT Karlsruhe).

Lang, P. T.: Pellet pacing/triggering and fuelling experiments from JET, ASDEX Upgrade and MAST. (26th Meeting of the ITPA Pedestal and Edge Physics Topical Group, 2014-04-15 to 2014-04-17, Prague).

Lang, P. T., Bernert, M., Casali, L., Fischer, R., Kardaun, O., Kocsis, G., Maraschek, M., Mlynek, A., Plöckl, B., Ryter, F., Szepesi, T., Tardini, G, Zohm, H., and ASDEX Upgrade Team: High density operation using pellet fuelling on ASDEX Upgrade. (78. DPG-Jahrestagung und Frühjahrstagung der Sektion AMOP, 2014-03-17 to 2014-03-21, Berlin).

Lang, P. T., Day, C., Fable, E., Igitkhanov, Y., Köchl, F., Pegourie, B., Plöckl, B., Wenninger, R., and Zohm, H.: Considerations on the DEMO pellet fuelling system. (28th Symposium on Fusion Technology (SOFT 2014), 2014-09-29 to 2014-10-03, San Sebastian).

Langer, H., Steinbicker, A., Meister, H., and Zauner, C.: Integrated Thermal FE Analyses and Testing of Prototype Components for the ITER Bolometer Diagnostic. (28th Symposium on Fusion Technology (SOFT 2014), 2014-09-29 to 2014-10-03, San Sebastian).

Laqua, H. P.: Plasmawellen und Heizung. (SS 2014. Vorlesung, Ernst-Moritz-Arndt-Universität Greifswald).

Laqua, H. P., Podoba, Y. Y., Otte, M., Stange, T., Dostal, M., Preinhaelter, J., Preynas, M., Marsen, S., Warr, G. B., Birus, D., Zhang, D., Zhang, X., Chlechowitz, E., Lingertat, J., Assmus, D., Horvath, K., Rodatos, A., Urban, J., and Wauters, T.: Overview of 13 years RF-experiments at the WEGA-Stellarator. (9th International Workshop "Strong Microwaves and Terahertz Waves: Sources and Applications", 2014-07-24 to 2014-07-30, Nizhny Novgorod).

Lauber, P.: Kinetic models for energetic particle physics in tokamaks – verification, validation and predictions for ITER. (Joint Varenna-Lausanne International Workshop on Theory of Fusion Plasmas, 2014-09-01 to 2014-09-05, Varenna).

Lawson, K. D., Groth, M., Belo, P., Brezinsek, S., Czarnecka, A., Drewelow, P., Harting, D., Ksiazek, I., Maggi, C. F., Meigs, A. G., Menmuir, S., Stamp, M. F., and JET-EFDA Contributors: Improved EDGE2D/EIRENE simulations of JET ITER-like wall L-mode discharges utilising poloidal VUV/visible spectral emission profiles. (21st International Conference on Plasma Surface Interactions 2014 (PSI 21), 2014-05-26 to 2014-05-30, Kanazawa).

Lebschy, A., Dux, R., Fischer, R., McDermott, R. M., and ASDEX Upgrade Team: Rekonstruktion der Elektronendichte mit Hilfe von Emissionsspektroskopie am Neutralstrahl.

(78. DPG-Jahrestagung und Frühjahrstagung der Sektion AMOP, 2014-03-17 to 2014-03-21, Berlin).

Lee, H. T., and Schwarz-Selinger, T.: Deuterium-hydrogen isotope exchange in self-damaged tungsten studied by in-situ nuclear reaction analysis. (19th International Conference on Ion Beam Modification of Materials (IBMM), 2014-09-14 to 2014-09-19, Leuven).

Lee, H. T., Ueda, Y., De Temmerman, G., Berg, M. A. v. d., Gao, L., and Schwarz-Selinger, T.: Deuterium retention in tungsten exposed to mixed D+N plasma at divertor relevant fluxes in Magnum-PSI. (21st International Conference on Plasma Surface Interactions 2014 (PSI 21), 2014-05-26 to 2014-05-30, Kanazawa).

Lemahieu, N., Greuner, H., Linke, J., Maier, H., Pintsuk, G., Van Ost, G., and Wirtz, M.: Synergistic effects of ELMs and steady state H and H/He irradiation on tungsten in plasma facing components. (28th Symposium on Fusion Technology (SOFT 2014), 2014-09-29 to 2014-10-03, San Sebastian).

Lennholm, M., Frigione, D., Graves, J., Beaumont, P. S., Blackman, T., Carvalho, I. S., Chapman, I., Dumont, R., Felton, R., Garzotti, L., Goniche, M., Goodyear, A., Grist, D., Jachmich, S., Johnson, T., Lang, P., Lerche, E., Luna, E. d. l., Monakhov, I., Mooney, R., Morris, J., Nave, M. F., Reich, M., Rimini, F. G., Sips, A., Sheikh, H., Sozzi, C., Tsalas, M., and JET-EFDA Contributors: Real-time Control of ELM and Saw-tooth Frequencies: Similarities and Differences. (25th IAEA Fusion Energy Conference (FEC 2014), 2014-10-13 to 2014-10-18, Saint Petersburg).

Lerche, E. A., Goniche, M., Jacquet, P., Van Eester, D., Bobkov, V., Colas, L., Monakhov, I., Noble, C., Blackman, T., Rimini, F., Brezinsek, S., Czarnecka, A., Crombé, K., Challis, C., Remi, D., Fedorczak, N., Giroud, C., Graves, J., Hobirk, J., Joffrin, E., Kiptily, V., Lennholm, M., Lomas, P., Maggi, C., Aho-Mantila, L., Mantica, P., Matthews, G., Mayoral, M.-L., Mlynar, J., Monier-Garbet, P., Nave, M. F., Ferreira Nunes, I. M., Petrzilka, V., Pütterich, T., Reich, M., Shaw, A., Sips, A., Tsalas, M., and Valisa, M.: ICRH for Mitigation of Core Impurity Accumulation in JET-ILW. (25th IAEA Fusion Energy Conference (FEC 2014), 2014-10-13 to 2014-10-18, Saint Petersburg).

Lerche, E., Goniche, M., Van Eester, D., Jacquet, P., Bobkov, V., Colas, L., Brezinsek, S., Czarnecka, A., Graham, M., Groth, M., Mathurin, T., Monakhov, I., Noble, C., Rimini, F., Shaw, A., and JET-EFDA Contributors: Impact of gas injection on ICRF coupling and SOL parameters in JET-ILW H-mode plasmas. (21st International Conference on Plasma Surface Interactions 2014 (PSI 21), 2014-05-26 to 2014-05-30, Kanazawa).

Lessig, A., Hölzl, M., Lackner, K., and Günter, S.: Towards non-linear simulations of full ELM crashes in ASDEX Upgrade. (78. DPG-Jahrestagung und Frühjahrstagung der Sektion AMOP, 2014-03-17 to 2014-03-21, Berlin).

Leuterer, F., Wagner, D., Schubert, M., Kasparek, W., and AUG-ECRH Group: Polarizer calibration for multifrequency high-power ECRH transmission lines. (9th International Workshop "Strong Microwaves and Terahertz Waves: Sources and Applications", 2014-07-24 to 2014-07-30, Nizhny Novgorod).

Li, C., Greuner, H., Yuan, Y., Zhao, S. X., Luo, G. N., Böswirth, B., Fu, B. Q., Jia, Y. Z., and Liu, W.: Surface modifications of W divertor components for EAST during high heat loads with He. (21st International Conference on Plasma Surface Interactions 2014 (PSI 21), 2014-05-26 to 2014-05-30, Kanazawa).

Li, X., Zhang, M., Yu, Q., and Chen, Z.: Overvoltage Protection for Magnetic Systems during Disruption in Tokamak. (28th Symposium on Fusion Technology (SOFT 2014), 2014-09-29 to 2014-10-03, San Sebastian).

Linsmeier, C., Allouche, A., Oberkofler, M., Reinelt, M., Schmid, K., and Piechoczek, R.: Hydrogen isotope retention and release in beryllium: The full picture from experiment and ab initio calculations. (2014 Joint ICTP-IAEA Conference on Models and Data for Plasma-Material Interaction in Fusion Devices, 2014-11-03 to 2014-11-07, Miramare, Trieste).

Linsmeier, C., Köppen, M., Oberkofler, M., Reinelt, M., and Vollmer, A.: Ion-induced chemistry and hydrogen retention mechanisms in fusion firstwall materials. (20th International Workshop on Inelastic Ion-Surface Collisions (IISC-20), 2014-02-16 to 2014-02-21, Wirrina Cove).

Lisgo, S., Harrison, J., Kocan, M., Pitts, R., Potzel, S., Reiter, D., and Stangeby, P.: Time-resolved kinetic modelling of ELM-induced tungsten influx in ITER. (56th Annual Meeting of the APS Division of Plasma Physics, 2014-10-27 to 2014-10-31, New Orleans, LA).

Lishev, S., Schiesko, L., Wünderlich, D., and Fantz, U.: Spatial Distribution of the Plasma Parameters in the rf Driven Negative Ion Source Prototype for Fusion. (4th International Symposium on Negative Ions, Beams and Sources (NIBS 2014), 2014-10-06 to 2014-10-10, Garching).

Litnovsky, A., Hellwig, M., Matveev, D., Komm, M., Berg, M. v. d., De Temmerman, G., Rudakov, D., Ding, F., Luo, G.-N., Krieger, K., Sugiyama, K., and Pitts, R. A.: Optimization of tungsten castellated structures for the ITER divertor. (21st International Conference on Plasma Surface Interactions 2014 (PSI 21), 2014-05-26 to 2014-05-30, Kanazawa).

Loewenhoff, T., Greuner, H., Linke, J., Maier, H., Pintsuk, G., Pitts, R. A., Riccardi, B., and De Temmerman, G.: Impact of combined transient plasma/heat loads on tungsten performance. (21st International Conference on Plasma Surface Interactions 2014 (PSI 21), 2014-05-26 to 2014-05-30, Kanazawa).

Loizu, J., Hudson, S., Bhattacharjee, A., and Helander, P.: Magnetic Islands and singular currents at rational surfaces in three-dimensional MHD equlibria. (56th Annual Meeting of the APS Division of Plasma Physics, 2014-10-27 to 2014-10-31, New Orleans, LA).

Lore, J. D., Reinke, M. L., LaBombard, B., Lipschultz, B., Pitts, R. A., and Feng, Y.: EMC3-EIRENE modelling of toroidally-localized divertor gas injection experiments on Alcator C-Mod. (21st International Conference on Plasma Surface Interactions 2014 (PSI 21), 2014-05-26 to 2014-05-30, Kanazawa).

Lowry, C., Wischmeier, M., Huber, A., Maggi, C. F., McCormick, K., Reinke, M., Drewelow, P., Brezinsek, S., Aho-Mantila, L., Arnoux, G., Sips, A., Meigs, A., Sergienko, G., Nave, M. F., Devaux, S., Marsen, S., and Stamp, M.: Impurity Seeding on JET to Achieve Power Plant Like Divertor Conditions. (25th IAEA Fusion Energy Conference (FEC 2014), 2014-10-13 to 2014-10-18, Saint Petersburg).

Lumsdaine, A., Boscary, J., Fellinger, J., Harris, J., Hölbe, H., König, R., McGinnis, D., Lore, J., Neilson, H., Peacock, A., Titus, P., and Tretter, J.: Instrumentation and Analysis of the W7-X Inertially Cooled Test Divertor Unit Scraper Element Design. (20th Topical Conference on High-Temperature Plasma Diagnostics (HTPD 2014), 2014-06-01 to 2014-06-05, Atlanta, GA).

Lumsdaine, A., Boscary, J., Harris, J., Hoelbe, H., König, R., McGinnis, D., Lore, J., Neilson, H., Peacock, A., Titus, P., and Tretter, J.: Design of the Wendelstein 7-X Inertially Cooled Test Divertor Unit Scraper Element. (28th Symposium on Fusion Technology (SOFT 2014), 2014-09-29 to 2014-10-03, San Sebastian).

Lunt, T., Canal, G., Feng, Y., and Reimerdes, H.: The snowflake divertor, physics of a new concept for power exhaust of fusion plasmas. (78. DPG-Jahrestagung und Frühjahrstagung der Sektion AMOP, 2014-03-17 to 2014-03-21, Berlin).

Lunt, T., Carralero, D., Birkenmeier, G., Feng, Y., Marné, P. d., Müller, H. W., Müller, S., Scarabosio, A., Sieglin, B., Wischmeier, M., and ASDEX Upgrade Team: EMC3-Eirene simulations of particle- and energy fluxes to main chamber- and divertor plasma facing components in ASDEX Upgrade compared to experiments. (21st International Conference on

Plasma Surface Interactions 2014 (PSI 21), 2014-05-26 to 2014-05-30, Kanazawa).

Maggi, C. F., Saarelma, S., Beurskens, M., Frassinetti, L., Matthew, L., Challis, C., Chapman, I., Elena, D. L. L., Joanne, F., Giroud, C., Hobirk, J., Joffrin, E., Lomas, P., Lowry, C., Maddison, G., Mailloux, J., Nunes Ferreira, I. M., Rimini, F., Simpson, J., Sips, A., and Urano, H.: Pedestal Confinement and Stability in JET-ILW ELMy H-Mode Scenarios. (25th IAEA Fusion Energy Conference (FEC 2014), 2014-10-13 to 2014-10-18, Saint Petersburg).

Maier, H., Greuner, H., Balden, M., Böswirth, B., Elgeti, S., Schmid, K., and Schwarz-Selinger, T.: Erosion and hydrogen retention of actively cooled tungsten components under high heat flux loading with H/He particles. (21st International Conference on Plasma Surface Interactions 2014 (PSI 21), 2014-05-26 to 2014-05-30, Kanazawa).

Makkonen, T., Airila, M. I., Dux, R., Groth, M., Hakola, A., Koivuranta, S., Kurki-Suonio, T., Likonen, J., Lindholm, V., Lunt, T., Mayer, M., Miettunen, J., Müller, H. W., Neu, R., Pettersson, P., Pütterich, T., Rohde, V., Rubel, M., Viezzer, E., and ASDEX Upgrade Team: Understanding material migration in the ASDEX Upgrade tokamak. (Physics Days 2014, 48th Annual Meeting of the Finnish Physical Society, 2014-03-11 to 2014-03-13, Tampere).

Manas, P., Camenen, Y., Benkadda, S., Angioni, C., and Casson, F. J.: Gyrokinetic modelling of light impurity transport in JET H-mode and hybrid discharges. (19th Joint EU-US Transport Task Force Meeting (TTF 2014), 2014-09-08 to 2014-09-11, Culham).

Manhard, A., Gao, L., Toussaint, U. v., Schmid, K., and Höschen, T.: Permeation of Hydrogen through Tungsten near Room Temperature. (21st International Conference on Plasma Surface Interactions 2014 (PSI 21), 2014-05-26 to 2014-05-30, Kanazawa).

Manhard, A., Schwarz-Selinger, T., Mayer, M., Markina, E., Kapser, S., and Schmid, K.: Investigations on Radiation Damaging of W at IPP Garching. (US-Japan Workshop, 2014-06-05, Kyoto).

Manhard, A., Schwarz-Selinger, T., and Schmid, K.: Simulation of D uptake by self-damged W at low ion fluxes and energies. (12th International Workshop on Hydrogen Isotopes in Fusion Reactor Materials (HWS-12), 2014-06-02 to 2014-06-04, Toyama).

Manhard, A., Schwarz-Selinger, T., Schmid, K., and Toussaint, U. v.: Comparison of a quantitative diffusion-trapping

model with experiments on D uptake in damaged W. (2014 Joint ICTP-IAEA Conference on Models and Data for Plasma-Material Interaction in Fusion Devices, 2014-11-03 to 2014-11-07, Miramare, Trieste).

Manhard, A., Lee, H. T., Ueda, Y., Toussaint, U. v., and Schmid, K.: Investigation of Hydrogen Diffusion in Tungsten below 500 K. (10th International Conference on Diffusion in Solids and Liquids (DSL-2014), 2014-06-23 to 2014-06-27, Paris).

Manz, P., Birkenmeier, G., Carralero, D., Fuchert, G., Müller, H. W., Müller, S. H., Scott, B. D., Stroth, U., Wolfrum, E., and ASDEX Upgrade Team: Influence of finite ion temperature on plasma blob dynamics. (41st EPS Conference on Plasma Physics, 2014-06-23 to 2014-06-27, Berlin).

Mardenfeld, M., Renard, S., Pablant, N., Langenberg, A., Ellis, R., Neilson, H., and Bykov, V.: Engineering Design of an X-Ray Imaging Crystal Spectrometer for the W7-X Stellarator. (20th Topical Conference on High-Temperature Plasma Diagnostics (HTPD 2014), 2014-06-01 to 2014-06-05, Atlanta, GA).

Markelj, S., Ogorodnikova, O., Zaloznik, A., Vavpetic, P., Schwarz-Selinger, T., Pelicon, P., and Cadez, I.: In situ of isotope exchange mechanism in self-ion damaged tungsten. (2014 Joint ICTP-IAEA Conference on Models and Data for Plasma-Material Interaction in Fusion Devices, 2014-11-03 to 2014-11-07, Miramare, Trieste).

Markelj, S., Zaloznik, A., Cadez, I., Pelicon, P., Vavpetic, P., Ogorodnikova, O., and Schwarz-Selinger, T.: Zadrzevanje devterija v poskodovanem volframu. (9. konference fizikov v osnovnih raziskavah, 2014-11-12 to 2014-11-12, Skofji Loki).

Martitsch, A. F., Kernbichler, W., Kasilov, S. V., Heyn, M. F., and Maassberg, H.: Evaluation of the toroidal torque driven by external non-resonant non-axisymmetric magnetic field perturbations in a tokamak. (19th Joint EU-US Transport Task Force Meeting (TTF 2014), 2014-09-08 to 2014-09-11, Culham).

Martone, M.: Auto-tuning shared memory parallel sparse BLAS operations with a recursive matrix layout. (8th International Workshop on Parallel Matrix Algorithms and Applications (PMAA 2014), 2014-07-02 to 2014-07-04, Lugano).

Marushchenko, N. B., Erckmann, V., Beidler, C. D., Geiger, J., Laqua, H. P., Helander, P., Maassberg, H., and Turkin, Y.: ECRH scenario with selective heating of trapped/passing electrons in the W7-X Stellarator. (18th Joint Workshop on Electron Cyclotron Emission and Electron Cyclotron Resonance Heating, 2014-04-22 to 2014-04-25, Nara).

Masiello, A., Agarici, G, Boilson, D., Bonicelli, T., Decamps, H., Fantz, U., Franzen, P., Graceffa, J., Heinemann, B., Hemsworth, R., Marcuzzi, D., Paolucci, F., Simon, M., Toigo, V., and Zaccaria, P.: Progress Status of the Activities in EU for the Development of the ITER Neutral Beam Injector and Test Facility. (25th IAEA Fusion Energy Conference (FEC 2014), 2014-10-13 to 2014-10-18, Saint Petersburg).

Matveev, D., Oberkofler, M., Reinelt, M., and Linsmeier, C.: Reaction-diffusion based modelling of deuterium retention in Be. (2014 Joint ICTP-IAEA Conference on Models and Data for Plasma-Material Interaction in Fusion Devices, 2014-11-03 to 2014-11-07, Miramare, Trieste).

Mayer, M.: Discussion: Hydrogen in Reduced Activation Ferritic-Martensitix (RAFM) Steels. (12th International Workshop on Hydrogen Isotopes in Fusion Reactor Materials (HWS-12), 2014-06-02 to 2014-06-04, Toyama).

Mayer, M.: Erosion and deposition studies in fusion devices. (International Summer School on the Physics of Plasma-Surface Interactions, 2014-07-28 to 2014-08-04, Moscow).

Mayer, M., Markina, E., Manhard, A., and Schwarz-Selinger, T.: Recovery temperatures of defects in tungsten created by self-implantation. (21st International Conference on Plasma Surface Interactions 2014 (PSI 21), 2014-05-26 to 2014-05-30, Kanazawa).

Mayer, M., Krat, S., Hakola, A., Coad, J. P., Gasparyan, Y., Koivuranta, S., Likonen, J., Neu, R., Pisarev, A., Rohde, V., Sugiyama, K., Widdowson, A., JET EFDA Contributors, and ASDEX Upgrade Team: JET and AUG experience with removable samples. (ITER Workshop on Erosion Depostion Dust Tritium, 2014-02-12 to 2014-02-14, Cadarache).

Mazon, D., Angioni, C., Pütterich, T., Vezinet, D., Sertoli, M., Belli, E. A., Bilato, R., Casson, F., Odstrcil, T., Bobkov, V., Dux, R., Gude, A., Guirlet, R., Igochine, V., Malard, P., and Kallenbach, A.: W Impurity Poloidal Assymmetries Observed at ASDEX Upgrade Using Soft-X-Ray Tomography Reconstruction. (25th IAEA Fusion Energy Conference (FEC 2014), 2014-10-13 to 2014-10-18, Saint Petersburg).

McClements, K., Dendy, R., Carbajal, L., Chapman, S., Cook, J., D'Inca, R., Harvey, B., Heidbrink, B., and Pinches, S.: Fast Particle-driven Ion Cyclotron Emission (ICE) in Tokamak Plasmas and the Case for an ICE Diagnostic in ITER. (25th IAEA Fusion Energy Conference (FEC 2014), 2014-10-13 to 2014-10-18, Saint Petersburg).

Medvedeva, A., Bottereau, C., Clairet, F., Conway, G., Heuraux, S., Molina, D., and Stroth, U.: Experimental study of the radial structure of turbulence with a ultra-fast sweeping reflectometer in ASDEX Upgrade. (78. DPG-Jahrestagung und Frühjahrstagung der Sektion AMOP, 2014-03-17 to 2014-03-21, Berlin).

Mehrenberger, M., Afeyan, B., Dodhy, A., and Sonnen-drücker, E.: The Birth of Kinetic Electrostatic Electron Nonlinear (KEEN) Waves Weakly Driven by the Pondero-motive Force of Crossing Laser Beams in High Energy Density Plasmas Compared to Strongly Driven KEEN Waves. (56th Annual Meeting of the APS Division of Plasma Physics, 2014-10-27 to 2014-10-31, New Orleans, LA).

Meisl, G., Schmid, K., Krieger, K., Lisgo, S., and ASDEX Upgrade Team: N migration in Be/W machines including the influence of toroidal asymmetries. (20th ITPA Scrape-off Layer & Divertor Topical Group Meeting, 2014-10-20 to 2014-10-23, Prague).

Meisl, G., Schmid, K., Oberkofler, M., Krieger, K., Lisgo, S. W., Aho-Mantila, L., Reimold, F., Rohde, V., and ASDEX Upgrade Team: Nitrogen migration and retention in ASDEX Upgrade. (78. DPG-Jahrestagung und Frühjahrstagung der Sektion AMOP, 2014-03-17 to 2014-03-21, Berlin).

Meisl, G., Schmid, K., Oberkofler, M., Krieger, K., Lisgo, S. W., Aho-Mantila, L., Reimold, F., Rohde, V., and ASDEX Upgrade Team: Nitrogen migration and retention in ASDEX Upgrade. (21st International Conference on Plasma Surface Interactions 2014 (PSI 21), 2014-05-26 to 2014-05-30, Kanazawa).

Meister, H., Kasparek, W., Zhang, D., Hirsch, M., Koll, J., and Zeitler, A.: Millimetre wave attenuation of prototype diagnostic components for the ITER bolometers. (28th Symposium on Fusion Technology (SOFT 2014), 2014-09-29 to 2014-10-03, San Sebastian).

Mendelevitch, B., Boscary, J., Peacock, A., Smirnow, M., and Stadler, R.: Water-cooling system of the W7-X plasma facing components. (28th Symposium on Fusion Technology (SOFT 2014), 2014-09-29 to 2014-10-03, San Sebastian).

Mendoza, L.: Solving Vlasov-like equations using the Semi-Lagrangian scheme on a 2D hexagonal mesh. (Numerical Methods for the Kinetic Equations of Plasma Physics (NumKin2014), 2014-10-20 to 2014-10-24, Garching).

Merli, S., Schulz, A., Walker, M., Stroth, U., and Hirth, T.: Großflächige Hochrateabscheidung von Kratzschutzschichten auf Polycarbonat mittels Mikrowellen-PECVD. (78. DPG-Jahrestagung und Frühjahrstagung der Sektion AMOP, 2014-03-17 to 2014-03-21, Berlin).

Meyer, H., Delabie, E., Hughes, J., Martin, Y., Maggi, C. F., Rimini, F., Ryter, F., Silva, C., Zoletnik, S., ASDEX Upgrade Team, JET-EFDA Contributors, and Alcator C-MOD Team: PEP-28 Effect of X-point height (divertor configuration) on L-H transitions. (27th Pedestal and Edge Physics Topical Group Meeting, 2014-10-20 to 2014-10-24, St. Paul Lez Durance).

Meyer-Spasche, R.: Communication of computational results around 1960. A case study. (6th International Conference of the European Society for the History of Science, 2014-09-04 to 2014-09-06, Lisbon).

Meyer-Spasche, R.: Confiscated classified secret and rejected manuscripts resp. of Oscar Buneman (1913-1993) and a citation classic. (12. Östereichisches Symposion zur Geschichte der Mathematik, 2014-05-04 to 2014-05-10, Miesenbach).

Miettunen, J., Airila, M. I., Groth, M., Lindholm, V., Makkonen, T., Äkäslompolo, S., and ASDEX Upgrade Team: Influence of toroidal field ripple and resonant magnetic perturbations on global impurity transport in ASDEX Upgrade. (21st International Conference on Plasma Surface Interactions 2014 (PSI 21), 2014-05-26 to 2014-05-30, Kanazawa).

Mink, F., Hopf, C., and Fantz, U.: Revision of the Spectroscopic Determination of Beam Parameters of the Neutral Beam Injection Systems on ASDEX Upgrade. (78. DPG-Jahrestagung und Frühjahrstagung der Sektion AMOP, 2014-03-17 to 2014-03-21, Berlin).

Mishchenko, A.: Gyrokinetics as a modern framework for fusion plasmas. (Seminar-Vortrag an der Karazin Kharkiv National University, 2014-10-17, Kharkiv).

Mishchenko, A.: How to model global electromagnetic modes with gyrokinetic codes? (Electromagnetic Gyrokinetic PIC Meeting, 2014-12-09 to 2014-12-11, Princeton, NJ).

Mishchenko, A., and Helander, P.: Fusion Energy, stellarators and the Wendelstein 7-X project. (Seminar-Vortrag an der Karazin Kharkiv National University, 2014-10-17, Kharkiv).

Mishchenko, A., Kleiber, R., Cole, M., Könies, A., Hatzky, R., Zocco, A., Feher, T., and Borchardt, M.: Global gyrokinetic particle-in-cell simulations of Alfvénic modes. (25th IAEA Fusion Energy Conference (FEC 2014), 2014-10-13 to 2014-10-18, Saint Petersburg).

Mlynar, J., Tomes, M., Imrisek, M., O'Mullane, M., Pütterich, T., Odstrcil, T., Alper, B., and JET EFDA Contributors: Soft X-ray tomographic reconstruction of JET ILW plasmas with tungsten impurity and different spectral response of detectors.

(28th Symposium on Fusion Technology (SOFT 2014), 2014-09-29 to 2014-10-03, San Sebastian).

Mlynek, A., Casali, L., Eixenberger, H., and ASDEX Upgrade Team: Finge jump analysis and correction by digital signal processing on the ASDEX Upgrade DCN interferometer and polarimeter. (20th Topical Conference on High-Temperature Plasma Diagnostics (HTPD 2014), 2014-06-01 to 2014-06-05, Atlanta, GA).

Mochalskyy, S., Lettry, J., Minea, T., Mattei, S., and Midttun, Ø.: Study of the different Cs conditioning states of the Linac4 negative hydrogen ion source by 3D PIC-MCC numerical simulations using ONIX code. (4th International Symposium on Negative Ions, Beams and Sources (NIBS 2014), 2014-10-06 to 2014-10-10, Garching).

Mochalskyy, S., Wünderlich, D., Fantz, U., Franzen, P., and Minea, T.: Towards a realistic 3D simulation of the meniscus in negative ion sources. (4th International Symposium on Negative Ions, Beams and Sources (NIBS 2014), 2014-10-06 to 2014-10-10, Garching).

Mollen, A., Landreman, M., and Smith, H.: On collisional impurity transport in nonaxisymmetric plasmas. (Joint Varenna-Lausanne International Workshop on Theory of Fusion Plasmas, 2014-09-01 to 2014-09-05, Varenna).

Müller, H. W.: Far SOL heat/particle fluxes on AUG/JET – link to detachment threshold. (20th ITPA Scrape-off Layer & Divertor Topical Group Meeting, 2014-10-20 to 2014-10-23, Prague).

Müller, H. W., and ASDEX Upgrade Team: Overview and comparison of resent results on plasma potential / Er diagnostic methods. (Workshop on Electric Fields, Turbulence and Self-Organisation in Magnetised Plasmas (EFTSOMP). Satellite Meeting of EPS Conference, 2014-06-30 to 2014-07-01, Berlin).

Müller, H. W., Carralero, D., Kallenbach, A., Marne, P. d., Guimarais, L., and ASDEX Upgrade Team: Far Scrape-off Layer Heat Fluxes in ITER Relevant High Density – High Power Scenarios. (21st International Conference on Plasma Surface Interactions 2014 (PSI 21), 2014-05-26 to 2014-05-30, Kanazawa).

Na, D., Na, Y.-S., Yang, S.-M., Kim, H.-S., Hahm, T. S., Jhang, H., Lee, S. G., Ko, W.-H., McDermott, R., Angioni, C., and Lee, W.: Investigation of Toroidal Rotation Reversal in KSTAR Ohmic Plasmas. (25th IAEA Fusion Energy Conference (FEC 2014), 2014-10-13 to 2014-10-18, Saint Petersburg).

Nagasaki, K., Yamamoto, S., Kobayashi, S., Nagaoka, K., Ascasibar, E., Osakabe, M., Yoshimura, Y., Mizuuchi, T.,

Okada, H., Minami, T., Kado, S., Ohshima, S., Konoshima, S., Shi, N., Sakamoto, K., Nakamura, Y., Zang, L., Kenmochi, N., Volpe, F., Marushchenko, N. B., Sano, F., and LHD Experiment Group: Control of Energetic-particle-driven MHD Modes by ECH/ECCD in Helical Systems. (18th Joint Workshop on Electron Cyclotron Emission and Electron Cyclotron Resonance Heating, 2014-04-22 to 2014-04-25, Nara).

Nakano, T., Shumack, A. E., Maggi, C. F., Reinke, M., Lawson, K. D., Pütterich, T., Brezinsek, S., Lipschultz, B., Matthews, G., Chernyshova, M., Jakubowska, K., Scholz, M., Rzadkiewicz, J., Czarski, T., Dominik, W., Kasprowicz, G., Pozniak, K., Zabolotny, W., Zastrow, K.-D., and JET EFDA Contributors: Determination of tungsten and molybdenum concentrations from an X-ray range spectrum in JET. (41st EPS Conference on Plasma Physics, 2014-06-23 to 2014-06-27, Berlin).

Nardon, E., Fil, A., Bécoulet, M., Dif-Pradalier, G., Grandgirard, V., Guirlet, R., Hölzl, M., Huijsmans, G. T. A., Latu, G., Lehnen, M., Monier-Garbet, P., Orain, F., Passeron, C., Pégourié, B., Reux, C., Saint-Laurent, F., and Tamain, P.: Investigating the Physics of Disruption Mitigation by Massive Gas Injection: 3D Non-Linear MHD Simulations and 1D Plasma-Gas Interaction Simulations. (25th IAEA Fusion Energy Conference (FEC 2014), 2014-10-13 to 2014-10-18, Saint Petersburg).

Neu, G., Cole, R., Gräter, A., Lüddecke, K., Rapson, C., Raupp, G., Treutterer, W., Zasche, D., Zehetbauer, T., and ASDEX Upgrade Team: The ASDEX Upgrade Parameter Server. (28th Symposium on Fusion Technology (SOFT 2014), 2014-09-29 to 2014-10-03, San Sebastian).

Neu, R., Herrmann, A., Kallenbach, A., Balden, M., Greuner, H., Krieger, K., Jaksic, N., Marné, P. d., Rohde, V., Schall, G., Scarabosio, A., Sieglin, B., and ASDEX Upgrade Team: Performance of the new ASDEX Upgrade bulk W divertor (Div III). (20th ITPA Scrape-off Layer & Divertor Topical Group Meeting, 2014-10-20 to 2014-10-23, Prague).

Nichols, J. H., Jaworski, M. A., Kaita, R., Abrams, T., Stotler, D. P., and Schmid, K.: Advances in global mixed-material surface evolution modeling for NSTX-U. (56th Annual Meeting of the APS Division of Plasma Physics, 2014-10-27 to 2014-10-31, New Orleans, LA).

Nielsen, S. K., Bongers, W., Fietz, S., Jacobsen, A. S., Korsholm, A. S., Leipold, F., Moseev, D., Rasmussen, J., Salewski, M., Schubert, M., Stejner, M., Stober, J., Wagner, D., Westerhof, E., TEXTOR Team, and ASDEX Upgrade Team: Strong scattering of mm waves in tokamaks. (9th International Workshop "Strong Microwaves and Terahertz Waves: Sources and Applications", 2014-07-24 to 2014-07-30, Nizhny Novgorod).

Nini, M., Abba, A., Germano, M., and Restelli, M.: Analysis of a Hybrid RANS/LES Model Using RANS Reconstruction. (iTi 2014 – Conference on Turbulence, 2014-09-21 to 2014-09-24, Darmstadt).

Nocentini, R., Bonomo, F., Pimazzoni, A., Fantz, U., Franzen, P., Fröschle, M., Heinemann, B., Pasqualoto, R., Riedl, R., Ruf, B., and Wünderlich, D.: Advanced ion beam calorimetry for the test facility ELISE. (4th International Symposium on Negative Ions, Beams and Sources (NIBS 2014), 2014-10-06 to 2014-10-10, Garching).

Norscini, C., Ghendrih, P., Milelli, D., Dif-Pradalier, G., Cartier-Michaud, T., Sarazin, Y., Abiteboul, J., Garbet, X., Grandgirard, V., and Esteve, D.: Turbulent transport close to marginal instability: role of the source driving the system out of equilibrium. (19th Joint EU-US Transport Task Force Meeting (TTF 2014), 2014-09-08 to 2014-09-11, Culham).

Nouailletas, R., Ravenel, N., Signoret, J., Guillerminet, B., Treutterer, W., Spring, A., Lewerentz, M., Rapson, C., Masand, H., Jasraj, D., Moreau, P., Brémond, S., Allegretti, L., Raupp, G., Werner, A., Saint Laurent, F., and Nardon, E.: From the conceptual design to the first mock-up of the new WEST plasma control system. (28th Symposium on Fusion Technology (SOFT 2014), 2014-09-29 to 2014-10-03, San Sebastian).

Oberkofler, M., Alegre, D., Aumayr, F., Brezinsek, S., Dittmar, T., Dobes, K., Douai, D., Drenik, A., Köppen, M., Kruezi, U., Linsmeier, C., Lungu, C. P., Mozetic, M., Porosnicu, C., Rohde, V., Romanelli, S., and ASDEX Upgrade Team: Plasma-wall interactions with nitrogen-seeding in all-metal fusion devices: formation of beryllium nitride and ammonia. (28th Symposium on Fusion Technology (SOFT 2014), 2014-09-29 to 2014-10-03, San Sebastian).

Oberparleiter, M., and Jenko, F.: Interaction between the neoclassical equilibrium and ITG turbulence in gyrokinetic simulations. (78. DPG-Jahrestagung und Frühjahrstagung der Sektion AMOP, 2014-03-17 to 2014-03-21, Berlin).

Odstrcil, T., Pütterich, T., Gude, A., Dux, R., Mazon, D., and ASDEX Upgrade Team: Poloidal asymmetries of heavy impurities in the ASDEX Upgrade plasma. (78. DPG-Jahrestagung und Frühjahrstagung der Sektion AMOP, 2014-03-17 to 2014-03-21, Berlin).

Ondac, P., Horacek, J., Seidl, J., Vondracek, P., Adamek, J., Müller, H. W., and ASDEX Upgrade Team: Comparison between the 2D turbulence model ESEL and experimental data from the ASDEX Upgrade and COMPASS tokamaks. (26th Symposium on Plasma Physics and Technology, 2014-06-16 to 2014-06-19, Prague).

Ongena, J., Messiaen, A., Krivska, A., Louche, F., Schweer, B., Vervier, M., Van Schoor, M., Borsuk, V., Neubauer, O., Wolf, R. C., Hartmann, D., and Birus, D.: Verification of the Simulated Radiated Power of the ICRH Antenna Design for Wendelstein 7-X with Experimental Results Using a Quarter Scale Mock-up Antenna. (25th IAEA Fusion Energy Conference (FEC 2014), 2014-10-13 to 2014-10-18, Saint Petersburg).

Oosterbeek, J. W., Udintsev, V. S., Vayakis, G., Sirinelli, A., Hirsch, M., Laqua, H. P., Gandini, F., Maassen, N., Ma, Y., Clough, M., Walsh, M. J., and Watt, C.: Loads due to Stray Microwave Radiation in ITER. (28th Symposium on Fusion Technology (SOFT 2014), 2014-09-29 to 2014-10-03, San Sebastian).

Orain, F., Becoulet, M., Huijsmans, G. T. A., Hölzl, M., Dif-Pradalier, G., Morales, J., Nardon, E., Pamela, S., Chapman, I., Cahyna, P., Fil, A., Grandgirard, V., Latu, G., Passeron, C., and Ratnani, A.: Non-linear MHD modeling of multi-ELM cycles and mitigation by RMPs. (41st EPS Conference on Plasma Physics, 2014-06-23 to 2014-06-27, Berlin).

Pablant, N. A., Bitter, M., Burhenn, R., Delgado-Aparicio, L., Ellis, R., Gates, D., Goto, M., Hill, K. W., Langenberg, A., Lazerson, S., Mardenfeld, M., Morita, S., Neilson, G. H., Oishi, T., and Pedersen, T. S.: Measurement of core plasma temperature and rotation on W7-X made available by the x-ray imaging crystal spectrometer (XICS). (41st EPS Conference on Plasma Physics, 2014-06-23 to 2014-06-27, Berlin).

Pablant, N., Bitter, M., Delgado Aparicio, L. F., Dinklage, A., Gates, D., Goto, M., Ido, T., Hill, K. H., Kubo, S., Morita, S., Nagaoka, K., Oishi, T., Satake, S., Takahashi, H., and Yokoyama, M.: Evolution of the radial electric field in high-Te ECH heated plasmas on LHD. (56th Annual Meeting of the APS Division of Plasma Physics, 2014-10-27 to 2014-10-31, New Orleans, LA).

Panea, M.: Site report – ein Bericht über die Aktivitäten des RZG im HPSS. (HPSS User Forum 2014 (HUF), 2014-10-27 to 2014-10-31, München).

Pardanaud, C., Addab, Y., Martin, C., Mellet, N., Giacometti, G., Roubin, P., Pegourie, B., Oberkofler, M., Koppen, M., Dittmar, T., Linsmeier, C., Hopf, C., Schwarz-Selinger, T., and Jacob, W.: Raman microscopy as a defect microprobe for hydrogen bonding characterization in materials used for thermonuclear fusion applications. (E-MRS 2014 Spring Meeting, 2014-05-26 to 2014-05-30, Lille).

Pardanaud, C., Martin, C., Giacometti, G., Roubin, P., Pégourié, B., Hopf, C., Schwarz-Selinger, T., and Jacob, W.: Thermal stability and long term hydrogen release from soft

to hard hydrogenated amorphous carbons analyzed using in-situ Raman spectroscopy: Application to tokamak deposits. (E-MRS 2014 Spring Meeting, 2014-05-26 to 2014-05-30, Lille).

Paris, P., Piip, K., Hakola, A., Laan, M., Aints, M., Koivuranta, S., Likonen, J., Lissovski, A., Mayer, M., Neu, R., Rohde, V., Sugiyama, K., and ASDEX Upgrade Team: Development of laser induced breakdown spectroscopy for studying erosion, deposition, and fuel retention in ASDEX Upgrade. (28th Symposium on Fusion Technology (SOFT 2014), 2014-09-29 to 2014-10-03, San Sebastian).

Pavei, M., Boilson, D., Bonicelli, T., Bigi, M., Boury, J., Bush, M., Ceracchi, A., Faso, D., Graceffa, J., Heinemann, B., Hemsworth, R., Lievin, C., Marcuzzi, D., Masiello, A., Pasqualotto, R., Pomaro, N., Rizzolo, A., Sczepaniak, B., Singh, M., and Zaccaria, P.: Manufacturing of the full size prototype of the ion source for the ITER neutral beam injector. The spider beam source. (28th Symposium on Fusion Technology (SOFT 2014), 2014-09-29 to 2014-10-03, San Sebastian).

Pedersen, T. S.: Plans for first plasma operation on Wendelstein 7-X. (56th Annual Meeting of the APS Division of Plasma Physics, 2014-10-27 to 2014-10-31, New Orleans, LA).

Pedersen, T. S.: Plans for first plasma operation on Wendelstein 7-X. (41st EPS Conference on Plasma Physics, 2014-06-23 to 2014-06-27, Berlin).

Pedersen, T. S., and Klinger, T.: Hochtemperaturplasma-physik I. (WS 2013/2014. Vorlesung, Ernst-Moritz-Arndt-Universität Greifswald).

Pedersen, T. S., and Klinger, T.: Fusionsphysik. Vorlesung (SS 2014. Vorlesung, Ernst-Moritz-Arndt-Universität Greifs-wald).

Penzel, F., Meister, H., Sehmer, T., and Koch, A. W.: Auto-matisierte Vermessung der Sichtliniencharakteristik von Bolometerkameras für die Fusionsforschung. (28. Messtech-nisches Symposium des Arbeitskreises der Hochschullehrer für Messtechnik (AHMT-2014), 2014-09-18 to 2014-09-20, Saarbrücken).

Penzel, F., Meister, H., Sehmer, T., Shalaby, S., Homner, N., Koll, J., and Koch, A. W.: Simulation of the ITER bolometer line of sight characteristics using Monte Carlo ray tracing methods. (28th Symposium on Fusion Technology (SOFT 2014), 2014-09-29 to 2014-10-03, San Sebastian).

Piovesan, P., Igochine, V., Kirk, A., Liu, Y., Maraschek, M., Marrelli, L., Ryan, D., Suttrop, W., Yadykin, D., Bogomolov, A.,

Cavedon, M., Classen, I. G. J., Gude, A., McDermott, R., Reich, M., Viezzer, E., Wolfrum, E., and ASDEX Upgrade Team: Measurement and modelling of plasma response to 3D fields at high-ß in ASDEX Upgrade. (13th Energetic Par-ticle Physics ITPA TG Meeting, 2014-10-21 to 2014-10-23, Padova).

Piovesan, P., Igochine, V., Kirk, A., Maraschek, M., Marrelli, L., Suttrop, W., Yadykin, D., Cavedon, M., Gude, A., Reich, M., Viezzer, E., Wolfrum, E., and ASDEX Upgrade Team: Mea-surement of plasma response to 3D fields at high-ß in ASDEX Upgrade. (56th Annual Meeting of the APS Divi-sion of Plasma Physics, 2014-10-27 to 2014-10-31, New Orleans, LA).

Piron, C., Felici, F., Kim, D., Piovesan, P., Rapson, C., Reich, M., Sauter, O., Treutterer, W., Van den Brand, H., and ASDEX Upgrade Team: Simulation and real-time estimation of sawtooth crash effects on ASDEX-Upgrade plasmas. (56th Annual Meeting of the APS Division of Plasma Physics, 2014-10-27 to 2014-10-31, New Orleans, LA).

Plaum, B., Lechte, C., Kasparek, W., Gaiser, S., Zeitler, A., Erckmann, V., Weißgerber, M., Bechtold, A., Busch, M., and Sczepaniak, B.: Design of a Remote Steering Antenna for ECRH Heating of the Stellarator Wendelstein 7-X. (28th Sym-posium on Fusion Technology (SOFT 2014), 2014-09-29 to 2014-10-03, San Sebastian).

Plöckl, B.: Definition and assessment of matter injection requirements. (Project Meeting 2 "Work Package Tritium, Fuelling and Vacuum", 2014-11-25, KIT Karlsruhe).

Plöckl, B.: IPP expertise in pellet experiments. (Kick-off Meeting of the DEMO Work Package Tritium, Fuelling and Vacuum, 2014-04-29, KIT Karlsruhe).

Plöckl, B.: Status report: Assessing the readiness of the ITER gas injection technology for DEMO. (Project Meeting 2 "Work Package Tritium, Fuelling and Vacuum", 2014-11-25, KIT Karlsruhe).

Plöckl, B., Day, C., Lamalle, P., Lang, P. T., Rohde, V., and ASDEX Upgrade Team: The enhanced pellet centrifuge launcher at ASDEX Upgrade: advanced operation and application as technology test facility for ITER and DEMO. (28th Sym-posium on Fusion Technology (SOFT 2014), 2014-09-29 to 2014-10-03, San Sebastian).

Plunk, G., Banon Navarro, A., and Jenko, F.: Nonlinear Satu-ration of Zonal-Flow-Dominated ITG Turbulence. (41st EPS Conference on Plasma Physics, 2014-06-23 to 2014-06-27, Berlin).

Plunk, G., Bird, T., Helander, P., and Xanthopoulos, P.: Proberties of ITG Turbulence in Wendelstein-7X. (Joint Varenna-Lausanne International Workshop on Theory of Fusion Plasmas, 2014-09-01 to 2014-09-05, Varenna).

Poli, E., Angioni, C., Casson, F. J., Farina, D., Figini, L., Goodman, T., Maj, O., Sauter, O., Weber, H., Zohm, H., Saibene, G., and Henderson, M.: On the criteria guiding the design of the upper electron-cyclotron launcher for ITER. (18th Joint Workshop on Electron Cyclotron Emission and Electron Cyclotron Resonance Heating, 2014-04-22 to 2014-04-25, Nara).

Porosnicu, C., Sugiyama, K., Lungu, C. P., Jacob, W., Jepu, I., Pompilian, O. G., and Stancu, C.: Deuterium Doped Beryllium Films Prepared by TVA. (21st International Conference on Plasma Surface Interactions 2014 (PSI 21), 2014-05-26 to 2014-05-30, Kanazawa).

Potzel, S., Wischmeier, M., Dux, R., Müller, H. W., Reimold, F., Scarabosio, A., Brezinsek, S., Clever, M., Huber, A., Meigs, A., Stamp, M., ASDEX Upgrade Team, and JET-EFDA Contributors: Formation of the high density front in the inner far SOL at ASDEX Upgrade and JET. (21st International Conference on Plasma Surface Interactions 2014 (PSI 21), 2014-05-26 to 2014-05-30, Kanazawa).

Predebon, I., Xanthopoulos, P., and Terranova, D.: Gyrokinetic investigation of ITG turbulence in helical RFPs. (56th Annual Meeting of the APS Division of Plasma Physics, 2014-10-27 to 2014-10-31, New Orleans, LA).

Preuss, R., and Toussaint, U. v.: Bayesian uncertainty quantification for an electrostatic plasma model. (34th International Workshop on Bayesian Inference and Maximum Entropy Methods in Science and Engineering (MaxEnt 2014), 2014-09-21 to 2014-09-24, Amboise).

Preuss, R., and Toussaint, U. v.: Prediction of SOLPS data employing Gaussian Processes. (41st EPS Conference on Plasma Physics, 2014-06-23 to 2014-06-27, Berlin).

Preynas, M., Kobayashi, S., Kubo, S., Laqua, H. P., Nagasaki, K., Shimozuma, T., Stange, T., Assmus, D., Igami, H., Kado, S., Mutoh, T., Otte, M., and Yoshimura, Y.: Experimental characterization of plasma start-up using ECRH in preparation of W7-X operation. (18th Joint Workshop on Electron Cyclotron Emission and Electron Cyclotron Resonance Heating, 2014-04-22 to 2014-04-25, Nara).

Preynas, M., Laqua, H. P., Otte, M., Stange, T., Wauters, T., Kim, H. T., Assmus, D., Igami, H., Kado, S., Kobayashi, S., Kubo, S., Mutoh, T., Nagasaki, K., Shimozuma, T., and

Yoshimura, Y.: Characterisation of plasma start-up using ECRH in preparation of W7-X operation. (78. DPG-Jahrestagung und Frühjahrstagung der Sektion AMOP, 2014-03-17 to 2014-03-21, Berlin).

Prisiazhniuk, D., Kramer-Flecken, A., Conway, G., and Stroth, U.: First Turbulence Measuremenents using Poloidal Correlation Reflectometry at AUG. (78. DPG-Jahrestagung und Frühjahrstagung der Sektion AMOP, 2014-03-17 to 2014-03-21, Berlin).

Proll, J. H. E.: Trapped-particle instabilities in quasi-isodynamic stellarators. (Stellarator Physics Meeting, 2014-04-17, Princeton, NJ).

Proll, J. H. E.: Trapped-particle instabilities in quasi-isodynamic stellarators. (Theory Seminar, 2014-05-12, Madison, WI).

Proll, J. H. E., Helander, P., Lazerson, S., Mynick, H., and Xanthopoulos, P.: TEM-turbulence in stellarators and its optimization. (56th Annual Meeting of the APS Division of Plasma Physics, 2014-10-27 to 2014-10-31, New Orleans, LA).

Pueschel, M. J., Terry, P. W., and Told, D.: Enhanced Magnetic Reconnection by Drift-wave Instabilities. (56th Annual Meeting of the APS Division of Plasma Physics, 2014-10-27 to 2014-10-31, New Orleans, LA).

Pueschel, M. J., Told, D., Terry, P. W., Jenko, F., Zweibel, E. G., Zhdankin, V., and Lesch, H.: Guide Field Reconnection Turbulence and Coronal Heating. (56th Annual Meeting of the APS Division of Plasma Physics, 2014-10-27 to 2014-10-31, New Orleans, LA).

Pütterich, T., Barrera Orte, L., Cavedon, M., Conway, G. D., McDermott, R. M., Ryter, F., Shao, L., Viezzer, E., Willensdorfer, M., Wolfrum, E., and ASDEX Upgrade Team: L-H Transition Physics Investigated at ASDEX Upgrade. (19th Joint EU-US Transport Task Force Meeting (TTF 2014), 2014-09-08 to 2014-09-11, Culham).

Pütterich, T., Dux, R., Neu, R., Vries, P. C. d., Bernert, M., Beurskens, M. N. A., Bobkov, V., Brezinsek, S., Challis, C., Coenen, J. W., Coffey, I., Czarnecka, A., Giroud, C., Jacquet, P., Joffrin, E., Kallenbach, A., Lehnen, M., Lerche, E., Luna, E. d. l., Matthews, G., Mayoral, M.-L., Mazon, D., McDermott, R. M., Meigs, A., Mlynar, J., Sertoli, M., Rooij, G. v., ASDEX Upgrade Team, and JET EFDA Contributors: W-Control in JET and AUG. (8th Workshop on Fusion Data Processing, Validation and Analysis, 2014-11-04 to 2014-11-06, Ghent).

Rahbarnia, K., Grulke, O., and Klinger, T.: Ion dynamics during magnetic reconnection. (78. DPG-Jahrestagung und Frühjahrstagung der Sektion AMOP, 2014-03-17 to 2014-03-21, Berlin).

Ramogida, G., Crisanti, F., Maddaluno, G., Albanese, R., Barbato, L., Mastrostefano, S., Villone, F., and Wenninger, R.: Disruption studies and simulations for the development of the DEMO physics basis. (28th Symposium on Fusion Technology (SOFT 2014), 2014-09-29 to 2014-10-03, San Sebastian).

Rampp, M., and Bockelmann, H.: Experiences with Intel Xeon Phi in the Max-Planck Society. (ENES Workshop on "Exascale Technologies & Innovation in HPC for Climate Models", 2014-03-17 to 2014-03-19, Hamburg).

Rampp, M.: Extreme scaling of the pseudospectral DNS code NSCOUETTE and some notes on high-performance-computing trends. (LSTM Seminar (Lehrstuhl für Strömungs-mechanik), 2014-11-28, Friedrich-Alexander-Universität Erlangen-Nürnberg).

Rampp, M., Lopez, J.-M., Shi, L., Hof, B., and Avila, M.: NSCOUETTE: A Hybrid MPI-OpenMP Parallel Implementation for Pseudospectral Simulations – Scaling experiments on SuperMUC. (28th International Conference on Supercomputing (ICS 2014), 2014-06-10 to 2014-06-13, München).

Rapson, C., Reich, M., Stober, J., Treutterer, W., and ASDEX Upgrade Team: Actuator management for ECRH at ASDEX Upgrade. (28th Symposium on Fusion Technology (SOFT 2014), 2014-09-29 to 2014-10-03, San Sebastian).

Ratnani, A.: CAID: A Python Computer Aided Design Tool for Computational Plasma Physics. (Numerical Methods for the Kinetic Equations of Plasma Physics (NumKin2014), 2014-10-20 to 2014-10-24, Garching).

Rauner, D., Kurutz, U., and Fantz, U.: Comparison of measured and modelled negative hydrogen ion densities at the ECR-discharge HOMER. (4th International Symposium on Negative Ions, Beams and Sources (NIBS 2014), 2014-10-06 to 2014-10-10, Garching).

Reich, M., Barrera, L., Behler, K., Buhler, A., Bock, A., Eixenberger, H., Fietz, S., Fischer, R., Giannone, L., Lackner, K., Lochbrunner, M., Maraschek, M., McCarthy, P., Monaco, F., Mlynek, A., Poli, E., Preuss, R., Rapson, C., Sauter, O., Schubert, M., Stober, J., Treutterer, W., Volpe, F., Wagner, D., Zohm, H., and ASDEX Upgrade Team: Real-time Control of NTMs Using ECCD at ASDEX Upgrade. (25th IAEA Fusion Energy Conference (FEC 2014), 2014-10-13 to 2014-10-18, Saint Petersburg).

Reimerdes, H., Canal, G. P., Duval, B. P., Labit, B., Lunt, T., Nespoli, F., Vijvers, W. A. J., De Temmerman, G., Lowry, C., Morgan, T. W., Tal, B., and Wischmeier, M.: Experimental investigation of neon seeding in the snowflake configuration in TCV.

(21st International Conference on Plasma Surface Interactions 2014 (PSI 21), 2014-05-26 to 2014-05-30, Kanazawa).

Reimold, F., Wischmeier, M., Aho-Mantila, L., Bernert, M., Bonnin, X., Coster, D., Kallenbach, A., Meisl, G., Potzel, S., and Reiter, D.: Experimental Studies and Modeling of Complete H-Mode Divertor Detachment in ASDEX Upgrade. (21st International Conference on Plasma Surface Interactions 2014 (PSI 21), 2014-05-26 to 2014-05-30, Kanazawa).

Reimold, F., Wischmeier, M., Bernert, M., Kallenbach, A., Lowry, C., ASDEX Upgrade Team, and JET Contributors: Integrated scenarios with radiative cooling. (European Fusion Physics Workshop (EFPW 2014), 2014-12-01 to 2014-12-03, Split).

Reinke, M., Angioni, C., Pütterich, T., Odstrcil, T., and ASDEX Upgrade Team: High-Z Impurity Asymmetries – Important for Radial Transport or Just a Diagnostic Nuisance. (19th Joint EU-US Transport Task Force Meeting (TTF 2014), 2014-09-08 to 2014-09-11, Culham).

Reux, C., Plyusnin, V., Alper, B., Alves, D., Bazylev, B., Belonohy, E., Brezinsek, S., Decker, J., Devaux, S., Vries, P. d., Fil, A., Gerasimov, S., Lupelli, I., Jachmich, S., Kiptily, V., Koslowski, R., Kruezi, U., Lehnen, M., Mlynar, J., Nardon, E., Nilsson, E., Riccardo, V., Saint-Laurent, F., Sozzi, C., and JET EFDA Contributors: Runaway beam studies during disruptions at JET-ILW. (21st International Conference on Plasma Surface Interactions 2014 (PSI 21), 2014-05-26 to 2014-05-30, Kanazawa).

Reux, C., Plyusnin, V. V., Koslowski, R., Alper, B., Alves, D., Bazylev, B., Belonohy, E., Brezinsek, S., Decker, J., Devaux, S., Drewelow, P., Vries, P. d., Fil, A., Gerasimov, S., Giacomelli, L., Lupelli, I., Jachmich, S., Kiptily, V., Kruezi, U., Lehnen, M., Manzanares, A., Mlynar, J., Nardon, E., Nilsson, E., Riccardo, V., Saint-Laurent, F., and Sozzi, C.: Runaway Electron Generation with the ITER-like Wall and Efficiency of Massive Gas Injection at JET. (25th IAEA Fusion Energy Conference (FEC 2014), 2014-10-13 to 2014-10-18, Saint Petersburg).

Revel, A., Mochalskyy, S., Caillault, L., Simonin, A., Esch, H. P. L. d., and Minea, T.: Numerical analysis of negative ion beam formation and aberrations in different plasma sources & accelerators by coupling two 3D PIC-MCC codes ONAC and ONIX. (4th International Symposium on Negative Ions, Beams and Sources (NIBS 2014), 2014-10-06 to 2014-10-10, Garching).

Ribeiro, T., Silva, F. d., Heuraux, S., and Scott, B. D.: Synthetic reflectometry probing of gyrofuid edge turbulence. (17th International Congress on Plasma Physics (ICPP 2014), 2014-09-15 to 2014-09-19, Lisbon).

Ricci, P., Halpern, F., Joaquim, L., Jolliet, S., Mosetto, A., Riva, F., Christoph, W., Fasoli, A., Furno, I., Labit, B., Nespoli, F., Theiler, C., Arnoux, G, Gunn, J. P., Horacek, J., Kocan, M., LaBombard, B., and Silva, C.: First-principle Theory-based Scaling of the SOL Width in Limited Tokamak Plasmas, Experimental Validation, and Implications for the ITER Start-up. (25th IAEA Fusion Energy Conference (FEC 2014), 2014-10-13 to 2014-10-18, Saint Petersburg).

Riesch, J., Höschen, C., Wurster, S., You, J.-H., Linsmeier, C., and Neu, R.: Brittle tungsten becomes tough: pseudo-ductility in tungsten fibre-reinforced tungsten composites. (The Nuclear Materials Conference (NuMat 2014), 2014-10-27 to 2014-10-30, Clearwater, FL).

Rodatos, A., Jakubowski, M., Greuner, H., Wurden, G. A., and Pedersen, T. S.: Algorithm development for safeguarding the Wendelstein 7-X divertor during steady state operation. (78. DPG-Jahrestagung und Frühjahrstagung der Sektion AMOP, 2014-03-17 to 2014-03-21, Berlin).

Rohde, V., Oberkofler, M., Meisl, G, and ASDEX Upgrade Team: Ammonia production in N seeded plasma discharges in ASDEX Upgrade. (21st International Conference on Plasma Surface Interactions 2014 (PSI 21), 2014-05-26 to 2014-05-30, Kanazawa).

Romanelli, M., Szepesi, G., Angioni, C., Peeters, A. G., Camenen, Y., Casson, F. C., Hornsby, W. A., Snodin, A. P., and Militello, F.: Impact of W on gradient driven micro-instabilities and heat/particle transport in JET-ILW plasma conditions. (19th Joint EU-US Transport Task Force Meeting (TTF 2014), 2014-09-08 to 2014-09-11, Culham).

Rondeau, A., Peillon, S., Roynette, A., Sabroux, J.-C., Gelain, T., Gensdarmes, F., Rohde, V., Grisolia, C., and Chassefière, E.: Characterization of tungsten particles in AUG tokamak which are potentially mobilizable by airflow. (28th Symposium on Fusion Technology (SOFT 2014), 2014-09-29 to 2014-10-03, San Sebastian).

Rondeau, A., Peillon, S., Roynette, A., Sabroux, J.-C., Gensdarmes, F., Rohde, V., Grisolia, C., and Chassefiere, E.: Etude des poussieres produites dans les tokamaks et potentiellement mobilisables lors d'un accident de perte de vide. (29. Congres Francais sur les Aerosols (CFA 2013), 2014-01-22 to 2014-01-23, Paris).

Rondeau, A., Peillon, S., Roynette, A., Sabroux, J.-C., Gelain, T., Gensdarmes, F., Rohde, V., Grisolia, C., and Chassefière, E.: Study of dust produced in tokamaks and potentially mobilized during a loss of vacuum accident. (International Aerosol Conference (CFA 2014), 2014-08-28 to 2014-09-02, Bexco, Busan).

Rondeau, A., Peillon, S., Roynette, A., Sabroux, J.-C., Gelain, T., Gensdarmes, F., Rohde, V., Grisolia, C., and Chassefière, E.: Study of dust produced in tokamaks and potentially mobilized during a loss of vacuum accident. (21st International Conference on Plasma Surface Interactions 2014 (PSI 21), 2014-05-26 to 2014-05-30, Kanazawa).

Rott, M., Arden, N., Eixenberger, H., Klädtke, K., Teschke, M., Suttrop, W., and ASDEX Upgrade Team: Electrical and mechanical adaptation of commercially available power inverter modules for BUSSARD – the power supply of ASDEX Upgrade in vessel saddle coils. (28th Symposium on Fusion Technology (SOFT 2014), 2014-09-29 to 2014-10-03, San Sebastian).

Rozhansky, V., Kaveeva, E., Veselova, I., Voskoboinikov, S., Coster, D., Fable, E., Pütterich, T., and Viezzer, E.: Understanding of Impurity Poloidal Distribution in Edge Pedestal by Modeling. (25th IAEA Fusion Energy Conference (FEC 2014), 2014-10-13 to 2014-10-18, Saint Petersburg).

Rozhansky, V., Sytova, E., Senichenkov, I., Veselova, I., Voskoboynikov, S., and Coster, D.: Momentum balance for impurities in SOLPS transport code. (21st International Conference on Plasma Surface Interactions 2014 (PSI 21), 2014-05-26 to 2014-05-30, Kanazawa).

Rualdo Soto-Chavez, A., Wang, G, Bhattacharjee, A., Fu, G.-y., and Smith, H.: A model for falling tone chorus in the Earth's magnetosphere. (56th Annual Meeting of the APS Division of Plasma Physics, 2014-10-27 to 2014-10-31, New Orleans, LA).

Rummel, T.: Commissioning Strategy of the Wendelstein 7-X Magnet System. (21st Topical Meeting on the Technology of Fusion Energy (TOFE), 2014-11-09 to 2014-11-13, Anaheim, CA).

Ryan, D. A., Liu, Y., Reinke, M., Dudson, B., Kirk, A., Garcia-Munoz, M., Piovesan, P., Suttrop, W., and ASDEX Upgrade Team: Simulations of a resonant plasma kink response to externally applied magnetic perturbations in the AUG tokamak. (19th Joint EU-US Transport Task Force Meeting (TTF 2014), 2014-09-08 to 2014-09-11, Culham).

Saarelma, S., Bottino, A., Chapman, I., Crocker, N., Diallo, A., Dunai, D., Dickinson, D., Hilleisheim, J., Kirk, A., McMillan, B., Roach, C., Scannell, R., Simpson, J., and Peebles, T.: Understanding the MAST H-Mode Pedestal through Experiments and Modelling. (25th IAEA Fusion Energy Conference (FEC 2014), 2014-10-13 to 2014-10-18, Saint Petersburg).

Saitoh, H., Pedersen, T. S., Hergenhahn, U., Stenson, E., and Paschkowski, N.: Injection and trapping of electrons in a dipole magnetic field: towards the formation of an electron-

positron plasma. (41ˢᵗ EPS Conference on Plasma Physics, 2014-06-23 to 2014-06-27, Berlin).

Salewski, M., Geiger, B., Heidbrink, W. W., Jacobsen, A. S., Korsholm, S. B., Leipold, F., Madsen, J., Moseev, D., Nielsen, S. K., Rasmussen, J., Stejner, M., Tardini, G., Weiland, M., and ASDEX Upgrade Team: Velocity-space tomography for magnetically confined plasmas and astrophysics. (41ˢᵗ EPS Conference on Plasma Physics, 2014-06-23 to 2014-06-27, Berlin).

Salmi, A., Tala, T., Bourdelle, C., Mantica, P., Meneses, L., Mordjick, S., Bufferand, H., Clever, M., Svensson, J., Tamain, P., Groth, M., Hillesheim, J., Maggi, C., Maslov, M., Naulin, V., Rasmussen, J. J., Sips, G., Sirinelli, A., Tsalas, M., Weisen, H., Wischmeier, M., and JET-EFDA Contributors: Particle transport via gas puff modulation experiments in JET. (19ᵗʰ Joint EU-US Transport Task Force Meeting (TTF 2014), 2014-09-08 to 2014-09-11, Culham).

Sarazin, Y., Abiteboul, J., Dif-Pradalier, G., McMillan, B., Bourdelle, C., Cartier-Michaud, T., Cottier, P., Est'eve, D., Garbet, X., Girardo, J.-B., Grandgirard, V., Ghendrih, P., Hariri, F., Latu, G., Newman, D., Norscini, C., Passeron, C., Reynolds-Barredo, J., Sanchez, R., Spineanu, F., Vlad, M., and Villard, L.: Understanding Momentum Transport in Tokamak Plasmas. (25ᵗʰ IAEA Fusion Energy Conference (FEC 2014), 2014-10-13 to 2014-10-18, Saint Petersburg).

Scarabosio, A.: New results on the S parameter. (20ᵗʰ ITPA Scrape-off Layer & Divertor Topical Group Meeting, 2014-10-20 to 2014-10-23, Prague).

Scarabosio, A., Eich, T., Hoppe, F., Sieglin, B., Rack, M., Groth, M., Wischmeier, M., Arnoux, G., Balboa, I., Marsen, S., ASDEX Upgrade Team, and JET-EFDA Contributors: Scaling of the divertor power spreading (S-factor) in open and closed divertor operation in JET and ASDEX Upgrade. (21ˢᵗ International Conference on Plasma Surface Interactions 2014 (PSI 21), 2014-05-26 to 2014-05-30, Kanazawa).

Schabinger, B., Biedermann, C., Clementson, J., König, S., Marx, G., and Schweikhard, L.: Experiments with the Greifswald EBIT. (Topical Workshop of the FLAIR Collaboration, 2014-05-15 to 2014-05-16, Heidelberg).

Schiesko, L., Cartry, G., Hopf, C., Höschen, C., Meisl, G., Encke, O., Franzen, P., Heinemann, B., Amsalem, P., Achkasov, K., and Fantz, U.: Cs doped Molybdenum as surface converter for H- / D- generation in NNBI sources: first steps and proof of principle. (4ᵗʰ International Symposium on Negative Ions, Beams and Sources (NIBS 2014), 2014-10-06 to 2014-10-10, Garching).

Schmid, B., Ramisch, M., and Stroth, U.: Untersuchung des Energietransfers in Zonalströmungen am Stellarator TJ-K. (78. DPG-Jahrestagung und Frühjahrstagung der Sektion AMOP, 2014-03-17 to 2014-03-21, Berlin).

S*chmid, K., Krieger, K., Lisgo, S. W., and Brezinsek, S.:* WALLDYN simulations of global impurity migration and fuel retention in JET and extrapolations to ITER. (25ᵗʰ IAEA Fusion Energy Conference (FEC 2014), 2014-10-13 to 2014-10-18, Saint Petersburg).

Schmid, K., Krieger, K., Lisgo, S. W., Brezinsek, S., and JET EFDA Contributors: Quantitative modeling of fuel retention in the JET-C and JET-ILW wall configurations by WallDyn and predictions for ITER. (21ˢᵗ International Conference on Plasma Surface Interactions 2014 (PSI 21), 2014-05-26 to 2014-05-30, Kanazawa).

Schneider, P. A., Burckhart, A., Dunne, M. G., Gude, A., Kurzan, B., Pütterich, T., Rathgeber, S. K., Suttrop, W., Viezzer, E., Wolfrum, E., and ASDEX Upgrade Team: Pedestal and ELM characteristics across first wall materials and nitrogen seeding. (41ˢᵗ EPS Conference on Plasma Physics, 2014-06-23 to 2014-06-27, Berlin).

Schneller, M., Lauber, P., and Briguglio, S.: The HAGIS-LIGKA model: current status, planned implementations and diagnostic techniques in progress. (4ᵗʰ Workshop "Fast Ion Modeling and Diagnostic" (FIMAD-4), 2014-02-19 to 2014-02-21, Innsbruck).

Schneller, M., Lauber, P., and Briguglio, S.: Study of Nonlinear Fast Particle Transport for the ITER 15MA Scenario. (Joint Varenna-Lausanne International Workshop on Theory of Fusion Plasmas, 2014-09-01 to 2014-09-05, Varenna).

Schneller, M., Lauber, P., Xin, W., Briguglio, S., Benedikt, G., Garcia-Munoz, M., Weiland, M., and Bilato, R.: Study of Nonlinear Fast Particle Transport and Losses in the Presence of Alfvén Waves. (25ᵗʰ IAEA Fusion Energy Conference (FEC 2014), 2014-10-13 to 2014-10-18, Saint Petersburg).

Schrittwieser, R., Ionita, C., Costea, S., Mehlmann, F., Grünwald, J., Schneider, B. S., Naulin, V., Rasmussen, J. J., Müller, H. W., and Adamek, J.: Probe diagnostics in various plasmas. (Interuniversity Attraction Poles Workshop (IAP), 2014-06-10 to 2014-06-11, Reims).

Schubert, M., Herrmann, A., Monaco, F., Schütz, H., Stober, J., Vierle, T., Vorbrugg, S., Wagner, D., Zasche, D., Zehetbauer, T., Zeidner, W., and ASDEX Upgrade Team: Machine safety issues with respect to the extension of ECRH system at ASDEX Upgrade. (18ᵗʰ Joint Workshop on Electron Cyclotron

Emission and Electron Cyclotron Resonance Heating, 2014-04-22 to 2014-04-25, Nara).

Schwarz-Selinger, T., Manhard, A., Schmid, K., and Jacob, W.: Deuterium penetration in self-damaged tungsten during low-flux plasma loading. (21st International Conference on Plasma Surface Interactions 2014 (PSI 21), 2014-05-26 to 2014-05-30, Kanazawa).

Schwarz-Selinger, T., Schmid, K., Toussaint, U. v., and Jacob, W.: Hydrogen isotope exchange in self-damaged tungsten: recent experiments and model approaches. (12th International Workshop on Hydrogen Isotopes in Fusion Reactor Materials (HWS-12), 2014-06-02 to 2014-06-04, Toyama).

Schweinzer, J., Bobkov, V., Dux, R., Kallenbach, A., Lang, P., Pütterich, T., Ryter, F., Stober, J., and Zohm, H.: Development of the Q=10 Scenario for ITER on ASDEX Upgrade (AUG). (25th IAEA Fusion Energy Conference (FEC 2014), 2014-10-13 to 2014-10-18, Saint Petersburg).

Scott, B.: Relaxation to neoclassical flow equilibrium in gyrofluid simulations. (56th Annual Meeting of the APS Division of Plasma Physics, 2014-10-27 to 2014-10-31, New Orleans, LA).

Serianni, G, Bonomo, F., Brombin, M., Cervaro, V., Chitarin, G, Cristofaro, S., Delogu, R., De Muri, M., Fasolo, D., Fonnesu, N., Franchin, L., Franzen, P., Ghiraldelli, R., Molon, F., Muraro, A., Pasqualotto, R., Ruf, B., Schiesko, L., and Veltri, P.: Negative Ion Beam Characterisation in BATMAN by mini-STRIKE: Improved Design and New Measurements. (4th International Symposium on Negative Ions, Beams and Sources (NIBS 2014), 2014-10-06 to 2014-10-10, Garching).

Sertoli, M., Bacharis, M., Brezinsek, S., Cackett, A., Coene, J. W., Coffey, I. H., Flannegan, J. C., Harting, D., Hodille, E., Jarvinen, A., Lazzaro, E., Marsen, S., Matthew, G. F., and JET-EFDA Contributors: Impact of W events and dust on JET-ILW operation. (21st International Conference on Plasma Surface Interactions 2014 (PSI 21), 2014-05-26 to 2014-05-30, Kanazawa).

Sertoli, M., Barrera, L., Igochine, V., and ASDEX Upgrade Team: New method for the evaluation of 2D impurity density in the presence of MHD instabilities in tokamak plasmas. (8th Workshop on Fusion Data Processing, Validation and Analysis, 2014-11-04 to 2014-11-06, Ghent).

Shi, Y., Wang, B., Scott, B., and Tang, W.: Computational Diagnostics for Extreme Scale Toroidal Gyrokinetic Particle Simulations. (56th Annual Meeting of the APS Division of Plasma Physics, 2014-10-27 to 2014-10-31, New Orleans, LA).

Shimozuma, T., Igami, H., Kubo, S., Yoshimura, Y., Takahashi, H., Osakabe, M., Mutoh, T., Nishiura, M., Idei, H., Nagasaki, K., Marushchenko, N., and Turkin, Y.: Optimization of High Harmonic ECRH Scenario to Extend a Heating Plasma Parameter Range in LHD. (25th IAEA Fusion Energy Conference (FEC 2014), 2014-10-13 to 2014-10-18, Saint Petersburg).

Sias, G., Aledda, R., Cannas, B., Fanni, A., Pau, A., and ASDEX Upgrade Team: Improvements in Disruption Prediction at ASDEX Upgrade. (28th Symposium on Fusion Technology (SOFT 2014), 2014-09-29 to 2014-10-03, San Sebastian).

Sigalov, A., Eixenberger, H., Käsemann, C.-P., and ASDEX Upgrade Team: Datenerfassungssystem des Vierquadranten-Stromrichters für die Plasma-Lageregelung von ASDEX Upgrade. (Virtuelle Instrumente in der Praxis (VIP 2014), 2014-10-22 to 2014-10-23, Fürstenfeldbruck).

Sips, A., Giruzzi, G., Ide, S., Kessel, C., Luce, T. C., Snipes, J., and Stober, J.: Progress in Preparing Scenarios for ITER Operation. (25th IAEA Fusion Energy Conference (FEC 2014), 2014-10-13 to 2014-10-18, Saint Petersburg).

Smirnow, M., Boscary, J., Peacock, A., Tittes, H., and Tretter, J.: Mechanical examination and analysis of W7-X divertor module sub-structures. (28th Symposium on Fusion Technology (SOFT 2014), 2014-09-29 to 2014-10-03, San Sebastian).

Smith, H., Gates, D. A., Gorelenkov, N. N., White, R. B., and Fredrickson, E.: Stochastic heating of thermal ions by compressional Alfvén eigenmodes in NSTX. (41st EPS Conference on Plasma Physics, 2014-06-23 to 2014-06-27, Berlin).

Sonato, P., Tran, M. Q., Franke, T., Simonin, A., Shivarova, A., Verhoeven, R., Franzen, P., Cernusak, I., and Furno, I.: The Development of the Neutral Beam Injector for DEMO within the EUROFUSION Activities. (4th International Symposium on Negative Ions, Beams and Sources (NIBS 2014), 2014-10-06 to 2014-10-10, Garching).

Sonnendrücker, E.: Monte Carlo Methods with applications to plasma physics. Vorlesung (SS 2014. Vorlesung, Technische Universität München).

Sonnendrücker, E.: Variance reduction in Monte Carlo PIC codes with collisions. (Numerical Methods for the Kinetic Equations of Plasma Physics (NumKin2014), 2014-10-20 to 2014-10-24, Garching).

Stadler, R. J., Peacock, A., Boscary, J., Mendelevitch, B., Czerwinski, M., Scholz, P., and Schubert, W.: Conceptual

design of the W7-X in vessel port protection for steady state operation. (28th Symposium on Fusion Technology (SOFT 2014), 2014-09-29 to 2014-10-03, San Sebastian).

Stange, T., Laqua, H. P., Dostal, M., and Otte, M.: Erzeugung relativistischer Elektronen über nichtresonante RF-Heizverfahren. (78. DPG-Jahrestagung und Frühjahrstagung der Sektion AMOP, 2014-03-17 to 2014-03-21, Berlin).

Stange, T., Laqua, H. P., Dostal, M., Otte, M., and Preynas, M.: Non resonant heating methods at the WEGA stellarator. (9th International Workshop "Strong Microwaves and Terahertz Waves: Sources and Applications", 2014-07-24 to 2014-07-30, Nizhny Novgorod).

Stanja, J., Hergenhahn, U., Niemann, H., Paschkowski, N., Pedersen, T. S., Saitoh, H., Stenson, E., Hugenschmidt, C., Marx, G. H., Schweikhard, L., Danielson, J. R., and Surko, C. M.: Progress toward positron-electron pair plasma experiments. (56th Annual Meeting of the APS Division of Plasma Physics, 2014-10-27 to 2014-10-31, New Orleans, LA).

Stechow, A. v., Grulke, O., and Klinger, T.: Guide field effects on magnetic reconnection. (78. DPG-Jahrestagung und Frühjahrstagung der Sektion AMOP, 2014-03-17 to 2014-03-21, Berlin).

Stegmeir, A.: Numerical Methods for 3D Tokamak Simulations using a Flux-surface independent Grid. (78. DPG-Jahrestagung und Frühjahrstagung der Sektion AMOP, 2014-03-17 to 2014-03-21, Berlin).

Stehouwer, H.: Making a Difference: RDA Working Groups. (RDA Third Plenary Meeting (Pre-Conference), 2014-03-25, Dublin).

Stehouwer, H.: RDA: Current Activities and Expected Impact. (2nd JTC 1 Study Group on Big Data (SGBD) Meeting, 2014-05-13 to 2014-05-16, Amsterdam).

Stehouwer, H.: Introduction to RDA. (5th Open Source GIS Conference (OSGIS 2014), 2014-09-02 to 2014-09-03, Nottingham).

Stehouwer, H.: Presentation on RDA Europe / MPG Science Workshop Outcome. (5th Open Source GIS Conference (OSGIS 2014), 2014-09-02 to 2014-09-03, Nottingham).

Stehouwer, H.: The Research Data Alliance. (RDA France Meeting, 2014-06-20, Paris).

Stehouwer, H.: The Research Data Alliance: Progress to Data. (RDA France Meeting, 2014-11-25, Paris).

Stehouwer, H.: Research Data Alliance: Research Data Sharing without Barriers. (Linking Geospatial Data Conference, 2014-03-05 to 2014-03-06, London).

Stehouwer, H.: Research Data Alliance: Research Data Sharing without Barriers. (Terena Networking Conference (TNC2014), 2014-05-19 to 2014-05-22, Dublin).

Stehouwer, H.: Sharing Ideas: RDA Interest Groups. (RDA Third Plenary Meeting (Pre-Conference), 2014-03-25, Dublin).

Stenson, E., Hergenhahn, U., Niemann, H., Paschkowski, N., Pedersen, T. S., Saitoh, H., Stanja, J., Marx, G. H., Schweikhard, L., Hugenschmidt, C., Danielson, J. R., and Surko, C. M.: Progress toward positron accumulation for use in pair plasmas. (56th Annual Meeting of the APS Division of Plasma Physics, 2014-10-27 to 2014-10-31, New Orleans, LA).

Stenson, E., Saitoh, H., Niemann, H., Paschkowski, N., Hergenhahn, U., Marx, G., Schweikhard, L., Danielson, J., Surko, C., Hugenschmidt, C., and Pedersen, T. S.: Progress towards making a plasma of positrons and electrons. (78. DPG-Jahrestagung und Frühjahrstagung der Sektion AMOP, 2014-03-17 to 2014-03-21, Berlin).

Stieglitz, R., Wolf, R., Boccaccini, L. V., Carloni, D., Gulden, W., Herb, J., Jin, X. Z., Pistner, C., Raeder, J., Taylor, N., and Weller, A.: Safety of Fusion Power Plants in View of Fission Regulations. (28th Symposium on Fusion Technology (SOFT 2014), 2014-09-29 to 2014-10-03, San Sebastian).

Stober, J., Bock, A., Fable, E., Sommer, F., Angioni, C., Leuterer, F., Monaco, F., Müller, S., Münich, M., Petzold, B., Poli, E., Schubert, M., Schütz, H., Wagner, D., Zohm, H., ASDEX Upgrade Team, Meier, A., Scherer, T., Strauß, D., Jelonnek, J., Thumm, M., Kasparek, W., Plaum, B., Litvak, A., Denisov, G. G., Chirkov, A. V., Tai, E. M., Popov, L. G., Nichiporenko, V. O., Myasnikov, V. E., Soluyanova, E. A., and Malygin, V.: High power ECRH and ECCD in moderately collisional ASDEX Upgrade H-modes and status of EC system upgrade. (18th Joint Workshop on Electron Cyclotron Emission and Electron Cyclotron Resonance Heating, 2014-04-22 to 2014-04-25, Nara).

Stober, J., and Pütterich, T.: Plasmaphysik I. (WS 2013/2014. Vorlesung/Übung, Ludwig-Maximilians-Universität München).

Stober, J., Rapson, C., Reich, M., Barrera Orte, L., Behler, K., Bock, A., Buhler, A., Eixenberger, H., Giannone, L., Monaco, F., Maraschek, M., Mlynek, A., Poli, E., Schubert, M., Treutterer, W., Wagner, D., Zohm, H., ASDEX Upgrade Team, and Kasparek, W.: Feedback-controlled NTM stabilization on ASDEX Upgrade.

(18th Joint Workshop on Electron Cyclotron Emission and Electron Cyclotron Resonance Heating, 2014-04-22 to 2014-04-25, Nara).

Stroth, U.: Experimental Turbulence Studies for Gyro-Kinetic Code Validation Using Advanced Microwave Diagnostics. (25th IAEA Fusion Energy Conference (FEC 2014), 2014-10-13 to 2014-10-18, Saint Petersburg).

Stroth, U., and Manz, P.: Turbulenter Transport in Fusionsplasmen. (SS 2014. Vorlesung/Übung, Technische Universität München).

Stroth, U., and Manz, P.: Turbulenz in neutralen Fluiden und Plasmen. (WS 2013/2014. Vorlesung/Übung, Technische Universität München).

Strumberger, E., Günter, S., Merkel, P., and Tichmann, C.: Linear stability studies including resistive wall effects with the CASTOR/STARWALL code. (Joint Varenna-Lausanne International Workshop on Theory of Fusion Plasmas, 2014-09-01 to 2014-09-05, Varenna).

Sugiyama, K., Roth, J., Alimov, V. K., Schmid, K., Balden, M., Elgeti, S., Koch, F., Höschen, T., Baldwin, M. J., Doerner, R. P., Maier, H., and Jacob, W.: Erosion study of Fe-W binary mixed layer prepared as model system of RAFM steel. (21st International Conference on Plasma Surface Interactions 2014 (PSI 21), 2014-05-26 to 2014-05-30, Kanazawa).

Suttrop, W., Barrera Orte, L., Fischer, R., Fietz, S., Fuchs, J. C., McDermott, R., Rathgeber, S., Viezzer, E., and Wolfrum, E.: Studies of Magnetic Perturbations in High-confinement Mode Plasmas in ASDEX Upgrade. (25th IAEA Fusion Energy Conference (FEC 2014), 2014-10-13 to 2014-10-18, Saint Petersburg).

Szepesi, T., Kocsis, G., Kovács, Á., Németh, J., Plöckl, B., and ASDEX Upgrade Team: Table-top pelletinjector (TATOP) for impurity pellet injection. (28th Symposium on Fusion Technology (SOFT 2014), 2014-09-29 to 2014-10-03, San Sebastian).

Tala, T., McDermott, R., Salmi, A., Angioni, C., Odstrcil, T., Pütterich, T., Ryter, F., Solomon, W., Tardini, G., and Viezzer, E.: Identification of Intrinsic Torques in ASDEX Upgrade H-Mode Plasmas. (25th IAEA Fusion Energy Conference (FEC 2014), 2014-10-13 to 2014-10-18, Saint Petersburg).

Tamain, P., Joffrin, E., Bufferand, H., Brezinsek, S., Beurskens, M., Ciraolo, G., Clever, M., Giroud, C., Dejarnac, R., Drewelow, P., Delabie, E., Devaux, S., Groth, G., Hacquin, S., Lipschutz, B., Marsen, S., Meigs, A., Lomas, P., Nunes, I., Oberkofler, M., Solano, E., Wiesen, S., and JET EFDA Contributors:

Investigation of the influence of divertor recycling on global plasma confinement in JET. (21st International Conference on Plasma Surface Interactions 2014 (PSI 21), 2014-05-26 to 2014-05-30, Kanazawa).

Telesca, G., Ivanova-Stanik, I., Zagorski, R., Brezinsek, S., Giroud, C., Marsen, S., Wischmeier, M., and JET EFDA Contributors: Numerical simulations of JET discharges with the ITER-like wall for different nitrogen seeding scenarios. (21st International Conference on Plasma Surface Interactions 2014 (PSI 21), 2014-05-26 to 2014-05-30, Kanazawa).

Teschke, M., Arden, N., Eixenberger, H., Rott, M., and Suttrop, W.: Electrical Design of the Inverter System BUSSARD for ASDEX Upgrade Saddle Coils. (28th Symposium on Fusion Technology (SOFT 2014), 2014-09-29 to 2014-10-03, San Sebastian).

Throumoulopoulos, G. N., Kuiroukidis, A., and Tasso, H.: On the Equilibrium and Stability of ITER Relevant Plasmas with Flow. (25th IAEA Fusion Energy Conference (FEC 2014), 2014-10-13 to 2014-10-18, Saint Petersburg).

Titus, P., Lumsdaine, A., McGinnis, J., Lore, J., Brown, T., Peacock, A., Boscary, J., and Tretter, J.: Analysis of the Wendelstein 7-X Inertially Cooled Test Divertor Unit Scraper Element. (28th Symposium on Fusion Technology (SOFT 2014), 2014-09-29 to 2014-10-03, San Sebastian).

Titus, P. H., Lumsdaine, A., McGinnis, W. D., Lore, J., Neilson, H., Brown, T., Boscary, J., and Peacock, A.: Analysis of the Wendelstein 7-X Test Divertor Unit Scraper Element with Radiation Shields. (21st Topical Meeting on the Technology of Fusion Energy (TOFE), 2014-11-09 to 2014-11-13, Anaheim, CA).

Told, D., Jenko, F., Görler, T., Casson, F. J., Fable, E., and ASDEX Upgrade Team: Characterizing turbulent transport in ASDEX Upgrade L-mode plasmas via nonlinear gyrokinetic simulations. (19th Joint EU-US Transport Task Force Meeting (TTF 2014), 2014-09-08 to 2014-09-11, Culham).

Toussaint, U. v.: Greens-function Monte Carlo Approaches in Plasma-wall-modelling. (Physik-Kolloquium, 2014-04-25, Helsinki).

Toussaint, U. v.: Non-intrusive uncertainty quantification for plasma modeling. (Numerical Methods for the Kinetic Equations of Plasma Physics (NumKin2014), 2014-10-20 to 2014-10-24, Garching).

Toussaint, U. v.: Robust phase estimation for signals with a low signal-to-noise-ratio. (34th International Workshop on Bayesian Inference and Maximum Entropy Methods in

Science and Engineering (MaxEnt 2014), 2014-09-21 to 2014-09-24, Amboise).

Toussaint, U. v.: Uncertainty quantification for computer model. (34th International Workshop on Bayesian Inference and Maximum Entropy Methods in Science and Engineering (MaxEnt 2014), 2014-09-21 to 2014-09-24, Amboise).

Toussaint, U. v., Manhard, A., Schwarz-Selinger, T., and Gori, S.: First-passage Kinetic Monte Carlo Study of Hydrogen Transport in Damaged Tungsten. (21st International Conference on Plasma Surface Interactions 2014 (PSI 21), 2014-05-26 to 2014-05-30, Kanazawa).

Treutterer, W., Raupp, G., Cole, R., Neu, G., Gräter, A., Lüddecke, K., Rapson, C., Zasche, D., Zehetbauer, T., and ASDEX Upgrade Team: Transforming the ASDEX Upgrade Discharge Control System to a General-Purpose Plasma Control Platform. (28th Symposium on Fusion Technology (SOFT 2014), 2014-09-29 to 2014-10-03, San Sebastian).

Tripsky, M., Wauters, T., Lyssoivan, A., TEXTOR Team, and ASDEX Upgrade Team: Monte Carlo simulation of ICRF discharge initiation at $w_{pe} < w$ and investigation of model validity at higher densities. (41st EPS Conference on Plasma Physics, 2014-06-23 to 2014-06-27, Berlin).

Tronko, N.: Exact conservation laws for gyrokinetic Vlasov-Poisson equations. (International Conference on Geometric Algorithms and Methods for Plasma Physics, 2014-05-13 to 2014-05-15, Hefei).

Tronko, N.: Systematic variational derivation of Gyrokinetic Maxwell-Vlasov equations: compare code and theory. (Numerical Methods for the Kinetic Equations of Plasma Physics (NumKin2014), 2014-10-20 to 2014-10-24, Garching).

Turnyanskiy, M., Neu, R., Albanese, R., Bachmann, C., Brezinsek, S., Eich, T., Falchetto, G., Federici, G., Kalupin, D., Mayoral, M.-L., McDonald, D. C., Reimerdes, H., Romanelli, F., and You, J.-H.: A roadmap to the realisationof fusion energy: – mission for solutions on heat-exhaust systems. (28th Symposium on Fusion Technology (SOFT 2014), 2014-09-29 to 2014-10-03, San Sebastian).

Valisa, M., Angioni, C., Mantica, P., Pütterich, T., Baruzzo, M., Silva Aresta Belo, P. d., Belli, E. A., Casson, F., Coffey, I., Drewelow, P., Giroud, C., Hawkes, N., Hender, T., Koskela, T., Lerche, E., Lauro Taroni, L., Maggi, C. F., Mlynar, J., O'Mullane, M., Puiatti, M. E., Reinke, M., and Romanelli, M.: Heavy Impurity Transport in the Core of JET Plasmas. (25th IAEA Fusion Energy Conference (FEC 2014), 2014-10-13 to 2014-10-18, Saint Petersburg).

Valovic, M., Lang, P. T., Plöckl, B., Kirk, A., Kocsis, G., Suttrop, W., Cseh, G., Classen, I., Garzotti, L., Guimarais, L., Szepesi, T., Mlynek, A., Wolfrum, E., and ASDEX Upgrade Team: Pellet fuelling with RMP ELM mitigation on ASDEX Upgrade. (ITPA Meeting on Transport and Confinement, 2014-10-20 to 2014-10-22, Cadarache).

Van Zeeland, M. A., Evans, T. E., Ferraro, N. M., Lanctot, M. J., Pace, D. C., Collins, C., Heidbrink, W. W., Garcia-Munoz, M., Hanson, J. M., Grierson, B. A., Kramer, G. J., Nazikian, R., Allen, S. L., Lasnier, C. J., and Meyer, W. H.: Measurements of Fast Ion Transport Due to n=3 Magnetic Perturbations on DIII-D. (56th Annual Meeting of the APS Division of Plasma Physics, 2014-10-27 to 2014-10-31, New Orleans, LA).

Van Zeeland, M., Ferraro, N. M., Heidbrink, W. W., Kramer, G. J., Pace, D. C., Allen, S. L., Chen, X., Evans, T. E., Grierson, B., Garcia-Munoz, M., Hanson, J., Lanctot, M. J., Lao, L., Lasnier, C. J., Moyer, R., Nazikian, R., Orlov, D. M., and Park, J.-K.: Fast Ion Transport during Applied 3D Magnetic Perturbations on DIII-D. (25th IAEA Fusion Energy Conference (FEC 2014), 2014-10-13 to 2014-10-18, Saint Petersburg).

Verdoolaege, G., McDermott, R., Angioni, C., and ASDEX Upgrade Team: Scaling of core intrinsic rotation in ASDEX Upgrade L-mode plasmas using a robust regression technique. (19th Joint EU-US Transport Task Force Meeting (TTF 2014), 2014-09-08 to 2014-09-11, Culham).

Verdoolaege, G., and Noterdaeme, J.-M.: A New Methodology for Scaling Laws with Arbitrary Error Distributions: Case Study for the H-mode Power Threshold. (25th IAEA Fusion Energy Conference (FEC 2014), 2014-10-13 to 2014-10-18, Saint Petersburg).

Vicente, J., Silva, F. d., Conway, G. D., Manso, M. E., Silva, C., Müller, H. W., and ASDEX Upgrade Team: Measurements of plasma filaments with fixed frequency reflectometry at the ASDEX Upgrade tokamak. (20th Topical Conference on High-Temperature Plasma Diagnostics (HTPD 2014), 2014-06-01 to 2014-06-05, Atlanta, GA).

Vicente, J., Silva, F. d., Heuraux, S., Manso, M. E., Conway, G. D., Silva, C., and ASDEX Upgrade Team: Numerical study of fixed frequency reflectometry measurements of plasma filaments with radial and polidal velocity components. (20th Topical Conference on High-Temperature Plasma Diagnostics (HTPD 2014), 2014-06-01 to 2014-06-05, Atlanta, GA).

Viezzer, E., Pütterich, T., Angioni, C., Bergmann, A., Cavedon, M., Dux, R., Fable, E., McDermott, R., Stroth, U., Wolfrum, E., and ASDEX Upgrade Team: Experimental evidence for the neo-classical nature of the edge radial electric field at ASDEX

Upgrade. (Workshop on Electric Fields, Turbulence and Self-Organisation in Magnetised Plasmas (EFTSOMP). Satellite Meeting of EPS Conference, 2014-06-30 to 2014-07-01, Berlin).

Viezzer, E., Pütterich, T., Fable, E., Bergmann, A., Dux, R., McDermott, R., Angioni, C., Cavedon, M., Churchill, R. M., Dunne, M. G., Lipschultz, B., Stroth, U., Wolfrum, E., and ASDEX Upgrade Team: Radial Electric Field and Poloidal Impurity Asymmetries in the Pedestal of ASDEX Upgrade: Quantitative Comparisons between Experiment and Theory. (25th IAEA Fusion Energy Conference (FEC 2014), 2014-10-13 to 2014-10-18, Saint Petersburg).

Vilbrandt, R.: Continuity and Enhancement of Quality Management during Commissioning of W7-X. (28th Symposium on Fusion Technology (SOFT 2014), 2014-09-29 to 2014-10-03, San Sebastian).

Voitsekhovitch, I., Ivanova-Stanik, I., Zagorski, R., Köchl, F., Belo, P., Fable, E., and Polevoi, A.: Integrated Core-SOL-Divertor Modelling for ITER Hybrid Scenario Including Impurities. (19th Joint EU-US Transport Task Force Meeting (TTF 2014), 2014-09-08 to 2014-09-11, Culham).

Volpe, F., Sweeney, R., Hender, T., Kirk, A., La Haye, R. J., Strait, E. J., Ding, Y. H., Rao, B., Fietz, S., Maraschek, M., Frassinetti, L., In, Y., Jeon, Y., Sakakibara, S., and Sabbagh, S.: Magnetic Control of Locked Modes in Present Devices and ITER. (56th Annual Meeting of the APS Division of Plasma Physics, 2014-10-27 to 2014-10-31, New Orleans, LA).

Vulliez, K., Ferlay, F., Helou, W., Hillairet, J., Mollard, P., Patterlini, J.-C., Argouarch, A., Bernard, J.-M., Zhaoxi, C., Delaplanche, J.-M., Lombard, G., Prou, M., Volpe, R., and Winkler, K.: The Mechanical Structure of the WEST Ion Cyclotron Resonant Heating Launchers. (28th Symposium on Fusion Technology (SOFT 2014), 2014-09-29 to 2014-10-03, San Sebastian).

Wagner, D.: High Power Microwave Technology: Generation, Mode Conversion and Transmission. (Vorlesung, Aix-Marseille Université, 2014-12-03 to 2014-12-05, Marseille).

Wagner, D., Bongers, W., Kasparek, W., Leuterer, F., Monaco, F., Münich, M., Schütz, H., Stober, J., Thumm, M., and Brand, H. v. d.: A Multifrequency Notch Filter for Millimeter Wave Plasma Diagnostics Based on Photonic Bandgaps in Corrugated Circular Waveguides. (18th Joint Workshop on Electron Cyclotron Emission and Electron Cyclotron Resonance Heating, 2014-04-22 to 2014-04-25, Nara).

Wagner, D., Kasparek, W., Plaum, B., Lechte, C., Wu, Z., Wang, H., Maraschek, M., Stober, J., Reich, M., Schubert, M.,

Grünwald, G., Monaco, F., Müller, S., Schütz, H., Erckmann, V., Doelman, N., van den Braber, R., Klop, W., van den Brand, H., Bongers, W., Krijger, B., Petelin, M., Koposova, L., Lubyako, L., Bruschi, A., Sakamoto, K., and Thumm, M.: Development of diplexers and millimeter wave filters for ECRH and diagnostics applications. (US-EU-JPN Workshop on RF Heating Technology, 2014-09-22 to 2014-09-24, Sedona).

Wagner, D., Stober, J., Leuterer, F., Monaco, F., Müller, S., Münich, M., Rapson, C., Reich, M., Ryter, F., Schubert, M., Schütz, H., Treutterer, W., Zohm, H., Thumm, M., Scherer, T., Meier, A., Gantenbein, G., Jelonnek, J., Kasparek, W., Lechte, C., Plaum, B., Litvak, A. G., Denisov, G. G., Chirkov, A., Popov, L. G., Nichiporenko, V. O., Myasnikov, V. E., Tai, E. M., Solyanova, E. A., Malygin, S. A., and ASDEX Upgrade Team: ECRH System and Experiments at ASDEX Upgrade. (9th International Workshop "Strong Microwaves and Terahertz Waves: Sources and Applications", 2014-07-24 to 2014-07-30, Nizhny Novgorod).

Wagner, D., Stober, J., Leuterer, F., Monaco, F., Müller, S., Münich, M., Rapson, C., Reich, M., Schubert, M., Schütz, H., Treutterer, W., Zohm, H., Thumm, M., Scherer, T., Meier, A., Gantenbein, G., Jelonnek, J., Kasparek, W., Lechte, C., Plaum, B., Litvak, A. G., Denisov, G. G., Chirkov, A., Popov, L. G., Nichiporenko, V. O., Myasnikov, V. E., Tai, E. M., Solyanova, E. A., Malygin, S. A., and ASDEX Upgrade Team: Operation and Upgrade of the ECRH System at ASDEX Upgrade. (39th International Conference on Infrared, Millimeter, and Terahertz Waves (IRMMW-THz 2014), 2014-09-14 to 2014-09-19 Tucson, AZ).

Wagner, F.: Comments to the German "Energiewende". (Vortrag, 2013-05-07, IVA's Conference Centre, Stockholm). (Addendum 2013)

Wagner, F.: Do we still need fusion? – A general view. (30 years of TEXTOR, 2014-03-28, Forschungszentrum Jülich).

Wagner, F.: Electricity by intermittent sources. (Almendalen-Woche, 2013-07-01, Gotland). (Addendum 2013)

Wagner, F.: Die Energiewende Deutschlands – wohin wird sie führen? (64. Jahrestagung der Österreichischen Physikalischen Gesellschaft, 2014-09-26 to 2014-09-27, Pöllau).

Wagner, F.: "Energiewende" in Germany – Issues and Problems. (2nd International Conference on Climate Change – The Environmental and Socio-economic Response in the Southern Baltic Region, 2014-05-12 to 2014-05-15, Szczecin).

Wagner, F.: Energiewende – wohin? (Physik am Sonnabend, 2014-06-21, Ernst-Moritz-Arndt-Universität Greifswald).

Wagner, F.: Energiewende – wohin? (Vortrag, Rotary Club Caspar-David-Friedrich, 2014-06-17, Greifswald).

Wagner, F.: Energiewende – wohin? Vortrag, Rotary Club Martinsried, 2014-01-14, München).

Wagner, F.: On an EU-wide use of RES for electricity generation. (RLPAT Seminar. Saint Petersburg State Polytechnic University (SPbSPU), 2014-09-15, St. Petersburg).

Wagner, F.: Features of electricity supply by REs. (Vortrag, Königlich Schwedische Akademie der Wissenschaften, 2013-05-06, Stockholm). (Addendum 2013)

Wagner, F.: Features of future electricity supply. (Vortrag, Czech Physical Society, 2013-03-06, Prague). (Addendum 2013)

Wagner, F.: Features of Intermittent Electricity Supply. (Joint EPS-SIF International School on Energy, 2014-07-17 to 2014-07-23, Varenna).

Wagner, F.: Fusion energy. (Vortrag, Academy University, 2013-05-15, Saint Petersburg). (Addendum 2013)

Wagner, F.: On the German "Energiewende". (EuroScience Open Forum 2014 (ESOF), 2014-06-21 to 2014-06-26, Copenhagen).

Wagner, F.: Introduction into stellarator physics. (Vorlesung in der Graduierten Schule des RLPAT, 2013-10-28 to 2013-10-29, Saint Petersburg). (Addendum 2013)

Wagner, F.: Möglichkeiten einer zukünftigen Energieversorgung. (Vortrag, Rotary Club, 2013-01-30, Hamm). (Addendum 2013)

Wagner, F.: Options of nuclear fusion beyond 2050. (European Academy Science Advisory Committee Meeting, 2013-04-07, IPP Greifswald). (Addendum 2013)

Wagner, F.: Properties of an electricity system with intermittent sources. (Seminar "Interdisciplinary energy prospective: towards a common toolbox for scenario assessment and design?", 2014-02-02 to 2014-02-07, Les Houches).

Wagner, F.: Properties of an electricity system with intermittent sources. (Vortrag, 2013-10-07, Kyushu University). (Addendum 2013)

Wagner, F.: Science of the future. (Fusion Research by the MEGA-Grant Laboratory RLPAT, 2014-09-17 to 2014-09-20, Saint Petersburg).

Wagner, F.: Sustainable Energy Supply Forms – Issues and Problems. (Lecture, 2014-05-26, Kyushu University, Fukuoka).

Wagner, F.: Supply of Europe with intermittent electricity. (Energy Group Meeting of the European Physical Society, 2014-11-13 to 2014-11-14, Lisbon).

Wagner, F.: The value of plasmas. (Opening Ceremony "Research Network on Non-equilibrium and Extreme State Plasma", 2014-05-22, Kyushu University, Fukuoka).

Wagner, F.: Zukunftsenergie Fusion. (Vortrag, 2013-04-10, Planetarium Mannheim). (Addendum 2013)

Walker, M., Ambrosino, G., De Tommasi, G., Humphreys, D., Mattei, M., Neu, G., Rapson, C., Raupp, G., Treutterer, W., Welander, A., and Winter, A.: The ITER plasma control system simulation platform. (28th Symposium on Fusion Technology (SOFT 2014), 2014-09-29 to 2014-10-03, San Sebastian).

Wang, P., Jacob, W., Gao, L., Elgeti, S., Balden, M., and Manhard, A.: Deuterium Retention in Tungsten Films Deposited on Different Substrates. (21st International Conference on Plasma Surface Interactions 2014 (PSI 21), 2014-05-26 to 2014-05-30, Kanazawa).

Wang, X.: Studies of nonlinear dynamics of wave-particle interactions in Tokamak plasmas based on Hamiltonian mapping techniques. (Joint Varenna-Lausanne International Workshop on Theory of Fusion Plasmas, 2014-09-01 to 2014-09-05, Varenna).

Warmer, F., Beidler, C. D., Dinklage, A., Egorov, K., Feng, Y., Geiger, J., Kemp, R., Knight, P., Schauer, F., Turkin, Y., Wolf, R., and Xanthopoulos, P.: Stellarator-Specific Developments for the Systems Code PROCESS. (28th Symposium on Fusion Technology (SOFT 2014), 2014-09-29 to 2014-10-03, San Sebastian).

Warmer, F., Beidler, C., Dinklage, A., Feng, Y., Geiger, J., Kemp, R., Knight, P., Schauer, F., Turkin, Y., Ward, D., Wolf, R., Xanthopoulos, P., and Torrisi, S.: The Way to Systems Studies of HELIAS Burning Plasma Devices. (Workshop on Systems Codes, 2014-09-04, Garching).

Warmer, F., Beidler, C. D., Dinklage, A., Feng, Y., Geiger, J., Kemp, R., Knight, P., Schauer, F., Xanthopoulos, P., and Torrisi, S.: Preliminary Approach to Tokamak/HELIAS Comparison within the Systems Code PROCESS. (German DEMO Working Group Meeting, 2014-09-02 to 2014-09-03, Garching).

Warmer, F., Knight, P., Beidler, C., Dinklage, A., Feng, Y., Geiger, J., Schauer, F., Turkin, Y., Ward, D., Wolf, R., and Xanthopoulos, P.: Stellarator-specific developments for the systems code PROCESS. (78. DPG-Jahrestagung und Frühjahrstagung der Sektion AMOP, 2014-03-17 to 2014-03-21, Berlin).

Warmer, F., Wolf, R. C., and Zohm, H.: Stellarators. (DPG Advanced School: The Physics of ITER, 2014-09-21 to 2014-09-26, Bad Honnef).

Wauters, T., Douai, D., Kogut, D., Lyssoivan, A., Brezinsek, S., Belonohy, E., Blackman, T., Bobkov, V., Crombé, K., Delabie, E., Drenik, A., Graham, M., Joffrin, E., Lerche, E., Loarer, T., Lomas, P. L., Manzanares, A., Mayoral, M.-L., Monakhov, I., Oberkofler, M., Philipps, V., Plyusnin, V., Sergienko, G., Van Eester, D., and JET EFDA Contributors: Isotope Exchange by Ion Cyclotron Wall Conditioning on JET. (21st International Conference on Plasma Surface Interactions 2014 (PSI 21), 2014-05-26 to 2014-05-30, Kanazawa).

Wauters, T., Lyssoivan, A., Douai, D., Brezinsek, S., Belohony, E., Blackman, T., Bobkov, V., Crombé, K., Delabie, E., Aleksander, D., Graham, M., Hartmann, D., Joffrin, E., Kogut, D., Lerche, E. A., Loarer, T., Lomas, P., Manzanares, A., Mayoral, M.-L., Monakhov, I., Noterdaeme, J.-M., Oberkofler, M., Ongena, J., Philipps, V. P., Plyusnin, V. V., Sergienko, G., Tripský, M., and Van Eester, D.: ICRF Discharge Production for Ion Cyclotron Wall Conditioning on JET. (25th IAEA Fusion Energy Conference (FEC 2014), 2014-10-13 to 2014-10-18, Saint Petersburg).

Weber, H., Maj, O., and Poli, E.: Scattering of diffracting beams of electron cyclotron waves by random density fluctuations in inhomogeneous plasmas. (18th Joint Workshop on Electron Cyclotron Emission and Electron Cyclotron Resonance Heating, 2014-04-22 to 2014-04-25, Nara).

Weidl, M. S., Teaca, B., and Jenko, F.: Acceleration of test particles in imbalanced magnetohydrodynamic turbulence. (78. DPG-Jahrestagung und Frühjahrstagung der Sektion AMOP, 2014-03-17 to 2014-03-21, Berlin).

Weidl, M. S., Teaca, B., and Jenko, F.: Turbulent heating of charged particles in imbalanced plasma turbulence. (78. DPG-Jahrestagung und Frühjahrstagung der Sektion AMOP, 2014-03-17 to 2014-03-21, Berlin).

Weiland, M., Geiger, B., Bilato, R., Schneider, P., Tardini, G., Lauber, P., Ryter, F., Schneller, M., and ASDEX Upgrade Team: Einfluss von Alfvén Eigenmoden und Ionenzyklotronheizung auf die schnelle Ionen-Verteilung im Tokamak ASDEX Upgrade. (78. DPG-Jahrestagung und Frühjahrstagung der Sektion AMOP, 2014-03-17 to 2014-03-21, Berlin).

Weinzettl, V., Pereira, T., Gomes, R., Odstrcil, T., Imrisek, M., Naydenkova, D., Varju, J., Panek, R., Melich, R., Jaspers, R., Ghosh, J., Pisarik, M., Shukla, G., and Van Oost, G.: Diagnostics of plasma rotation using high-resolution spectroscopy on the COMPASS tokamak. (28th Symposium on Fusion Technology (SOFT 2014), 2014-09-29 to 2014-10-03, San Sebastian).

Wenninger, R., Aho-Mantila, L., Angioni, C., Fasoli, A., Garcia, J., Giruzzi, G., Jenko, F., Wischmeier, M., Zohm, H., Albanese, R., Ambrosino, R., Artaud, J.-F., Bernert, M., Fable, E., Federici, G., Maget, P., Mattei, M., Ramogida, G., Sieglin, B., and Villone, F.: Advances in the Physics Basis for the European DEMO Design. (25th IAEA Fusion Energy Conference (FEC 2014), 2014-10-13 to 2014-10-18, Saint Petersburg).

Wenzel, U.: Two Types of Marfes in Tokamaks and Stellarators. (21st International Conference on Plasma Surface Interactions 2014 (PSI 21), 2014-05-26 to 2014-05-30, Kanazawa).

Werner, A.: Archiving, Analysis Modeling of Wendelstein 7-X Experiment Data. (RZG Workshop, 2014-02-05 to 2014-02-07, Schloss Ringberg, Tegernsee).

Willensdorfer, M., Fable, E., Wolfrum, E., Aumayr, F., Fischer, R., Reimhold, F., Ryter, F., and ASDEX Upgrade Team: The role of convective and diffusive particle transport in the plasma edge during the density build-up following the L-H transition. (21st International Conference on Plasma Surface Interactions 2014 (PSI 21), 2014-05-26 to 2014-05-30, Kanazawa).

Willensdorfer, M., Laggner, F., Manz, P., Carralero, D., Wolfrum, E., Zoletnik, S., Stroth, U., and ASDEX Upgrade Team: Blob Filament Measurements with Lithium Beam Emission Specroscopy in the SOL of ASDEX Upgrade. (KSTAR Conference, 2014-02-24 to 2014-02-26, Gangwon-do).

Wimmer, C., Fantz, U., Schiesko, L., and NNBI Team: Dependence of the Source Performance on Plasma Parameters at the BATMAN Test Facility. (4th International Symposium on Negative Ions, Beams and Sources (NIBS 2014), 2014-10-06 to 2014-10-10, Garching).

Winter, A., Ambrosino, G., DeTommasi, G., Humphreys, D., Mattei, M., Neto, A., Raupp, G., Stephen, A., Snipes, J., Treutterer, W., Walker, M., and Zabeo, L.: Implementation Strategy for the ITER Plasma Control System. (28th Symposium on Fusion Technology (SOFT 2014), 2014-09-29 to 2014-10-03, San Sebastian).

Wischmeier, M.: Grundlagen der Plasmaspektroskopie. (WS 2013/2014. Vorlesung, Universität Augsburg).

Wischmeier, M.: Maximum achievable radiated fraction with med-Z seeding in the JET-ILW. (20th ITPA Scrape-off Layer & Divertor Topical Group Meeting, 2014-10-20 to 2014-10-23, Prague).

Wischmeier, M.: Methoden der Plasmadiagnostik. (SS 2014. Vorlesung, Universität Augsburg).

Wischmeier, M., Aho-Mantila, L., Matthias, B., Eich, T., Kallenbach, A., Carralero, D., Coster, D., Lunt, T., Müller, H. W., Potzel, S., Scarabosio, A., Bernhard, S., and Reimold, F.: Advancing Power Exhaust Studies from Present to Future Tokamak Devices. (25th IAEA Fusion Energy Conference (FEC 2014), 2014-10-13 to 2014-10-18, Saint Petersburg).

Wischmeier, M., ASDEX Upgrade Team, and JET EFDA Contributors: High density divertor operation for reactor-relevant power exhaust. (CCFE Exhaust Plasma Forum, 2014-08-14, Culham).

Wischmeier, M., ASDEX Upgrade Team, and JET EFDA Contributors: High density divertor operation for reactor-relevant power exhaust. (21st International Conference on Plasma Surface Interactions 2014 (PSI 21), 2014-05-26 to 2014-05-30, Kanazawa).

Wolf, R. C.: Controlled thermonuclear fusion – from the stars to the laboratory. (SS 2014. Vorlesung, Technische Universität Berlin).

Wolf, R. C.: Hot plasmas in the universe. (WS 2013/2014. Vorlesung, Technische Universität Berlin).

Wolf, R. C.: Wendelstein 7-X – Ingenieurskunst und Physikexperiment. (DESY-Veranstaltung, 2014-12-17, Hamburg).

Wolfrum, E., Burckhart, A., Dunne, M. G., Schneider, P. A., Willensdorfer, M., Fable, E., Fischer, R., Hatch, D., Jenko, F., Kurzan, B., Viezzer, E., Rathgeber, S. K., and Manz, P.: Overview of Recent Pedestal Studies at ASDEX Upgrade. (25th IAEA Fusion Energy Conference (FEC 2014), 2014-10-13 to 2014-10-18, Saint Petersburg).

Wünderlich, D., Franzen, P., and Fantz, U.: Erste Resultate des ITER-relevanten Teststands ELISE für negative Wasserstoffionen. (78. DPG-Jahrestagung und Frühjahrstagung der Sektion AMOP, 2014-03-17 to 2014-03-21, Berlin).

Wünderlich, D., Wimmer, C., and Friedl, R.: A Collisional Radiative Model for Caesium and its Application to an RF Source for Negative Hydrogen Ions. (4th International Symposium on Negative Ions, Beams and Sources (NIBS 2014), 2014-10-06 to 2014-10-10, Garching).

Wünderlich, D., Wimmer, C., Schiesko, L., Fantz, U., Franzen, P., and NNBI Team: Negative hydrogen ion sources for NBI: diagnostics of electronegative plasmas with high relevance for fusion experiments. (22nd Europhysics Conference on Atomic and Molecular Physics of Ionized Gases (ESCAMPIG), 2014-07-15 to 2014-07-19, Greifswald).

Wurden, G., Jakubowski, M., and Baldzuhn, J.: A Specialized IR Endoscope for High Resolution Views in the W7-X Stellarator. (56th Annual Meeting of the APS Division of Plasma Physics, 2014-10-27 to 2014-10-31, New Orleans, LA).

Xanthopoulos, P., Helander, P., Mynick, H., Turkin, Y., Jenko, F., Görler, T., Told, D., Plunk, G. G., Bird, T., and Proll, J. H. E.: Simulation and optimisation of turbulence in stellarators. (78. DPG-Jahrestagung und Frühjahrstagung der Sektion AMOP, 2014-03-17 to 2014-03-21, Berlin).

Xiang, L., Guo, H. Y., Wischmeier, M., Wu, Z. W., Wang, L., Duan, Y. M., Wang, H. Q., Chen, Y. L., and EAST Team: Investigation of argon seeding in different divertor configurations in EAST with SOLPS 5.0 modeling. (25th IAEA Fusion Energy Conference (FEC 2014), 2014-10-13 to 2014-10-18, Saint Petersburg).

Xufei, X., Nocente, M., Bonomo, F., Franzen, P., Fröschle, M., Grosso, G., Grünauer, F., Pasqualotto, R., Tardocchi, M., and Gorini, G.: Neutron measurements from beam-target reactions at the ELISE neutral beam test facility. (20th Topical Conference on High-Temperature Plasma Diagnostics (HTPD 2014), 2014-06-01 to 2014-06-05, Atlanta, GA).

Yamoto, S., Homma, Y., Hoshino, K., Sawada, Y., Bonnin, X., Coster, D., Schneider, R., and Hatayama, A.: Effects of Background Plasma Characteristics on Tungsten Impurity Transport in the SOL/Divertor Region using IMPGYRO Code. (21st International Conference on Plasma Surface Interactions 2014 (PSI 21), 2014-05-26 to 2014-05-30, Kanazawa).

You, J.-H.: Divertor PFC concepts considered in the DEMO divertor project. (European Fusion Programe Workshop (EFPW 2014), 2014-12-01 to 2014-12-03, Split).

You, J.-H.: Nuclear Fusion Power & Safety Issues. (7th EU Korea Conference on Science and Technology 2014 (EKC 2014), 2014-07-22 to 2014-07-25, Vienna).

You, J.-H., Brendel, A., Herrmann, A., Kimmig, S., Linsmeier, C., Riesch, J., and Zivelonghi, A.: Novel composite materials for innovative design of high-heat-flux components of fusion reactors. (The Nuclear Materials Conference (NuMat 2014), 2014-10-27 to 2014-10-30, Clearwater, FL).

You, J.-H., Li, M., Visca, E., Crescenzi, F., Li Puma, A., Richou, M., Timmis, W., Barrett, T. R., McIntosh, S., Hancock, D., Fursdon, M., Keech, G., and Bachmann, C.: Design assessment of water-cooled divertor target concepts for the European DEMO. (28th Symposium on Fusion Technology (SOFT 2014), 2014-09-29 to 2014-10-03, San Sebastian).

Yu, J. H., Baldwin, M. J., Doerner, R. P., Dittmar, T., Hakola, A., Höschen, T., Likonen, J., Nishijima, D., and Toudeshki, H. H.: Transient heating effects on tungsten: Be ablation, alloying, and enhanced fuzz growth. (21st International Conference on Plasma Surface Interactions 2014 (PSI 21), 2014-05-26 to 2014-05-30, Kanazawa).

Yuan, Y., Wang, P., Greuner, H., Böswirth, B., Zou, D. R., Luo, G.-N., Lu, G.-H., and Liu, W.: D retention in molten W and W-La$_2$O$_3$ induced by high heat flux. (21st International Conference on Plasma Surface Interactions 2014 (PSI 21), 2014-05-26 to 2014-05-30, Kanazawa).

Zagorski, R., Voitsekhovitch, I., Ivanova-Stanik, I., Köchl, F., Citrin, J., Fable, E., Garcia, J., Garzotti, L., Hobirk, J., Hogeweij, D., Joffrin, E., Litaudon, X., Polevoi, A., and Telesca, G.: Integrated Core-SOL-Divertor Modelling for ITER Including Impurity: Effect of Tungsten on Fusion Performance in H-Mode and Hybrid Scenario. (25th IAEA Fusion Energy Conference (FEC 2014), 2014-10-13 to 2014-10-18, Saint Petersburg).

Zammuto, I., Giannone, L., Herrmann, A., Kallenbach, A., and ASDEX Upgrade Team: Long term project in ASDEX Upgrade: implementation of ferritic steel as in vessel wall. (28th Symposium on Fusion Technology (SOFT 2014), 2014-09-29 to 2014-10-03, San Sebastian).

Zarzoso, D.: Verification of gyrokinetic codes with energetic particle driven global instabilities. (Numerical Methods for the Kinetic Equations of Plasma Physics (NumKin2014), 2014-10-20 to 2014-10-24, Garching).

Zarzoso, D., Biancalani, A., Bottino, A., Lauber, P., Poli, E., Sarazin, Y., Garbet, X., Dumont, R., and Girardo, J. B.: Turbulent transport of energetic particles in gyrokinetic simulations and impact on the excitation and nonlinear saturation of global instabilities. (19th Joint EU-US Transport Task Force Meeting (TTF 2014), 2014-09-08 to 2014-09-11, Culham).

Zarzoso, D., Hornsby, W. A., Casson, F., Poli, E., and Peeters, G.: Implementation of magnetic islands in gyrokinetics and impact of rotating islands on turbulence. (Joint Varenna-Lausanne International Workshop on Theory of Fusion Plasmas, 2014-09-01 to 2014-09-05, Varenna).

Zastrow, T.: PID Information Types – An RDA Working Group. (DASISH Workshop on Persistent Identifiers – Services and Policies, 2014-12-08 to 2014-12-09, Köln).

Zastrow, T., and Gross, K.: Taco: A Metadata System for Hierarchical Structured Data Collections. (Digital Humanities Conference 2014 (DH 2014), 2014-07-07 to 2014-07-12, Lausanne.

Zhang, X., Zhao, Y., Lu, L., Wan, B., Gong, X., Mao, Y., Lin, Y., Li, J., Hu, L., Song, Y., Kumazawa, R., Wukitch, S., Noterdaeme, J.-M., Braun, F., and Kasahara, H.: High Power ICRF Systems and Heating Experiments in EAST. (25th IAEA Fusion Energy Conference (FEC 2014), 2014-10-13 to 2014-10-18, Saint Petersburg).

Zibrov, M., Mayer, M., Gao, L., Elgeti, S., Kurishita, H., Gasparyan, Y., and Pisarev, A.: Deuterium retention in TiC and TaC doped tungsten at high temperatures. (21st International Conference on Plasma Surface Interactions 2014 (PSI 21), 2014-05-26 to 2014-05-30, Kanazawa).

Zohm, H.: Magnetohydrodynamische Beschreibung heißer Fusionsplasmen. (SS 2014. Vorlesung, Ludwig-Maximilians-Universität München).

Zohm, H.: Recent ASDEX Upgrade Research in Support of ITER and DEMO. (25th IAEA Fusion Energy Conference (FEC 2014), 2014-10-13 to 2014-10-18, Saint Petersburg).

Zohm, H.: Status and Prospects of Nuclear Fusion Using Magnetic Confinement. (78. DPG-Jahrestagung und Frühjahrstagung der Sektion AMOP, 2014-03-17 to 2014-03-21, Berlin).

Teams

ASDEX Upgrade Team

J. Ahn*, L. Aho-Mantila*, S. Äkäslompolo*, C. Angioni, O. Asunta*, M. de Baar*, M. Balden, L. Barrera Orte, F. Bastian, K. Behler, A. Bergmann, J. Bernardo*, M. Bernert, M. Beurskens*, A. Biancalani, R. Bilato, G. Birkenmeier, V. Bobkov, A. Bock, A. Bogomolov*, T. Bolzonella*, J. Boom*, B. Böswirth, C. Bottereau*, A. Bottino, H. van den Brand*, F. Braun, S. Brezinsek*, F. Brochard*, A. Buhler, A. Burckhart, Y. Camenen*, P. Carvalho*, G. Carrasco*, C. Cazzaniga*, D. Carralero, L. Casali, M. Cavedon, C. Challis*, A. Chankin, I. Chapman*, F. Clairet*, I. Classen*, S. Coda*, R. Coelho*, J. W. Coenen*, L. Colas*, G. Conway, S. Costea*, D. P. Coster, G. Croci*, G. Cseh*, A. Czarnecka*, C. Day*, P. de Marné, P. Denner*, M. Dibon, R. D'Inca, D. Douai*, R. Drube, M. Dunne, B. P. Duval*, R. Dux, T. Eibert*, T. Eich, K. Engelhardt, B. Esposito*, E. Fable, M. Faitsch, U. Fantz, H. Faugel, F. Felici*, S. Fietz, A. Figueredo*, R. Fischer, P. Franzen, L. Frassinetti*, M. Fröschle, G. Fuchert, H. Fünfgelder, J. C. Fuchs, J. Galdon*, K. Gál-Hobirk*, S. Garavaglia*, M. Garcia-Muñoz*, B. Geiger, L. Giannone, E. Giovannozzi*, C. Gleason-González*, T. Görler, T. Goodman*, G. Gorini*, S. da Graca*, A. Gräter, G. Granucci*, H. Greuner, J. Grießhammer, M. Groth*, A. Gude, S. Günter, L. Guimarais*, G. Haas, A. H. Hakola*, T. Happel, J. Harrison*, V. Hauer*, B. Heinemann, S. Heinzel, T. Hellsten*, P. Hennequin*, A. Herrmann, E. Heyn*, J. Hobirk, M. Hölzl, T. Höschen, J. H. Holm*, C. Honoré*, C. Hopf, L. Horvath*, A. Huber*, V. Igochine, T. Ilkei*, W. Jacob, A. S. Jacobsen*, J. Jacquot, F. Jaulmes*, F. Jenko, T. Jensen*, E. Joffrin*, C. Käsemann, A. Kallenbach, S. Kálvin*, M. Kantor*, A. Kappatou, O. Kardaun, J. Karhunen*, D. Kim*, A. Kirk*, F. Koch, G. Kocsis*, A. Köhn*, C. Koenen*, J. Kötterl, R. Koslowski*, M. Koubiti*, M. Kraus, K. Krieger, A. Krivska*, D. Kogut*, A. Krämer-Flecken*, T. Kurki-Suonio*, B. Kurzan, K. Lackner, F. Laggner*, P. T. Lang, P. Lauber, N. Lazányi*, A. Lazaros*, A. Lebschy, F. Leuterer, Y. Liang*, B. Lipschultz*, A. Litnovski*, A. Lohs, N. C. Luhmann*, T. Lunt, A. Lyssoivan*, J. Madsen*, M. L. Magnussen*, H. Maier, O. Maj, J. Mailloux*, E. Maljaars*, A. Mancini*, A. Manhard, K. Mank, M.-E. Manso*, P. Mantica*, M. Mantsinen*, P. Manz, M. Maraschek, C. Martens, P. Martin*, A. Mayer, M. Mayer, D. Mazon*, P. J. McCarthy*, R. McDermott, A. Medvedeva, G. Meisl, H. Meister, G. Meisl, R. Merkel, V. Mertens, H. Meyer*, O. Meyer*, D. Milanesio*, J. Miettunen*, A. Mlynek, D. Molina*, F. Monaco, A. Moro*, D. Moseev, H. W. Müller, S. Müller*, F. Nabais*, V. Naulin*, A. Nemes-Czopf*, G. Neu, R. Neu, A. H. Nielsen*, V. Nikolaeva*, S. K. Nielsen*, M. Nocente*, B. Nold*, J.-M. Noterdaeme, S. Nowak*, M. Oberkofler, R. Ochoukov, T. Odstrcil, G. Papp, H. K. Park*, A. Pau*, G. Pautasso, F. Penzel, P. Petersson*, P. Piovesan*, C. Piron*, B. Plaum*, B. Plöckl, V. Plyusnin*, G. Pokol*, E. Poli, L. Porte*, S. Potzel, R. Preuss, D. Prisiazhniuk, T. Pütterich, M. Ramish*, C. Rapson, J. Rasmussen*, J. Juul Rasmussen*, G. Raupp, D. Réfy*, M. Reich, F. Reimold, M. Reinke*, T. Ribeiro, R. Riedl, D. Rittich, G. Rocchi*, M. Rodriguez-Ramos*, V. Rohde, M. Rott, M. Rubel*, F. Ryter, S. Saarelma*, M. Salewski*, A. Salmi*, L. Sanchis-Sanchez*, G. Santos*, J. Santos*, O. Sauter*, A. Scarabosio, G. Schall, K. Schmid, O. Schmitz*, P. A. Schneider, W. Schneider, M. Schneller, R. Schrittwieser*, M. Schubert, T. Schwarz-Selinger, J. Schweinzer, B. Scott, T. Sehmer, M. Sertoli, A. Shalpegin*, L. Shao, U. Siart*, G. Sias*, B. Sieglin, A. Sigalov, A. Silva*, C. Silva*, P. Simon, J. Simpson*, A. Snicker*, F. Sommer, C. Sozzi*, M. Spolaore*, M. Stejner*, J. Stober, F. Stobbe, U. Stroth, E. Strumberger, K. Sugiyama, H.-J. Sun, W. Suttrop, T. Szepesi*, B. Tál*, T. Tala*, G. Tardini, C. Tichmann, D. Told, L. Tophøj*, O. Tudisco*, U. von Toussaint, G. Trevisan*, W. Treutterer, M. Tripský*, M. Valisa*, M. Valovic*, P. Varela*, S. Varoutis*, D. Vezinet, N. Vianello*, J. Vicente*, T. Vierle, E. Viezzer, C. Vorpahl, D. Wagner, X. Wang, T. Wauters*, I. Weidl, M. Weiland, A. Weller, R. Wenninger, M. Wiesinger*, M. Willensdorfer, B. Wiringer, M. Wischmeier, R. Wolf, E. Wolfrum, D. Wünderlich, E. Würsching, O. Yadikin*, Q. Yu, I. Zammuto, D. Zarzoso, D. Zasche, M. van Zeeland*, T. Zehetbauer, M. Zilker, S. Zoletnik*, H. Zohm.

ITED Team

U. Fantz, P. Franzen, M. Fröschle, B. Heinemann, D. Holtum, C. Hopf, W. Kraus, C. Martens, H. Meister, R. Nocentini, S. Obermayer, G. Orozco, F. Penzel, D. Rittich, R. Riedl, J. Schäffler, T. Sehmer, A. Stäbler, D. Wünderlich.

NBI Team

F. Bonomo*, S. Briefi, U. Fantz, H. Falter, P. Franzen, R. Friedl*, M. Fröschle, B. Heinemann, S. Heinrich, D. Holtum, C. Hopf, R. Kairys, W. Kraus, U. Kurutz, C. Martens, A. Mimo, S. Mochalskyy, P. McNeely, R. Nocentini, S. Obermayer, G. Orozco, M. Ricci, R. Riedl, D. Rittich, P. Rong, B. Ruf, N. Rust, J. Schäffler, R. Schroeder, L. Schiesko, E. Speth, A. Stäbler, C. Wimmer, D. Wünderlich.

NNBI Team

F. Bonomo*, S. Briefi, H. Falter, U. Fantz, P. Franzen, R. Friedl*, M. Fröschle, B. Heinemann, W. Kraus, U. Kurutz, C. Martens, A. Mimo, S. Mochalskyy, R. Nocentini, S. Obermayer, G. Orozco, M. Ricci, R. Riedl, B. Ruf, L. Schiesko, C. Wimmer, D. Wünderlich.

W7-X Team

J. Adldinger, J. Ahmels, Y. Altenburg, T. Andreeva, D. Aßmus, M. Balden, J. Baldzuhn, M. Banduch, H. Bandt, H. Bau, D. Beiersdorf, A. Benndorf, C. Biedermann, D. Birus, T. Bluhm, R. Blumenthal, J. Boscary, H.-S. Bosch, B. Böswirth, S. Bozhenkov, A. Braatz, T. Bräuer, R. Brakel, M. Braun, H. Braune, T. Broszat, B. Brucker, R. Burhenn, B. Buttenschön, V. Bykov, A. Carls, D. Chauvin*, M. Czerwinski, N. Dekorsky, C. P. Dhard, A. Dinklage, A. Domscheidt, P. Drewelow*, A. Dudek, H. Dutz, P. van Eeten, K. Egorov, G. Ehrke, S. Elgeti, A. Eller, M. Endler, V. Erckmann, N. Fahrenkamp, H. Faugel, W. Fay, J. H. Feist, J. Fellinger, F. Fischer, O. Ford, S. Freundt, F. Füllenbach, H. Fünfgelder, K. Gallowski, S. Geißler, G. Gliege, M. Gottschewsky, M. Grahl, H. Greuner, H. Greve, S. Groß, K. Grosser, H. Grote, O. Grulke, H. Grunwald, M. Haas, M. Hagen, H.-J. Hartfuß, D. Hartmann, D. Hathiramani, D. Haus, B. Heinemann, St. Heinrich, G. Hemmann, K. Henkelmann, C. Hennig, U. Herbst, U. Hergenhahn, F. Herold, R. Herrmann, K. Hertel, M. Hirsch, H. Hölbe, A. Hölting, F. Hollmann, D. Holtum, A. Holtz, R. Holzthüm, C. Hopf, A. Hübschmann, M. Ihrke, N. Jaksic, M. Jakubowski, D. Jassmann, H. Jensen, H. Jenzsch, A. John, L. Jonitz, P. Junghanns, R. Kairys, J. Kallmeyer, U. Kamionka, T. Klinger, S. Klose, T. Kluck, C. Klug, J. Knauer, F. Koch, R. König, M. Köppen, P. Kornejev, M. Kostmann, R. Krampitz, W. Kraus, J. Krom*, M. Krychowiak, G. Kühner, F. Kunkel, B. Kursinski, A. Kus, A. Langenberg, H. Laqua, H.-P. Laqua, R. Laube, M. Laux, H. Lentz, M. Lewerentz, C. Li, K. Liesenberg, A. Lorenz, J. Maier, M. Marquardt, G. Matern, M. Mayer, P. McNeely, B. Mendelevitch, U. Meyer, G. Michel, B. Missal, H. Modrow, S. Mohr, St. Mohr, A. Möller, T. Mönnich, A. Müller, I. Müller, J. Müller, M. Müller, S. Nack, K. Näckel, M. Nagel, D. Naujoks, R. Neu, U. Neumann, U. Neuner, M. Nitz, R. Nocentini, F. Noke, J.-M. Noterdaeme, S. Obermayer, G. Orozco, M. Otte, E. Pasch, A. Pasyutina, A. Peacock*, T. Sunn Pedersen, M. Pietsch, D. Pilopp, S. Pingel, H. Pirsch, M. Preynas, F. Purps, D. Rademann, K. Rahbarnia, O. Raths, L. Reinke, S. Renard*, T. Richert, R. Riedl, H. Riemann, K. Riße, A. Rodatos*, V. Rohde, P. Rong, K. Rummel, Th. Rummel, N. Rust, N. Rüter, H. Saitoh*, A. Scarabosio, J. Schacht, J. Schäffler, F. Schauer, D. Schinkel, M. Schneider, W. Schneider, P. Scholz, M. Schröder, R. Schroeder, M. Schülke, H. Schürmann, A. Schütz, U. Schultz, T. Schulz, E. Schwarzkopf, R. Schwibbe, C. von Sehren, O. Sellmeier, T. Sieber, G. Siegl, M. Smirnov, A. Spring, J. Springer, R. Stadler, B. Standley, T. Stange, J. Stanja, M. Steffen, E. Stenson, M. Stöcker, U. Stridde, T. Suhrow, J. Svensson, S. Thiel, H. Thomsen, H. Tittes, J. Tretter, P. Uhren, I. Unmack, S. Valet, H. Viebke, R. Vilbrandt, O. Volzke, A. Vorköper, F. Wagner*, F. Warmer, L. Wegener, D. Wegner, M. Weissgerber, J. Wendorf, U. Wenzel, A. Werner, K.-D. Wiegand, D. Wieseler, T. Windisch, E. Winkler, M. Winkler, A. Wölk, R. Wolf, T. Xu*, G. Zangl, H. Zeplien, D. Zhang, M. Zilker.

W7-X ECRH Team

K. Baumann*, G. Dammertz*, G. Gantenbein*, V. Erckmann, F. Hollmann, E. Holzhauer*, H. Hunger*, S. Illy*, J. Jelonnek*, W. Kasparek*, Th. Kobarg*, M. Krämer, R. Lang*, H.-P. Laqua, C. Lechte*, W. Leonhardt*, M. Losert*, A. Meier*, D. Mellein*, R. Munk*, F. Noke, A. Papenfuß*, B. Plaum*, M. Preynas, F. Purps, F. Remppel*, H. Röhlinger*, B. Roth*, A. Samartsev*, T. Scherer*, A. Schlaich*, K.-H. Schlüter*, T. Schulz, W. Spiess*, T. Stange, M. Thumm*, P. Uhren, S. Wadle*, J. Weggen*, S. Wolf*, A. Zeitler*.

W7-X NBI Team

B. Heinemann, D. Holtum, C. Hopf, R. Kairys, C. Martens, P. McNeely, R. Nocentini, S. Obermayer, R. Riedl, N. Rust, R. Schroeder.

---

external authors

Appendix

How to reach IPP in Garching

Nürnberg A9

A92 Deggendorf

Neufahrn

Munich Airport

Bus 690

Exit
Garching
Nord

IPP

Garching-
Research Center

Garching

A9 9

Stuttgart A8

S1

U6

S8

A9 9

München

Lindau

Passau

A9 6

A9 4

A9 9

Garmisch A9 5

A8 Salzburg
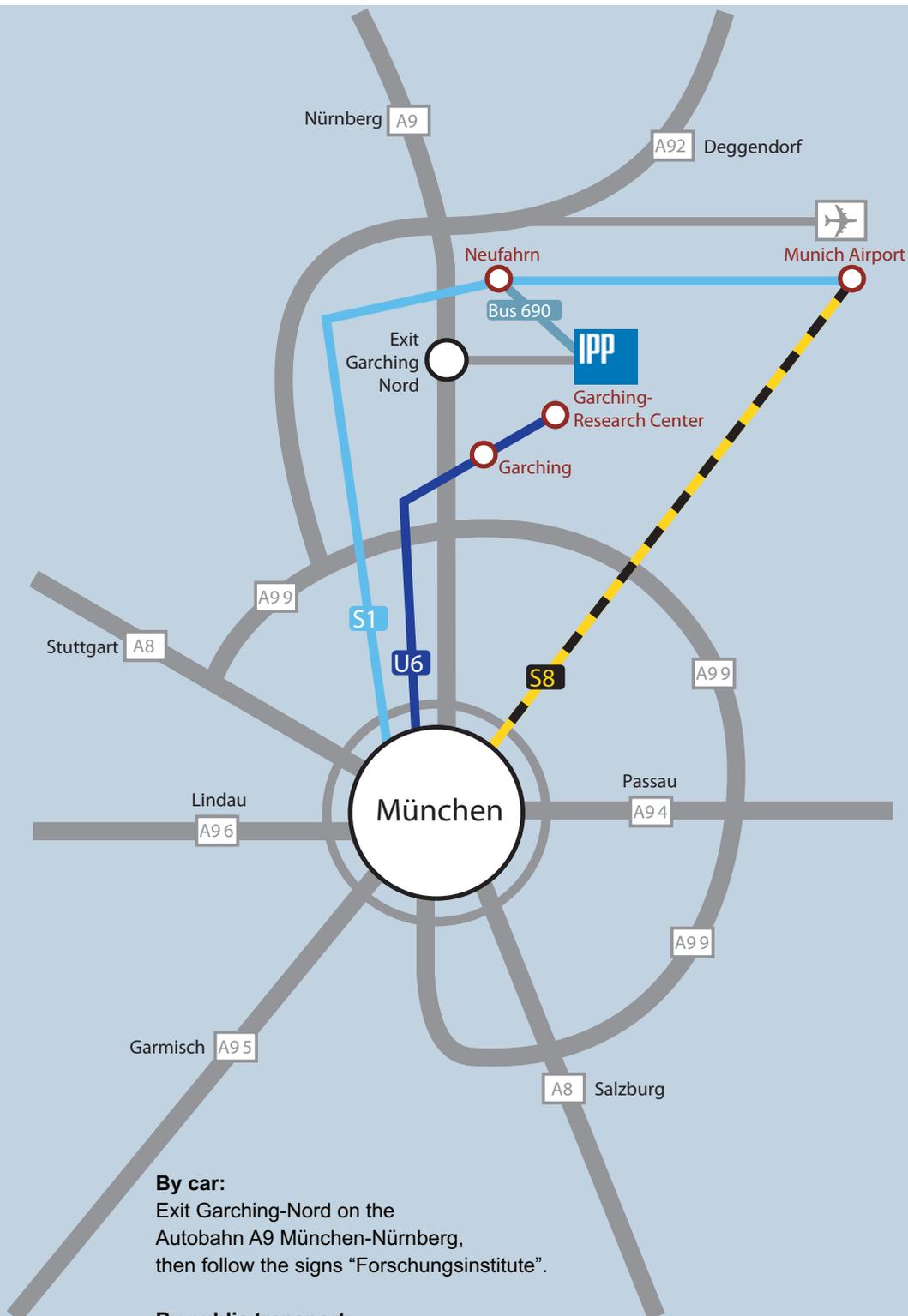
By car:
Exit Garching-Nord on the
Autobahn A9 München-Nürnberg,
then follow the signs "Forschungsinstitute".

By public transport:
Any S metro from Munich Main Station to Marienplatz,
metro U6 to Garching-Forschungszentrum;
or from Airport Munich: S1 to Neufahrn, then bus 690
to "Garching Forschungszentrum" (only on weekdays).

How to reach Greifswald Branch Institute of IPP
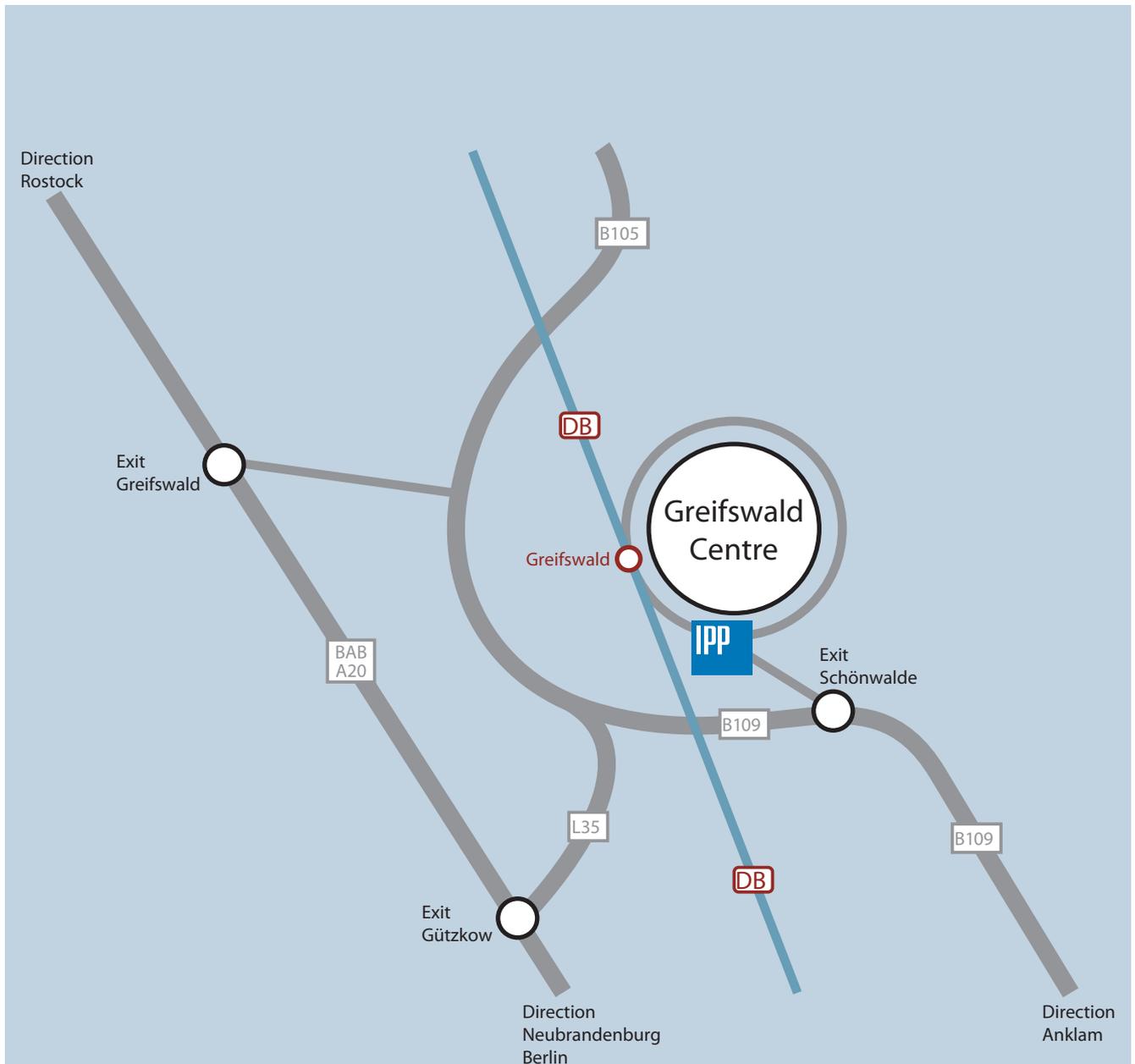
By air and train:
Via Berlin: from Berlin Tegel Airport by bus "JetExpressBus" to Hauptbahnhof (central station), by train to Greifswald.
Via Hamburg: from the airport to main Railway Station, by train to Greifswald main station.

By bus:
From Greifswald-Railway Station (ZOB) by bus No. 3 to the "Elisenpark" stop.

By car:
Via Berlin, Neubrandenburg to Greifswald **or** via Hamburg, Lübeck, Stralsund to Greifswald, in Greifswald follow the signs "Max-Planck-Institut".

IPP in Figures

Funding

In 2014 IPP received approx. 19 % of its total funding from EURATOM. Of the basic national funding 90 % is met by the Federal Government and 10 % by the states of Bavaria and Mecklenburg-West Pomerania. EURATOM funding and national funding amounted to approx. 132 million euros.

Scientific Staff

At the end of the year IPP had a total of 1.076 members of staff, 390 of them worked at IPP's Greifswald site. The work-force comprised 259 researchers and scientists, 56 post-graduates and 71 postdocs.

Organisational Structure

```
                         Max Planck Society                    Helmholtz Association


Advisory Board           Supervisory Board
Dr. R. Hawryluk          Prof. Dr. M. Stratmann
(Chair)                  (Chair)


Board of                 Directorate
Scientific Directors     Prof. Dr. S. Günter (Chair)
Prof. Dr. S. Günter      Prof. Dr. T. Klinger
(Chair)                  Prof. Dr. H. Zohm
                         Dr. J. Schweinzer (Administrator)
```

			Staff Representative Councils G. Kißling (Garching) Dr. H. Grote (Greifswald)
Scientist Representative Council Dr. J. Geiger	Office of the Director Dr. W. Dyckhoff	Organisation Auditing Data Protection	
Tokamak Scenario Development Prof. Dr. H. Zohm	Stellarator Dynamics and Transport Prof. Dr. T. Klinger	Stellarator Heating and Optimization Prof. Dr. R. Wolf	Integrated Technical Center W. Lösch
Plasma Edge and Wall Prof. Dr. U. Stroth	Stellarator Edge and Divertor Physics Prof. Dr. T. S. Pedersen	Wendelstein 7-X Operations Dr. H.-S. Bosch	Technical Services Greifswald R. Krampitz
Tokamak Theory Dr. E. Poli (acting)	Stellarator Theory Prof. Dr. P. Helander		Administration General Services Dr. J. Schweinzer
ITER Technology and Diagnostics Prof. Dr. U. Fantz (acting)	Numerical Methods in Plasma Physics Prof. Dr. E. Sonnendrücker		Administration Greifswald K. Küttler

Last update: 31/01/2015

■ Garching   ■ Greifswald   □ cross-sectional tasks

210

Imprint